FOODS and raw materials

Volume 14
Issue 2
2026

ISSN 2308-4057 (print)
ISSN 2310-9599 (online)

FRM

food production technology

food production processes and equipment

nutrition

veterinary

biotechnology

biological sciences

chemistry and ecology

standardization, certification, quality and safety

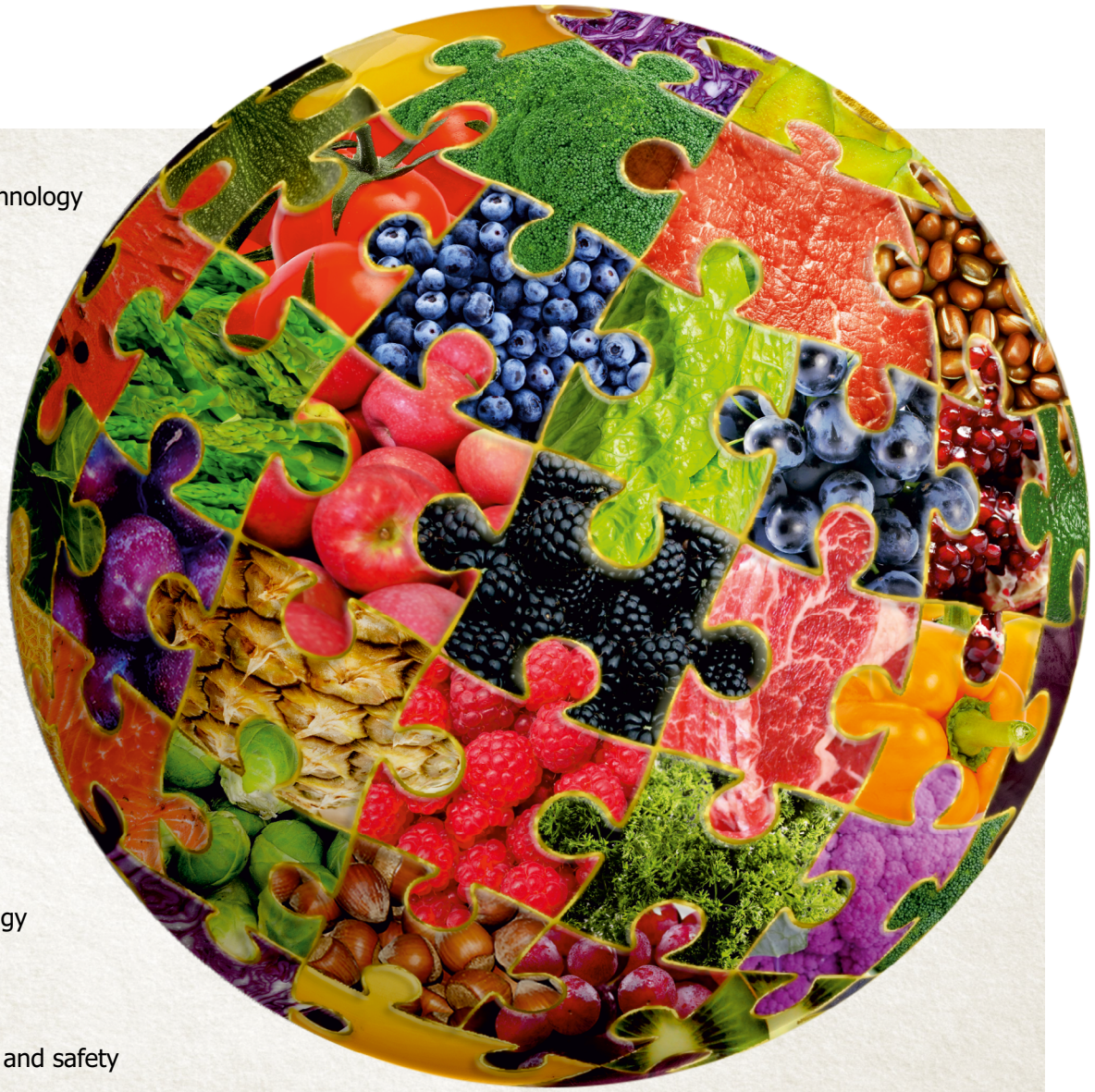

FOODS AND RAW MATERIALS

Kemerovo State University

Vol. 14, no. 2, 2026

ISSN 2308-4057 (Print) ISSN 2310-9599 (Online)

Foods and Raw Materials reports pioneering research in the food industry and agricultural science. We publish the results of fundamental and applied research as scientific papers, peer reviews, brief scientific reports, etc. The Journal is a single platform for scientific communication.

Foods and Raw Materials has been published in the English language since 2013. Two volumes a year come out in print and online.

All submitted manuscripts are checked for plagiarisms via *antiplagiat.ru* and undergo a double-blind peer review. Authors are responsible for the content of their article.

Foods and Raw Materials is supported by the Kemerovo State University. Authors are charged an Article Publication Charge (APC).

Foods and Raw Materials is an open access journal (CC BY 4.0). Our open access policy follows the Budapest Open Access Initiative (BOAI), which means that all our articles are available online immediately upon publication. Full-text electronic versions of all published materials appear in open access on *jfrm.ru/en* and *elibrary.ru*

Foods and Raw Materials is included in the following international data-bases: Scopus, Emerging Sources Citation Index (Web of Science Core Collection), CAS, FSTA, WJCI, Dimensions, LENS.ORG, Scilit, CNKI, ProQuest, CABI, Agricola, Ulrich's, Google Schoar, OCLC WorldCat, and "White list" (Russia) – 1 level.

For submission and subscription instructions, please visit us online at *jfrm.ru/en*

Editor-in-Chief

Alexander Yu. Prosekov, Dr. Sci. (Eng.), Dr. Sci. (Biol.), Professor, Academician of RAS, Kemerovo State University, Kemerovo, Russia.

Deputy Editor-in-Chief

Olga O. Babich, Dr. Sci. (Eng.), Associate Professor, Immanuel Kant Baltic Federal University, Kaliningrad, Russia.

Editorial Board

Levent Bat, Ph.D., Professor Dr., University of Sinop, Sinop, Turkey;

Yogesh Shrinivas Gat, Ph.D., Institute of Chemical Technology, Mumbai, India;

Irina M. Donnik, Dr. Sci. (Biol.), Professor, Academician of RAS, Kurchatov Institute, Moscow, Russia;

Nishant Kumar, Ph.D., National Institute of Food Technology Entrepreneurship and Management, Sonepat, India;

Fatumetuzzehra Küçükbay, Ph.D., Professor Dr., İnönü University, Malatya, Turkey;

Andrey B. Lisitsyn, Dr. Sci. (Eng.), Professor, Academician of RAS, V. M. Gorbatov Federal Research Center for Food Systems of Russian Academy of Sciences, Moscow, Russia;

Yang Li, Dr. Sci. (Eng.), Professor, College of Food Science, Northeast Agricultural University, Harbin, China;

Abdalbasit Adam Mariod, Ph.D., Professor, University of Jeddah, Alkamil, Saudi Arabia;

Philippe Michaud, Ph.D., Professor, Universite Clermont Auvergne, Polytech Clermont Ferrand, Aubiere, France;

Mehran Moradi, Doctor of Veterinary Medicine, Ph.D., Urmia University, Urmia, Iran;

Gláucia Maria Pastore, Ph.D., Professor, Campinas University, Campinas, Brazil;

Shirish Hari Sonawane, Ph.D., Professor, National Institute of Technology Warangal, Telangana, India;

Diako Khodaei, Ph.D., Technical University of Dublin, Dublin, Ireland.

Scientific Editor

Galina V. Gurinovich, Dr. Sci. (Eng.), Professor, Kemerovo State University, Kemerovo, Russia;

Tatyana F. Kiseleva, Dr. Sci. (Eng.), Professor, Kemerovo State University, Kemerovo, Russia;

Alexey M. Osintsev, Dr. Sci. (Eng.), Professor, Kemerovo State University, Kemerovo, Russia.

Executive Editor

Anna I. Loseva, Dr. Sci. (Eng.), Kemerovo State Universty, Kemerovo, Russia.

Founder and Publisher: Kemerovo State University, 6, Krasnaya St., Kemerovo, Kemerovo region – Kuzbass, 650000, Russia

Editorial Office: Kemerovo State University, 6, Krasnaya St., Kemerovo, Kemerovo Region – Kuzbass, 650000, Russia; phone: +7(3842)58-81-19; e-mail: fjournal@mail.ru

Printing Office: Kemerovo State University, 73, Sovetskiy Ave., Kemerovo, Kemerovo Region – Kuzbass, 650000, Russia

Publishing editor: Ekaterina V. Dmitrieva

Translators: Oxana Yu. Pavlova, Nadezda V. Rabkina

Literary editor: Ksenia A. Nikolaeva

Computer layout and design: Elena V. Volkova

Photos credits: contributors

Date of publishing

April 22, 2026

16+

Circulation 500 ex. Open price.

Subscription index in the Ural-Press online catalog – 40539.

The Federal Service for Supervision of Communications, Information Technology, and Mass Media (Roskomnadzor)

Media registration number PI series No. FS77-72606

© Layout, accompanying text, editorial and publishing design, Kemerovo State University, 2026

Foods and Raw Materials. 2026;14(2)

ISSN 2308-4057 (Print)
ISSN 2310-9599 (Online)

Editorial Article
Open Access

Available online at http://jfrm.ru/en
https://doi.org/10.21603/2308-4057-2026-2-679
https://elibrary.ru/MPSBPX

Food security and globalization

Alexander Yu. Prosekov

Kemerovo State University, Kemerovo, Russia

e-mail: aprosekov@rambler.ru

Received 12.05.2025; Revised 20.06.2025; Accepted 01.07.2025; Published online 21.08.2025

Abstract:
Food security goes far beyond the traditional concept of food availability: it is a global challenge of intertwined geopolitics, economics, technology, and ecology. The current international and climate changes cause unpredictable fluctuations on food markets. As a result, sustainable food supply and a powerful agro-industrial complex have become a national priority. The North-South and East-West directions in traffic and logistics open up new, more cost-effective transit routes into a new geopolitical environment, which requires an active development of all related industries. Russia and China have excellent cooperation prospects in a wide range of areas, from agriculture and logistics to R&D and quality standardization. The Belt and Road Initiative creates additional infrastructural opportunities in mutual trade and Eurasian integration. In this respect, food security is a key factor of national and global stability, and it needs a robust agro-industrial complex, advanced infrastructure, active R&D investments, and international cooperation.

Keywords: Food availability, sustainable food supply, international cooperation, transport corridors, food systems, agricultural exports

Please cite this article in press as: Prosekov AYu. Food security and globalization. Foods and Raw Materials. 2026;14(2): 247–251. https://doi.org/10.21603/2308-4057-2026-2-679

Food security is much more than supermarket shelves that burst with food. This global challenge is a maze of geopolitics, economics, technology, and climate. The FAO defines food security as a situation when all people, at all times, have physical, social, and economic access to sufficient safe and nutritious food that meets their dietary needs and food preferences for an active and healthy life [1].

The paradox is that the 21st century with all its advanced technologies and unprecedented food production capacity still sees food shortage epicenters all over the world. A shocking 828 million people worldwide experienced famine in 2021 while another 2.3 billion (29% global population) faced moderate or severe food insecurity [2]. That means that one in ten people on the planet goes to bed hungry. Despite all global efforts, famine remains a looming threat in Africa, South Asia, and Latin America [1].

In 2020–2023, epicenters of abnormal or moderate food insecurity clustered in Africa, Asia, and Latin America (Fig. 1). Africa and Asia had the highest number of people facing famine. Even Europe and North America still demonstrate areas affected by food insecurity. These data clearly show the major imbalance and uneven distribution of food risks across the globe. While the so-called Western world enjoys a relatively stable basic food supply, most developing regions face critical food shortages. This situation obviously requires urgent measures.

By 2050, the working-age population will double in 52 countries, most of which are in Africa, not to mention Iraq, Afghanistan, Guatemala, and Papua New Guinea. Asia will give its title of the most overpopulated continent to Africa with its 50% of the global population growth. By 2100, African population will have increased from 1.1 billion to 4.2 billion people.

China's population is expected to peak around 2030 and begin to decline. India will have surpassed China by 2028. Both countries are projected to have approximately 1.45 billion people at that point. These processes are fueled by uneven distribution of resources and food availability. While some countries have to scrape by the basic food minimum, others enjoy food surplus of such a scale that it results in a mass food waste crisis. The FAO estimates that about 1.3 billion tons of food is discarded as wastes annually at different stages of the product life cycle [3], i.e., as much as one third of all global food production. In some places, people live in constant threat of

Copyright © 2025, Prosekov. This is an open access article distributed under the terms of the Creative Commons Attribution 4.0 International License (https://creativecommons.org/licenses/by/4.0/), allowing third parties to copy and redistribute the material in any medium or format and to remix, transform, and build upon the material for any purpose, even commercially, provided the original work is properly cited and states its license.

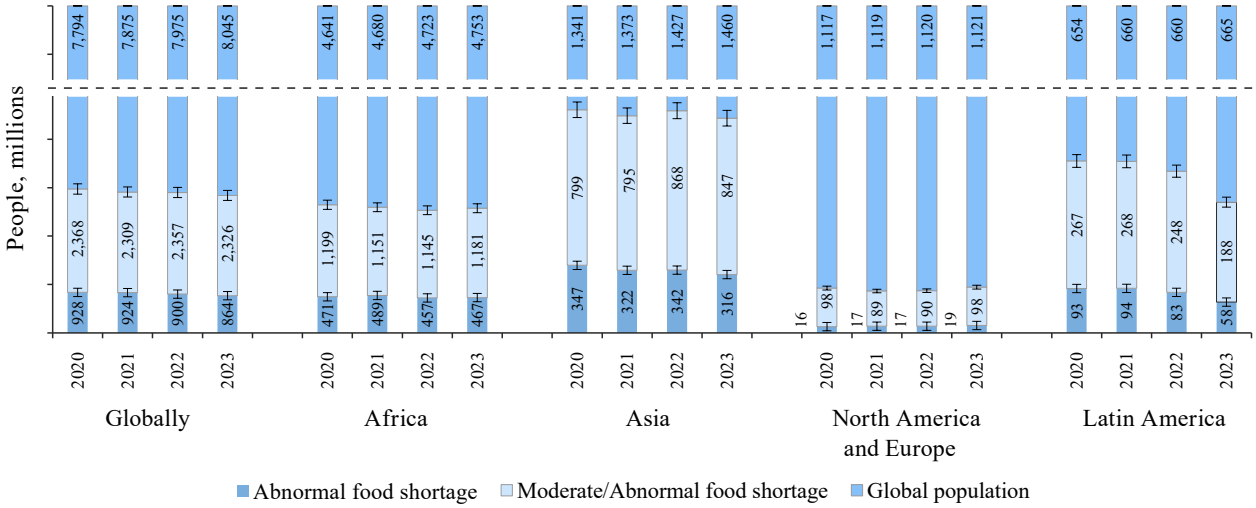

Figure 1 Moderate and abnormal food insecurity, 2020–2023

famine and starvation; in other places, excess consumption is seen as a national disaster. Big agricultural countries are also at risk. For instance, the countries of the Eurasian Economic Union keep lagging behind world leaders in agricultural land use efficiency.

The situation is aggravated by such global factor as climate change, which directly affects food systems. While food demand continues to grow, maize and wheat yields may drop by 10–25%, the Intergovernmental Panel on Climate Change (IPCC) prognoses for 2050 [4]. But in fact, droughts, floods, soil degradation, and desertification are not matters of some distant future but the reality that millions of farmers have to face every day.

Geopolitical instability is another important factor that affects global food security. Conflicts, trade wars, and unstable supply chains wear out national food systems. The FAO-WHO Food Price Index reached a historical maximum of 159.7 points in 2022 [5]. The situation could not but affects food availability because the global agri-food market is a complex system where everything is interconnected.

The recent COVID-19 pandemic revealed all the fragility of the traditional food supplies and logistics, especially in metropolitan cities. Mobility restrictions, border closures, agricultural job cuts, and disruptions in international logistics resulted in temporary shortages even in the countries with the most reliable food security. The pandemic demonstrated that even highly developed countries are not immune to food vulnerability [1].

The food insecurity map for 2015–2022 shows a steady increase in both moderate and abnormal food insecurity (Fig. 2). In Africa, the total share of food insecurity victims reached 60% in 2022, with 24% suffering from severe food shortage. In Latin America, the total moderate and abnormal food shortage exceeded 37% the same year. Even Asia, with its robust agricultural sector, had 20% of population facing food restrictions. Europe and North America slowed down at 6–8%, but these figures also demonstrate major risks [1].

Food security is rightly associated with poverty, health, and education. Poor diet affects the cognitive development of children, reduces labor performance of adults, and increases health care costs for all population groups. According to the World Bank, starvation and malnutrition annually cost $3.5 trillion of global GDP in low productivity and high morbidity [6].

Sustainable food supply is much more than production figures. It is a matter of fair access to means that could boost the development of local farming, agricultural technologies, storage techniques, and distribution systems. The current gap between rural and urban areas is as big as that between the global North and South. Even countries with advanced agriculture have areas where people get no access to fresh food due to poverty, remoteness, or logistical constraints.

Food security is a major priority task of Russian national policy, just like in any other country. Its priority has significantly increased in recent years, fueled by international challenges, climate change, and global fluctuations in food markets. The national food independence and agro-industrial sustainability are especially relevant issues. In Russia, they are regulated by the Food Security Doctrine, first approved in 2010 and updated in 2020 and 2025. In its latest version, the focus has shifted from strong domestic production to sustainable food systems that are resistant to external and internal challenges.

In 2023, Russia achieved high self-sufficiency indicators in some key food categories, the Ministry of Agriculture reports. In percentage from domestic demand, the results were 185.5 for grain production, 221.1 for vegetable oil, 153.2 for fish products, 103.2 for sugar, and 101.6% for meat [7]. The national food market apparently proved its stability in the face of global challenges. Grain production has achieved the best results. In 2022–2023, Russia hit a record of 156 million tons, thus strengthening its position as a leading wheat exporter. Having become a leader in a number of other commodity

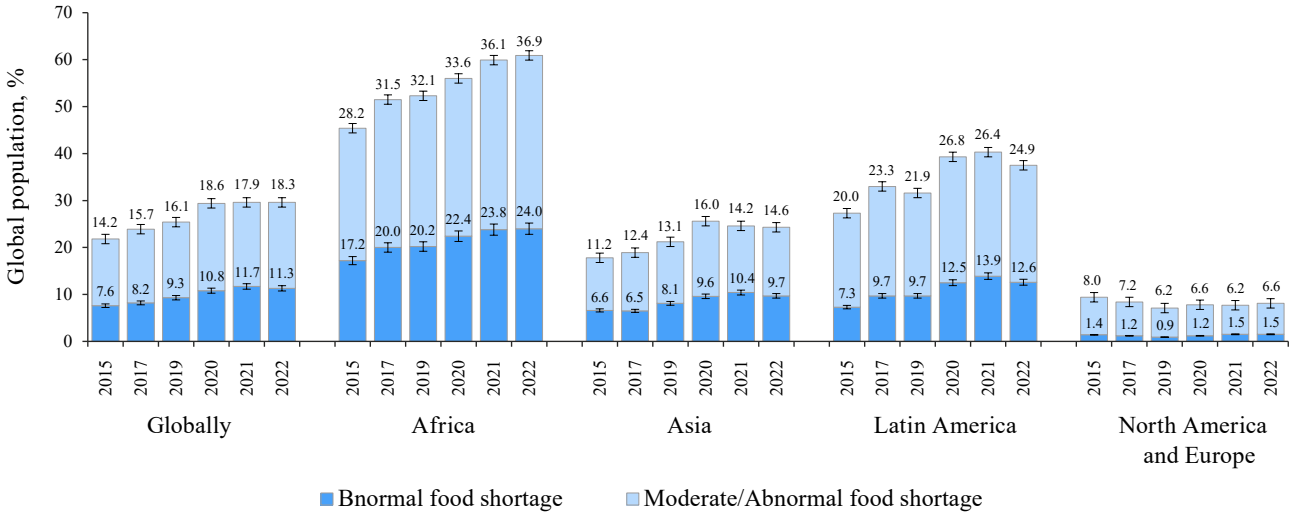

Figure 2 Moderate and abnormal food insecurity across the globe in 2015–2022

groups, Russia has been able to increase its agricultural exports, which reached $43 billion in 2023 [8].

Yet a number of areas are experiencing difficulties. Dairy self-sufficiency remains a major concern: it was as low as 85.7% in 2023. An even worse situation was observed the same year on the domestic market of vegetables (82%) and fruits and berries (60%) [9]. The seed sector also remains particularly vulnerable since Russia still relies on imported seeds. The share of domestic seeds is 3 for sugar beets, 9 for potatoes, 22 for sunflowers, and 42% for maize [10]. Should this situation persist, agricultural sustainability will find itself in jeopardy from the increasing international pressure.

The Western sanctions make Russia adjust its logistics to improve the national food security. The new transport corridors offer new logistics chains. The North-South and East-West transport and logistics corridors open up new opportunities for cheap transit, facilitating the trade in the actual geopolitical conditions and developing other economic sectors. As Russian agri-food exports are redirected to friendly countries, their total share has increased to 90%. In 2023, our largest importers were China, Turkey, Egypt, Kazakhstan, Belarus, South Korea, India, and Saudi Arabia. These new trade corridors simplify the import of agricultural equipment, vaccines, vitamins, animal feed, and seedlings to support the domestic agricultural production.

Climate change is another major stress factor to Russia's food security. As droughts, floods, and other extreme weather events strike the traditional centers of agricultural production (Volga Valley, South-Western Siberia, Central Black Earth Region), the crop yields go down while the production costs go up [10]. The national response includes melioration projects, drought-resistant cultivars, and advanced agricultural technologies.

Social availability of food is by no doubt a national priority. As the real income of some social strata continues to plummet, the state has to keep basic foods affordable. The current share of food expenses in the overall structure of consumer spending is about 35% [9]. However, some regions that are going through a difficult socio-economic phase are facing severe food insecurity with 20% of households struggling to purchase the basic food products [11].

In these conditions, the country tries to stimulate its export of agricultural products with high added value. Processed foods, organic products, and functional foods are to stabilize the domestic agricultural sector by reducing its dependence on fluctuations in raw materials markets. Another export option is R&D in biotechnology, agroecology, and climate-resistant varieties [8].

Food security requires an effective monitoring system for prompt response to internal and external threats. It includes an ongoing analysis of food market, supply and demand forecasts, and strategic food reserves. The new federal projects in veterinary and agro-industrial biotechnology launched in 2024 are aimed at producing domestic veterinary drugs, plant protection, enzymes, feed additives, etc. In addition, the State Program of Agrarian Science for the Future of Agro-Industrial Complex is to merge with another major State Project on Independence and Competitiveness of National Agro-Industrial Complex.

Investment projects in food security can be divided into four groups. Firstly, the transport and logistics infrastructure projects include the North-South corridor, terminals in the Far East, the Caspian Sea, and the Baltic Sea, as well as hubs, linear elevators, and wholesale distribution centers. Secondly, the storage projects include silo elevators and vegetable/fruit storage facilities in consumer regions. Thirdly, the agro-industrial R&D projects include the development of agricultural science in selection, seed production, livestock breeding, complex fertilizers, veterinary drugs, feed additives, agricultural machinery, etc. Finally, the list of import substitution projects in transport engineering includes a larger merchant fleet, as well as producing more storage

containers and refrigerated cars. These areas may reduce food security risks, both nationally and globally.

Russia and China are both world's largest powers with rapidly developing economies. As food security is becoming a major aspect of strategic planning, they are striving to build a sustainable food security system both in the national and cross-regional contexts. The current agricultural cooperation between Russia and China covers investment, scientific, technological, and infrastructure projects. Both countries see agricultural cooperation as an important step to a stronger economic stability and national independence.

Agricultural investment projects between Russian and Chinese companies are a rapidly developing area. The main efforts are concentrated in the Russian Far East and Eastern Siberia: despite their significant land potential, they are short of investments. Chinese investments in Russian agriculture account for 13% of China's total foreign investments [12]. Chinese agricultural technologies and seeds increase Russian crop yields and reduce production costs. These projects facilitate the implementation the Food Doctrine, which secures the growth of domestic agricultural production [9].

Russia and China also focus on logistics infrastructure to optimize food supplies. The international agricultural logistics center in Blagoveshchensk is a perfect example in this sphere. The center is supported by the Russian Export Center and Chinese enterprises. It will include elevators, warehouses, storage terminals, and transport hubs for agricultural products [13]. When integrated into transport routes, it will speed up deliveries between Russia and China, as well as expand the export capabilities of Russian producers in the Asian market.

Our participation in the global Chinese Belt and Road Initiative also strengthens our national food security. Launched in 2013, the Initiative presupposes new infrastructure and trade corridors to connect Asia, Europe, and Africa. The land and sea trade routes of the Belt and Road Initiative (Fig. 3) go across Asia, Europe, and Africa, with major hubs that proved global integration [14]. Due to its geographical location, Russia becomes the central link in the New Silk Road, which opens up broad prospects for boosting the international agricultural trade. When modernized, the railways and highways across Siberia and the Far East will reduce the delivery time and maintain the quality of agricultural products transported to China and other Asian countries. Other joint projects make it possible to create a more sustainable food supply chain, minimizing the risks associated with unreliable global logistics.

Organic farming is an important cooperation area. The Chinese demand for organic products grows annually by 10–15% [1]. Russia, with its vast unpolluted land resources, is a promising partner in the field of organic crop production. In 2022, Russian and Chinese companies sighed several cooperation agreements to export organic grain cultivation and oilseed crops to China. The products are to be certified and labelled in line with Chinese and international standards.

The ongoing R&D cooperation also strengthens food security in both countries. Joint research projects are aimed at developing highly productive agricultural cultivars that are resistant to adverse climate, e.g., soya, potatoes, and maize adapted to the harsh environment of the Far East and Siberia [15]. The research results increase the yields and reduce the national dependence on imported seeds.

Biosecurity in mutual food trade is a relevant aspect of international cooperation. In 2024, Russia and China signed an agreement on the mutual recognition of veterinary and phytosanitary certificates to simplify the export- agricultural import [16]. A weaker red tape and a stronger food quality control will improve the food security in both countries.

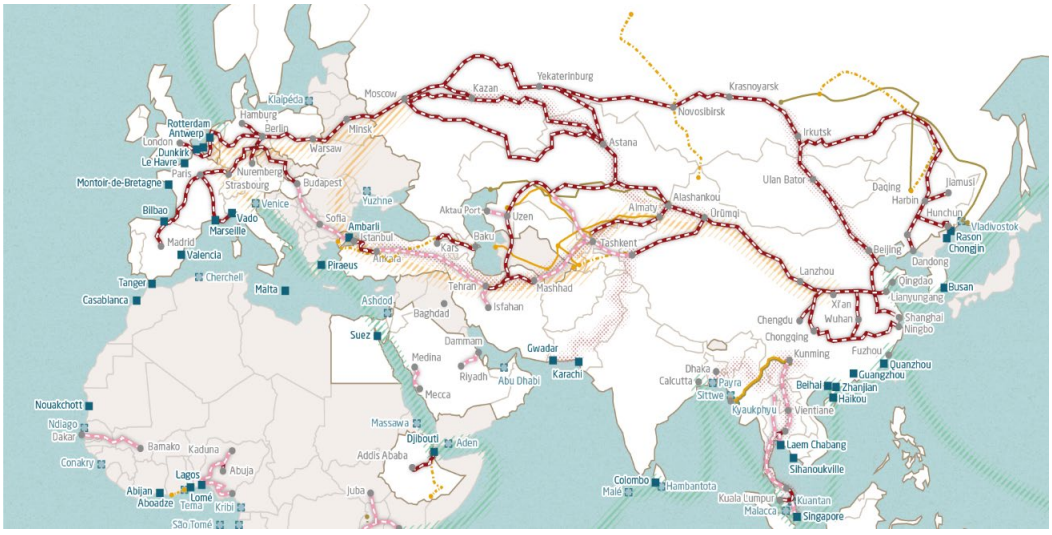

Figure 3 The Belt and Road Initiative: Red lines – economic corridors that link China with Central Asia, Russia, Europe and the Middle East; yellow lines – extra transport routes and branches; blue lines – maritime trade routes across the Indian Ocean, the Suez Canal, and the Mediterranean Sea

The joint projects between Russia and China in the field of food security range from agricultural production and logistics to R&D and quality standardization. The Belt and Road Initiative creates additional infrastructure opportunities, strengthening the trade ties and promoting the integration processes in Eurasia. In the context of global instability and increased competition, the strategic partnership between Russia and China is important for both countries. Major prospects lie in mutual agro-industrial investments, robust R&D cooperation, and strong foreign food trade regulations.

Food security is an integral part of national and global stability. In the context of overpopulation, climate change, geopolitical conflicts, and disrupted global supply chains, food security has become an (inter)national priority. As counties strive to improve their domestic agriculture, technologies, food storage infrastructure, and transport logistics, they seek international cooperation to create sustainable food systems.

CONFLICT OF INTEREST

The author declare no conflict of interest.

REFERENCES

1. The State of Food Security and Nutrition in the World 2023. Urbanization, agrifood systems transformation and healthy diets across the rural–urban continuum. Rome: FAO; 2023. 283 p. https://doi.org/10.4060/cc3017en
2. UN Report: Global hunger numbers rose to as many as 828 million in 2021. World Health Organization. [cited 2025 Apr 26]. Available from: https://www.who.int/ru/news/item/06-07-2022-un-report--global-hunger-numbers-rose-to-as-many-as-828-million-in-2021
3. FAO. The State of Food and Agriculture 2019. Moving forward on food loss and waste reduction. Rome: FAO; 2019. 192 p. https://doi.org/10.4060/ca6030en
4. IPCC. Climate Change 2022: Impacts, adaptation and vulnerability. Contribution of Working Group II to the Sixth Assessment Report of the Intergovernmental Panel on Climate Change. Cambridge, NY: Cambridge University Press; 2023. 3056 p. https://doi.org/10.1017/9781009325844
5. World Food Situation. Food and Agriculture Organization of the United Nations. [cited 2025 Apr 26]. Available from: https://www.fao.org/worldfoodsituation/foodpricesindex/ru
6. The Cost of Hunger: The Social and Economic Impact of Child Undernutrition on Lesotho Vision 2020. Reliefweb. [cited 2025 Apr 26]. Available from: https://reliefweb.int/report/lesotho/cost-hunger-social-and-economic-impact-child-undernutrition-lesotho-vision-2020
7. Sergey Semenov. Welcome to our table. Bulletin of the Agro-Industrial Complex. 2024;(2):52–57. [cited 2025 Apr 26]. (In Russ.) Available from: https://vestnikapk.ru/articles/aktualno/prosim-k-nashemu-stolu/
8. Shchetinina I. Has Russia gained food security? ECO. 2024;54(6):258–280. https://doi.org/10.30680/ECO0131-7652-2024-6-258-280
9. Consumption of basic foodstuffs by the population of the Russian Federation. Federal State Statistics Service. [cited 2025 Apr 26]. (In Russ.) Available from: https://rosstat.gov.ru/compendium/document/13278
10. Vershinina DD, Makarova IV. Improving Russia's food security under sanctions: Results and prospects. The Eurasian Scientific Journal. 2024;16(s6). (In Russ.) https://esj.today/PDF/47FAVN624.pdf
11. Rosselkhoznadzor held a Board meeting on the results of its activities in 2023. [cited 2025 Apr 26]. (In Russ.) Available from: https://fsvps.gov.ru/news/rosselhoznadzor-provel-zasedanie-kollegii-po-itogam-dejatelnosti-v-2023-godu/
12. Russia and China will jointly develop agriculture in the border areas. [cited 2025 Apr 26]. (In Russ.) Available from: https://mcx.gov.ru/press-service/news/rossiya-i-kitay-budut-sovmestno-razvivat-selskoe-khozyaystvo-na-prigranichnykh-territoriyakh/
13. A resident of the Amurskaya Priority Development Area has launched a key logistics complex on the border with China. Far East Development Corporation. [cited 2025 Apr 26]. (In Russ.) Available from: https://erdc.ru/news/rezident-tor-amurskaya-zapustil-klyuchevoy-logisticheskiy-kompleks-na-granitse-s-kitaem/
14. Li N. "One belt, one road" initiative as a new cooperation model of the PRC with Russia and central Asia countries. RUDN Journal of World History. 2018;10(4):382–392. https://doi.org/10.22363/2312-8127-2018-10-4-382-392
15. The Chinese tested the seeds of Amur soybeans and potatoes. National Agrarian Agency. [cited 2025 Apr 26]. (In Russ.) Available from: https://rosng.ru/post/kitaycy-protestirovali-semena-amurskoy-soi-i-kartofelya
16. Following the results of the Russian-Chinese talks in Beijing, five documents were signed. Alfa-Soft. [cited 2025 Apr 26]. (In Russ.) Available from: https://www.alta.ru/external_news/100778/

ORCID IDs
Alexander Yu. Prosekov https://orcid.org/0000-0002-5630-3196

Foods and Raw Materials. 2026;14(2)

ISSN 2308-4057 (Print)
ISSN 2310-9599 (Online)

Research Article
Open Access

Available online at http://jfrm.ru/en
https://doi.org/10.21603/2308-4057-2026-2-672
https://elibrary.ru/FIGHAE

Alternative sweets from cooked pulses and date products: Nutritional and quality characteristics

Azza A. Omran*, Nadra S.Y. Hassan, Abd Elaziz M. Hanaa

Food Technology Research Institute, Agricultural Research Center, Giza, Egypt

* e-mail: azzaa_omran@yahoo.com

Received 26.07.2024; Revised 25.11.2024; Accepted 27.11.2024; Published online 27.06.2025

Abstract:
Nowadays, the worldwide market includes a wide variety of sweets with processed sugar. The food industry has been developing alternatives based on health products. This study aimed to formulate alternative, highly-nutritional date-based sweets filled with cooked pulses and sweetened with date products without using processed sugar. Different cooked pulses (red cowpea, soybean, and chickpea seeds) sweetened with date powder or date syrup (dips) were used to prepare alternative date sweets. They were exposed to physicochemical and microbiological analyses and sensory evaluation. Adding pulses to the pulse-date sweet samples significantly raised their contents of protein, fats, crude fibers, total sugars, calcium, iron, and zinc, as well as caloric values, lightness, and water activity. Compared to the control (date paste mixed with dark chocolate), the sweets with cooked pulses had lower contents of ash, carbohydrates, phenolics, and caffeine, as well as lower antioxidant activity and hardness values. Following storage for three months, the water activity and microbiological counts slightly declined. The date sweets filled with cooked pulses had high sensory acceptability. The samples containing cooked red cowpeas and chickpeas were the most acceptable, while those sweetened with date powder had maximum antioxidant activity. Our study revealed that enriching date sweets with cooked pulses increases their nutritional value without involving processed sugar in the final product.

Keywords: Date palm products, soybeans, chickpea, dark chocolate, alternative sweets, nutritional quality, sensory attributes

Please cite this article in press as: Omran AA, Hassan NSY, Hanaa AEM. Alternative sweets from cooked pulses and date products: Nutritional and quality characteristics. Foods and Raw Materials. 2026;14(2):252–263. https://doi.org/10.21603/2308-4057-2026-2-672

INTRODUCTION

Legumes, or pulses, are a low-cost, natural source of protein and phenolic compounds such as tannins, phenolic acids, and flavonoids. In addition, they are rich in antioxidants and minerals, which could prevent mineral deficiencies [1, 2]. Cowpea seeds (*Vigna unguiculata* L.) are an important pulse crop grown in Africa and in some parts of America and Asia. They are widely consumed as an affordable source of protein, potassium, and polyphenols. Also, they have very low contents of lipids and sodium [3].

Soybeans (*Glycine max* L.) are a significant source of protein and lipids worldwide, with high nutritional and commercial value. They contain considerable amounts of folic acid, isoflavones, and saponins. Soybean products are gaining more attention due to their benefits for human health. In particular, they can reduce cholesterol and prevent multiple chronic diseases such as obesity, diabetes, and cardiovascular disease, as well as some types of cancer [4].

The chickpea (*Cicer arietinum* L.) is a major pulse crop cultivated and consumed all over the world. It has a high content of protein, crude fibers, and dietary fibers, as well as a lower content of carbohydrates than cereals. Chickpeas are rich in bioactive compounds such as saponins, carotenoid, tocopherol, and phenolic acids. Adding chickpeas to food products can increase their nutritional value. Additionally, the pulse nutrients' availability can be enhanced by different processing methods such as soaking and cooking [5, 6].

The date palm (*Phoenix dactylifera* L.) is one of the most significant cultivars worldwide. Its fruit has a high nutritional value and an abundance of minerals, dietary fibers, and other healthy metabolites [7]. Date fruit is also rich in antioxidants, proteins, carbohydrates, and a vitamin B complex (riboflavin, thiamine, pantothenic, niacin, folate, and pyridoxine). According to Aljaloud *et al.* [8], 70% of the date fruit is made up of carbohydrates, specifically fructose and glucose. The nutritional and sensory qualities of palm dates are enhanced by the pres-

Copyright © 2025, Omran *et al.* This is an open access article distributed under the terms of the Creative Commons Attribution 4.0 International License (https://creativecommons.org/licenses/by/4.0/), allowing third parties to copy and redistribute the material in any medium or format and to remix, transform, and build upon the material for any purpose, even commercially, provided the original work is properly cited and states its license.

ence of phytochemicals, such as flavonoids, carotenoids, and phenolic components.

Dates have found multiple applications in the food industry due to their enormous production worldwide [9]. According to the Bulletin of Food Balance Sheet [10], Egypt produced 523,000 tons of dried dates and date paste in 2021. Date fruits provide a wide range of potential health advantages. This has created a need for novel food products incorporating dates as a source of nutrients [8].

Candies and sweets may contain fruits, chocolate, nuts, honey, sugar, or other sweeteners. Chocolate is one of the most common and highly desired foods in the world market [11, 12]. Its consumption as a daily snack has increased among all age groups [11, 13]. Dark chocolate consumed for two weeks may boost microbiological activity in the gut and normalize the effects of stress on human metabolism [14]. Children most commonly favor chocolate biscuits, chocolate bars, chocolate cake, chocolate ice cream, and cocoa milk [15]. However, sweet products, particularly chocolates, have long been thought to be unhealthy because of their high sugar content (processed sugar). Consequently, food researchers have been working hard to modify recipes in the hope to improve the nutritional profile of sweet-based chocolate. This has included lowering the amount of sugar or adding ingredients without changing the texture or sensory aspects of the product [11].

The most significant changes in the food industry have been motivated by the consumers' rising demand for functional or health-promoting foods with bioactive components that positively modulate the immune system [16]. Since consumers are becoming increasingly concerned about their well-being and good health, they are changing their eating habits in favor of nutritious foods with functional components [1]. This drives the food industry and inspires the development of novel products [17]. In particular, the consumers' demand for healthier sweeteners has promoted a switch from sucrose, the most common sweetener used in chocolate, to other alternatives such as coconut- or palm-based sugar [18].

The core target of fortification is to enhance the nutritional value of products while also making them more self-sufficient and complementary to food products [16]. A strategy that is now being encouraged is the use of natural ingredients with an abundance of bioactive substances and beneficial nutritional contents. Fortifying food products with high-value-added seeds or plant-based materials may alter their nutritional qualities, overall consumer acceptance, and shelf life [16, 19].

Therefore, in this study, we aimed to produce alternative sweets from cooked pulses sweetened with date powder or date syrup (dips). The pulses were used as a filling in the sweets coated with date paste and dark chocolate. The sweet products were analyzed for their physicochemical, nutritional, microbiological, and sensory properties.

STUDY OBJECTS AND METHODS

Materials. Soya bean seeds (*Glycine max* L., Giza 111 variety) were provided by the Field Crops Research Institute, Agricultural Research Center, Egypt. Red cowpea seeds (*Vigna unguiculate* L. Walp, *Leguminasae* family) were purchased from the markets in Cairo and then botanically recognized and authenticated by the Flora and Phytotaxonomy Research Department, Horticulture Research Institute, Agricultural Research Center, Egypt. Chickpea (*Cicer arietinum* L.), date powder, date dips (68% TSS) and dark chocolate were purchased from markets in Cairo and all of the other chemicals were analytical grade.

Pulses processing. Different pulse seeds were exposed to certain technological treatments. They had been thoroughly cleaned and freed of any extraneous materials and broken seeds before being soaked in water (1:2, w/v) for 12 h (the soaking water was changed twice). The soaked seeds were then cooked in water (1:3, w/v) for 60–70 min, drained, and hulled. Then, the cotyledons were mashed, filtrated through a cloth to remove excessive water, packed in polyethylene bags, and frozen for further use.

Pulse-date sweet preparation. The cooked pulses were heated for 10 min until the appropriate consistency was achieved. Then, 120 g of date paste was mixed with 80 g of dark chocolate and filled with 100 g of the cooked pulses sweetened with 20 g of date powder or date dips (based on preliminary experiments). The weight of each sweet sample was 12 g (8 g of date paste mixed with dark chocolate and 4 g of cooked pulses). Then, the samples were shaped, stored in polypropylene metalized bags, and refrigerated at 4 ± 1°C for 90 days until further investigation (Fig. 1).

Proximate analysis. The moisture, protein, fat, crude fibers, and ash contents of raw materials, cooked pulses, and pulse-date sweet samples were estimated using the methods of the Association of Official Analytical Chemists (AOAC) [20]. Carbohydrates were determined as follows: [carbohydrates = 100 – (ash + fats + crude fibers + protein)]. The calcium, iron, and zinc contents were measured by Model-4210 MP-AES Microwave Plasma Atomic Emission Spectrometers (Agilent Technologies, USA) using the method established by the AOAC [20]. Total calories in the pulse-date chocolate samples were calculated by multiplying the fat, protein, and carbs values on the basis of 9, 4, and 4 kcal/g, respectively [20]. The total sugar content was measured by the Somogyi-Nelson method, as described by the AOAC [20]. The pH of the samples was measured with a pH meter. The daily intakes, %, of protein, calories, calcium, iron, and zinc in the pulse-date sweets were calculated using the Dietary Reference Intakes (DRI) [21] and the Recommended Dietary Allowances (RDA) [22] using the Eq. 1:

$$\text{The calculated daily intake} = \frac{\text{Value of the nutrient in each sample}}{\text{DRI or RDA for each age group for the same nutrient}} \quad (1)$$

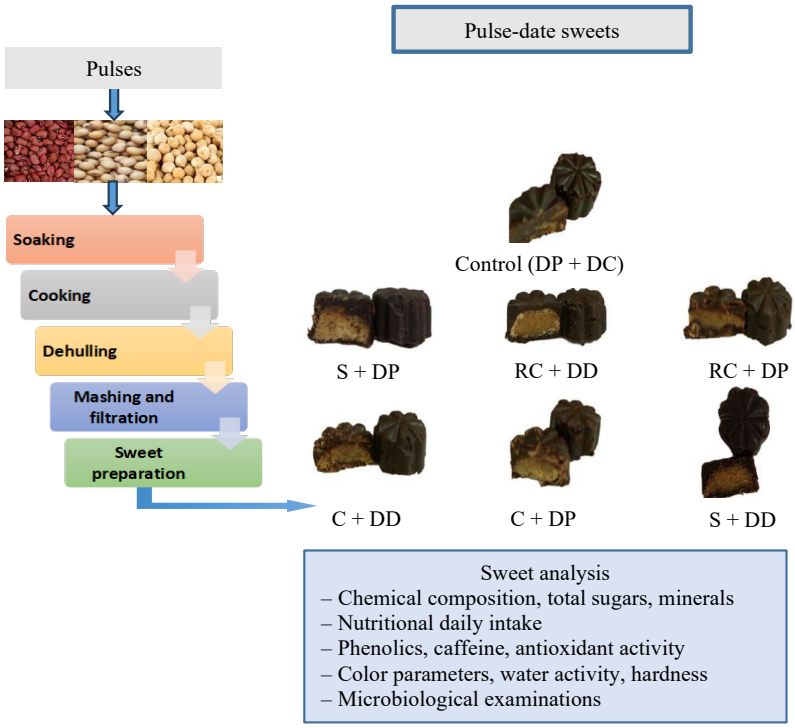

Control (DP + DC) – date paste mixed with dark chocolate, RC + DP – red cowpea with date powder, RC + DD – red cowpea with date dips, S + DP – soybean with date powder, S + DD – soybean with date dips, C + DP – chickpea with date powder, and C + DD – chickpea with date dips

Figure 1 The pulse-date sweet preparation

Determination of total phenolics. The total phenolic content in the pulse-date sweet samples was extracted and evaluated based on the Folin-Ciocalteu phenol method [23]. The samples' absorbance was measured at 725 nm by a Jenway spectrophotometer Model-6715-UV/Vis (Cole-Parmer Ltd, UK), and the data was presented as mg/100 g of gallic acid equivalent.

Caffeine determination. To determine the caffeine content, 2 g of a sample and 20 mL of H_2O were boiled in a water bath for 10 min, then 2 g of sodium carbonate was added to the mix (to precipitate tannins), and filtered. The samples were concentrated by heating and added to 5 mL of chloroform in the separator funnel. The bottom layer was separated and 0.10 mL of each sample was diluted with 10 mL of chloroform [24]. The absorbance of the samples was measured at 274 nm against the blank, and the results were expressed as mg/100 g of caffeine equivalent.

Free radical scavenging by DPPH. The antioxidant activity of the phenolic sample extract was measured by mixing 0.10 mL of the extract with 3.90 mL of DPPH methanol solution (2.40 mg of DPPH dissolved in 100.0 mL of methanol) [25]. The mixture was left in the dark for 30 min and then measured at 515 nm, and the radical scavenging, %, as DPPH was calculated using the Eq. (2):

$$\text{Radical scavenging} = \left[\frac{A_0 - A_1}{A_0}\right] \times 100 \qquad (2)$$

where A_0 is the absorbance of the control reaction and A_1 is the absorbance of the tested sample after 30 min.

Sensory evaluation. The pulse-date sweet samples and the control (DP + DC) were cooled to room temperature (23 ± 2°C) before a sensory evaluation by ten panelists from the Food Technology Research Institute. The samples were assessed for color, sweetness, mouthfeel, odor, taste, aftertaste, and overall acceptability. The panelists were informed about the study and the products to be tasted before they gave their consent. We used the nine-point hedonic test (9 – extremely like; 5 – neither like nor dislike; 1 – extremely dislike) [26].

Color measurement. The color characteristics of the sweet samples (for outer and inner color) were determined with a hand-held Tristimulus reflectance colorimeter Minolta Chroma Meter CR-400 (Konica Minolta, Japan). The color parameters were recorded as L^* [lightness = (100 for lightness and zero for darkness)]; a^* [redness = red (+) to green (–)]; and b^* [yellowness = yellow (+) to blue (–)], by means of three replicate measurements.

Water activity. The water activity (a_w) of the sweet samples (before and after storage for three months) was measured at 18 ± 2°C using a Rotronic HygroLab 3 analyzer (CH-8303, Switzerland) [27].

Hardness. The hardness of the sweet samples was assessed at 23 ± 2°C using a Universal Testing Machine (Cometech, B type, Taiwan) equipped with software [28]. Three replicates of each pulse-date sweet sample were cut with a flat-ended probe (2.50 mm thick) at a cross-head speed of 1 mm/s and 20% compression. The hardness values were expressed in Newton.

Microbiological analysis. The total plate, as well as yeasts and molds in the sweet samples were counted before and after storage using a method developed by the American Public Health Association [29]. The microbiological analysis results were presented as log CFU/g.

Statistical analysis. The data was statistically analyzed for means and standard deviations using CoStat statistical software [30]. The data was analyzed by one-way analysis of variance (ANOVA, $p > 0.05$) and then by Duncan's new multiple range tests to evaluate variations of the means.

RESULTS AND DISCUSSION

Proximate composition of ingredients. Table 1 displays the proximate composition of the ingredients used in the study, namely red cowpea, soy bean, chickpea, dark chocolate, date paste, date powder, and date dips.

As can be seen, soybeans had a higher content of protein, ash, fats, and crude fibers than the other pulses. Date dips, how-ever, had a higher content of carbohydrates and a lower content of protein, ash, fats, and crude fibers.

The results of our study were partially close to those reported by Ferweez *et al.* [31], Rabie *et al.* [32], USDA [33], Xiao *et al.* [34] and Zewudie & Gemede [35], who analyzed dried dates, date syrup, black-eyed peas, chickpeas and soybeans.

Table 1 also shows that the soaking, cooking, and dehulling of pulses (red cowpea, soy bean, and chickpea) led to a slight increase in protein and carbohydrates and a decrease in fats, ash, and crude fibers. Different processing methods indicated a high moisture content in all the cooked pulses compared to the raw seeds.

Sensory acceptability of pulse-date sweets. Table 2 exhibits the sensory acceptability scores of the cooked pulse-date sweet samples and the control. The samples were evaluated for their overall acceptability based on their color, sweetness, odor, taste, mouthfeel, and aftertaste scores.

There were no significant differences between the control and the cooked pulse samples in terms of color, sweetness, odor, mouthfeel, aftertaste, and overall acceptability. The taste scores, however, were higher for the pulse-date sweets compared to the control, except for the soybean-date samples, which had the lowest scores. The chickpea-date powder sample and the red cowpea-date dips sample recorded the highest scores (8.60 and 8.55). They were followed by the red cowpeadate powder sweet, the chickpea-date dips sweet, the control, and the soybean-date powder sample, respectively.

Table 1 Proximate composition of sweet ingredients and cooked pulses

Constituents / Samples	Moisture	Protein	Fats	Ash	Crude fibers	Carbohydrates
Raw materials						
Red cowpea	7.38 ± 0.14^{d}	21.71 ± 0.99^{b}	2.77 ± 0.09^{d}	3.96 ± 0.37^{b}	6.09 ± 0.70^{b}	65.47 ± 2.10^{e}
Soybean	5.78 ± 0.44^{e}	33.63 ± 0.40^{a}	21.95 ± 0.59^{a}	4.85 ± 0.74^{a}	9.41 ± 0.17^{a}	30.16 ± 1.86^{f}
Chickpea	10.37 ± 0.57^{c}	20.61 ± 0.33^{c}	5.53 ± 0.16^{c}	1.98 ± 0.02^{d}	3.28 ± 0.19^{c}	68.60 ± 0.69^{d}
Dark chocolate	1.20 ± 0.04^{g}	6.69 ± 0.13^{d}	19.21 ± 2.49^{b}	2.81 ± 0.02^{c}	0 ± 0^{e}	71.29 ± 2.63^{c}
Date paste	14.92 ± 0.47^{b}	2.79 ± 0.16^{f}	0.75 ± 0.03^{e}	1.66 ± 0.01^{de}	2.05 ± 0.18^{d}	92.75 ± 0.37^{b}
Date powder	3.18 ± 0.10^{f}	3.64 ± 0.12^{e}	1.32 ± 0.08^{de}	2.03 ± 0.12^{d}	1.88 ± 0.09^{d}	91.13 ± 0.72^{b}
Date dips	26.24 ± 0.08^{a}	0.82 ± 0.06^{g}	0 ± 0^{e}	1.18 ± 0.34^{e}	0.02 ± 0.01^{e}	97.98 ± 0.41^{a}
Hulled cooked pulses						
Cooked red cowpea	53.50 ± 1.09^{b}	23.09 ± 0.18^{b}	1.91 ± 0.11^{c}	1.43 ± 0.01^{b}	2.38 ± 0.55^{b}	71.19 ± 0.83^{a}
Cooked soybean	55.52 ± 0.11^{a}	34.22 ± 0.70^{a}	21.12 ± 0.15^{a}	3.66 ± 0.05^{a}	4.04 ± 0.10^{a}	36.96 ± 0.99^{b}
Cooked chickpea	50.95 ± 0.20^{c}	21.05 ± 0.17^{c}	4.77 ± 0.57^{b}	1.06 ± 0.03^{c}	1.42 ± 0.72^{b}	71.70 ± 1.44^{a}

Moisture content and caloric value were calculated as fresh weight. Means of three replicates ± SD, the number in the same column followed by a different letter is significantly different at 0.05 level

Table 2 Sensory acceptability of pulse-date sweets

Samples	Color	Sweet-ness	Odor	Taste	Mouth-feel	After-taste	Overall acceptability
Control (DP + DC)	8.65 ± 0.41^{a}	7.85 ± 0.62^{a}	8.80 ± 0.42^{a}	7.90 ± 0.74^{ab}	8.45 ± 0.59^{a}	8.15 ± 0.74^{a}	7.95 ± 0.68^{a}
RC + DP	8.40 ± 0.52^{a}	8.45 ± 0.68^{a}	8.60 ± 0.70^{a}	8.35 ± 0.53^{ab}	8.50 ± 0.97^{a}	8.40 ± 0.65^{a}	8.20 ± 0.58^{a}
RC + DD	8.40 ± 0.52^{a}	8.20 ± 0.79^{a}	8.70 ± 0.67^{a}	8.55 ± 0.49^{a}	8.60 ± 0.69^{a}	8.60 ± 0.46^{a}	8.45 ± 0.49^{a}
S + DP	8.15 ± 0.81^{a}	8.20 ± 0.67^{a}	8.60 ± 0.69^{a}	7.85 ± 1.03^{ab}	8.50 ± 0.70^{a}	8.25 ± 1.03^{a}	7.90 ± 0.94^{a}
S + DD	8.35 ± 0.58^{a}	8.00 ± 0.94^{a}	8.50 ± 0.84^{a}	7.55 ± 0.80^{b}	8.50 ± 0.71^{a}	8.30 ± 0.78^{a}	8.10 ± 0.87^{a}
C + DP	8.40 ± 0.66^{a}	8.45 ± 0.68^{a}	8.70 ± 0.48^{a}	8.60 ± 0.52^{a}	8.60 ± 0.51^{a}	8.40 ± 0.52^{a}	8.60 ± 0.53^{a}
C + DD	8.30 ± 0.78^{a}	8.40 ± 0.70^{a}	8.70 ± 0.48^{a}	8.10 ± 0.73^{ab}	8.20 ± 0.78^{a}	8.30 ± 0.67^{a}	8.35 ± 0.63^{a}

Control (DP + DC) – date paste mixed with dark chocolate, RC + DP – red cowpea with date powder, RC + DD – red cowpea with date dips, S + DP – soybean with date powder, S + DD – soybean with date dips, C + DP – chickpea with date powder, and C + DD – chickpea with date dips. Moisture content and caloric value were calculated as fresh weight. Means of ten replicates ± SD, the number in the same column followed by a different letter is significantly different at 0.05 level

After three months of storage, there were no variations in any of the attributes between the values at the start of manufacturing and at the end of storage. It is generally acknowledged that adding cooked pulses to sweets has no substantial influence on their qualities. Incorporating various seeds into chocolate products is regarded as acceptable. In some studies, different chocolate formulations with plant-based sources had a noticeable variation in texture and flavor [36, 37]. According to Radia *et al.* [38] and Erukainure *et al.* [39], date paste can be utilized as a natural flavoring ingredient to improve consumer perceptions (flavor and taste) of the final product.

Proximate composition, phenolics, antioxidant activity, and pH of pulse-date sweets. Table 3 and Fig. 2 exhibit the proximate chemical composition of seven pulse-date sweet samples, including the control. We found that the addition of pulses significantly increased the contents of protein, fats, and crude fibers, as well as the caloric value of the samples relative to the control. The highest protein content was observed in the soybean-date powder sample followed by the soybean-date dips sample, which included cooked soybeans sweetened with date powder and syrup, respectively. Adding cooked pulses also led to a decrease in ash and carbohydrates compared to the control with a higher carbohydrate content in date paste.

The results of Ibrahim *et al.* [40] were close to those reported by us. In addition, dried fruits are a great material for chocolate formation and have strong nutritional qualities and health benefits [41]. Ripnar *et al.* [42] found that their cluster bean-chocolate products were similar in protein contents, higher in fats and energy, and lower in carbohydrates. They also contained sufficient amounts of nutrients compared to other common chocolate products on the market.

Regarding minerals, the contents of calcium, iron, and zinc in the pulse-date sweets (121.54–137.13, 5.45–6.69, and 1.31–1.54 mg/100 g, respectively) were higher than in the control, except for the lower zinc content in the soybean-date samples. Likewise, the samples containing cooked chickpea had the highest iron content compared to the sweets with red cowpea and soybean. In general, adding cooked pulses to the date products raised their contents of the above minerals. Kumari *et al.* [36] mentioned that the chocolate product made from different ingredients had a good overall nutritional quality.

Table 3 Proximate composition, phenolics, antioxidant activity, and pH of pulse-date sweets

Samples / Constituents	Control (DP + DC)	RC + DP	RC + DD	S + DP	S + DD	C + DP	C + DD
Moisture, %	11.86 ± 0.55^{e}	20.75 ± 0.04^{b}	20.70 ± 0.05^{b}	19.00 ± 0.11^{d}	21.34 ± 0.12^{a}	19.32 ± 0.25^{cd}	19.50^{c}±0.33
Protein, % on dry weight basis	4.01 ± 0.16^{f}	6.77 ± 0.14^{d}	6.38 ± 0.27^{e}	7.79 ± 0.08^{a}	7.53 ± 0.29^{ab}	7.30 ± 0.18^{bc}	7.12^{c}±0.12
Fats, % on dry weight basis	3.85 ± 0.03^{c}	9.11 ± 0.17^{b}	9.07 ± 0.17^{b}	11.90 ± 0.28^{a}	11.50 ± 0.05^{a}	8.85 ± 0.17^{b}	8.73^{b}±0.69
Ash, % on dry weight basis	2.11 ± 0.03^{a}	1.79 ± 0.03^{a}	1.68 ± 0.20^{a}	1.76 ± 0.05^{a}	1.67 ± 0.04^{a}	1.80 ± 0.30^{a}	1.6688 ± 0.50^{a}
Crude fibers, % on dry weight basis	3.61 ± 0.27^{b}	4.13 ± 0.15^{a}	3.91 ± 0.27^{ab}	4.17 ± 0.05^{a}	4.03 ± 0.12^{a}	4.05 ± 0.10^{a}	3.88 ± 0.08^{ab}
Carbohydrates, % on dry weight basis	86.42 ± 0.50^{a}	78.20 ± 0.61^{a}	78.96 ± 0.94^{c}	74.38 ± 0.45^{b}	75.27 ± 0.48^{c}	77.99 ± 0.74^{c}	78.61 ± 0.96^{c}
Caloric value, kcal/100 g	396.39 ± 1.06^{b}	431.60 ± 8.63^{b}	422.9 ± 1.19^{a}	437.91 ± 0.89^{b}	441.43 ± 8.37^{a}	419.90 ± 1.17^{a}	419.61 ± 4.97^{a}
Calcium, mg/100 g	116.67 ± 1.61^{d}	126.92 ± 3.49^{b}	121.54 ± 2.31^{c}	137.10 ± 2.31^{a}	133.90 ± 1.85^{a}	134.82 ± 4.38^{a}	134.02 ± 2.29^{a}
Iron, mg/100 g	5.18 ± 0.75^{b}	5.74 ± 0.84^{ab}	5.54 ± 0.14^{b}	5.80 ± 1.02^{ab}	5.45 ± 0.19^{b}	6.69 ± 0.10^{a}	6.61 ± 0.06^{a}
Zinc, mg/100 g	1.50 ± 0.05^{ab}	1.54 ± 0.41^{a}	1.51 ± 0.08^{a}	1.35 ± 0.15^{a}	1.31 ± 0.38^{a}	1.45 ± 0.09^{a}	1.39 ± 0.04^{a}
Total phenolics, mg/100 g, as gallic acid	135.66 ± 0.78^{a}	108.86 ± 1.37^{b}	96.40 ± 0.72^{de}	104.70 ± 0.72^{c}	98.35 ± 0.29^{d}	94.56 ± 1.09^{e}	86.29 ± 4.26^{f}
Antioxidant activity, %, as DPPH	73.38 ± 0.35^{a}	73.21 ± 0.26^{a}	67.35 ± 0.26^{c}	71.85 ± 0.18^{b}	62.39 ± 0.05^{d}	57.54 ± 0.05^{e}	49.20 ± 1.38^{f}
pH	7.36 ± 0.38^{a}	6.78 ± 0.10^{b}	6.83 ± 0.05^{b}	6.68 ± 0.07^{b}	6.64 ± 0.05^{b}	6.72 ± 0.07^{b}	6.66 ± 0.03^{b}

Control (DP + DC) – date paste mixed with dark chocolate, RC + DP – red cowpea with date powder, RC + DD – red cowpea with date dips, S + DP – soybean with date powder, S + DD – soybean with date dips, C + DP – chickpea with date powder, and C + DD – chickpea with date dips. Means of three replicates ± SD, the number in the same row followed by a different letter is significantly different at 0.05 level

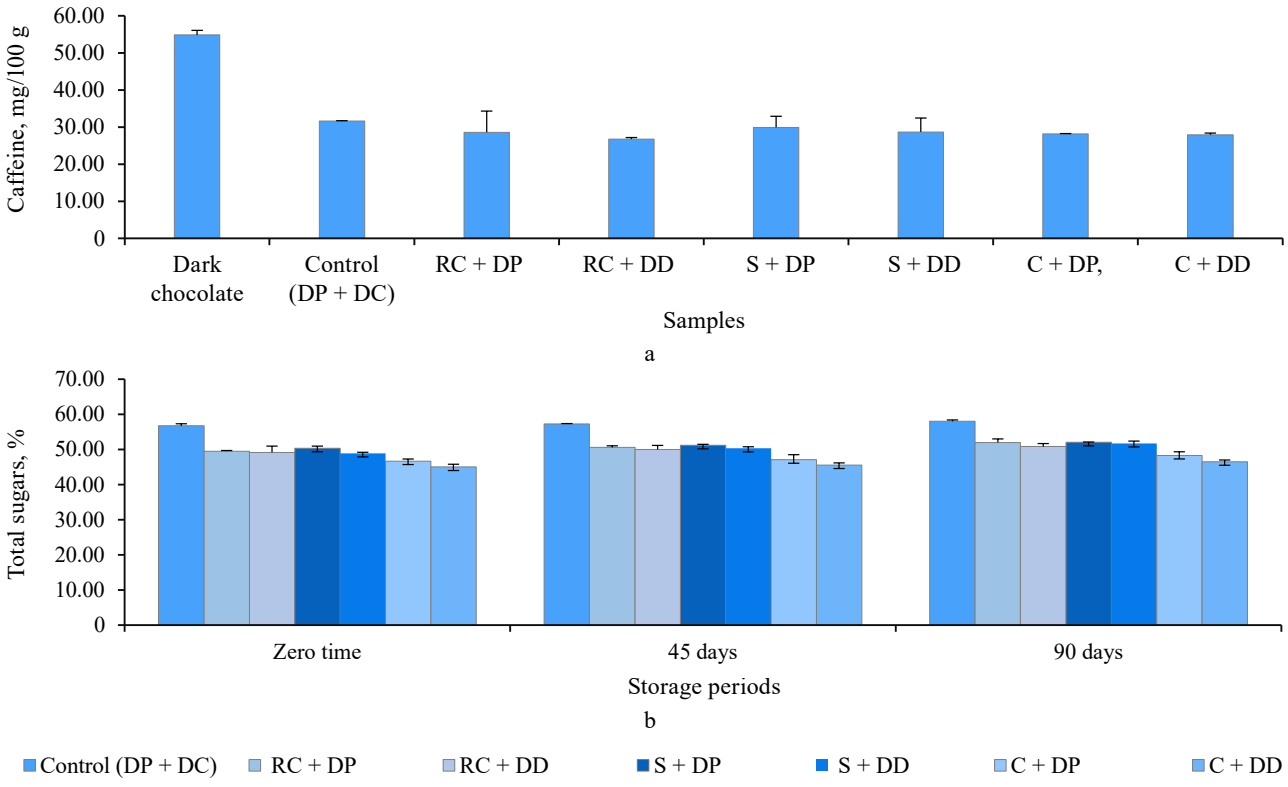

Control (DP + DC) – date paste mixed with dark chocolate, RC + DP – red cowpea with date powder, RC + DD – red cowpea with date dips, S + DP – soybean with date powder, S + DD – soybean with date dips, C + DP – chickpea with date powder, and C + DD – chickpea with date dips. Values are means of three replicates ± SD

Figure 2 Caffeine (a) and total sugars (b) in pulse-date sweet samples

As for phenolics, their contents varied between 86.29 and 108.86 mg/100 g sample. The control sample, which contained only date paste and dark chocolate, had a higher content of phenolics (135.66 mg/100 g) than the other samples. The highest antioxidant activity was in both the control and the red cowpea-date powder sample (73.38 and 73.21%, respectively). This might be due to the type of phytochemicals in those samples [12]. It was clear that the samples sweetened with date powder had higher antioxidant activity than those sweetened with date dips.

Figure 2a shows the caffeine content in dark chocolate and the date sweets prepared from cooked pulses. Dark chocolate, which was used for comparison, contained 54.82 mg caffeine/100 g, which was significantly ($p < 0.05$) higher than in the other sweet samples (26.76–29.92 mg/100 g). This variation in caffeine contents may be due to the differences in the pulse and date types, as well as moisture content. Since the control sample contained only dark chocolate and date paste, its caffeine level was higher (31.62 mg/100 g) than in the other samples. The lowest caffeine level was found in the red cowpea-date dips sweet. Overall, the sweet samples had lower caffeine contents than the maximum allowed concentrations. According to Vuletić *et al.* [26], food labels have to specify the exact amount of caffeine in the product (beverages and chocolate) to avoid overdose health risks. The Food and Drug Administration limits the maximum amount of caffeine to 45 mg/day for children aged 4–6 years, 62.50 mg/day for children aged 7–9, and 85 mg/day for those aged 10–12 [43]. Caffeine intoxication and an overstimulated central nervous system may result from an acute caffeine overdose, often exceeding 250 mg per day [44].

Regarding pH values, the control sample (date paste mixed with dark chocolate) had a significantly ($p < 0.05$) higher pH value (7.36) than the other samples. The sweets had varying pH values depending on their ingredients and processing methods. The measurement of pH in food products ensures consumer health and acceptability since it affects two key aspects of food safety: consistency and quality [45].

As for total sugars, the findings revealed a significant ($p < 0.05$) decrease in total sugars across all the samples compared to the control (Fig. 2b). Likewise, the pulse-date samples containing chickpeas and sweetened with date powder or syrup had the lowest amount of sugars compared to the other pulses. Conversely, as storage times extended, the overall sugar content somewhat increased.

Daily intake of some nutrients in pulse-date sweets. The daily intakes of protein, calories, calcium, iron, and zinc were calculated for females and males aged 4–18 years (schoolchildren) based on the proximate chemical composition (Table 2) for the control and pulse-date sweets (Table 4). According to the results,

Table 4 The daily intake of some nutrients in pulse-date sweets (100 g) for different age groups

Children age group	Nutrients	DRI	Control (DP + DC)	RC + DP	RC + DD	S + DP	S + DD	C + DP	C + DD
From 4–8 y. o.	Protein, g/day	19	21.11	35.63	33.58	41.00	39.63	38.42	37.47
	Calories, kcal/day,								
	Female	1200	33.03	35.97	35.25	36.49	36.79	34.99	34.97
	Male	1500	26.43	28.78	28.20	29.19	29.43	27.99	27.97
	Calcium, mg/day	1000	11.67	12.70	12.15	13.71	13.39	13.48	13.40
	Iron, mg/day	10	51.80	57.40	55.40	58.00	54.50	66.90	66.10
	Zinc, mg/day	5	30.00	30.80	30.20	27.00	26.20	29.00	27.80
From 9–13 y. o.	Protein, g/day	34	13.63	19.91	18.74	22.91	22.15	21.47	20.94
	Calories, kcal/day								
	Female	1600	24.77	26.98	26.43	27.37	27.59	26.24	26.23
	Male	1800	22.02	23.98	23.50	24.33	24.52	23.32	23.31
	Calcium, mg/day	1300	8.97	9.76	9.35	10.55	10.30	10.37	10.31
	Iron, mg/day	8	64.75	71.75	69.25	72.25	68.12	83.62	82.62
	Zinc, mg/day	8	18.75	19.25	18.89	16.87	16.37	18.12	17.37
From 14–18 y. o.	Protein, g/day								
	Female	46	8.72	14.72	13.87	16.93	16.37	15.87	15.48
	Male	52	7.71	13.02	12.27	14.98	14.48	14.04	13.69
	Calories, kcal/day								
	Female	1800	22.02	23.98	23.50	24.33	24.52	23.32	23.31
	Male	2800	14.16	15.52	15.11	15.64	15.77	14.99	14.99
	Calcium, mg/day	1300	8.97	9.76	9.35	10.55	10.30	10.37	10.31
	Iron, mg/day								
	Female	15	34.53	39.27	36.93	38.67	36.33	44.60	44.07
	Male	11	47.09	52.18	50.36	52.72	49.54	60.81	60.09
	Zinc, mg/day								
	Female	9	16.67	17.11	16.78	15.00	14.55	16.11	15.44
	Male	11	13.64	14.00	13.73	12.27	11.91	13.18	12.63

DRI – Dietary Reference Intake [21], calories were calculated based on RDA – Recommended Dietary Allowance [22], Control (DP + DC) – date paste mixed with dark chocolate, RC + DP – red cowpea with date powder, RC + DD – red cowpea with date dips, S + DP – soybean with date powder, S + DD – soybean with date dips, C + DP – chickpea with date powder, and C + DD – chickpea with date dips

Table 5 Color values of pulse-date sweet samples

Parameters / Samples	Outer color			Inner color		
	*L**	*a**	*b**	*L**	*a**	*b**
Control (DP + DC)	43.70 ± 0.15^{e}	2.67 ± 0.16^{abc}	1.62 ± 0.08^{bc}	46.31 ± 0.05^{d}	3.72 ± 0.04^{f}	3.64 ± 0.40^{g}
RC + DP	46.36 ± 0.33^{a}	1.92 ± 0.08^{d}	1.00 ± 0.02^{e}	57.86 ± 1.56^{a}	4.30 ± 0.035^{e}	16.74 ± 0.13^{c}
RC + DD	45.79 ± 0.31^{b}	1.97 ± 0.04^{d}	1.22 ± 0.02^{de}	51.03 ± 1.01^{b}	5.78 ± 0.05^{a}	9.00 ± 0.29^{f}
S + DP	44.76 ± 0.11^{c}	$3.06 \pm 0.3.06^{ab}$	2.10 ± 0.42^{a}	58.06 ± 0.85^{a}	5.21 ± 0.06^{c}	21.69 ± 0.24^{a}
S + DD	44.10 ± 0.34^{de}	3.26 ± 0.56^{a}	1.88 ± 0.22^{ab}	49.00 ± 0.07^{c}	5.43 ± 0.18^{b}	14.44 ± 0.23^{d}
C + DP	45.35 ± 0.29^{b}	2.11 ± 0.02^{cd}	1.52 ± 0.09^{cd}	59.45 ± 0.13^{a}	5.01 ± 0.04^{d}	18.40 ± 0.09^{b}
C + DD	44.26 ± 0.11^{d}	2.51 ± 0.02^{bcd}	1.78 ± 0.06^{abc}	50.81 ± 0.12^{b}	5.35 ± 0.02^{b}	12.86 ± 0.56^{e}

Control (DP + DC) – date paste mixed with dark chocolate, RC + DP – red cowpea with date powder, RC + DD – red cowpea with date dips, S + DP – soybean with date powder, S + DD – soybean with date dips, C + DP – chickpea with date powder, and C + DD – chickpea with date dips, *L** – lightness, *a** – redness, and *b** – yellowness. Means of three replicates ± SD, the number in the same column followed by a different letter is significantly different at 0.05 level

schoolchildren aged 4–18 years can eat about 3 sweets per day as a snack to cover some part of their daily requirements in protein, calories, calcium, iron, and zinc. The sweets prepared from cooked pulses were higher in these minerals, especially iron, which was consistent with [46]. As for zinc, the pulse-date sweets can provide 4–8-year-olds (both females and males) with 26.20 to 30.80% of their daily requirement, the highest zinc content compared to the other age groups. Abedini *et al.* [19] found that high-value plant-based constitutes could be added to chocolate-based products to enhance their nutritional value. The qualitative characteristics of date-based products enhance their potential as nutritious snacks [47].

Color of pulse-date sweets. Various optical phenomena, such as scattering and the shape of the food surface, can influence the color of the food being consumed [48]. Table 5 displays the color measurements for the pulse-date sweet samples. As can be seen, adding cooked pulses considerably raised the lightness (*L**)

values of the inner and outer colors in all the sweet samples compared to the control. This might be attributed to the light color of cooked pulses in comparison with dark chocolate. Furthermore, the inner color of the sweets had higher brightness values than the outer color. Similarly, addingdate dips lowered the lightness. In terms of redness (a^*) and yellowness (b^*), adding date dips increased the redness values across all the samples while decreasing their yellowness. Additionally, the yellowness values of the soybean samples were higher than those of the other pulse samples and the control, which might be due to the yellow color of soybean seeds. The color of food products is affected by many factors, such as processing methods, the presence of pigments, variety type, as well as packaging and storage conditions. Consequently, the food's quality can be managed by examining its color parameters and assessing the changes in its chemical composition [49].

Water activity of pulse-date sweets. Water is an essential component in food. It is crucial for the industry to monitor free water since it can be used for microbiological growth and chemical reactions. The measurement of water activity (a_w) can have a significant impact on the product's quality and is highly useful in food preservation [50]. Figure 3 presents the a_w values of the pulse-date sweet samples during storage. The data demonstrated that using cooked pulses in sweets had a significant ($p < 0.05$) effect on the water activity before storage (at zero time) compared to the control. In particular, the water activity varied between 0.757 and 0.793, which might be due to the moisture content in the cooked pulses. These results were close to those reported by Ibrahim *et al.* [51]. The water activity slightly decreased in all the samples after storage for three months, ranging within 0.755–0.787 and 0.754–0.782 during 45 and 90 days, respectively. The control sample recorded the lowest water activity (0.512, 0.509, and 0.507 after storage for 0, 45, and 90 days, respectively). The relationship between the level of water activity and the sample's humidity levels should be considered as these two parameters are highly proportional [52]. Preetha & Narayanan [53] found that chocolate candies, dried fruit (e.g., dates and figs), nuts, rolled oats, and malt extract had water activity values ranging between 0.650 and 0.750.

Hardness. Figure 4 illustrates a side view of the pulse-date sweets' texture during a three-month storage period. We found that the hardness of the sweets was significantly reduced when part of the dates and dark chocolate mixture was replaced with cooked pulses. In particular, the hardness values reached 4.02, 3.53, 2.82, 2.48, 4.41, and 2.84 N at zero time for the red cowpea samples sweetened with date powder and date dips, the soybean samples sweetened with date powder and date dips, and the chickpea samples sweetened with date powder and date dips, respectively. The control sample recorded the highest hardness value of 24.81 N. After storage for 90 days, the results showed an increase in hardness in the control and a further slight decrease in the samples [54]. Additionally, the samples that contained date dips were softer than those containing date powder. This could be due to different moisture contents in both the ingredients and the pulses affecting the texture of the final product, which aligned with the findings of Sayas-Barberá *et al.* [55].

Microbiological examination. The microbiological quality of food is essential for consumers' health and safety. Figure 5 shows changes in the microbial counts (total plate count, yeasts and molds) of the pulse-date sweet samples before and after storage periods (90 days). There was a decrease in molds and yeasts after storage in all the samples. This reduction could be attributed to the decrease in water activity and the content of total sugars, as well as to the presence of phytochemicals with antioxidant properties acting as antimicrobial agents [56].

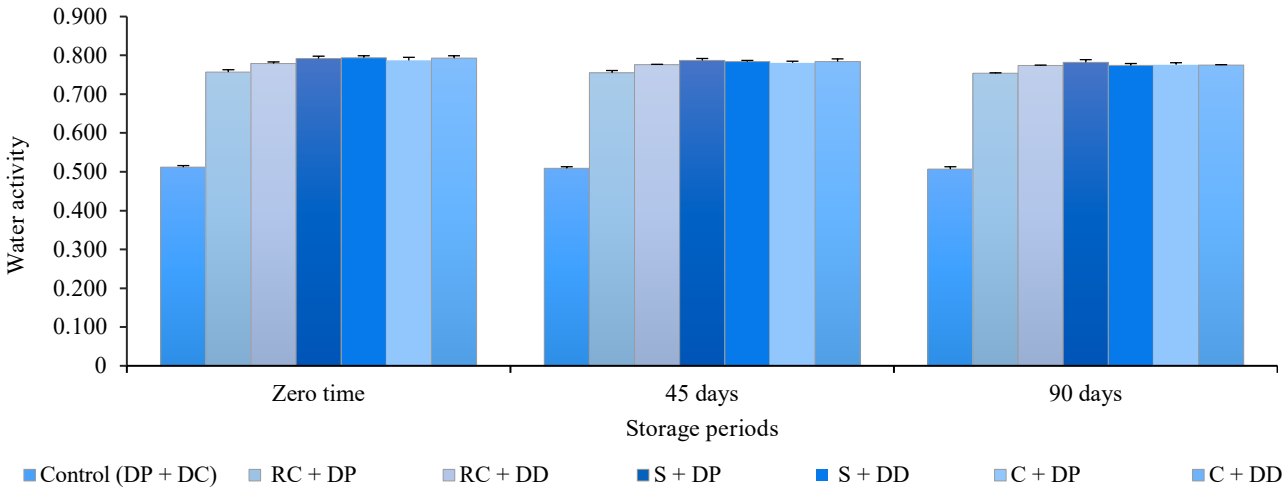

Control (DP + DC) – date paste mixed with dark chocolate, RC + DP – red cowpea with date powder, RC + DD – red cowpea with date dips, S + DP – soybean with date powder, S + DD – soybean with date dips, C + DP – chickpea with date powder, and C + DD – chickpea with date dips. Values are means of three replicates ± SD

Figure 3 Water activity of pulse-date sweet samples

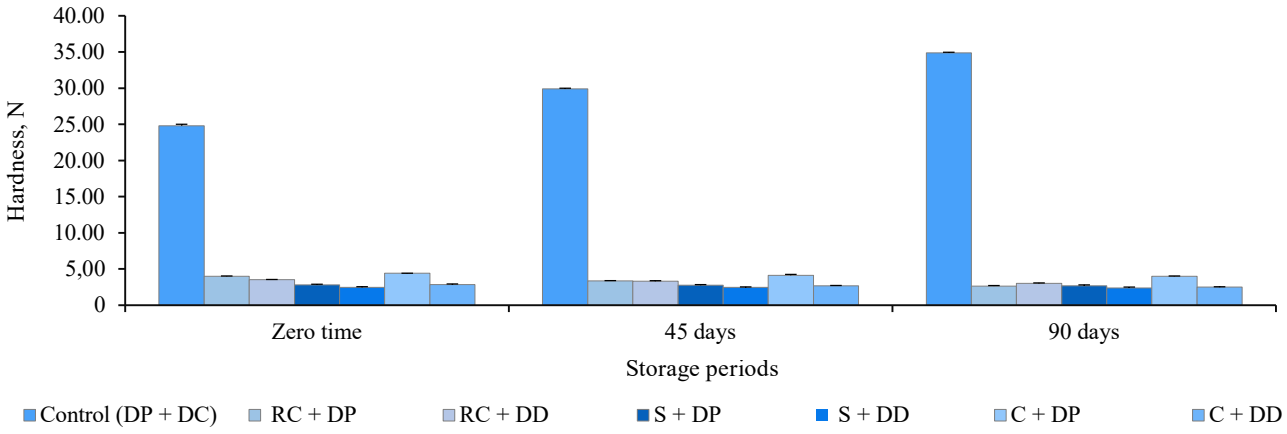

Control (DP + DC) – date paste mixed with dark chocolate, RC + DP – red cowpea with date powder, RC + DD – red cowpea with date dips, S + DP – soybean with date powder, S + DD – soybean with date dips, C + DP – chickpea with date powder, and C + DD – chickpea with date dips. Values are means of three replicates ± SD

Figure 4 Hardness of pulse-date sweet samples during storage

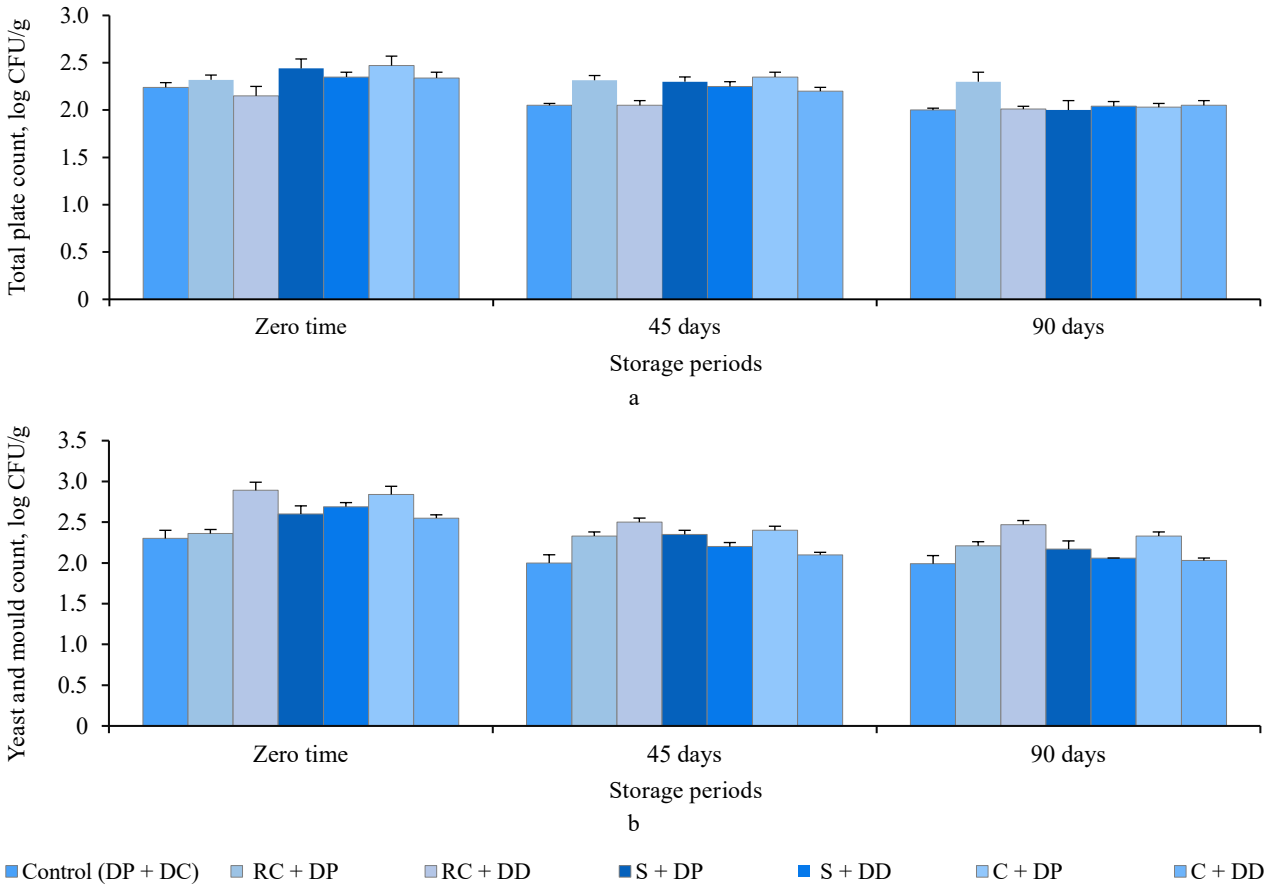

Control (DP + DC) – date paste mixed with dark chocolate, RC + DP – red cowpea with date powder, RC + DD – red cowpea with date dips, S + DP – soybean with date powder, S + DD – soybean with date dips, C + DP – chickpea with date powder, and C + DD – chickpea with date dips. Values are means of three replicates ± SD

Figure 5 Total plate (a) and yeast and mold (b) counts of pulse-date sweets during storage

Agamy *et al.* [47], who studied dates and date-based products, reported values of below 10^4 CFU/g for yeasts and molds and 10^5 CFU/g for the total plate count. According to Snyder *et al.* [57], microorganism growth could occur in food products with water activity up to 0.850. Abedini *et al.* [19] reported that the shelf life of chocolate-based products could be extended by fortifying them with some plant-based ingredients. Foods high in carbs are susceptible to spoilage by microbes that ferment carbohydrates, such as yeasts and molds [55].

CONCLUSION

There is a growing demand for highly-nutritious healthy products, including alternatives to sweets without processed sugar. In response to this demand, we formulated date-based sweets filled with cooked pulses, such as red cowpeas, soybeans, and chickpeas, using date powder or date dips as alternative sweeteners. The pulses improved the nutritional characteristics and flavor of the samples and proved a reasonable source of protein, bioactive components, calcium, iron, and zinc. The sweet products also had high sensory acceptability, especially the samples containing red cowpeas and chickpeas.

Thus, these constituents can be effectively applied to prepare pulse-date sweets with functional properties. Overall, our study revealed an efficient technique for mixing different cooked pulses with dates to create new nutritious food products in a variety of shapes and textures for all consumer categories.

CONTRIBUTION

All the authors contributed to the design and concept of this study and were equally involved in the data collection and analysis, investigation, preparation, writing, and revision of the manuscript. All the authors have read and approved the final manuscript.

CONFLICT OF INTEREST

The authors declare no conflict of interest.

ETHICS APPROVAL AND CONSENT TO PARTICIPATION

The sensory evaluation was conducted following the rules and criteria of the Food Technology Research Institute, Agricultural Research Center. The participants were provided with full information about the study and the products to be tasted before they gave their consent to participate in the research

REFERENCES

1. Singh P, Pandey VK, Sultan Z, Singh R, Dar AH. Classification, benefits, and applications of various anti-nutritional factors present in edible crops. Journal of Agriculture and Food Research. 2023;14:100902. https://doi.org/10.1016/j.jafr.2023.100902
2. Lisciani S, Marconi S, Le Donne C, Camilli E, Aguzzi A, *et al.* Legumes and common beans in sustainable diets: Nutritional quality, environmental benefits, spread and use in food preparations. Frontiers in Nutrition. 2024;11:1385232. https://doi.org/10.3389/fnut.2024.1385232
3. Affrifah NS, Phillips RD, Saalia FK. Cowpeas: Nutritional profile, processing methods and products – A review. Legume Science. 2021;4(3):e131. https://doi.org/10.1002/leg3.131
4. Dukariya G, Shah S, Singh G, Kumar A. Soybean and its products: Nutritional and health benefits. Journal of Nutritional Science. 2020;1(2):22–29.
5. Kumari U. Chickpea (*Cicer arietinum* L.): Nutrition beyond protein, bioactives and associated health benefits. The Pharma Innovation Journal. 2023;12(9):134–142.
6. Koul B, Sharma K, Sehgal V, Yadav D, Mishra M, *et al.* Chickpea (*Cicer arietinum* L.) biology and biotechnology: From domestication to biofortification and biopharming. Plants. 2022;11:2926. https://doi.org/10.3390/plants11212926
7. Al-Shwyeh HA. Date palm (*Phoenix dactylifera* L.) fruit as potential antioxidant and antimicrobial agents. Journal of Pharmacy and Bioallied Sciences. 2019;11(1):1–11.
8. Aljaloud S, Colleran HL, Ibrahim SA. Nutritional value of date fruits and potential use in nutritional bars for athletes. Food and Nutrition Sciences. 2020;11(6):463–480. https://doi.org/10.4236/fns.2020.116034
9. Hussain MI, Farooq M, Syed QA. Nutritional and biological characteristics of the date palm fruit (*Phoenix dactylifera* L.) – A review. Food Bioscience. 2020;34:100509. https://doi.org/10.1016/j.fbio.2019.100509
10. Bulletin of Food Balance Sheet. Economic Affairs Sector. Ministry of Agriculture and Land Reclamation, Egypt; 2021. 60 p. https://www.agri.gov.eg/uploads/topics/16819017944659.pdf
11. Bhattacharya S. Sugars, sweeteners, chocolates, and sweet snacks. In: Snack Foods Processing and Technology. London: Elsevier, Academic Press; 2023. pp. 211–249. https://doi.org/10.1016/B978-0-12-819759-2.00003-3
12. Faccinetto-Beltrán P, Gómez-Fernández AR, Santacruz A, Jacobo-Velázquez DA. Chocolate as carrier to deliver bioactive ingredients: Current advances and future perspectives. Foods. 2021;10(9):2065. https://doi.org/10.3390/foods10092065
13. Rajeswari P. Can chocolate be addictive. Food and Agriculture Spectrum Journal. 2020;1(2):108–115.
14. Shin J-H, Kim C-S, Cha J, Kim S, Lee S, *et al*. Consumption of 85% cocoa dark chocolate improves mood in association with gut microbial changes in healthy adults: A randomized controlled trial. The Journal of Nutritional Biochemistry. 2022;99:108854. https://doi.org/10.1016/j.jnutbio.2021.108854
15. Wang S, Dong Y. Applications of life cycle assessment in the chocolate industry: A state-of-the-art analysis based on systematic review. Foods. 2024;13(6):915. https://doi.org/10.3390/foods13060915

16. Samanta S, Sarkar T, Chakraborty R, Rebezov M, Shariati MA, *et al*. Dark chocolate: An overview of its biological activity, processing, and fortification approaches. Current Research in Food Science. 2022;5:1916–1943. https://doi.org/10.1016/j.crfs.2022.10.017
17. Onyeaka H, Nwaiwu O, Obileke K, Miri T, Al-Sharify ZT. Global nutritional challenges of reformulated food: A review. Food Science & Nutrition. 2023;11(6):2483–2499. https://doi.org/10.1002/fsn3.3286
18. Arshad S, Rehman T, Saif S, Rajoka MSR. Replacement of refined sugar by natural sweeteners: Focus on potential health benefits. Heliyon. 2022;8(9):e10711. https://doi.org/10.1016/j.heliyon.2022.e10711
19. Abedini A, Dakhili S, Bazzaz S, Moghaddam SK, Mahmoudzadeh M, *et al*. Fortification of chocolates with high-value-added plant-based substances: Recent trends, current challenges, and future prospects. Food Science & Nutrition. 2023;11(7):3686–3705. https://doi.org/10.1002/fsn3.3387
20. Latimer Jr GW. Official methods of analysis, 22nd edition. AOAC International. Washington DC; 2023. 322 p.
21. Dietary reference intakes for energy, carbohydrate, fiber, fat, fatty acids, cholesterol, protein, and amino acids. Institute of Medicine of the National Academies. Washington DC: The National Academies Press; 2005. 1332 p. https://nap.nationalacademies.org/read/10490/chapter/1#xxi
22. National Research Council. Recommended Dietary Allowances: 10th edition. Washington DC: National Academy Press; 1989. 302 p. https://doi.org/10.17226/1349
23. Kupina S, Fields C, Roman MC, Brunelle SL. Determination of total phenolic content using the folin-C assay: Single-laboratory validation, first action 2017.13. Journal of AOAC International. 2018;101(5):1466–1472. https://doi.org/10.5740/jaoacint.18-0031
24. Vuletic N, Bardic L, Odžak R. Spectrophotometric determining of caffeine content in the selection of teas, soft and energy drinks available on the Croatian market. Food Research. 2021;5(2):325–330. https://doi.org/10.26656/fr.2017.5(2).482
25. Brand-Williams W, Cuvelier ME, Berset C. Use of a free radical method to evaluate antioxidant activity. LWT – Food Science and Technology. 1995;28(1):25–30. https://doi.org/10.1016/S0023-6438(95)80008-5
26. Yadav AK, Kumar S, Janghu S, Chaudhary C. Sensory evaluation techniques. In: Mehra R, Pandey AK, Guiné RPF. Sensory Science Applications for Food Production. Hershey, PA: IGI Global; 2024. pp. 177–196. https://doi.org/10.4018/979-8-3693-2121-8.ch009
27. Zhang L, Sun D-W, Zhang Z. Methods for measuring water activity (a_w) of foods and its applications to moisture sorption isotherm studies. Critical Reviews in Food Science and Nutrition. 2017;57(5):1052–1058. https://doi.org/10.1080/10408398.2015.1108282
28. Nishinari K. Textural Characteristics of World Foods. Hoboken, NJ: John Wiley & Sons; 2020. pp. 424. https://doi.org/10.1002/9781119430902
29. Kaysner CA, Angelo D. Compendium of methods for the microbiological examination of foods (Fourth Edition). Washington DC: American Public Health Association; 2001. 676 p. https://doi.org/10.2105/MBEF.0222
30. Heumann C, Schomaker M, Shalabh S. Introduction to statistics and data analysis. (Second Edition). Cham: Springer Nature Switzerland AG; 2022. 584 p. https://doi.org/10.1007/978-3-031-11833-3
31. Ferweez H, Elsyaid SI, Abd Elaal HA, Salh YMS. Optimal method for added value increase of low quality dates obtained from dates packaging factories as by-products. Journal of Food Dairy Sciences, Mansoura University. 2020;11(9):241–246. https://doi.org/10.21608/jfds.2020.117361
32. Rabie SM, Salem E, Assous M, Afifi M, Mohamed A. Technological and economical studies on production of date powder and paste from some low quality Egyptian dates. Egyptian International Journal of Palms. 2021;1(1):109–123. https://doi.org/10.21608/ESJP.2021.233544
33. USDA. Food Data Central: official website [Internet]. [cited 2024 Jun 11]. Available from: https://fdc.nal.usda.gov/
34. Xiao S, Li Z, Zhou K, Fu Y. Chemical composition of kabuli and desi chickpea (*Cicer arietinum* L.) cultivars grown in Xinjiang, China. Food Science & Nutrition. 2023;11(1):236–248. https://doi.org/10.1002/fsn3.3056
35. Zewudie KG, Gemede HF. Assessment of nutritional, antinutritional, antioxidant and functional properties of different soybean varieties: Implications for soy milk development. Cogent Food & Agriculture. 2024;10(1):2380496. https://doi.org/10.1080/23311932.2024.2380496
36. Kumari A, Pandey S, Chauhan AK, Singh M. Optimization and characterization of functional chocolate with addition of butter fruit milkshake powder as a source of phenolic, flavonoid and carotenoid. Indian Journal of Dairy Science. 2021;74(1):54–60. https://doi.org/10.33785/IJDS.2021.v74i01.007
37. Patel H, Bains A, Sridhar K, Ali N, Najda A, *et al*. An approach to manufacturing well-being milk chocolate in partial replacement of lecithin by the functional plant-based combination. Food Science & Nutrition. 2024;12(6):3920–3934. http://doi.org/10.1002/fsn3.4051

38. Radia A, Boukhiar A, Kechadi K, Benamara S. Preparation of a natural candy from date (*Phoenix dactylifera* L.), olive (*Olea europaea* L.), and carob (*Ceratonia siliqua* L.) fruits. Journal of Food Quality. 2018;2018(3):1–9. https://doi.org/10.1155/2018/9565931

39. Erukainure OL, Egagah TI, Bolaji PT, Ajibboye AJ. Development and quality assessment of date chocolate products. American Journal of Food Technology. 2010;5(5):324–330. https://doi.org/10.3923/ajft.2010.324.330

40. Ibrahim SA, Fidan H, Aljaloud SO, Stankov S, Ivanov G. Application of date (*Phoenix dactylifera* L.) fruit in the composition of a novel snack bar. Foods. 2021;10(5):918. https://doi.org/10.3390/foods10050918

41. Çağındı Ö, Ötleş S. The health benefits of chocolate enrichment with dried fruits. Acta Scientiarum Polonorum Technologia Alimentaria. 2009;8(4):63–69.

42. Ripnar CK, Hiremath US, Anitha S. Development and nutrient analysis of cluster bean chocolate. Ecology, Environment and Conservation. 2017;23(1):283–286.

43. Spilling the beans: How much caffeine is too much? [Internet]. [cited 2024 Jun 11]. Available from: https://www.fda.gov/consumers/consumer-updates/spilling-beans-how-much-caffeine-too-much

44. Khalid A, Ahmad S, Raza H, Batool M, Khan Lodhi R, *et al*. Determination of caffeine in soft and energy drinks available in market by using UV/visible spectrophotometer. Family Medicine and Medical Science Research. 2016;5(4):1000206. https://doi.org/10.4172/2327-4972.1000206

45. Abdo NH, Mounir SMM, El-Shewey MT, Omar MM. Sensory, physico-chemical, and functional properties of lupin-based chocolate dessert formulations prepared from Egyptian-sweet white lupin seeds. Zagazig Journal of Agricultural Research. 2022;49(5):637–652. https://doi.org/10.21608/zjar.2022.269599

46. Alkurd RA, AL-Akayleh FT, AL-Remawi MM, Hasan MR, Maqousi A, *et al*. Evaluation of a Jordanian commercial chocolate brand fortified with micronutrients of vitamins B_{12} and D_3, iron and zinc. Food Science and Technology. 2023;43(6):e105122. https://doi.org/10.1590/fst.105122

47. Agamy NF, Hegazy EM, Younes NM, El-Hossainy AM. Nutritional, safety and sensory evaluation of innovative siwi date snacks with flavors and fillings. Journal of High Institute of Public Health. 2023;53(3):114–125. https://dx.doi.org/10.21608/jhiph.2024.345880

48. Rao P, Yu Z, Han H, Xu Y, Ke L. Dynamic light scattering for food quality evaluation. In: Zhong J, Wang X. Evaluation Technologies for Food Quality. Elsevier; 2019. pp. 535–557. https://doi.org/10.1016/B978-0-12-814217-2.00020-2

49. Pandiselvam R, Mitharwal S, Rani P, Shanker MA, Kumar A, *et al*. The influence of non-thermal technologies on color pigments of food materials: An updated review. Current Research in Food Science. 2023;6:100529. https://doi.org/10.1016/j.crfs.2023.100529

50. Escobedo-Avellaneda Z, Rodríguez-Martínez V, Serment-Moreno V, Velázquez G, Welti-Chanes J, *et al*. Selected applications of water activity management in the food industry. In: Barbosa-Cánovas GV, Fontana Jr AJ, Schmidt SJ, Labuza TP. Water Activity in Foods: Fundamentals and Applications, Second Edition. Hoboken, NJ: John Wiley & Sons; 2020. pp. 465–482. https://doi.org/10.1002/9781118765982.ch19

51. Ibrahim SF, Dalek NSEM, Raffie QAFM, Faridatul Ain MR. Quantification of physicochemical and microstructure properties of dark chocolate incorporated with palm sugar and dates as alternative sweetener. Materials Today: Proceedings. 2020;31(Part 1):366–371. https://doi.org/10.1016/j.matpr.2020.06.235

52. Figura LO, Teixeira AA. Water activity. In: Food Physics. Physical Properties – Measurement and Applications. Cham: Springer Nature Switzerland AG; 2023. pp. 1–57. https://doi.org/10.1007/978-3-031-27398-8

53. Preetha SS, Narayanan R. Factors influencing the development of microbes in food. International Journal of Arts, Science and Humanities. 2020;7(3):57–77. https://doi.org/10.34293/sijash.v7i3.473

54. Sayas-Barberá E, Paredes C, Salgado-Ramos M, Pallarés N, *et al*. Approaches to enhance sugar content in foods: Is the date palm fruit a natural alternative to sweeteners? Foods. 2024;13(1):129. https://doi.org/10.3390/foods13010129

55. Sayas-Barberá E, Martín-Sánchez AM, Cherif S, Ben-Abda J, Pérez-Álvarez JÁ. Effect of date (*Phoenix dactylifera* L.) pits on the shelf life of beef burgers. Foods. 2020;9(1):102. https://doi.org/10.3390/foods9010102

56. Prakash B, Kumar A, Singh PP, Songachan LS. Antimicrobial and antioxidant properties of phytochemicals: Current status and future perspective. In: Functional and Preservative Properties of Phytochemicals. Elsevier; 2020. pp. 1–45. https://doi.org/10.1016/B978-0-12-818593-3.00001-4

57. Snyder AB, Martin N, Wiedmann M. Microbial food spoilage: Impact, causative agents and control strategies. Nature Reviews Microbiology. 2024;22:528–542. https://doi.org/10.1038/s41579-024-01037-x

ORCID IDs
Azza A. Omran https://orcid.org/0000-0002-9328-8087
Nadra S.Y. Hassan https://orcid.org/0009-0007-8370-4028
Abd Elaziz M. Hanaa https://orcid.org/0009-0005-3733-990X

Foods and Raw Materials. 2026;14(2)

ISSN 2308-4057 (Print)
ISSN 2310-9599 (Online)

Research Article
Open Access

Available online at http://jfrm.ru/en
https://doi.org/10.21603/2308-4057-2026-2-673
https://elibrary.ru/GCLICJ

Carcinogenesis of malignant neoplasms in cats: Development factors

Anatoly P. Kaledin[1], Marina V. Stepanova[2,*], Larisa F. Sotnikova[2], Sergei Yu. Zaitsev[2], Yulia N. Melikova[2], Anastasia S. Kuryndina[2], Daria A. Vilmis[2]

[1] Russian State Agrarian University – Moscow Timiryazev Agricultural Academy, Moscow, Russia
[2] Russian Biotechnological University, Moscow, Russia

* e-mail: stepanova-marina@bk.ru

Received 20.08.2024; Revised 10.10.2024; Accepted 06.05.2025; Published online 27.06.2025

Abstract:
An effective and timely prevention of diseases in animal companions is a major task faced by the modern veterinary science. This research featured the correlation between malignant neoplasms and ophthalmological diseases in cats. The authors studied the multifactorial effect on the neoplastic proliferation and cancer-related ophthalmopathy to develop a general scheme of neoplastic proliferation in cats.

The effect of exogenous and endogenous factors on neoplastic proliferation was described based on experimental studies of numerous samples taken from 192 cats, including 67 cancer patients.

The comprehensive methodological approach included anamnestic data sampling, clinical examination, examination of the pathological area, hematology, cytomorphology, and chemical-toxicological tests.

The cats with various ophthalmopathies were simultaneously diagnosed with one or more of the following cancer types: carcinoma (37.13%), squamous cell carcinoma (32.83%), lymphoma (29.85%), sarcoma (20.89%), melanoma (2.98%), and mastocytoma (1.49%).

The main factors of neoplastic proliferation included diet, care, living conditions, physical activity, stress, chronic inflammation, repeated cases, the rate of increase/decrease in clinical signs, previous therapies, etc. In most cases, the cancer-related ophthalmopathy developed as a result of tumor metabolites or as a side-effect of chemotherapy. The incidence of cancer-related ophthalmopathy increased with age.

Cancer was found to correlate with the amounts of zinc, iron, and lead in the fur. Another correlation occurred between carcinomas, especially mammary tumors, and the high copper content in the fur.

Keywords: *Felis catus,* hematology, cytomorphology, visual diagnostics, oncological study, ophthalmological study, biochemistry, microelement

Funding: The research was part of Project no. FSMF-2022-0003 supported by the Ministry of Higher Education and Science of the Russian Federation: *Etiopathogenesis and development of methods for diagnosis, prevention, and treatment of immune-mediated paraneoplastic ophthalmopathy in animals.* It was conducted on the premises of the Research Laboratory of Ophthalmology, Oncology, and Animal Biochemistry, Russian Biotechnological University (ROSBIOTECH), Moscow, Russia.

Please cite this article in press as: Kaledin AP, Stepanova MV, Sotnikova LF, Zaitsev SYu, Melikova YuN, *et al.* Carcinogenesis of malignant neoplasms in cats: Development factors. Foods and Raw Materials. 2026;14(2):264–275. https://doi.org/10.21603/2308-4057-2026-2-673

INTRODUCTION

Carcinogenesis is a popular and multifaceted research problem, but all attempts to trace the chain of processes that cause cell degeneration down to its cause have failed so far. The nature of neoplastic proliferation remains a scientific mystery [1–3]. Cancer is one of the main causes of morbidity and mortality in domestic cats. A correct understanding of the oncogenome for each particular cancer type is critically important because it affects all aspects of patient care, from diagnosis and prognosis to targeted therapy [4]. However, the frequency of tumor formation means that cell neotransformation is not unique, i.e., it needs no exceptional phenomena to occur. Yet, the current trend towards the autonomous assessment of oncogenesis factors and the ultra-detailed biology of tumor cells hinders any attempts of synchronous perception and prevents antitumor resistance [5].

Copyright © 2025, Kaledin *et al.* This is an open access article distributed under the terms of the Creative Commons Attribution 4.0 International License (https://creativecommons.org/licenses/by/4.0/), allowing third parties to copy and redistribute the material in any medium or format and to remix, transform, and build upon the material for any purpose, even commercially, provided the original work is properly cited and states its license.

Carcinogenesis is a complex multi-stage process that involves exogenous factors (environment, lifestyle, etc.), endogenous factors (heredity, hormones, immune issues, etc.), and their combinations. These factors change the genetic material of cells and disturb the immune system [6–8]. Depending on the nature and severity of risk factors, the carcinogenesis progresses, accelerates, or decelerates [9].

Local veterinary centers provide assistance to animal companions that share the same ecosystem with humans. These centers prevent and treat new and recurring diseases in pets, as well as conduct research on relevant issues.

Cancer-associated ophthalmopathy is a major problem in veterinary and human medicine [10–16]. Poor knowledge of the fundamental principles of carcinogenesis in ophthalmopathy prevents early diagnostics. This research project aimed at solving this problem.

A comprehensive review of medical publications made it possible to outline some important research results [15–27].

Liu *et al.* [17] described a case series of paraneoplastic neuromyelitis optica, including two new histological types of cancer and their histological rationale.

Recurrent optic neuritis and extensive longitudinal and transverse myelitis seem to dominate the clinical picture [18]. In most cases, paraneoplastic neuromyelitis optica is associated with autoantibodies that target the aquaporin-4 (AQP-4) water channel. Neuromyelitis optica spectrum disorder (NMOSD) in senior-age patients is associated with paraneoplastic etiology because NMOSD usually affects the young. NMOSD cases could be associated with squamous cell carcinoma of the lung or with anti-AQP-4 in the serum and cerebrospinal fluid. However, the method of immunohistological staining revealed no AQP-4 on the surface of tumor cells [18].

Cohen *et al.* [19] analyzed neuro-ophthalmologic data and macrophotography in a large cohort of CRMP-5 IgG-positive patients to describe their clinical phenotype and treatment response. They linked the response of collapsing response-mediator protein-5 immunoglobulin G (CRMP-5) with paraneoplastic optic neuritis, vitritis, retinitis, or a combination of those. However, such findings are scarce in scientific literature.

Garibaldi *et al.* [20] reported extensive clinical, serological, and morphological data on middle-aged male patients with isolated bilateral ptosis and external ophthalmoplegia caused by immune checkpoint inhibitors.

Gordon & Dinkin [21] described different paraneoplastic syndromes with neuro-ophthalmologic manifestations, their diagnostics, and therapeutic options.

Graus & Dalmau [22] featured paraneoplastic neurological syndromes, i.e., disorders that affect any part of the nervous system in cancer patients, usually as a result of autoimmune reactions caused by ectopic expression of neuronal proteins in cancer cells.

Paraneoplastic neurological syndromes are rare. However, the method of immune checkpoint inhibitors (ICIs) in cancer treatment algorithms triggered the scientific interest in paraneoplastic neurological syndromes. Immune checkpoint inhibitors demonstrate a much higher incidence of immunological toxicity than conventional cancer therapy, e.g., immune-related neurological adverse events (IRAEs) that may manifest as paraneoplastic neurological syndromes [22]. In theory, immune checkpoint inhibitors may increase the risk of paraneoplastic neurological syndromes, especially in patients with some particular types of cancer, e.g., small-cell lung cancer. A prompt diagnosis and early treatment of paraneoplastic neurological syndromes may prevent irreversible neurological deficits [21]. To diagnose these disorders in the context of immune checkpoint inhibition, the authors also reviewed paraneoplastic neurological syndromes with underlying syndromes, types of neuronal autoantibodies, and associated immunological mechanisms. They studied scenarios when immune-nerelated neurological adverse events met the criteria for paraneoplastic neurological syndromes, as well as examined their incidence and clinical manifestations. The research yielded a set of recommendations for the prevention and treatment of paraneoplastic neurological syndromes that may arise during immune checkpoint blockade therapy.

Becquart *et al.* [23] reported that immune checkpoint inhibitors improved the prognosis of metastatic melanoma and other cancer types. While studying the side effect of myasthenia, they described 34 cases of myasthenia associated with anti-programmed cell death protein 1 checkpoint inhibitor and melanoma.

Scientific publications [15–26] are scarce on clinical ophthalmopathy in animals and feature no clinical forms of the course of pathological changes.

The morphological picture of regeneration mechanisms also remains understudied. We found neither statistics nor risk factor analysis for immune-mediated paraneoplastic ophthalmopathy in dogs, cats, or horses. Other understudied areas include clinical differential diagnostic criteria for immune-mediated paraneoplastic ophthalmopathy, classification of clinical forms, diagnostically substantiated criteria, clinical risk factors for blindness in various animal species, etc. Treatment methods for ophthalmopathy need further development.

Tumor metabolism, chemotherapeutic drugs, and internal protective factors affect the damage and regeneration of retina, choroid, iris, ciliary body. Ophthalmopathy protocols cannot be applied to cancer patients without establishing the cause of the vision loss associated with a long-term effect of chemotherapeutic drugs. In this regard, new ways of early diagnosis of cancer-related ophthalmopathy are a relevant research task.

Our review of domestic and foreign publications proved that this research direction is fundamental, relevant, and understudied. This research contributes to effective prevention and treatment of diseases in cats as animal companions that share the same ecosystem with humans. We studied the ophthalmology-related neoplastic proliferation in cats to analyze the effect of all factors on ocular carcinogenesis and develop a general scheme of neoplastic proliferation in animals.

STUDY OBJECTS AND METHODS

The research was conducted at the laboratory of Ophthalmology, Oncology, and Animal Biochemistry, Russian Biotechnological University, Moscow, Russia. The exogenous and endogenous factors of neoplastic proliferation were studied experimentally. The experiments involved samples obtained from 192 cats, including animals with various oncological diseases (n = 67).

The comprehensive methodological approach covered data sampling, clinical examination, examination of pathological area, hematological and cytomorphological studies, visual diagnostics, and a complete oncological and ophthalmological examination.

The final diagnosis relied on such methods as magnetic resonance imaging, computed tomography, hematological blood indices, and morphological conclusions.

The autopsy samples and antemortem materials were subjected to standard histological processing.

After extraction, the eyeballs or their fragments were immediately placed in labeled sealed containers with 10% neutral buffered formalin. The fixation lasted at least seven days with a single solution change. The material-to-formalin ratio was ≥ 1:10. After fixation, the pathological material was excised for macroscopy. In every case, we obtained 1–2 sections for each eyeball, a total of 2–4 sections, and four sections of organ tissue.

After the histological examination, the tissues were embedded in paraffin and subjected to microtomy, during which we stained 5-µm-thick sections with hematoxylin and eosin in line with the official protocol.

A sample of wool (1–3 g) was taken from a 1-cm^2 area on the back, below the projection of the shoulder blades. The accumulation levels of zinc, copper, iron, lead, cadmium, and arsenic were studied using an AQUILON AAS A2 atomic absorption spectrometer.

The cats were grouped based on their diagnosis and further subdivided into severity cohorts. The monitoring relied on the medical histories of the most common oncological diseases in cats. The monitoring made it possible to calculate the share of animals with cancer accompanied by visual impairment in the anamnesis against the total number of cancer patients.

The anamnestic data included the following criteria: breed, age, sex, living conditions, bad habits of the owners, oncological heredity, chronic diseases, long-term drug treatment, e.g., immunosuppressants, hormone replacement therapy, etc.

The statistic processing revealed the arithmetic mean values (M), average errors (m), and standard deviations (δ). The nonparametric Shapiro-Wilk criterion W made it possible to identify reliable differences between the groups, the contingency between the features, and the nature of the compatibility data distribution.

To verify the differences between two samples, we used Student's test and Fisher's criterion; to verify the difference between several independent samples for one feature, we applied the one-way variance analysis and the nonparametric variance analysis based on the Kruskal-Wallis test. The regression analysis and Spearman's rank correlation coefficient clarified the correlation between two or more samples.

The statistical significance level was 0.05 for all statistical analyses. The databases were compiled in Microsoft Office Excel 2010 and Statistica 10.0.

RESULTS AND DISCUSSION

Etiology. About 34.9% of cats aged 3–15 y.o. had cancer at different stages, the most common localization being the oral cavity and phalanges. According to the morphological studies, the most common cases included carcinoma (31.35%), squamous cell carcinoma (28.35%), lymphoma (23.88%), and sarcoma (13.44%) (Fig. 1).

Other malignant tumors were much less common: melanoma and mastocytoma were responsible for 1.49% of all cases (Fig. 1). Benign tumors accounted for 11.9% of all tumors and tumor-like lesions. These results correlated with the data published by Ludwig *et al.* [4].

Some sporadic cases of sarcoma are associated with implants and injections in humans and animals [24–28]. However, cats appear to have a unique predilection for trauma and/or inflammation-related sarcoma. Injection-site sarcoma is a well-known phenomenon in cats, often associated with vaccination. In the USA and the UK, the estimates range from one case per 1,000–12,500 vaccinated cats [29, 30]. Most post-injection or post-traumatic sarcomas in cats are fibrosarcoma. Its histologic features include multinucleated giant cells, myofibroblast differentiation, and inflammatory infiltrates (lymphocytes and macrophages), which are typically absent from non-injection fibrosarcomas in cats [31–33]. Cats also may develop an intraocular sarcoma after an eye injury or an eye disease [34].

Researchers report no particular risk factors that could trigger a post-injection or post-traumatic sarcoma in cats. Potential chemopreventive strategies can probably be assessed in a relatively timely manner. Most cancers develop within three years after vaccination, although some researchers report a decade-long latency period [35–38].

Inflammation caused by post-traumatic and/or post-injection conditions is the main prerequisite for soft tissue sarcoma in cats. It develops in the withers, popliteal

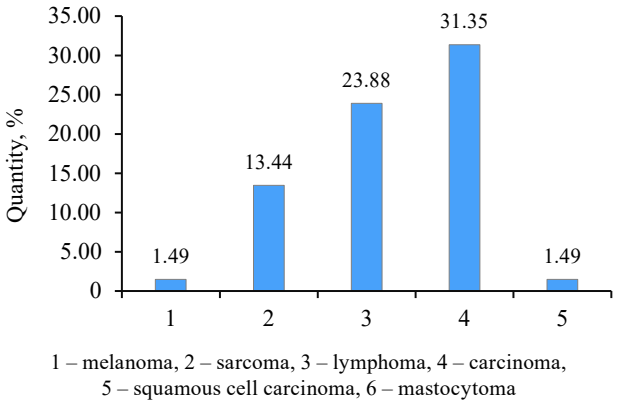

1 – melanoma, 2 – sarcoma, 3 – lymphoma, 4 – carcinoma, 5 – squamous cell carcinoma, 6 – mastocytoma

Figure 1 Classification of neoplasms in cats

folds (injection sites), in the eye, and other soft tissues (trauma sites). Post-injection and post-traumatic sarcomas usually occur 2–10 months after the event. Ophthalmologic neoplasms can be multimodal or monomodal.

Animals with poor genetic or individual medical history are at high risk of cancer. Other risk factors associated with paraneoplastic ophthalmopathy may include poor diet and care, low physical activity, high stress, chronic inflammation, etc. Some previous medical treatments also may become risk factors. Cancerous ophthalmopathy could be triggered by biologically active substances in the tumor or may develop as a complication after chemotherapy.

Genetic and individual anamnesis. Breed is an important carcinogenic risk factor. Cancer often affects Siamese, Japanese, Somali, and Abyssinian cats, as well as some other shorthair breeds [24]. In our sampling, 34.3% of cancer cases belonged to pets adopted from animal shelters; in 16.3%, the owners failed to specify the breed. The diseased cats were crossbreeds (50.7%), British (26.9%), Maine Coons (10.4%), and Persians (7.5%). Exotic breeds were responsible for as little as 4.5% (Fig. 2).

Cats with one first-degree diseased relative in family history (parents, siblings, offsprings) were reported to develop cancer twice as often [8].

In our case, the data analysis revealed a strong hereditary nature: 19.4% of cancer cats had relatives with neoplasms (carcinoma, squamous cell carcinoma, lymphoma, sarcoma, melanoma, mastocytoma). About 15.4% of this number had a certain connection between subsequent generations in the first line. However, we failed to establish the correlation between types of inherited tumors across lines.

Mammary cancer is known to be of hereditary nature in felines. It is associated with point mutations in the BRCA2 tumor suppressor gene, which contains eight BRC repeats in exon 11. The BRCA2 protein interacts through the BRC (mammary cancer) domain with RAD51. This cellular component is important for genome stability and repairing double-strand breaks [25–27]. Feline mammary carcinomas are molecularly heterogeneous. An RNA-Seq-based comparative transcriptome profiling identified recurrent and exceptional differentially expressed (DEGs) genes used as a cancer marker in cats [28].

Immune response. Inflammation can be a major risk factor for the development of several types of cancer in animals [30]. Probably, the immune response to injection or trauma in cats is insufficient and excessive [30]. Eventually, it leads to chronic inflammation, causing proliferation and malignant transformation in fibroblasts. Chronic inflammation often leads to sarcoma, e.g., Kaposi's sarcoma, which is often associated with an inflammatory infiltrate [29]. Herpesvirus proteins associated with Kaposi's sarcoma activate such factors as Th2 lymphocytes, cyclooxygenase 2, and nuclear factor kappa B, which develop a pro-tumor inflammatory microenvironment [29].

According to Oh & Cho [29], injection-site sarcoma in cats may serve as a general model of inflammation-associated tumorigenesis due to the pathways shared by many different tumor histologies. Of course, not every vaccinated cat develops injection-site sarcoma. In the US and the UK, it occurs only in 0.1–0.01% of vaccinated cats. A strict control of living conditions, environment, diet, etc., may help reduce the risk. Biochemical and genomic screening is required to study the development of injection-site sarcoma and other tumors in cats. A recent example of best care for a cat with injection-site sarcoma is the approval of feline recombinant canarypox virus interleukin-2 (Oncept Il-2). It reduces local recurrence after standard therapy [29].

We attempted to identify cancer markers in cats using a clinical blood analysis and white blood cell count (Tables 1 and 2).

The white blood cell counts obtained from the cancer cats revealed a reliable 3.58-time decrease in eosinophils (Table 2) while the general clinical analysis showed a reliable ($p < 0.05$) increase in monocytes (2.94 times).

High monocyte count (monocytosis) is a marker of infectious diseases of viral, fungal, rickettsial, or protozoal nature; blood parasitic diseases, e.g., piroplasmosis; granulomatosis, e.g., tuberculosis, brucellosis, ulcerative colitis, enteritis; and tissue inflammation. In addition, monocytes may increase after surgery.

We detected low eosinophil and lymphocyte counts and high neutrophils; the red blood cell count exceeded the standard by 0.8%. High neutrophil counts (neutrophilia) accompany various bacterial infections, tissue inflammation or necrosis, progressive tumors with necrosis, acute and chronic leukemia, intoxication, etc.

The neutrophil-to-lymphocyte ratio may be a useful prognostic predictor for various types of cancer. However, it is seldom used for pre-surgery prognosis in feline cancer [30].

Biochemistry of blood serum. In addition to the clinical and leukocyte blood tests (Tables 1 and 2), we examined some key serum biochemical parameters (Table 3).

The biochemistry of blood serum reflects the state of metabolism in animals, i.e., the functional activity of individual organs and systems, as well as the general homeostasis. The biochemical analysis of blood serum shows the severity of the disease and the treatment effecti-

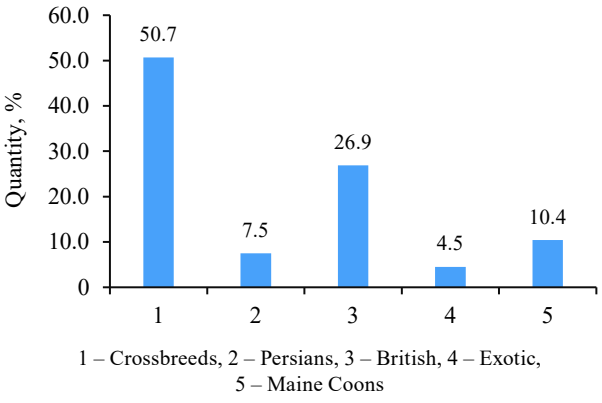

Figure 2 Paraneoplastic ophthalmopathy in cats by breed

Table 1 General clinical blood analysis of cats' blood samples (M ± SD)

Group	Neutrophils, %	Eosinophils, %	Basophils, %	Monocytes, %	Leukocyte count, $\times 10^9$/L	Lymphocytes, %	Red blood cell count, $\times 10^9$/L
Cancer patients (n = 67)	71.98 ± 9.63*	1.47 ± 0.35	0.34 ± 0.74	11.29 ± 2.55*	9.40 ± 6.08	20.03 ± 12.61	10.05 ± 1.39
Healthy cats (n = 125)	65.87 ± 14.52*	4.57 ± 0.46	0.48 ± 0.63	3.84 ± 1.13*	11.95 ± 3.64	42.18 ± 6.53	6.55 ± 1.70
Standard (reference data) [39]	60–75	2–8	0–1	1–4	5.5–13	36–51	5.28–9.97

* Significant differences between cancer and healthy patients are marked with an asterisk ($p < 0.05$)

Table 2 Leukocyte formula of cats' blood samples (M ± SD)

Group	Leukocytes, thousand/mcL	Lymphocytes, $\times 10^9$/L	Monocytes, $\times 10^9$/L	Neutrophils, $\times 10^9$/L	Eosinophils, $\times 10^9$/L	Basophils, $\times 10^9$/L
Cancer patients (n = 67)	9.40 ± 4.99	1.58 ± 0.98	0.52 ± 0.37	7.35 ± 4.49	0.12 ± 0.15*	0.01 ± 0.01
Healthy cats (n = 125)	8.61 ± 1.87	3.35 ± 1.28	0.01 ± 0.01	4.82 ± 1.95	0.43 ± 0.11*	0.00 ± 0.01
Standard (reference data) [39]	5.0–19.5	1.5–7.0	0–0.85	2.5–12.5	0–1.5	–

* Significant differences between cancer and healthy patients are marked with an asterisk ($p < 0.05$)

Table 3 Key biochemical parameters of cats' blood serum

Parameters	Group		Standard [39]
	Cancer patients	Healthy cats (control)	
Total protein, g/L	67.52 ± 9.72	55.96 ± 9.35	54–77
Indirect bilirubin, µmol/L	22.60 ± 29.02*	5.27 ± 1.35*	3–12
Direct bilirubin, µmol/L	12.92 ± 20.02*	5.13 ± 1.64*	0–5.5
Globulins, g/L	34.73 ± 8.67	23.43 ± 7.25	–
Alanine aminotransferase, m/L	123.34 ± 111.89*	55.27 ± 11.37*	17–79
Aspartate aminotransferase, m/L	83.73 ± 80.91*	14.84 ± 3.23*	9–29
Lactate dehydrogenase, m/L	145.04 ± 60.40	57.28 ± 20.37	55–155
Amylase, m/L	1505.26 ± 257.66	1387.32 ± 136.92	780–1720
Alkaline phosphatase, m/L	73.88 ± 61.11*	43.28 ± 23.48*	39–55
Urea, µmol/L	10.28 ± 2.80	5.85 ± 1.28	2–8
Creatinine, µmol/L	128.37 ± 34.07	103.28 ± 22.84	70–165
Glucose, µmol/L	6.16 ± 1.71	4.28 ± 2.01	3.2–6.4
Alanine aminotransferase vs. aspartate aminotransferase, RU	0.78 ± 0.39*	3.72 ± 0.45*	–
Calcium, mmol/L	2.84 ± 0.52	2.21 ± 0.33	2–2.7
Phosphorus, mmol/L	1.51 ± 0.23	1.34 ± 0.32	1.1–2.3
Sodium, mmol/L	154.01 ± 3.56	144.26 ± 23.74	143–165
Potassium, mmol/L	4.43 ± 0.38	5.01 ± 0.45	3.8–5.4

* Significant differences between cancer patients and control are marked with an asterisk ($p < 0.05$)

veness. In some cases, the biochemical parameters of blood serum may clarify the diagnosis made using other research methods.

The data obtained showed high total protein (by 20.7%) and globulin contents (by 48.2%). The increase in the synthesis of proteins and, especially, globulins, is a factor of immune response, which is typical for cancer patients. These data were confirmed by the content of bilirubin fractions in the blood samples. The direct bilirubin increased 2.51 times whereas the indirect bilirubin rose 4.28 times. The accelerated protein metabolism was manifested in the excretion of its derivatives, i.e., bilirubin.

A bilirubin molecule can bind with two molecules of glucuronic acid to form a water-soluble conjugate, i.e., direct bilirubin. Bilirubin enters bile mainly in its indirect form. Bilirubin count shows liver function and hemolytic processes. High bilirubin in blood plasma, especially its direct fraction, means a liver cell damage.

In this research, the cancer patients had the urea level increased by 75.7% compared to the control. The total amount of residual nitrogen and individual substances is another diagnostic tool. Low residual nitrogen in the plasma indicates poor liver function while high residual nitrogen means poor kidney function. Some diseases affect the total amount of residual nitrogen in the blood

plasma and its individual components. Poor excretory function of the kidneys results in a sharp increase in urea, i.e., uremia. In adult animals, high total nitrogen in the blood plasma is associated with increased breakdown of tissue proteins.

Creatine is important for energy metabolism as it provides for the synthesis of creatine phosphate in muscles and brain cells. As a result of dephosphorylation, creatine phosphate converts into creatinine. The standard amount of creatinine is 103.28 ± 22.8 μM for healthy cats. In the cancer patients, the amount of creatinine increased by 24.3% to reach 128.37 ± 34.1 μM. Since the level of creatine phosphate is proportional to the muscle tissue, the level of creatine in the blood plasma of young animals is always higher than that of creatinine.

The glucose content increased as well (by 43.9%) but remained within the standard range (3.2–6.4 mM). A carbohydrate diet boosts the concentration of glucose in the blood. The glucokinase (hexokinase) of the liver develops glucose-6-phosphate, the level of which depends on glucagon and insulin. High blood glucose inhibits glucagon synthesis and boosts insulin. This hormonal ratio is a direct allosteric effect of glucose.

We also detected an increase in the total amount of alanine aminotransferase and aspartate aminotransferase. These enzymes participate in the metabolism of amino acids, as well as intracellular metabolic processes. Membrane permeability, necrosis, and cellular lysis may increase the level of enzymes.

In this research, the main biochemical parameters of cat blood serum deviated from the standard values in cancer patients.

Oncological ophthalmopathy was established in 7.5% of all clinical cases. Approximately 16.4% demonstrated secondary inflammatory processes, manifested as serous and fibrinous posterior uveitis. About 1.5% had malignant neoplasms in the following forms: the invasion of surrounding tissues, lysis of bone structures, displacement or lysis of eye structures, invasion into the retrobulbar space, an inflammatory component, etc.

We also detected random cases of multimodal tissue damage of various organ systems, namely lung cancer and iris melanocytoma. There, the ophthalmopathy was of a primary long-term homogeneous limited nature with no inflammation.

We enucleated the eyeballs and removed the retrobulbar tissues, as well as sampled the damaged organs (Fig. 3a, b). The sclera, limbus, and damaged organs were macrophotographed (Fig. 3c, d).

The case below had a combined lesion of the eyeball choroid (melanocytoma), lung (sarcoma), and lymphatic system (lymphoma) (Table 4).

The micromorphological examination of iris melanocytoma revealed its thickness and changes in the layer ratio. The focal thickening was the morphological equivalent of the lesion. It was a well-defined, highly cellular mass that consisted of round and polygonal melanocytes with strongly pigmented cytoplasm (Fig. 4b). The nuclear details of the cells were partially invisible because of pigmentation. However, the signs of nuclear atypia were minor (Fig. 4a), with a mild scleral infiltration.

Old age was one of the most significant cancer risks. About 90% of all new cancer cases occur in ten-plusers. In our research, the average age of tumor onset in cats was 12.7 ± 6.1 years. This result exceeded the average age of oncology development in cats in Portugal [40] and Mexico City [41] by 3 years.

Pérez-Enriquez *et al.* [41] reported a late first development of benign tumors compared to malignant ones.

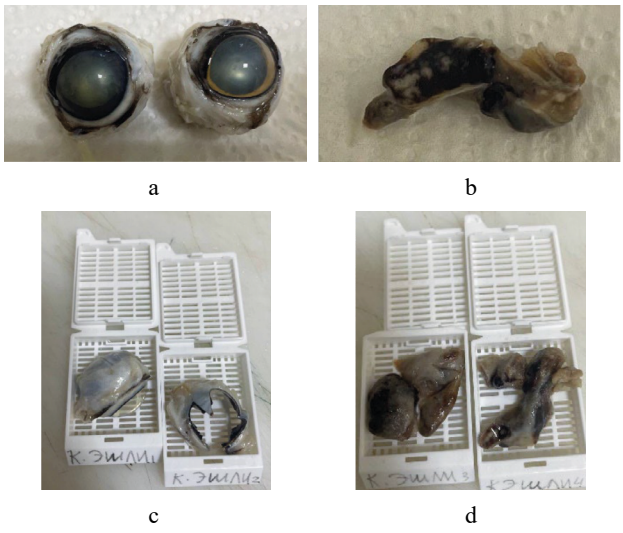

Figure 3 Macrophotographs: (a) eyeballs, (b) lung and sections, (c) sclera and limbus, and (d) lung

Table 4 Histopathology of feline eyeballs

Structure	Histopathology
Cornea	The corneal wall is deformed (artifact); the thickness was not measured. The corneal wall consists of 5–8 epithelium layers with no significant histological changes. The corneal stroma consists of keratinocytes with no histological changes. Descemet's membrane and corneal endothelium demonstrate no histological changes
Choroid	The anterior part is represented by clusters of melanocytes with no histological changes. The blood vessels are not dilated. The ciliary body demonstrates no histological changes. The pectineal ligament is indistinguishable
Tapetum	Not available
Iris	The iris is focally thickened by a round well-defined highly cellular mass that consists of round and polygonal melanocytes with pigmented cytoplasm. The nuclear details being partly obscured by pigmentation, the cells show only mild nuclear atypia. Mild scleral infiltration is observed
Retina	The vessels are not dilated, with no histological changes
Optic nerve	Not available

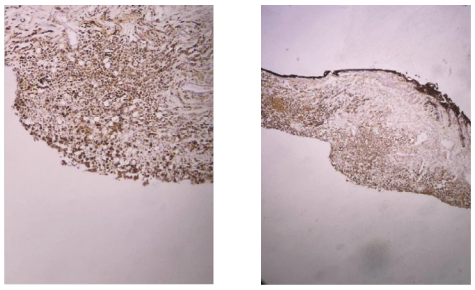

Figure 4 Microphotography of the iris: (a) nuclear details partially obscured by pigmentation (400× magnification), (b) focal thickening (100× magnification) after hematoxylin and eosin staining

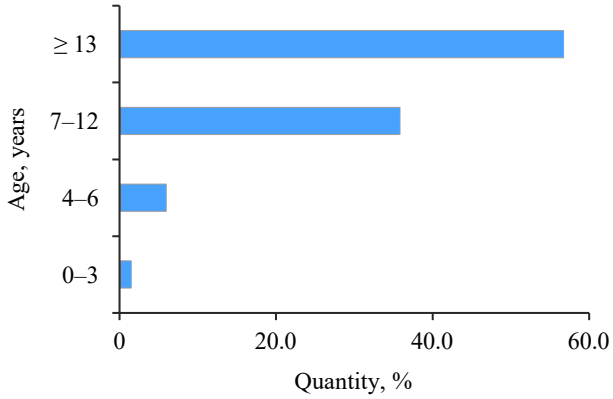

Figure 5 Age profile of cats

They calculated the correlation between the histological type and age, as well as summarized the age-related features of hematopoietic and lymphoreticular tumors. The authors statistically confirmed a high risk of lymphoma in young cats. Cancer patients of 7–12 y.o. and 13-plusers developed ophthalmopathy more often than other age groups. The frequency was 35.82 and 56.72% of all cases, respectively (Fig. 2). In cats under 3 y.o. and between 4 and 6 y.o., ophthalmopathy was the least common: 1.49 and 5.97% of all cases, respectively.

Our data confirmed other reports on the correlation between age and the overall incidence of malignant tumors in animals [8, 24, 34]. However, our data on the high incidence of neoplasms in adult and old cats were by 8.28% lower than those in Mexico City [41]. The main group demonstrated a significant increase in tumor incidence by 21.02%; the geriatric and young groups showed a decrease of 6.23 and 3.91%, respectively. The research included a quantitative sample of animals and studies based on animal shelters.

Domestic cats can serve as models for various non-neoplastic diseases and are particularly valuable for studying inherited ophthalmologic diseases. Cats and humans demonstrate a significant homology for certain genes [29]. Natural tumors in domestic cats make it possible to model cancer development in humans because they share some characteristics. Such studies include spontaneous cancers that develop in immunocompetent animals living in the same environment as humans. In addition, the relatively short lifespans facilitate research completion and data collection. A lot of cancer types have no treatment standards that could provide evaluation of treatment methods.

Feline oral squamous cell carcinoma is common and shares some clinical and molecular characteristics with human head and neck cancer. These similarities make it an attractive model for new treatment trials. Feline mammary tumors are typically malignant and aggressive, with a triple negative phenotype being more common than in humans. They also provide an opportunity to explore potential targets and treatments. Feline injection-site sarcoma may be a model for inflammatory tumorigenesis, although no definitive results are available for humans. However, there are good prospects for studying individual differences in treatment susceptibility, as well as developing preventive and therapeutic strategies [29].

If we interpret the age of cats to human age, these data correlate with the results of studies of neoplastic proliferation in middle-aged people.

In 65-plusers, the colorectal cancer risk is approximately three times as high as in people aged 50–64 y.o. and approximately 30 times as high as in people aged 25–49 y.o. For cats, the correlating age is 13, 9–12, and 2.5–8 y.o., respectively [31]. The average age of diagnosis is 68 and 72 for men and women, respectively, and 13–14 for male and female cats, respectively (Fig. 5).

The age-related character of colorectal cancer is especially obvious in developed countries, where the incidence of colorectal cancer is the highest. There, the incidence of colorectal cancer is associated, among other things, with a longer life expectancy, resulting in a higher proportion of senior citizens in the population [31].

However, some recent studies demonstrated an increase in the incidence of colorectal cancer in young people aged 20–49 y.o. in the USA and Europe (i.e., 2–8 years on the cats' age scale) [33]. The current recommendation is to conduct the first colorectal cancer screening at 50 y.o. (9 y.o. for cats). If the trend perseveres, these screening recommendations will have to be revised.

The sex dimorphism shows that male cats are more likely to get cancer, i.e., 57.14% of the total number of oncological diseases. However, most researchers deny the effect of sex on cancer development in cats [40]. Females are more likely to develop mammary cancer: its incidence is 17 times higher in females than in males, i.e., 25.40 vs. 1.50%. These data confirm other reports [24]. Moreover, males have a worse survival prognosis and an almost 40.00% higher mortality [8]. On the other hand, females have a higher proportion of right-sided tumors, which are often diagnosed at a late stage and tend to be more aggressive than left-sided tumors.

This sex-related difference remains a mystery. It may be related to the differences in the risk factors, diet, and

sex hormones [8]. In our research, castrated males were more common than sterilized females. The castrated males with cancer developed ophthalmopathy in 47.62% while for uncastrated males it was only 9.52%. Unsterilized females with oncological diseases and ophthalmopathy were more common than sterilized ones: 33.33 and 9.53%, respectively.

Early ovariohysterectomy (≤ 2 y.o.) significantly reduces the risk of mammary tumors, its effect depending on the timing [24].

The type of neoplasm was found to correlate with the vascular tract inflammation. Our morphological research made it possible to identify the most common malignant neoplasms with ophthalmopathy in cats. The cats with an ophthalmopathy were simultaneously diagnosed with one or more of the following diseases: carcinoma (25 cats; 37.13%), squamous cell carcinoma (22 cats; 32.83%), lymphoma (20 cats; 29.85%), and sarcoma (14 cats; 20.89%). Other malignant tumors were much less common: melanoma (2.98%) and mastocytoma (1.49%). In other words, cats with two or three types of tumors were rather common.

Considering the ratio of inflammation of the anterior uveal tract (Table 5), the acute fibrinous or hemorrhagic iridocyclitis and chorioretinitis in cats were much less frequent than, e.g., in dogs.

Cancerous ophthalmopathy manifested itself as separate neoplasms and metastases under the effect of substances that accumulated in the vessels or nerves. They triggered an inflammatory or degenerative reaction on the part of the vascular or nervous tissue of the choroid.

Figure 6 illustrates the course of anterior uveitis. Mydriasis and hyperpigmentation of the iris were present in 74.6 and 85.1%, respectively. The cornea was transparent (97.0%), the conjunctiva was pigmented (85.1%). The fluid of the anterior chamber was opalescent (47.8%).

Figure 7 shows chronic lesions of the posterior uveal tract in cats: they occurred more often in the chronic form of serofibrinous (52.2%) or hemorrhagic (31.3%) chorioretinitis, as well as hemorrhagic irido-cyclitis (7.5%).

About 6.0% of posterior uveal tract lesions were fibrinous (52.2%) or hemorrhagic (31.3%) inflammations, as well as retinal detachment (Fig. 8). Chronic chorioretinitis paired with vitreous adhesions (26.9%), posterior capsular false cataract (68.7%), posterior synechiae (7.5%), or posterior margin ruptures (7.5%).

Lymphomas usually have a multifactorial etiology. Chronic viral diseases, poor immune system, or immunodeficiency may be prerequisites for the development of some lymphomas in cats [6].

The cats with lymphoma were more likely to acquire chronic issues of the posterior uveal tract, i.e., fibrinous and hemorrhagic chorioretinitis (Table 5).

Carcinoma in cats is usually triggered by hormonal imbalance, genetic predisposition, or carcinogens [8]. In the six-plusers, mammary tumors were the most common, followed by skin neoplasms. Carcinoma was most often accompanied by chronic damage to the posterior uveal tract, i.e., fibrinous or hemorrhagic chorioretinitis. Chronic inflammation in the posterior uveal tract led to irreversible morphological changes.

Table 5 Clinical forms of inflammation in the uveal tract in cats with neoplasms

Clinical forms	Cats, %			
	Sarcoma (n = 9)	Lymphoma (n = 16)	Squamous cell carcinoma (n = 19)	Carcinoma (n = 21)
Fibrinous iridocyclitis	–	12.50	5.26	9.52
Hemorrhagic iridocyclitis	11.11	6.25	10.53	4.76
Fibrinous chorioretinitis	66.67	50.00	52.63	47.62
Hemorrhagic chorioretinitis	22.22	31.25	31.58	38.10

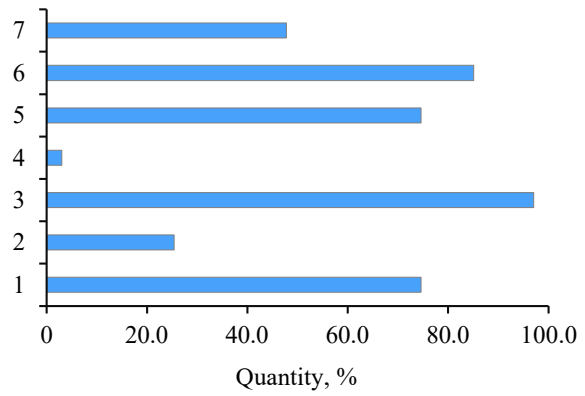

Figure 6 Clinical course of anterior uveal tract lesions in cats: conjunctiva (1 – pigmentation, 2 – no pigmentation), cornea (3 – transparent, 4 – posterior keratitis), iris (5 – mydriasis, 6 – iris hyperpigmentation), and anterior chamber fluid (7 – opalescence)

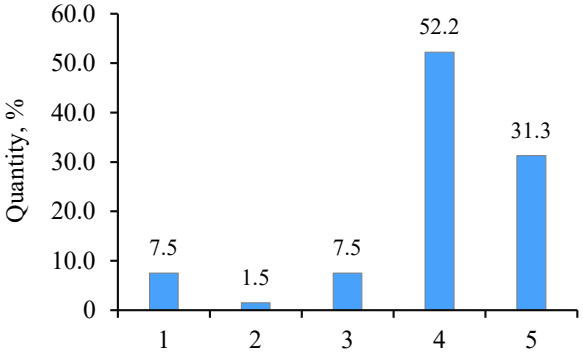

1 – fibrinous iridocyclitis, 2 – chorioretinitis, 3 – hemorrhagic iridocyclitis, 4 – fibrinous chorioretinitis, 5 – hemorrhagic chorioretinitis

Figure 7 Clinical forms of inflammation in the posterior uveal tract in cats

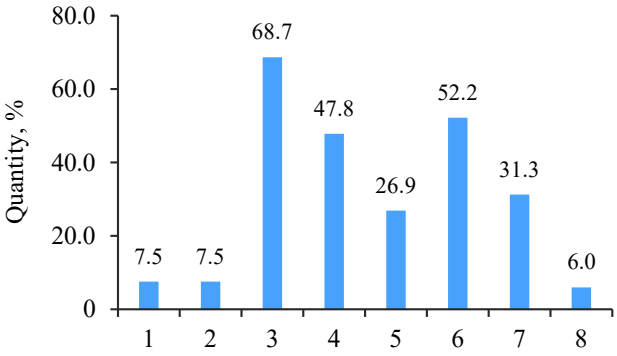

1 – posterior synechiae, 2 – pupillary ruptures, 3 – posterior capsular false cataract, 4 – vitreous opalescence, 5 – vitreous adhesions, 6 – fibrinous inflammation, 7 – hemorrhagic inflammation, 8 – retinal detachment

Figure 8 Clinical course of posterior uveal tract lesions in cats



a b

Figure 9 Chorioretinitis in cats with preretinal opacification of the vitreous body: fundus and vitreous body (a), anterior segment of the eyeball unchanged (b)

Posterior uveal tract inflammation dominated in the cases of uveal inflammation in paraneoplastic ophthalmopathy: fibrinous inflammation (47.62% carcinoma, 66.67% sarcoma) and hemorrhagic inflammation (22.22% sarcoma, 47.62% carcinoma) in all cases of cancer.

Posterior uveal tract inflammation proved to be a quite common form of uveal inflammation in the cats with paraneoplastic ophthalmopathy.

Figure 9 describes the chronic chorioretinitis. The eyelids were of normal size; the palpebral fissure was normal; the conjunctiva was pale pink; the cornea was shiny, transparent, spherical, and moist; the anterior chamber was deep; the aqueous humor of the anterior chamber was transparent. The iris was yellow-green, with a normal pupillary edge. The ophthalmoscopy showed that the lens was unaffected, but the vitreous body demonstrated some opacity; the optic disc and retinal vessels were normal.

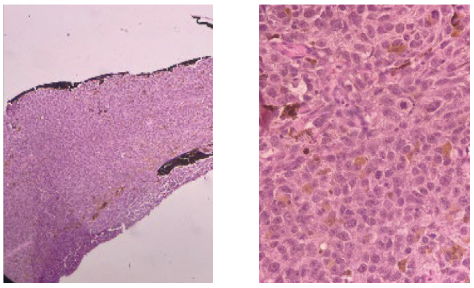

a b

Figure 10 Microphotography of neoplasm after hematoxylin and eosin staining: (a) neoplasm (10× lens, 20× ocular lens), (b) mitotic activity and cells with melanin (10× lens, 40× ocular lens)

In the case illustrated in Fig. 9, the oncological lesion of the iris (melanocytoma) was not accompanied by neoplasms in other organs (Table 6). Unlike multimodal lesions, monolesions of the iris were more likely to occur together with severe anisocytosis and anisokaryosis.

The microarchitecture of iris melanoma demonstrated focal proliferation caused by the abundant cellularity of the tumor. It consisted of polygonal and rounded cells with moderate eosinophilic cytoplasm and melanin. The nuclei were round and irregular, of medium and large in size, with pronounced karyomegaly, coarse-grained chromatin, and 1–3 clearly visible large nucleoli. The mitoses were abundant, with severe anisocytosis and anisokaryosis. The tumor slightly infiltrated the underlying sclera (Fig. 10).

We revealed a significant correlation between cancer and the accumulation of zinc, iron, and lead (Table 7).

Table 6 Pathohistological changes in cats' eyeballs

Eyeball structure	Histology
Cornea	The corneal wall is deformed (artifact); the thickness was not measured. The corneal wall consists of 5–8 epithelium layers with no significant histological changes. The corneal stroma consists of keratinocytes with no histological changes. Descemet's membrane and corneal endothelium demonstrate no histological changes
Choroid	The anterior part is represented by clusters of melanocytes with no histological changes. The blood vessels are not dilated. The ciliary body demonstrates no histological changes. The pectineal ligament is indistinguishable
Tapetum	Not available
Iris	The iris is focally thickened by a highly cellular mass that consists of round and polygonal melanocytes. The cells have a moderately eosinophilic cytoplasm; most cells in the cytoplasm are rich in black granular pigment (melanin). The nuclei are round and irregular, of medium and large size, with pronounced karyomegaly, coarse-grained chromatin, and 1–3 clearly visible large nucleoli. The mitoses are abundant (≤ 20 per 10×400). The anisocytosis and anisokaryosis are pronounced, with a weak infiltrative growth of the tumor into the underlying sclera. The tumor demonstrated no necrosis
Retina	The vessels are not dilated, with no histological changes
Optic nerve	Not available

Table 7 Macro- and microelements in cats with different health status, μg/g

Health status	Macro- and microelements					
	Zn	Cu	Fe	Pb	Cd	As
Paraneoplastic ophthalmopathy	43.78 ± 9.85*	23.84 ± 8.54*	254.84 ± 98.42	5.961 ± 2.513	0.174 ± 0.027	1.521 ± 0.242
Healthy	191.67 ± 47.43*	12.71 ± 1.83*	157.82 ± 38.74	4.580 ± 1.554	0.140 ± 0.058	0.991 ± 0.692

* Reliable differences in the level of macro- and microelements in cancer patients and healthy animals were marked with an asterisk ($p < 0.05$)

The animals with paraneoplastic ophthalmopathy demonstrated a statistically significant increase ($p < 0.05$) in the copper level (Table 11), which confirmed the data published elsewhere [35–37]. The high copper concentration in the fur was associated with a low zinc content. This correlation may be due to carcinoma and mammary tumors, which predominated in the sample [38, 42–44].

Due to the small sampling for each particular type of cancer, we revealed no correlations between other macronutrients and paraneoplastic ophthalmopathy.

Although scientists associate cancer with high lead content, our study did not confirm the well-established cancerogenic effect of lead [45]. The low zinc levels in paraneoplastic ophthalmopathies may be associated with its need for optimal metabolism of retinal cells, modification of plasma membranes of photoreceptors, regulation of the light-rhodopsin reaction, modulation of synaptic transmission, and maintenance of taurine in the retina [3]. The elevated copper levels are associated with the proliferation and metastasis of cancer cells, which need copper [3].

CONCLUSION

In this research, the cats with ophthalmopathy were simultaneously diagnosed with one or more of the following cancers: carcinoma (37.13%), squamous cell carcinoma (32.83%), lymphoma (29.85%), sarcoma (20.89%), melanoma (2.98%), and mastocytoma (1.49%). Evidently, cats with two or three types of cancer are a common veterinarian case.

The main factors of neoplastic proliferation included the diet, care, living conditions, physical activity, stress, chronic inflammation, repeated cases, the rate of increase/decrease in clinical signs, previous therapeutic measure, etc. Cancer-related ophthalmopathy could be triggered by biologically active substances in the tumor or chemotherapeutic drugs, i.e., as a therapy complication. The incidence of cancer-related ophthalmopathy increased with age. Cancer correlated with the accumulation of zinc, iron, and lead in the fur. Carcinomas, especially mammary tumors, correlated with high copper concentration in the fur.

CONTRIBUTION

A.P. Kaledin, M.V. Stepanova, L.F. Sotnikova, and S.Yu. Zaytsev developed the research concept; M.V. Stepanova, S.Yu. Zaytsev, and L.F. Sotnikova designed the methodology; A.S. Kuryndina, D.A. Vilmis, and Yu.N. Melikova worked with the software; A.S. Kuryndina, D.A. Vilmis, Yu.N. Melikova, M.V. Stepanova, and L.F. Sotnikova were responsible for the data validation; A.S. Kuryndina, D.A. Vilmis, Yu.N. Melikova, L.F. Sotnikova, and S.Yu. Zaytsev provided the formal analysis; M.V. Stepanova, S.Yu. Zaytsev, and L.F. Sotnikova wrote the review; A.S. Kuryndina, D.A. Vilmis, Yu.N. Melikova, S.Yu. Zaitsev, and L.F. Sotnikova performed the data curation; M.V. Stepanova and S.Yu. Zaitsev drafted the article; M.V. Stepanova, S.Yu. Zaitsev, and L. F. Sotnikova proofread the manuscript; M.V. Stepanova, S.Yu. Zaitsev, and L.F. Sotnikova supervised the project; M.V. Stepanova, S.Yu. Zaitsev, and L.F. Sotnikova were responsible for the project administration; L.F. Sotnikova acquired the funding. All authors approve of the final version of the manuscript.

CONFLICT OF INTEREST

The authors declared no conflict of interest regarding the publication of this article.

REFERENCES

1. Cheng YQ, Wang SB, Liu JH, Jin L, Liu Y, *et al*. Modifying the tumour microenvironment and reverting tumour cells: New strategies for treating malignant tumours. Cell Proliferation. 2020;53(8):e12865. https://doi.org/10.1111/cpr.12865
2. Baghban R, Roshangar L, Jahanban-Esfahlan R, Seidi K, Ebrahimi-Kalan A, *et al*. Tumor microenvironment complexity and therapeutic implications at a glance. Cell Communication and Signaling. 2020;18:59. https://doi.org/10.1186/s12964-020-0530-4
3. Stepanova MV, Sotnikova LF, Zaitsev SYu. Relationships between the content of micro- and macroelements in animal samples and diseases of different etiologies. Animals. 2023;13(5):852. https://doi.org/10.3390/ani13050852
4. Ludwig L, Dobromylskyj M, Wood GA, van der Weyden L. Feline oncogenomics: What do we know about the genetics of cancer in domestic cats? Veterinary Sciences. 2022;9(10):547. https://doi.org/10.3390/vetsci9100547

5. Denicoff AM, McCaskill-Stevens W, Grubbs SS, Bruinooge SS, Comis RL, *et al*. The National Cancer Institute-American society of Clinical Oncology Cancer Trial accrual symposium: Summary and recommendations. Journal of Oncology Practice. 2013;9(6):267–276. https://doi.org/10.1200/JOP.2013.001119
6. Rolph KE, Cavanaugh RP. Infectious causes of neoplasia in the domestic cat. Veterinary Sciences. 2022;9(9):467. https://doi.org/10.3390/vetsci9090467
7. Shishin MV, Prosekov AYu. Investigation of morphological and antimicrobial properties of intestinal tract microorganisms. Food Processing: Techniques and Technology. 2015;39(4):134−137. (In Russ.)
8. Sawicki T, Ruszkowska M, Danielewicz A, Niedźwiedzka E, Arłukowicz T, *et al*. A review of colorectal cancer in terms of epidemiology, risk factors, development, symptoms and diagnosis. Cancers. 2021;13(9):2025. https://doi.org/10.3390/cancers13092025
9. Pham AT, van Dijk BAC, van der Valk ES, van der Vegt B, van Rossum EFC, *et al*. Chronic stress related to cancer incidence, including the role of metabolic syndrome components. Cancers. 2024;16(11):2044. https://doi.org/10.3390/cancers16112044
10. Dutta Majumder P, Marchese A, Pichi F, Garg I, Agarwal A. An update on autoimmune retinopathy. Indian Journal of Ophthalmology. 2020;68(9):1829–1837. https://doi.org/10.4103/ijo.IJO_786_20
11. Henry K. Paraneoplastic syndromes: Definitions, classification, pathophysiology and principles of treatment. Seminars in Diagnostic Pathology. 2019;36(4):204–210. https://doi.org/10.1053/j.semdp.2019.01.002
12. Naramala S, Ahmad J, Adapa S, Gavini F, Konala VM. Case series of cancer-associated retinopathy (CAR). Cureus. 2019;11(6):e4872. https://doi.org/10.7759/cureus.4872
13. Uemura A, Fruttiger M, d'Amore PA, de Falco S, Joussen AM, *et al*. VEGFR1 signaling in retinal angiogenesis and microinflammation. Progress in Retinal and Eye Research. 2021;84:100954 https://doi.org/10.1016/j.preteyeres.2021.100954
14. Thomas AS. Paraneoplastic retinopathies: An update on pathogenesis, diagnosis and management. Annals of Eye Science. 2024;9:2. https://doi.org/10.21037/aes-23-14
15. Maeda A, Maeda T, Liang Y, Yenerel M, Saperstein DA. Effects of cytotoxic T lymphocyte antigen 4 (CTLA4) signaling and locally applied steroid on retinal dysfunction by recoverin, cancer-associated retinopathy antigen. Molecular vision. 2006;12:885–891.
16. Serrano NC, Millan P, Páez M-C. Non-HLA associations with autoimmune diseases. Autoimmunity Reviews. 2006;5(3):209–214. https://doi.org/10.1016/j.autrev.2005.06.009
17. Liu P, Wang S, Zhang C, Li Y. Paraneoplastic neuromyelitis optica spectrum disorder associated with ovarian dysgerminoma: A case report and literature review. Frontiers in Immunology. 2024;15:1424243. https://doi.org/10.3389/fimmu.2024.1424243
18. Maiorca C, Moret F, Martines V, Tramontano D, Papassifachis MA, *et al*. Paraneoplastic neuromyelitis optica spectrum disorder associated with lung adenocarcinoma: A case report. Frontiers in Immunology. 2022;8:743798. https://doi.org/10.3389/fmed.2021.743798
19. Cohen DA, Bhatti MT, Pulido JS, Lennon VA, Dubey D, *et al*. Collapsin response-mediator protein 5-associated retinitis, vitritis, and optic disc edema. Ophthalmology. 2020;127(2):221–229. https://doi.org/10.1016/j.ophtha.2019.09.012
20. Garibaldi M, Calabrò F, Merlonghi G, Pugliese S, Ceccanti M, *et al*. Immune checkpoint inhibitors (ICIs)-related ocular myositis. Neuromuscular Disorders. 2020;30(5):420–423. https://doi.org/10.1016/j.nmd.2020.02.013
21. Gordon L, Dinkin M. Paraneoplastic syndromes in neuro-ophthalmology. Continuum. 2019;25(5):1401–1421. https://doi.org/10.1212/CON.0000000000000788
22. Graus F, Dalmau J. Paraneoplastic neurological syndromes in the era of immune-checkpoint inhibitors. Nature Reviews Clinical Oncology. 2019;16(9):535–548. https://doi.org/10.1038/s41571-019-0194-4
23. Becquart O, Lacotte J, Malissart P, Nadal J, Lesage C, *et al*. Myasthenia gravis induced by immune checkpoint inhibitors. Journal of Immunotherapy. 2019;42(8):309–312. https://doi.org/10.1097/CJI.0000000000000278
24. Dyulger GP, Dyulger PG, Alikhanov O, Sedletskaya ES, Latynina ES, *et al*. Epidemiology, risk factors and pathomorphological features of mammary tumors in cats. Bulletin of the National academy of sciences of the Republic of Kazakhstan. 2020;(6):78–84. https://doi.org/10.32014/2020.2518-1467.185
25. Govoni VM, da Silva TC, Guerra JM, Pereira IVA, Queiroga FL, *et al*. Genetic variants of *BRCA1* and *BRCA2* genes in cats with mammary gland carcinoma. Veterinary and Comparative Oncology. 2021;19(2):404–408. https://doi.org/10.1111/vco.12685
26. Nosalova N, Huniadi M, Ľubica H, Valenčáková A, Horňák S, *et al*. Canine mammary tumors: Classification, biomarkers, traditional and personalized therapies. International Journal of Molecular Sciences. 2024;25(5):2891. https://doi.org/10.3390/ijms25052891

27. Zhu Z, Kitano T, Morimatsu M, Ochiai K, Ishiguro-Oonuma T, *et al*. A highly conserved region in BRCA2 suppresses the RAD51-interaction activity of BRC repeats. Veterinary Sciences. 2023;10(2):145. https://doi.org/10.3390/vetsci10020145
28. Granados-Soler J-L, Taher L, Beck J, Bornemann-Kolatzki K, Brenig B, *et al*. Transcription profiling of feline mammary carcinomas and derived cell lines reveals biomarkers and drug targets associated with metabolic and cell cycle pathways. Scientific Reports. 2022;12:17025. https://doi.org/10.1038/s41598-022-20874-5
29. Oh JH, Cho J-Y. Comparative oncology: Overcoming human cancer through companion animal studies. Experimental & Molecular Medicine. 2023;55(4):725–734. https://doi.org/10.1038/s12276-023-00977-3
30. Naito E, Yuki M, Hirano T, Kainuma D, Aoyama R. Prognostic utility of preoperative neutrophil-lymphocyte ratio in cats with malignant mammary tumors. Research in Veterinary Science. 2021;135:349–354. https://doi.org/10.1016/j.rvsc.2020.10.015
31. Rawla P, Sunkara T, Barsouk A. Epidemiology of colorectal cancer: Incidence, mortality, survival, and risk factors. Gastroenterology Review. 2019;14(2):89–103. https://doi.org/10.5114/pg.2018.81072
32. Goodarzi E, Beiranvand R, Naemi H, Momenabadi V, Khazaei Z. Worldwide incidence and mortality of colorectal cancer and human development index (HDI): An ecological study. World Cancer Research Journal. 2019;6:e1433. https://doi.org/10.32113/wcrj_201911_1433
33. Peterse EFP, Meester RGS, Siegel RL, Chen JC, Dwyer A, *et al*. The impact of the rising colorectal cancer incidence in young adults on the optimal age to start screening: Microsimulation analysis I to inform the American Cancer Society colorectal cancer screening guideline. Cancer. 2018;124(14):2964–2973. https://doi.org/10.1002/cncr.31543
34. Zhang S, Xiao X, Yi Y, Wang X, Zhu L, *et al*. Tumor initiation and early tumorigenesis: Molecular mechanisms and interventional targets. Signal Transduction and Targeted Therapy. 2024;9:149. https://doi.org/10.1038/s41392-024-01848-7
35. Capriotti G, Piccardo A, Giovannelli E, Signore A. Targeting copper in cancer imaging and therapy: A new theragnostic agent. Journal of Clinical Medicine. 2022;12(1):223. https://doi.org/10.3390/jcm12010223
36. Lener MR, Scott RJ, Wiechowska-Kozłowska A, Serrano-Fernández P, Baszuk P, *et al*. Serum concentrations of selenium and copper in patients diagnosed with pancreatic cancer. Cancer Research and Treatment: Official Journal of Korean Cancer Association. 2016;48(3):1056–1064. https://doi.org/10.4143/crt.2015.282
37. Wittung-Stafshede P. A copper story: From protein folding and metal transport to cancer. Israel Journal of Chemistry. 2016;56(9–10):671–681. https://doi.org/10.1002/ijch.201600019
38. Golovin TS, Tolkachev VA, Everstova EA, Vanina NV. Clinic – laborantorny indicators status of cancer patients of cats. Bulletin of the Kursk State Agricultural Academy. 2017;(1):28–30. (In Russ.)
39. Mitrokhina NV. Methods of Laboratory Diagnostics. Moscow: Veterinarnyj centr patomorfologii i laboratornoj diagnostiki doktora N.V. Mitrokhinoj; 2022. 89 p.
40. Pinello K, Amorim I, Pires I, Canadas-Sousa A, Catarino J, *et al*. Vet-OncoNet: Malignancy analysis of neoplasms in dogs and cats. Veterinary Sciences. 2022;9(10):535. https://doi.org/10.3390/vetsci9100535
41. Pérez-Enriquez JM, Romero-Romero L, Alonso-Morales RA, Fuentes-Pananá EM. Tumor prevalence in cats: Experience from a reference diagnostic center in Mexico City (2006–2018). Veterinaria México OA. 2020;7(4). https://doi.org/10.22201/fmvz.24486760e.2020.4.837
42. Pereira AM, Maia MRG, Fonseca AJM, Cabrita ARJ. Zinc in dog nutrition, health and disease: A review. Animals. 2021;11(4):978. https://doi.org/10.3390/ani11040978
43. Enginler SO, Toydemir TSF, Ates A, Ozturk B, Erdogan O, *et al*. Examination of oxidative /Antioxidative status and trace element levels in dogs with mammary tumors. Bulgarian Journal of Agricultural Science. 2015;21(5):1086–1091.
44. Harro CC, Smedley RC, Buchweitz JP, Langlois DK. Hepatic copper and other trace mineral concentrations in dogs with hepatocellular carcinoma. Journal of Veterinary Internal Medicine. 2019;33(5):2193–2199. https://doi.org/10.1111/jvim.15619
45. Shahrokh M, Alsultan M, Kabalan Y. The relationship between papillary thyroid carcinoma and preoperative TSH level: A cross-sectional study from Syria. Medicine. 2023;102(28):e34283. https://doi.org/10.1097/MD.0000000000034283

ORCID IDs
Anatoly P. Kaledin https://orcid.org/0000-0002-1769-5043
Marina V. Stepanova https://orcid.org/0000-0002-0041-1091
Larisa F. Sotnikova https://orcid.org/0000-0001-7138-6463
Sergei Yu. Zaitsev https://orcid.org/0000-0003-1533-8680
Yulia N. Melikova https://orcid.org/0000-0002-9322-1464
Anastasia S. Kuryndina https://orcid.org/0009-0009-6201-8250
Daria A. Vilmis https://orcid.org/0009-0007-0921-627X

Foods and Raw Materials. 2026;14(2)

ISSN 2308-4057 (Print)
ISSN 2310-9599 (Online)

Research Article
Open Access

Available online at http://jfrm.ru/en
https://doi.org/10.21603/2308-4057-2026-2-671
https://elibrary.ru/FQDYGY

Effect of cultivation conditions on polysaccharide synthesis by *Skeletonema pseudocostatum*

Vyacheslav F. Dolganyuk[1,2], Egor V. Kashirskikh[1], Stanislav A. Sukhikh[1,*], Olga E. Kremleva[3], Elena V. Ulrikh[4], Danil I. Malkov[1], Olga O. Babich[1]

[1] Immanuel Kant Baltic Federal University, Kaliningrad, Russia
[2] Kemerovo State University, Kemerovo, Russia
[3] Yanka Kupala State University of Grodno, Grodno, Belarus
[4] Kaliningrad State Technical University, Kaliningrad, Russia

* e-mail: stas-asp@mail.ru

Received 24.05.2024; Revised 26.06.2024; Accepted 06.05.2025; Published online 21.08.2025

Abstract:
Microalgae are a source of biologically active substances, e.g., polysaccharides. Their commercial potential attracts a lot of scientific attention. This research featured the effect of various nutrient media on the biomass of the psychrophilic microalga *Skeletonema pseudocostatum* and its ability to synthesize polysaccharides.

The Tamiya nutrient medium was used as the standard one. Its composition was improved to accelerate biomass cultivation. Optimization principles were based on the unconventional mathematical method for multidimensional modeling and involved the ANETR 21 software. The qualitative and quantitative assessment of microalgal polysaccharides relied on the anthrone sulfate method. The concentration of uronic acids was determined by the carbazole method while neutral sugars were studied by the resorcinol sulfate method in a microalgal suspension. The growth index of the *S. pseudocostatum* biomass was represented as a ratio of the maximal mass to the initial mass.

The maximal growth index was achieved by adding to the standard Tamiya medium: 10.00 g/cm^3 potassium nitrate ($MgSO_4 \times 7H_2O$), 2.50 g/cm^3 potassium dihydrogen phosphate, 1 cm^3 Fe^+ ethylenediaminetetraacetic acid (EDTA), and a mix of 4.29 g/cm^3 boric acid and 0.9 g/cm^3 manganese (II) chloride tetrahydrate ($MnCl_2 \times 4H_2O$) in an amount of 1.00 cm^3. The maximal polysaccharide biosynthesis was observed when the nutrient medium was modified as follows: 5.00 g/m^3 potassium nitrate, 3.75 g/cm^3 magnesium sulfate, 2.50 g/cm^3 potassium dihydrogen phosphate, 1 mm^3 solution of Fe^+ ethylenediaminetetraacetic acid, and solution of 1.0 g/cm^3 boric acid and 1.81 g/cm^3 $MnCl_2 \times 4H_2O$ (1.00 mm^3 each). The maximal accumulation of microalgal biomass was 2.88 ± 0.08 µg/100 mg dry solids; the maximal yield of polysaccharides was 3.16 ± 0.09 µg/100 mg dry solids. These results were obtained at 5°C.

The yield of polysaccharides by *S. pseudocostatum* depended on such cultivation parameters as temperature and pH. At cultivation temperatures of 0, 5, and 10°C, the yield of polysaccharides reached 2.13 ± 0.06, 3.16 ± 0.09, and 2.04 ± 0.06 µg/100 mg dry solids, respectively. The yield of exopolysaccharides represented by uronic acids and neutral sugars was 106.3 ± 3.1 mg/g and 806.6 ± 24.0 mg/g, respectively. In this research, polysaccharides synthesized by *S. pseudocostatum* demonstrated good prospects for the food industry and sustainable organic agriculture.

Keywords: Microalgae, *Skeletonema pseudocostatum*, polysaccharides, optimization parameters, nutrient medium

Funding: The research was supported by the Ministry of Science and Higher Education of the Russian Federation as part of grant from the President of the Russian Federation, project no. MK-484.2022.1.4 (agreement no. 075-15-2022-393).

Please cite this article in press as: Dolganyuk VF, Kashirskikh EV, Sukhikh SA, Kremleva OE, Ulrikh EV, *et al.* Effect of cultivation conditions on polysaccharide synthesis by *Skeletonema pseudocostatum*. Foods and Raw Materials. 2026;14(2): 276–284. https://doi.org/10.21603/2308-4057-2026-2-671

INTRODUCTION

Microalgae are photosynthetic microorganisms that use light, energy, and carbon dioxide to produce biomass and bioactive compounds, e.g., polysaccharides [1]. They can convert solid waste from thermoelectric plants [2, 3] and other emissions, e.g., sulfur oxides, nitrogen oxides, or hydrocarbons, in order to use them as nutrients for growth. Microalgae are considered as excellent sources of functional and biologically-active nutrients to meet human nutritional needs [4]. *Porphyridium* sp.,

Copyright © 2025, Dolganyuk *et al.* This is an open access article distributed under the terms of the Creative Commons Attribution 4.0 International License (https://creativecommons.org/licenses/by/4.0/), allowing third parties to copy and redistribute the material in any medium or format and to remix, transform, and build upon the material for any purpose, even commercially, provided the original work is properly cited and states its license.

Chlorella sp., *Spirulina* sp., and *Nostoc* sp. are the most well-studied sources in polysaccharide production [5].

Microalgae can grow under extremely unfavorable conditions due to their ability to synthesize polysaccharides [6]. However, some environmental and nutritional factors of microalgae technology may interfere with polysaccharide production [7]. For instance, salinity, nutrient deficiency, temperature, growth phase, as well as ions of magnesium, potassium, or calcium may affect polysaccharide synthesis [8]. Production conditions and infrastructure have to be optimized to cultivate microalgae with rapid cell growth rate, increased biomass, and high polysaccharide yield [9].

Polysaccharides obtained from microalgae consist mainly of galactose, xylose, and glucose, as well as some other sugars and glucuronic or galacturonic acid residues. Their composition depends on such factors as species, strain, and cultivation conditions. Acidic compounds, as well as sulfate and carboxyl groups, are also known to contribute to the anionic nature and, therefore, to the diverse biological activities of polysaccharides [10]. Exopolysaccharides are, perhaps, the most well-known microalgal polysaccharides due to their antioxidant, anti-inflammatory, antitumor, and antimicrobial properties. As a result, polysaccharides can be applied in different industries. Polysaccharides are necessary for the creation of new functional products, biologically active additives, pharmaceuticals, etc. [2, 5, 8, 10, 11].

Numerous publications on microalgal polysaccharides focus on their production, structure, and biological properties, which have direct application in various sectors. For example, Morais *et al*. [12] studied various aspects of obtaining exopolysaccharides from microalgae. Chanda *et al*. [13] reviewed microalgae polysaccharides as plant biostimulants. Moreira *et al*. [14] reported the use of microalgal exopolysaccharides in flocculation. These studies are crucial for commercial production of polysaccharides from microalgae. They explain the potential of microalgal polysaccharides for the food industry, animal feed, and agriculture.

Skeletonema pseudocostatum is a diatom microalga that can produce polysaccharides [15]. *Skeletonemae* are common phytoplankters and proliferate in coastal marine areas [16]. *S. pseudocostatum* is morphologically variable, genotypically diverse, and physiologically versatile. It lives in all seas and oceans, except Antarctica. The list of *Skeletonema* species includes *Skeletonema*, namely *S. ardens, S. dohrnii, S. grethae, S. japonicum, S. marinoi, S. menzelii, S. subsalsum,* and *S. tropicum* [17]. They differ in morphology and SSU/LSU rDNA sequence. In some cases, regional varieties may demonstrate environmentally-induced differences [17]. However, very little reliable information is available on the effect of the nutrient medium on the yield of exopolysaccharides.

Like others of its kind, *S. pseudocostatum* also possesses some exopolysaccharide prospects. This study featured the effect of various nutrient media on the biomass growth rate of *S. pseudocostatum*, as well as on its ability to synthesize polysaccharides.

In case of microalgae, the yield of exopolysaccharides depends on the modification of the standard nutrient medium and such cultivation variables as temperature, time, extractant, etc. Some studies [18, 19] confirmed that low nutrient content in a culture media encourages microalgae to produce more exopolysaccharides. Since *S. pseudocostatum* is a photosynthetic microorganism, an experiment with extremely low nutrient concentrations seems quite promising.

Exopolysaccharides develop as microalgae grow in mass. Their synthesis depends on particular conditions that occur as a result of nutrient depletion, high salinity, light pollution, etc. [20]. Depending on the photosynthetic microorganism, exopolysaccharides can be completely released into the medium or remain more or less bound to the cells.

Exopolysaccharides possess some unique rheological properties that make them promising gelling agents and thickeners. Microalgal exopolysaccharides may find a lot of prospective applications due to their unique properties and cheap production. They possess antibacterial, antioxidant, anti-inflammatory, antiparasitic, immunomodulatory, antitumor, and anticoagulant biological activities, which makes them a popular subject of *in-vitro* and *in-vivo* studies. To sum up, microalgal exopolysaccharides have a lot of advantages: a wide range of microalgal species to be used as raw material, unique structures, physicochemical properties, biological activity, etc. As a result, compounds like microalgal exopolysaccharides are attractive for many industries [21].

Exopolysaccharides are usually extracted from the culture medium by ethanol precipitation. Their yield depends on the length of the alcohol radical, as well as on the deposition temperature. Therefore, producers have to choose from ethanol, butanol, or isopropanol and apply optimal temperatures in the range from –30 to +30°C. Exopolysaccharides are thermally stable, which opens up opportunities for their use in the food, pharmaceutical, and cosmetic industries. Exopolysaccharides obtained using alcohols with different radical lengths differ in water solubility and water-holding capacity. As a result, they are quite predictable when used as hydrocolloids or stabilizers [22–25].

This research was the first of its kind to introduce the possibilities of producing polysaccharides by the psychrophilic microalga of *S. pseudocostatum* isolated from the Baltic Sea under various cultivation conditions. The study rationalized the composition of the nutrient medium and optimized the cultivating conditions with the maximal biomass and polysaccharide yield. The article also introduces data on the yield of uronic acids and neutral sugars.

STUDY OBJECTS AND METHODS

The research featured psychrophilic *Skeletonema pseudocostatum* from the Baltic Sea. The microalgae were cultivated at 0°C at night and +26°C during the day at a lighting intensity of 2,000–3,000 lux, 12-hour photoperiod, and an active acidity of 6.0–9.0. The cultivation

process took place in a refrigeration chamber on a laboratory orbital shaker Unimax 1010 (Heidolph) with a cooling module and a 267 mm box with a stirring speed of 120 rpm.

The first stage involved a standard Tamiya nutrient medium. The rationalized composition for accelerated biomass growth was determined using the unconventional method for constructing multidimensional models on a PC using the ANETR 21 software.

The growth index was represented as a ratio of the maximal yield to the mass registered at the cultivation onset.

Determining the rational composition of the nutrient medium. When using traditional methods, the final model is a polynomial that does not identify the effect of each individual factor on the final result. The ANETR 21 program [26] allows for mathematical multidimensional modelling and presupposes a special procedure that measures the effect of each factor, thus facilitating the optimization task.

We determined the composition of the nutrient medium for accelerated biomass cultivation under the following fixed conditions:

– the inoculum was 20% of the total suspension volume;
– the active acidity of the suspension was 6.0–9.0; and
– the photoperiod was 12 h and involved the LED SENAT Flora plant lamp (25 W).

The cell concentration was determined in a Goryaev chamber. The cultivation process consisted of two periods. During the first stage, microalgal biomass accumulated to ≥ 55–60 million cells/mL. During the second stage, we created stressful conditions to inhibit the proliferation of microalgae in the suspension and trigger the accumulation of polysaccharides in cells.

This method resulted in an analytical expression of the required multidimensional function. We also obtained graphs and analytical expressions of paired dependencies, a graph of changes in standard deviation (%), and deviations of the calculated values from the original value, all numbered and ranked in ascending order. The data about the model were generated into a form table.

To conduct a complete factorial experiment, we used a design matrix for nutrient media variants. We chose five arguments, i.e., components of the culture media.

The sequence of experiments correlated to the minimal costs on changing the level of the selected argument. The design matrix below involves $m = 4–6$; $n = 5$, where m is the number of arguments while n is the number of equations for each argument:

111111 122222 133333 144444 155555
215243 221435 234512 242351 253124
314325 323541 331254 345132 352413
413452 425314 432145 441523 454231
512534 524153 535421 543215 551342

The experiment followed the design matrix for 25 experiments.

If the required number of arguments (m) was ≤ 6, we removed the last columns of each minor rectangle from the matrix.

The matrix showed that at $6 = F(1,2,3,4,5)$, the factors that affected the growth index by optical density (%) ranked in order of effect priority as 3, 2, 5, 4, and 1.

Next, we performed a comparative analysis of the cultivation parameters on standard and optimized nutrient media. The analysis included the maximal density of the culture on the standard medium (P_{max}), as well as the initial (B_0) and maximal (B_{max}) densities of the culture on the optimized medium.

Quantitative analysis of polysaccharides. We determined the presence and quantity of polysaccharides using the anthrone sulfate method at each stage of parameter selection. According to the method, we added 150 μm of anthrone agent (0.1% recrystallized anthrone in concentrated sulfuric acid) to each microplate well (DV-expert, Moscow, Russia) with 50 μm of each sample. The plates spent 10 min at 4°C in a Pozis RK-102 S refrigerator (Diamond Elektrik, Moscow, Russia). After cooling, the samples were incubated in an A-24 thermostat (Millab, Moscow, Russia) at 70°C for 20 min and then cooled back to room temperature. The optical density was measured at 620 nm. The standard curve involved sucrose solutions [27].

Quantitative analysis of uronic acids. We applied the carbazole method to determine the level of uronic acids. To reduce the effect of neutral sugars, we added 10 μm^3 of sulfanilic acid in sulfuric acid (1%) to a 250 μm^3 suspension of microalgae. Then, we placed the tubes in a PE-4300 ice bath (PiterLab, St. Petersburg, Russia) and added 1.5 cm^3 of sodium tetraborate in sulfuric acid (0.1%) dropwise along the wall. After that, the samples underwent a boiling PE4300 water bath (PiterLab, St. Petersburg, Russia) for 6 min. Following this procedure, we added 50 μm^3 of carbazole solution in ethanol (0.1%) to the samples and again subjected them to the water bath for 10 min. The tubes were then cooled to room temperature to measure the optical density of the solutions at 525 nm. The concentration of uronic acids was determined using a calibration curve of galacturonic acid [28].

Quantitative analysis of neutral sugars. We used the resorcinol sulfate method to determine neutral sugars. We added 200 μm^3 of resorcinol recrystallized in butanol (6 mg/cm^3) and 1 mm^3 of 75% sulfuric acid to a 200 μm^3 of microalgae suspension. The tubes were shaken on a vortex (DV-expert, Moscow, Russia) and heated in the PE-4300 water bath at 90°C for 30 min. Subsequently, we cooled the samples in a PE-4300 ice bath in the dark for 30 min to measure the optical density at 480 nm. The concentration of neutral sugars was determined with a calibration curve of glucose solutions [29].

The reagents and chemicals were of analytical or higher grade (Diadema, Moscow, Russia).

Statistical analysis. All experiments and measurements were carried out in triplicates. The results were presented as a combination of mean and standard deviation (M ± SD). ANOVA was followed by Student's and Tukey's tests to identify statistically significant differences between different groups ($p < 0.05$). The statistical

analysis involved IBM SPSS Statistics 28.0.1 (IBM Corporation, USA) while the graphs were generated in Excel (Microsoft 300 Office, Microsoft Corporation, USA).

RESULTS AND DISCUSSION

The ANETR 21 software uses the Turbo Pascal language to process data bulks. The program makes it possible to introduce various restrictions depending on the nature of the phenomenon under investigation. Its paired dependencies include 15 equations. They describe curves that vary monotonically without extreme inflections, those with one inflection only, symmetrical/asymmetrical curves, and S-shaped curves.

The method is deterministic because the choice of the type of paired dependencies is limited for each argument, the passage of the paired dependency curve through a given point is mandatory, and a neutralization sequence is provided. The program includes some other restrictions that provide significant flexibility and versatility.

Table 1 shows calculations of the relative impact of the first three arguments on the required function.

The calculations in Table 1 provide the following data:

– Argument 3: 100.0 – 90.6 = 9.4%;
– Argument 2: 90.6 – 81.3 = 9.3%; and
– Argument 1: 81.3 – 76.2 = 5.1%.

The reliability of the models was assessed by several indicators, including the mean standard deviation of the calculated values from the original one (MSD) and from the mean intervals (RMS_{mean}) in absolute or relative units, %, the multiple correlation coefficient (*R*), and Fisher's criterion.

The design matrix data revealed the changes in the mean standard deviation (%). It was 6.2% while Fisher's coefficients were $F = 1.8086$, $F(001) = 2.697$, and $F(005) = 2.007$.

Table 2 represents the arguments and their values.

Two remaining factors 4 and 1 accounted for only 75.0 – 74.4 = 0.6% while the error caused by other unspecified factors was 6.2%.

As a result, factors 3, 2, and 5 proved significant for rationalizing the nutrient medium and physicochemical conditions for cultivating *Skeletonema pseudocostatum*.

When K_2HPO_4 (factor 3) grew from 0 to 3.62 g/cm^3, the biomass growth index increased from 69.3 to 90.6%, as in the equation $Y = 1/(0.0154 – 1.26\times10^{-6}\times X_3)$.

As the content of $MgSO_4\times2H_2O$ (factor 2) increased from 0 to 5.0 g/cm^3, the function initially grew from 61.0 to 96.0%, peaked at 2.50 g/cm^3, then dropped to 79.0%, as in $Y = –1.006 \times 10^{-7} \times X_2^2 + 4.18 \times 10^{-4} \times X_2 + 0.7104$.

As KNO_3 rose from 0 to 10.0 g/cm^3 (factor 1), the required function increased linearly from 66.0 to 84.5%, as in $Y = 0.8565 + 8.268 \times 10^{-4} \times X_6$.

In this experiment, the maximal growth index was observed at KH_2PO_4 – 8.4 g/cm^3, $MgSO_4\times7H_2O$ – 0.5 g/cm^3, and KNO_3 – 1.0 g/cm^3.

Table 2 made it possible to substantiate the effectiveness of a multifactorial experiment to rationalize the macrosalt composition of the nutrient medium. When *S. pseudocostatum* grew on a nutrient medium with an optimal macrosalt balance, its growth characteristics increased by a factor of 1.4, compared to the standard Tamiya medium.

Table 3 summarizes the experimental data.

Tables 4 compares the cultivation parameters of *S. pseudocostatum* on the standard and optimized nutrient media.

We registered a 1.5-time increase in biomass in the optimized medium, compared to the standard one.

Table 1 Model form

Argument	Equation	Coefficient			Mean standard deviation from the original, %	Multiple correlation coefficient	Mean standard from the mean intervals, %
		A	B	C			
3	7	1.539E-2	–1.263E-6	–	90.6	0.376	44.8
2	11	–1.006E-7	4.179E-4	7.104E-1	81.3	0.525	43.5
1	1	8.565E-1	8.268E-4	–	76.2	0.577	70.7
4	11	–9.704E-7	6.189E-4	9.688E-1	75.0	0.664	97.3
5	11	–5.483E-7	4.994E-4	9.398E-1	74.4	0.542	48.9

Table 2 Arguments (complete factorial experiment) and their values

No.	Argument, g/cm^3				
	1 KNO_3	2 K_2HPO_4	3 $MgSO_4\times2H_2O$	4 $(NH_2)_2CO$	5 $FeSO_4\times7H_2O$
1	0	0	0	0	0
2	0.09	0.009	0.009	0.9	0.0027
3	0.10	0.010	0.010	1.0	0.0030
4	0.11	0.011	0.011	1.1	0.0033
5	0.20	0.020	0.020	2.0	0.0060
Range	0–33.60	0–2.00	0–5.00	0–2.00	0–2.00

Table 3 Summary of experiments (n = 25) (complete factorial experiment)

Functions							
Values in design matrix						Experimental results	
						Growth index, %	Polysaccharides μg/ 100 mg
No.	1	2	3	4	5	6	7
1	0	0	0	0	0	0.757	0.01
2	0.09	0	0.0200	0.90	0.0030	1.442	2.08
3	0.10	0	0.0011	0.01	0.0027	0.980	2.02
4	0.11	0	0.0010	1.10	0.0060	1.105	2.41
5	0.20	0	0.0090	2.00	0.0030	1.143	2.02
6	0	0.009	0.0090	0.90	0.0027	0.676	2.12
7	0.09	0.009	0	1.10	0.0030	0.755	2.08
8	0.10	0.009	0.0100	2.00	0.0033	1.180	2.03
9	0.11	0.009	0.0200	1.00	0	1.187	2.01
10	0.20	0.009	0.0110	0	0.0060	1.210	2.01
11	0	0.010	0.0100	1.00	0.0030	0.708	2.02
12	0.09	0.010	0.0110	2.00	0	0.707	2.07
13	0.10	0.010	0	0.90	0.0060	0.790	1.02
14	0.11	0.010	0.0090	0	0.0033	1.302	2.02
15	0.20	0.010	0.0200	1.10	0.0027	1.341	2.52
16	0	0.011	0.0110	1.10	0.0033	0.686	2.19
17	0.09	0.011	0.0090	1.00	0.0060	0.790	2.10
18	0.10	0.011	0.0200	0	0.0030	1.302	2.63
19	0.11	0.011	0	2.00	0.0027	1.167	1.12
20	0.20	0.011	0.0100	0.90	0	1.076	2.09
21	0	0.020	0.0200	2.00	0.0060	0.757	1.43
22	0.09	0.020	0.0100	0	0.0027	0.797	1.87
23	0.10	0.020	0.0090	1.10	0	1.110	2.11
24	0.11	0.020	0.0110	0.90	0.0030	1.120	2.56
25	0.20	0.020	0	1.00	0.0033	1.208	2.15
Min	0	0	0	0	0	0.676	0.01
Max	0.20	0.020	0.0200	2.00	0.0060	1.341	2.63

Table 4 Comparative analysis of *Skeletonema pseudocostatum* cultivation parameters on standard medium

Strain	Maximal culture density on standard medium (P_{max}), %	Initial culture density on optimized medium (B_0), %	Maximal culture density on standard medium (B_{max}), %	Magnification coefficient
Skeletonema pseudocostatum	0.96	0.59	1.32	1.50

Therefore, the conditions improved in line with the complete factorial experiment proved to be optimal.

In this study, we rationalized the nutrient composition and optimized the physicochemical conditions for cultivating the microalgae. The maximal growth index was detected under the following nutrient composition: 10.00 g/L of potassium nitrate, 2.50 g/cm^3 magnesium sulfate, 2.50 g/cm^3 potassium dihydrogen phosphate, 1 mm^3 solution of Fe^+ EDTA (ethylenediaminetetraacetic acid), and 1.00 mm^3 solution of trace elements (4.29 g/cm^3 boric acid, 0.9 g/cm^3 $MnCl_2 \times 4H_2O$). The maximal polysaccharide biosynthesis in the antioxidant complex occurred under the following nutrient composition: 5.00 g/L potassium nitrate, 3.75 g/cm^3 magnesium sulfate, 2.50 g/cm^3 potassium dihydrogen phosphate, 1 mm^3 solution Fe^+ EDTA, and 1.00 mm^3 solution of trace elements (0 g/cm^3 boric acid, 1.81 g/cm^3 $MnCl_2 \times 4H_2O$).

S. pseudocostatum has received little scientific attention, most publications dating back to the 1970s and 1980s. However, there is another *Skeletonema Skeletonemataceae* microalga that found its way into research articles [30, 31]. Since both *S. pseudocostatum* and *S. costatum* belong to the same genus, we found it necessary to dwell upon the way *S. costatum* accumulates polysaccharides.

Myklestad [30] studied the effect of nitrogen:phosphorus ratio in the nutrient medium on the yield of *S. costatum*. The scientist varied the nitrogen:phosphorus ratio in six steps from 0.4 to 100 in batch cultures of the marine diatom of *S. costatum* (Greville) Cleve. The publication reports the effect of these changes on growth rate, nitrogen and phosphorus assimilation coefficient, yield of cellular and extracellular polysaccharides, protein, cellular phosphorus, and cell size in exponential and stationary growth phases.

At 10–100, the growth rate dropped from 1.7 to 1.1 divisions per day, and the rate of nitrate absorption from the nutrient medium also went down. At the lowest nitrogen:phosphorus ratios, the phosphorus content per cell was almost constant in both exponential and stationary phases and decreased as the ratio increased.

The fast-growing *S. costatum* cells proved to be poor polysaccharide producers whereas the slow-growing cells appeared to be much more prolific, as a result of media optimization.

As the nitrogen:phosphorus ratio grew, the ratio of cellular protein to polysaccharides decreased in the exponential phase and increased in the stationary phase. The *β*-1,3-glucan content was especially effective in boosting cellular polysaccharide synthesis. Myklestad [30] proposed the ratio of cellular polysaccharide to cellular phosphorus (15–675) as an indicator of the physiological state of marine diatoms. The study also casts light upon the potential ecological significance of *S. costatum* as a polysaccharide producer.

pH is an important factor for microalgal cultivation on optimized nutrient media. As a chemical property of the growing medium, pH affects the CO_2 hydrolysis and biodegradation of water-soluble sulfur-containing pollutants.

Low pH inhibits the growth of microalgae. However, CO_2 has a rather limited effect on pH while sulfur-containing ions can change pH significantly, thus reducing the biomass accumulation. In this research, we calibrated the pH values using a buffered medium.

Table 5 illustrates the effect of pH on *S. pseudocostatum* biomass growth rate at the initial and final stages of cultivation. The greatest increase in biomass and, therefore, polysaccharides was detected when the medium remained neutral throughout the entire cultivation process.

For *S. pseudocostatum*, the optimal ratio of initial and final pH values was 6.9/6.9. At this ratio, the biomass yield of *S. pseudocostatum* increased by 67.3 ± 0.14%.

Taraldsvik & Myklestad [31] grew *S. costatum* at different pH. They used a semi-continuous culture system that maintained a preset pH value. At pH 6.5–8.5, the growth rate was almost constant (2.4 divisions per day on average) and decreased at pH > 9. Organic carbon (C) production dropped from 5.3 mg/cm^3 to 2.0 at pH 6.5–8.5 and to 1.0 mg/cm^3 at pH 9.0 and 9.4. The content of *β*-1,3-linked glucan decreased from 7.1 mg/L at pH 6.5 to 0.2 mg/L at pH 9.4. The content of total organic carbon in the form of glucan decreased from 60 to 10%. At pH 8.0–9.0, the cellular concentration of amino acids varied from approximately 62 to 84 mM. At pH 9.4, the glutamine concentration sank below the detection limit. At pH 6.5–8.5, the content of extracellularly synthesized polysaccharides averaged as low as 3.7% of the total carbon but increased at pH 9.0 and 9.4. The down growth and biosynthesis of polysaccharides at pH > 9.0 might have been related to the decrease in the rate of some important biochemical reactions, as well as the changes in the properties of cell membranes in this pH range [31].

In our research, we defined the rational cultivation temperature after selecting the optimal pH. We varied it from 0 to 10°C. Table 6 summarizes the effect of temperature on the biomass growth and polysaccharide synthesis by *S. pseudocostatum*.

Table 6 shows it quite clearly that the largest yield of polysaccharides was detected at 5°C. At this temperature, exopolysaccharides entered the intercellular space most actively.

The biggest biomass accumulation (2.88 ± 0.08 g/cm^3) and polysaccharide yield (3.16 ± 0.09 μg/100 mg dry solids) were observed at 5°C. When we reduced the cultivation temperature to 0°C and increased it to 10°C, the biomass accumulation dropped to 1.92 ± 0.06 g/cm^3 and 2.13 ± 0.06 μg/100 mg dry solids, respectively, and the polysaccharide yield went as low as 1.71 ± 0.05 g/cm^3 and 2.04 ± 0.06 μg/100 mg dry solids, respectively.

Table 7 introduces the experimental data on the content of uronic acids and neutral sugars.

The optimized medium raised the yield of polysaccharides and uronic acids by a factor of 1.1. Neutral sugars demonstrated the greatest difference. In the optimized medium, they experienced a 1.48-time increase, probably, because the optimized environment provided the most favorable conditions for their accumulation.

Granum *et al*. [32] studied the cellular and extracellular synthesis of polysaccharides and amino acids by the marine diatom of *S. costatum* (Grev.) Cleve in different growth phases. They grew batch cultures on a 10/14 dark/light cycle in nitrogen-limited media at two different nutrient concentrations. The exponential

Table 5 Effect of cultivation medium pH on *Skeletonema pseudocostat*

Sample	Initial pH/final pH					
	5.0/4.9	6.2/6.2	6.9/6.9	7.5/7.8	8.0/7.9	8.3/7.9
Skeletonema pseudocostatum	55.20 ± 0.12	56.30 ± 0.14	67.30 ± 0.14	56.70 ± 0.13	58.10 ± 0.11	36.10 ± 0.08

Table 6 Effect of cultivation temperature on *Skeletonema pseudocostatum* growth and polysaccharide yield (antioxidant complex)

Sample	Biomass, g/cm^3			Polysaccharide yield, μg/100 mg dry solids		
	Cultivation temperature, °C					
	0	5	10	0	5	10
*Skeletonema pseudocostatu*m	1.92 ± 0.06	2.88 ± 0.08	1.71 ± 0.05	2.13 ± 0.06	3.16 ± 0.09	2.04 ± 0.06

Table 7 Effect of nutrient media on polysaccharide synthesis of *Skeletonema pseudocostatum*

Compound	Exopolysaccharides	
	Standard medium	Optimized medium
Polysaccharides, g/cm^3	2.88 ± 0.08	3.16 ± 0.09
Uronic acids, mg/g exopolysaccharides	96.90 ± 2.80	106.30 ± 3.10
Neutral sugars, mg/g exopolysaccharides	273.90 ± 8.10	406.60 ± 24.00

growth rate was 2.0 divisions per day. The growth rate was quite balanced, except for some significant changes in chemical composition. During the photophase, inorganic carbon and nitrogen were absorbed, and the number of elementary cells went down. At the end of the light phase of photosynthesis, the amount of *β*-1.3-glucan polysaccharide was 17% cellular organic carbon; at the end of the dark phase, it was 42%. The protein:glucan ratio was 2.3:0.7.

In the same study, cell wall polysaccharides accounted for 6–10% cellular organic carbon. The cellular pool of free amino acids rose from 8 at the end of the light phase to 22 at the end of the dark phase (% cellular organic nitrogen). Glutamine is the main amino acid in photosynthesis: its amount increased from 0.2 to 12 mmol per cell whereas the glutamine:glutamate ratio increased from 0.05 to 2. After depletion of nitrogen ions NO_3, the level of glucan increased rapidly within 3–4 days to settle down at the level of 75–80% cellular organic polysaccharide. On the contrary, the amount of cellular nitrogen decreased by 80%, and the amount of cell wall polysaccharides dropped by 35%. Consequently, the protein:glucan ratio dropped as low as < 0.1. The pool of cellular free amino acids decreased by 90% within 24 h of nitrogen depletion and continued to decrease steadily throughout the stationary phase. Glutamine decreased most rapidly and accounted for < 1% free amino acids in the stationary phase. Extracellular production accounted for 4% of total photosynthetic production during both exponential and stationary growth phases. However, the absolute release rate per cell was significantly higher in the exponential phase. In one case, a transient high release occurred during the transition phase, probably as a result of cell leakage. The extracellular production of healthy cells contained 33% of polysaccharides, 15% monosaccharides, and 5% free amino acids. The composition of extracellular amino acids differed from intracellular ones and experienced significant changes between the exponential and the stationary phases. To sum up, Granum *et al*. [32] reported the rapid response of the diatom *S. costatum* to ambient nitrogen and light conditions, which affected the carbohydrate and amino acid dynamics at the cellular level.

Biomass accumulation and polysaccharide synthesis by *Microchloropsis salina* reported by Ocaranza *et al*. [33] can serve as a comparison. *M. salina* is a source of various biomolecules, e.g., lipids and carbohydrates. Such polysaccharides as *β*-glucans are the most important synthesized carbohydrates to be used as antioxidants, antiseptics, and immunomodulators. Ocaranza *et al*. [33] assessed *M. salina* for its polysaccharide production potential under two different culture conditions: a high-density batch and a simulated high-density fed batch. The simulated high-density fed-batch culture improved the biomass growth. It was $8.00\times10^{-2} \pm 2.00\times10^{-3}$ g/cm^3 per 24 h; in the loading state, it was $-5.13\times10^{-2} \pm 4.00\times10^{-4}$ g/cm^3 per 24 h. The same dependence occurred for *β*-glucans: their volumetric production reached $5.96\times10^{-3} \pm 2.00\times10^{-4}$ g of product/cm^3 per 24 h vs. $4.10\times10^{-3} \pm 2.00\times10^{-4}$ g product/cm^3 per 24 h under batch conditions. These data establish the basic conditions for optimizing and boosting polysaccharide biosynthesis and biomass growth. This new raw material source of *β*-glucans can be applied in the production of nutraceuticals for people and animals. To sum up, Ocaranza *et al*. [33] described the accumulation of polysaccharides by *M. salina* in standard and modified media.

S. pseudocostatum is a promising alternative for polysaccharide synthesis in the sense that it can mitigate the effects of industrial pollution [34]. *S. pseudocostatum* is known to grow faster than any land plant, and it requires no fertile soil. Therefore, it does not compete with food production. Its carbon fixation efficiency is 10–50 times greater than that of any plant. Microalgae help reduce greenhouse gases by sequestering carbon dioxide from industrial processes. *S. pseudocostatum* can grow in fresh, sea, subsaline, and waste water [35]. Microalgal polysaccharides have important rheological and biological properties for food and sustainable agriculture applications.

CONCLUSION

The improved nutrient medium and pH ratio at the onset and end of cultivation (6.9/6.9) yielded 2.13 ± 0.06, 3.16 ± 0.09, and 2.04 ± 0.06 μg polysaccharides per 100 mg dry solids at 0, 5, and 10°C, respectively. When we reduced the cultivation temperature to 0°C or brought it up to 10°C, the *Skeletonema pseudocostatum* biomass and the polysaccharide yield decreased. Similar results occurred when we lowered or raised the ratio of pH values at the two cultivation stages. The polysaccharide synthesis in the optimized medium demonstrated a 1.3-time increase. The polysaccharide yield in the optimized medium was 1.1 times greater than in the standard medium. The uronic acid synthesis demonstrated the same 1.1-time increase in the optimized medium. The neutral sugars showed the largest 1.48-fold difference between the standard and the optimized media. The optimized nutrient medium provided the most favorable conditions for the accumulation of neutral sugars.

It had no hydrodynamic factors that would inhibit the cell growth, which allowed it to boost the polysaccharide synthesis.

Polysaccharides obtained from *S. pseudocostatum* can be used to design new types of foods, e.g., healthy bakery products, special nutrition for sports and weight correction, age-inhibiting products, new dietary supplements, pharmaceuticals, etc.

CONTRIBUTION

V.F. Dolganyuk – 25%, E.V. Kashirskikh – 10%, S.A. Sukhikh – 20%, O.E. Kremleva – 10%, E.V. Ulrikh – 10%, D.I. Malkov – 10%, O.O. Babich – 25%.

CONFLICT OF INTEREST

The authors declared no conflict of interest related to this publication.

REFERENCES

1. de Carvalho Silvello MA, Gonçalves IS, Azambuja SPH, Costa SS, Silva PGP, *et al*. Microalgae-based carbohydrates: A green innovative source of bioenergy. Bioresource Technology. 2022;344(Part B):126304. https://doi.org/10.1016/j.biortech.2021.126304
2. Dolganyuk V, Belova D, Babich O, Prosekov A, Ivanova S, *et al*. Microalgae: A promising source of valuable bioproducts. Biomolecules. 2020;10(8):1153. https://doi.org/10.3390/biom10081153
3. Hu J, Nagarajan D, Zhang Q, Chang JS, Lee DJ. Heterotrophic cultivation of microalgae for pigment production: A review. Biotechnology Advances. 2018;36(1):54–67. https://doi.org/10.1016/j.biotechadv.2017.09.009
4. Dolganyuk V, Sukhikh S, Kalashnikova O, Ivanova S, Kashirskikh E, *et al.* Food Proteins: Potential resources. Sustainability. 2023;15(7):5863. https://doi.org/10.3390/su15075863
5. Gonçalves AL. The use of microalgae and cyanobacteria in the improvement of agricultural practices: A review on their Biofertilising, Biostimulating and biopesticide roles. Applied Sciences. 2021;11(2):871. https://doi.org/10.3390/app11020871
6. López-Hernández JF, Kean-Meng T, Asencio-Alcudia GG, Asyraf-Kassim M, Alvarez-González CA, *et al*. Sustainable microalgae and cyanobacteria biotechnology. Applied Sciences. 2022;12(14):6887. https://doi.org/10.3390/app12146887
7. Coulombier N, Blanchier P, Le Dean L, Barthelemy V, Lebouvier N, *et al*. The effects of CO_2-induced acidification on Tetraselmis biomass production, photophysiology and antioxidant activity: A comparison using batch and continuous culture. Journal of Biotechnology. 2021;325:312–324. https://doi.org/10.1016/j.jbiotec.2020.10.005
8. Paliwal C, Mitra M, Bhayani K, Bharadwaj SVV, Ghosh T, *et al*. Abiotic stresses as tools for metabolites in microalgae. Bioresource Technology. 2017;244(Part 2):1216–1226. https://doi.org/10.1016/j.biortech.2017.05.058
9. Marques AEML, Balen RE, da Silva Pereira Fernandes L, Motta CM, de Assis HCS, *et al*. Diets containing residual microalgae biomass protect fishes against oxidative stress and DNA damage. Journal of Applied Phycology. 2019;31:2933–2940. https://doi.org/10.1007/s10811-019-01825-6
10. Gürlek C, Yarkent Ç, Köse A, Tuğcu B, Gebeloğlu IK, *et al*. Screening of antioxidant and cytotoxic activities of several microalgal extracts with pharmaceutical potential. Health and Technology. 2020;10:111–117. https://doi.org/10.1007/s12553-019-00388-3
11. Chaplygina TV, Prosekov AU, Babich OO, Pavsky VA, Ivanova SA. Functional dairy products are protection during pandemic. Dairy industry. 2020;(6):26–28. https://doi.org/10.31515/1019-8946-2020-06-26-28
12. Morais MG, Santos TD, Moraes L, Vaz BS, Morais EG, *et al*. Exopolysaccharides from microalgae: Production in a biorefinery framework and potential applications. Bioresource Technology Reports. 2022;18:101006. https://doi.org/10.1016/j.biteb.2022.101006.
13. Chanda MJ, Merghoub N, Arroussi HE. Microalgae polysaccharides: The new sustainable bioactive products for the development of plant bio-stimulants? World Journal of Microbiology and Biotechnology. 2019;35:177. https://doi.org/10.1007/s11274-019-2745-3
14. Moreira JB, Kuntzler SG, Bezerra PQM, Cassuriaga APA, Zaparoli M, *et al*. Recent advances of microalgae exopolysaccharides for application as bioflocculants. Polysaccharides 2022;3(1):264–276. https://doi.org/10.3390/polysaccharides3010015
15. Gerecht A, Romano G, Ianora A, d'Ippolito G, Cutignano A, *et al*. Plasticity of oxylipin metabolism among clones of the marine diatom *Skeletonema marinoi* (Bacillariophyceae). Journal of Phycology. 2011;47(5):1050–1056. https://doi.org/10.1111/j.1529-8817.2011.01030.x
16. McKenzie CH, Bates SS, Martin JL, Haigh N, Howland KL, *et al*. Three decades of Canadian marine harmful algal events: Phytoplankton and phycotoxins of concern to human and ecosystem health. Harmful Algae. 2021;102:101852. https://doi.org/10.1016/j.hal.2020.101852
17. Kooistra WHCF, Sarno D, Balzano S, Gu H, Andersen RA, *et al*. Global diversity and biogeography of *Skeletonema* species (Bacillariophyta). Protist. 2008;159(2):177–193. https://doi.org/10.1016/j.protis.2007.09.004

18. Aremu AO, Nemény M, Stirk WA, Ördög V, van Staden J. Manipulation of nitrogen levels and mode of cultivation are viable methods to improve the lipid, fatty acids, phytochemical content, and bioactivities in *Chlorella minutissima*. Journal of Phycology. 2015;51(4):659–669. https://doi.org/10.1111/jpy.12308
19. Coulombier N, Jauffrais T, Lebouvier N. Antioxidant compounds from microalgae: A Review. Marine Drugs. 2021;19(10):549. https://doi.org/10.3390/md19100549
20. Paradis-Hautcoeur J, Gosselin M, Villeneuve V, Tremblay J, Lévesque D, *et al*. Effects of riverine nutrient inputs on the sinking fluxes of microbial particles in the St. Lawrence Estuary. Estuarine, Coastal and Shelf Science. 2023;284:108270. https://doi.org/10.1016/j.ecss.2023.108270
21. Azizan A, Bustamam MSA, Maulidiani M, Shaari K, Ismail IS, *et al*. Metabolite profiling of the microalgal diatom chaetoceros calcitrans and correlation with antioxidant and nitric oxide inhibitory activities via ^{1}H NMR-based metabolomics. Marine Drugs. 2018;16(5):154. https://doi.org/10.3390/md16050154
22. Jaroszuk-Ściseł J, Nowak A, Komaniecka I, Choma A, *et al*. Differences in production, composition, and antioxidant activities of exopolymeric substances (EPS) obtained from cultures of endophytic *Fusarium culmorum* strains with different effects on cereals. Molecules. 2020;25(3):616. https://doi.org/10.3390/molecules25030616
23. Koçer AT, İnan B, Usul SK, Özçimen D, Yılmaz MT, *et al*. Exopolysaccharides from microalgae: Production, characterization, optimization and techno-economic assessment. Brazilian Journal of Microbiology. 2021;52:1779–1790. https://doi.org/10.1007/s42770-021-00575-3
24. Ahmed Z, Wang Y, Anjum N, Ahmad H, Ahmad A, *et al*. Characterization of new exopolysaccharides produced by coculturing of *L. kefiranofaciens* with yoghurt strains. International Journal of Biological Macromolecules. 2013;59:377–383. https://doi.org/10.1016/j.ijbiomac.2013.04.075
25. Martirosyan VV, Kostyuchenko MN, Reynov MV, Tyurina OE, Savkina OA. Study of exopolysaccharide production by lactic acid bacteria used in the baking industry and comparison of methods for their determination. Food Metaengineering. 2024;2(4):13–25. (In Russ.) https://doi.org/10.37442/fme.2024.4.67
26. Pérez-Lechuga G, Venegas-Martínez F, Martínez-Sánchez JF. Mathematical modeling of manufacturing lines with distribution by process: A Markov chain approach. Mathematics. 2021;9(24):3269. https://doi.org/10.3390/math9243269
27. Papuga S, Pećanac I, Stojković M, Savić A, Velemir A. Mead fermentation parameters: Optimization by response surface methodology. Foods and Raw Materials. 2022;10(1):137–147. https://doi.org/10.21603/23084057-2022-1-137-147
28. Taylor KA, Buchanan-Smith JG. A colorimetric method for the quantitation of uronic acids and a specific assay for galacturonic acid. Analytical Biochemistry. 1992;201(1):190–196. https://doi.org/10.1016/0003-2697(92)90194-C
29. Monsigny M, Petit C, Roche AC. Colorimetric determination of neutral sugars by a resorcinol sulfuric acid micromethod. Analytical Biochemistry. 1988;175(2):525–530. https://doi.org/10.1016/0003-2697(88)90578-7
30. Myklestad S. Production of carbohydrates by marine planktonic diatoms. II. Influence of the NP ratio in the growth medium on the assimilation ratio, growth rate, and production of cellular and extracellular carbohydrates by Chaetoceros *affinis* var. *willei* (Gran) Hustedt and *Skeletonema costatum* (Grev.) Cleve. Journal of Experimental Marine Biology and Ecology. 1977;29(2):161–179. https://doi.org/10.1016/0022-0981(77)90046-6
31. Taraldsvik M, Myklestad S. The effect of pH on growth rate, biochemical composition and extracellular carbohydrate production of the marine diatom *Skeletonema costatum*. European Journal of Phycology 2000;35(2):189–194. https://doi.org/10.1080/09670260010001735781
32. Granum E, Kirkvold S, Myklestad SM. Cellular and extracellular production of carbohydrates and amino acids by the marine diatom *Skeletonema costatum*: Diel variations and effects of N depletion. Marine Ecology-progress Series. 2002;242:83–94. https://doi.org/10.3354/meps242083
33. Ocaranza D, Balic I, Bruna T, Moreno I, *et al*. A modeled high-density fed-batch culture improves biomass growth and *β*-glucans accumulation in *Microchloropsis salina*. Plants. 2022;11(23):3229. https://doi.org/10.3390/plants11233229
34. Sathasivam R, Ki J. A review of the biological activities of microalgal carotenoids and their potential use in healthcare and cosmetic industries. Marine Drugs. 2018;16(1):26. https://doi.org/10.3390/md16010026
35. Yue F, Zhang J, Xu J, Niu T, Lü X, *et al*. Effects of monosaccharide composition on quantitative analysis of total sugar content by phenol-sulfuric acid method. Frontiers in Nutrition. 2022;9:963318. http://doi.org/10.3389/fnut.2022.963318

ORCID IDs
Vyacheslav F. Dolganyuk https://orcid.org/0000-0003-0603-7456
Egor V. Kashirskikh https://orcid.org/0000-0003-0442-5471
Stanislav A. Sukhikh https://orcid.org/0000-0001-7910-8388
Elena V. Ulrikh https://orcid.org/0000-0003-4107-7277
Olga O. Babich https://orcid.org/0000-0002-4921-8997

Foods and Raw Materials. 2026;14(2)

ISSN 2308-4057 (Print)
ISSN 2310-9599 (Online)

Research Article
Open Access

Available online at http://jfrm.ru/en
https://doi.org/10.21603/2308-4057-2026-2-674
https://elibrary.ru/GJWJWQ

Hematological profile of wild boar *Sus scrofa* (Linnaeus 1758) (*Suina, Suidae*) in the Kirov Region, Russia

Maria A. Perevozchikova*, Igor A. Domsky, Alexey A. Sergeev, Alexander V. Economov, Mikhail A. Dolgikh, Alexander V. Dolgikh

Professor Zhitkov Russian Research Institute of Game Management and Fur Farming, Kirov, Russia

* e-mail: mperevozchikova@mail.ru

Received 17.12.2024; Revised 29.01.2025; Accepted 06.05.2025; Published online 21.08.2025

Abstract:
Physiological blood parameters help assess the health, feeding, immune, and reproductive status of wild animals. However, complicated sampling procedures make it difficult to establish the reference intervals for hematological parameters. Wild boar (*Sus scrofa*, Linnaeus 1758) is a popular game species. As a result, its population in Russia has been declining for the last decade. The wild boar is fertile and ecologically flexible; it responds well to biotechnical measures and have high population density. The research renders new data on the biology and physiology of wild boars.

The blood samples were obtained from 68 juvenile and adult wild boars in the Kirov Region in 2017–2023. The body weight varied from 30 to 211 kg. Blood from the jugular vein was collected into anticoagulant test tubes. The laboratory tests involved a veterinary version of a MicroCC-20 Plus automatic analyzer (High Technology, USA). The stained smears were examined using a MEIJI TECHNO light microscope (Japan) under an immersion system with a ×100 lens. The red blood cell parameters were measured using the Vision Bio software (Epi, Austria).

The research revealed the hematological profile of wild boars; the data were statistically processed, including, for the first time, the effect of sex and age on various hematological parameters. The significant differences ($p < 0.05$) between juvenile and adult females included the relative red cell distribution width by volume (standard deviation) and red blood cell thickness. The significant differences ($p < 0.05$) between juvenile and adult males were in hemoglobin, hematocrit, lymphocytes, and segmented neutrophils, as well as in such red blood cell parameters as total count, relative width by volume, area, perimeter, diameter, and sphericity index. The significant differences ($p < 0.05$) between juvenile females and males referred to hemoglobin and such parameters of red blood cells as total count, area, perimeter, and diameter. In adult males and females, it was the red blood cell thickness and platelet count. The research also yielded the lymphocytic profile of wild boar blood. The age affected such parameters as hematocrit ($p = 0.02$), segmented neutrophils ($p = 0.00$), and lymphocytes ($p = 0.00$). The body weight affected the hematocrit ($p = 0.02$) and mean red blood cell volume ($p = 0.04$).

The differences in *Sus scrofa* hematological profile depended on the physiological status, diet, minerals, age, sex, and stress. The reference intervals may help interpret the hematological profiles of other wild boar populations and optimize the game resource management.

Keywords: *Sus scrofa*, wild animals, hematology, blood cells, blood parameters, platelets, cell morphology

Funding: The research was carried out at the Professor Zhitkov Russian Research Institute of Game Management and Fur Farming, Kirov, Russia with the support of the Fundamental Scientific Research Program of the State Academies of Sciences FSZZ-2019-0001 (AAAA-A19-119020190132-5).

Please cite this article in press as: Perevozchikova MA, Domsky IA, Sergeev AA, Economov AV, Dolgikh MA, *et al.* Hematological profile of wild boar *Sus scrofa* (Linnaeus 1758) (*Suina, Suidae*) in the Kirov Region, Russia. Foods and Raw Materials. 2026;14(2):285–299. https://doi.org/10.21603/2308-4057-2026-2-674

INTRODUCTION

Hematological profile reveals the physiological status of mammals: its parameters characterize the exposure to infection, parasites, and ecotoxicants. Game managers and breeders use blood tests to determine the diet, immune, and reproductive status of the animals to take effective biotechnical, therapeutic, and preventive measures. Blood tests are especially important when other methods are unavailable [1–7]. Sampling becomes a very complex procedure in the wild, which makes it a serious limiting factor for ecological, veterinary, and biochemical studies [8–9]. Large, strong, dangerous, or nervous

Copyright © 2025, Perevozchikova *et al.* This is an open access article distributed under the terms of the Creative Commons Attribution 4.0 International License (https://creativecommons.org/licenses/by/4.0/), allowing third parties to copy and redistribute the material in any medium or format and to remix, transform, and build upon the material for any purpose, even commercially, provided the original work is properly cited and states its license.

animals are difficult to immobilize. In addition, drug administration and stress can affect the test results [10–12].

Establishing reference values for physiological parameters of wild animals are a difficult and expensive task. The strict standards for sampling make them time-consuming. Healthy animal physiology is affected by a number of factors, e.g., stress, food shortage, predators, injuries, diseases, anthropogenic triggers, migration, reproduction, etc. This list also includes procedures for capturing and handling [4]. Reference values for morphophysiological parameters have probably never been obtained for any biological species, including humans [13]. In this respect, the reference ranges we used in this research rely on the best approximation to the physiological norm and can be considered guidelines for interpretation.

The blood parameters for wild boars are rarely published in scientific journals [2, 4, 14–19]. As a rule, scientists focus on a limited sampling [14, 19], age group [2, 15], or parameter set. Since they usually pursue veterinary purposes [1–2], animals are anesthetized [4] and not classified by sex [1–2, 4, 10, 14–15]. The material obtained in this way has significant scientific value but cannot be considered representative.

Wild boar (*Sus scrofa*, Linnaeus 1758) is an important game species. In Russia, its population has halved since 2012 [20–22], mostly as a result of African swine fever [23].

The wild boar is a popular hunting object. Of all wild ungulates, wild boars are the most responsive to biotechnical measures. In addition, they are fertile, ecologically flexible, and have high population density. In semi-free conditions or an artificial habitat, veterinary care is necessary to prevent outbreaks that may be caused by the transfer of parasites or pathogens to native populations [2, 24–26]. On game farms, improper diet and poor reproduction management trigger metabolic changes that increase mortality as well as reduce fertility and life expectancy in the herd [27–28]. Unfortunately, metabolic changes are difficult to diagnose.

Hematological tests are the most informative ones in terms of physiological status and early diagnosis [29]. However, they are unpopular in nature management and conservation because the sampling complexity and wild habitat differences make their practical application particularly difficult.

Currently, the blood parameters of wild animals are taken mostly *postmortem* as venous blood from large vessels. This method provides high-quality samples in sufficient quantities. In wild boar studies, this method is simple, fast, reliable, clean, and human-safe.

Arenas-Montes *et al.* [3] offered an alternative sampling method. Based on dural venous system, it involved blood from intracavernous venipuncture from the cavernous sinus. This method is far from perfect because the delay between the death and the sampling may be several hours: blood tends to clot and becomes contaminated, which results in autolytic, cytotoxic, and/or hemolytic sera [30].

Blood parameter studies are important for wild boar breeding. This research provided an insight into the biology and physiology of wild boars, which made it possible to identify the reference values of hematological parameters in different age and sex groups in different environments.

STUDY OBJECTS AND METHODS

The study featured 68 wild boars shot in 2017–2023 by hunters issued with scientific collecting permits that authorized the lethal collection of wildlife. The animals lived on the scientific and experimental hunting grounds of the scientific and experimental hunting farm of the All-Russian Research Institute of Wildlife Management. The hunting grounds cover 66,250 ha in the Slobodskoy, Belaya Kholunitsa, and Zuevka districts of the Kirov Region, Russia (58.502270 N, 50.835894 E).

The animals were divided into those under 1 year of age (juveniles), which were even visually different from the adult animals (adults). The biomaterial was harvested during the hunting season, i.e., from October to December. The local climate is continental, with mild winters and warm summers. All wild boars moved freely within the hunting grounds. In addition to their natural diet, the boars received seasonal supplementary feeding, e.g., grain purchased from local farmers.

The blood obtained from these animals served as research material. The latest mandatory veterinary examination revealed no signs of disease, and all animals were considered clinically healthy.

The biomaterial was collected from the jugular vein (*v. jugularis*) into 4 mL UNIVAC vacuum tubes immediately after shooting. The tubes contained an anticoagulant, namely, dipotassium ethylenediaminetetraacetic acid (K2EDTA). The sampling, storage, and preparation followed Protocol no. 346n established by the Ministry of Health and Social Development, May 12, 2010 and adapted to wild animals [31]. Prior to laboratory tests, the tubes remained in a refrigerator at +4 °C.

The hematological studies were performed after 1–3 days using a veterinary version of a MicroCC-20 Plus automatic analyzer (High Technology, USA). The white blood cell count was obtained by the microscopy of blood smears stained with May-Grünwald's eosin methylene blue and Romanovsky's azure eosin (MiniMed-M-G, Russia).

The hematological profile consisted of the following parameters: total red blood cell count, hemoglobin concentration, hematocrit, mean corpuscular volume, mean corpuscular hemoglobin content, mean corpuscular hemoglobin concentration, red cell distribution width, red blood cell distribution width (standard deviation), platelet volume, platelet distribution width, plateletcrit, platelet count, large platelet count, total white blood cell, proportion of lymphocytes, monocytes, band neutrophils, segmented neutrophils, granulocyte eosinophils, and basophils. The morphological parameters of erythrocytes included area, perimeter, diameter, thickness, and global sphericity index.

The red blood cell sphericity index was calculated by the standard formula:

$$IRS = D / T = D / (V/S)$$

where D is the mean diameter, μm; T is the mean thickness, μm; V is the mean volume, fl; and S is the mean base area, μm.

The blood smears were air-dried and stained with May-Grünwald's eosin methylene blue and Romanovsky's azure eosin. Each stained smear was examined using a MEIJI TECHNO light microscope (Japan) under an immersion system with a ×100 objective. To determine the red blood cell parameters, we took 10–20 clear view fields with adequate morphology for each blood smear. The parameters were processed using the Vision Bio software (Epi, Austria). The total red blood cell pool more than 13,000.

The statistical analysis involved MS Excel (Office 2019) and Statgraphics (19-X64) with standard methods [32]. The hematological parameters were expressed as mean (M), error of the mean (m), standard deviation (SD), median (Me), 25 and 75% percentiles. Since the distribution of values in some cases differed from the standard, we used nonparametric Mann-Whitney U test and Kruskal-Wallis H tests to compare the parameters between groups.

The relationship between parameters was assessed by Spearman's correlation coefficient.

The one- and multifactorial analysis of variance (ANOWA-test) made it possible to assess the effect of age, sex, and weight on the hematological parameters. The effect was considered significant at $p < 0.05$.

RESULTS AND DISCUSSION

The body weight of wild boars varied from 30 to 211 kg. Young females tend to grow in weight faster than males, but eventually males become larger (Table 1).

Table 2 summarizes the red blood cell parameters in the wild boars under study.

We determined the area, perimeter, and diameter for 13,450 red blood cells. Table 3 shows their minimal and maximal values.

Table 4 shows the main parameters for 350 red blood cells, i.e., the mean values of area, perimeter, and diameter.

The red blood cell thickness and sphericity index were calculated for the blood samples that underwent a general blood test and had a smear taken (Table 5).

Table 6 describes the platelet indices, including the mean platelet volume, the relative platelet distribution width by volume, palatelcrit, platelet count, and large platelet content.

Table 7 gives the total count of white blood cells, as well as the share of lymphocytes, monocytes, band neutrophils, segmented neutrophils, eosinophils, granulocytes, and basophils.

The single- and multifactorial analysis of variance revealed the effect of such physiological factors as age, sex, and weight on the hematological profile. The age had a reliable effect on hematocrit ($p = 0.02$), segmental neutrophils ($p = 0.00$), and lymphocytes ($p = 0.00$). The weight affected such parameters as hematocrit ($p = 0.02$) and mean corpuscular volume ($p = 0.04$).

For hematological parameters, the reference intervals describe the dispersion of variables in animal blood samples and are true for 95% of all healthy individuals in the population [33]. However, healthy animals at different stages of ontogenesis may have variations in hematological parameter values even under stable conditions. This is true for most mammals, including humans. Accurate and adapted reference intervals provide the correct interpretation of blood tests from animals that lived in different parts of the habitat.

Reference intervals for hematological parameters in wild boars are difficult to determine because they depend on many factors associated with the high ecological plasticity of this species. These factors include age, season, habitat, diet, hunting, inheritance, pregnancy, lactation, etc. Available publications provide no stable reference values for hematological parameters in wild boars because they usually rely on small samplings and refer to different regions of the world.

To compensate for the lack of data, we compared our results with physiological values available both for wild boars and domestic pigs (Table 8).

Red blood cell parameters. Modern hematological analyzers show not only the red blood cell and platelet counts in peripheral blood, but also erythrocyte indices. Automatic calculation of red blood cell parameters provides more accurate information about hematological profile than manual counting.

We detected reliable differences ($p < 0.05$) between juvenile and adult animals for the following red blood cell parameters: cell count (males), hemoglobin (males), hematocrit (males), relative distribution width by volume (coefficient of variation, males), relative distribution width by volume (standard deviation, females), area (males), perimeter (males), diameter (males), thickness (females), and sphericity index (males) (Tables 2–6).

Both age groups demonstrated reliable sex differences: red blood cell count, hemoglobin, area, perimeter, and diameter in juveniles and thickness in adults.

Kukharenko *et al.* [14] studied the hematological profile of wild boars in the game reserves of the Amur Region, Russian Far East. The animals were classified by sex, not age. The blood tests revealed signs of anmia, i.e., low red blood cell count, hemoglobin, color index, and hematocrit. Moreover, they detected severe poikilocytosis, with a large proportion of spiky (23%) and indefinite shape (35.3%) red blood cells. As for the diameter, the red blood cells were represented by microcytes. Anemia, probably caused by bone marrow failure, reduces the population of Amur wild boars.

In this study, both adult and juvenile boars had higher values for red cell count: by 9.41 and 1.93%, respectively (Table 2). The concentration of hemoglobin was increased by 13.70% in the juvenile boars and by 28.78% in the adult boars. The hematocrit value was

Table 1 Body weight of wild boars from the Kirov Region, Russia

Parameter \ Group	Females		Males	
	Juveniles	Adults	Juveniles	Adults
n	13	9	21	25
M ± m	52.47 ± 5.54	105.00 ± 7.07	47.43 ± 11.35	127.50 ± 40.97
lim	42.50–60.00	100.00–110.00	30.00–64.50	80.00–211.00

Table 2 Erythrocyte parameters in juvenile and adult wild boars (n = 51)

Parameters \ Group	Females		Males	
	Juvenile (n = 8) M ± SD Me 25–75%	Adult (n = 9) M ± SD Me 25–75%	Juvenile (n = 14) M ± SD Me 25–75%	Adult (n = 20) M ± SD Me 25–75%
Red blood cells, 10^{12}/L	4.11–8.11 6.33 ± 1.31 [B] 6.13 5.77–7.12	4.44–7.16 5.61 ± 0.93 5.38 4.79–5.90	3.67–6.45 5.12 ± 0.86 [A, B] 5.30 4.37–5.59	3.67–9.40 6.18 ± 1.46 [A] 6.32 5.35–7.14
Hemoglobin, g/L	105.00–200.00 153.00 ± 30.18 151.50 [B] 137.75–162.75	109.00–169.00 133.33 ± 19.77 124.00 120.00–150.00	89.00–162.00 115.76 ± 22.28 115.00 [A, B] 96.00–132.00	89.00–210.00 147.10 ± 31.72 154.00 [A] 127.50–162.25
Hematocrit, %	26.70–44.40 37.02 ± 6.69 37.50 32.45–42.92	26.80–55.70 37.45 ± 9.52 39.80 28.50–42.60	20.00–46.30 33.00 ± 7.19 32.10 [A] 27.70–38.50	20.00–68.90 43.07 ± 12.01 42.95 [A] 34.95–52.10
Mean corpuscular volume, fl	48.20–74.30 60.36 ± 9.54 59.85 53.00–67.17	53.00–79.20 66.36 ± 9.35 67.80 58.30–72.60	49.70–73.60 64.25 ± 7.17 66.00 60.00–68.90	53.50–80.30 68.17 ± 7.12 70.35 63.27–73.42
Mean concentration hemoglobin, pg	22.60–25.50 24.07 ± 1.07 24.00 23.47–24.85	20.00–27.90 23.85 ± 2.89 23.60 22.20–26.10	16.60–31.00 22.78 ± 3.39 22.20 21.70–24.10	15.60–31.00 23.47 ± 3.74 24.15 21.70–25.27
Mean corpuscular hemoglobin concentration, g/L	341.00–471.00 406.00 ± 57.86 418.00 342.75–454.25	296.00–448.00 365.88 ± 54.52 352.00 342.00–382.00	241.00–495.00 359.23 ± 67.53 348.00 328.00–383.00	194.00–495.00 354.8 ± 74.93 368.00 320.50–387.75
Red blood cell distribution width (coefficient of variation), %	13.60–17.70 16.01 ± 1.59 16.25 15.12–17.30	12.40–17.80 15.12 ± 1.69 15.40 14.30–15.80	12.90–21.80 15.22 ± 2.24 14.50 [A] 14.00–15.60	12.90–20.50 16.22 ± 2.11 16.65 [A] 14.20–17.70
Red blood cell distribution width (standard deviation), fl	41.10–52.50 48.17 ± 3.59 47.80 [A] 47.30–50.40	39.20–50.60 44.41 ± 4.20 45.50 [A] 40.95–46.85	37.90–69.30 46.77 ± 9.00 45.50 41.65–47.22	38.70–54.70 45.43 ± 4.69 45.30 41.75–47.45

Reliable differences between juveniles and adults are marked with superscript A ($p < 0.05$); reliable differences between males and females are marked with superscript B ($p < 0.05$)

Table 3 Area, perimeter, and diameter of red blood cells in wild boars (n = 38): Minimal and maximal values

Group \ Parameters		min			max		
		Area, μm²	Perimeter, μm	Diameter, μm	Area, μm²	Perimeter, μm	Diameter, μm
Females	Juvenile	12.27–21.30	14.15–18.57	4.68–5.75	36.25–46.11	23.78–28.93	8.02–8.98
	Adult	17.38–21.65	16.29–18.56	5.27–5.95	42.19–45.55	26.47–28.72	8.43–9.45
Males	Juvenile	11.73–18.08	13.28–16.81	4.22–5.41	35.92–46.67	23.77–36.26	7.90–10.35
	Adult	16.97–22.34	16.15–19.21	5.08–5.89	37.20–46.64	26.14–28.98	8.44–9.51

Table 4 Area, perimeter, and diameter of red blood cells in wild boars (n = 38)

Parameters \ Group	Females		Males	
	Juvenile (n = 10) M ± SD Me 25–75%	Adult (n = 4) M ± SD Me 25–75%	Juvenile (n = 16) M ± SD Me 25–75%	Adult (n = 8) M ± SD Me 25–75%
Area, μm²	21.96–31.18 28.36 ± 2.76 29.13 [B] 27.36–30.29	26.95–33.11 29.67 ± 2.56 29.31 28.49–30.48	20.80–30.78 26.59 ± 2.37 26.42 [A, B] 25.77–27.32	27.80–32.63 29.19 ± 1.67 28.79 [A] 27.92–29.44
Perimeter, μm	18.51–22.92 21.41 ± 1.29 21.52 [B] 20.90–22.33	20.57–22.89 21.61 ± 0.95 21.50 21.26–21.85	18.21–22.12 20.56 ± 0.94 20.38 [A, B] 20.20–20.96	20.72–23.38 21.67 ± 0.89 21.46 [A] 20.98–22.08
Diameter, μm	6.03–7.13 6.77 ± 0.34 6.82 [B] 6.66–7.04	6.58–7.24 6.83 ± 0.28 6.76 6.71–6.88	5.77–6.95 6.51 ± 0.28 6.49 [A, B] 6.35–6.65	6.55–7.30 6.81 ± 0.24 6.80 [A] 6.62–6.87

Reliable differences between juveniles and adults are marked with superscript A ($p < 0.05$); reliable differences between males and females are marked with superscript B ($p < 0.05$)

Table 5 Thickness and sphericity index of red blood cells in wild boars (n = 21)

Parameters \ Group	Females		Males	
	Juvenile (n = 5) M ± SD Me 25–75%	Adult (n = 3) M ± SD Me 25–75%	Juvenile (n = 8) M ± SD Me 25–75%	Adult (n = 5) M ± SD Me 25–75%
Thickness, μm	1.74–3.02 2.33 ± 0.56 2.54 [A] 1.75–2.61	1.76–2.93 2.38 ± 0.59 2.45 [A, B] 2.10–2.69	2.16–2.86 2.56 ± 0.24 2.53 2.43–2.79	2.04–2.63 2.30 ± 0.23 2.25 [B] 2.15–2.42
Sphericity index	1.99–4.06 3.05 ± 0.94 2.61 2.54–4.05	2.23–4.11 3.03 ± 0.96 2.76 2.50–3.43	2.22–2.96 2.50 ± 0.25 2.45 [A] 2.32–2.60	2.48–3.41 3.02 ± 0.39 3.03 [A] 2.79–3.38

Reliable differences between juveniles and adults are marked with superscript A ($p < 0.05$); reliable differences between males and females are marked with superscript B ($p < 0.05$)

Table 6 Platelet parameters in juvenile and adult wild boars (n = 51)

Parameters \ Group	Females		Males	
	Juvenile females (n = 8) M ± SD Me 25%–75%	Adult females (n = 9) M ± SD Me 25%–75%	Juvenile males (n = 14) M ± SD Me 25%–75%	Adult males (n = 20) M ± SD Me 25%–75%
Platelets, 10^9/L	71.00–321.00 206.87 ± 97.95 227.50 124.00–291.00	37.00–174.00 116.55 ± 41.47 129.00 [B] 108.00–141.00	89.00–450.00 159.85 ± 93.21 138.50 103.25–174.50	65.00–436.00 198.55 ± 96.98 181.00 [B] 156.75–225.75
Plateletcrit, %	0.04–0.79 0.23 ± 0.24 0.15 0.08–0.26	0.02–0.17 0.10 ± 0.04 0.10 [B] 0.09–0.11	0.06–0.35 0.12 ± 0.07 0.10 0.07–0.12	0.05-0.46 0.18 ± 0.11 0.16 [B] 0.11–0.20
Mean platelet volume, fl	6.90–9.80 8.07 ± 1.03 8.05 7.15–8.70	3.40–10.60 7.91 ± 2.09 8.30 6.90–8.70	6.50–9.80 7.61 ± 0.91 7.50 7.02–8.02	5.90–72.10 10.89 ± 14.43 7.70 7.05–8.62
Platelet distribution width, %	3.20–22.80 13.00 ± 6.45 11.10 9.77–16.92	9.90–22.80 15.08 ± 4.74 13.90 11.00–18.30	3.40–23.20 13.11 ± 6.40 11.95 10.40–18.10	2.70–23.90 15.82 ± 5.51 16.80 14.00–18.82
Platelet large cell ratio, %	8.50–42.20 25.71 ± 13.20 23.4 16.10–36.90	13.30–55.70 35.50 ± 15.76 36.6 25.45–45.95	5.50–50.20 20.43 ± 14.59 14.3 11.20–28.80	10.20–44.30 21.97 ± 11.25 18.25 14.60–27.65

Reliable differences between males and females are marked with superscript B ($p < 0.05$)

Table 7 While blood cell parameters in juvenile and adult wild boars (n = 68)

Parameters \ Group	Females		Males	
	Juvenile (n = 13) M ± SD Me 25–75%	Adult (n = 9) M ± SD Me 25–75%	Juvenile (n = 21) M ± SD Me 25–75%	Adult (n = 25) M ± SD Me 25–75%
White blood cells, 10^9/L	4.00–7.40 5.51 ± 1.23 5.30 4.50–6.47	3.30–9.00 5.85 ± 2.24 5.50 4.20–8.10	1.20–15.30 6.98 ± 4.52 5.40 4.30–10.60	1.60–14.20 6.71 ± 3.30 5.60 4.42–9.10
Lymphocytes, %	28.00–93.00 75.54 ± 19.05 83.00 71.00–85.50	34.00–88.00 63.40 ± 26.36 71.00 37.00–87.00	62.00–95.00 82.93 ± 9.40 83.50 [A] 75.00–91.00	49.00–96.00 70.50 ± 10.96 68.50 [A] 63.75–76.00
Monocytes, %	0–4.00 1.54 ± 1.50 1.00 0–3.00	0–8.00 2.00 ± 3.39 1.00 0–1.00	0–3.00 0.81 ± 0.91 1.00 0–1.00	0–3.00 0.95 ± 1.04 1.00 0–2.00
Band neutrophils, %	0–2.00 0.72 ± 1.00 0 0–2.00	0–2.00 1.00 ± 1.00 1.00 0–2.00	0–4.00 1.31 ± 1.25 1.00 0–2.00	0–6.00 1.33 ± 1.71 1.00 0–2.00
Segmental neutrophils, %	2.00–66.00 17.27 ± 18.64 9.00 6.50–21.50	4.00–57.00 29.60 ± 24.96 22.00 10.00–55.00	2.00–28.00 10.75 ± 7.63 7.50 [A] 5.00–16.25	2.00–39.00 21.70 ± 9.42 23.00 [A] 15.50–28.25
Eosinophils, %	1.00–10.00 4.72 ± 2.57 4.00 3.50–5.50	0–8.00 3.60 ± 2.96 4.00 2.00–4.00	0–11.00 4.00 ± 2.68 4.00 2.00–5.00	0–16.00 5.37±4.16 5.00 2.75–6.25
Basophils, %	0–1.00 0.18 ± 0.40 0 0–0	0–1.00 0.40 ± 0.54 0 0–1.00	0–1.00 0.12 ± 0.34 0 0–0	0–2.00 0.20 ± 0.50 0 0–0

Reliable differences between juveniles and adults are marked with superscript A ($p < 0.05$)

Table 8 Hematological parameters in wild boars and domestic pigs across the world

M ± SD (min–max)		Species	Region	Reference
Juveniles	Adults			
Red blood cells, 10^{12}/L				
5.60 ± 0.00	5.30 ± 0.42	Wild boars	Amur Region, Russia	Kukharenko *et al*. [14]
6.40 ± 0.96	–	Wild boars	Iberian Peninsula, Spain, France	López-Olvera *et al.* [2]
–	8.00 ± 0.68 (6.87–9.03)	Wild boars	Croatia	Harapin *et al.* [15]
6.70 ± 1.38	6.02 ± 0.76	Feral pigs	Texas, USA	Shender *et al.* [1]
5.80 ± 0.35	5.60 ± 0.22	Domestic pigs	Amur Region, Russia	Kukharenko *et al.* [34]
♀ 5.70 ± 0.38 ♂ 7.90 ± 0.57	♀ 7.80 ± 0.99 ♂ 6.10 ± 1.20	Danish Landrace pigs	Amur Region, Russia	Semenova *et al.* [35]
5.71–8.47	♀ 5.46–7.20 ♂ 7.12–11.83	Large White pigs	European Russa	Gimadeeva *et al.* [36]
6.38 ± 0.93 (4.38–8.54)	–	Yorkshire pigs	Massachusetts, USA	Dimitrakakis *et al.* [37]
Hemoglobin, g/L				
115.00 ± 0.60	99.00 ± 5.00	Wild boars	Amur Region, Russia	Kukharenko *et al.* [14]
–	156.60 ± 17.32 (123.00–183.00)	Wild boars	Croatia	Harapin *et al.* [15]
126.87 ± 15.16 (101.00–172.00)	140.29 ± 13.24 (109.00–157.00)	Wild boars	Spain	Casas-Diaz *et al.* [4]
118.50 ± 21.6	120.30 ± 1.25	Feral pigs	Texas, USA	Shender *et al.* [1]

Continuation of Table 8

M ± SD (min–max)		Species	Region	Reference
Juveniles	Adults			
Hemoglobin, g/L				
92.00 ± 4.70	90.00 ± 5.40	Domestic pigs	Amur Region, Russia	Kukharenko *et al.* [34]
♀ 119.10 ± 9.77 ♂ 121.70 ± 3.00	♀ 122.80 ± 6.47 ♂ 118.30 ± 3.98	Danish Landrace pigs	Amur Region, Russia	Semenova *et al.* [36]
105.60–137.70	♀ 107.70–134.70 ♂ 106.40–162.30	Large White pigs	European Russia	Gimadeeva *et al.* [36]
	♀ 95.20–135.10	Domestic pigs	Chili	Baeza *et al*. [27]
99.90 ± 144.00 (80.00–140.00)	–	Yorkshire pigs	Massachusetts, USA	Dimitrakakis *et al*. [37]
Hematocrit, %				
36.40 ± 0.78	36.40 ± 1.72	Wild boars	Amur Region, Russia	Kukharenko *et al.* [14]
44.00 ± 6.00	–	Wild boars	Iberian Peninsula, Spain, France	López-Olvera *et al*. [2]
–	60.98 ± 4.20 (55.40–69.40)	Wild boars	Croatia	Harapin *et al*. [15]
36.00 ± 4.00 (30.00–51.00)	38.00 ± 3.00 (31.00–45.00)	Wild boars	Spain	Casas-Diaz *et al*. [4]
37.38 ± 6.85	37.86 ± 3.85	Feral pigs	Texas, USA	Shender *et al*. [1]
36.70 ± 1.74	36.90 ± 2.47	Domestic pigs	Amur Region, Russia	Kukharenko *et al.* [34]
42.67–57.00	♀ 41.55–49.94 ♂ 49.60–78.70	Large White pigs	European Russia	Gimadeeva *et al.* [36]
–	♀ 30.30–40.90	Domestic pigs	Chile	Baeza *et al*. [27]
34.47 ± 4.78 (25.25–47.00)	–	Yorkshire pigs	Massachusetts, USA	Dimitrakakis *et al*. [37]
Mean corpuscular volume, fl				
–	77.50 ± 5.13 (70.00–86.00)	Wild boars	Croatia	Harapin *et al.* [15]
Mean concentration hemoglobin, pg				
19.52 ± 0.58 (18.80–20.60)	21.13 ± 1.32 (18.10–22.90)	Wild boars	Spain	Casas-Diaz *et al.* [4]
13.64–18.62	♀ 17.91–20.68 ♂ 13.21–17.60	Large White pigs	European Russia	Gimadeeva *et al.* [36]
Mean corpuscular hemoglobin concentration, g/L				
347.10±11.80 (322.00–370.00)	355.00 ± 9.40 (339.00–376.00)	Wild boars	Spain	Casas-Diaz *et al.* [4]
Diameter, μm				
5.30 ± 0.60	7.20 ± 0.50	Wild boars	Amur Region, Russia	Kukharenko *et al.* [14]
Platelets, 10^9/L				
–	289.20–917.20	Domestic pigs	Chile	Baeza *et al.* [27]
359.00 ± 87.85 (180.00–559.00)	–	Yorkshire pigs	Massachusetts, USA	Dimitrakakis *et al.* [37]
White blood cells, 10^9/L				
21.50 ± 1.40	25.80 ± 1.90	Wild boars	Amur Region, Russia	Kukharenko *et al.* [14]
6.90 ± 2.94	–	Wild boars	Iberian Peninsula, Spain, France	López-Olvera *et al.* [2]
–	9.79 ± 4.27 (6.00–20.35)	Wild boars	Croatia	Harapin *et al.* [15]
22.10 ± 0.38	18.60 ± 0.54	Domestic pigs	Amur Region, Russia	Kukharenko *et al.* [34]
♀ 12.30 ± 2.25 ♂ 10.00 ± 0.57	♀ 10.90 ± 1.71 ♂ 7.90 ± 1.69	Danish Landrace pigs	Amur Region, Russia	Semenova *et al.* [35]
6.58–38.69	♀ 11.64–17.47 ♂ 5.46–24.78	Large White pigs	European Russia	Gimadeeva *et al.* [36]
–	♀ 11.06–19.64	Domestic pigs	Chile	Baeza *et al.* [27]
16.17 ± 3.33 (10.94–22.14)	–	Yorkshire pigs	Massachusetts, USA	Dimitrakakis *et al.* [37]
Band neutrophils, %				
8.50 ± 0.02	11.30 ± 1.60	Wild boars	Amur Region, Russia	Kukharenko *et al.* [14]
5.20 ± 0.02	4.00 ± 0.05	Domestic pigs	Amur Region, Russia	Kukharenko *et al.* [34]

End of Table 8

M ± SD (min–max)		Species	Region	Reference
Juveniles	Adults			
Segmental neutrophils, %				
29.00 ± 1.20	28.70 ± 3.80	Wild boars	Amur Region, Russia	Kukharenko *et al.* [14]
36.40 ± 1.21	33.20 ± 2.24	Domestic pigs	Amur Region, Russia	Kukharenko *et al.* [34]
–	43.50–76.20	Domestic pigs	Chile	Baeza *et al.* [27]
Monocytes, %				
6.50 ± 0.01	4.00 ± 0.60	Wild boars	Amur Region, Russia	Kukharenko *et al.* [14]
4.80 ± 0.23	4.20 ± 1.47	Domestic pigs	Amur Region, Russia	Kukharenko *et al.* [34]
–	1.40–7.60	Domestic pigs	Chile	Baeza *et al.* [27]
Lymphocytes, %				
52.00 ± 0.95	52.2 ± 4.60	Wild boars	Amur Region, Russia	Kukharenko *et al.* [14]
61.30 ± 1.56	55.90 ± 2.81	Domestic pigs	Amur Region, Russia	Kukharenko *et al.* [34]
	15.80–47.00	Domestic pigs	Chile	Baeza *et al*. [27]
Eosinophils, %				
4.00 ± 0.01	3.00 ± 0.10	Wild boars	Amur Region, Russia	Kukharenko *et al.* [14]
1.25 ± 0.04	1.40 ± 0.54	Domestic pigs	Amur Region, Russia	Kukharenko *et al.* [34]
	♀ 0–11.20	Domestic pigs	Chile	Baeza *et al*. [27]
Basophils, %				
0	0.70 ± 0.02	Wild boars	Amur Region, Russia	Kukharenko *et al.* [14]
0	0.50 ± 0.02	Domestic pigs	Amur Region, Russia	Kukharenko *et al.* [34]

lower by 4.51% in the juveniles and higher by 12.02% in the adults. The diameter of red cells was increased by 20.19% in the juveniles and reduced by 5.84% in the adults (Tables 3 and 4).

A comparative analysis of hematological parameters in the domestic pigs (*Sus scrofa domesticus*, Linnaeus, 1758) from the Amur Region [34] yielded similar results. However, the hemoglobin value in the Amur pigs (30.96%) was lower than in the wild boars from the Kirov Region (35.26%). The hematocrit in the juvenile Amur pigs was by 5.29% higher than in this study while in the adult pigs it was by 10.81% lower. The red cell diameter was by 20.19% smaller in the juveniles and by 5.84% larger in the adults.

The Iberian juvenile wild boars had higher red cell count (10.79%) and hematocrit content (21.00%) than in our research [2]. The Croatian adult boars demonstrated higher red cell count (26.88%), hemoglobin (11.24%), hematocrit (32.16%), and mean corpuscular volume (10.88%) [15].

The Texan feral pigs had higher red cell count: by 14.78% in the juveniles and 2.78% in the adults. The hemoglobin was by 11.07 and 13.46% lower in the juveniles than in the adults, respectively. The hematocrit was by 7.01% higher in the juveniles and by 8.49% lower in the adults [1].

The Spanish juvenile wild boars [2] demonstrated lower hemoglobin (by 4.70%) while the adults showed similar results to ours. The hematocrit was higher by 3.45% in the juveniles and by 8.15% lower in the adults. The mean content hemoglobin was lower by 12.94% in the juveniles and 10.70% in the adults. The hemoglobin concentration in red blood cells was also lower than in our studies: by 9.26% lower in the juveniles and 1.39% in the adults. The Spanish research did not classify the animals by sex. The boars were anesthetized with a combination of tiletamine-zolazepam (6 mg/kg) and xylazine (3 mg/kg).

The differences in hematological parameters could be associated with the habitat, e.g., the absolute geographic altitude (Fig. 1).

The Amur valley is about 250 m above sea level [14]. The Sant Llorenç del Munt i L'Obac Natural Park in the Northeast of Spain is 400–1,140 m above sea level. The Croatian hunting grounds of Sisak-Moslavina is over 500 m above sea level. The Texan feral pigs lived in the southeast of the state, 200 m above sea level. In our research, the wild boars lived at absolute altitudes of 160–200 m.

Adaptation to different altitudes, i.e. to the amount of oxygen available, causes anatomical, physiological, and biochemical changes [38]. High altitudes affect the oxygen transport system. At high altitudes, the partial pressure of oxygen in the air is insufficient to saturate the blood. As a result, the total capacity of the oxygen transporting system increases. Hemoglobin's lower affinity for oxygen requires an increase in the total amount of circulating hemoglobin. The regulatory effect of 2,3-diphosphoglycerate is enhanced to facilitate the release of oxygen by hemoglobin in tissues.

Behavioral and physiological adaptation pathways include the following mechanisms. Low muscle activity reduces the need for oxygen; increased heart rate and breathing raise the amount of oxygen delivered to tissues. However, these mechanisms are no longer necessary when adaptive shifts occur at the molecular level. The first change is an increase in the red blood cell count. It increases the ability of hemoglobin to carry oxygen to tissues as the concentration of 2,3-diphosphoglycerate in red blood cells grows [38].

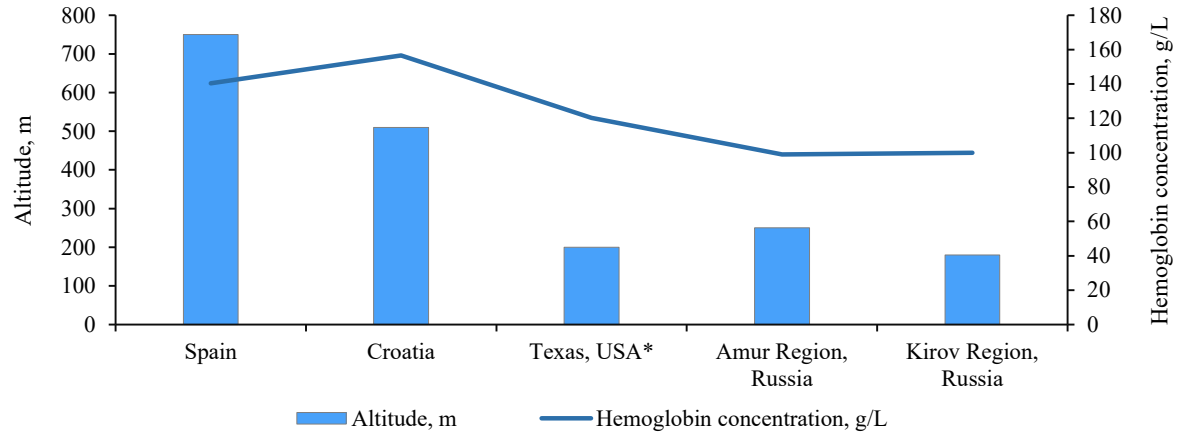

Figure 1 Mean hemoglobin concentration vs. habitat altitude based on our data and [1, 4, 14, 15]: Wild boars and Texan feral pigs*

A comprehensive comparative hematological analysis should take into account the difference in climatic conditions. The blood parameters in Table 8 were obtained from animals that inhabited different climatic zones, from the Mediterranean climate of the Iberian Peninsula, Spain, and Croatia to the oceanic climate of Massachusetts, USA, and the extremely continental climate of Russia's forest zone.

The hematology of domestic pigs depends on the low motor activity in farm stalls, dreary diet, population density stress, and regular veterinary and zootechnical measures. Yet, given the lack of information on the hematology of wild boars, domestic pigs remain a valuable source.

Juvenile domestic Landrace pigs from the Altai Region, Russia [35], demonstrated a higher red blood cell count in juvenile males (by 32.92%) and adult females (by 32.95%). Compared to the wild boars from the Kirov Region, Altai juvenile females and adult males had lower red blood cell counts (by 7.02% and 3.49%, respectively). As for hemoglobin, it was by 21.39, 6.36, and 23.19% lower in the juvenile females, adult females, and adult males, respectively. The data for young males, however, were similar to ours.

According to Semenova *et al.* [35], an age-related decrease in the hemoglobin level by 5.9–6.0% is a common feature shared by all pigs. At the age of 4–6 months, the hemoglobin level and red blood cell count in males are higher by 2.2–2.4 and 18.6–38.6%, respectively. At 8 months, the difference in red blood cell count between female wild boars and domestic pigs drops down to 1.6%. Pregnant sows have a slightly higher hemoglobin level (by 7.5%) because of increased metabolism.

The young Large White domestic pigs of both sexes and the adult females and males [35] from European Russia demonstrated much higher values of red blood cell count and hematocrit than those obtained in this study. On the other hand, the hemoglobin concentrations and mean hemoglobin content were lower.

Gimadeeva *et al.* [36] reported higher red blood cell counts, hemoglobin concentration, and hematocrit in adult males than in other age and sex groups. In the breeding boars, the red blood cell content was by 33.6, 21.4, and 20.9% higher in the barren sows, sows in recent pregnancy, and sows in late pregnancy, respectively. The pregnant sows had a 10.1–10.5% higher red blood cell content than the barren sows. The mean hemoglobin content per erythrocyte decreased by 6.8–7.6% while the hematocrit increased by 5.3–7.6%.

The lowest red blood cell count (3.43×10^{12}/L), hemoglobin (24.86 g/L), and hematocrit (8.71%) belonged to the suck-ling piglets. In terms of hemoglobin per erythrocyte, the suckling piglets exceeded other animals by 8.66–29.78%. The oxidation and reduction processes during active growth require a lot of red cells, white cells, hemoglobin, hematocrit, lymphocytes, monocytes, and granulocytes.

In the juvenile Yorkshire pigs from Massachusetts, USA [37], anesthetized with intramuscular injections of atropine (0.04 mg/kg), tiletamine-zolazepam (4.4 mg/kg), and xialzine (2.2 mg/kg), the red blood cell count was by 10.51% higher in our research while the hematocrit concentration was the same. The total hemoglobin concentration in the adult female domestic pigs from Chile [27] was lower than that in the wild boars from the Kirov Region whereas the hematocrit values were within similar ranges.

Baeza *et al.* [27] reported a decrease in hematocrit in older sows ($p = 0.00$). The underweight sows had lower hematocrit and hemoglobin levels ($p = 0.02$) than those with standard weight. The high hematocrit in the youngest sows could be caused by the increased bone marrow activity during growth [39]. Young animals might be more susceptible to stress, which triggers polycythemia [40, 41].

Other researchers [42, 43] see physiological anemia with a decrease in red blood cells, hemoglobin, hematocrit, and white blood cells as typical of young animals. The increased red blood cell count, erythrocyte mass, and hemoglobin in males compared to females are associated with erythropoietin and testosterone, especially during the mating season [44, 45]. The hematocrit fluctuations may depend on water consumption, intestinal disorders, etc. [44].

The adult wild boars from northeastern Spain demonstrated higher mean hemoglobin content, hema-

tocrit, and hemoglobin concentration in red blood cells than the juveniles [7], as was the case with the wild boars from the Kirov Region.

In Harapin *et al.* [15], the hematocrit and mean corpuscular volume in wild boars exceeded the upper limits for domestic pigs. Wild boars need more oxygen as they are more physically active [16]. When hunted, they experience tress and increased oxygen demand: the spleen contracts and raises the hematocrit level, as well as the total red cell count and hemoglobin. The same phenomenon is typical of canines [46].

For instance, the wild boars with helminthiasis demonstrated significant changes in blood parameters [47]. Poor diet also affects hematological parameters. The wild boars that lost a lot of weight had low hemoglobin and hematocrit concentration, especially during the late stages of starvation [48].

The fat content in bone marrow correlated with the concentrations of hemoglobin, hematocrit, albumin, total globulin, gamma globulin, alkaline phosphatase, and urea in the blood of 26 young boars [49]. This correlation was probably associated with the level of fat reserves and the efficiency of their use.

Platelet parameters. Hematological analyzers define platelet count in peripheral blood and such parameters as relative platelet distribution width by volume, mean platelet volume, and large platelet ratio vs. total platelets.

Automatic calculations provide reliable information on platelet count and their morphological properties [50–52]. Low mean platelet volumes and relative distribution width by volume indicate the predominance of microplatelets in the total platelet count, i.e., inhibited thrombopoiesis, while their growth indicates increased thrombopoiesis. The index of large platelet content indicates the rate of platelet formation in the bone marrow [53–58].

We found no publications on platelet count and their parameters in wild boars. We determined reliable sex differences ($p < 0.05$) in platelet count in adult wild boars (Table 6).

In the domestic pigs, the platelet count was 2–4 times as high as in the boars from the Kirov Region [27, 36]. The sows with insufficient body weight demonstrated below-standard platelet indices [27].

In humans, a drop in platelet count in the peripheral blood or changes in their morphology occur as a result of severe diseases, after surgery with complications, etc. [50].

Leukocyte parameters. We obtained new data for a comprehensive assessment of cellular immunity in wild boars (Table 7). Their lymphocytes were of average size, with a low share of small and large forms. In some juvenile females, the lymphocyte content exceeded 90%. Segmented neutrophils had polysegmented nuclei and poor granularity.

The males demonstrated reliable age differences ($p < 0.05$) in the percentage of lymphocytes and segmented neutrophils. Both juveniles and adults had fewer neutrophils than lymphocytes. The adults had more band and segmented neutrophils than the juveniles, which was consistent with other reports [10, 15].

Eosinophils contain a lot of small granules. Wild animals have more eosinophils than domestic ones [33] because eosinophils counteract parasitic infection. In this research, wild boars had ≥ 20% eosinophils.

The white blood cell count in the Kirov wild boars was at the bottom of the value ranges reported for boars from elsewhere [1–2, 10, 13, 15] and domestic pigs [27, 33, 35–36, 59]. In addition to environmental factors, the differences may be associated with the methods for determining the while blood cell count or the stress that the animals experienced during sampling.

The correlation between the white blood cell indicators, sex, and age was detected in domestic pigs [35, 41]. In the adult males, the leukocyte content in the peripheral blood was by 12–29% higher in females.

In the pre-weaning piglets, the white blood cell count was the lowest. Their body was protected mainly by the antibodies that they received with milk. As they grew and turned to adult diet, the count of blood cells that protected the body from pathogens increased. During this period, they had more leukocytes and lymphocytes than adults, but the count decreased with age [36].

Old females have a lot of lymphocytes, eosinophils, and monocytes [27]. During labor, sows develop neutrophilia and lymphopenia as a result of cortisol increase [59]. Lymphocytes and segmented neutrophils grow in number during early pregnancy, which is typical of other species [56–57, 60–61]. Probably, this phenomenon is connected with lower immune function of maternal cells, suppression of specific immune functions, and a compensatory increase in non-specific immunity [62–63]. Different ranges of eosinophils in farm pigs may be explained by different ventilation conditions because ammonia irritates the respiratory system [40].

Stress reactions. Physical restraint, transportation, chase, and trapping induce a biphasic pattern typical of stress reactions. The biochemistry of stress is described in [59]. Acute stress caused by physical struggle, restraint, or injury may cause significant changes in a number of hematological parameters [64]. Piglets demonstrate increased lymphocyte counts under stress [65]; stress affects the immune response in domestic pigs [1, 66]. Some publications report the effect of anesthetics during live capture on total blood counts in several wild animal species [4, 13, 67–70].

Baeza *et al.* [27] described young animals as more susceptible to stress: it makes the spleen contract, causing relative polycythemia [40]. This hypothesis is supported by the white blood cell count, which is higher in juveniles and may indicate a stress-induced change in the leukogram [39, 59].

Cortisol affects blood cells, reduces lymph flow, and increases segmented neutrophils and total while blood cell counts [71]. In this regard, leukogram stress is more neutrophilic than lymphophilic and is associated with increased hematocrit [59].

Stress during sampling is the largest source of hematological changes in pigs: it develops within minutes and affects the leukogram [4, 59]. In lactating animals, the

increase in segmented neutrophils may be explained by their role in eliminating pathogens in mammary glands by phagocytosis [72].

We obtained most blood samples from wild boars ambushed and killed at feeding sites, which eliminated the stress associated with fright and pursuit induced by other hunting methods.

Diseases and parasites. Parasites also affect hematological parameters; in case of wild boars, this issue remains understudied.

These studies [46, 73] indicated a possible connection between parasites and blood parameters in wild boars. In particular, *Metastrongylus* nematodes in the lungs cause metostrongillosis, which then affects hemoglobin concentration.

Statistically significant differences were established for white blood cells, triglycerides, lactic acid, creatinine, urea, aspartate aminotransferase, and lactate dehydrogenase in helminth-infected (*Ascaris* sp., *Physocephalus sexalatus*, *Ascarops strongylina*) and healthy boars [2]. Another study [1] revealed no changes in hematological parameters of feral pigs with helminths. However, the results may be caused by the differences in sampling methods. Some animals were shot while others were trapped and subjected to severe stress during capture and transportation.

The parasite-induced hematological and biochemical changes in blood serum are probably related to different nutrient absorption, physical activity, and immune response. Bacteremia may affect hematological parameters, in particular, *Borrelia* spirochetes in the blood. These spirochetes are quite common in wild boars and feral pigs, but this issue requires further study [74–77].

The hematology of wild boar depends on habitat, diet, age, and sex. Proteolytic enzymes of neutrophils are important for protein digestion while lipolytic enzymes of lymphocytes are important for fat digestion. In wild animals, the blood composition depends on the season [78]. In Spanish red deer (*Cervus elaphus*) [79], the seasonal hematological fluctuations in erythrocytes, white blood cells, and platelets could be connected with body weight, body growth, antler development, and reproductive cycle. A sudden weather change is stressful because it might complicate foraging process. As a result, lymphocytes enter peripheral blood. Red blood cell parameters increase in autumn rather than in spring as animals prepare for winter.

This paper describes the initial data on the hematology of wild boars from the Kirov Region, Russia. Comparative studies should take into account other limiting factors, e.g., different hematological analyzers, diagnostic methods, habitats, etc. [80]. Moreover, a gap of $\geq$ 72 h between sampling and analysis reduces the data for platelets, white blood cells, lymphocytes, monocytes, and basophils [81]. Their decrease explains the hematocrit growth.

Our results should be interpreted based on these factors. In our research, the morphological parameters depended on sex and age. The resulting clinical profile may help interpret other hematological profiles.

Our data demonstrate an urgent need for further comprehensive research of the hemogram parameters in wild boars.

CONCLUSION

Hemogram reference intervals expand our knowledge in the field of wildlife biology. In this study, we established the hematological profile for the wild boars (*Sus scrofa*, Linnaeus 1758) of different age and sex living in the Kirov Region, Russia. The research revealed reliable differences ($p < 0.05$) between the young and adult females in relative erythrocyte distribution width by volume (standard deviation) and red blood cell thickness. For the juvenile and adult boars, the reliable differences ($p < 0.05$) included the red blood count, hemoglobin, hematocrit, relative red cell distribution width by volume (variation coefficient), erythrocyte area, erythrocyte perimeter, erythrocyte diameter, erythrocyte sphericity index, lymphocyte, and segmented neutrophils. As for the juvenile females and males, the reliable differences ($p < 0.05$) included the red blood cell count and hemoglobin, as well as the area, perimeter, and diameter of red blood cells. In the adult males and females, the difference was in the thickness of red blood cells and platelet count. We also determined the lymphocytic profile.

The single- and multifactorial analysis of variance revealed the effect of age, sex, and weight on the hematological profile. The age affected hematocrit ($p = 0.02$), segmented neutrophils ($p = 0.00$), and lymphocytes ($p = 0.00$). The weight affected hematocrit ($p = 0.02$) and mean corpuscular volume ($p = 0.04$).

The comparative analysis with other domestic and foreign studies revealed certain features typical of wild boars from the Kirov Region, Russia. The variability of blood indicators depended on the living conditions, diet, age, and sex, as well as on the laboratory equipment.

The reference intervals identified in this research may help interpret hematological profiles of other wild boar populations to optimize the game resource management.

CONTRIBUTION

All the authors contributed equally to the study and bear equal responsibility for information published in this article. We also acknowledge the vital participation of A.V. Dolgikh in field research, collection and processing of scientific materials, and dedicate this article to his memory.

CONFLICT OF INTEREST

The authors declared no conflict of interest regarding the publication of this article.

ACKNOWLEDGEMENTS

The authors express their gratitude to the hunters of the Russian Research Institute of Game Management and Fur Farming for their help in sampling for assisting with data collection.

REFERENCES

1. Shender LA, Botzler RG, George TL. Analysis of serum and whole blood values in relation to helminth and ectoparasite infections of feral pigs in Texas. Journal of Wildlife Diseases. 2002;38:385–394. https://doi.org/10.7589/0090-3558-38.2.385
2. López-Olvera JR, Höfle U, Vicente J, Fernández-de-Mera IG, Gortázar C. Effects of parasitic helminths and ivermectin treatment on clinical parameters in the European wild boar (*Sus scrofa*). Parasitology Research. 2006;98:582–587. https://doi.org/10.1007/s00436-005-0099-2
3. Arenas-Montes A, García-Bocanegra I, Paniagua J, Franco JJ, Miró F, *et al*. Blood sampling by puncture in the cavernous sinus from hunted wild boar. European Journal of Wildlife Research. 2013;59:299–303. https://doi.org/10.1007/s10344-013-0701-3
4. Casas-Díaz E, Closa-Sebastià F, Marco I, Lavín S, Bach-Raich E, *et al*. Hematologic and biochemical reference intervals for wild boar (*Sus scrofa*) captured by cage trap. Veterinary Clinical Pathology. 2015;44(2):215–222. https://doi.org/10.1111/vcp.12250
5. Maceda-Veiga A, Figuerola J, Martínez-Silvestre A, Viscor G, Ferrari N, *et al*. Inside the redbox: Applications of haematology in wildlife monitoring and ecosystem health assessment. Science of The Total Environment. 2015;514:322–332. https://doi.org/10.1016/j.scitotenv.2015.02.004
6. Didkowska A, Klich D, Anusz K, Wojciechowska M, Kloch M, *et al*. Determination of hematological and biochemical values blood parameters for European bison (*Bison bonasus*). Plos One. 2024;19(5):e0303457. https://doi.org/10.1371/journal.pone.0303457
7. Perevozchikova MA, Domsky IA, Sergeyev AA. Hematological parameters of free-ranging moose *Alces alces* (Linnaeus 1758) (*Ruminantia, Cervidae*). Foods and Raw Materials. 2024;12(1):80–90. https://doi.org/10.21603/2308-4057-2024-1-592
8. Geffré A, Friedrichs K, Harr K, Concordet D, Trumel C, *et al*. Reference values: A review. Veterinary Clinical Pathology. 2009;38(3):288–298. https://doi.org/10.1111/j.1939-165X.2009.00179.x
9. General information. In: OIE Terrestrial Manual editor. Collection and shipment of diagnostic specimens. Chapter 1.1.1. Paris: OIE; 2008. 14 p.
10. Morelli J, Rossi S, Fuchs B, Richard E, Barros DSB, *et al*. Evaluation of three medetomidine-based anesthetic protocols in free-ranging wild boars (*Sus scrofa*). Frontiers in Veterinary Science 2021;(8):655345. https://doi.org/10.3389/fvets.2021.655345
11. Casas-Díaz E, Marco I, López-Olvera JR, Mentaberre G, Lavín S. Comparison of xylazine–ketamine and medetomidine–ketamine anaesthesia in the Iberian ibex (*Capra pyrenaica*). European Journal of Wildlife Research. 2011;57:887–893. https://doi.org/10.1007/s10344-011-0500-7
12. Perevozchikova MA, Domskiy IA, Sergeev AA, Berezina YuA, Bespyatykh OYu, *et al*. A study of post-mortem hematological parameters of arctic foxes, *Vulpes Lagopus* (Linnaeus, 1758). Transactions of the Karelian Research Centre RAS. 2023;(7):83–96. (In Russ.) https://elibrary.ru/MRLDYD
13. Tryland M. 'Normal' serum chemistry values in wild animals. Veterinary Record. 2006;158(6):211–212. https://doi.org/10.1136/vr.158.6.211-b
14. Kukharenko NS, Kukharenko AA, Kovalchuk IV. Anemia as the reason for wild boar livestock reduction in the Amur region. Bulliten KrasSAU. 2011;(10):177–180. (In Russ.) https://elibrary.ru/OIGGUP
15. Harapin I, Bedrica L, Hahn V, Šoštarić B, Gračner D. Haematological and biochemical values in blood of wild boar (*Sus scrofa ferus*). Veterinarski Arhiv. 2003;73(6):333–343.
16. Tušek T, Mihelić D, Firšt L, Janicki Z, Opančar D. A comparative survey of the red blood count in the boar and native European pig. Veterinarska Stanica. 1994;25(2):81–84.
17. Vidal D, Naranjo V, Mateo R, Gortazar C, de la Fuente J. Analysis of serum biochemical parameters in relation to *Mycobacterium bovis* infection of European wild boars (*Sus scrofa*) in Spain. European Journal of Wildlife Research. 2006;52:301–304. https://doi.org/10.1007/s10344-006-0062-2
18. Vitic J, Tosic L, Stevanovic J. Comparative studies of the serum lipoproteins and lipids in domestic swine and wild boar. Acta Veterinaria. 1994;44:49–56.
19. Barasona JA, López-Olvera JR, Beltrán-Beck B, Gortázar C, Vicente J. Trap-effectiveness and response to tiletamine-zolazepam and medetomidine anaesthesia in Eurasian wild boar captured with cage and corral traps. BMC Veterinary Research. 2013;(9):107. https://doi.org/10.1186/1746-6148-9-107
20. Danilkin AA. Trends of wild ungulate population dynamics in Russia. Biology Bulletin. 2019;46(10):1368–1373. https://doi.org/10.1134/S106235901910008X

21. Ekonomov AV, Kolesnikov VV, Dolinin VV, Sergeev AA. Wild boar (*Sus scrofa* L., 1758) resources in the range of the amur tiger (*Panthera tigris* L., 1758) in the far east of the Russian Federation Far Eastern Agricultural Journal. 2022;16(2)2:98–107. (In Russ.) https://doi.org/10.22450/19996837_2022_2_98
22. Domskiy IA, Sergeyev AA, Ekonomov AV, Kolesnikov VV, Makarov VV, Tselykhova EK. Current status of the wild boar population in Russia in relation to the spread of African swine fever. Contributions to hunting and game research. 2020;(45):33–46. (In German.) https://elibrary.ru/CJSUCK
23. Makarov VV, Domsky IA, Sergeev AA. To the problem of the «boar-African swine pest» Vestnik of the Russian agricultural science. 2020;(6):58–62. (In Russ.) https://doi.org/10.30850/vrsn/2020/6/58-62
24. Vicente J, Segalés J, Höfle U, Balasch M, Plana-Durán J, *et al*. Epidemiological study on porcine circovirus type 2 (PCV2) infection in the European wild boar (*Sus scrofa*). Veterinary Research. 2004;35(2):243–253. https://doi.org/10.1051/VETRES:2004008
25. Fernandez-de-Mera IG, Gortazar C, Vicente J, Höfle U, Fierro Y. Wild boar helminths: Risks in animal translocations. Veterinary Parasitology. 2003;115(4):335–341. https://doi.org/10.1016/s0304-4017(03)00211-5
26. Höfle U, Vicente J, Nagore D, Hurtado A, Peña A, *et al*. The risks of translocating wildlife: Pathogenic infection with *Theileria* sp. and *Elaeophora elaphi* in an imported red deer. Veterinary Parasitology. 2004;126:387–395. https://doi.org/10.1016/j.vetpar.2004.07.026
27. Baeza C, Gädicke P, Ruiz A. Determination of new hematologic reference intervals for sows with optimal reproductive performance, according to reproductive stage, parity and body condition: A cohort study. Preprint (Version 1) available at Research Square. 2021:1–16. https://doi.org/10.21203/rs.3.rs-317100/v1
28. Žvorc Z, Mrljak V, Sušić V, Pompe Gotal J. Haematological and biochemical parameters during pregnancy and lactation in sows. Veterinarski arhiv. 2006;76(3):245–253.
29. Perri AM, O'Sullivan TL, Harding JCS, Wood RD, Friendship RM. Hematology and biochemistry reference intervals for Ontario commercial nursing pigs close to the time of weaning. Canadian Journal of Veterinary Research. 2017;58(4):371–376.
30. Boadella M, Gortazar C. Effect of haemolysis and repeated freeze-thawing cycles on wild boar serum antibody testing by ELISA. BMC Research Notes. 2011;4:498. https://doi.org/10.1186/1756-0500-4-498
31. Koshurnikova MA, Domskiy IA. Sample collection, storage and laboratory analysis of biological material derived from hunter harvested wild animals. Transactions of the Karelian Research Centre of the Russian Academy of Sciences. 2022;(7):75–84. (In Russ.) https://elibrary.ru/DFYMXW
32. Ivanter EV, Korosov AV. Elementary biometrics. In: Obarchuk OV, editor. Petrozavodsk: Petrozavodsk State University, 2005. 104 p.
33. Friedrichs KR, Harr KE, Freeman KP, Szladovits B, Walton RM, *et al*. ASVCP reference interval guidelines: Determination of de novo reference intervals in veterinary species and other related topics. Veterinary Clinical Pathology. 2012;41(4):441–453. https://doi.org/10.1111/vcp.12006
34. Kukharenko NS, Kukharenko AA, Kovalchuk IV. Comparative analysis of hematological parameters of wild boars and pigs in Amur region. Actual Questions of Veterinary Biology. 2011;(3):7–10. (In Russ.) https://elibrary.ru/OBEXKH
35. Semenova ID, Rudishin OYu, Burtseva SV, Klemin VP. Hematologic indices of various age-sex groups of pigs of newly bred landrace breed type. Bulletin of Altai State Agricultural University. 2013;10:90–92. (In Russ.) https://elibrary.ru/RDKETL
36. Gimadeeva LS, Gusev IV, Ryzhkov VA, Rykov RA. Comparative assessment of hematological profile of pigs of different technological groups. Bulletin of Orenburg State Agrarian University. 2015;(5):148–151. (In Russ.) https://elibrary.ru/UZBYIL
37. Dimitrakakis N, Waterhouse A, Lightbown S, Leslie DC, Jiang A, *et al*. Biochemical and hematologic reference intervals for anesthetized, female, juvenile Yorkshire swine. Journal of the American Association for Laboratory Animal Science. 2022;61(1):21–30. https://doi.org/10.30802/AALAS-JAALAS-21-000014
38. Giraud-Billoud M, Rivera-Ingraham GA, Moreira DC, Burmester T, Castro-Vazquez A, *et al*. Twenty years of the 'Preparation for Oxidative Stress' (POS) theory: Ecophysiological advantages and molecular strategies. Comparative Biochemistry and Physiology Part A: Molecular & Integrative Physiology. 2019:234. https://doi.org/10.1016/j.cbpa.2019.04.004
39. Estienne MJ, ClarkDeener SG, Williams KA. Growth performance and hematology characteristics in pigs treated with iron at weaning as influenced by nursery diets supplemented with copper. Journal of Swine Health and Production. 2020;28(4):190–203. https://doi.org/10.54846/jshap/1165
40. Stockham SL, Scott MA. Fundamentals of veterinary clinical pathology. Hoboken, NJ: John Wiley & Sons, 2013. 928 p.

41. Zhang S, Yu B, Liu Q, Zhang Y, Zhu M, *et al*. Assessment of hematologic and biochemical parameters for healthy commercial pigs in china. Animals. 2022;12(18):2464. https://doi.org/10.3390/ani12182464

42. Moyseenko NA. Components of red blood in young moose. Alces. 2002;(2):93–97.

43. Taylor JA, Feldman BF, Zinki JG, Jain NC. Leukocyte responses in ruminants. Schalm's veterinary hematology. Baltimore, Maryland: Lippincott Williams & Wilkins; 2000. p. 391–393.

44. Revsbech IG, Fago A. Regulation of blood oxygen transport in hibernating mammals. Journal of Comparative Physiology B. 2017;187:847–856. https://doi.org/10.1007/s00360-017-1085-6

45. Lee S, Lee SC, Jeon Y. Analysis of blood composition by porcine breeding cycle. Veterinary Medicine and Science. 2024;10(2):e31376. https://doi.org/10.1002/vms3.1376

46. Erjavec V, Vovk T, Nemec Svete A. The effect of two acute bouts of exercise on oxidative stress, hematological, and biochemical parameters, and rectal temperature in trained canicross dogs. Frontiers in Veterinary Science. 2022;2:767482. https://doi.org/10.3389/fvets.2022.767482

47. López-Olvera JR, Höfle U, Vicente J, Fernández-de-Mera IG, Gortázar C. Effects of parasitic helminths and ivermectin treatment on clinical parameters in the European wild boar (*Sus scrofa*). Parasitology Research. 2006;98:582–587. https://doi.org/10.1007/s00436-005-0099-2

48. Wolkers J, Wensing T, Groot Bruinderink GWTA, Schonewille JT. The effect of undernutrition on haematological and serum biochemical variables in wild boar (*Sus scrofa*). Comparative Biochemistry and Physiology. 1994; 108(2–3):431–437. https://doi.org/10.1016/0300-9629(94)90115-5

49. Wolkers J, Wensing T, Groot Bruinderink GW, Schonewille AT. Comparative nutrition papers: Nutritional status of wild boar (*Sus scrofa*): II. Body fat reserves in relation to haematology and blood chemistry. Comparative Biochemistry and Physiology Part A: Physiology. 1993;105(3):539–542. https://doi.org/10.1016/0300-9629(93)90431-3

50. Petrova OV, Shashin SA, Tarasov DG. Significance of platelet indices determination in patients after coronary artery bypass grafting. Russian Journal of Cardiology and Cardiovascular Surgery. 2014;7(3):58–62. (In Russ.) https://elibrary.ru/SUCVCB

51. Balakrishnan A, Shetty A, Vijaya C. Estimation of platelet counts: Auto analyzer versus counts from peripheral blood smear based on traditional and platelet: Red blood cell ratio method. Tropical Journal of Pathology and Microbiology. 2018;4(5):389–395. https://doi.org/10.17511/jopm.2018.i05.04

52. Mabood A, Chaturvedi V, Gupta S, Alam MQ, Dwivedi N, *et al*. Thrombocyte estimation based on blood smear and its comparison using automated haematology analysers. Journal of Evolution of Medical and Dental Sciences. 2019;8(19):1588–1591. https://doi.org/10.14260/jemds/2019/351

53. Dolgov VV, Svirin PV. Laboratory diagnostics of hemostasis disorders. Moscow–Tver: Triada, 2005. 227 p. (In Russ.)

54. Momot AP. Pathology of hemostasis. Principles and algorithms of clinical and laboratory diagnostics. St. Petersburg: FormaT; 2006. 208 p. (In Russ.)

55. Mininkova AI. A review of analytical capabilities of hematological analyzers in platelet assessment. Clinical Laboratory Diagnostics. 2012;(3):27–34. (In Russ.) https://www.elibrary.ru/PFHMRN

56. Puchinskaya MV, Pochtovtsev AYu. Clinical significance of platelet indices in cardiology. Military Medicine. 2011;(2):77–81. (In Russ.) https://www.elibrary.ru/RQDYIL

57. Brækkan SK, Mathiesen EB, Njølstad I, Wilsgaard T, Størmer J, *et al*. Mean platelet volume is a risk factor for venous thromboembolism: The Tromsø study. Journal of Thrombosis and Haemostasis. 2010;8(1):157–162. https://doi.org/10.1111/j.1538-7836.2009.03498.x

58. Buttarello M, Plebani M. Automated blood cell counts: State of the art. American Journal of Clinical Pathology. 2008;130(1):104–116. https://doi.org/10.1309/ek3c7ctdknvpxvtn

59. Thorn CE. Hematology of the pig. In: Weiss DJ, Wardrop KJ, Schalm OW, editors. Schalm's Veterinary Hematology. Wiley Blackwell, 2010. pp. 843–851.

60. Bazzano M, Giannetto C, Fazio F, Rizzo M, Giudice E, *et al*. Physiological adjustments of haematological profile during the last trimester of pregnancy and the early post-partum period in mares. Animal Reproduction Science. 2014;149(3–4):199–203. https://doi.org/10.1016/j.anireprosci.2014.07.005

61. Bakrim S, Motiaa Y, Ouarour A, Masrar A. Hematological parameters of the blood count in a healthy population of pregnant women in the Northwest of Morocco (Tetouan-M'diq-Fnideq provinces). Pan African Medical Journal. 2018;29:205. https://doi.org/10.11604/pamj.2018.29.205.13043

62. Bhattarai S, Framstad T, Nielsen JP. Stillbirths in relation to sow hematological parameters at farrowing: A cohort study. Journal of Swine Health and Production. 2018;26(4):215–222. https://doi.org/10.54846/jshap/1052

63. Ježek J, Starič J, Nemec M, Plut J, Golinar Oven I, *et al*. The influence of age, farm, and physiological status on pig hematological profiles. Journal of Swine Health and Production. 2018;26(2):72–78. https://doi.org/10.54846/jshap/1049

64. Martínez-Miró S, Tecles F, Ramón M, Escribano D, Hernández F, *et al*. Causes, consequences and biomarkers of stress in swine: An update. BMC Veterinary Research. 2016;12:171. https://doi.org/10.1186/s12917-016-0791-8
65. Zhang S, Yu B, Liu Q, Zhang Y, Zhu M, *et al*. Assessment of hematologic and biochemical parameters for healthy commercial pigs in China. Animals. 2022;12(18):2464. https://doi.org/10.3390/ani12182464
66. Perri AM, O'Sullivan TL, Harding JCS, Wood RD, Friendship RM. Hematology and biochemistry reference intervals for Ontario commercial nursing pigs close to the time of weaning. The Canadian Veterinary Journal. 2017;58(4): 371–376.
67. Alves MH, Kluyber D, Alves AC, Yogui DR, Pereira FMAM, *et al*. Hematology and biochemistry reference intervals in chemically immobilized free-ranging giant anteaters (*Myrmecophaga tridactyla*). European Journal of Wildlife Research. 2023;69:37. https://doi.org/10.1007/s10344-023-01663-5
68. Zeiler GE, Meyer LCR. Chemical capture of impala (*Aepyceros melampus*): A review of factors contributing to morbidity and mortality. Veterinary Anaesthesia and Analgesia. 2017;44(5):991–1006. https://doi.org/10.1016/j.vaa.2017.04.005
69. Barić R, Rafaj R, Tončić J, Vicković I, Šoštarić B. Haematological and biochemical values of farmed red deer (*Cervus elaphus*). Veterinarski arhiv. 2011;81(4):513–523.
70. Miller AL, Evans AL, Os Ø, Arnemo JM. Biochemical and hematologic reference values for free-ranging, chemically immobilized wild Norwegian reindeer (*Rangifer Tarandus Tarandus*) during early winter. Journal of Wildlife Diseases. 2013;49(2):221–228. https://doi.org/10.7589/2012-04-115
71. Harvey JW, Pate MG, Kivipelto J, Asquith RL. Clinical biochemistry of pregnant and nursing mares. Veterinary Clinical Pathology. 2005;34(3):248–254. https://doi.org/10.1111/j.1939-165x.2005.tb00049.x
72. Czech A, Grela ER. Biochemical and haematological blood parameters of sows during pregnancy and lactation fed the diet with different source and activity of phytase. Animal Feed Science and Technology. 2004;116(3–4):211–223. https://doi.org/10.1016/j.anifeedsci.2004.07.013
73. Wolkers J, Wensing Th, Groot Bruinderink GWTA, Schonewille JTh. Lungworm and stomach worm infection in relation to body fat reserves and blood composition in wild boar (*Sus scrofa*). Veterinary Quarterly. 1994;16(4):193–195. https://doi.org/10.1080/01652176.1994.9694446
74. Juřicová Z, Hubálek Z. Serologic survey of the wild boar (*Sus scrofa*) for *Borrelia Burgdorferi* sensu lato. Vector-Borne and Zoonotic Diseases. 2009;9(5):479–482. https://doi.org/10.1089/vbz.2008.0125
75. Faria AS, Paiva-Cardoso MDN, Nunes M, Carreira T, Vale-Gonçalves HM, *et al*. First detection of *Borrelia burgdorferi* sensu lato DNA in serum of the wild boar (*Sus scrofa*) in northern Portugal by Nested-PCR. EcoHealth. 2015;12: 183–187. https://doi.org/10.1007/s10393-014-0973-4
76. Mays Maestas SE, Campbell LP, Milleson MP, Reeves LE, Kaufman PE, *et al*. Ticks and tick-borne pathogens from wild pigs in northern and central Florida. 2023;14(7):612. https://doi.org/10.3390/insects14070612
77. Perevozchikova MA, Domsky IA, Berezina YuA, Sergeev AA. Blood biochemical parameters in reservoir hosts under ixodid tick-borne borreliosis. Agricultural Biology. 2023;58(4):757–772. (In Russ.) https://doi.org/10.15389/agrobiology.2023.4.757rus
78. Karpiński M, Czyżowski P, Beeger S, Flis M. Hematological and serum biochemical values of free-ranging roe deer (*Capreolus capreolus*) in Poland. Animals. 2023;13(2):242. https://doi.org/10.3390/ani13020242
79. Gaspar-López E, Landete-Castillejos T, Estevez JA, Ceacero F, Gallego L, *et al*. Seasonal variations in red deer (*Cervus elaphus*) hematology related to antler growth and biometrics measurements. Journal of Experimental Zoology. 2011;315A(4):242–249. https://doi.org/10.1002/jez.670
80. Kazakova MS, Lugovskaya SA, Dolgov VV. The reference values of indicators of total blood analysis of adult working population. Clinical Laboratory Diagnostics. 2012;(6):43–49. (In Russ.) https://elibrary.ru/PFHTLR
81. Bleul U, Bleul U, Sobiraj A, Bostedt H. Effects of duration of storage and storage temperature on cell counts of bovine blood samples as determined by an automated haematology analyser. Comparative Clinical Pathology. 2002;11: 211–216. https://doi.org/10.1007/s005800200021

ORCID IDs
Maria A. Perevozchikova https://orcid.org/0000-0003-3638-3712
Igor A. Domsky https://orcid.org/0000-0003-1633-1341
Alexey A. Sergeev https://orcid.org/0000-0002-9461-5131
Alexander V. Economov https://orcid.org/0000-0002-0242-8954
Mikhail A. Dolgikh https://orcid.org/0009-0004-2573-5721

Foods and Raw Materials. 2026;14(2)

ISSN 2308-4057 (Print)
ISSN 2310-9599 (Online)

Research Article
Open Access

Available online at http://jfrm.ru/en
https://doi.org/10.21603/2308-4057-2026-2-676
https://elibrary.ru/BNUUXB

Synergistic anti-glycation and antioxidant interaction among different mushroom extract combinations

Kimberly Weng Kuan Tan[1], Phaik Har Yong[2], Zhi Xiang Ng[1,*]

[1] University of Nottingham Malaysia, Semenyih, Selangor, Malaysia
[2] MAHSA University, Jenjarom, Selangor, Malaysia

* e-mail: zhixiang.ng@nottingham.edu.my

Receive 20.09.2024; Revised 11.11.2024; Accepted 06.05.2025; Puplished online 21.08.2025

Abstract:
Although the nutrient compositions of edible mushrooms are well-studied, the effect of combining different mushrooms on their anti-glycation and antioxidant activities remains unknown. This study therefore aimed to identify mushroom combinations that exhibit synergistic anti-glycation and antioxidant activities.

Five edible mushroom species, namely *Agaricus bisporus*, *Lentinula edodes*, *Pleurotus ostreatus*, *Pleurotus eryngii*, and *Flammulina velutipes*, were evaluated both individually and in pairwise combinations. Their bioactive profile (phenolics, tannins, flavonoids, and polysaccharides), as well as antioxidant and anti-glycation activities were analyzed to determine the types of activity interaction: synergism, addition, or antagonism.

A. bisporus (7.5 mg/mL) showed the highest reducing capacity and tannin content. *L. edodes* demonstrated the strongest radical scavenging potential, while *F. velutipes* displayed the highest anti-glycation activity and phenolic content. Despite its high polysaccharide level, *P. eryngii* showed low antioxidant activity. Pairwise combinations revealed synergistic anti-glycation and antioxidant effects at low sample concentrations, while antagonistic anti-glycation and antioxidant effects were observed at high sample concentrations. The mushrooms' polyphenols, tannins, and flavonoids were positively correlated with their antioxidant activity (r = 0.325 to 0.825, $p < 0.05$). However, they showed an inverse relationship (r = –0.349 to –0.644, $p < 0.05$) with polysaccharides and anti-glycation activity. The principal component analysis revealed that the types of bioactive content and mushroom combinations contributed to respective 53 and 23% of total activity variances.

The best-performing mushroom combinations with synergistic anti-glycation and antioxidant activities were the mixtures of 7.5 mg/mL *A. bisporus* + 15 mg/mL *F. velutipes*, 7.5 mg/mL *L. edodes* + 7.5 mg/mL *F. velutipes*, and 7.5 mg/mL L. edodes + 15 mg/mL *F. velutipes*.

Keywords: Flavonoid, fungi, phytochemical, phenolic, polysaccharide, tannin

Funding: This study was supported by the Malaysian Allied Health Sciences Academy [RP202-04/23].

Please cite this article in press as: Tan KWK, Yong PH, Ng ZX. Synergistic anti-glycation and antioxidant interaction among different mushroom extract combinations. Foods and Raw Materials. 2026;14(2):300–320. https://doi.org/10.21603/2308-4057-2026-2-676

INTRODUCTION

Oxidation is an essential process in biological systems that facilitates the production of energy [1]. However, numerous reactive nitrogen species and reactive oxygen species are generated as by-products during the oxidation process [1]. The formation of excessive reactive radicals is further accelerated by the production of advanced glycation end-products (AGEs) under pathological conditions. AGEs are a chemically heterogenous group of compounds, including crossline, pentosidine (Pent), Nε-(carboxymethyl)lysine (CML), and pyrroline [2]. Various reactive radicals, such as hydrogen peroxide, hydroxyl, and superoxide anion, as well as AGEs, interact with biological systems in a cytotoxic manner [2]. This leads to cell death and other degenerative processes associated with ageing [3]. Excessive deposition of AGEs and free radicals in a human body is a catalyst for a multitude of detrimental diseases such as cancer, atherosclerosis, diabetes, neurological disorders, and cardiovascular diseases [4]. However, a significant proportion of these chronic diseases could be prevented with the use of antioxidants [5] and AGE inhibitors [2].

Copyright © 2025, Tan *et al.* This is an open access article distributed under the terms of the Creative Commons Attribution 4.0 International License (https://creativecommons.org/licenses/by/4.0/), allowing third parties to copy and redistribute the material in any medium or format and to remix, transform, and build upon the material for any purpose, even commercially, provided the original work is properly cited and states its license.

Foods with a natural abundance of antioxidants and AGE inhibitors hold the potential to mitigate the detrimental effects of oxidative damage [2, 5]. These exogenous antioxidants and AGE inhibitors effectively hinder the generation of AGEs by scavenging free radicals produced during glycation, while inhibiting advanced oxidation protein products [2]. Epidemiological studies have revealed a strong positive association between plant-based foods and a decreased risk of chronic illnesses [6]. Bioactive constituents within food can lower the risk of chronic diseases and thus improve human well-being by reducing blood cholesterol or neutralizing reactive species, as well as through anti-carcinogenic, anti-hypertensive, or anti-glycemic responses [7]. Food scientists are increasingly exploring natural sources that are rich in bioactive compounds and have antioxidant and anti-glycation effects. These compounds contribute to lesser adverse side effects and a minimized likelihood of developing resistance to them [8].

In recent years, the incorporation of mushrooms as dietary supplements has garnered considerable attention within the realm of food nutrition [7]. Mushrooms have been consumed by humans since ancient times due to their ideal nutritional compositions, appealing sensory characteristics, and amenable cultivate conditions [7]. They have been recognized for their crucial role in mitigating and preventing an array of health complications [7, 9, 10]. Mushrooms are rich in bioactive compounds such as flavonoids, lycopene, phenolic acids, ascorbic acid, tocopherols, carboxylic acids, β-carotene, and various dietary fibers [11]. Based on their intended applications, mushroom species can be classified into edible and medicinal categories [7]. Despite the growing interest in medicinal varieties, edible cultivated species such as *Lentinula edodes* and *Agariscus bisporus* continue to dominate the market [7]. *Lentinula edodes* (shiitake), *Agaricus bisporus* (button mushroom), *Pleurotus ostreatus* (grey oyster), *Flammulina velutipes* (golden needle), and *Pleurotus eryngii* (king oyster) represent some of the most prominent commercially cultivated mushrooms [12]. Among the major types of edible mushrooms, shiitake leads in production volume, followed by oyster mushroom (*Pleurotus* spp.) and button mushroom [13]. According to numerous studies, these mushroom species display various bioactivities, including anti-mutagenic, antioxidant, anti-tumor, anti-dementia, hypoglycemic, acetylcholinesterase-inhibitory, anti-microbial, and anti-inflammatory potentials [14–17].

Phytochemical extracts derived from plant-based foods have been reported to exhibit potent anti-proliferative and antioxidant activities. Antioxidant activity is significantly due to the interaction of phytochemicals, leading to synergistic, additive, or antagonistic effects [18]. This may explain why isolated antioxidants cannot supplant combinations of natural phytochemicals in foods and replicate their health advantages [9]. The interaction among phytochemicals, such as flavonoids, within a given plant extract can substantially contribute to human health by alleviating disease-related cellular damage, as the bioactive compounds involved rarely function independently [18]. Wang *et al.* [18] defined an additive effect as a food combination that yields the cumulative impact of individual components. A synergistic effect arises when the outcome surpasses the sum of individual components, whereas antagonism takes place when the combined effect is less than the anticipated mathematical sum of individual components. Although multiple studies have reported that many plant-based foods possessed numerous bioactive compounds with functional activities [19, 20], only few have investigated the synergism related to the use of fungi species. For instance, Wang *et al.* [18] did not observe any synergistic effect when *A. bisporus* was combined with other fruits, vegetables, and legumes. However, Mallard *et al.* [21] showed that a combination of β-glucans from *Lentinula edodes*, *Grifola frondosa*, and *Ganoderma lucidum* exhibited a synergistic immunomodulatory effect in human macrophages.

To the best of our knowledge, there has been no research into the effects of *L. edodes*, *A. bisporus*, *F. velutipes*, *P. eryngii,* and *P. ostreatus* combinations on antioxidant and anti-glycation activities. Assessing synergistic effect is a challenging endeavor, since various available bioassays are based on distinct chemical mechanisms [18]. Given the diversity of phytochemical classes and types of mushrooms, a multitude of bioassays are required to assess their overall antioxidant and anti-glycation capacity [15]. The sensitivity and specificity of a singular method cannot ensure a comprehensive evaluation of all dietary bioactive compounds. Therefore, a combination of multiple tests can be a more precise indicator of antioxidant and anti-glycation activities [18].

In this study, we aimed to explore the effects of *L. edodes*, *A. bisporus*, *F. velutipes*, *P. eryngii,* and *P. ostreatus* combinations. For this, we adopted seven distinct bioassays, namely ferric reducing antioxidant power, total flavonoid content, total tannins, total phenolic content, 2,2-diphenyl-1-picrylhydrazyl radical scavenging capacity, AGE inhibition analysis, and polysaccharide assays. These assays were employed to discern the types of interactions between the phytochemicals, antioxidant and anti-glycation activities in the selected mushroom species, as well as to identify the best mushroom combinations that yield synergistic antioxidant and anti-glycation effects.

STUDY OBJECTS AND METHODS

Chemicals. All the reagents used in this study were of analytical grade. Iron(III) chloride hexahydrate, 2,2-diphenyl-1-picrylhydrazyl, sodium azide, iron(II) sulphate heptahydrate, 3,4,5-trihydroxybenzoic acid (gallic acid), sodium acetate, bovine serum albumin, sodium carbonate, 2-(3,4-dihydroxyphenyl)-3,5,7-trihydroxy-4H-1-benzopyran-4-one (quercetin), 2,4,6-tripyridyl-s-triazine, trichloroacetic acid, Folin-Ciocalteu's reagent, tannic acid, D-glucose, phenol, and starch were obtained from Sigma-Aldrich (USA). Aminoguanidine hydrochloride was sourced from Tokyo Chemical Industry

(Japan). Potassium acetate ($C_2H_3KO_2$), aluminum chloride ($AlCl_3$), and polyvinylpolypyrrolidone were purchased from Thermo Fisher-Scientific (USA). Absolute ethanol, glacial acetic acid, hydrochloric acid, methanol, and concentrated sulphuric acid were obtained from Merck (Germany). L-ascorbic acid was purchased from HmbG Chemicals (Germany).

Equipment. The assays were performed on the following equipment: a hot air oven (Memmert GmbH & Co. KG, Germany), a vortex mixer (IKA-Werke GmbH & Co. KG, Germany), an Alpha 1-2 LSC basic laboratory freeze dryer (Germany), an Epoch microplate spectrophotometer (Biotek Instrument Inc., USA), a centrifuge (Eppendorf AG, Germany), an electrical blender (Philips, Netherlands), a hotplate (Harmony, Japan), a water bath (Memmert GmbH & Co. KG, Germany), and a digital analytical balance (Sartorius Corporate Administration GmbH, Germany).

Sample collection. Five fresh commercial cultivated mushrooms, namely *Agaricus bisporus, Flammulina velutipes, Lentinula edodes, Pleutorus eryngii,* and *Pleurotus ostreatus,* were purchased from a local grocery store in Selangor, Malaysia. Mushroom samples with complete fruiting bodies (gills, caps, stipe, and tubes) in various sizes were randomly selected from the store's shelves. Prior to processing, all the samples were washed with distilled water and dried.

Sample processing. The mushroom samples were extracted according to Midoh *et al.* [22] with slight modifications. Briefly, clean mushrooms were blended with 80°C distilled water in a solid-to-solvent ratio of 1:5 for 15 min. The extract was subsequently filtered using cheesecloth, and the filtrates were centrifuged at 16,000 × g for 10 min at room temperature. The collected supernatant was further filtered through Whatman filter paper, and the remaining filtrates were frozen before being subjected to a 72-hour freeze-drying process. The resulting lyophilized powders were stored in airtight containers at –20°C until analysis. For experimental analysis, lyophilized powders of an individual mushroom were reconstituted in 1 mL of distilled water to achieve concentrations of 7.5, 15.0, and 30.0 mg/mL for *A. bisporus, F. velutipes,* and *L. edodes,* and 25.0, 50.0, and 100.0 mg/mL for *P. eryngii* and *P. ostreatus*. These sample concentrations were determined based on a previous pilot study finding (unpublished data). The mushroom extracts were then combined in pairs at a 1:1 (v/v) ratio to produce 90 distinct combinations (Table 2) to evaluate their antioxidant and anti-glycation interactions.

Water content. The water content in the selected mushroom samples was determined according to Li *et al*. [23]. Each mushroom sample (100 g) was cut into smaller pieces and spread in a single layer on trays in triplicates. The samples were dried in a hot air oven at 50 ± 2°C until constant weight was obtained. To monitor water loss, the sample trays were removed from the hot air oven every 12 h and weighed using a digital analytical balance. The water content, %, was calculated with the following formula:

$$\text{Water content} = \frac{W_0 - W_1}{W_0} \times 100 \quad (1)$$

where W_0 is the fresh weight of mushroom sample, g; W_1 is the dry weight of mushroom sample, g.

Extraction yield. The extraction yield, %, of each mushroom sample was determined according to Tepsongkroh *et al*. [24] via the following formula:

$$\text{Yield} = \frac{W_3}{W_0} \times 100 \quad (2)$$

where W_3 is the weight of lyophilized sample powder.

Antioxidant activities. ***Ferric-reducing antioxidant power.*** A sample's ferricreducing antioxidant power (FRAP) was measured based on Ranneh *et al.* [25]. Briefly, the FRAP reagent consisted of 300 mM acetate buffer (pH 3.6), 10 mM 2,4,6-tripyridyl-s-triazine, and 20 mM iron(III) chloride hexahydrate in a 10:1:1 (v/v/v) ratio. Following the addition of the FRAP reagent to the mushroom sample, the sample's absorbance was measured at 593 nm after 4 min of incubation at room temperature. The FRAP values were expressed as millimole ferrous ion equivalent per 100 g of a fresh weight sample (mmol Fe^{2+}/100g FW), using a standard curve of iron(II) sulphate (0–1000 μM).

DPPH radical scavenging activity. A sample's 2,2-diphenyl-1-picrylhydrazyl (DPPH) radical scavenging activity was measured according to Gerhauser *et al.* [26] with minor modifications. 100 μM of the DPPH reagent was mixed with the sample and the change in reaction absorbance was measured for 60 min, with 15 min intervals at 515 nm. The DPPH radical scavenging capacity was expressed as milligram ascorbic acid equivalent per 100 g of a fresh weight sample (mg AA/100g FW), using a standard curve of ascorbic acid (0–1000 μM).

Advanced glycation end-products inhibition activity. A sample's anti-glycation activity was determined according to Ho *et al*. [27]. The mushroom samples were mixed with 1M glucose and 10 mg/mL bovine serum albumin in 50 mM of phosphate buffer (pH 7.4). The reaction mixtures were incubated at 80°C for 7 days, while the negative control was kept at 4°C. All the reactions were then stopped with 100% trichloroacetic acid and centrifuged for 10 min at 15,000 × g. Pellets of advanced glycation end-products and bovine serum albumin were dissolved with phosphate-buffered saline (pH 10.0), and the reaction fluorescence intensity was determined at 360 nm excitation and 450 nm emission wavelength. The sample's anti-glycation activity was expressed as milligram of aminoguanidine hydrochloride per 100 g of a fresh weight sample (mg AH/100g FW), with aminoguanidine (0–10 mg/mL) used as a standard.

Bioactive compounds. ***Total phenolic content.*** A sample's total phenolic content (TPC) was measured using Folin-Ciocalteu's method, as previously described by Yong *et al.* [19]. Briefly, 10% of Folin–Ciocalteu's reagent was added to each mushroom sample and incubated for 3 min prior to the addition of 10% sodium carbonate. The reaction was incubated at room temperature

in the dark for 60 min prior to measuring the absorbance at 750 nm. Gallic acid (0–100 µg/mL) was used as the standard. The TPC value was expressed as milligram of gallic acid equivalent per 100 g of a fresh weight sample (mg GAE/100 g FW).

Total tannin content. A sample's total tannin content was measured according to Siddhuraju & Manian [28]. Tannic acid (0 to 100 µg/mL) was used as the standard. Briefly, mushroom samples were incubated with and without polyvinylpolypyrrolidone (PVPP) at 4°C for 15 min. The sample mixtures were centrifuged for 10 min at 15,000 × g. The total phenolic content (TPC) was determined in the collected sample supernatants. The total tannin content in each sample corresponded to the difference in TPC values between the PVPP-treated sample and the water-treated sample. Tannic acid (0 to 100 µg/mL) was used as the standard. The total tannin value was expressed as milligram of tannic acid equivalent per 100 g of a fresh weight sample (mg TAE/100 g FW).

Total flavonoid content. A sample's total flavonoid content (TFC) was measured with aluminum chloride as outlined by Yong *et al.* [19]. Briefly, each mushroom sample was mixed with 95% ethanol, 1M $C_2H_3KO_2$, 10% (w/v) $AlCl_3$, and distilled water and then incubated for 30 min in the dark prior to measuring the absorbance at 415 nm. Quercetin (0–300 µg/mL) was used as the standard. The TFC value was expressed as milligram of quercetin equivalent per 100 g of a fresh weight sample (mg QE/100 g FW).

Polysaccharides. A sample's polysaccharide content was measured according to Masuko *et al.* [29]. Briefly, the mushroom sample was mixed with concentrated sulphuric acid and incubated for 30 min on a plate shaker. 5% phenol was then added to the mixture and incubated for 5 min at 90°C. The reaction plate was cooled for 5 min prior to measuring the absorbance at 590 nm. Starch (0–1.2 mM) was used as the standard. The carbohydrate value was expressed as milligrams of polysaccharide equivalent per 100 g of a fresh weight sample (mg PE/100g FW).

Bioactivity interaction. The experimental sample capacity (ESC) for individual mushroom samples and combined mushroom mixtures was determined via the following equation [30]:

$$ESC = 100 - \frac{\left(Abs_{sample} - Abs_{blank}\right)}{Abs_{control}} \times 100 \quad (3)$$

where Abs_{sample} is the absorbance of the sample reaction, Abs_{blank} is the sample blank, and $Abs_{control}$ is the absorbance of the reagent control [30].

The theoretical sample capacity (TSC) was calculated for combined sample mixtures and was described as a cumulative sum of individual sample capacities of each constituent found in the mushroom mixtures. It was determined via the following equation:

$$TSC = \left(ESC_A + ESC_B\right) - \frac{\left(ESC_A \times ESC_B\right)}{100} \quad (4)$$

where ESC_A and ESC_B are the ESC values of each individual mushroom sample in the combined mushroom mixture.

For the combinational study, individual mushroom samples were combined in a 1:1 ratio. A mathematical model for deriving synergism evaluation (SE) values [30] was used to determine the types of interaction among various mushroom combinations as follows:

$$SE = \frac{ESC_{mixture}}{TSC_{mixture}} \quad (5)$$

Interactions were categorized as synergism (SE > 1), antagonism (SE < 1), or additive (SE ≈ 1) based on the SE value.

Statistical analysis. All the analyses were carried out in triplicate, and the final data were presented as mean values ± standard deviations. One-way analysis of variance and Tukey's post hoc test were used to compare the sample values, with $p \leq 0.05$ deemed as statistically significant. Pearson's correlation and regression tests were employed to evaluate the relationship among the activity variables. Data analyses were performed with XLSTAT 2021 (Addinsoft Inc., USA) and GraphPad Prism 6 Software (GraphPad Software, USA).

RESULTS AND DISCUSSION

Mushroom extraction yield and water content. The extraction yields of the selected five mushrooms varied from 1.3 to 3.4% in the following order: *Flammulina velutipes* > *Agaricus bisporus* > *Lentinula edodes* > *Pleurotus eryngii* > *Pleurotus ostreatus* (Table 1). Among the five mushroom species, *F.velutipes* demonstrated the highest extraction yield, suggesting the presence of water-soluble phytochemicals such as phenolic compounds [31], amino acids, oligosaccharides, and monosaccharides. This speculation was substantiated by the high total phenolic content (TPC) in *F. velutipes* (Table 2).

The water content in the mushrooms ranged from 87.6 to 93.6 % (Table 1). *A. bisporus* showed the highest moisture content (93.6 ± 0.6%), followed by *P. ostreatus* (89.8 ± *0.5%)*, *F. velutipes* (88.8 ± 0.3%), *L. edodes* (87.8 ± 0.4%), and *P. eryngii* (87.6 ± 0.0%) (Table 1). These values agreed with a previous report by Yong *et al.* [19] that highlighted similar moisture values for *A. bisporus* (94.8 ± 0%) and *F. velutipes* (89.8 ± 0.1%). The differences in water content for other mushrooms, when compared to

Table 1 The extraction yield and water content of the selected edible mushrooms

Samples	Extraction yield, %	Water, %
Agaricus bisporus	3.06[a]	93.60 ± 0.59[c]
Lentinula edodes	2.53[b]	87.80 ± 0.35[a]
Flammulina velutipes	3.35[c]	88.83 ± 0.25[ab]
Pleurotus ostreatus	1.25[d]	89.75 ± 0.46[b]
Pleurotus eryngii	2.24[e]	87.60 ± 0.00[a]

Values indicate mean ± standard deviations of three independent measurements. Values within the same column followed by the same superscript lower-case letters do not differ significantly ($p > 0.05$)

Table 2 Polyphenol, polysaccharide, antioxidant, and anti-glycation values in the mushroom species under study

Mushroom species	Concentration, mg/mL	Antioxidant activity		Anti-glycation activity	Polyphenols			Polysaccharides, mg PE/100 g
		FRAP, mmol Fe^{2+}/100 g	DPPH, mgAA/100 g	Anti-AGE, mgAH/100 g	TFC, mg QE/100 g	TT, mg TAE/100 g	TFC, mg QE/100 g	
Agaricus bisporus	7.5	3.9 ± 0.0^{b}	501.0 ± 0.0^{a}	43.3 ± 0.5^{f}	626.8 ± 0.0^{a}	246.4 ± 0.0a	36.9 ± 0.0^{a}	6576.2 ± 0.0^{a}
	15	3.9 ± 0.0^{c}	446.2 ± 0.0^{b}	20.9 ± 0.6^{a}	484.6 ± 0.0^{b}	102.0 ± 0.0^{b}	30.4 ± 0.0^{b}	4848.2 ± 0.0^{b}
	30	3.4 ± 0.0^{d}	427.3 ± 0.0^{c}	9.2 ± 0.4^{b}	352.8 ± 0.0^{c}	87.3 ± 0.0^{c}	29.5 ± 0.0^{c}	3861.8 ± 0.1^{c}
Lentinula edodes	7.5	2.7 ± 0.0^{e}	548.0 ± 0.0^{d}	53.6 ± 0.8^{g}	623.5 ± 0.0^{d}	55.8 ± 0.0^{d}	4.3 ± 0.0^{d}	10773.7 ± 0.0^{d}
	15	2.6 ± 0.0^{f}	523.2 ± 0.0^{e}	22.6 ± 0.8^{a}	520.4 ± 0.0^{e}	86.8 ± 0.0^{e}	16.3 ± 0.0e	8633.0 ± 0.0^{e}
	30	2.5 ± 0.0g	431.8 ± 0.0^{f}	10.0 ± 0.5^{b}	386.6 ± 0.0^{f}	63.6 ± 0.0^{f}	27.4 ± 0.0^{f}	7650.0 ± 0.1^{f}
Flammulina velutipes	7.5	2.0 ± 0.0h	430.5 ± 0.0g	84.2 ± 1.4^{h}	688.5 ± 0.0^{g}	115.2 ± 0.0^{g}	2.2 ± 0.0^{g}	3344.1 ± 0.0^{g}
	15	2.2 ± 0.0^{i}	383.6 ± 0.0^{h}	37.5 ± 1.1^{i}	540.3 ± 0.0^{h}	149.9 ± 0.0^{h}	23.3 ± 0.0^{h}	2119.8 ± 0.0^{h}
	30	2.2 ± 0.0^{j}	379.0 ± 0.0^{i}	19.7 ± 0.7^{a}	390.1 ± 0.0^{i}	71.3 ± 0.1^{i}	34.7 ± 0.0^{i}	2406.6 ± 0.0^{i}
Pleurotus ostreatus	25	0.6 ± 0.0^{a}	115.1 ± 0.0^{j}	12.6 ± 0.8^{c}	391.5 ± 0.0^{j}	202.1 ± 0.0^{j}	7.8 ± 0.0^{j}	21256.4 ± 0.0^{j}
	50	0.6 ± 0.0^{a}	122.5 ± 0.0^{k}	5.9 ± 0.7^{d}	247.2 ± 0.0^{k}	118.1 ± 0.0^{k}	4.9 ± 0.0^{k}	20887.0 ± 0.0^{k}
	100	0.8 ± 0.0^{k}	112.7 ± 0.0^{l}	2.7 ± 0.1^{e}	134.0 ± 0.0^{l}	57.1 ± 0.0^{l}	16.8 ± 0.0^{l}	19417.9 ± 0.0^{l}
Pleurotus eryngii	25	0.6 ± 0.0^{a}	173.0 ± 0.0^{m}	14.8 ± 0.4^{c}	328.8 ± 0.0^{m}	70.1 ± 0.0^{m}	1.6 ± 0.0^{m}	24300.0 ± 0.1^{m}
	50	0.6 ± 0.0^{a}	153.0 ± 0.0^{n}	6.7 ± 0.4^{d}	236.1 ± 0.0^{n}	88.8 ± 0.0^{n}	3.7 ± 0.0^{n}	38533.5 ± 0.0^{n}
	100	0.5 ± 0.0^{l}	144.6 ± 0.0^{o}	3.5 ± 0.1^{e}	132.3 ± 0.0^{o}	45.8 ± 0.0^{o}	7.3 ± 0.0^{o}	49479.5 ± 0.0^{o}

Values indicate mean ± standard deviation of three independent measurements. Values within the same column accompanied by the same superscript lower-case letter do not differ significantly ($p > 0.05$). FRAP – ferric-reducing antioxidant power; DPPH – 2,2-Diphenyl-1-picrylhydrazyl radical scavenging activity; TPC – total phenolic content; TT – total tannins; TFC – total flavonoid content; AGE – advanced glycation end-product; AA – ascorbic acid; AH – aminoguanidine hydrochloride; GAE – gallic acid equivalent; TAE – tannic acid equivalent; QE – quercetin equivalent; PE – polysaccharide equivalent

those reported by Yong *et al.* [20], could be attributed to variations in environmental conditions, such as humidity and temperature during the cultivation period [32].

Antioxidant activity of individual mushroom extracts. A three-sample concentration model was adopted for each mushroom species to comprehensively evaluate their phytochemical, antioxidant, and anti-glycation activities. This concentration gradient approach enabled a thorough investigation into the potency and efficacy of individual mushrooms and their combinations across a range of concentrations as recommended by Hengst *et al.* [33].

The concentrations of *L. edodes, A. bisporus,* and *F. velutipes* were selected within a 7.5–30.0 mg/mL range based on the previous pilot study and literature suggesting that this concentration range could yield observable phytochemical activity pertinent to antioxidant and anti-glycation activities [34–36]. This approach aimed to identify the lowest and highest effective sample concentration that demonstrates significant functional activity. However, an exception was made for both *P. ostreatus* and *P. eryngii,* in which the concentration series were adjusted to a higher range of 25–100 mg/mL. This modification stemmed from the pilot study conducted prior to the current experimental phase, which revealed that *Pleurotus spp.* exhibited noticeable functional activity exclusively at a threshold concentration of 25 mg/mL. This finding agreed with Reis *et al.* [37] where lower antioxidant activity was observed in *Pleutorus spp.* when compared to other cultivated mushrooms at the same concentration. The observed variance could be due to the unique phytochemical composition in each mushroom species, resulting in divergent antioxidant effects and profiles of phenolic acids [37]. Therefore, the concentration range for *Pleutorus spp.* was elevated to accurately assess the potential and ensure a fair comparison among all the mushroom species. This decision was validated by subsequent assays, which demonstrated more pronounced phytochemical, antioxidant, and anti-glycation activities in *Pleutorus* spp. within the adjusted concentration range.

The mushrooms' antioxidant activity was assessed through ferric reducing antioxidant power (FRAP) and 2,2-diphenyl-1-picrylhydrazyl (DPPH) assays. The FRAP assay relies on the reduction of the ferric to ferrous ions complex by combining with 2,4,6-tripyridyl-s-triazine (TPTZ) in an acetate buffer [38]. The resulting ferrous ion-TPTZ complex produces a blue color, with intensity dependent on the quantity of reduced ferric ions [38]. The DPPH method is a widely utilized protocol for screening antioxidants, involving the scavenging of DPPH free radicals in an alcoholic solution [38]. In this process, the presence of antioxidants changes the color from purple to yellow in the DPPH solution [38]. Given the diverse nature of antioxidant compounds and numerous reaction mechanisms, it is not possible to evaluate the antioxidant properties of natural products using a single antioxidant assay [30, 38]. Thus, we employed multiple methods to provide a comprehensive evaluation of the antioxidant properties of these compounds.

Among the five mushroom species (Table 2), *A. bisporus* showed the highest reducing potential for all three concentrations investigated. At 7.5 mg/mL, *A. bisporus* displayed a FRAP value of 3.9 mmol Fe^{2+} per 100 g, which

corresponded to the relatively high total phenolic, total tannin, and total flavonoid contents (626.8 mg GAE/100 g, 246.4 mg TAE /100 g, and 36.9 QE/100 g, respectively). This suggested an association of phenolic compounds and flavonoids to the antioxidant activity. These phytochemicals possessed an ability to disrupt the free radical chain by donating an electron to stabilize and terminate radical chain reactions [39]. Our findings align with a previous study [20] where *A. bisporus* demonstrated the highest reducing power, followed by *L. edodes* and *F. velutipes*.

The DPPH radical scavenging finding revealed that, at a concentration of 7.5 mg/mL, *L. edodes* displayed the highest DPPH scavenging capacity at 548.0 mg AA/100g, followed by 15 mg/mL of *L. edodes* (523.2 mg AA/100 g) and 7.5mg/mL of *A. bisporus* (501.0 mg AA/100g). A significant difference ($p < 0.05$) in the DPPH radical scavenging capacity was observed across all the concentrations of the aqueous mushroom extracts. This finding was consistent with that of Shah and Modi [40], who reported higher radical scavenging activity in the aqueous extracts of *L. edodes* when compared to *A. bisporus*. The relatively high radical scavenging activity in *L. edodes* could be attributed to the presence of additional hydrogen-donating components such as phenolic compounds in the mushroom extract [39]. This finding also suggested that the phytochemicals in *L. edodes* extracts were effective hydrogen atom donors. The difference between the DPPH and FRAP values may be due to the distinct mechanisms of each assay, which also highlights the diversity of antioxidant activities in different mushroom species.

Anti-glycation activity of individual mushroom extracts. The formation of endogenous advanced glycation end-products (AGEs) plays a critical role in the development of pathologies related to aging and metabolic diseases [41]. A previous study has demonstrated that a daily intake of 150–300 mg of aminoguanidine could inhibit the progression of diabetic retinopathy [42]. Expanding from this notion, Ishioka *et al.* [36] conducted a study to determine the daily intake of different vegetable samples to achieve anti-glycation activity equivalent to that of aminoguanidine. This comparison not only highlights the potential of dietary intervention with potent anti-glycation activity but also paves the way for exploring other natural sources with similar health benefits. Thus, investigating individual mushrooms and their combinations with good anti-glycation activities could lead to the discovery of new therapeutic agents to prevent diabetic complications.

The anti-glycation activity of the mushroom samples in this study was evaluated with a bovine serum albumin-glucose glycation model. We found that the water extract of 7.5 mg/mL *F. velutipes* showed the strongest inhibition of protein glycation at 84.2 mg AH/100g, followed by 7.5 mg/mL *L. edodes* (53.6 mg AH/100g) and 7.5 mg/mL *A. bisporus* (43.3 mg AH/100 g) (Table 2). Interestingly, these three mushroom samples not only displayed high anti-glycation activity but also possessed the highest total phenolic contents among the five mushroom samples. This provided further evidence to support the correlation between total phenolics and anti-glycation activity in the mushrooms. The mushroom's phenolic constituents, particularly their hydroxyl groups, may play a crucial role as AGE inhibitors by intercepting the glycation process [27].

Polyphenols and polysaccharides in individual mushroom extracts. Phenolics and tannins are secondary metabolites that possess antioxidant properties in the mushrooms [43]. The selected five mushrooms revealed substantial phenolic contents in the following order: 7.5 mg/mL *F. velutipes* > 7.5 mg/mL *A. bisporus* > 7.5 mg/mL *L. edodes* (Table 2). This was in agreement with Bach *et al.* [44] who observed higher phenolic contents in *F. velutipes* and *A. bisporus* when compared to other edible mushrooms. Kozarski *et al.* [45] previously identified ten types of phenolic compounds in *F. velutipes,* namely pyrogallol, quercetin, as well as homogentisic, protocatechuic, gallic, 5-sulfosalicylic, chlogenic, p-hydroxybenzoic, caffeic, and ferulic acids. They also identified 15 types of phenolic compounds in *Agaricus* spp., including pyrogallol, catechin, myricetin, and naringin, as well as trans-cinnamic, sulfosalicylic, rosmarinic, syringic, chlorogenic, p-hydroxybenzoic, ferulic, p-coumaric, caffeic, protocatechuic, and gallic acids. Conversely, 7.5 mg/mL *A. bisporus* showed the highest total tannin content (246.6 mg TAE/100 g), followed by 25 mg/mL *P. ostreatus* (202.1 mg TAE/100 g) and 15 mg/mL *F. velutipes* (149.9 mg TAE/100 g). The variation in total phenolic and tannin contents among the mushrooms could be due to the variation in their phenolic compositions, which are generally determined by genetic, environmental, and other factors [46]. The presence of flavonoids within the biological membranes, in conjunction with their interactions at the lipid bilayer surface, may restrict oxidant access and thereby preserve the integrity and functionality of cell membranes [43]. Therefore, the flavonoid contents in the mushrooms were pertinent to assessing their antioxidant properties. The highest flavonoid content was observed in 7.5 mg/mL *A. bisporus* (36.9 mg QE/100 g), while 25 mg/mL *P. eryngii* showed the lowest flavonoid content at 1.6 mg QE/100 g. This corresponded to the previous reports of *A. bisporus* having the highest total phenolic content among the edible mushrooms [19, 20].

Plant and fungi-derived polysaccharides, such as chitin, α-glucans, and β-glucans, constitute a promising group of antioxidants that are primary sources of bioactive compounds [16]. The consumption of polysaccharides has been associated with various health benefits, including improved gastrointestinal health, management of cardiovascular diseases, and treatment of specific cancer [11]. Therefore, polysaccharides are emerging as potential candidates for dietary supplements and treatments targeting oxidative stress-mediated conditions [11]. In our study, *P. eryngii* displayed the highest total carbohydrate content at 100 mg/mL (49479.5 mg PE/100 g). However, this mushroom showed

the lowest FRAP value (0.5 mmol Fe^{2+}/100 g) and a low DPPH value (144.6 mg AA/100 g), implying that its polysaccharides may not be associated with its antioxidant capacities. Most mushroom extracts in our study showed a decreasing trend in their bioactive contents, as well as antioxidant and anti-glycation activities, with increasing sample concentrations (Table 2). However, the increased FRAP and TFC values in *F. velutipes* and *P. ostreatus* supported the association between flavonoids and the reducing potential of both mushrooms.

Hengst *et al*. [33] have previously highlighted that a food extract concentration is a major determining factor of their functional values. They showed a decrease in antioxidant capacities for tomato extract, white tea, and strawberry nectar with increasing sample concentrations [33]. Similarly, Nowak *et al.* [47] observed a decreasing trend in antioxidant activities with increasing concentrations of polyphenols using a Fe^{2+}-EGTA-H_2O_2 system. Zhou *et al*. [48] also observed a decrease in antioxidant activity with increasing concentrations of green tea and maté extracts. The above findings may be explained by the pro-oxidant properties of plants with high polyphenol concentrations [48]. Certain dietary phenolic compounds, including phenolic acids, flavonoids, and non-flavonoids, are known to exhibit pro-oxidant behavior under specific conditions [49]. Factors such as the phenolic compound structure, high pH, and the sample's concentration may contribute to the pro-oxidant activity leading to reduced antioxidant activity [49]. Another plausible reason for the reduced antioxidant activity at high sample concentrations may be the autoxidation of flavonoids and phenolic compounds by transition metals, leading to the production of superoxide anions radicals [48]. Thus, it is crucial to account for the potential influence of pro-oxidant effects when assessing the antioxidant activity in mushroom extracts.

Antioxidant interaction in different mushroom mixtures. The theoretical sample capacity (TSC) and the experimental sample capacity (ESC) for antioxidant activity and phytochemicals in 90 combined mushroom mixtures are presented in Table 3 and Table 4, respectively. The synergism evaluation (SE) values of these mixtures are displayed in Table 5. Three best-performing mushroom combinations were selected out of 90 mixtures based on their collective phytochemical assay values and synergistic performance across all seven assays. In general, 7.5 mg/mL *A. bisporus* + 15 mg/mL *F. velutipes*, 7.5 mg/mL *L. edodes* + 7.5 mg/mL *F. velutipes,*

Table 3 Theoretical sample capacity values for polyphenols, polysaccharides, antioxidant and anti-glycation activities in different mushroom combinations

Mushrooms mixtures (A+B), mg/mL		Antioxidant activity		Anti-glycation activity	Polyphenols			Polysaccharides, mg PE/100 g
Mushroom A	Mushroom B	FRAP, mmol Fe^{2+}/100 g	DPPH, mg AA/100 g	Anti-AGE value, mg AH/100 g	TPC, mg GAE/100 g	TT, mg TAE/100 g	TFC, mg QE/100 g	
Agaricus bisporus	*Lentinula edodes*							
7.5	7.5	6.6 ± 0.0^{a}	1049.0 ± 0.0^{a}	96.9 ± 1.0^{a}	1250.2 ± 0.0^{a}	302.2 ± 0.0^{a}	41.2 ± 0.0^{a}	17349.9 ± 0.0^{a}
7.5	15	6.6 ± 0.0^{ab}	1024.2 ± 0.0^{b}	65.9 ± 0.9^{b}	1147.1 ± 0.0^{b}	333.2 ± 0.0^{b}	53.1 ± 0.0^{b}	15209.1 ± 0.1^{b}
7.5	30	6.4 ± 0.0^{c}	932.8 ± 0.0^{c}	53.3 ± 0.7^{c}	1013.4 ± 0.0^{c}	319.0 ± 0.0^{c}	64.23± 0.0^{c}	14226.2 ± 0.1^{c}
15	7.5	6.6 ± 0.0^{ab}	994.2 ± 0.0^{d}	74.5 ± 1.1^{g}	1108.0 ± 0.0^{d}	157.9 ± 0.0^{d}	34.7 ± 0.0^{d}	15621.9 ± 0.0^{d}
15	15	6.5 ± 0.0^{b}	969.4 ± 0.0^{e}	43.5 ± 1.0^{h}	1004.9 ± 0.0^{e}	188.8 ± 0.0^{e}	46.6 ± 0.0^{e}	13481.1 ± 0.0^{e}
15	30	6.4 ± 0.0^{c}	878.0 ± 0.0^{f}	30.9 ± 0.8^{i}	871.2 ± 0.0^{f}	165.6 ± 0.0^{f}	57.7 ± 0.0^{f}	12498.2 ± 0.1^{f}
30	7.5	6.1 ± 0.0^{e}	975.2 ± 0.0^{g}	62.9 ± 0.9^{b}	976.2 ± 0.0^{g}	143.1 ± 0.0^{g}	33.9 ± 0.0^{g}	14635.5 ± 0.1^{g}
30	15	6.1 ± 0.0^{e}	950.5 ± 0.0^{h}	31.8 ± 0.9^{ik}	873.2 ± 0.0^{h}	174.0 ± 0.0^{h}	45.8 ± 0.0^{h}	12494.7 ± 0.1^{h}
30	30	5.9 ± 0.0^{d}	859.1 ± 0.0^{i}	19.3 ± 0.6^{n}	739.4 ± 0.0^{i}	150.8 ± 0.0^{i}	56.9 ± 0.0^{i}	11511.8 ± 0.1^{i}
Agaricus bisporus	*Flammulina velutipes*							
7.5	7.5	5.9 ± 0.0^{d}	931.5 ± 0.0^{j}	127.5 ± 1.5^{x}	1315.2 ± 0.0^{j}	361.6 ± 0.0^{j}	39.0 ± 0.0^{j}	9920.2 ± 0.0^{j}
7.5	15	6.1 ± 0.0^{e}	884.6 ± 0.0^{k}	80.8 ± 1.2^{w}	1167.1 ± 0.0^{k}	396.3 ± 0.1^{k}	60.2 ± 0.0^{k}	8695.9 ± 0.0^{k}
7.5	30	6.1 ± 0.0^{e}	880.0 ± 0.0^{l}	63.0 ± 0.9^{bd}	1016.9 ± 0.0^{l}	317.7 ± 0.1^{l}	71.5 ± 0.0^{l}	8982.8 ± 0.1^{l}
15	7.5	5.9 ± 0.0^{d}	876.7 ± 0.0^{m}	105.1 ± 1.6^{j}	1173.1 ± 0.0^{m}	217.2 ± 0.0^{m}	32.5 ± 0.0^{m}	8192.2 ± 0.0^{m}
15	15	6.1 ± 0.0^{e}	829.8 ± 0.0^{n}	58.4 ± 1.3^{e}	1024.9 ± 0.0^{n}	251.9 ± 0.0^{n}	53.7 ± 0.0^{n}	6967.9 ± 0.0^{n}
15	30	6.1 ± 0.0^{e}	825.2 ± 0.0^{o}	40.6 ± 0.9^{h}	874.7 ± 0.0^{o}	173.3 ± 0.1^{o}	65.0 ± 0.0^{o}	7254.8 ± 0.0^{o}
30	7.5	5.4 ± 0.0^{w}	857.8 ± 0.0^{p}	93.5 ± 1.5^{ao}	1041.3 ± 0.0^{p}	202.5 ± 0.0^{p}	31.7 ± 0.0^{p}	7205.8 ± 0.1^{p}
30	15	5.6 ± 0.0^{j}	810.9 ± 0.0^{q}	46.8 ± 1.2^{fh}	893.1 ± 0.0^{q}	237.2 ± 0.1^{q}	52.9 ± 0.0^{q}	5981.5 ± 0.1^{q}
30	30	5.7 ± 0.0^{j}	806.3 ± 0.0^{r}	28.9 ± 0.8^{il}	742.9 ± 0.0^{r}	158.6 ± 0.1^{r}	64.2 ± 0.0^{r}	6268.4 ± 0.1^{r}

Continuation of Table 3

Mushrooms mixtures (A+B), mg/mL		Antioxidant activity		Anti-glycation activity	Polyphenols			Polysaccharides, mg PE/100 g
Mushroom A	Mushroom B	FRAP, mmol Fe^{2+}/100 g	DPPH, mg AA/100 g	Anti-AGE value, mg AH/100 g	TPC, mg GAE/100 g	TT, mg TAE/100 g	TFC, mg QE/100 g	
Agaricus bisporus	*Pleurotus ostreatus*							
7.5	25	4.5 ± 0.0^{f}	616.1 ± 0.0^{s}	55.8 ± 0.9^{cc}	1018.2 ± 0.0^{s}	448.5 ± 0.0^{s}	44.7 ± 0.0^{s}	27832.6 ± 0.0^{s}
7.5	50	4.5 ± 0.0^{f}	623.5 ± 0.0^{t}	49.1 ± 0.9^{f}	874.0 ± 0.0^{t}	364.5 ± 0.0^{t}	41.7 ± 0.0^{t}	27463.2 ± 0.0^{t}
7.5	100	4.7 ± 0.0^{g}	613.7 ± 0.0^{u}	46.0 ± 0.5^{f}	760.7 ± 0.0^{u}	303.5 ± 0.0^{u}	53.0 ± 0.0^{u}	25994.1 ± 0.0^{u}
15	25	4.5 ± 0.0^{fh}	561.3 ± 0.0^{v}	33.4 ± 1.0^{ik}	876.1 ± 0.0^{v}	304.2 ± 0.0^{v}	38.2 ± 0.0^{v}	26104.6 ± 0.0^{v}
15	50	4.5 ± 0.0^{fh}	568.7 ± 0.0^{w}	26.7 ± 0.9^{l}	731.8 ± 0.0^{x}	220.1 ± 0.0^{w}	35.2 ± 0.0^{w}	25735.2 ± 0.0^{w}
15	100	4.7 ± 0.0^{g}	558.9 ± 0.0^{x}	23.5 ± 0.6^{m}	618.5 ± 0.0^{y}	159.2 ± 0.0^{x}	46.5 ± 0.0^{x}	24266.1 ± 0.0^{x}
30	25	4.0 ± 0.0^{k}	542.4 ± 0.0^{y}	21.8 ± 0.9^{mn}	744.3 ± 0.0^{w}	289.4 ± 0.0^{y}	37.3 ± 0.0^{y}	25118.2 ± 0.1^{y}
30	50	4.0 ± 0.0^{k}	549.8 ± 0.0^{z}	15.1 ± 0.80^{p}	600.0 ± 0.0^{z}	205.4 ± 0.0^{z}	34.4 ± 0.0^{z}	24748.8 ± 0.1^{z}
30	100	4.3 ± 0.0^{x}	540.0 ± 0.0^{A}	11.9 ± 0.4^{p}	486.7 ± 0.0^{A}	144.4 ± 0.0^{A}	45.7 ± 0.0^{A}	23279.6 ± 0.1^{A}
Agaricus bisporus	*Pleurotus eryngii*							
7.5	25	4.5 ± 0.0^{f}	674.0 ± 0.0^{B}	58.0 ± 0.7^{cc}	955.5 ± 0.0^{B}	316.5 ± 0.0^{B}	38.5 ± 0.0^{B}	30876.2 ± 0.1^{B}
7.5	50	4.5 ± 0.0^{f}	654.0 ± 0.0^{C}	49.9 ± 0.7^{f}	862.9 ± 0.0^{C}	335.2 ± 0.0^{C}	40.6 ± 0.0^{C}	45109.7 ± 0.0^{C}
7.5	100	4.5 ± 0.0^{h}	645.6 ± 0.0^{D}	46.7 ± 0.6^{f}	759.0 ± 0.0^{D}	292.2 ± 0.0^{D}	44.2 ± 0.0^{D}	56055.6 ± 0.1^{D}
15	25	4.5 ± 0.0^{i}	619.2 ± 0.0^{E}	35.6 ± 0.7^{k}	813.3 ± 0.0^{E}	172.1 ± 0.0^{E}	32.0 ± 0.0^{E}	29148.2 ± 0.1^{E}
15	50	4.5 ± 0.0^{fi}	599.2 ± 0.0^{F}	27.5 ± 0.7^{il}	720.7 ± 0.0^{F}	190.8 ± 0.0^{F}	34.1 ± 0.0^{F}	43381.7 ± 0.0^{F}
15	100	4.4 ± 0.0^{fh}	590.8 ± 0.0^{G}	24.3 ± 0.6^{lm}	616.8 ± 0.0^{G}	147.8 ± 0.0^{G}	37.7 ± 0.0^{G}	54327.6 ± 0.0^{G}
30	25	4.0 ± 0.0^{k}	600.3 ± 0.0^{H}	24.0 ± 0.5^{lm}	681.5 ± 0.0^{H}	157.4 ± 0.0^{H}	31.2 ± 0.0^{H}	28161.8 ± 0.1^{H}
30	50	4.0 ± 0.0^{k}	580.3 ± 0.0^{I}	15.9 ± 0.6^{np}	588.9 ± 0.0^{I}	176.1 ± 0.0^{I}	33.3 ± 0.0^{I}	42395.3 ± 0.1^{I}
30	100	4.0 ± 0.0^{y}	571.9 ± 0.0^{J}	12.7 ± 0.4^{p}	485.0 ± 0.0^{J}	133.1 ± 0.0^{J}	36.9 ± 0.0^{J}	53341.2 ± 0.1^{J}
Lentinula edodes	*Flammulina velutipes*							
7.5	7.5	4.7 ± 0.0^{l}	978.5 ± 0.0^{K}	137.9 ± 1.7^{v}	1311.9 ± 0.0^{K}	171.0 ± 0.0^{K}	6.5 ± 0.0^{K}	14117.8 ± 0.0^{K}
7.5	15	4.8 ± 0.0^{m}	931.5 ± 0.0^{L}	91.2 ± 1.4^{o}	1163.8 ± 0.0^{L}	205.7 ± 0.0^{L}	27.6 ± 0.0^{L}	12893.5 ± 0.0^{L}
7.5	30	4.9 ± 0.0^{m}	927.0 ± 0.0^{M}	73.3 ± 1.1^{g}	1013.6 ± 0.0^{M}	127.1 ± 0.1^{M}	39.0 ± 0.0^{M}	13180.3 ± 0.0^{M}
15	7.5	4.6 ± 0.0^{l}	953.7 ± 0.0^{N}	106.8 ± 1.6^{j}	1208.9 ± 0.0^{N}	202.0 ± 0.0^{N}	18.4 ± 0.0^{N}	11977.0 ± 0.0^{N}
15	15	4.8 ± 0.0^{m}	906.7 ± 0.0^{O}	60.1 ± 1.4^{d}	1060.7 ± 0.0^{O}	236.6 ± 0.0^{O}	39.6 ± 0.0^{O}	10752.7 ± 0.0^{O}
15	30	4.8 ± 0.0^{m}	902.2 ± 0.0^{P}	42.3 ± 1.1^{h}	910.5 ± 0.0^{P}	158.0 ± 0.1^{P}	51.0 ± 0.0^{P}	11039.6 ± 0.1^{P}
30	7.5	4.5 ± 0.0^{hi}	862.4 ± 0.0^{Q}	94.3 ± 1.5^{ao}	1075.1 ± 0.0^{Q}	178.8 ± 0.0^{Q}	29.5 ± 0.0^{Q}	10994.1 ± 0.1^{Q}
30	15	4.6 ± 0.0^{l}	815.4 ± 0.0^{R}	47.6 ± 1.2^{f}	927.0 ± 0.0^{R}	213.4 ± 0.1^{R}	50.7 ± 0.0^{R}	9769.8 ± 0.1^{R}
30	30	4.7 ± 0.0^{l}	810.9 ± 0.0^{S}	29.7 ± 0.9^{il}	776.8 ± 0.0^{S}	134.8 ± 0.1^{S}	62.1 ± 0.0^{S}	10056.6 ± 0.1^{S}
Lentinula edodes	*Pleurotus ostreatus*							
7.5	25	3.2 ± 0.0^{n}	663.0 ± 0.0^{T}	66.2 ± 1.1^{d}	1014.9 ± 0.0^{T}	258.0 ± 0.0^{T}	12.1 ± 0.0^{T}	32030.1 ± 0.0^{T}
7.5	50	3.2 ± 0.0^{n}	670.5 ± 0.0^{U}	59.5 ± 1.1^{d}	870.7 ± 0.0^{U}	173.9 ± 0.0^{U}	9.2 ± 0.0^{U}	31660.8 ± 0.0^{U}
7.5	100	3.5 ± 0.0^{o}	660.7 ± 0.0^{V}	56.3 ± 0.8^{cc}	757.4 ± 0.0^{V}	112.9 ± 0.0^{V}	20.5 ± 0.0^{V}	30191.6 ± 0.0^{V}
15	25	3.2 ± 0.0^{np}	638.2 ± 0.0^{X}	35.2 ± 1.1^{k}	911.9 ± 0.0^{W}	288.9 ± 0.0^{W}	24.1 ± 0.0^{W}	29889.4 ± 0.1^{W}
15	50	3.2 ± 0.0^{p}	645.7 ± 0.0^{Y}	28.5 ± 1.1^{il}	767.6 ± 0.0^{X}	204.8 ± 0.0^{X}	21.1 ± 0.0^{X}	29520.0 ± 0.1^{X}
15	100	3.4 ± 0.0^{o}	635.9 ± 0.0^{Z}	25.3 ± 0.8^{l}	654.3 ± 0.0^{Y}	143.9 ± 0.0^{Y}	32.4 ± 0.0^{Y}	28050.9 ± 0.1^{Y}
30	25	3.0 ± 0.0^{q}	546.9 ± 0.0^{W}	22.6 ± 0.9^{mn}	778.1 ± 0.0^{Z}	265.7 ± 0.0^{Z}	35.2 ± 0.0^{Z}	28906.5 ± 0.1^{Z}
30	50	3.0 ± 0.0^{q}	554.4 ± 0.0^{A1}	15.9 ± 0.9^{np}	633.9 ± 0.0^{A1}	181.6 ± 0.0^{A1}	32.3 ± 0.0^{A1}	28537.1 ± 0.1^{A1}
30	100	3.3 ± 0.0^{n}	544.6 ± 0.0^{B1}	12.7 ± 0.5^{p}	520.6 ± 0.0^{B1}	120.7 ± 0.0^{B1}	43.6 ± 0.0^{B1}	27067.9 ± 0.1^{B1}
Lentinula edodes	*Pleurotus eryngii*							
7.5	25	3.2 ± 0.0^{n}	721.0 ± 0.0^{C1}	68.4 ± 0.9^{b}	952.2 ± 0.0^{C1}	125.9 ± 0.0^{C1}	6.0 ± 0.00^{C1}	35073.7 ± 0.1^{C1}
7.5	50	3.3 ± 0.0^{n}	701.0 ± 0.0^{D1}	60.3 ± 0.9^{d}	859.6 ± 0.0^{D1}	144.6 ± 0.0^{D1}	8.1 ± 0.00^{D1}	49307.3 ± 0.0^{D1}
7.5	100	3.2 ± 0.0^{p}	692.6 ± 0.0^{E1}	57.1 ± 0.9^{e}	755.7 ± 0.0^{E1}	101.6 ± 0.0^{E1}	11.7 ± 0.0^{E1}	60253.2 ± 0.0^{E1}

End of Table 3

Mushrooms mixtures (A+B), mg/mL		Antioxidant activity		Anti-glycation activity	Polyphenols			Polysaccharides, mg PE/100 g
Mushroom A	Mushroom B	FRAP, mmol Fe^{2+}/100 g	DPPH, mg AA/100 g	Anti-AGE value, mg AH/100 g	TPC, mg GAE/100 g	TT, mg TAE/100 g	TFC, mg QE/100 g	
15	25	3.2 ± 0.0^{np}	696.2 ± 0.0^{F1}	37.4 ± 0.9^{q}	849.1 ± 0.0^{F1}	156.8 ± 0.0^{F1}	17.9 ± 0.0^{F1}	32933.0 ± 0.1^{F1}
15	50	3.2 ± 0.0^{np}	676.2 ± 0.0^{G1}	29.3 ± 0.9^{il}	756.5 ± 0.0^{G1}	175.6 ± 0.0^{G1}	20.0 ± 0.0^{G1}	47166.5 ± 0.1^{G1}
15	100	3.1 ± 0.0^{p}	667.8 ± 0.0^{H1}	26.1 ± 0.8^{lmq}	652.6 ± 0.0^{H1}	132.5 ± 0.0^{H1}	23.6 ± 0.0^{H1}	58112.4 ± 0.1^{H1}
30	25	3.0 ± 0.0^{q}	604.8 ± 0.0^{I1}	24.8 ± 0.6^{lm}	715.4 ± 0.0^{I1}	133.6 ± 0.0^{I1}	29.0 ± 0.0^{I1}	31950.1 ± 0.1^{I1}
30	50	3.1 ± 0.0^{q}	584.9 ± 0.0^{J1}	16.7 ± 0.7^{np}	622.7 ± 0.0^{J1}	152.4 ± 0.0^{J1}	31.1 ± 0.0^{J1}	46183.6 ± 0.1^{J1}
30	100	3.0 ± 0.0^{z}	576.5 ± 0.0^{K1}	13.5 ± 0.5^{p}	518.9 ± 0.0^{K1}	109.3 ± 0.0^{K1}	34.7 ± 0.0^{K1}	57129.5 ± 0.1^{K1}
Flammulina velutipes	*Pleurotus ostreatus*							
7.5	25	2.6 ± 0.0^{r}	545.6 ± 0.0^{L1}	96.8 ± 1.6^{ao}	1080.0 ± 0.0^{L1}	317.3 ± 0.0^{L1}	10.0 ± 0.0^{L1}	24600.5 ± 0.0^{L1}
7.5	50	2.6 ± 0.0^{r}	553.1 ± 0.0^{M1}	90.1 ± 1.6^{o}	936.0 ± 0.0^{M1}	233.3 ± 0.0^{M1}	7.1 ± 0.0^{M1}	24231.1 ± 0.0^{M1}
7.5	100	2.8 ± 0.0^{s}	543.3 ± 0.0^{N1}	86.9 ± 1.4^{t}	822.4 ± 0.0^{N1}	172.3 ± 0.0^{N1}	18.4 ± 0.0^{N1}	22761.9 ± 0.0^{N1}
15	25	2.7 ± 0.0^{t}	498.6 ± 0.0^{O1}	50.1 ± 1.4^{cef}	931.8 ± 0.0^{O1}	352.0 ± 0.1^{O1}	31.1 ± 0.0^{O1}	23376.2 ± 0.0^{O1}
15	50	2.7 ± 0.0^{t}	506.1 ± 0.0^{P1}	43.4 ± 1.3^{h}	787.6 ± 0.0^{P1}	268.0 ± 0.0^{P1}	28.2 ± 0.0^{P1}	23006.8 ± 0.0^{P1}
15	100	3.0 ± 0.0	496.3 ± 0.0^{Q1}	40.2 ± 1.1^{hq}	674.3 ± 0.0^{Q1}	207.0 ± 0.0^{Q1}	39.5 ± 0.0^{Q1}	21537.7 ± 0.0^{Q1}
30	25	2.8 ± 0.0st	494.1 ± 0.0^{R1}	32.3 ± 1.0^{ik}	781.6 ± 0.0^{R1}	273.4 ± 0.1^{R1}	42.5 ± 0.0^{R1}	23663.0 ± 0.1^{R1}
30	50	2.8 ± 0.0st	501.5 ± 0.0^{S1}	25.6 ± 1.0^{lm}	637.4 ± 0.0^{S1}	189.4 ± 0.1^{S1}	39.6 ± 0.0^{S1}	23293.6 ± 0.1^{S1}
30	100	3.0 ± 0.0^{q}	491.7 ± 0.0^{T1}	22.4 ± 0.7^{n}	524.1 ± 0.0^{T1}	128.4 ± 0.1^{T1}	50.9 ± 0.0^{T1}	21824.5 ± 0.0^{T1}
Flammulina velutipes	*Pleurotus eryngii*							
7.5	25	2.6 ± 0.0^{r}	603.5 ± 0.0^{U1}	99.0 ± 1.5^{a}	1017.2 ± 0.0^{U1}	185.3 ± 0.0^{U1}	3.8 ± 0.0^{U1}	27644.1 ± 0.1^{U1}
7.5	50	2.6 ± 0.0^{r}	583.6 ± 0.0^{V1}	90.9 ± 1.5^{o}	924.6 ± 0.0^{V1}	204.0 ± 0.0^{V1}	5.9 ± 0.0^{V1}	41877.6 ± 0.0^{V1}
7.5	100	2.5 ± 0.0^{A}	575.2 ± 0.0^{W1}	87.7 ± 1.4^{u}	820.7 ± 0.0^{W1}	161.0 ± 0.0^{W1}	9.5 ± 0.0^{W1}	52823.5 ± 0.0^{W1}
15	25	2.8 ± 0.0^{t}	556.6 ± 0.0^{X1}	52.3 ± 1.2^{cf}	869.1 ± 0.0^{X1}	220.0 ± 0.0^{X1}	24.9 ± 0.0^{X1}	26419.8 ± 0.1^{X1}
15	50	2.8 ± 0.0^{t}	536.6 ± 0.0^{Y1}	44.2 ± 1.2^{h}	776.4 ± 0.0^{Y1}	238.7 ± 0.1^{Y1}	27.1 ± 0.0^{Y1}	40653.3 ± 0.0^{Y1}
15	100	2.7 ± 0.0^{B}	528.2 ± 0.0^{Z1}	41.0 ± 1.1^{h}	672.6 ± 0.0^{Z1}	195.6 ± 0.0^{Z1}	30.6 ± 0.0^{Z1}	51599.2 ± 0.0^{Z1}
30	25	2.8 ± 0.0st	552.0 ± 0.0^{A2}	34.5 ± 0.8^{kq}	718.9 ± 0.0^{A2}	141.4 ± 0.1^{A2}	36.3 ± 0.0^{A2}	26706.6 ± 0.1^{A2}
30	50	2.8 ± 0.0st	532.0 ± 0.0^{B2}	26.3 ± 0.8^{lm}	626.2 ± 0.0^{B2}	160.1 ± 0.1^{B2}	38.4 ± 0.0^{B2}	40940.1 ± 0.1^{B2}
30	100	2.7 ± 0.0^{t}	523.6 ± 0.0^{C2}	23.2 ± 0.7^{m}	522.4 ± 0.0^{C2}	117.1 ± 0.1^{C2}	42.0 ± 0.0^{C2}	51886.1 ± 0.1^{C2}
Pleurotus ostreatus	*Pleurotus eryngii*							
25	25	1.2 ± 0.0^{u}	288.1 ± 0.0^{D2}	27.4 ± 0.9^{il}	720.3 ± 0.0^{D2}	272.2 ± 0.0^{D2}	9.4 ± 0.0^{D2}	45556.4 ± 0.1^{D2}
25	50	1.2 ± 0.0^{u}	268.1 ± 0.0^{E2}	19.2 ± 0.9^{n}	627.6 ± 0.0^{E2}	290.9 ± 0.0^{E2}	11.5 ± 0.0^{E2}	59790.0 ± 0.0^{E2}
25	100	1.1 ± 0.0^{C}	259.7 ± 0.0^{F2}	16.0 ± 0.8^{n}	523.7 ± 0.0^{F2}	247.9 ± 0.0^{F2}	15.1 ± 0.0^{F2}	70735.9 ± 0.0^{F2}
50	25	1.2 ± 0.0^{u}	295.5 ± 0.0^{G2}	20.6 ± 0.8^{mn}	576.0 ± 0.0^{G2}	188.2 ± 0.0^{G2}	6.5 ± 0.0^{G2}	45187.1 ± 0.1^{G2}
50	50	1.2 ± 0.0^{u}	275.6 ± 0.0^{H2}	12.5 ± 0.8^{r}	483.3 ± 0.0^{H2}	206.9 ± 0.0^{H2}	8.6 ± 0.0^{H2}	59420.6 ± 0.0^{H2}
50	100	1.1 ± 0.0^{D}	267.1 ± 0.0^{I2}	9.3 ± 0.7^{r}	379.5 ± 0.0^{I2}	163.8 ± 0.0^{I2}	12.2 ± 0.0^{I2}	70366.5 ± 0.1^{I2}
100	25	1.4 ± 0.0^{v}	285.7 ± 0.0^{J2}	17.5 ± 0.4^{n}	462.7 ± 0.0^{J2}	127.2 ± 0.0^{J2}	17.8 ± 0.0^{J2}	43717.9 ± 0.1^{J2}
100	50	1.4 ± 0.0^{v}	265.8 ± 0.0^{K2}	9.3 ± 0.4^{rs}	370.1 ± 0.0^{K2}	145.9 ± 0.0^{K2}	19.9 ± 0.0^{K2}	57951.4 ± 0.0^{K2}
100	100	1.3 ± 0.0^{E}	257.4 ± 0.0^{L2}	6.1 ± 0.2^{s}	266.2 ± 0.0^{L2}	102.9 ± 0.0^{L2}	23.5 ± 0.0^{L2}	68897.4 ± 0.0^{L2}

Values represent mean ± standard deviations of three independent measurements. Mean values in a column with the same letter do not differ significantly ($p > 0.05$). TSC – theoretical sample capacity; FRAP – ferric-reducing antioxidant power; DPPH – 2,2-Diphenyl-1-picrylhydrazyl radical scavenging activity; TPC – total phenolic content; TT – total tannins; TFC – total flavonoid content; AGE – advanced glycation end-product; AA – ascorbic acid; AH – aminoguanidine hydrochloride; GAE – gallic acid equivalent; TAE – tannic acid equivalent; QE – quercetin equivalent; PE – polysaccharide equivalent

and 7.5 mg/mL *L. edodes* + 15 mg/mL *F. velutipes* were identified as three best mushroom combinations that consistently demonstrated significant synergistic effects in most bioassays, particularly in the ferric reducing antioxidant power (FRAP), 2,2-diphenyl-1-picrylhydrazyl (DPPH), and total tannins (TT) assays. In addition, these mushroom combinations also showed minimal antagonism in the total phenolic content (TPC) when compared to the others. In the polysaccharide assay, the three mushroom combinations exhibited the lowest

synergistic effect. This characteristic is deemed beneficial, considering that a lower polysaccharide level is preferable for a diabetic individual. Beyond the observed synergistic effects, the selection criteria also considered the phytochemical values obtained in each bioassay. Remarkably, the three chosen combinations displayed some of the best values in the FRAP, DPPH, TPC, TT, polysaccharide and anti-glycation assays, marking them as superior in terms of their potential health benefits.

Based on synergism evaluation in the FRAP assay, most mushroom mixtures displayed synergistic interaction at low sample concentrations (Table 5). Out of them, the three selected mushroom mixtures (7.5 mg/mL *A. bisporus* + 15 mg/mL *F. velutipes*, 7.5 mg/mL *L. edodes* + 7.5 mg/mL *F. velutipes,* and 7.5 mg/mL *L. edodes* + 15 mg/mL *F. velutipes*) demonstrated synergistic FRAP interaction. However, their interaction depended on their concentrations, with antagonism arising in the samples with higher concentrations. This was evident in the mixtures of *A. bisporus* + *L. edodes, A. bisporus* + *P. ostreatus*, *A. bisporus* + *P. eryngii, L. edodes* + *P. ostreatus,* and *L. edodes* + *P. eryngii* (Table 5). A similar transition in antioxidant activity interaction was observed by Rúa *et al.* [50], where a higher concentration of carvacrol and thymol led to increased antagonism. This finding could be attributed to the oxidation of antioxidants with higher effectiveness by free radicals when compared to those with lower effectiveness [38]. Such

Table 4 Experimental sample capacity values for polyphenols, polysaccharides, antioxidant and anti-glycation activities in different mushroom combinations

Mushrooms mixtures (A+B), mg/mL		Antioxidant activity		Anti-glycation activity	Polyphenols			Polysaccharides, mg PE/100 g
Mushroom A	Mushroom B	FRAP, mmol Fe^{2+}/100 g	DPPH, mg AA/100 g	Anti-AGE value, mg AH/100 g	TPC, mg GAE/100 g	TT, mg TAE/100 g	TFC, mg QE/100 g	
Agaricus bisporus	*Lentinula edodes*							
7.5	7.5	7.3 ± 0.0^{B}	1025.5 ± 0.0^{a}	16.4 ± 0.8^{a}	1039.9 ± 0.0^{y}	499.2 ± 0.0^{c}	39.0 ± 0.0^{e}	18161.4 ± 0.0^{a}
7.5	15.0	7.0 ± 0.0^{C}	970.7 ± 0.0^{b}	8.8 ± 0.2^{b}	935.3 ± 0.0^{c}	420.3 ± 0.0^{d}	60.7 ± 0.0^{a}	17779.0 ± 0.0^{b}
7.5	30.0	6.2 ± 0.0^{a}	829.8 ± 0.0^{c}	4.8 ± 0.7^{c}	682.6 ± 0.0^{d}	250.2 ± 0.0^{e}	88.9 ± 0.0^{f}	17047.7 ± 0.0^{c}
15.0	7.5	6.8 ± 0.0^{D}	925.4 ± 0.0^{d}	9.1 ± 0.9^{bd}	842.0 ± 0.0^{e}	318.3 ± 0.0^{f}	52.8 ± 0.0^{g}	14178.4 ± 0.0^{d}
15.0	15.0	6.3 ± 0.0^{a}	880.7 ± 0.0^{e}	6.0 ± 0.8^{bc}	749.6 ± 0.0^{f}	241.6 ± 0.0^{g}	69.4 ± 0.0^{h}	14271.7 ± 0.0^{e}
15.0	30.0	5.5 ± 0.0^{b}	794.1 ± 0.0^{f}	4.7 ± 0.6^{bce}	564.8 ± 0.0^{g}	132.2 ± 0.0^{h}	78.4 ± 0.0^{i}	15661.5 ± 0.1^{f}
30.0	7.5	6.0 ± 0.0^{c}	946.7 ± 0.0^{g}	9.2 ± 0.7^{bd}	622.9 ± 0.0^{h}	211.4 ± 0.0^{i}	64.2 ± 0.0^{j}	10230.8 ± 0.0^{g}
30.0	15.0	6.0 ± 0.1^{c}	831.5 ± 0.0^{h}	8.1 ± 0.9^{bd}	560.8 ± 0.0^{i}	158.3 ± 0.0^{j}	60.3 ± 0.0^{k}	11072.2 ± 0.0^{h}
30.0	30.0	5.2 ± 0.1^{E}	743.7 ± 0.0^{i}	5.7 ± 0.7^{c}	444.0 ± 0.0^{j}	90.1 ± 0.1^{k}	95.1 ± 0.0^{l}	12837.5 ± 0.1^{i}
Agaricus bisporus	*Flammulina velutipes*							
7.5	7.5	7.6 ± 0.0^{F}	884.6 ± 0.0^{j}	16.8 ± 1.0^{a}	980.3 ± 0.0^{k}	562.84 ± 0.0^{l}	37.9 ± 0.0^{m}	5876.6 ± 0.0^{j}
7.5	15.0	7.1 ± 0.0^{G}	774.1 ± 0.0^{k}	11.0 ± 0.8^{bd}	836.8 ± 0.0^{l}	488.5 ± 0.0^{m}	59.3 ± 0.0^{n}	6660.1 ± 0.0^{k}
7.5	30.0	6.3 ± 0.0^{H}	754.6 ± 0.0^{l}	5.8 ± 0.6^{c}	608.7 ± 0.0^{m}	324.7 ± 0.0^{n}	72.4 ± 0.0^{o}	5865.4 ± 0.0^{l}
15.0	7.5	6.8 ± 0.0^{I}	828.0 ± 0.0^{m}	10.7 ± 0.8^{bd}	813.2 ± 0.0^{n}	366.2 ± 0.0^{o}	57.8 ± 0.0^{p}	10055.5 ± 0.0^{m}
15.0	15.0	6.6 ± 0.0^{J}	812.8 ± 0.0^{n}	5.7 ± 0.7^{bc}	729.6 ± 0.0^{o}	321.8 ± 0.0^{p}	47.7 ± 0.0^{q}	8171.2 ± 0.0^{n}
15.0	30.0	6.00 ± 0.0^{c}	772.4 ± 0.0^{o}	3.5 ± 0.5^{ce}	557.1 ± 0.0^{p}	182.2 ± 0.0^{q}	63.6 ± 0.0^{r}	7686.2 ± 0.1^{o}
30.0	7.5	6.23 ± 0.0^{a}	774.5 ± 0.0^{p}	12.9 ± 0.7^{d}	603.1 ± 0.0^{q}	218.7 ± 0.0^{r}	78.1 ± 0.0^{s}	8439.2 ± 0.0^{p}
30.0	15.0	6.1 ± 0.0^{c}	788.0 ± 0.0^{q}	10.8 ± 2.0^{bd}	541.3 ± 0.0^{r}	93.6 ± 0.1^{s}	65.7 ± 0.0^{t}	8628.3 ± 0.0^{q}
30.0	30.0	5.7 ± 0.0^{K}	729.3 ± 0.0^{r}	6.5 ± 0.7^{bc}	431.2 ± 0.0^{s}	82.0 ± 0.0^{t}	77.5 ± 0.0^{u}	7667.5 ± 0.0^{v}
Agaricus bisporus	*Pleurotus ostreatus*							
7.5	25.0	3.1 ± 0.0^{d}	3823.0 ± 0.0^{s}	6.9 ± 0.8^{bcd}	662.3 ± 0.0^{t}	427.8 ± 0.0^{u}	44.0 ± 0.0^{v}	41717.2 ± 0.0^{w}
7.5	50.0	2.4 ± 0.0^{e}	317.2 ± 0.0^{t}	4.0 ± 0.6^{c}	435.4 ± 0.0^{u}	270.2 ± 0.0^{v}	37.6 ± 0.0^{w}	35507.7 ± 0.1^{x}
7.5	100.0	2.5 ± 0.0^{j}	262.2 ± 0.0^{u}	2.3 ± 0.2^{ce}	249.0 ± 0.0^{v}	130.7 ± 0.0^{a}	38.1 ± 0.0^{x}	44466.7 ± 0.0^{y}
15.0	25.0	3.1 ± 0.0^{d}	434.5 ± 0.0^{v}	6.4 ± 0.6^{bc}	564.0 ± 0.0^{w}	293.6 ± 0.0^{w}	36.2 ± 0.0^{y}	25752.0 ± 0.0^{z}
15.0	50.0	2.4 ± 0.0^{ef}	340.2 ± 0.0^{w}	4.0 ± 0.2^{ce}	387.8 ± 0.0^{x}	191.1 ± 0.0^{b}	42.3 ± 0.0^{z}	34458.7 ± 0.0^{A}
15.0	100.0	2.5 ± 0.0^{fh}	301.2 ± 0.0^{x}	2.1 ± 0.3^{e}	225.2 ± 0.0^{b}	86.3 ± 0.1^{x}	50.8 ± 0.0^{A}	41683.5 ± 0.0^{B}
30.0	25.0	3.6 ± 0.0^{L}	525.9 ± 0.0^{y}	11.6 ± 0.1^{b}	446.4 ± 0.0^{z}	184.9 ± 0.0^{y}	71.8 ± 0.0^{B}	21415.2 ± 0.0^{C}
30.0	50.0	2.8 ± 0.0^{k}	412.4 ± 0.0^{z}	7.7 ± 0.5^{b}	327.2 ± 0.0^{A}	128.1 ± 0.0^{z}	57.9 ± 0.0^{C}	27305.1 ± 0.0^{D}
30.0	100.0	2.5 ± 0.0^{ghj}	338.4 ± 0.0^{A}	4.2 ± 0.3^{ce}	207.7 ± 0.0^{B}	67.2 ± 0.0^{A}	67.9 ± 0.0^{D}	30777.8 ± 0.0^{E}

Continuation of Table 4

Mushrooms mixtures (A+B), mg/mL		Antioxidant activity		Anti-glycation activity	Polyphenols			Polysaccharides, mg PE/100 g
Mushroom A	Mushroom B	FRAP, mmol Fe^{2+}/100 g	DPPH, mg AA/100 g	Anti-AGE value, mg AH/100 g	TPC, mg GAE/100 g	TT, mg TAE/100 g	TFC, mg QE/100 g	
Agaricus bisporus	*Pleurotus eryngii*							
7.5	25.0	3.5 ± 0.0^{M}	480.5 ± 0.0^{B}	24.0 ± 0.5^{f}	588.2 ± 0.0^{C}	360.7 ± 0.0^{B}	32.5 ± 0.0^{E}	55717.7 ± 0.1^{F}
7.5	50.0	2.9 ± 0.0^{k}	388.0 ± 0.0^{C}	13.4 ± 0.2^{ad}	412.2 ± 0.0^{D}	249.2 ± 0.0^{C}	23.2 ± 0.0^{F}	54517.1 ± 0.0^{G}
7.5	100.0	2.1 ± 0.0^{n}	321.5 ± 0.0^{D}	6.6 ± 0.2^{bc}	241.2 ± 0.0^{a}	130.6 ± 0.0^{a}	19.2 ± 0.0^{G}	52151.2 ± 0.0^{H}
15.0	25.0	3.9 ± 0.0^{N}	503.9 ± 0.0^{E}	18.5 ± 0.2^{a}	529.6 ± 0.0^{E}	266.7 ± 0.0^{D}	36.6 ± 0.0^{H}	40611.3 ± 0.1^{I}
15.0	50.0	3.0 ± 0.0^{m}	414.3 ± 0.0^{F}	11.5 ± 0.2^{bd}	375.0 ± 0.0^{F}	182.7 ± 0.0^{E}	27.5 ± 0.0^{I}	50293.2 ± 0.0^{J}
15.0	100.0	2.4 ± 0.0^{o}	347.2 ± 0.0^{G}	5.1 ± 0.1^{c}	217.3 ± 0.1^{G}	85.1 ± 0.1^{F}	23.8 ± 0.0^{J}	49786.6 ± 0.2^{K}
30.0	25.0	4.0 ± 0.0^{O}	589.2 ± 0.0^{H}	14.0 ± 0.3^{ad}	443.8 ± 0.0^{H}	186.9 ± 0.0^{G}	52.6 ± 0.0^{K}	30619.3 ± 0.0^{L}
30.0	50.0	3.2 ± 0.0^{P}	469.7 ± 0.0^{I}	8.9 ± 0.6^{b}	317.6 ± 0.0^{I}	122.1 ± 0.0^{H}	48.4 ± 0.0^{L}	40716.3 ± 0.0^{M}
30.0	100.0	2.3 ± 0.0^{Q}	371.8 ± 0.0^{J}	5.2 ± 0.2^{c}	205.5 ± 0.0^{J}	69.3 ± 0.0^{I}	28.4 ± 0.0^{b}	46121.4 ± 0.1^{N}
Lentinula edodes	*Flammulina velutipes*							
7.5	7.5	5.9 ± 0.0^{R}	1476.9 ± 0.0^{K}	60.4 ± 1.9^{h}	1105.4 ± 0.0^{K}	328.2 ± 0.0^{J}	8.7 ± 0.0^{M}	5792.6 ± 0.0^{O}
7.5	15.0	5.6 ± 0.0^{S}	1252.5 ± 0.0^{L}	36.5 ± 1.7^{i}	939.9 ± 0.0^{L}	313.1 ± 0.0^{K}	23.9 ± 0.0^{N}	9290.6 ± 0.0^{P}
7.5	30.0	5.5 ± 0.0^{I}	1076.1 ± 0.0^{M}	25.7 ± 0.9^{f}	646.1 ± 0.0^{M}	304.9 ± 0.0^{L}	60.7 ± 0.0^{a}	8238.4 ± 0.0^{Q}
15.0	7.5	5.5 ± 0.0^{bl}	1238.6 ± 0.0^{N}	40.2 ± 1.5^{j}	917.7 ± 0.0^{N}	261.0 ± 0.0^{N}	21.7 ± 0.0^{O}	16566.3 ± 0.0^{R}
15.0	15.0	5.5 ± 0.0^{b}	1088.1 ± 0.0^{O}	29.4 ± 2.3^{k}	800.2 ± 0.0^{O}	188.4 ± 0.0^{O}	39.6 ± 0.0^{P}	14397.6 ± 0.1^{S}
15.0	30.0	5.4 ± 0.0^{T}	972.4 ± 0.0^{P}	15.3 ± 1.0^{a}	575.7 ± 0.0^{P}	103.7 ± 0.1^{P}	60.0 ± 0.0^{c}	10923.0 ± 0.0^{T}
30.0	7.5	4.7 ± 0.0^{U}	886.1 ± 0.0^{Q}	22.3 ± 0.7^{f}	651.4 ± 0.0^{Q}	139.7 ± 0.0^{Q}	59.4 ± 0.0^{Q}	15088.8 ± 0.1^{U}
30.0	15.0	4.9 ± 0.0^{x}	844.6 ± 0.0^{R}	18.6 ± 0.8^{a}	578.3 ± 0.0^{R}	113.8 ± 0.0^{V}	60.0 ± 0.0^{c}	14906.0 ± 0.0^{V}
30.0	30.0	4.9 ± 0.0^{x}	771.7 ± 0.0^{S}	11.6 ± 0.9^{bd}	440.3 ± 0.0^{S}	77.6 ± 0.0^{W}	99.5 ± 0.1^{R}	12564.7 ± 0.0^{W}
Lentinula edodes	*Pleurotus ostreatus*							
7.5	25.0	2.2 ± 0.0^{pq}	615.4 ± 0.0^{T}	26.2 ± 1.0^{f}	680.7 ± 0.0^{T}	124.1 ± 0.0^{X}	29.0 ± 0.0^{S}	25314.5 ± 0.1^{X}
7.5	50.0	1.8 ± 0.0^{r}	392.1 ± 0.0^{U}	11.5 ± 0.2^{bd}	426.8 ± 0.0^{U}	101.7 ± 0.0^{Y}	42.1 ± 0.0^{T}	31419.6 ± 0.0^{Y}
7.5	100.0	2.1 ± 0.0^{o}	238.9 ± 0.0^{V}	6.6 ± 0.8^{c}	241.2 ± 0.0^{a}	119.7 ± 0.0^{Z}	79.7 ± 0.0^{U}	27301.7 ± 0.0^{Z}
15.0	25.0	2.6 ± 0.0^{hij}	616.5 ± 0.0^{W}	16.6 ± 0.4^{a}	615.3 ± 0.0^{V}	184.3 ± 0.0^{R}	29.3 ± 0.0^{V}	29445.8 ± 0.0^{A1}
15.0	50.0	1.8 ± 0.0^{r}	411.9 ± 0.0^{X}	10.2 ± 0.9^{bd}	393.0 ± 0.0^{W}	108.8 ± 0.0^{S}	40.8 ± 0.0^{d}	32030.6 ± 0.0^{B1}
15.0	100.0	2.0 ± 0.0^{t}	261.7 ± 0.0^{Y}	4.7 ± 0.6^{ce}	228.3 ± 0.0^{X}	56.6 ± 0.0^{T}	71.7 ± 0.0^{W}	34354.2 ± 0.0^{C1}
30.0	25.0	2.5 ± 0.0^{fgj}	564.3 ± 0.0^{Z}	10.0 ± 0.6^{bd}	468.8 ± 0.0^{Y}	88.7 ± 0.0^{U}	52.0 ± 0.0^{X}	29581.3 ± 0.0^{D1}
30.0	50.0	2.1 ± 0.0^{n}	409.0 ± 0.0^{A1}	6.4 ± 1.0^{bc}	335.7 ± 0.0^{Z}	62.1 ± 0.0^{A1}	51.0 ± 0.0^{Y}	28522.4 ± 0.0^{E1}
30.0	100.0	1.9 ± 0.0^{tu}	271.3 ± 0.0^{B1}	3.3 ± 0.3^{ce}	225.2 ± 0.0^{b}	42.9 ± 0.0^{B1}	74.9 ± 0.0^{Z}	29021.2 ± 0.1^{F1}
Lentinula edodes	*Pleurotus eryngii*							
7.5	25.0	2.5 ± 0.0^{gij}	728.6 ± 0.0^{C1}	23.0 ± 0.7^{f}	624.5 ± 0.0^{A1}	141.8 ± 0.0^{C1}	18.5 ± 0.0^{A1}	35956.9 ± 0.0^{G1}
7.5	50.0	2.0 ± 0.0^{t}	489.4 ± 0.0^{D1}	14.5 ± 0.8^{a}	415.6 ± 0.0^{B1}	110.9 ± 0.0^{D1}	35.1 ± 0.0^{B1}	40413.3 ± 0.0^{H1}
7.5	100.0	1.5 ± 0.0^{v}	355.4 ± 0.0^{E1}	8.7 ± 0.8^{bd}	230.0 ± 0.0^{C1}	85.4 ± 0.0^{E1}	37.2 ± 0.0^{C1}	33705.4 ± 0.0^{I1}
15.0	25.0	2.6 ± 0.0^{i}	696.7 ± 0.0^{F1}	23.3 ± 1.0^{f}	578.1 ± 0.0^{D1}	175.5 ± 0.0^{F1}	27.6 ± 0.0^{D1}	16566.3 ± 0.0^{J1}
15.0	50.0	2.0 ± 0.0^{t}	496.8 ± 0.0^{G1}	15.3 ± 0.7^{a}	373.9 ± 0.0^{E1}	103.6 ± 0.0^{G1}	29.5 ± 0.0^{E1}	14397.6 ± 0.1^{K1}
15.0	100.0	1.4 ± 0.0^{w}	368.3 ± 0.0^{H1}	8.6 ± 0.5^{bd}	222.3 ± 0.0^{F1}	56.0 ± 0.0^{H1}	33.4 ± 0.0^{F1}	10923.0 ± 0.0^{L1}
30.0	25.0	3.0 ± 0.0^{m}	617.7 ± 0.0^{I1}	18.1 ± 0.9^{g}	459.3 ± 0.0^{G1}	91.4 ± 0.1^{I1}	40.8 ± 0.0^{d}	15088.8 ± 0.1^{M1}
30.0	50.0	2.4 ± 0.0^{e}	500.5 ± 0.0^{J1}	12.4 ± 0.6^{d}	330.7 ± 0.0^{H1}	64.1 ± 0.0^{J1}	35.0 ± 0.0^{G1}	14906.0 ± 0.0^{N1}
30.0	100.0	1.8 ± 0.0^{rs}	350.5 ± 0.0^{K1}	7.4 ± 0.4^{bc}	207.0 ± 0.0^{I1}	38.1 ± 0.0^{K1}	43.7 ± 0.0^{H1}	12564.7 ± 0.0^{O1}
Flammulina velutipes	*Pleurotus ostreatus*							
7.5	25.0	1.9 ± 0.0^{tu}	510.6 ± 0.0^{L1}	22.3 ± 1.2^{f}	670.1 ± 0.0^{J1}	448.3 ± 0.0^{L1}	15.5 ± 0.0^{I1}	31488.1 ± 0.0^{P1}
7.5	50.0	1.5 ± 0.0^{v}	332.2 ± 0.0^{M1}	11.6 ± 0.5^{bd}	437.6 ± 0.0^{K1}	277.2 ± 0.0^{M1}	16.4 ± 0.0^{J1}	33609.6 ± 0.0^{Q1}
7.5	100.0	2.1 ± 0.0^{n}	220.3 ± 0.0^{N1}	6.0 ± 0.4^{bc}	249.8 ± 0.0^{L1}	136.8 ± 0.0^{N1}	38.6 ± 0.0^{K1}	36017.0 ± 0.0^{R1}
15.0	25.0	2.3 ± 0.0^{q}	549.9 ± 0.0^{O1}	19.3 ± 0.0^{g}	147.7 ± 0.0^{M1}	364.4 ± 0.0^{O1}	32.9 ± 0.0^{L1}	26150.8 ± 0.0^{S1}

End of Table 4

Mushrooms mixtures (A+B), mg/mL		Antioxidant activity		Anti-glycation activity	Polyphenols			Polysaccharides, mg PE/100 g
Mushroom A	Mushroom B	FRAP, mmol Fe^{2+}/100 g	DPPH, mg AA/100 g	Anti-AGE value, mg AH/100 g	TPC, mg GAE/100 g	TT, mg TAE/100 g	TFC, mg QE/100 g	
15.0	50.0	1.8 ± 0.0^{r}	352.9 ± 0.0^{P1}	11.5 ± 0.4^{ag}	116.6 ± 0.0^{N1}	228.5 ± 0.0^{P1}	28.5 ± 0.0^{M1}	33864.6 ± 0.1^{T1}
15.0	100.0	2.2 ± 0.0^{op}	249.8 ± 0.0^{Q1}	6.7 ± 0.4^{bd}	140.8 ± 0.0^{O1}	115.3 ± 0.0^{Q1}	54.7 ± 0.0^{N1}	33434.4 ± 0.0^{U1}
30.0	25.0	2.8 ± 0.0^{k}	591.4 ± 0.0^{V1}	14.7 ± 0.4^{a}	459.7 ± 0.0^{P1}	191.0 ± 0.0^{b}	43.5 ± 0.0^{O1}	22850.0 ± 0.0^{V1}
30.0	50.0	2.3 ± 0.0^{q}	425.7 ± 0.0^{W1}	10.2 ± 1.0^{bd}	327.7 ± 0.0^{Q1}	121.7 ± 0.0^{R1}	37.0 ± 0.0^{P1}	27892.7 ± 0.0^{W1}
30.0	100.0	2.2 ± 0.0^{pq}	313.1 ± 0.0^{X1}	4.3 ± 0.1^{ce}	214.2 ± 0.0^{R1}	80.0 ± 0.1^{S1}	59.0 ± 0.0^{Q1}	32366.4 ± 0.0^{X1}
Flammulina velutipes	*Pleurotus eryngii*							
7.5	25.0	2.1 ± 0.0^{n}	601.0 ± 0.0^{Y1}	18.0 ± 0.8^{ag}	632.5 ± 0.0^{S1}	259.1 ± 0.0^{T1}	13.0 ± 0.0^{R1}	41045.6 ± 0.0^{Y1}
7.5	50.0	1.7 ± 0.0^{y}	432.2 ± 0.0^{Z1}	16.6 ± 1.1^{ag}	413.4 ± 0.0^{T1}	244.1 ± 0.0^{U1}	17.3 ± 0.0^{S1}	46180.4 ± 0.0^{Z1}
7.5	100.0	1.4 ± 0.0^{w}	334.6 ± 0.0^{A2}	8.4 ± 0.1^{bd}	235.5 ± 0.0^{U1}	123.1 ± 0.0^{V1}	21.2 ± 0.0^{T1}	49527.2 ± 0.0^{A2}
15.0	25.0	2.6 ± 0.0^{zij}	644.8 ± 0.0^{B2}	21.8 ± 0.6^{f}	166.1 ± 0.0^{V1}	345.9 ± 0.0^{W1}	19.1 ± 0.0^{U1}	35028.6 ± 0.0^{B2}
15.0	50.0	2.0 ± 0.0^{nt}	479.3 ± 0.0^{C2}	15.3 ± 0.8^{ag}	130.8 ± 0.0^{W1}	205.0 ± 0.0^{X1}	22.3 ± 0.0^{V1}	41898.0 ± 0.0^{C2}
15.0	100.0	1.5 ± 0.0^{v}	362.1 ± 0.0^{D2}	7.7 ± 0.1^{bc}	99.9 ± 0.0^{X1}	85.6 ± 0.0^{Y1}	25.3 ± 0.0^{W1}	45319.0 ± 0.0^{D2}
30.0	25.0	3.1 ± 0.0^{dm}	686.7 ± 0.0^{E2}	18.1 ± 0.9^{ag}	459.3 ± 0.0^{Y1}	176.8 ± 0.0^{Z1}	34.9 ± 0.0^{X1}	25383.8 ± 0.0^{E2}
30.0	500.0	2.4 ± 0.0^{e}	523.5 ± 0.0^{F2}	12.4 ± 0.6^{d}	321.8 ± 0.0^{Z1}	90.0 ± 0.0^{A2}	30.1 ± 0.0^{Y1}	34147.1 ± 0.0^{F2}
30.0	100.0	1.7 ± 0.0^{rsy}	396.8 ± 0.0^{G2}	7.4 ± 0.6^{bc}	207.5 ± 0.0^{A2}	48.3 ± 0.0^{B2}	28.4 ± 0.0^{b}	39999.5 ± 0.1^{G2}
Pleurotus ostreatus	*Pleurotus eryngii*							
25.0	25.0	0.4 ± 0.0^{V}	341.3 ± 0.0^{H2}	19.3 ± 1.1^{ag}	471.4 ± 0.0^{B2}	317.3 ± 0.0^{C2}	16.6 ± 0.0^{Z1}	80089.3 ± 0.1^{H2}
25.0	50.0	0.5 ± 0.0^{W}	296.4 ± 0.0^{I2}	11.2 ± 0.3^{bd}	332.8 ± 0.0^{C2}	181.6 ± 0.0^{D2}	16.5 ± 0.0^{A2}	88115.0 ± 0.1^{I2}
25.0	100.0	0.6 ± 0.0^{X}	263.3 ± 0.0^{J2}	7.0 ± 0.1^{bc}	204.5 ± 0.0^{D2}	90.6 ± 0.0^{E2}	25.8 ± 0.0^{B2}	57946.4 ± 0.0^{J2}
50.0	25.0	1.0 ± 0.0^{z}	260.9 ± 0.0^{K2}	13.3 ± 0.7^{ad}	337.5 ± 0.0^{E2}	211.4 ± 0.0^{F2}	21.0 ± 0.0^{C2}	35169.9 ± 0.0^{K2}
50.0	50.0	1.0 ± 0.0^{zA}	228.2 ± 0.0^{L2}	9.9 ± 0.5^{bd}	265.4 ± 0.0^{F2}	159.0 ± 0.0^{G2}	25.0 ± 0.0^{D2}	40363.7 ± 0.1^{L2}
50.0	100.0	1.0 ± 0.0^{A}	215.8 ± 0.0^{R1}	6.3 ± 0.6^{bc}	184.3 ± 0.0^{G2}	81.3 ± 0.1^{H2}	24.9 ± 0.0^{E2}	55430.1 ± 0.1^{r}
100.0	25.0	3.6 ± 0.0^{Y}	197.3 ± 0.0^{S1}	7.2 ± 0.1^{bc}	211.3 ± 0.0^{H2}	107.8 ± 0.0^{I2}	49.7 ± 0.0^{F2}	38630.9 ± 0.2^{s}
100.0	50.0	2.6 ± 0.0^{hij}	195.2 ± 0.0^{T1}	5.9 ± 0.1^{bc}	190.2 ± 0.0^{I2}	98.9 ± 0.0^{J2}	45.8 ± 0.0^{G2}	42344.9 ± 0.1^{t}
100.0	100.0	1.6 ± 0.0^{iy}	191.4 ± 0.0^{U1}	5.4 ± 0.8^{c}	157.1 ± 0.0^{J2}	79.3 ± 0.0^{K2}	35.6 ± 0.0^{H2}	52385.5 ± 0.1^{u}

Values represent mean ± standard deviations of three independent measurements. Mean values in a column with the same letter do not differ significantly ($p > 0.05$) ESC – experimental sample capacity; FRAP – ferric-reducing antioxidant power; DPPH – 2,2-Diphenyl-1-picrylhydrazyl radical scavenging activity; TPC – total phenolic content; TT – total tannins; TFC – total flavonoid content; AGE – advanced glycation end-product; AA – ascorbic acid; AH – aminoguanidine hydrochloride; GAE – gallic acid equivalent; TAE – tannic acid equivalent; QE – Quercetin equivalent; PE – polysaccharide equivalent

interactions have been previously observed between the phenolic and flavonoid compounds such as anthocyanins and quercetin [38]. It is plausible that these flavonoids formed hydrogen bonds which reduced the availability of hydroxyl groups contributing to the flavonoids' antioxidant activity and ultimately led to an antagonistic effect [38].

In contrast to the FRAP, the combined mushroom mixtures predominantly showed either synergistic or additive interactions in the DPPH radical scavenging system. Different mechanisms, such as sacrificial oxidation, metal chelation, spatial distribution, regeneration, and mutual protection, may have contributed to the observed synergism [51]. Nevertheless, a transition from synergism to antagonism with increasing sample concentrations was apparent in the sample mixtures of *L. edodes* + *P. ostreatus, F. velutipes* + *P. ostreatus,* and *P. eryngii* + *P. ostreatus.* The most likely explanation for the above observation was that the phenolic antioxidants lose their activities at higher sample concentrations by acting as pro-oxidants [52]. It is noteworthy that the 7.5 mg/mL *L. edodes* +7.5 mg/mL *F. velutipes* mixture with the highest DPPH scavenging activity also possessed the highest TPC (Table 4). Further correlation analysis (Table 6) revealed a strong positive association between the TPC and the total antioxidant activity. This implies that the phenolic compounds partly contributed to the radical scavenging capacity of the edible mushrooms. The antioxidant interactions among the mushroom mixtures vary, depending on their chemical

Table 5 Synergism evaluation values of phytochemicals, polysaccharides, antioxidant and anti-glycation activities in different mushroom combinations

Mushrooms mixtures (A+B), mg/mL		Antioxidant activity		Anti-glycation activity	Polyphenols			Polysaccharides, mg PE/100 g
Mushroom A	Mushroom B	FRAP, mmol Fe^{2+}/100 g	DPPH, mg AA/100 g	Anti-AGE value, mg AH/100 g	TPC, mg GAE/100 g	TT, mg TAE/100 g	TFC, mg QE/100 g	
Agaricus bisporus	*Lentinula edodes*							
7.5	7.5	1.1	1.1	0.2	0.9	1.1	1.2	1.1
7.5	15.0	1.1	1.0	0.3	0.9	1.0	1.6	1.1
7.5	30.0	1.1	1.0	0.7	0.8	0.9	1.6	1.3
15.0	7.5	1.0	1.1	0.2	0.9	1.7	1.1	0.9
15.0	15.0	1.0	1.0	0.2	0.8	1.3	1.5	1.0
15.0	30.0	0.9	1.0	0.4	0.7	0.9	1.4	1.4
30.0	7.5	0.9	1.2	0.2	0.8	1.3	1.4	0.9
30.0	15.0	1.0	1.1	0.3	0.7	0.9	1.2	1.1
30.0	30.0	0.9	1.1	0.2	0.6	0.7	1.6	1.0
Agaricus bisporus	*Flammulina velutipes*							
7.5	7.5	1.3	1.1	0.2	0.8	0.9	0.6	0.7
7.5	15.0	1.3	1.0	0.2	0.8	0.9	1.3	0.8
7.5	30.0	1.2	1.0	0.4	0.8	0.8	1.0	0.8
15.0	7.5	1.0	1.0	0.2	0.8	1.6	1.5	1.2
15.0	15.0	1.1	1.1	0.3	0.8	1.4	0.8	1.2
15.0	30.0	1.1	1.1	0.2	0.7	1.1	1.1	1.1
30.0	7.5	1.0	1.0	0.5	0.8	1.2	1.5	1.0
30.0	15.0	1.0	1.1	0.6	0.7	0.3	0.9	1.2
30.0	30.0	1.0	1.1	0.8	0.6	0.5	1.3	1.1
Agaricus bisporus	*Pleurotus ostreatus*							
7.5	25.0	1.1	1.1	0.2	0.9	0.9	1.5	1.1
7.5	50.0	1.2	1.0	0.3	0.8	0.8	1.8	0.9
7.5	100.0	1.2	1.0	0.2	0.8	0.8	1.1	1.2
15.0	25.0	0.8	1.0	0.5	0.7	0.9	0.8	0.9
15.0	50.0	0.9	1.0	0.6	0.7	0.8	1.8	1.0
15.0	100.0	1.0	1.1	0.8	0.7	0.7	1.4	1.2
30.0	25.0	0.8	1.0	0.3	0.6	0.7	1.8	0.9
30.0	50.0	0.9	1.0	0.7	0.6	0.6	2.1	1.1
30.0	100.0	1.1	1.1	0.2	0.9	1.1	1.2	1.1
Agaricus bisporus	*Pleurotus eryngii*							
7.5	25.0	1.3	1.1	0.4	0.9	1.1	1.7	0.9
7.5	50.0	1.4	1.1	0.5	0.8	0.8	1.4	1.4
7.5	100.0	1.4	1.1	0.6	0.8	0.8	1.2	1.0
15.0	25.0	1.1	1.0	0.8	0.7	1.5	1.4	0.9
15.0	50.0	1.1	1.1	0.3	0.7	1.0	1.5	1.0
15.0	100.0	1.1	1.1	0.7	0.6	0.9	1.2	1.0
30.0	25.0	0.9	1.1	1.1	0.7	1.1	1.7	1.0
30.0	50.0	1.0	1.1	0.1	0.6	0.7	2.0	1.1
30.0	100.0	0.9	1.1	0.6	0.6	0.6	1.1	1.0
Lentinula edodes	*Flammulina velutipes*							
7.5	7.5	1.3	1.0	0.9	0.9	2.2	1.8	0.9
7.5	15.0	1.2	1.1	0.1	0.9	1.3	0.5	0.5
7.5	30.0	1.2	1.1	0.2	0.8	1.3	1.2	1.0

Continuation of Table 5

Mushrooms mixtures (A+B), mg/mL		Antioxidant activity		Anti-glycation activity		Polyphenols		Polysaccharides, mg PE/100 g
Mushroom A	Mushroom B	FRAP, mmol Fe^{2+}/100 g	DPPH, mg AA/100 g	Anti-AGE value, mg AH/100 g	TPC, mg GAE/100 g	TT, mg TAE/100 g	TFC, mg QE/100 g	
15.0	7.5	1.1	1.1	0.3	0.9	1.5	0.5	1.0
15.0	15.0	1.2	1.1	0.5	0.8	0.8	1.3	1.2
15.0	30.0	1.1	1.1	0.6	0.7	0.6	1.1	1.1
30.0	7.5	1.0	1.1	0.6	0.8	0.9	1.3	1.2
30.0	15.0	1.0	1.1	0.4	0.7	0.6	1.3	1.0
30.0	30.0	1.0	1.1	0.3	0.6	0.6	1.2	1.2
Lentinula edodes	*Pleurotus ostreatus*							
7.5	25.0	1.0	1.2	0.2	0.8	1.1	1.9	1.2
7.5	50.0	1.1	1.1	0.5	0.8	1.0	4.0	0.8
7.5	100.0	1.1	0.9	0.6	0.8	0.9	2.6	1.0
15.0	25.0	1.0	1.1	0.6	0.7	0.6	1.3	0.9
15.0	50.0	0.9	1.0	0.4	0.7	0.5	3.0	1.0
15.0	100.0	0.9	0.9	0.3	0.6	0.5	2.2	1.2
30.0	25.0	0.8	1.2	0.2	0.6	0.4	1.4	1.2
30.0	50.0	0.8	1.1	0.1	0.6	0.3	2.1	1.2
30.0	100.0	0.8	1.0	03	0.6	0.4	1.9	0.9
Lentinula edodes	*Pleurotus eryngii*							
7.5	25.0	1.2	1.1	0.4	0.8	1.4	3.5	0.9
7.5	50.0	1.2	1.1	0.3	0.8	0.7	4.5	0.9
7.5	100.0	1.1	1.1	0.2	0.7	0.6	3.2	0.8
15.0	25.0	1.0	1.0	0.1	0.8	1.2	1.9	0.9
15.0	50.0	0.9	1.1	0.3	0.6	0.6	2.2	1.7
15.0	100.0	0.9	1.1	0.8	0.6	0.5	2.2	1.2
30.0	25.0	0.9	1.1	1.1	0.7	0.8	1.3	1.0
30.0	50.0	0.9	1.2	1.5	0.6	0.4	1.4	1.1
30.0	100.0	0.9	1.1	2.1	0.6	0.4	1.6	1.0
Flammulina velutipes	*Pleurotus ostreatus*							
7.5	25.0	1.0	1.2	0.3	0.8	1.2	1.2	1.0
7.5	50.0	1.0	1.1	0.5	0.8	1.2	1.6	1.2
7.5	100.0	1.2	0.9	0.6	0.8	1.1	1.3	1.2
15.0	25.0	1.0	1.1	0.5	0.7	1.0	1.5	1.0
15.0	50.0	1.0	1.0	0	0.6	0.9	1.4	1.3
15.0	100.0	1.1	0.9	0.1	0.6	0.8	1.5	1.2
30.0	25.0	1.0	1.0	0.6	0.6	0.7	1.0	1.1
30.0	50.0	1.0	1.0	0.7	0.6	0.6	1.3	1.3
30.0	100.0	1.0	1.0	1.0	0.6	0.7	1.5	1.3
Flammulina velutipes	*Pleurotus eryngii*							
7.5	25.0	1.1	1.0	0.5	0.8	2.5	4.5	1.2
7.5	50.0	1.1	1.1	0	0.7	1.3	2.2	1.1
7.5	100.0	1.1	1.1	0.1	0.7	1.2	1.9	1.2
15.0	25.0	1.1	1.1	0.6	0.7	1.6	0.8	1.3
15.0	50.0	1.1	1.1	0.7	0.6	1.0	1.2	1.1
15.0	100.0	1.1	1.1	1.0	0.6	0.7	1.1	1.2
30.0	25.0	1.0	1.0	0.3	0.7	1.3	1.1	1.1
30.0	500.0	1.0	1.1	0	0.6	0.5	1.1	1.1
30.0	100.0	1.0	1.1	0.3	0.6	0.5	0.9	1.2

End of Table 5

Mushrooms mixtures (A+B), mg/mL		Antioxidant activity		Anti-glycation activity	Polyphenols			Polysaccharides, mg PE/100 g
Mushroom A	Mushroom B	FRAP, mmol Fe^{2+}/100 g	DPPH, mg AA/100 g	Anti-AGE value, mg AH/100 g	TPC, mg GAE/100 g	TT, mg TAE/100 g	TFC, mg QE/100 g	
Pleurotus ostreatus	*Pleurotus eryngii*							
25.0	25.0	0.8	1.1	0.1	0.7	1.2	1.6	2.0
25.0	50.0	0.9	1.1	1.1	0.6	0.7	1.4	2.3
25.0	100.0	0.9	1.1	0.9	0.6	0.6	1.4	1.5
50.0	25.0	0.8	1.1	0	0.6	1.0	2.4	1.1
50.0	50.0	0.9	1.0	0.1	0.6	0.8	2.6	1.2
50.0	100.0	0.9	1.0	0.6	0.6	0.6	2.1	1.7
100.0	25.0	0.9	0.9	0.5	0.6	0.9	1.9	1.4
100.0	50.0	0.9	1.0	1.1	0.6	0.7	1.9	1.5
100.0	100.0	0.8	1.0	0.9	0.6	0.8	1.5	2.0

The synergism evaluation values of 90 different mushroom mixtures across seven assays. SE – synergistic evaluation; FRAP – ferric-reducing antioxidant power; DPPH – 2,2-Diphenyl-1-picrylhydrazyl radical scavenging activity; TPC – total phenolic content; TT – total tannin; TFC – total flavonoid content

nature and on the reactivity of bioactive compounds that undergo polymerization and structural changes [9]. For instance, the radical scavenging capacity of phenolic compounds is closely linked to their hydrogen-donating ability: the more hydroxyl groups are present, the greater their free radical scavenging activity [39].

Anti-glycation interaction in different mushroom mixtures. We also found that most combined mushroom mixtures demonstrated antagonism in their anti-glycation activity (Table 5), except for several combined mixtures containing *P. ostreatus* and *P. eryngii* which displayed synergistic effects at higher sample concentrations. The synergism was evidenced by a marked reduction in the fluorescence signal associated with the formation of advanced glycation end-products. The anti-glycation activity of the mushrooms could be attributed to the presence of bioactive compounds such as t-cinnamic, ferulic, 4-hydroxybenzoic, p-coumaric, protocatechuic, and vanillic acids, as well as myricetins, in *P. ostreatus* [53, 54] and *P. eryngii* [54]. The effectiveness of these bioactive compounds (particularly, t-cinnamic, p-coumaric, protocatechuic, ferulic, and vanillic acids) in attenuating glycation has been corroborated in recent studies [53]. Our findings agree with those of Atta *et al.* [55], who reported an increase in dose-dependent synergism in the functional activities of natural polyphenolic extracts combined with cefixime.

Bioactive compound interactions in different mushroom mixtures. Due to the positive correlation between the total antioxidant capacity and the total phenolic content (TPC) in the combined mushroom mixtures (Table 6), we anticipated that increasing the proportion of an extract with a high phenolic content in a binary mixture would increase the overall TPC in the mushroom mixture. However, most mushroom mixtures showed antagonistic effects in the TPC with increasing sample concentrations (Table 5). The least antagonistic effect was displayed by three combined mushroom mixtures (7.5 mg/mL *A. bisporus* + 15 mg/mL *F. velutipes*, 7.5 mg/mL *L. edodes* + 7.5 mg/mL *F. velutipes,* and 7.5 mg/mL *L. edodes* + 15 mg/mL *F. velutipes*). This finding contradicted that of Benamar-Aissa *et al.* [52], who reported synergism in the antioxidant activity of the combined plant extracts, possibly due to different plant species. The above finding also suggested that increasing the biological diversity of a plant mixture may not always lead to synergism. A possible explanation would be the formation of complexes and adducts among the phenolic compounds, which reduces their antioxidant capacity [56].

The combination study based on the total tannin (TT) content revealed that the mixture of 7.5 mg/mL *A. bisporus* + 7.5 mg/mL *F. velutipes* had the highest synergistic antioxidant and TT values (Table 4). This mushroom mixture also recorded the highest ferric reducing antioxidant power (FRAP) value (7.6 mmol Fe^{2+}/100 g) (Table 3), partly due to the formation of new phenolic compounds [4]. Similarly, 7.5 mg/mL *A. bisporus* + 7.5 mg/mL *L. edodes* was ranked second in the TT (499.2 mg TAE/100 g) and FRAP (7.3 mmol Fe^{2+}/100 g) values (Table 4). The moderate positive correlation between total tannins and total antioxidant activity (Table 6) justified the antioxidant role of high molecular weight polyphenols in the mushroom mixtures.

Approximately 90% of the combined mushroom mixtures displayed synergism in the total flavonoid content

Table 6 Correlation and regression among bioactive compounds, antioxidant and anti-glycation variables

Assays	*r*	R^2	Significance
Between TPC and anti-oxidant activity			
TPC versus FRAP	0.753	0.567	****
TPC versus DPPH	0.825	0.680	****
Between TT and anti-oxidant activity			
TT versus FRAP	0.509	0.260	****
TT versus DPPH	0.473	0.224	****
Between TFC and anti-oxidant activity			
TFC versus FRAP	0.585	0.342	****
TFC versus DPPH	0.325	0.106	***
Between polysaccharides and anti-oxidant activity			
Polysaccharide versus FRAP	–0.644	0.414	****
Polysaccharide versus DPPH	–0.557	0.311	****
Between reducing power and radical scavenging activity			
FRAP versus DPPH	0.841	0.708	****
Between anti-oxidant activity and anti-glycation activity			
FRAP versus anti-glycation	0.048	0.002	n.s.
DPPH versus anti-glycation	0.421	0.177	****
Between polyphenols and anti-glycation activity			
TPC versus anti-glycation	0.469	0.220	****
TT versus anti-glycation	0.153	0.023	n.s.
TFC versus anti-glycation	–0.397	0.158	****
Polysaccharide versus anti-glycation	–0.154	0.024	n.s.
Between polyphenols and polysaccharide			
TPC versus TT	0.650	0.422	****
TPC versus TFC	0.129	0.017	n.s.
TPC versus polysaccharides	–0.545	0.297	****
TT versus TFC	–0.009	0.065	n.s.
TT versus polysaccharides	–0.161	0.026	n.d.
TFC versus polysaccharides	–0.349	0.122	***

The r value denotes the Pearson's correlation value and R^2 value denotes the coefficient of determination; the level of significance was expressed as either not significant – n.s., $p < 0.005$ (***), or $p < 0.001$ (****)

(TFC) (Table 5). The mushroom mixtures containing *P. ostreatus*, *P. eryngii,* or both exhibited double or quadruple synergism in the TFC. Flavonoids, particularly catechin, quercetin, and chrysin, are the primary phenolic compounds in *Pleurotus* spp. [19]. Flavonoids possess heterocyclic structures which confer antioxidant activity by enabling conjugation between the aromatic rings [57]. These aromatic rings allow delocalization of electrons within the molecules and create resonance structures [30]. Combining various aromatic compounds could delocalize the bioactive compounds via electron transfer, allowing for more efficient reactions with free radicals and thus resulting in a synergistic effect [30]. Given the inverse correlation found between total antioxidant activity and polysaccharides, we favored the mushroom mixtures with lower carbohydrate values and antagonistic effects on polysaccharides.

In general, the combined mushroom mixtures containing 7.5 mg/mL *A. bisporus* + 15 mg/mL *F. velutipes*, 7.5 mg/mL *L. edodes* + 7.5 mg/mL *F. velutipes,* and 7.5 mg/mL *L. edodes* + 15 mg/mL *F. velutipes* displayed synergism in most antioxidant variables, except for polysaccharides, TPC, and anti-glycation values. These mushroom mixtures presented relatively high TPC, antioxidant and anti-glycation properties (Table 4), as previously discussed. All the above findings collectively suggested that the antioxidant activities and interactions in the mushroom mixtures were not solely dependent on their bioactive components but also determined by their proportions within the mixture [52].

Correlation and principal component analysis. Table 6 presents the linear correlation and regression analysis of the investigated antioxidant and anti-glycation variables in individual and combined mushroom samples. To date, the relationship between antioxidant and anti-glycation activities in plant samples is yet to be studied extensively. A few studies have reported the absence of correlation between antioxidant activity and anti-glycation values [58], while others suggested that antioxidant compounds effectively inhibited advanced glycation end-products (AGEs) [27, 55]. Our study confirmed a moderate correlation between the 2,2-Diphenyl-1-picrylhydrazyl (DPPH) radical scavenging activity and anti-glycation activity ($r = 0.4211$, $p < 0.001$). However, a similar correlation between the ferric-reducing antioxidant power (FRAP) and anti-glycation activity was non-significant ($p > 0.05$). Intagliata *et al.* [58], on the other hand, reported no direct relationship between

the antioxidant and anti-glycation activities of resveratrol. The observed discrepancy may be explained by the distinct pathways involved in AGE formation, including lipid peroxidation and the Namiki and Wolff pathways, which include various precursors and intermediates not directly influenced by the antioxidant mechanisms [58].

Our study also showed that the total phenolic content (TPC) was positively correlated ($p < 0.001$) with both the DPPH radical scavenging ($r = 0.825$) and the FRAP ($r = 0.753$) variables, while a moderate correlation existed between the TPC and anti-glycation activity ($r = 0.469$). For polyphenols, total tannins (FRAP, $r = 0.509$ and DPPH, $r = 0.473$) and total flavonoids (FRAP, $r = 0.585$ and DPPH, $r = 0.325$) were positive correlated with total antioxidant activities in the mushroom samples. These findings agreed with the previous studies [59] which highlighted a similar role of phenolics and flavonoids in the mushrooms' antioxidant properties. On the contrary, the total flavonoid content was inversely correlated with anti-glycation activity ($r = –0.397$, $p < 0.001$), possibly due to the degradation of certain flavonoids (such as quercetin) by oxidation at a high sample concentration [60]. Besides, the mushrooms' polysaccharides were inversely correlated with the total antioxidant activity (FRAP, $r = –0.644$, $p < 0.001$; DPPH, $r = –0.557$, $p < 0.001$). This could be attributed to the fact that protein components and phenolic compounds, rather than carbohydrates, mainly contributed to the overall antioxidant effect in mushrooms [59]. In addition, a strong positive correlation between the FRAP and the DPPH radical scavenging activity ($r = 0.841$, $p < 0.001$) showed the mushrooms as good reducing agents and radical scavengers.

Finally, we performed the principal component analysis (PCA) to identify the key variables that influence the mushrooms' functional characteristics under study [61]. The variables under analysis included the antioxidant parameters (FRAP and DPPH radical scavenging), anti-glycation value, polyphenols (TPC, TT, TFC), and polysaccharides. As illustrated in Fig. 1, the PCA biplot provides an overview of the relationships, as well as a distinction, between the variables for both individual and combined mushroom samples. The first principal component (F1) accounts for 52.7% of the data's variability, predominantly capturing the variance in antioxidant attributes, polyphenols and polysaccharides. The second principal component (F2) explains another 23% of the data variance, aligning positively with the TFC and inversely with anti-glycation activities. F1 effectively segregates over half of the samples to its left. These samples are characterized by a higher carbohydrate composition, as can be seen in the mixtures with *P. ostreatus* and *P. eryngii*. In contrast, the right side of F1 is populated by the mixtures containing *F. velutipes, A. bisporus*, and *L. edodes*, which were associated with high antioxidant activity and phenolic content. The biplot positions polysaccharides on the left, indicating that the mushrooms with a higher carbohydrate content tend to show lower phenolic and antioxidant activity. This trend was sup-

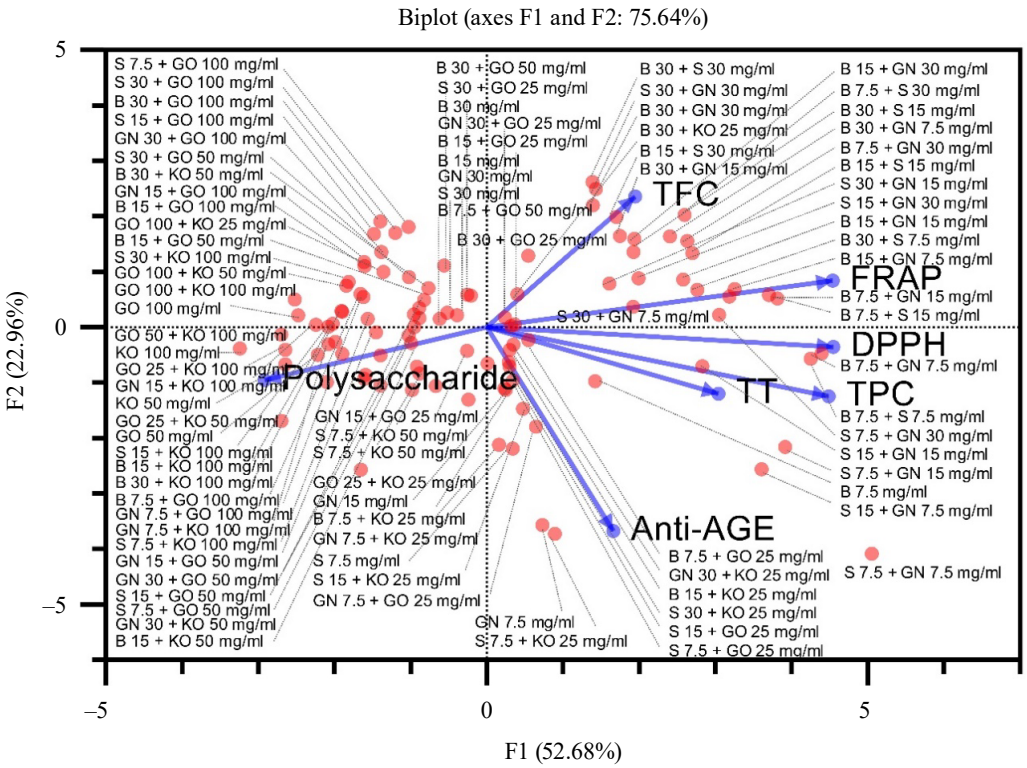

Figure 1 Biplot of different bioactive compounds with antioxidant and anti-glycation activities in the mushroom samples; FRAP – ferric-reducing antioxidant power; DPPH – 2,2-Diphenyl-1-picrylhydrazyl radical scavenging activity; TPC – total phenolic content; TT – total tannin; TFC – total flavonoid content; AGE – advanced glycation end-product; B – button; S – shiitake; GN – golden needle; GO – grey oyster; KO – king oyster

ported by previous studies highlighting that polyphenols were integral to the antioxidant properties of plant-based foods [61]. The biplot further revealed that certain mushroom combinations (particularly, 7.5 mg/mL *A. bisporus* + 15 mg/mL *F. velutipes*, 7.5 mg/mL *L. edodes* + 7.5 mg/mL *F. velutipes,* and 7.5 mg/mL *L. edodes* + 15 mg/mL) displayed synergistic interaction that enhanced the observed activity variables, as suggested by their proximity to the vectors representing antioxidant activities. In addition, the inverse relationship between the TFC and anti-glycation activity suggested a need for further exploration into the stability and function of flavonoids in the combined mushroom mixtures. The biplot also showed a strong positive relationship between the FRAP and DPPH radical scavenging activities. This reinforced the premise that the selected mushroom mixtures were not only effective reducing agents but also potent radical scavengers.

CONCLUSION

Our study showed that *Agaricus bisporus* exhibited the highest reducing potential, total flavonoids, and total tannin values, while *Lentinula edodes* demonstrated the strongest radical scavenging capacity among the five selected edible mushrooms. Although *Flammulina velutipes* displayed the highest total phenolic content and anti-glycation activity, the highest polysaccharide content was observed in *Pleurotus eryngii,* which had low antioxidant activity. The combinational study evaluated all three types of interactions: synergism, addition, and antagonism. Three mushroom mixtures with the best performance in antioxidant and anti-glycation values were 7.5 mg/mL *A. bisporus* + 15 mg/mL *F. velutipes*, 7.5 mg/mL *L. edodes* + 7.5 mg/mL *F. velutipes,* and 7.5 mg/mL *L. edodes* + 15 mg/mL *F. velutipes*. These findings suggested that the bioactivity interactions in the mushroom samples could induce both positive and negative impacts on their total antioxidant capacity and anti-glycation activity.

The polyphenols (phenolics, tannins, and flavonoids) were positively associated with the mushrooms' total antioxidant activity, while an inverse association occurred between the polysaccharides and total antioxidant activity, as well as between the flavonoids and anti-glycation activity. A nutrigenomic investigation needs to be conducted into specific molecular targets to understand the underlying mechanisms behind the observed synergistic and antagonistic effects in the edible mushroom mixtures. The utilization of an *in vivo* model could further confirm the synergistic and antagonistic interactions between the mushroom phytochemicals in the biological systems. Given the widespread consumption of mushrooms, understanding the antioxidant and anti-glycation interactions among their bioactive compounds could valorize these edible fungi as a worthy functional food for developing a potential nutraceutical product.

CONTRIBUTION

Tan Weng Kuan Kimberly conducted the investigation and formal analysis, as well as wrote the original draft. Phaik Har Yong wrote, reviewed, and edited the manuscript. Zhi Xiang Ng developed the study concept and methodology, supervised the research, and was involved in writing, reviewing, and editing of the manuscript.

CONFLICT OF INTEREST

The authors declare no conflict of interest.

REFERENCES

1. Juan CA, Pérez de la Lastra JM, Plou FJ, Pérez-Lebeña E. The chemistry of reactive oxygen species (ROS) revisited: Outlining their role in biological macromolecules (DNA, lipids and proteins) and induced pathologies. International Journal of Molecular Sciences. 2021;22(9):4642. https://doi.org/10.3390/ijms22094642
2. Sadeghi M, Miroliaei M, Kamyabiamineh A, Taslimi P, Ghanadian M. The impact of AGEs on human health and the development of their inhibitors based on natural compounds. Arabian Journal of Chemistry. 2023;16(10):105143. https://doi.org/10.1016/j.arabjc.2023.105143
3. Shields HJ, Traa A, Van Raamsdonk JM. Beneficial and detrimental effects of reactive oxygen species on lifespan: A comprehensive review of comparative and experimental studies. Frontiers in Cell and Developmental Biology. 2021;9:628157. https://doi.org/10.3389/fcell.2021.628157
4. Olszowy-Tomczyk M. Synergistic, antagonistic and additive antioxidant effects in the binary mixtures. Phytochemistry Reviews. 2020;19:63–103. https://doi.org/10.1007/s11101-019-09658-4
5. Rahaman MM, Hossain R, Herrera-Bravo J, Islam MT, Atolani O, *et al*. Natural antioxidants from some fruits, seeds, foods, natural products, and associated health benefits: An update. Food Science & Nutrition. 2023;11(4):1657–1670. https://doi.org/10.1002/fsn3.3217
6. Thompson AS, Tresserra-Rimbau A, Karavasiloglou N, Jennings A, Cantwell M, *et al*. Association of healthful plant-based diet adherence with risk of mortality and major chronic diseases among adults in the UK. JAMA Network Open. 2023;6(3):e234714. https://doi.org/10.1001/jamanetworkopen.2023.4714
7. Kozarski MS, Klaus AS, Vunduk JĐ, Jakovljević DM, Jadranin MB, *et al*. Health impact of the commercially cultivated mushroom Agaricus bisporus and wild-growing mushroom Ganoderma resinaceum – A comparative overview. Journal of the Serbian Chemical Society. 2020;85(6):721–735. https://doi.org/10.2298/JSC190930129K

8. Ćilerdžić J, Alimpić Aradski A, Stajić M, Vukojević J, Duletić-Laušević S. Do *Ganoderma lucidum* and *Salvia officinalis* extracts exhibit synergistic antioxidant and antineurodegenerative effects? Journal of Food Measurement and Characterization. 2019;13(4):3357–3365. https://doi.org/10.1007/s11694-019-00258-6
9. Fogarasi M, Nemeș SA, Fărcaș A, Socaciu C, Semeniuc CA, *et al*. Bioactive secondary metabolites in mushrooms: A focus on polyphenols, their health benefits and applications. Food Bioscience. 2024;62:105166. https://doi.org/10.1016/j.fbio.2024.105166
10. Ba DM, Gao X, Al-Shaar L, Muscat J, Chinchilli VM, *et al*. Prospective study of dietary mushroom intake and risk of mortality: Results from continuous National Health and Nutrition Examination Survey (NHANES) 2003–2014 and a meta-analysis. Nutrition Journal. 2021;20(1):80. https://doi.org/10.1186/s12937-021-00738-w
11. Chun S, Gopal J, Muthu M. Antioxidant activity of mushroom extracts/polysaccharides–Their antiviral properties and plausible antiCOVID-19 properties. Antioxidants. 2021;10(12):1899. https://doi.org/10.3390/antiox10121899
12. Das AK, Nanda PK, Dandapat P, Bandyopadhyay S, Gullón P, *et al*. Edible mushrooms as functional ingredients for development of healthier and more sustainable muscle foods: A flexitarian approach. Molecules. 2021;26(9):2463. https://doi.org/10.3390/molecules26092463
13. Okuda Y. Sustainability perspectives for future continuity of mushroom production: The bright and dark sides. Frontiers in Sustainable Food Systems. 2022;6:1026508. https://doi.org/10.3389/fsufs.2022.1026508
14. Liu X, Luo D, Guan J, Chen J, Xu X. Mushroom polysaccharides with potential in anti-diabetes: Biological mechanisms, extraction, and future perspectives: A review. Frontiers in Nutrition. 2022;9:1087826. https://doi.org/10.3389/fnut.2022.1087826
15. Thu ZM, Myo KK, Aung HT, Clericuzio M, Armijos C, *et al*. Bioactive phytochemical constituents of wild edible mushrooms from Southeast Asia. Molecules. 2020;25(8):1972. https://doi.org/10.3390/molecules25081972
16. Flores GA, Cusumano G, Venanzoni R, Angelini P. The glucans mushrooms: Molecules of significant biological and medicinal value. Polysaccharides. 2024;5(3):212–224. https://doi.org/10.3390/polysaccharides5030016
17. Liuzzi GM, Petraglia T, Latronico T, Crescenzi A, Rossano R. Antioxidant compounds from edible mushrooms as potential candidates for treating age-related neurodegenerative diseases. Nutrients. 2023;15(8):1913. https://doi.org/10.3390/nu15081913
18. Wang S, Meckling KA, Marcone MF, Kakuda Y, Tsao R. Synergistic, additive, and antagonistic effects of food mixtures on total antioxidant capacities. Journal of Agriculture and Food Chemistry. 2011;59(3):960–968. https://doi.org/10.1021/jf1040977
19. Yong PH, Zin Yii SL, Azzani M, Anbazhagan D, Ng ZX. Potential of medicinal plants to ameliorate retinopathy events in diabetes: A systematic review. Journal of Young Pharmacists. 2024;16(4):633–641. http://dx.doi.org/10.5530/jyp.2024.16.81
20. Yong PH, Yi WX, Azzani M, Guad RM, Ng ZX. Potential of medicinal plants to inhibit neurodegenerative activities in diabetes: A systematic review. Journal of Young Pharmacists. 2024;16(4):620–632. http://dx.doi.org/10.5530/jyp.2024.16.80
21. Mallard B, Leach DN, Wohlmuth H, Tiralongo J. Synergistic immuno-modulatory activity in human macrophages of a medicinal mushroom formulation consisting of Reishi, Shiitake and Maitake. 2019;14(11):e0224740. https://doi.org/10.1371/journal.pone.0224740
22. Midoh N, Miyazawa N, Eguchi F. Effects of a hot-water extract of porcini (*Boletus aestivalis*) mushrooms on the blood pressure and heart rate of spontaneously hypertensive rats. Bioscience, Biotechnology and Biochemistry. 2013;77(8):1769–1772. https://doi.org/10.1271/bbb.130085
23. Li Y, Chen J, Lai P, Tang B, Wu L. Influence of drying methods on the physicochemical properties and nutritional composition of instant *Tremella fuciformis*. Food Science and Technology. 2020;40(3):741–748. https://doi.org/10.1590/fst.20519
24. Tepsongkroh B, Jangchud K, Trakoontivakorn G. Antioxidant properties and selected phenolic acids of five different tray-dried and freeze-dried mushrooms using methanol and hot water extraction. Journal of Food Measurement and Characterization. 2019;13:3097–3105. https://doi.org/10.1007/s11694-019-00232-2
25. Ranneh Y, Abu Bakar MF, Ismail NA, Kormin F, Mohamed M, *et al*. Anti-aging and antioxidant of four traditional malaysian plants using simplex centroid mixture design approach. Saudi Journal of Biological Sciences. 2021;28(12):6711–6720. https://doi.org/10.1016/j.sjbs.2021.07.048
26. Gerhäuser C, Klimo K, Heiss E, Neumann I, Gamal-Eldeen A, *et al*. Mechanism-based in vitro screening of potential cancer chemopreventive agents. Mutation Research/Fundamental and Molecular Mechanisms of Mutagenesis. 2003;523–524:163–172. https://doi.org/10.1016/s0027-5107(02)00332-9
27. Ho KL, Yong PH, Lim SH, Ng ZX. *Peperomia pellucida* (L.) Kunth suppresses glycation-induced inflammatory response in human retinal pigment epithelial cell line ARPE-19 via JAK-STAT3 signaling. Archiv der Pharmazie. 2024;357(10):e2400299. https://doi.org/10.1002/ardp.202400299

28. Siddhuraju P, Manian S. The antioxidant activity and free radical-scavenging capacity of dietary phenolic extracts from horse gram (*Macrotyloma uniflorum* (Lam.) Verdc.) seeds. Food Chemistry. 2007;105(3):950–958. https://doi.org/10.1016/j.foodchem.2007.04.040

29. Masuko T, Minami A, Iwasaki N, Majima T, Nishimura S-I, *et al*. Carbohydrate analysis by a phenol-sulfuric acid method in microplate format. Analytical Biochemistry. 2005;339(1):69–72. https://doi.org/10.1016/j.ab.2004.12.001

30. Luís Â, Duarte AP, Pereira L, Domingues F. Interactions between the major bioactive polyphenols of berries: Effects on antioxidant properties. European Food Research and Technology. 2017;244(1):175–185. https://doi.org/10.1007/s00217-017-2948-5

31. Yong PH, New SY, Azzani M, Wu YS, Chia VV, *et al*. Potential of medicinal plants to ameliorate neovascularization activities in diabetes: A systematic review. Endocrine Regulations. 2024;58(1):26–39. https://doi.org/10.2478/enr-2024-0004

32. Hamwenye KKN, Ueitele ISE, Kadhila NP, Embashu W, Nantanga KKM. Towards medicinal tea from untapped Namibian Ganoderma: Phenolics and in vitro antioxidant activity of wild and cultivated mushrooms. South African Journal of Science. 2022;118(3/4):1–7. https://doi.org/10.17159/sajs.2022/9357

33. Hengst C, Werner S, Müller L, Fröhlich K, Böhm V. Determination of the antioxidant capacity: Influence of the sample concentration on the measured values. European Food Research and Technology. 2009;230(2):249–254. http://dx.doi.org/10.1007/s00217-009-1166-1

34. Mwangi RW, Macharia JM, Wagara IN, Bence RL. The antioxidant potential of different edible and medicinal mushrooms. Biomedicine & Pharmacotherapy. 2022;147:112621. https://doi.org/10.1016/j.biopha.2022.112621

35. Rangel-Vargas E, Rodriguez JA, Domínguez R, Lorenzo JM, Sosa ME, *et al*. Edible mushrooms as a natural source of food ingredient/additive replacer. Foods. 2021;10(11):2687. https://doi.org/10.3390/foods10112687

36. Ishioka Y, Yagi M, Ogura M, Yonei Y. Antiglycation effect of various vegetables: Inhibition of advanced glycation end product formation in glucose and human serum albumin reaction system. Glycative Stress Research. 2015;2(1):22–34. https://doi.org/10.24659/gsr.2.1_022

37. Reis FS, Martins A, Barros L, Ferreira ICFR. Antioxidant properties and phenolic profile of the most widely appreciated cultivated mushrooms: A comparative study between *in vivo* and *in vitro* samples. Food and Chemical Toxicology. 2012;50(5):1201–1207. https://doi.org/10.1016/j.fct.2012.02.013

38. Tashim NA-Z, Lim SA, Basri AM. Synergistic antioxidant activity of selected medicinal plants in Brunei Darussalam and its application in developing fortified pasta. Journal of the Science of Food and Agriculture. 2022;102(15):7331–7342. https://doi.org/10.1002/jsfa.12099

39. Maina S, Ryu DH, Bakari G, Misinzo G, Nho CW, *et al*. Variation in phenolic compounds and antioxidant activity of various organs of african cabbage (*Cleome gynandra* L.) accessions at different growth stages. Antioxidants. 2021;10(12):1952. https://doi.org/10.3390/antiox10121952

40. Shah P, Modi HA. Comparative study of DPPH, ABTS and FRAP assays for determination of antioxidant activity. International Journal for Research in Applied Science and Engineering. 2015;3(VI):636–641.

41. Rungratanawanich W, Qu Y, Wang X, Essa MM, Song B-J. Advanced glycation end products (AGEs) and other adducts in aging-related diseases and alcohol-mediated tissue injury. Experimental & Molecular Medicine. 2021;53(2):168–188. https://doi.org/10.1038/s12276-021-00561-7

42. Jud P, Sourij H, Therapeutic options to reduce advanced glycation end products in patients with diabetes mellitus: A review. Diabetes Research and Clinical Practice. 2019;148:54–68. https://doi.org/10.1016/j.diabres.2018.11.016

43. Sifat N, Lovely F, Zihad SMNK, Hossain MG, Shilpi JA, *et al*. Investigation of the nutritional value and antioxidant activities of common Bangladeshi edible mushrooms. Clinical Phytoscience. 2020;6:88. https://doi.org/10.1186/s40816-020-00235-3

44. Bach F, Zielinski AAF, Helm CV, Maciel GM, Pedro AC, *et al*. Bio compounds of edible mushrooms: *in vitro* antioxidant and antimicrobial activities. LWT. 2019;107:214–220. https://doi.org/10.1016/j.lwt.2019.03.017

45. Kozarski M, Klaus A, van Griensven L, Jakovljevic D, Todorovic N, *et al*. Mushroom *β*-glucan and polyphenol formulations as natural *immunity* boosters and *balancers*: Nature of the application. Food Science and Human Wellness. 2023;12(2):378–396. https://doi.org/10.1016/j.fshw.2022.07.040

46. Bristy AT, Islam T, Ahmed R, Hossain J, Reza HM, *et al*. Evaluation of total phenolic content, HPLC analysis, and antioxidant potential of three local varieties of mushroom: A comparative study. International Journal of Food Science. 2022;2022:3834936. https://doi.org/10.1155/2022/3834936

47. Nowak M, Tryniszewski W, Sarniak A, Wlodarczyk A, Nowak PJ, *et al*. Concentration dependence of anti- and pro-oxidant activity of polyphenols as evaluated with a light-emitting Fe^{2+}-EGTA-H_2O_2 system. Molecules. 2022;27(11):3453. https://doi.org/10.3390/molecules27113453

48. Zhou F, Jongberg S, Zhao M, Sun W, Skibsted LH. Antioxidant efficiency and mechanisms of green tea, rosemary or maté extracts in porcine *Longissimus dorsi* subjected to iron-induced oxidative stress. Food Chemistry. 2019;298:125030. https://doi.org/10.1016/j.foodchem.2019.125030

49. Ng ZX, Yong PH. Myricetin: The resources, biosynthesis, physicochemical, pharmacokinetic, bioavailability, pharmacology, and toxicology. In: Xiao, J, editor. Handbook of Dietary Flavonoids. Switzerland: Springer Cham; 2023. pp. 1–43. https://doi.org/10.1007/978-3-030-94753-8_19-1

50. Rúa J, del Valle P, de Arriaga D, Fernández-Álvarez L, García-Armesto MR. Combination of carvacrol and thymol: Antimicrobial activity against *Staphylococcus aureus* and antioxidant activity. Foodborne Pathogens and Disease. 2019;16(9):622–629. https://doi.org/10.1089/fpd.2018.2594

51. Farooq S, Sehgal A. Synergistic antioxidant interactions between green tea and *Ocimum gratissimum*. Asian Pacific Journal of Tropical Biomedicine. 2019;9(8):333–338. https://doi.org/10.4103/2221-1691.262081

52. Benamar-Aissa B, Gourine N, Ouinten M, Harrat M, Benarfa A, *et al*. Synergistic effects of essential oils and phenolic extracts on antioxidant activities responses using two *Artemisia species* (*A. campestris* and *A. herba alba*) combined with *Citrus aurantium*. Biocatalyst and Agricultural Biotechnology. 2023;47:102570. https://doi.org/10.1016/j.bcab.2022.102570

53. Macwan D, Patel HV. Inhibitory effect of bioassay-guided fractionation of mushroom (Pleurotus ostreatus) extract on fructose-induced glycated hemoglobin and aggregation in vitro. Pharmacognosy Research. 2023;15(4):776–784. https://doi.org/10.5530/pres.15.4.082

54. Cateni F, Gargano ML, Procida G, Venturella G, Cirlincione F, *et al*. Mycochemicals in wild and cultivated mushrooms: Nutrition and health. Phytochemical Reviews. 2022;21:339–383. https://doi.org/10.1007/s11101-021-09748-2

55. Atta S, Waseem D, Fatima H, Naz I, Rasheed F, *et al*. Antibacterial potential and synergistic interaction between natural polyphenolic extracts and synthetic antibiotic on clinical isolates. Saudi Journal of Biological Sciences. 2023;30(3):103576. https://doi.org/10.1016/j.sjbs.2023.103576

56. Yong KT, Yong PH, Ng ZX. Tomato and human health: A perspective from post-harvest processing, nutrient bioaccessibility, and pharmacological interaction. Food Frontiers. 2023;4(4):1702–1719. https://doi.org/10.1002/fft2.299

57. Huynh TTH, Wongmaneepratip W, Vangnai K. Relationship between flavonoid chemical structures and their antioxidant capacity in preventing polycyclic aromatic hydrocarbons formation in heated meat model system. Foods. 2024;13(7):1002. https://doi.org/10.3390/foods13071002

58. Intagliata S, Spadaro A, Lorenti M, Panico A, Siciliano EA, *et al*. In vitro antioxidant and anti-glycation activity of resveratrol and its novel triester with trolox. Antioxidants. 2021;10(1):12. https://doi.org/10.3390/antiox10010012

59. Chu M, Khan RD, Zhou Y, Agar OT, Barrow CJ, *et al*. LC-ESI-QTOF-MS/MS characterization of phenolic compounds in common commercial mushrooms and their potential antioxidant activities. Processes. 2023;11(6):1711. https://doi.org/10.3390/pr11061711

60. Bernacka K, Bednarska K, Starzec A, Mazurek S, Fecka I. Antioxidant and antiglycation effects of *Cistus* × *incanus* water infusion, its phenolic components, and respective metabolites. Molecules. 2022;27(8):2432. https://doi.org/10.3390/molecules27082432

61. Singh V, Singh J, Kushwaha R, Singh M, Kumar S, *et al*. Assessment of antioxidant activity, minerals and chemical constituents of edible mahua (*Madhuca longifolia*) flower and fruit of using principal component analysis. Nutrition & Food Science. 2020;51(2):387–411. https://doi.org/10.1108/NFS-04-2020-0129

ORCID IDs
Kimberly Weng Kuan Tan https://orcid.org/0009-0000-4185-8714
Phaik Har Yong https://orcid.org/0000-0002-5888-9856
Zhi Xiang Ng https://orcid.org/0000-0002-9423-7206

Foods and Raw Materials. 2026;14(2)

ISSN 2308-4057 (Print)
ISSN 2310-9599 (Online)

Research Article
Open Access

Available online at http://jfrm.ru/en
https://doi.org/10.21603/2308-4057-2026-2-678
https://elibrary.ru/DDIVNN

Controlled fermentation in improving the functional properties of *Brassica* with *Undaria*

Romina B. Parada[1,2,*], Emilio R. Marguet[1], Carmen A. Campos[3,4], Marisol Vallejo[1]

[1] National University of Patagonia San Juan Bosco, Chubut, Argentina
[2] National Scientific and Technical Research Council, Buenos Aires, Argentina
[3] University of Buenos Aires, Buenos Aires, Argentina
[4] Institute of Food Technology and Chemical Processes, CONICET – University of Buenos Aires, Buenos Aires, Argentina

* e-mail: parada.ro91@gmail.com

Received 12.07.2024; Revised 10.12.2024; Accepted 06.05.2025; Published online 21.08.2025

Abstract:
Fermentation improves the nutritional and sensory properties of food. Despite the challenges of fermenting algae individually, incorporating it into vegetable matrices offers a great opportunity for the development of new products.
This study aimed to investigate changes in the antioxidant capacity and total phenolic content of Chinese, white, and red cabbages supplemented with *Undaria pinnatifida* throughout controlled fermentation. These values were then compared to those for the respective spontaneous process (mixed models), as well as to previously published data on cabbage fermentation without algae (simple models). Controlled fermentation was carried out in a two-step process using previously selected autochthonous starter cultures. Antioxidant activity was measured using the DPPH scavenging assay and the CUPRAC assay. The total phenolic content was determined using the Folin-Ciocalteu method.
The total phenolic content varied across the different fermentation processes depending on the vegetable matrix. The antioxidant capacity was significantly higher in the controlled process than in the spontaneous one in all mixed models. Red cabbage with algae exhibited higher total phenolics and antioxidant capacity than white and Chinese cabbages with algae. Furthermore, all the mixed models showed higher or comparable total phenolics and antioxidant capacity compared to the respective simple models under similar controlled fermentation and extraction conditions, except for Chinese cabbage with *Undaria* under the CUPRAC method.
Controlled fermentation of the studied cabbages improved their antioxidant capacity to a greater extent than spontaneous in all mixed models. In general, the mixed models showed higher nutritional properties than the simple models.

Keywords: *Brassica*, family, *Lactiplantibacillus* sp., *Leuconostoc* sp., algae, total phenolics, antioxidant capacity, lactic fermentation

Funding: This study was supported by the National Agency for the Promotion of Research, Technological Development and Innovation (grants No. PICT-2019-01348 and PICT-2020-00437), the National Council for Scientific and Technical Research of the Argentine Republic (grant No. 11220150100042CO), and the University of Buenos Aires (grant No. 20020220200033BA).

Please cite this article in press as: Parada RB, Marguet E, Campos CA, Vallejo M. Controlled fermentation in improving the functional properties of *Brassica* with *Undaria*. Foods and Raw Materials. 2026;14(2):321–330. https://doi.org/10.21603/2308-4057-2026-1-678

INTRODUCTION

Undaria pinnatifida (Harvey) Suringar (*Laminariales*, *Phaeophyta*) is native to the coast of Japan, China, and Korea [1]. This is a highly invasive species that has colonized different coastal areas worldwide [2]. In 1992, it was introduced to the coast of Golfo Nuevo (Puerto Madryn, Argentina) by shipping traffic [3], causing a significant impact on the ecosystem [4]. Currently, this alga is distributed continuously from Puerto Deseado, Province of Santa Cruz, to the west bank of the San Matías Gulf, Province of Río Negro [4]. As its invasion progresses and abundance increases, its eradication becomes a challenge. In this sense, *Undaria* becomes an alternative source for use in industries such as textile, food, cosmetics, and pharmaceuticals, among others.

U. pinnatifida is mainly consumed in Asia as wakame (dried seaweed), which is used as a supplement in soups and salads [5]. This seaweed is a natural source of nutritional compounds such as fatty acids, dietary fiber, protein, polysaccharides, minerals, vitamins, and

Copyright © 2025, Parada *et al.* This is an open access article distributed under the terms of the Creative Commons Attribution 4.0 International License (https://creativecommons.org/licenses/by/4.0/), allowing third parties to copy and redistribute the material in any medium or format and to remix, transform, and build upon the material for any purpose, even commercially, provided the original work is properly cited and states its license.

sterols. Furthermore, this alga also contains bioactive compounds, such as carotenoids and polyphenols, with high antioxidant activity [6]. The nutritive properties of *U. pinnatifida* exert numerous health benefits, making the alga a potential source of functional foods [7]. These powerful properties may contribute to formulating innovative natural alternatives that cater to the customers' growing demand for healthier products.

In response to this trend, seaweed fermentation has gained considerable interest due to its potential to promote the products' nutritional and sensory qualities [8]. Furthermore, this biotechnological approach can enhance the products' safety, health-promoting properties, and overall appeal [9]. Uchida *et al.* [10] used starter cultures for *U. pinnatifida* fermentation and, in all the treatments relying on native microflora, observed spoilage due to a slight decrease in the pH values. *U. pinnatifida* contains complex polysaccharides, such as fucoidans, laminarins, and alginates, which are challenging to hydrolyze by the metabolism of lactic acid bacteria (LAB) [11]. However, it could be used in a seaweed-sauerkraut style product with a broader spectrum of bioactive molecules [12], generating an alternative for vegans, vegetarians, lactose intolerants, and those requiring a cholesterol-free diet.

Sauerkraut is mainly consumed in Central and Eastern Europe. This traditional food is developed through the natural lactic fermentation of shredded white cabbage (*Brassica oleracea* var. *capitata* f. *alba*) preserved in salt, with sugars transformed to lactic acid by the action of LAB. However, this fermentation process has been adapted globally to include different types of cabbage, such as red cabbage (*B. oleracea* var. *capitata* f. *rubra*) and Chinese cabbage (*B. rapa* ssp. *pekinensis* (Lour.) Hanelt). These vegetables differ in their physicochemical properties due to variations in structure and composition. White and red cabbage have a moderate carbohydrate content between 6 and 7 g/100 g FW (fresh weight), primarily as simple sugars, whereas Chinese cabbage has a lower carbohydrate concentration, 3 g/100 g FW [13, 14]. Chinese cabbage stands out for calcium and iron. In addition, it exhibits diversity in the polyphenolic contents, with the outer leaves having the highest levels, and related antioxidant activities. In contrast, white and red cabbage are rich in Vitamin C, potassium, and glucosinolates, with red cabbage containing additional anthocyanins and polyphenols, enhancing its antioxidant properties [14]. Nevertheless, the profile and concentration of phytochemicals are influenced by such factors as cultivar, agricultural conditions, and environment [15], while fermentation can variably affect total phenolic compounds and antioxidant activity [13].

Sauerkraut is recognized for its numerous health benefits, which stem from the fermentation process used to produce it [9]. For example, the hydrolysis of polyphenols, naturally present in raw cabbage, enhances antioxidant activity, and organic acid production inhibits the development of pathogenic or spoilage bacteria [16]. Red cabbage, which is also used to produce sauerkraut, has an advantage over white cabbage due to its high concentration of anthocyanins [17]. These naturally occurring flavonoid pigment molecules have health-promoting properties such as antioxidant, anti-inflammatory, and anti-diabetic activities [14, 17]. Chinese cabbage, widely used to make kimchi, is also linked to health-promoting properties. Its effectiveness has been demonstrated in treating obesity and irritable bowel syndrome [18].

While many manufacturers incorporate seaweed in sauerkraut, it is used primarily as a seasoning to enhance flavor rather than as a fundamental ingredient. Unlike cabbage, seaweed does not contain simple carbohydrates and has a high buffering capacity, which affects the lactic fermentation process [11]. The LAB, which play a key role in this fermentation, are Generally Recognized as Safe (GRAS) and have a Qualified Presumption of Safety (QPS) status according to the U.S. Food and Drug Administration (FDA) and the European Food and Safety Authority (EFSA), respectively [19, 20]. The species belonging to *Lactiplantibacillus*, *Lactobacillus*, *Leuconostoc*, *Enterococcus*, *Pediococcus*, and *Weissella* genera are often involved in the spontaneous fermentation of vegetables [21]. Even though spontaneous fermentation is widely used to preserve raw vegetables, it can exhibit alterations during the process. These risks include inadequate inhibition of pathogenic and spoilage microorganisms, the development of undesirable sensory characteristics, and changes in the nutrient composition [22].

An alternative approach is to use selected starter cultures for controlled fermentation. Unlike other traditional products (cheese, sausages), starter cultures in vegetable matrixes have only been developed in recent years [23]. Previous studies widely recommend autochthonous cultures, which adapt quickly to the fermentation matrix, guarantee safety, and improve the fermented product's sensory and functional properties [21, 23].

In this study, we aimed to assess the development of fermentation, total phenolic content, and antioxidant capacity (DPPH and CUPRAC methods) of three varieties of *Brassica* vegetables (Chinese cabbage, white cabbage, red cabbage) supplemented with *U. pinnatifida* (mixed models). The fermentation process was controlled and included two steps. In addition, we compared these parameters with those for the respective spontaneous processes (mixed models) and previously published data for cabbage fermentation without algae (simple models).

STUDY OBJECTS AND METHODS

Cabbage and *Undaria* samples. White cabbage (*Brassica oleracea* var. *capitata* f. *alba*), red cabbage (*B. oleracea* var. *capitata* f. *rubra*), and Chinese cabbage (*Brassica rapa* subsp. *pekinensis* (Lour.) Hanelt) were grown in autumn (March–June 2022) in the Valle Inferior del Río Chubut, Patagonia, Argentina (−43.31 latitude, −65.53 longitude). The cabbages were bought from a local farm and stored for less than three days at 4°C before fermentation. *U. pinnatifida* algae were

provided by the National Technological University, Puerto Madryn-Chubut, Argentina. The seaweeds were harvested in winter (July–August 2022) in the coastal areas of Golfo Nuevo at a depth of 3–15 m. After that, the samples were placed in sterile bags and stored at –20°C until used. Only the blade structure was used for the experiments.

Bacterial strains. *Leuconostoc mesenteroides* ssp. *jonggajibkimchii* RCTw1.1, *Ln. mesenteroides* ssp. *dextranicum* RBTw100, *Lactiplantibacillus plantarum* ssp. *argentoratensis* RBTw102*, L. plantarum* AKTw180, and *L. pentosus* AKTw332 were obtained from the Bacterial Biotechnology Laboratory (BBL, Trelew-Chubut, Argentina). The strains were previously isolated from the three spontaneously fermented cabbages and selected based on their technological properties [24]. They were propagated in MRS broth and incubated overnight at 30°C. After centrifugation (4,000×g, 10 min), the microbial cells were washed twice in a sterile saline solution (0.9% NaCl) before their inoculation.

Fermentation trial. A controlled fermentation trial was carried out with Chinese, white, and red cabbage supplemented with 20% (w/w) of shredded *U. pinnatifida* blades and 3% (w/w) of common salt. The cabbage heads were processed according to the methodology proposed by Parada *et al*. [24]. The algae blades were previously sanitized for 5 min (NaClO, 100 ppm) and washed. After removing the algae midrib, the blades were shredded for 2 min using a processor (Atma LM852, 400 Watt). Each salted cabbage jar (2 L) supplemented with the algae was heated at 100°C for 5 min and cooled at room temperature. The inoculation process was completed in two stages as described by Parada *et al.* [24]. At the same time, the spontaneous fermentation of Chinese, white, and red cabbage was carried out under the same conditions mentioned by Parada *et al*. [24]. The assays were performed in triplicate.

Fermentation parameters. The LAB count and pH were determined according to Parada *et al.* [24]. These parameters were monitored on days 0, 1, 3, 5, 10, 15, 20, 25, and 30 of the fermentation process. The results of the LAB count were expressed as CFU/g sample. All the trials were performed in triplicate.

Antioxidant analysis. ***Sample preparation.*** The samples collected on days 0, 1, 3, 5, 10, 15, 20, 25, and 30 were processed following the recommendation of Parada *et al.* [24]. They were dried at 37°C until constant weight and ground. Water extracts (1:10 dilution, w/v) were obtained using an autoclave at 120°C for 15 min. After centrifuging the extracts (12,000×g for 15 min), the supernatants were stored at –20°C.

Total phenolic content. The total phenolic content was determined by the Folin-Ciocalteu method with slight modifications [25]. For this, 50 µL of the extract was added to 100 µL of the Folin-Ciocalteu phenol reagent (Sigma Aldrich, St. Louis, USA). After 10 min incubation, 2 mL of Na_2CO_3 (1.0%, w/v) was added to the mixture and allowed it to react for 90 min. The absorbance was measured at 750 nm using a spectrophotometer (Jenway, ColePalmer, St. Neots, UK). Gallic acid was used as a standard (50–800 µg/mL). The results were expressed as milligram gallic acid equivalents per 100 g dry weight (mg GAE/100 g DW).

DPPH radical scavenging assay. The determination of DPPH (2.2-Diphenyl-1-picrylhydrazyl) radical scavenging capacities was carried out in agreement with the method outlined by Chen *et al.* [26] with some modifications. For this, 100 µL of the extract was mixed with a DPPH ethanolic solution (900 µL, 100 µM) (Sigma Aldrich, St. Louis, USA) and incubated at 25°C for 30 min in darkness. The absorbance was measured at 517 nm using a spectrophotometer, and ascorbic acid was used as a standard (10.5–176 µg/mL). The results were expressed as milligram ascorbic acid (Sigma Aldrich, St. Louis, USA) equivalents per 100 g dry weight (mg AAE/100 g DW).

Cupric reducing antioxidant capacity. The antioxidant capacity of the water extracts was determined according to the cupric reducing antioxidant capacity (CUPRAC) method described by Gouda and Amin [27] with minor modifications. The reaction mixture was prepared with 3 mL of an acetate buffer (50 mM, pH 5.0) (Sigma Aldrich, St. Louis, USA), 2 mL of a neocuproine solution (5 mM) (Sigma Aldrich, St. Louis, USA), and 1 mL of 0.01 M $CuCl_2$ (Cicarelli, Cordoba, Argentina). Then, 100 µL of the extract and 900 µL of the reaction mixture were mixed and manually shaken. After 1 h of incubation in darkness, the absorbance was measured at 450 nm in a spectrophotometer. Ascorbic acid was used as a standard (10.5–176 µg/mL). The results were expressed as mg AAE/100 g DW.

Statistical data analysis. The numerical values represent mean values derived from triplicate samples and presented as mean ± standard deviation. The data were subjected to two- and one-way ANOVA, and significant differences between the means ($p < 0.05$) were determined by Tukey's test. InfoStat statistical software was used for all data analysis.

RESULTS AND DISCUSSION

The fermentation processes were monitored through LAB count and pH measurement. The spontaneous and controlled fermentations exhibited a similar trend, namely an increase in LAB during the initial period and a decrease in pH caused by organic acid production during carbohydrate metabolism (Fig. 1).

The spontaneous processes exhibited pH of ≈ 6 and LAB counts of ≈ 4 log CFU/g at the initial time for the three cabbages. These results are consistent with prior research on fermented cabbage [23, 24]. The LAB population increased (≈ 7.8 log CFU/g), while the pH values dropped (≈ 4.6) after three days for all the cases. Later, the pH values continued to decrease in the three vegetables, exhibiting values of ≈ 4 after 30 days of the assay. At the same time, the LAB count dropped gradually to ≈ 6.6 log CFU/g after 15 and 20 days of fermentation in Chinese cabbage supplemented with *U. pinnatifida* and red cabbage supplemented with *U. pinnatifida*, respectively ($p \leq 0.05$). Meanwhile, the decrease of LAB was

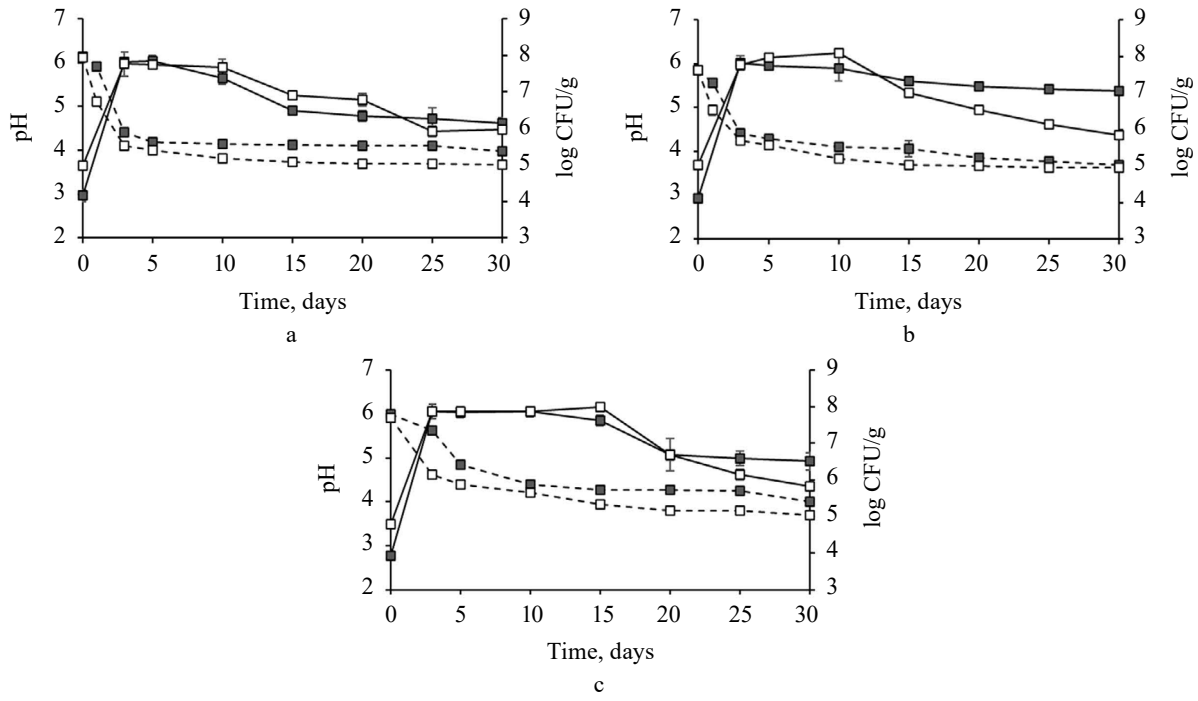

Figure 1 Total lactic acid bacteria (–) and pH changes (– – –) determined in cabbage during controlled (□) and spontaneous (■) fermentation of: a – Chinese cabbage, b – white cabbage, and c – red cabbage, each supplemented with *U. pinnatifida*

slighter in white cabbage supplemented with *U. pinnatifida* than in the other mixed models, at ≈ 7.3 log CFU/g after 15 days of the process ($p \leq 0.05$). These values remained stable until the end of the trial for the three vegetables ($p > 0.05$).

The controlled fermentation showed pH of ≈ 6 and LAB counts of ≈ 5 log CFU/g at the initial fermentation period. The indigenous biota was previously reduced by the thermal treatment, and a starter culture with *Leuconostoc* species was added, as suggested by Parada *et al*. [24]. This process showed a significant drop in pH after one day for all the cabbages supplemented with *Undaria* ($p \leq 0.05$). Recent studies have observed a notable decrease in pH levels when *Ln. mesenteroides* strains were used as starter cultures in vegetable fermentations [24, 28]. Later, a second starter culture with selected *Lactiplantibacillus* strains was added after three days, when the pH values dropped to ≈ 4, and the LAB cell counts increased to ≈ 8 log CFU/g. Then, LAB populations decreased gradually in all the samples, exhibiting values of ≈ 5.8 log CFU/g at the end of the assay. Meanwhile, the pH reached < 4, which was lower than in the spontaneous fermentation of the Chinese and red cabbages supplemented with *U. pinnatifida* ($p \leq 0.05$), with the white cabbage sample showing no differences ($p > 0.05$).

Previous reports showed a maximum LAB count on the seventh day of fermentation followed by a slight decrease [29, 30]. We observed a similar trend in the three mixed models. According to Brochu [29], the algae significantly affected LAB development in sauerkraut due to the presence of complex polysaccharides that are difficult to metabolize. However, the fermentation conditions in our study did not significantly affect LAB growth, which showed similar values to those obtained in the previously published research on cabbage fermentations (simple model) [24]. Even though *Undaria* did not provide fermentable carbohydrates to the matrices [29], it did increase the content and diversity of vitamins and minerals [31, 32], contributing to the complex nutritional requirement of LAB.

The beneficial effects of cabbage on human health have been linked to phytochemicals, mainly phenolic compounds [13]. Furthermore, previous reports stressed the effect of polyphenols in *U. pinnatifida* on human health, highlighting their antioxidant activity [6, 7, 31]. In this study, we evaluated the evolution of the total phenolic content in the water extracts obtained from the Chinese, white, and red cabbages supplemented with *Undaria* during spontaneous and controlled fermentation processes (Fig. 2).

The red cabbage sample showed higher values of the total phenolic content (TPC) than the Chinese and white samples, regardless of the fermentation type ($p \leq 0.05$). Similar differences were reported for the fresh samples of Chinese cabbage (347.46 mg GAE/100 g DW) [33], white cabbage (980–1220 mg GAE/100 g DW) [34], and red cabbage (1851 mg GAE/100 g DW) [35], as well as for their fermented samples without seaweed (simple model) [24]. The *Brassica* vegetables contain a great diversity of phenolic compounds, with over 30 anthocyanin pigments previously identified only in red cabbage extract [17].

The evolution of the TPC in the supplemented Chinese cabbage was similar between the spontaneous and controlled processes (Fig. 2a). The TPC increased during the first three days of fermentation and then

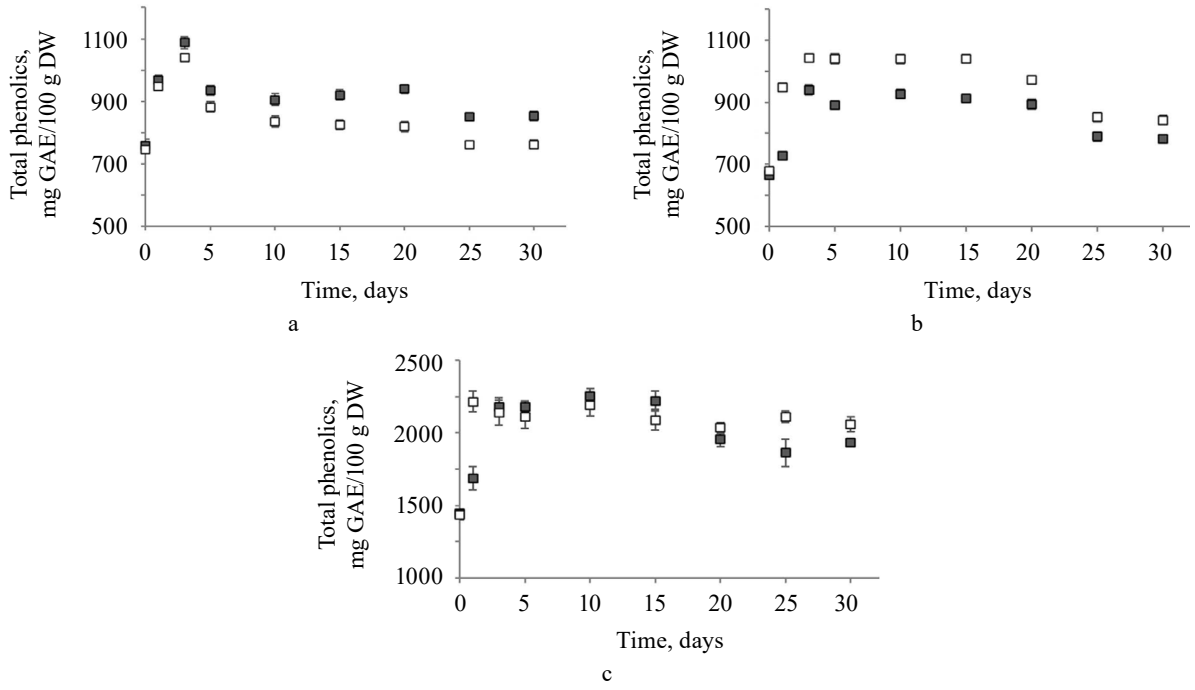

Figure 2 Total phenolic content in water extracts of: a – Chinese cabbage, b – white cabbage, and c – red cabbage during spontaneous (■) and controlled (□) fermentation, each supplemented with *U. pinnatifida*

gradually decreased ($p \leq 0.05$). The spontaneous fermentation exhibited higher TPC values than the controlled process at 30 days. When comparing both models (mixed and simple) during controlled fermentation, we found higher TPC values in the Chinese cabbage with *U. pinnatifida* compared to the one without the algae during the initial period. After that, the difference was no longer significant ($p > 0.05$) (761.9 ± 14.2 and 726.5 ± 25.1 mg GAE/100 g DW for the Chinese cabbage with and without *U. pinnatifida*, respectively, on day 30) [24].

The controlled fermentation of the white cabbage with *U. pinnatifida* showed a significant increase in the TPC on day one of the fermentation. These values remained stable until day 20 and then decreased until the end of the assay. However, the values were significantly higher than the ones for the fresh vegetables. Parada *et al.* [24] reported a similar tendency in the simple model of while cabbage (without algae) fermented with the same starter strains. Meanwhile, the spontaneous fermentation of the supplemented white cabbage showed a significant increase in the TPC on day three of the process, followed by a gradual decrease after 20 days. The controlled fermentation of the WCU showed higher TPC values than the spontaneous process after the end of the assay ($p \leq 0.05$). These TPC values were not significantly different ($p > 0.05$) from the values previously reported in the simple model of white cabbage (without algae) during the controlled process (842.9 ± 15.0 and 847.7 ± 37.5 mg GAE/100 g DW for the white cabbage with and without *U. pinnatifida*, respectively, on day 30) [24].

Lastly, the red cabbage supplemented with *U. pinnatifida* had significantly higher TPC values on the first day of controlled fermentation, and these values remained stable until day 30. Meanwhile, the spontaneous process showed similar TPC values after three days, with a decrease on day 20. However, the TPC values achieved on day 30 did not show a significant difference between both fermentations ($p > 0.05$). Parada *et al.* [24] reported lower TPC values in the simple model of red cabbage compared to the model mixed with *U. pinnatifida*. These differences were exhibited from day five to the end of the controlled fermentation trial ($p \leq 0.05$) (2059.4 ± 62.7 and 1657.1 ± 118.2 mg GAE/100 g DW for the red cabbage with and without *U. pinnatifida*, respectively, on day 30). Notably, the TPC values at the end of fermentation were higher than the ones for the fresh vegetables.

The TPC showed a similar tendency during controlled fermentation of the mixed models, increasing in the first days and, in some cases, decreasing significantly during the intermediate and final stages of the process. Meanwhile, the LAB count was high and pH values were low. However, variations in the TPC values were observed between the vegetable species. Hunaefi *et al.* [36], who used an *L. plantarum* strain to ferment red cabbage, reported a similar tendency. Furthermore, the controlled fermentations of the same vegetables (without adding *Undaria*), with the inoculation of identical starter cultures in a two-step process, exhibited similar variations [24]. Lactobacilli have been observed to exhibit a higher tolerance towards phenolic compounds compared to other bacterial groups.

The strains of *L. plantarum* stand out mainly because of their mechanisms for mitigating the impact of these metabolites [37]. In this study, the strains used in the second inoculum exhibited tolerance to phenol, gallic acid, and tannic acid, as well as pectinase and tannase activity in the previous trials [24]. Thus, the selected strains could contribute to the metabolization of the phenolics in the vegetable matrix (*U. pinnatifida* and *Brassica*), as well as an increment in organic acids, consequently causing a decrease in TPC values and an increase in other biologically active compounds [33, 36–38].

Undaria contains a wide variety of bioactive compounds, such as phenolic compounds and carotenoids [31, 32], while cabbages can also display glucosinolates, anthocyanins, and tocopherols [39]. However, most antioxidant compounds in plants are phenols that act as reducing agents, metal chelators, and singlet oxygen inhibitors [40].

In this study, we used the DPPH radical scavenging method and the CUPRAC reduction assay to determine the antioxidant capacity. These electron transfer-based methods are commonly employed to assess phenolic compounds' antioxidant capacity in various food sources [41]. Due to its versatility and accuracy, the DPPH radical scavenging assay is one of the most frequently used methods for evaluating antioxidant activity. This method is based on the electron donation of antioxidants that induces the loss of color in the DPPH. The change in the optical density is proportional to the antioxidant activity. The CUPRAC method, a variant of the FRAP (ferric reducing antioxidant power) assay, measures the reduction of cupric (Cu^{2+}) to cuprous (Cu^{+}) ions by antioxidants [41, 42].

The antiradical activity of the cabbage samples against the DPPH radical can be observed in Figure 3. In the Chinese cabbage supplemented with *U. pinnatifida*, the controlled fermentation exhibited a higher reducing power than the spontaneous process ($p \leq 0.05$) (Fig. 3a). The antioxidant capacity of the supplemented Chinese cabbage sample increased significantly during the first ten days, remaining stable until the end of the controlled process. In contrast, the spontaneous fermentation of the CCU did not exhibit significant variations during all the assays ($p > 0.05$). According to Parada *et al.* [24], the antioxidant capacity of the simple model of fermented Chinese cabbage was comparable with that of the mixed model (with *U. pinnatifida*) in similar conditions ($p > 0.05$) (219.1 ± 6.7 and 199.6 ± 7.7 mg AAE/100 g DW for the Chinese cabbage with and without *U. pinnatifida*, respectively, on day 30).

In the white cabbage supplemented with *U. pinnatifida*, the antioxidant capacity increased significantly during both fermentation types ($p \leq 0.05$). However, the controlled process exhibited a higher reducing power than the spontaneous fermentation ($p \leq 0.05$) (Fig. 3b). In the controlled and spontaneous processes, the extract displayed a significant increase in the reduction power until day ten and day three, respectively ($p \leq 0.05$). Then, the values obtained in each process remained stable until day 30.

The antioxidant capacity of the mixed model of white cabbage was higher than that of the simple model, as previously reported by [24], during both controlled processes ($p \leq 0.05$) (319.3 ± 12.3 and 202.9 ± 7.2 mg AAE/100 g DW for the white cabbage with and without *U. pinnatifida*, respectively, on day 30).

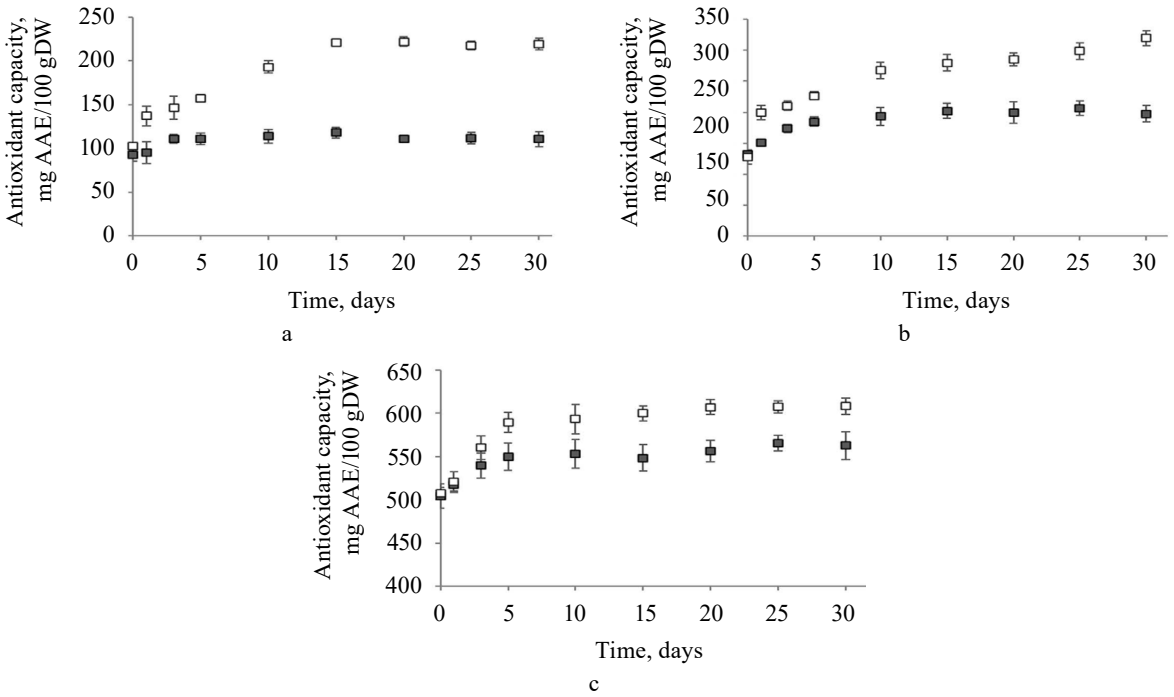

Figure 3 Antioxidant capacity (DPPH method) in water extracts of: a – Chinese cabbage, b – white cabbage, and c – red cabbage supplemented with *U. pinnatifida* during spontaneous (■) and controlled (□) fermentation

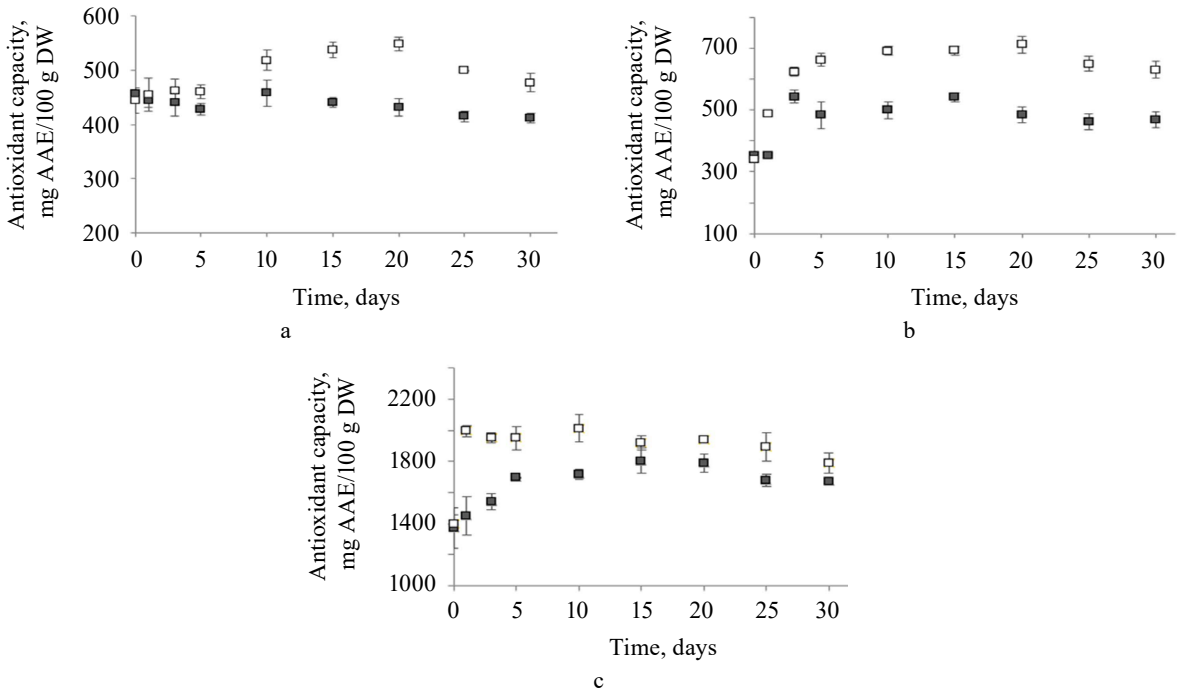

Figure 4 Antioxidant capacity (CUPRAC method) in water extracts of: a – Chinese cabbage, b – white cabbage, and c – red cabbage supplemented with *U. pinnatifida* during spontaneous (■) and controlled (□) fermentation

Regarding the supplemented red cabbage, its water extracts exhibited a higher reducing power than the CCU and WCU, regardless of the fermentation type. Parada *et al*. [24] showed a similar tendency between the fermented simple models. In the controlled fermentation, the supplemented red cabbage sample showed a significant increase in the antioxidant capacity until day five, with no changes observed afterwards. However, the spontaneous process showed an increase during the last period of the assay (25 days) (Fig. 3c). After 20 days, the controlled fermentation of the RCU exhibited higher antioxidant capacity than the spontaneous process ($p \leq 0.05$). The antioxidant capacity of the mixed model of red cabbage during controlled fermentation was comparable with the values previously reported for the simple model under similar process conditions [24] ($p > 0.05$) (608.0 ± 9.3 and 567.5 ± 16.8 mg AAE/100 g DW for the red cabbage with and without *U. pinnatifida*, respectively, on day 30).

In all the cases, the DPPH radical scavenging capacity increased as natural and inoculated fermentation progressed. This tendency agrees with the results reported by other authors [29, 38]. Furthermore, in all the cases, controlled fermentation displayed higher values of antioxidant activity than spontaneous fermentation at the end of the process ($p \leq 0.05$). According to previous reports, the inoculation with *L. plantarum* has a significative effect on antioxidant activity [24, 36]. *Lactiplantarum* spp. strains as a starter culture can hydrolyze the ester bonds in hydrolysable tannins, releasing potent antioxidant compounds, such as gallic acid and pyrogallol, through the tannase activity [38]. In addition, the pectinase activity can modify the texture of cabbage during fermentation [33], allowing the release of phenolic compounds.

The antiradical activity of the samples determined by the CUPRAC method can be observed in Fig. 4. The AAE values obtained through the CUPRAC assay were higher than those exhibited by DPPH in all the cases ($p \leq 0.05$). These dissimilarities were related to the capacity of each method. The CUPRAC method can detect hydrophilic and lipophilic antioxidants in the sample, whereas the DPPH method can determine only those molecules which are soluble in organic solvents [42].

The water extracts of the Chinese cabbage supplemented with *U. pinnatifida* exhibited different antioxidant capacity depending on the type of fermentation (Fig. 4a). In the controlled process, their antioxidant capacity increased significantly until day 20, followed by a decrease in the last days of the assay ($p \leq 0.05$). However, the spontaneous fermentation did not exhibit significant differences during the process ($p > 0.05$). The controlled fermentation displayed higher reduction power than the spontaneous process ($p \leq 0.05$). Parada *et al*. [24] reported higher antioxidant capacity in the Chinese cabbage simple model (without algae) than in the mixed model exposed to similar controlled fermentation conditions ($p \leq 0.05$) (477.6 ± 16.9 and 676.4 ± 37.2 mg AAE/100 g DW for the Chinese cabbage with and without *U. pinnatifida*, respectively, on day 30).

In the spontaneous and controlled fermentation, the white cabbage samples supplemented with *U. pinnatifida* showed increasing antioxidant capacity until day three

and day five, respectively ($p \leq 0.05$) (Fig. 4b). Then, the antioxidant capacity remained constant until day 30 ($p > 0.05$) for both types of fermentation. Notably, the controlled process displayed a higher antioxidant capacity than the spontaneous fermentation ($p \leq 0.05$). The mixed model of white cabbage exhibited a comparable evolution of the antioxidant activity to the one of the simple model, as previously reported [24], under similar controlled fermentation conditions ($p > 0.05$) (631.1 ± 28.5 and 694.5 ± 21.9 mg AAE/100 g DW for the white cabbage with and without *U. pinnatifida*, respectively, on day 30).

Lastly, the supplemented red cabbage extracts displayed similar tendencies during the controlled and spontaneous fermentation (Fig. 4c), with an increase in antioxidant capacity observed on days one and five, respectively ($p \leq 0.05$). Then, these values remained stable until day 30 in both processes ($p > 0.05$). Only during the initial stage did the controlled fermentation show higher values of the antioxidant capacity than the spontaneous process ($p \leq 0.05$). In the controlled fermentation, the mixed model of red cabbage showed similar values to those for the simple model, as previously reported [24], ($p > 0.05$) (1788.2 ± 63.2 and 1890.7 ± 77.4 mg AAE/100 g DW for the red cabbage with and without *U. pinnatifida*, respectively, on day 30).

The red cabbage supplemented with *U. pinnatifida* exhibited a higher antioxidant capacity than the supplemented Chinese and white cabbage samples, regardless of the fermentation type or method (DPPH/CUPRAC). This tendency was observed previously in the simple-model fermentations (without *Undaria*) [24]. Additionally, the antioxidant capacity of the fermented cabbages at the end of the assay was significantly higher than that for the fresh vegetables, except for the spontaneously fermented Chinese cabbage.

After analyzing the simple and mixed models under controlled fermentation conditions, we found that adding *U. pinnatifida* did not significantly increase the antioxidant capacity of any of the fermented vegetable matrices studied. However, *U. pinnatifida* supplementation in these types of matrices provides a greater diversity of available minerals and metabolic compounds (fucoidans, alginates, polyphenols, fucosterols, and carotenoids, among others) with nutritional, functional, and biological properties beneficial to the consumer's health [5, 6, 31]. Furthermore, controlled fermentation exhibited significantly higher antioxidant activity than spontaneous fermentation in all the mixed models, which was consistent with Parada's analysis [24] for the simple model.

CONCLUSION

Current research aimed to improve the nutritional properties of foods and develop functional foods through supplementation with seaweed to increase their health benefits. This study was the first to use *U. pinnatifida* in the fermentation of cabbages in Argentina. Notably, supplementing the vegetable matrix with 20% of the algae did not affect the development of lactic fermentation. While the total phenolic content varied between the cabbages and fermentation types, the antioxidant capacity obtained by both methods (DPPH and CUPRAC) was significantly higher in the controlled process than in the spontaneous one in all the cases. All the mixed models (Chinese, white, and red cabbages supplemented with *Undaria*) exhibited higher or similar values of the total phenolic content and antioxidant capacity compared to the simple models (without the algae) under similar conditions of controlled fermentation and extraction (except for the supplemented Chinese cabbage when applying the CUPRAC method). The high total phenolic content and antioxidant activity exhibited by the supplemented red cabbage sample suggest its use as a functional food product and a new alternative for consuming *Undaria* algae, taking advantage of the scarcely exploited resources on our coasts.

CONTRIBUTION

Romina B. Parada – conceptualization, methodology, software, validation, formal analysis, investigation, writing – reviewing and editing, and visualization. Emilio R. Marguet – conceptualization, methodology, formal analysis, investigation, and writing the original draft. Carmen A. Campos – conceptualization, software, formal analysis, writing-reviewing and editing. Marisol Vallejo – conceptualization, methodology, writing-reviewing and editing, and visualization. All the authors participated in developing the research concept and writing the original draft. All the authors approved the final version of the manuscript.

CONFLICT OF INTEREST

The authors declare that there is no conflict of interest.

REFERENCES

1. Saito Y. *Undaria*. In: Toshida J, Hirose H, editors. Advance of Phycology in Japan. Jena: Gustav Fischer Verlag; 1975. pp. 304–320.
2. Epstein G, Smale DA. *Undaria pinnatifida:* A case study to highlight challenges in marine invasion ecology and management. Ecology and Evolution. 2017;7(20):8624–8642. https://doi.org/10.1002/ece3.3430
3. Casas GN, Piriz ML. Surveys of *Undaria pinnatifida* (Laminariales, Phaeophyta) in Golfo Nuevo, Argentina. Hydrobiologia. 1996;326:213–215. https://doi.org/10.1007/BF00047809
4. Dellatorre FG, Orensanz JML, Amoroso R, Saravia J. Rapid expansion and potential range of the invasive kelp *Undaria pinnatifida* in the Southwest Atlantic. Aqua Invasions. 2014;9(4):467–478. https://elibrary.ru/UQMUYR

5. Wells ML, Potin P, Craigie JS, Raven JA, Merchant SS, *et al*. Algae as nutritional and functional food sources: Revisiting our understanding. Journal of Applied Phycology. 2017;29:949–982. https://doi.org/10.1007/s10811-016-0974-5
6. Kumar CS, Ganesan P, Suresh PV, Bhaskar N. Seaweeds as a source of nutritionally beneficial compounds – A review. Journal of Food Science and Technology. 2008;45(1):1–13. https:/elibrary.ru/LMMJAZ
7. Zhang H, Pang Z, Han C. *Undaria pinnatifida* (Wakame): A seaweed with pharmacological properties. Science International. 2014;2(2):32–36. https://doi.org/10.17311/sciintl.2014.32.36
8. Monteiro P, Lomartire S, Cotas J, Pacheco D, Marques JC, *et al*. Seaweeds as a fermentation substrate: A challenge for the food processing industry. Processes. 2021;9(11):1953. https://doi.org/10.3390/pr9111953
9. Di Cagno R, Filannino P, Gobbetti M. Fermented foods: Fermented vegetables and other products. In: Caballero B, Finglas PM, Toldrá F, editors. Encyclopedia of Food and Health. London: Academic Press; 2016. pp. 668–674. https://doi.org/10.1016/B978-0-12-384947-2.00284-1
10. Uchida M, Murata M, Ishikawa F. Lactic acid bacteria effective for regulating the growth of contaminant bacteria during the fermentation of *Undaria pinnatifida* (Phaeophyta). Fisheries Science. 2007;73:694–704. https://doi.org/10.1111/j.1444-2906.2007.01383.x
11. Uchida M, Miyoshi T. Algal fermentation – The seed for a new fermentation industry of foods and related products. Japan Agricultural Research Quarterly: JARQ. 2013;47(1):53–63. https://doi.org/10.6090/jarq.47.53
12. Skonberg DI, Fader S, Perkins LB, Perry JJ. Lactic acid fermentation in the development of a seaweed sauerkraut-style product: Microbiological, physicochemical, and sensory evaluation. Journal of Food Science. 2021; 86(2):334–342. https://doi.org/10.1111/1750-3841.15602
13. Manchali S, Murthy KNC, Patil BS. Crucial facts about health benefits of popular cruciferous vegetables. Journal of Functional Foods. 2012;4(1):94–106. https://doi.org/10.1016/j.jff.2011.08.004
14. Ağagündüz D, Şahin TÖ, Yılmaz B, Ekenci KD, Özer ŞD, *et al*. Cruciferous vegetables and their bioactive metabolites: From prevention to novel therapies of colorectal cancer. Evidence-Based Complementary and Alternative Medicine. 2022;2022:1534083. https://doi.org/10.1155/2022/1534083
15. Aires A, Fernandes C, Carvalho R, Bennett RN, Saavedra MJ, *et al*. Seasonal effects on bioactive compounds and antioxidant capacity of six economically important *Brassica* vegetables. Molecules. 2011;16(8)6816–6832. https://doi.org/10.3390/molecules16086816
16. Peñas E, Martínez-Villaluenga C, Pihlava JM, Frias J. Evaluation of refrigerated storage in nitrogen-enriched atmospheres on the microbial quality, content of bioactive compounds and antioxidant activity of sauerkrauts. LWT – Food Science and Technology. 2015;61(2):463–470. https://doi.org/10.1016/j.lwt.2014.11.049
17. Ghareaghajlou N, Hallaj-Nezhadi S, Ghasempour Z. Red cabbage anthocyanins: Stability, extraction, biological activities and applications in food systems. Food Chemistry. 2021;365:130482. https://doi.org/10.1016/j.foodchem.2021.130482
18. Song E, Ang L, Lee HW, Kim MS, Kim YJ, *et al*. Effects of kimchi on human health: A scoping review of randomized controlled trials. Journal of Ethnic Foods. 2023;10:7. https://doi.org/10.1186/s42779-023-00173-8
19. Wessels S, Axelsson L, Hansen EB, De Vuyst L, Laulund S, *et al*. The lactic acid bacteria, the food chain, and their regulation. Trends in Food Science & Technology. 2004;15(10):498–505. https://doi.org/10.1016/j.tifs.2004.03.003
20. Koutsoumanis K, Allende A, Alvarez-Ordóñez A, Bolton D, Bover-Cid S, *et al*. Update of the list of QPS-recommended biological agents intentionally added to food or feed as notified to EFSA 15: Suitability of taxonomic units notified to EFSA until September 2021. EFSA Journal. 2022;20(1):1–40. https://doi.org/10.2903/j.efsa.2022.7045
21. Torres S, Verón H, Contreras L, Isla MI. An overview of plant-autochthonous microorganisms and fermented vegetable foods. Food Science and Human Wellness. 2020;9(2):112–123. https://doi.org/10.1016/j.fshw.2020.02.006
22. Sajjad N, Rasool A, Bakr A, Fazili A, Bhat EA. Fermentation of fruits and vegetables a review. Plant Archives. 2020;20(2):1338–1342.
23. Di Cagno R, Coda R, De Angelis M, Gobbetti M. Exploitation of vegetables and fruits through lactic acid fermentation. Food Microbiology. 2013;33(1):1–10. https://doi.org/10.1016/j.fm.2012.09.003
24. Parada RB, Marguet E, Campos C, Vallejo M. Improved antioxidant capacity of three *Brassica* vegetables by two-step controlled fermentation using isolated autochthone strains of the genus *Leuconostoc* spp. and *Lactiplantibacillus* spp. Food Chemistry: Molecular Sciences. 2023;6:100163. https://doi.org/10.1016/j.fochms.2023.100163
25. Agbor G, Vinson JA, Donnelly PE. Folin-ciocalteau reagent for polyphenolic assay. International Journal of Food Science, Nutrition and Dietetics. 2014;3(8)147–156. https://doi.org/10.19070/2326-3350-1400028
26. Chen YC, Sugiyama Y, Abe N, Kuruto-Niwa R, Nozawa R, *et al*. DPPH radical-scavenging compounds from Dou-Chi, a soybean fermented Food. Bioscience, Biotechnology and Biochemistry. 2005;69(5):999–1006. https://doi.org/ https://doi.org/10.1271/bbb.69.999

27. Gouda AA, Amin AS. Copper (II) – neocuproine reagent for spectrophotometric determination of captopril in pure form and pharmaceutical formulations. Arabian Journal of Chemistry. 2010;3(3):159–165. https://doi.org/10.1016/j.arabjc.2010.04.004
28. Gardner NJ, Savard T, Obermeier P, Caldwell G, Champagne CP. Selection and characterization of mixed starter cultures for lactic acid fermentation of carrot, cabbage, beet and onion vegetable mixtures. International Journal of Food Microbiology. 2001;64(3):261–275. https://doi.org/10.1016/S0168-1605(00)00461-X
29. Brochu SD. Development and shelf life evaluation of a novel fermented seaweed sauerkraut utilizing commercially important maine seaweeds. Electronic Theses and Dissertations. 2018;2891.
30. Kim MJ, Lee HW, Lee ME, Roh SW, Kim TW. Mixed starter of *Lactococcus lactis* and *Leuconostoc citreum* for extending kimchi shelf-life. Journal of Microbiology. 2019;57:479–484. https://doi.org/10.1007/s12275-019-9048-0
31. Kolb N, Luciana V, Milanovi N, Stocchi V. Evaluation of marine algae wakame (*Undaria pinnatifida*) and kombu (*Laminaria digitata japonica*) as food supplements. Food Technology and Biotechnology, 2004;42:57–61.
32. Afonso NC, Catarino MD, Silva AMS, Cardoso SM. Brown macroalgae as valuable food ingredients. Antioxidants. 2019;8(9):365. https://doi.org/10.3390/antiox8090365
33. Seong GU, Hwang IW, Chung SK. Antioxidant capacities and polyphenolics of Chinese cabbage (*Brassica rapa* L. ssp. Pekinensis) leaves. Food Chemistry. 2016;199:612–618. https://doi.org/10.1016/j.foodchem.2015.12.066
34. Vicas SI, Teusdea AC, Carbunar M, Socaci SA, Socaciu C. Glucosinolates profile and antioxidant capacity of Romanian *Brassica* vegetables obtained by organic and conventional agricultural practices. Plant Foods for Human Nutrition. 2013;68:313–321. https://doi.org/10.1007/s11130-013-0367-8
35. Tabart J, Pincemail J, Kevers C, Defraigne JO, Dommes J. Processing effects on antioxidant, glucosinolate, and sulforaphane contents in broccoli and red cabbage. European Food Research and Technology. 2018;244:2085–2094. https://doi.org/10.1007/s00217-018-3126-0
36. Hunaefi D, Akumo DN, Smetanska I. Effect of fermentation on antioxidant properties of red cabbages. Food Biotechnology. 2013;27(1):66–85. https://doi.org/10.1080/08905436.2012.755694
37. López de Felipe F, de las Rivas B, Muñoz R. Molecular responses of *Lactobacilli* to plant phenolic compounds: A comparative review of the mechanisms involved. Antioxidants. 2022;11(1):18. https://doi.org/10.3390/antiox11010018
38. Hur SJ, Lee SY, Kim YC, Choi I, Kim GB. Effect of fermentation on the antioxidant activity in plant-based foods. Food Chemistry. 2014;160:346–356. https://doi.org/10.1016/j.foodchem.2014.03.112
39. Favela-González KM, Hernández-Almanza AY, De la Fuente-Salcido NM. The value of bioactive compounds of cruciferous vegetables (*Brassica*) as antimicrobials and antioxidants: A review. Journal of Food Biochemistry. 2020;3:e13414. https://doi.org/10.1111/jfbc.13414
40. Olszowy M. What is responsible for antioxidant properties of polyphenolic compounds from plants? Plant Physiology and Biochemistry. 2019;144:135–143. https://doi.org/10.1016/j.plaphy.2019.09.039
41. Shahidi F, Zhong Y. Measurement of antioxidant activity. Journal of Functional Foods. 2015;18(Part B):757–781. https://doi.org/10.1016/j.jff.2015.01.047
42. Apak R, Özyürek M, Güçlü K, Çapanoğlu E. Antioxidant activity/capacity measurement. 1. "Classification" with a capital letter, physicochemical principles, mechanisms, and electron transfer (ET)-based assays. Journal of Agricultural and Food Chemistry. 2016;64(5):997–1027. https://doi.org/10.1021/acs.jafc.5b04739

ORCID IDs
Romina B. Parada https://orcid.org/0000-0002-1089-9625
Emilio R. Marguet https://orcid.org/0000-0002-9790-8511
Carmen A. Campos https://orcid.org/0000-0002-6665-8011
Marisol Vallejo https://orcid.org/0000-0002-4393-3615

Foods and Raw Materials. 2026;14(2)

ISSN 2308-4057 (Print)
ISSN 2310-9599 (Online)

Research Article
Open Access

Available online at http://jfrm.ru/en
https://doi.org/10.21603/2308-4057-2026-2-675
https://elibrary.ru/GSYOUN

Empirical predicting permeate flux in skim milk microfiltration

Dmitriy S. Mamay*, Sergey P. Babenyshev, Ivan A. Evdokimov, Angelina V. Mamay, Vyacheslav A. Lisitsyn

North-Caucasus Federal University, Stavropol, Russia

* e-mail: dima-mamaj@yandex.ru

Received 14.01.2025; Revised 10.02.2025; Accepted 03.06.2025; Published online 11.09.2025

Abstract:
Native micellar casein and whey proteins can be obtained from skim milk by microfiltration. It is a popular method that yields high-quality dairy products. The article introduces an empirical approach to predicting the permeate flux value during microfiltration of skim milk. The research objective was to produce retentates with a target ratio of protein fractions in the true protein.

The physicochemical profile of skim milk was studied by standard methods. The experimental microfiltration involved a Spectrum Labs KrosFlo® Research II TFF System.

The research revealed the optimal operating modes of microfiltration and diafiltration for 0.1 μM membranes (Vladisart, Russia): operating pressure 0.2–2.5 bar, circulation rate 65–140 mL/min, temperature 50 ± 1°C. These modes made it possible to obtain a ratio of casein to whey proteins that exceeded 95:5. At the optimal ratios of pressure, circulation rate, and temperature, the amount of casein proteins grew from 2.2 to 4.0% in relation to whey proteins.

The grid search analysis confirmed a set of similar values of $Y = f(X_1, X_2, X_3)$. Microfiltration of skim milk proved effective at different combinations of pressure, circulation rate, and temperature, depending on the production technology, target products, and target ratio of mass fractions of casein and whey proteins in the true protein.

Keywords: Filtration, separation, dairy industry, casein, whey proteins, empirical approach

Funding: The research was supported by the Russian Science Foundation, grant no. 24-26-20084, https://rscf.ru/en/project/24-26-20084/

Please cite this article in press as: Mamay DS, Babenyshev SP, Evdokimov IA, Mamay AV, Lisitsyn VA. Empirical predicting permeate flux in skim milk microfiltration. Foods and Raw Materials. 2026;15(2):331–338. https://doi.org/10.21603/2308-4057-2026-2-675

INTRODUCTION

High-quality foods based on animal proteins have always attracted consumers' attention. The ever-growing demand creates prerequisites for new, more efficient processing methods. For instance, the method of membrane separation divides milk into fractions – casein, whey proteins, lactose, etc. – to be used in functional foods [1, 2]. Microfiltration-derived micellar casein is a popular raw material in the dairy industry. Microfiltration separates permeate from enzymes and technological ingredients to use it in cheese or cottage cheese formulations. Microfiltration-derived permeate contains all native whey proteins, including *β*-lactoglobulin and *α*-lactalbumin [3, 4]. However, the permeate flux depends on the properties of raw materials and membranes, as well as on the operating parameters. As the membrane fouling increases, the equipment performance goes down while the operating cost goes up. As a result, the method of membrane filtration has serious industrial limitations. Permeate flux, or the permeate flow rate, is the volume per unit of time and membrane area. Its prediction and optimization are crucial for effective baromembrane separation.

Forecasting and optimizing involve two methodological approaches. The first one relies on optimization and planning that determine the most effective processing options and the highest yield across the entire process line [5]. The main disadvantage of this approach is that the result depends on special criteria, e.g., the physicochemical profile of the raw materials, product range, environmental safety, etc. [6–8]. As a rule, these criteria are individual for each dairy enterprise. The second approach presupposes creating optimal conditions for microfiltration and fractionation by using selected modes of

Copyright © 2025, Mamay *et al.* This is an open access article distributed under the terms of the Creative Commons Attribution 4.0 International License (https://creativecommons.org/licenses/by/4.0/), allowing third parties to copy and redistribute the material in any medium or format and to remix, transform, and build upon the material for any purpose, even commercially, provided the original work is properly cited and states its license.

preparatory technological operations. The physicochemical and sensory indicators of the separation products should comply with the technological requirements. The main disadvantage is that the operating microfiltration parameters have to be optimized for many variables, and their characteristics depend on the specific requirements for the target product. The physicochemical properties of raw materials and membrane materials, as well as the membrane separation modes, are to be compared for a number of quantitative and quantitative characteristics.

To calculate the future permeate flux, dairy producers use different models for membrane processes [9–11]. The models can be divided into phenomenological (concentration polarization, osmotic counterpressure, series resistance, film, etc.) and non-phenomenological ones [12–16]. Phenomenological predictions are highly variable. However, they provide information on the effect of various parameters on the permeate flux, which is very important for scaling. Non-phenomenological models can be empirical, semi-empirical, or statistical. They are more accurate, but only if the membrane and raw materials have a limited physicochemical variability.

Some researchers believe that membrane separation can be optimized for only one type of liquid high-molecular polydisperse systems [17, 18]. The Box-Jenkins model of autoregressive integrated moving average (ARIMA) predicts the permeate flux for fruit juice ultrafiltration: it provides a 99% correlation between the precalculated and experimentally obtained values [19]. However, it does not reveal the patterns between the membrane characteristics, the physicochemical parameters of the system, the hydrodynamic phenomena during filtration, and the operating parameters.

The choice of microfiltration method for fractionating skim milk, i.e., technology, design, and processing conditions, relies on expert knowledge and empirical data [20–27]. Modeling also relies on the analysis of experimental data and is usually limited by the design of the baromembrane device and/or the operational properties of the membranes [28]. During skim milk microfiltration, the effect of each operating parameter on the permeate flux depends on the type of membrane [27]. As a result, no general theoretical model of skim milk microfiltration has been obtained so far to satisfy the needs of practical engineering.

The baromembrane separation of liquid polydisperse high-molecular systems is a complex of interrelated physical and chemical phenomena. Their accurate mathematical description is complicated by the complexity or impossibility of determining the patterns for individual stages and their interrelations. Considering the time-to-time variability, all membrane processes are stochastic, which means that the output values do not reliably correlate with the input ones.

Such processes are usually described by means of probabilistic statistics. Full factorial experiment is the most popular method applied to baromembrane separation of skim milk. It determines the effect of the main external deterministic factors on a certain optimization parameter. This method reveals the optimal permeability (Q) of microfiltration membranes for particular values of operating variables, e.g., pressure (ΔP) and the circulation rate of the separated system (V). Our own experience [29, 30] in experimental baromembrane separation of various dairy raw materials shows that the effect of pressure or circulation rate on the optimal permeability depends on the temperature of the separated system.

To predict the permeate flux during skim milk microfiltration, we used experimentally-obtained regression equations combined with grid search calculations. This approach makes it possible to justify the use of microfiltration separation at various combinations of variables, i.e., pressure, circulation rate, and temperature. In addition, our method also reveals the permeability values for microfiltration membranes.

The protocol was as follows:

– the determination of the operating parameters for the skim milk microfiltration, at which the true protein in the microfiltration retentate has at least a 95:5 mass fraction ratio of casein and whey proteins;

– the establishment of the conditions and modes for the skim milk microfiltration/diafiltration process to obtain a 97:3 ratio of casein to whey proteins in the true protein of the microfiltration retentate.

STUDY OBJECTS AND METHODS

The research involved skim milk supplied by a Stavropol milk factory (MK Stavropolsky LLC, Russia), pretreated as in State Standard GOST 31449-2013: Raw cow's milk. Technical conditions (Table 1).

The physicochemical profile of skim milk to be subjected to microfiltration was described using standard methods. An IRF-454B2M universal laboratory refractometer served to reveal the solids in the separated systems. A UDK-149 VELP protein analyzer determined the protein fractions in line with the Kjeldahl method. A Brand® Titrette® electronic titrator measured the titratable acidity.

All experiments were replicated 3–5 times; the standard research methods also contributed to the reliability and reproducibility (Table 2).

The microfiltration involved polymer membrane elements with an average pore diameter of 0.1 μM [29–34].

The separation process relied on a Spectrum Labs KrosFlo® Research II TFF System with a Novaset-LS-LHV SS316 cassette device (Fig. 1). The device

Table 1 Composition and physicochemical profile: Whole vs. skim milk ($p = 0.95$)

Indicator	Whole milk	Skim milk
Protein, %	3.0	3.0
Fat, %	3.80	0.02
Non-protein nitrogen, %	0.1	0.1
Lactose, %	4.7	4.7
Minerals, %	0.7	0.7
Titratable acidity, °T	17	17
Density, kg/m^3	1,029	1,034

Table 2 Research methods

Indicator	Source
Titratable acidity, °T	State Standard GOST 3624-92: Milk and dairy products. Titrimetric methods for acidity determination
Solids, %	State Standard GOST 34128-2017: Juice products. Refractometric method for determining the mass fraction of soluble solids
Total nitrogen, %	AOAC 991.20-1994 Nitrogen (total) in milk. Kjeldahl method
Casein nitrogen, %	AOAC 998.07 Casein nitrogen content of milk. Kjeldahl method, Indirect method
Whey protein nitrogen, %	Velp Scientifica Application Note F&F-K-005-2013/A1: Whey protein determination in milk according to the Kjeldahl method
Temperature, °C	State Standard GOST 26754-85: Milk. Methods of temperature measurement
Protein composition	State Standard GOST P 53761-2009: Milk. Identification of protein composition by electrophoresis in polyakrilamide gel

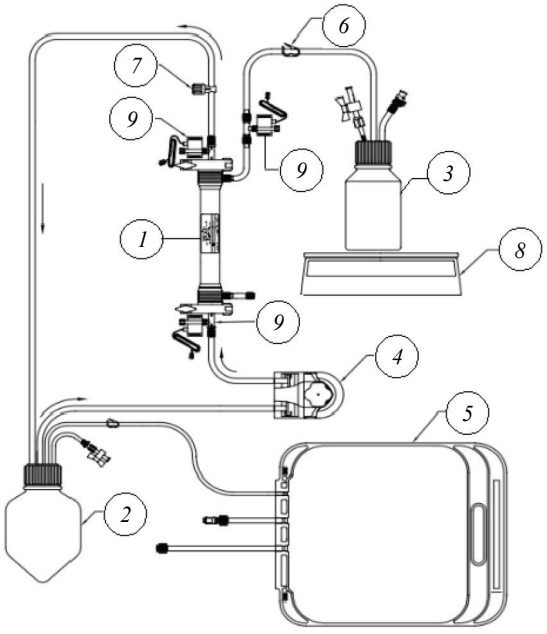

Figure 1 KrosFlo® Research IIi TFF tangential filtration system: *1* – membrane module, *2* – skim milk tank, *3* – permeate tank, *4* – peristaltic pump, *5* – control unit, *6* – permeate flow throttle, *7* – retentate flow throttle, *8* – permeate flow scale, *9* – pressure sensors

had 0.1 μM industrial polyethersulfone microfiltration membranes (Vladisart, Russia). The membranes worked at 40–55°C of skim milk and required 0.1–3.5 bar of operating pressure.

The mode limits were in line with the technical characteristics of the laboratory equipment:

– ΔP_{max} = 2.5 bar (Spectrum Labs KrosFlo® Research II TFF System);

– V_{max} = 140 mL/min (Spectrum Labs KrosFlo® Research II TFF System);

– $t_{max} \leq 50$°C.

Each experimental run lasted for 7–8 h; the permeate and the retentate returned to the initial tank after each processing circle. To measure the effect of pressure (ΔP) and circulation rate (V) on the optimal membrane permeability (Q), Stage 1 followed a 2^2 full factorial experiment (Table 3) [35]. We defined permeate flux J by weighing the permeate on a digital scale. The Eq. (1) was as follows:

$$J = \frac{W_p}{\tau \times A_p} \quad (1)$$

where W_p is the weight of the permeate that went through the membrane per unit of time τ; A_p is the operating area of the membrane surface.

The amount of permeate was checked every 5 min with an accuracy of ± 0.1 g at a constant temperature of the separated system t_1 = 50 ± 1°C.

Stage 2 yielded a matrix for regression equation with various pressures (ΔP), circulation rates (V), and temperatures (t) at a constant solids mass fraction in the separated system (Table 4).

The laboratory work was divided into the following stages to obtain retentate with a 95:5 ratio of casein to whey proteins:

1. We filtered skim milk through 0.1 μM membranes in a closed cycle for 7–8 h to achieve the maximal value of membrane selectivity for casein. After that, we continuously removed permeate at a concentration factor of 3–6. The main operating parameters corresponded to 2^2 or 2^3 full factorial experiments.

2. The microfiltered retentate and permeate were tested for mass fractions of total protein, casein, and whey proteins in the true protein. The mass fraction of true protein in each sample was the difference in the mass fractions of total and non-protein nitrogen.

3. The mass fractions of total, casein, and whey proteins in the true protein in the retentates and permeates were summarized in tables.

To obtain a microfiltration retentate with a 96:4 ratio of casein to whey proteins in the true protein, we planned and performed the following stages:

1. We microfiltered the skim milk in a closed cycle for 7–8 h to reach the maximal value of the membrane selectivity index for casein. Then, we continued to remove the permeate at a concentration factor of 3–6. The operating parameters followed a 2^3 full factorial experiment.

2. Upon completion, we mixed the microfiltered retentate with deionized water at a ratio of 1.0:1.0–3.0. The diafiltration involved the same basic parameters as microfiltration: the permeate was removed until the concentration factor was 3–6.

Table 3 Matrix for 2^2 full factorial experiment

Indicators		Basic level	Variability interval	Bottom level	Top level	Variable
Pressure, bar	Natural value	1.6	1.4	0.2	2.5	X_1
	Encoded value, X_1	0	–	–1	+1	
Circulation rate, mL/min	Natural value	105	35	70	140	X_2
	Encoded value, X_2	0	–	–1	+1	

Table 4 Matrix for 2^3 full factorial experiment

Indicators		Basic level	Variability interval	Bottom level	Top level	Variable	Conversion formula
Pressure (ΔP), bar	Natural value	1.6	1.4	0.2	2.5	X_1	$=\frac{\Delta P-1.6}{1.4}$
	Encoded value, X_1	0	–	–1	+1		
Circulation rate (V), mL/min	Natural value	105	35	70	140	X_2	$=\frac{V-105}{35}$
	Encoded value, X_2	0	–	–1	+1		
Temperature (t), °C	Natural value	40	10	30	50	X_3	$=\frac{t-50}{10}$
	Encoded value, X_3	0	–	–1	+1		

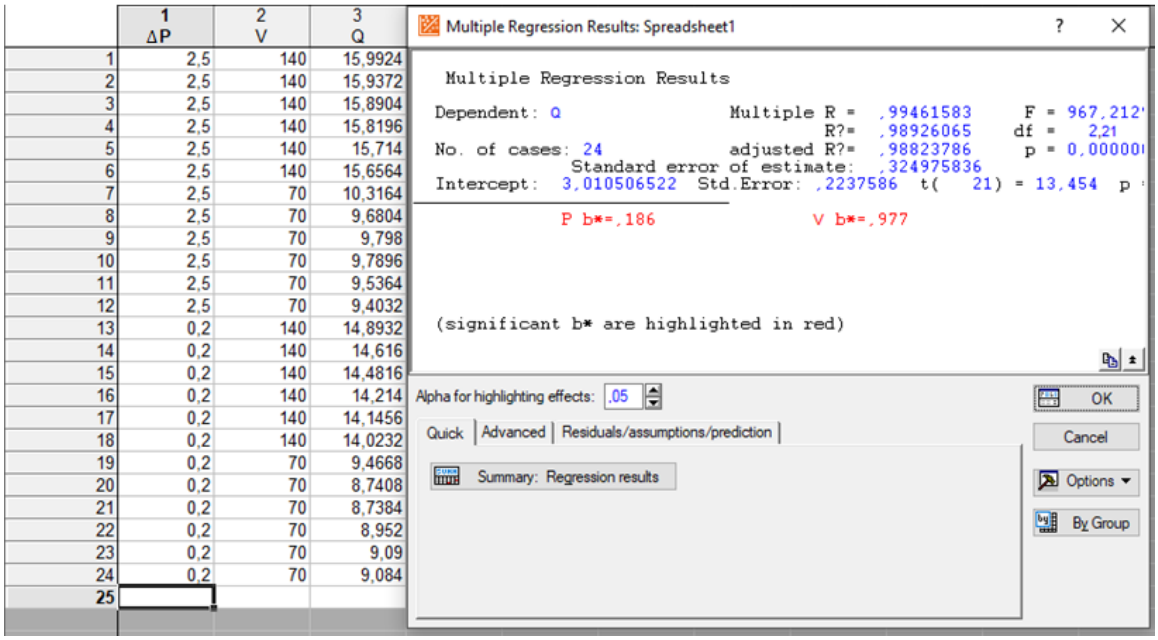

	1 ΔP	2 V	3 Q
1	2,5	140	15,9924
2	2,5	140	15,9372
3	2,5	140	15,8904
4	2,5	140	15,8196
5	2,5	140	15,714
6	2,5	140	15,6564
7	2,5	70	10,3164
8	2,5	70	9,6804
9	2,5	70	9,798
10	2,5	70	9,7896
11	2,5	70	9,5364
12	2,5	70	9,4032
13	0,2	140	14,8932
14	0,2	140	14,616
15	0,2	140	14,4816
16	0,2	140	14,214
17	0,2	140	14,1456
18	0,2	140	14,0232
19	0,2	70	9,4668
20	0,2	70	8,7408
21	0,2	70	8,7384
22	0,2	70	8,952
23	0,2	70	9,09
24	0,2	70	9,084
25			

Figure 2 Multiple regression for a 0.1-μM membrane

3. The resulting mass fractions of total, casein, and whey proteins in the true protein in the retentates and permeates were summarized in tables.

RESULTS AND DISCUSSION

The 2^2 full factorial experiment was represented as a data set matrix (n × k) of four observations and two factors, i.e., pressure ΔP and circulation rate V, at constant temperature of the separated system $t_1 = 50 \pm 1$°C. Stage 1, which involved microfiltration with 0.1 μM membranes, yielded the necessary experimental data. The membrane permeability values and the mass fractions of casein and whey proteins in the retentate were determined every 10 min. Statistica 10.0 provided regression equations (Eq. (2), (3)) and their response surfaces (Figs 3 and 4). The method of multiple linear regression analysis (Fig. 2) made it possible to verify the regression equations with determination coefficient $R^2 = 0.989$.

To facilitate the prediction of permeate flux, we used the most visual numerical method, i.e., the trial-and-error method with target function grid search in Python.

The data obtained for a 0.1 μM membrane as a result of the 2^2 full factorial experiment (Eq. (2), (3)) and response surfaces (Fig. 3) showed that the value of the transmembrane pressure was the main factor that affected the 0.1 μM and 0.2 μM membrane permeability:

$$Q = 3.0105 + 0.4742\Delta P + 0.0819V \quad (2)$$

$$K = 21.7978 - 3.7391\Delta P + 0.0043V \quad (3)$$

where Q is the optimal permeability; V is circulation rate; K is a ratio of the mass fractions of casein and whey proteins in the retentate.

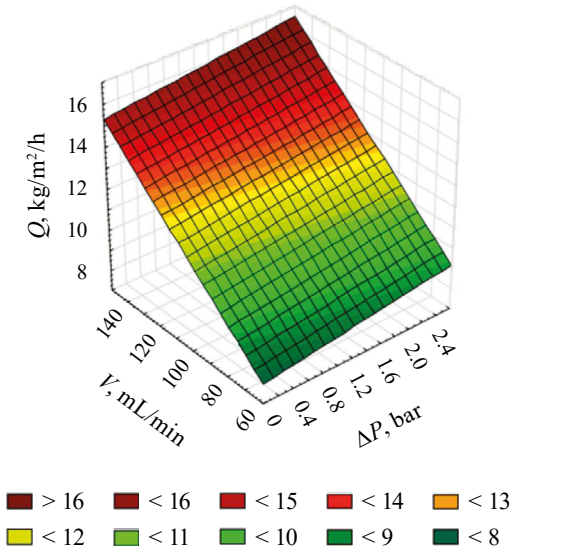

Figure 3 Effect of operating pressure (ΔP) and circulation rate (V) on permeability (Q) of 0.1 μm membranes

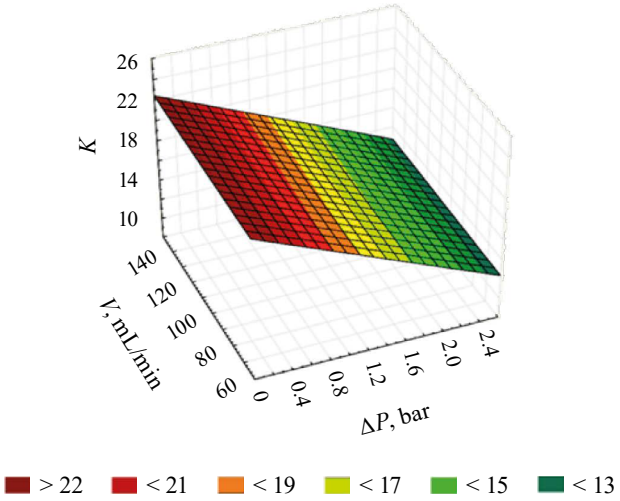

Figure 4 Effect of operating pressure (ΔP) and circulation rate (V) on the ratio of casein vs. whey proteins in microfiltration retentate (K) for 0.1 μM membranes

The qualitative (Fig. 5), quantitative (Table 5), and calculated data (Eq. (4)) for response surface (Fig. 4) showed that the highest ratio (93:7) of the mass fractions of casein and whey proteins in the retentate for a 0.1 μM membrane were obtained at $\Delta P_{min} = 0.20 \pm 0.01$ bar and $V_{min} = 70 \pm 5$ mL/min. However, a comparable ratio of 92:8 was achieved at ΔP_{min} and V_{max}, i.e., the higher the increase rate of circulation rate in the separated system, the lower the mass fraction of casein in the retentate. A higher operating pressure at V_{min} and V_{max} did not increase the mass fraction of casein either. Consequently, the ratio of 95:5 for the given operating parameters could be achieved only by changing the conditions of microfiltration and diafiltration.

Microfiltration and diafiltration made it possible to increase the content of casein fractions in the retentate.

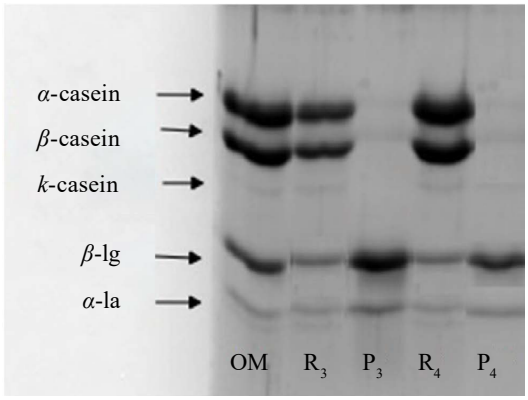

Figure 5 Electrophoresis of retentates and permeates (microfiltration, 0.1 μM membrane). OM – original skim milk, R_3 – retentate, Sample 3; P_3 – permeate, Sample 3; R_4 – retentate, Sample 4; P_4 – permeate, Sample 4 (Table 4)

Table 5 Mass fractions of casein and whey proteins in true protein of microfiltered retentate for 0.1 μM membranes

Sample	Pressure (ΔP), bar	Circulation rate (V), mL/min	Casein, %	Whey protein, %
1	2.5	140	90	10
2	2.5	70	91	9
3	0.2	140	93	4
4	0.2	70	92	8

Table 6 Mass fractions of casein and whey proteins in the true protein in retentates after defiltration

Sample	Pressure (ΔP), bar	Circulation rate (V), mL/min	Casein, %	Whey protein, %
5	0.2	140	95	5
6	0.2	70	96	4

The proportion of casein protein fractions increased from 94:6 to 95:5 in relation to whey protein fractions in the total protein (Table 6).

The results of the 2^2 full factorial experiment revealed nonlinear dependencies of the objective function Y_i on factors X_1 and X_2. The effect of the third factor, i.e., the temperature of the system after microfiltration, was highly probable for the following reasons:

– the interaction of micellar casein with whey proteins grew more intensive;

– the viscosity of the skim milk decreased as the temperature reached 50°C due to storage conditions and the permeate permeability of the membrane increased.

To raise the ratio of casein and whey protein above 95:5, the separation process had to be carried out in the microfiltrate/deionized water mode or by varying the three operating parameters, i.e., pressure, circulation rate, and temperature of the microfiltered system. As a result, the research proceeded in line with the 2^3 full factorial experiment.

The final regression equations were obtained in encoded variables for 0.1 μM membranes:

$$Y = 11.0 + 1.26X_1 + 2.46X_2 + 0.44X_3 + 0.39X_1X_2 + \\ + 0.11X_1X_3 + 0.06X_2X_3 + 0.09X_1X_2X_3 \quad (4)$$

where Y is the permeability; X_1 is the pressure; X_2 is the circulation rate; X_3 is the temperature.

At 10–50°C of the separated system (t), the greatest effect on the output parameter Y_i belonged not to X_1, but to X_2. As for paired interactions, the combined effect of X_1 and X_3 on Y_i was important for optimizing the external microfiltration parameters. To predict the membrane permeability (Q) for permeate, we substituted the encoded variables (X_i) in Eq. (4) with natural variables (Table 4):

$$Q = 1.22 + 1.11 + 0.058V + 0.06t - 0.002 - \\ - 0.00002Vt - 0.021 + 0.0002 \quad (5)$$

The optimal result for the ratio of casein and whey proteins in the true protein of the retentate after diafiltration was 96:4. We performed a theoretical analysis of Eq. (4) and determined the extremum of the function as $Y_{0.1} = f_1(X_1, X_2, X_3)$.

The tangent point was $M_0(X_{10}, X_{20}, X_{30})$; its region ($\delta$) was a sphere centered in point M_0 of radius $\delta > 0$. After that, we analyzed the partial derivatives of the first and second orders:

$$Y_i^{'} = \frac{dY_{0.1}}{dX_i} \text{ and } Y_i^{''} = \frac{dY_{0.1}^{'}}{dX_i}$$

The analysis revealed that $\delta_1 = 0$; $\delta_2 > 0$; $\delta_3 < 0$. Since $\delta_3 \neq 0$, point $M_0(11.436, 2.419, 10.659)$ was the saddle point. Obviously, $Y_{0.1} = f(X_1, X_2, X_3)$ excluded any visual three-dimensional geometric interpretation of the obtained result. However, the mere fact of a saddle point hinted at a possibility of multiple combinations of different values of variables $X_1(\Delta P)$, $X_2(V)$, and $X_3(t)$, at which $Y(Q)$ was close to the maximum in the established region of discrete variation.

The further analysis involved grid search values of $Y(Q)$. It confirmed a set of numerically close values $Y = f(X_1, X_2, X_3)$. The skim milk microfiltration could be performed at various combinations of pressure, circulation rate, and temperature, depending on the technology requirements for target products and the required ratio of the mass fractions of casein and whey proteins in the true protein of the microfiltered retentate.

CONCLUSION

In the baromembrane separation of skim milk, the transmembrane pressure proved to be the most important variable to affect the membrane permeate for 0.1 μM membranes, if the goal was to obtain a ratio of casein to whey proteins in the true protein below 95:5.

When the goal was to obtain a ratio over 95:5, all three variables, i.e., pressure, circulation rate (V), and temperature (t), should be taken into account. In that case, the permeability of 0.1 μM membranes was affected by the circulation rate, not operating pressure.

When the experiment involved an industrial sample of a 0.1 μM microfiltration membrane (Vladisart, Russia), the operating modes were experimentally determined as follows: $\Delta P = 2.5$ bar; $V = 140$ mL/min; $t = 50 \pm 1$°C and $\Delta P = 0.20 \pm 0.01$ bar; $V = 70 \pm 5$ mL/min; $t = 50 \pm 1$°C. The resulting retentates had casein and whey protein mass fraction ratios of 96:4 and 95:5, respectively.

The regression equation of $Q = f(\Delta P, V, t)$ made it possible to calculate the permeability of the microfiltration membrane, depending on the main operating parameters in specified variation intervals.

The mathematical model of the skim milk microfiltration revealed a variety of combinations of values for variables $X_1(\Delta P)$, $X_2(V)$, and $X_3(t)$, for which the parameter $Y(Q)$ approached the maximal values in the experimentally established area.

For 0.1 μM membranes, the transition from microfiltration to diafiltration resulted in the overall efficiency of the membrane separation process that demonstrated a 2.2 to 4.0% increase in casein proteins in the retentate in relation to whey proteins.

CONTRIBUTION

All the authors contributed equally to the study and bear equal responsibility for the information published in this article.

CONFLICT OF INTEREST

The author declared no potential conflict of interest regarding the research, authorship, and/or publication of this article.

ACKNOWLEDGEMENTS

The authors express their gratitude to G.S. Anisimov, Director of the Center for Biotechnological Engineering, North Caucasus Federal University.

REFERENCES

1. Charcosset C. Classical and recent applications of membrane processes in the food industry. Food Engineering Reviews. 2021;13:322–343. https://doi.org/10.1007/s12393-020-09262-9
2. Staszak K, Wieszczycka K. Membrane applications in the food industry. Physical Sciences Reviews. 2023;8(9):2647–2677. https://doi.org/10.1515/psr-2021-0050
3. Agarkova EYu, Kruchinin AG, Zolotaryov NA, Pryanichnikova N, Belyakova ZYu, *et al*. Processing cottage cheese whey components for functional food production. Foods and Raw Materials. 2020;8(1):52–59. https://doi.org/10.21603/2308-4057-2020-1-52-59

4. Jørgensen CE, Abrahamsen RK, Rukke E-O, Johansen A-G, Schüller RB, *et al*. Optimization of protein fractionation by skim milk microfiltration: Choice of ceramic membrane pore size and filtration temperature. Journal of Dairy Science. 2016;99(8):6164–6179. https://doi.org/10.3168/jds.2016-11090
5. Sel C, Bilgen B, Bloemhof-Ruwaard J. Planning and scheduling of the make-and-pack dairy production under lifetime uncertainty. Applied Mathematical Modelling. 2017;51(3):129–144. https://doi.org/10.1016/j.apm.2017.06.002
6. Gésan-Guiziou G, Sobańtka AP, Omont S, Froelich D, Rabiller-Baudry M, *et al*. Life cycle assessment of a milk protein fractionation process: Contribution of the production and the cleaning stages at unit process level. Separation and Purification Technology. 2019;224:591–610. http://dx.doi.org/10.1016/j.seppur.2019.05.008
7. Depping V, Grunow M, Kulozik U. A methodological framework for comparing fractionated and non-fractionated products in life cycle assessments: The case of milk concentrates. Journal of Cleaner Production. 2020;257:120478. https://doi.org/10.1016/j.jclepro.2020.120478
8. Madoumier M, Azzaro-Pantel C, Gésan-Guiziou G. Including cleaning and production phases in the eco-design of a milk evaporation process. Food and Bioproducts Processing. 2020;123:427–436. http://dx.doi.org/10.1016/j.fbp.2020.07.023
9. Mestawet AT, France TC, Mulcahy PGJ, O'Mahony JA. Component partitioning during microfiltration and diafiltration of whey protein concentrate in the production of whey protein isolate. International Dairy Journal. 2024;157:106006. https://doi.org/10.1016/j.idairyj.2024.106006
10. Mardal F, Parjikolaei BR, Corredig M. Effect of diafiltration media and filtration modes on fouling and performance in skim milk microfiltration: A comparative study. Journal of Dairy Science. 2024;107(12):10414–10425. https://doi.org/10.3168/jds.2024-25107
11. Trystram G. Modelling of food and food processes. Journal of Food Engineering. 2012;110(2):269–277. https://doi.org/10.1016/j.jfoodeng.2011.05.001
12. Field RW, Wu JJ. Permeate flux in ultrafiltration processes–Understandings and misunderstandings. Membranes. 2022;12(2):187. https://doi.org/10.3390/membranes12020187
13. Cheng T-W, Wu J-G. Modified boundary layer resistance model for membrane ultrafiltration. Tamkang Journal of Science and Engineering. 2001;4(2):111–117. https://doi.org/10.6180/jase.2001.4.2.05
14. Cheng T-W, Yeh H-M. Complete momentum-balance analysis of permeate flux for ultrafiltration in hollow-fiber modules. Tamkang Journal of Science and Engineering. 2008;11(3):239–246. https://doi.org/10.6180/jase.2008.11.3.02
15. Beicha A, Zaamouch R, Sulaiman NM. Permeate flux in ultrafiltration membrane: A review. Journal of Applied Membrane Science & Technology. 2017;14(1):9–20. https://doi.org/10.11113/amst.v14i1.91
16. Bhattacharjee C, Datta S. Simulation of continuous stirred ultrafiltration process: An approach based on analytical solution coupled with turbulent back transport. Journal of Chemical Technology and Biotechnology. 2003;78:1135–1141. https://doi.org/10.1002/jctb.912
17. Ruby-Figueroa RA, Nardi M, Sindona G, Conidi C, Cassano A. A multivariate statistical analyses of membrane performance in the clarification of citrus press liquor. ChemEngineering. 2019;3(1):10.
18. Ruby-Figueroa RA, Cassano A, Drioli E. Ultrafiltration of orange press liquor: Optimization for permeate flux and fouling index by response surface methodology. Separation and Purification Technology. 2011;80(1):1–10. https://doi.org/10.1016/j.seppur.2011.03.030
19. Ruby-Figueroa RA, Saavedra J, Bahamonde N, Cassano A. Permeate flux prediction in the ultrafiltration of fruit juices by ARIMA models. Journal of Membrane Science. 2017;524:108–116. https://doi.org/10.1016/j.memsci.2016.11.034
20. Adams MC, Hurt EE, Barbano DM. Effect of ceramic membrane channel geometry and uniform transmembrane pressure on limiting flux and serum protein removal during skim milk microfiltration. Journal of Dairy Science. 2015;98(11):7527–7543. http://dx.doi.org/10.3168/jds.2015-9753
21. Granger-Delacroix M, Leconte N, Grassin C, Le Goff F, Garnier-Lambrouin F, *et al*. Skimmed milk microfiltration in diafiltration mode: Impact of solvent nature and concentration factor on spiral-wound membrane performance operated at low temperature. Separation and Purification Technology. 2023;304:122326. https://doi.org/10.1016/j.seppur.2022.122326
22. Gésan-Guiziou G, Daufin G, Boyaval E. Critical stability conditions in skimmed milk crossflow microfiltration: Impact on operating modes. Le Lait. 2000;80(1):129–138. https://doi.org/10.1051/lait:2000114
23. Jørgensen CE, Abrahamsen RK, Rukke E-O, Johansen A-G, Schüller RB, *et al*. Optimization of protein fractionation by skim milk microfiltration: Choice of ceramic membrane pore size and filtration temperature. Journal of Dairy Science. 2016;99(8):6164–6179. https://doi.org/10.3168/jds.2016-11090
24. Tremblay-Marchand D, Doyen A, Britten M, Pouliot Y. A process efficiency assessment of serum protein removal from milk using ceramic graded permeability microfiltration membrane. Journal of Dairy Science. 2016;99(7):5230–5243. https://doi.org/10.3168/jds.2016-10914

25. Zulewska J, Barbano DM. Influence of casein on flux and passage of serum proteins during microfiltration using polymeric spiral-wound membranes at 50°C Spiral-wound microfiltration. Journal of Dairy Science. 2013;96(4):2048–2060. https://doi.org/10.3168/jds.2012-6032
26. Zulewska J, Barbano DM. The effect of linear velocity and flux on performance of ceramic graded permeability membranes when processing skim milk at 50°C. Journal of Dairy Science. 2014;97(5):2619–2632. https://doi.org/10.3168/jds.2013-7635
27. Zulewska J, Newbold M, Barbano DM. Efficiency of serum protein removal from skim milk with ceramic and polymeric membranes at 50°C. Journal of Dairy Science. 2009;92(4):1361–1377. http://dx.doi.org/10.3168/jds.2008-1757
28. Astudillo-Castro CL. Limiting flux and critical transmembrane pressure determination using an exponential model: The effect of concentration factor, temperature, and cross-flow velocity during casein micelle concentration by microfiltration. Industrial & Engineering Chemistry Research. 2015;54(1):414–425. https://doi.org/10.1021/ie5033292
29. Mamay DS, Babenyshev SP, Mamay AV, Ivanets VA, Bratsikhin AA. Microfiltration processing of raw materials for the fermented milk product making. In: Kurchenko V, Lodygin A, Machado da Costa RM, Samoylenko I, editors. Intelligent Biotechnologies of Natural and Synthetic Biologically Active Substances. ICAETT 2021. Lecture Notes in Networks and Systems. 2022;408:10–17. https://doi.org/10.1007/978-3-030-96641-6_2
30. Babenyshev SP, Nesterenko PG, Bratsikhin AA, Zhidkov VE, Mamay DS, *et al*. Hydrodynamics and mass transfer with gel formation in a roll type ultrafiltration membrane. Foods and Raw materials. 2018;6(2):350–357. https://doi.org/10.21603/2308-4057-2018-2-350-357
31. Hurt EE, Adams MC, Barbano DM. Microfiltration of skim milk and modified skim milk using a 0.1-μm ceramic uniform transmembrane pressure system at temperatures of 50, 55, 60, and 65°C. Journal of Dairy Science. 2015;98(2):765–780. https://doi.org/10.3168/jds.2014-8775
32. Carter BG, Cheng N, Kapoor R, Meletharayil GH, Drake MA. Invited review: Microfiltration-derived casein and whey proteins from milk. Journal of Dairy Science. 2021;104(3):2465–2479. https://doi.org/10.3168/jds.2020-18811
33. Gavazzi-April C, Benoit S, Doyen A, Britten M, Pouliot Y. Preparation of milk protein concentrates by ultrafiltration and continuous diafiltration: Effect of process design on overall efficiency. Journal of Dairy Science. 2018;101(11):9670–9679. https://doi.org/10.3168/jds.2018-14430
34. Alanood AA, Abbas TK, Alaswad S, e-Guld S, Bajoga A. Remove liquid radioactive wastes utilizing nanofiltration, ultrafiltration, and microfiltration membranes. Engineering and Technology Journal. 2022;40(9):1231–1259. https://doi.org/10.30684/etj.2022.134025.1218
35. Jankovic A, Chaudhary G, Goia F. Designing the design of experiments (DOE) – An investigation on the influence of different factorial designs on the characterization of complex systems. Energy and Buildings. 2021;250:111298. https://doi.org/10.1016/j.enbuild.2021.111298

ORCID IDs
Dmitriy S. Mamay https://orcid.org/0000-0001-6221-8230
Sergey P. Babenyshev https://orcid.org/0000-0002-1784-0837
Ivan A. Evdokimov https://orcid.org/0000-0002-5396-1548

Foods and Raw Materials. 2026;14(2)

ISSN 2308-4057 (Print)
ISSN 2310-9599 (Online)

Brief Communication
Open Access

Available online at http://jfrm.ru/en
https://doi.org/10.21603/2308-4057-2026-2-677
https://elibrary.ru/CRGELC

Prospects for livestock farming in Siberia and Far East of Russia

Vladimir A. Soloshenko*, Sergey N. Mager

Siberian Federal Scientific Center of Agro-BioTechnologies of the Russian Academy of Sciences, Krasnoobsk, Russia

* e-mail: soloshenko@sfsca.ru

Received 14.04.2025; Revised 16.05.2025; Accepted 03.06.2025; Published online 11.09.2025

Abstract:
This article describes the current state and prospects of cattle farming in remote areas of Russia with a focus on the role of the Siberian Research Institute of Animal Husbandry in developing the dairy and beef cattle breeding industries between 1930 and 2025. It highlights new approaches to cattle breeding that adapt conventional breeds to extreme environment, and lists local R&D projects aimed at increasing meat and dairy productivity.
By outlining the faults and errors of animal husbandry in northern latitudes, we define the current priorities in agricultural science and practice that could improve forage production, thus leading to high-quality organic livestock products in the risk farming areas of Siberia and the Far East.
We propose to develop a net of independent food supply areas that would provide the local population with essential foods and create jobs for new rural settlers.

Keywords: Food independence, animal selection, breeds, extreme conditions, organic food production

Please cite this article in press as: Soloshenko VA, Mager SN. Prospects for livestock farming in Siberia and Far East of Russia. Foods and Raw Materials. 2026;14(2):339–343. https://doi.org/10.21603/2308-4057-2026-2-677

The rapidly changing geopolitical situation affects the economy of nations and entire continents [1]. National independence relies on certain economic sectors, and countries can reach economic sovereignty only by boosting their development.

Russian agriculture still depends on imports in such spheres as seed production, monogerm beet seeds, vegetable and fruit storage technologies, breeding and hybridization in broiler poultry farming, meat and dairy cattle breeding, etc. High-quality animal feeds and livestock processing lag behind the global standards. The domestic pedigree livestock farming has lost its scientific, experimental, material, and technical foundations. While struggling to regain quantity indicators in milk, meat, wool, and eggs, the agricultural science has abandoned its previous research achievements in primary agricultural aspects (food quality, fertility, productive longevity, economically valuable breeds, etc.) and secondary products. As a result, the contemporary R&D budget distribution relies on the wrong priorities, state funds being directed to projects of doubtful demand. The market is saturated with low-quality livestock foods while what Russian scientific agriculture really needs is to focus on improving the quality of bread, milk, meat, and eggs. And to do that, Russia has all necessary resources, i.e., land, energy, water, equipment, and scientific knowledge.

The underdeveloped remote regions beyond the Urals occupy more than 60% of Russia. Their agricultural development depends on a number of important conditions that are hard to meet. The exploration of Siberia and the Far East was a long and complex process; today, the colossal resources of the Russian Antarctic are on the real-time national agenda. Historically, only a few major attempts to develop the Russian frontier proved successful. Here, we could mention Stolypin's project of reclaiming Siberia and the Baikal-Amur Mainline, but the efficiency of the latter remains biased.

When it comes to developing remote territories with harsh climate, the strategizing depends not so much on the income of extractive industries and raw material sale options as on the geopolitics, i.e., population density, sedentary lifestyle vs. nomadism, local production of essential foods, footwear, and clothing, etc. The bioclimatic parameters of the Russian North and Far East are incomparable with the black earth belt of its European part, which means a total absence of any competitiveness between them.

Copyright © 2025, Soloshenko *et al.* This is an open access article distributed under the terms of the Creative Commons Attribution 4.0 International License (https://creativecommons.org/licenses/by/4.0/), allowing third parties to copy and redistribute the material in any medium or format and to remix, transform, and build upon the material for any purpose, even commercially, provided the original work is properly cited and states its license.

In 2023, the domestic milk production was at its lowest while beef farming demonstrated zero profit [2]. The government did its best to support beef breeding by issuing various decrees in 2009–2012, but the industry keeps shrinking, the only exception being the Miratorg Holding that receives considerable financial injections from the government. However, the company's price policy fails to recognize the needs of the lower middle class, retirees, and other financially-challenged social strata.

The development of livestock farming in remote areas remains as challenging as any attempts to encourage the working migration to the underpopulated North. Fur, wool, skins, feed grain, meat, timber, and other industries are seldom profitable if they are provincial. The only way out seems to be a closed production cycle that ends with high-quality primary and secondary goods with high added value. For example, coats, hats, and mantles from high-quality pelts could bring more profit than the sheer breeding of minks, nutria, foxes, or sables. Wood processed into luxury furniture, finishing materials, environmentally friendly tableware, and other green utensils is a huge market that generates high profit from renewable raw materials. Processed wool, fleece, and skins of horses, deer, yaks, and other small and large cattle are a source of a wide range of goods, from clothes and footwear to carpets, and they are in high demand on domestic and foreign markets.

If combined with hi-tech processing facilities, livestock farms provide new year-round jobs. However, such full-circle enterprises require a stable cooperation of proactive entrepreneurs with the state. In the Russian North and Far East, it is the bioclimatic potential and the geopolitical situation that dictate the business conditions. The only profitable variant seems to be small and medium-sized livestock family farms of 10–100 cattle heads that are serviced by local feed and fattening cooperatives. These small businesses are then linked by strict contractual terms with processing enterprises and regional retail chains.

Russian North and Far East are huge territories with a remarkable diversity of agricultural production. Such far-sighted scientists and statesmen of the Russian Empire as Dmitry Mendeleyev and Pyotr Stolypin [3] believed that agriculture needed much more capital than other production sectors. Prime Ministers of the Russian Federation Valentin Pavlov and Egor Gaidar, on the contrary, proved short-sighted in their conviction that Russia's abundant resources could buy us everything we need. They reduced the domestic agriculture to a "bottomless barrel" and a "black hole" that would swallow any serious investments. As a result, Russia started to lag behind the global standards in plant and animal breeding, feed production, agricultural engineering, farm and storage design, etc. What is even more important, this attitude did enormous harm to agricultural science. However, when the foreign sanctions turned Russia's food independence into a national economic priority, domestic agricultural scientists and managers made invaluable contributions to the national poultry and pig breeding. Thanks to their efforts, these areas of animal husbandry started to receive state loans to purchase highly productive animals, quality feeds, and hi-tech farm equipment. Thanks to them, Russian consumers can now buy high-quality livestock products instead of unhealthy, fatty pork. However, these achievements became feasible only due to some R&D developed by foreign scientists, who, unlike their Russian colleagues, received much better funding from their national state budgets.

Yet, this approach has also brought about some major failures. For instance, we built 61 no-grass fattening cattle complexes for 10,000 heads each using Italian G&G technology, but they all closed down as a result of poor product quality. The monotonous feeds, aggravated by the lack of sunlight and active exercise, degraded the sensory profile of commercial-scale beef.

Although the R&D work goes on, the quality of products yielded by large industrial complexes remains below the standard level, especially their taste properties. As the country abandoned the system of state standards (GOST) and all-union standards (OST) in favor of technical specifications (TU), the quality of foods and feeds fell victims to all sorts of additives, fillers, and leavening agents. In such conditions, consumers of meat and dairy products turn to private farms, and this trend indicates the low quality of products obtained by large-scale industrial technologies.

Microorganisms that come with feed and environment play a crucial role in animal metabolism, thus affecting the quality of meat products [4, 5, 6]. Since foreign consultants encouraged stagnation in the chemical and microbiological industries, biologically active feed additives have become scarce in the domestic cattle farming. Combined with long-term stall keeping, the poor diet ignores the typical needs of farm ruminants. The weak microbiome literally raises the demand for animal products of satisfactory quality and lowers the profitability of industrial cattle farming.

Considering that Russian North and Far East are risk farming areas, foreign plant cultivars, animal breeds, technologies, and projects have to be subjected to profound testing in local conditions before being introduces on industrial scale. Moreover, different regions of Russian North, Siberia, and the Far East have different climates and thus require different agricultural strategies.

The current geopolitical situation demands independent agriculture, textile and footwear industry, pharmacy, construction materials, etc. Undoubtedly, Russia has enough resources to gain sovereignty in all these areas. The Siberian Research Institute of Animal Husbandry (1930) is the oldest agricultural institute in Siberia. Its teams assess the current trends in agriculture, trying to adjust the research to actual consumer demands. However, state support for regional agricultural science is limited mainly to covering salaries. As a result, agricultural engineering, seed selection, animal breeding, and farming technology lag behind the global standards with no coordination of science and management

to boost cattle and crop farming. Agricultural producers have to spend their income on import products. Their expectations of robust extra-budgetary financing of agricultural production and science have failed. For instance, the mass Holsteinization of dairy cattle requires a radical revision of the structure and technology of forage production.

Cow breeds with high milk and meat yield need a lot of energy and essential nutrients, i.e., protein and fast-digesting carbohydrates. As a result, the proportion of grain feed in their diet has reached 45–60%. However, a long-term diet like that is bad for ruminants since it fails to provide optimal conditions for symbiotic microflora and microfauna in the forestomach, thus preventing absorption of essential nutrients. The resulting epidemic of metabolic disorders in purebred Holstein dairy cattle caused a sharp decrease in productive longevity and calf yield. Obviously, this inevitably affects milk composition [7].

The most urgent task of modern agricultural science is to monitor not only the state of the improved dairy cattle but also livestock products and production economy. Siberia and the Far East possess much poorer bioclimatic resources than the European part of Russia, and it would be impractical to develop here large dairy complexes because they would demand large volumes of transported roughage and succulent feed. These territories are more appropriate for small farms of gourmet marbled beef, young lamb, horsemeat, yakmeat, and venison. With sustainable processing of main and by-products, such small businesses could facilitate the development of remote territories and resolve a lot of social and political issues in the area.

The late XX century saw the development of a complex net of central and regional research institutions, breeding enterprises, multiplying farms, experimental production farms, and test facilities. Working together as a system, they created improved stock breeds adapted to local conditions: one breed and four new types of dairy cattle, three types and five specialized ecotypes of the Hereford meat cows, two types of the Simmental meat breed, one type of the Kazakh white-headed breed, two new breeds of herd horses, one new type of yaks, one new type of meat sheep, two breeds of wool-producing goats, two breeds and four types of pigs, as well as two breeds of fish. By organizing a large Siberian bank of semen and embryos of wild, endemic, and experimental breeds, the government could ensure the continuity of breeding work and improve the arrays of domestic animals in the Regional Center for Breeding and Genetics, which is part of the Siberian R&D and Technological Institute of Animal Husbandry with its 95 years of coordinating breeding work across Siberia and the Far East.

Unfortunately, all new centers for breeding and genetics are located in the European part of Russia, including two in the Moscow Region. Moreover, they belong to agricultural organizations with poor results in dairy cattle breeding. It would be much more expedient to scatter new selection centers across the Russian Federation, preferably in the regions with research laboratories that have successful breeding experience. For instance, the breeding center in Novosibirsk has good results in dairy cattle and pig breeding; Barnaul is famous for beef cattle and maral breeding; Yakutia successfully deals with herd horse and reindeer; Transbaikalia is known for its yaks and sheep, etc. A wide all-Russian net of experimental production centers would support the principle of regional specialization in animal husbandry, preserve achievements of local scientific schools, provide the regions with domestic breeding material, maintain coordinated breeding work, and develop a continuous system of personnel training.

The industrial curse of Russian cattle farming is that the improvements in the feed sphere never catch up with those in the animal breeding, both in terms of quantity and quality. As a result of this gap, inappropriate diet degenerates highly productive cattle breeds, even those purchased abroad, and it does so in several generations. Across Siberia, the feed stock could vary from 4 centners of feed units per head in Tuva and Buryatia to 40–45 in Tomsk, Kemerovo, Omsk, Novosibirsk, Krasnoyarsk, and Altai regions. With an average milk yield of over 6,000 kg per cow, one Russian cow needs at least 50–55 feed units.

Most bulk feeds belong to grades 2 and 3 while the specific weight of rough and succulent silage feeds of grade 1 rarely rises above 10%. As a result, farmers turn to concentrates (45–50%), which are bad for digestion: such a diet cannot be routine since it prevents nutrient absorption. A long-term lack of high-quality hay, straw, and fast-digesting carbohydrates inhibits the upper-rumen microbiome that destroys fiber and forms microbial protein.

We need a new generation of feed additives to normalize the digestion of cattle, which, in its turn, will improve the taste of milk and meat. These new additives improve the microbiome and facilitate the digestion of low-quality feed, e.g., straw, crop waste, overripe natural grass during long-term grazing of beef cattle, herd horses, sheep, yaks, etc. Given the national priority of food independence, these R&D projects are conducted by several institutes powered by the Siberian Branch of the Russian Academy of Sciences, i.e., Institutes of Solid-State Chemistry, Organic Chemistry, Cytology and Genetics, as well as by the Sibbiopharm Production Association. Their combined efforts provide mutual theoretical, financial, and production support. The pilot samples of new feed additives contain enzyme compositions, rumen microbial complexes, sets of cheap fast-digesting carbohydrates, capsuled urea, immune system stimulants, etc. However, most experimental facilities located in pilot production farms have gone bankrupt, which complicates the R&D work. These facilities provided equipped experimental base where experiments could be conducted together with students' field practice and personnel retraining. No breakthroughs in animal husbandry are possible without such facilities, which makes their financial maintenance a state priority. New experi-

mental facilities will provide for the much-needed creativity in fundamental and applied science to boost the domestic feed production, without which all other agricultural work is futile.

We need a new, more effective forage production system to yield high-quality artificially dried forage based on the regional long-term green conveyor principle. We need a comprehensive study that would compare – both biologically and economically – the standard diets oversaturated with forage grain and silage forages with alternative diets based on granules or briquettes of artificially dried alfalfa, rye, triticale, goat's rue, mallow, rape, and other promising plant species. These raw materials can fortify the deficient cattle diets with vitamins, fast-digesting carbohydrates, and valuable proteins preserved by special drying modes. Such additives normalize metabolic processes and improve the quality of final meat and dairy products.

The above-mentioned green crops are a much more favorable variant of agricultural land use than wheat, and they could be sold at higher prices than low-quality wheat grain. Should this approach prove feasible, it could change the structure of the national livestock feed production. Today, grain feed mixes consist of mostly poor-quality hay and soft wheat. Artificially dried green grass, harvested in the optimal vegetation phase, is more biologically valuable than silage, haylage, or moldy hay rolls. Structural fiber could be obtained from high-quality straw combined with the above-mentioned new-generation feed additives to reduce the rate of concentrate-related metabolic diseases.

According to foreign best practice, artificially dried granulated or briquetted green feed is good for highly productive cattle of all types. This product is in demand on the world market, e.g., China even has to import it from the USA. Some agricultural entrepreneurs from the Voronezh Region have been applying a new drying technology to green plants for several years, and now they sell their products to other Russian regions. Several Russian enterprises have learnt to manufacture equipment for green mass drying from domestic components. In terms of energy consumption and drying modes, this new technology is much better than the old one that relied on diesel fuel. Supported by the enormous land and energy resources, the combined efforts of fundamental and applied science to improve the drying technology for green plants may bring about a breakthrough in the domestic agricultural production. Even in the risky farming areas, Russia may become a leader in the novel feed that could boost the productivity of farm animals, thereby improving the quality of milk, meat, eggs, etc.

The recent rise in the productive potential of farm animals has led to predictable consequences worldwide: high productivity suppresses reproductive functions [4]. For the Holstein dairy cows with a milk yield of 7,000–8,000 kg per lactation, the calf output has plummeted to 76 per 100 cows while their productive age is as short as 2.67 calvings [7]. The negative changes presumably affect the milk quality and the development of young animals. We need comprehensive analytical report on the state of beef and dairy herds, with monitoring and forecasts of breed development. These projects should be given scientific priority, with the management and coordination organized by professionals.

Beef cattle breeding in risky farming areas, i.e., 50% of Russia, can become the beacon of economic recovery in remote and underpopulated regions. Eventually, it could catalyze the settlement of sparsely populated areas. The specialized beef cattle breeding industry first attracted the state attention and funds in the early 1970s. Since then, the Siberian Institute of Animal Husbandry, together with regional science and breeding enterprises, has created eight new types of the Hereford beef cows, one new type of the Simmental breed, and one new Kazakh white-headed cattle breed, by combining local cattle with foreign specimen. The most successful new ecotype was a combination of Siberian Simmentals with German meat Simmentals, crossed with improved Herefords (Figs. 1 and 2). They are highly adaptable to steppe, mountain-taiga, and forest-steppe environment,



Figure 1 A 18-month-old Simmental bull of Baganskiy type: 705 kg of post-fattening live weight



Figure 2 First generation crossbred calves (♀Simmental × ♂Hereford)

providing up to 1.5 kg of daily live weight gain during final fattening. The cows demonstrate good maternal qualities, and the bulls are quite placid. Their semen is available in many breeding enterprises across Siberia.

In addition to marbled beef, regions with intensive farming have good prospects for long-term storage feed production and elite livestock products from herd horses, yaks, deer, meat sheep, and pigs. Their semen and other bio-products should be stored in special storage banks as state property.

Siberia and the Far East need new breeding and genetic centers for new ecotypes and breeds. With academic and state support, they could develop environmentally friendly organic products to be exported to China, India, and Africa. This type of export is likely to turn out more profitable than grain trade. In addition, an agile meat livestock industry with vast grazing areas and pastures could fortify the national independence in the eastern regions, as well as stop the neighboring countries from "friendly" attempts to claim underdeveloped territories.

Most proposals listed in this article are being implemented right now in the Altai Region (AltaiMyas Association, KFK Nauka, OOO Pharm, OOO Lebyazhye), in the Omsk Region (Tyukalinsky Butter and Cheese Factory, OOO Osha Food Corporation), and in Yakutia (AO Tuimada, Verte Agricultural Production Cooperative) [8, 9]. These enterprises use new technologies that render their livestock products with unique sensory qualities and ensure a meat potential of 0.9–1.1 kg/day. However, their profitability remains below 18–20%, which indicates a gap between energy prices and the bioclimatic potential of the region. The profitability of agricultural enterprises should be high enough to guarantee a constant production improvement and high wages for all their employees.

REFERENCES

1. Serafimovich AE, Prosekov AYu. Food Security: International legal aspects and Russian law enforcement practice. Law. Journal of the higher school of economics. 2018(4):235–253. (In Russ.) https://doi.org/10.17323/2072-8166.2018.4.235.254
2. Yearbook of beef cattle breeding in farms of the Russian Federation (2022). In: Moroz TA, editor. Moscow: All-Russian Research Institute of Breeding; 2023. 218 p.
3. Kravchenko NA. Breeding of agricultural animals. Moscow: Kolos; 1973. 485 p.
4. Chirvinsky NP. General animal husbandry. Saint Petersburg: Izdatel Devrien A. F.; 1903. 365 p.
5. Krasnikov GYa, Makarov NA. Russian Academy of Sciences: 300 years of history. Vol. 2. Moscow: Nauka; 2024. 816 p.
6. Lisitsyn AB, Shumakova IA. Fatty acids in meat quality and human nutrition. Moscow: V. M. Gorbatov All-Russian Scientific Research Institute of Meat Industry; 2002. 41 p.
7. Felorenko VF, Mishurov NP, *et al.* Advanced practices in domestic livestock breeding: A scientific analytical review. Moscow: 2018. 69 p.
8. Drakunov V. Natural products for Omsk residents. Rural Siberia. 2018;(4):8–9.
9. Rybchenko TV. Producing safe and high-quality cheeses in Siberia. Rural Siberia. 2018;4:22–24.

Foods and Raw Materials. 2026;14(2)

ISSN 2308-4057 (Print)
ISSN 2310-9599 (Online)

Research Article
Open Access

Available online at http://jfrm.ru/en
https://doi.org/10.21603/2308-4057-2026-2-681
https://elibrary.ru/ETGLCB

Developing composite films from carboxymethyl starch, polyvinyl alcohol, and kaolin for sustainable packaging applications

Bright A. Omoike[1,*], Felix E. Okieimen[2], Chinyere Imoisi[1]

[1] Mewar International University, Masaka, Nigeria
[2] University of Benin, Benin City, Nigeria

* e-mail: brightomoike@yahoo.com

Received 27.09.2024; Revised 21.11.2024; Accepted 03.06.2025; Published online 20.10.2025

Abstract:
Health and environmental problems are rising by the day due to an increasing use of synthetic plastics. However, biobased packaging from starch, with its numerous advantages, or its derivatives offers a promising solution to this problem. In this study, we aimed to explore a sustainable approach to developing a bioplastic film from carboxymethyl starch, polyvinyl alcohol, and kaolin to serve as a substitute for synthetic packaging.

The study objects included carboxymethyl starch, polyvinyl alcohol, glycerol, and kaolin. All the materials were heated in water to form viscous solutions. The solution was then cast into films using a mold and the water was evaporated through oven-drying. The cast films were characterized via scanning electron microscopy, X-ray diffraction, and thermogravimetric analysis. They were analyzed for their tensile mechanical, barrier, sorption, and biodegradability properties. We also investigated the effects of polyvinyl alcohol and kaolin on the morphology and functional properties of the films.

The micro-surface morphology of the carboxymethyl starch/polyvinyl alcohol blend revealed a smooth and homogenous structure, while the film reinforced with kaolin had a more compact structure with zones of particle aggregations. The highest thermal stability was observed in the composite films containing carboxymethyl starch, polyvinyl alcohol, and kaolin. Higher contents of polyvinyl alcohol and kaolin significantly improved the films' thermal, tensile mechanical, barrier, and sorption properties. The films also demonstrated a substantial rate of biodegradability. The best properties were observed in the films containing 40% of carboxymethyl starch, 60% of polyvinyl alcohol, and 4.5 per hundred resin (phr) of kaolin.

The composite films made from carboxymethyl starch, polyvinyl alcohol, and kaolin had good biodegradability, renewability, and improved functional material properties. Therefore, they can be considered a sustainable alternative to the traditional synthetic plastics in packaging applications.

Keywords: Biobased packaging, bioplastics, sustainable, mechanical tensile, barrier properties, biodegradability, composites

Please cite this article in press as: Omoike BA, Okieimen FE, Imoisi C. Developing composite films from carboxymethyl starch, polyvinyl alcohol, and kaolin for sustainable packaging applications. Foods and Raw Materials. 2026;14(2):344–356. https://doi.org/10.21603/2308-4057-2026-2-681

INTRODUCTION

In the face of escalating global concerns about environmental degradation and waste management, sustainable development has emerged as a paramount priority in the pursuit of a circular economy and waste minimization strategies [1]. This imperative has inspired researchers to seek innovative and greener solutions to conventional plastics in the packaging industry [2]. The plastics industry is a significant sector globally, boasting a massive market of $348 billion and playing a crucial role in shaping the global economy [3]. The demand for plastics is expected to continue rising, with a projected annual growth of 4.2% from 2021 to 2026 [4].

However, the environmental impact of conventional plastics has become a major concern, driving the need for sustainable alternatives. Moreover, the natural sources of these conventional plastics are not renewable and hence are becoming depleted as a result of the increasing demand for plastics [2]. Bioplastic is a novel, eco-friendly, and sustainable substitute for the traditional petroleum-based plastic [5]. It is obtained from renewable bio-natural resources such as starch, cellulose, gelatin, chitin, etc. [6]. The use of bioplastic offers advantages of biodegradability, biocompatibility, and renewability in addition to nearly comparable material strength properties of conventional plastics.

Starch-based bioplastics are promising alternatives to conventional plastics but further modifications are needed to enhance their mechanical and barrier properties for competitive use [7]. Previous studies have shown various

Copyright © 2025, Omoike *et al.* This is an open access article distributed under the terms of the Creative Commons Attribution 4.0 International License (https://creativecommons.org/licenses/by/4.0/), allowing third parties to copy and redistribute the material in any medium or format and to remix, transform, and build upon the material for any purpose, even commercially, provided the original work is properly cited and states its license.

techniques for modifying starch-based films. These include modifying native starch [8], blending with other biomaterials sources [9], or reinforcing with nanofillers [10].

Carboxymethyl starch (CMS) is a versatile green polymer with a wide range of applications in pharmacy, medicine, cosmetics, food, environmental protection, and other industries [11]. It is a chemically modified starch derived from native starch through a reaction with monochloroacetic acid. This process leads to the replacement of some hydroxyl groups with carboxymethyl groups and is known as the Williamson synthesis [12]. This modification enhances the properties of starch, making it a promising material for packaging applications. Introducing a bulky hydrophilic group into the starch chains results in improved thermal stability and film-forming properties, as well as in decreased susceptibility to microbial degradation [13, 14]. Additionally, CMS demonstrates a low tendency for retrogradation, a low gelatinization temperature, and a good freeze-thaw behavior, which further expands its potential applications [11, 15].

The blending of polyvinyl alcohol (PVA or PVOH) with starch has been reported as a good approach to improve the properties of starch-based films [16]. Polyvinyl alcohol is the most widely produced biodegradable synthetic polymer in the world because of its exceptional physical characteristics, resistance to chemicals, and full biodegradability [17]. It is a polymer with a linear structure that is non-toxic and non-carcinogenic. Its remarkable film-forming ability and good compatibility with other materials have led to a wide range of industrial applications [18], especially in food packaging. Due to their semicrystalline structure, PVOH films exhibit excellent oxygen and aromatic barrier qualities, a reduced capacity for water adsorption, high tensile strength, and flexibility [19]. Adding PVOH to biodegradable packaging enhances its mechanical characteristics and water resistance [16, 6]. Highly-polar hydroxyl groups (-OH) in starch and PVOH can create intra- and intermolecular hydrogen interactions, which can change the functional properties of blended films and enhance their integrity [20].

Kaolinite, also known as Kaolin clay, is a naturally occurring clay mineral with various applications in different industries, such as adhesives, paints, pharmaceuticals, fiberglass, paper, rubber, ceramics, electronics, plastics, coatings, and agriculture [21]. Its chemical composition consists of hydrated aluminum silicate with a structure of 1:1 dioctahedral asymmetric layers linked through apical oxygen [21]. Adding kaolin clay to starch films improves their mechanical and thermal stability. Kaolin clay also acts as an effective barrier to moisture transmission, which makes it suitable for use in packaging materials [22, 23]. This cost-effective and versatile material offers a wide surface area and reactive surface for OH-groups, making it an interesting alternative for incorporating into various products [4].

Despite extensive research on developing native starch-based composites for packaging applications, limited studies have explored the potential of carboxymethyl starch and Wilpiszewska *et al.* [25] have demonstrated the potential of CMS derivatives in pharmaceutical and food packaging applications. However, further research is urgently needed to improve the properties and viability of CMS for packaging uses.

In this study, we aimed to develop a CMS/PVA/kaolin composite film with enhanced properties for packaging applications through the synergistic effect of PVA and kaolin (Fig. 1). We also investigated the impact of PVA and kaolin on the morphological, thermal, mechanical, barrier, sorption, and biodegradability properties of CMS/PVA/kaolin composite films. A comprehensive review of the current literature revealed no previous research in this area, highlighting the need to explore the properties and potential applications of this composite material.

STUDY OBJECTS AND METHODS

Chemicals and materials. Carboxymethyl starch (degree of substitution = 0.71), polyvinyl alcohol, and glycerol of analytical grades were supplied by a chemical store in Benin City. Kaolin clay was obtained from a factory in Auchi, Edo State. All the other chemicals and reagents in this study were of analytical grade.

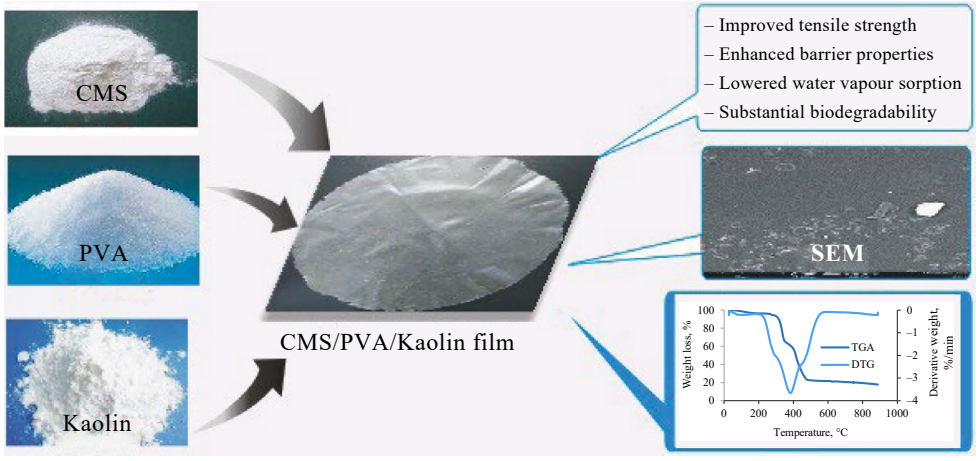

Figure 1 Graphical representation for the preparation and characterization of composite films

Preparation of a carboxymethyl starch/polyvinyl alcohol blend. Carboxymethyl starch (CMS)/polyvinyl alcohol (PVA) blend was prepared by the solution casting method as described by Patil *et al.* with slight modifications [16]. First, different masses of PVA were heated at 90°C in distilled water until complete dissolution. Then, we added a slurry of CMS to the PVA solution and heated at 80–90°C with continuous stirring to ensure complete gelatinization and homogenization. Glycerol was then added to the mixture and stirred for another 20 min. The viscous polymer solution was cast on a glass plate at room temperature for 24 h. The films were further dried in an oven at 60°C for 16 h before being peeled off the plates and kept in a desiccator for analysis. The composition of the films varied depending on the mass of PVA and CMS in the blend.

Preparation of carboxymethyl starch/polyvinyl alcohol/kaolin composites. Carboxymethyl starch (CMS)/polyvinyl alcohol (PVA) films reinforced with kaolin clay were prepared using a modified method described in the study by Garavand *et al.* [26]. First, kaolin clay was dispersed in distilled water and then placed in a mechanical shaker to ensure even distribution of the clay particles. Separately, a slurry of CMS was prepared in water. Meanwhile, PVA was heated at 90°C in distilled water until complete dissolution. Once PVA was fully dissolved, it was mixed with the kaolin clay/CMS mixture and then with glycerol. The entire mixture was then stirred using a magnetic stirrer at 80–90°C for 30 min to ensure complete gelatinization and homogenization. This step was crucial to achieve a uniform filmogenic solution. The filmogenic solution was then cast onto a glass plate and dried in an oven at 60°C for 16 h. The dried films were subsequently peeled off and stored in a desiccator for further analysis. To control the thickness of the films, a known volume of the film solution was measured and poured into the glass plate mold.

The composition of the films is presented in Table 1, which outlines the specific proportions of carboxymethyl starch, polyvinyl alcohol, kaolin clay, and glycerol used in the study.

Characterization of carboxymethyl starch-based composite films. The surface morphological properties of the carboxymethyl starch-based composite films were analyzed using a Phenom ProX scanning electron microscope (Phenom-World, Eindhoven, Netherlands) at an accelerating voltage of 10 kV. Prior to scanning, the samples were mounted on a brass stub and sputtered with gold to ensure electrical conductivity. The scanning electron microscopy (SEM) micrographs were taken at magnifications ranging from 1500 to 2000 times, with the microscope focused on the upper surface of the films. SEM allows for a detailed visualization of the surface morphology, topography, and structure of materials at a microscopic level, enabling researchers to observe the characteristics and arrangement of the components within the composite films.

X-ray diffraction. The crystallinity of the carboxymethyl starch-based composite films was determined using a Miniflex 600 X-ray diffractometer (Rigaku, Japan). This instrument utilizes copper (Kα) anode radiation, which has a wavelength of 1.5444 Å, to examine the crystal structure of the films. The emitted anode radiation produced at 40 kV and 50 mA was passed through a monochromator to produce a focused incident beam. This beam was directed onto the film sample through a one-degree (1°) divergence slit, ensuring a precise and controlled measurement. The diffraction intensity was measured over a range of 2θ = 2 to 70° at room temperature. This allowed for a comprehensive assessment of the crystal structure and order within the composite films. The level of crystallinity for each film was evaluated by visual inspection of the strongest peak in the X-ray diffraction pattern.

Table 1 Composition of the films used for preparation.

Films (Coded)	CMS, g	PVA, g	CMS, %	PVA, %	Kaolin, phr
Pure CMS	10.0	0.0	100	0	–
CMS/PVA1	8.0	2.0	80	20	–
CMS/PVA2	7.0	3.0	70	30	–
CMS/PVA3	6.0	4.0	60	40	–
CMS/PVA4	5.0	5.0	50	50	–
CMS/PVA5	4.0	6.0	40	60	–
CMS/PVA/K1	4.0	6.0	40	60	1.5
CMS/PVA/K2	4.0	6.0	40	60	2.5
CMS/PVA/K3	4.0	6.0	40	60	3.5
CMS/PVA/K4	4.0	6.0	40	60	4.5
CMS/PVA/K5	4.0	6.0	40	60	5.5

CMS is the carboxymethyl starch; PVA is the polyvinyl alcohol; Amount of glycerol used (1 mL = 10% of CMS & PVA) for all films, phr = per hundred resin of filmogenic solution

Thermal stability. The thermal stability of the films was determined via thermogravimetric analysis. This analysis was conducted using a TGA 4000 thermal analyzer (PerkinElmer, Netherland) in a nitrogen gas environment at 10°C/min in the temperature range of 30–950°C. The thermogravimetric and derivative thermogravimetric curves were obtained to assess the thermal stability of the composite films. These curves provide valuable information about the weight loss of the films over a range of temperatures, indicating their thermal degradation behavior.

Evaluation of properties of carboxymethyl starch-based composites. ***Tensile mechanical properties.*** The tensile mechanical properties of the composite films were determined using a universal testing machine (TecQuipment, India) following standard procedures as described in [7]. Prior to the test, the films were cut into rectangular 3 × 15 cm strips and conditioned in a desiccator (0% relative humidity) for 48 h. The films' thickness was measured by means of a digital caliper and was used to obtain the cross-sectional area of the films (the film's thickness multiplied by its width). Subsequently, the ultimate tensile strength, percentage of

elongation at break, and tensile modulus of the films were determined by subjecting them to a controlled tension of 1 kN load at a cross-head speed of 50 mm/min. Their responses to the applied force just before breaking were measured.

Barrier properties. The barrier properties of the carboxymethyl starch-based composite films were determined using ASTM E96-95 standard procedures as described in earlier publications with slight modifications [27]. The water vapor permeability (WVP) of the films was evaluated by a gravimetric approach. A permeation cup with specific dimensions (4 cm in diameter and 3.5 cm in height) was utilized for the measurement. The films were cut into circular discs and mounted on the top surface of the cup using a collar-type lid supported with a rubber washer. The cup contained activated silica gel to maintain 0% relative humidity inside. The cup was then placed in a desiccator containing a saturated solution of NaCl (75% relative humidity). The test cup with the film was periodically weighed at a 24 h (1 day) interval for 5 days under room temperature, and the amount of water vapor that permeated through the film was calculated from the weight gain. The water vapor transmission rate (WVTR) through the film was determined from the plot of water vapor permeated as a function of time (Eq. (1)). The WVP was then calculated by considering various factors such as the film's thickness, area, and the partial pressure difference across the film (Eq. (2)). This method provides a comprehensive understanding of the barrier properties of the composite films in terms of their ability to prevent the permeation of water vapor.

$$\mathrm{WVTR} = \frac{S}{A} \tag{1}$$

$$\mathrm{WVP} = \frac{\mathrm{WVTR}}{S^1\left(R_2 - R_1\right)} \times L \tag{2}$$

where S is the slope of a plot; A is the cross-sectional area of the films, L is the film's mean thickness, mm; S^1 is the saturation vapor pressure at test temperature, Pa; R_1 is the relative humidity in the test chamber expressed as a fraction, and R_2 is the relative humidity in the vapor sink expressed as a fraction.

Determination of water sorption characteristics. The method used for this study is in accordance with that described in previous publications [28]. The films were first cut into pieces of 3 × 3 cm and dried in an oven at 60°C for 4 h to obtain a constant weight. One side of each film was covered with aluminum foil to allow absorption only on one side and prevent moisture permeation from the other side. The moisture sorption was measured at 25°C (75% relative humidity) in a desiccator containing a saturated solution of NaCl. The weight of the films was measured every 6 h for 7 days to reach the equilibrium weight. A control was set up to account for any moisture adsorbed on the aluminum foil surface. The mass of the water vapor absorbed was expressed as a weight fraction and plotted against the square root of time. The sorption, diffusion, and permeability coefficients were calculated using the Fickian equations (Eq. 3). The sorption coefficient was determined using the simplified Henry's law, where the concentration of absorbed water vapor in the film is linearly dependent on the water vapor partial pressure, and was calculated as a proportionality constant (Eq. 4). The sorption, diffusion, and permeability coefficients were calculated to understand the sorption properties of the composite films.

$$\frac{m_t}{m_\infty} = 1 - \sum_{n=0}^{\infty} \frac{8}{(2n+1)^2 x n^2} \times e^{\frac{-D x (2n+1)^2 x n^2 x t}{l^2}} \tag{3}$$

For short exposure times, the simplified Fickian equation (Eq. 4) holds:

$$\frac{m_t}{m_\infty} = \frac{4}{h}\sqrt{\frac{Dt}{\pi}} \tag{4}$$

where $\frac{m_t}{m_\infty}$ is the mass fraction of absorbed water vapour (i.e m_t is the mass absorbed at time t and m_∞ is the mass of moisture absorbed at equilibrium), h is the thickness of the film, π = 3.142, D is the diffusion coefficient, t is the time. The application of these equations to polymer composite materials involves simplifications, and thus, D should be considered as an effective diffusion coefficient, D_{eff} [29] can be determined experimentally from the initial slope (s) of the sorption curve (Eq. (5)).

$$D_{eff} = \pi\left[\frac{s}{4}\right]^2 \tag{5}$$

The sorption or solubility coefficient was determined using a mathematical expression based on Henry's law which assumes a linear relationship between the concentration of absorbed water vapour, C_{water} (i. e. in the film and the partial pressure of water vapour ($C_{water} = m_\infty \rho$) as described in Eq. (6) [18, 31].

$$S_{eff} = \frac{C_{water}}{P_{water}} = \frac{m_\infty}{\Delta P}\rho \tag{6}$$

where S_{eff} is the sorption coefficient; ρ is the density of the film and ΔP is the saturation vapour pressure at 75% relative humidity.

The water vapour permeability coefficient (P_{eff}) of the films as determined by sorption kinetics can be calculated using the relationship:

$$P_{eff} = D_{eff} \times S_{eff} \tag{7}$$

Determination of biodegradation. The biodegradability of the composite films was evaluated using the soil burial degradation method, as described by Chaisuwan *et al.* [30] with slight modifications. This method involved burying the film samples in compost soil to assess their degradation over time. The composite films were cut into rectangular pieces of 3 × 5 cm. These pieces were then buried in garden buckets filled

with compost soil at a depth of 10 cm. The buckets were kept at room temperature, and the soil was maintained in a moist state through regular watering. This ensured a consistent environment for the degradation process. The degradation of the films was assessed by measuring their weight at regular intervals of 7 days over a total period of 8 weeks (56 days). After removal from the soil, the films were gently washed to remove adhered soil, and the weight of the dry residual film was determined. The degree of soil burial degradation (DSBD), %, was calculated from the percentage weight loss of each film sample over time (Eq. 8). This equation provided a numerical value representing the extent of degradation, allowing for a comprehensive evaluation of the films' biodegradability.

$$\text{DSBD} = \frac{W_i - W_n}{W_i} \times 100 \qquad (8)$$

where W_i is the initial weight of the films before burial and W_n is the residual weight of the films after soil burial degradation over 7 successive days.

Tools and equipment manufacturers. The instruments used in this study, such as the digital caliper, oven, analytical balance, desiccator, and other equipment, were obtained from well-known manufacturers, including Hanna Instruments (Woonsocket, Rhode Island, USA), Thermo Fisher Scientific (Waltham, Massachusetts, USA), and Mettler Toledo (Columbus, Ohio, USA), among others.

Statistical analysis. Statistical analysis was carried out using the BMDP 2R software (version 7.0) for stepwise multiple regressions. The data were presented as a mean of three replicate measurements. The findings were considered statistically significant at $p < 0.05$.

RESULTS AND DISCUSSION

Scanning electron microscopy. Scanning electron microscopy (SEM) reveals important insights into the surface structural characteristics of composite materials in terms of the topography, distribution, and interaction of the components within the material [31]. The SEM image of carboxymethyl starch (CMS) powder (Fig. 2a) exhibited a porous granular structure, whereas the CMS film (Fig. 2b) displayed a smooth and continuous surface. This indicates effective gelatinization and plastification of CMS upon dispersion and heating in water during preparation [7].

The SEM image of the CMS/polyvinyl alcohol (PVA) blend (Fig. 2c) revealed a smooth and continuous surface structure, with particle domains having diameters in the micron range, possibly due to phase separation. However, the predominantly continuous phase indicated good miscibility and homogeneity between CMS and PVA. The indistinct interface between the two polymers suggested strong intermolecular interactions between CMS and PVA molecules, which were possibly facilitated by hydrogen bonding [16]. This observation indicates a high degree of compatibility and interaction between the two polymers [9].

The SEM images of the CMS/PVA/kaolin composite (Fig. 2d) exhibited a smooth surface homogenous morphology with no cracks or defects. However, there were some visible particle aggregates and zones of agglomeration due to the presence of kaolin in the blend. This distribution of kaolin aggregates in the homogenous matrix of CMS/PVA had a positive impact on the interfacial interaction between the kaolin particles and the polymer phase [4, 22].

X-ray diffraction (XRD) is a powerful technique used to assess the structural properties of materials by analyzing the diffraction intensity. It provides valuable information about the crystalline regions within the material [32]. In this study, XRD was employed to investigate the crystallinity and structural changes induced by PVA and kaolin additives in carboxymethyl starch (CMS)-based composite films. The results revealed significant changes in the crystalline peak patterns upon plasticization of CMS and blending with polyvinyl alcohol (PVA), indicating modifications of the material's crystalline structure. Specifically, the XRD diffractogram of the CMS powder (Fig. 3a) exhibited a characteristic peak intensity at 20.4°, indicating a high degree of crystallinity. In contrast, the CMS film (Fig. 3b) showed a decrease in peak intensity, suggesting disruption of the granular structure during heating and gelatinization [9].

When CMS was blended with PVA, an increase in peak intensity was observed in the XRD diffractogram of the film (Fig. 3c). This enhancement in peak intensity suggested strengthening of intermolecular bonding via additional hydroxyl groups on the PVA chains [9, 33]. The hydroxyl groups on the PVA chains can form hydrogen bonds with CMS, leading to improved crystallinity and structural stability.

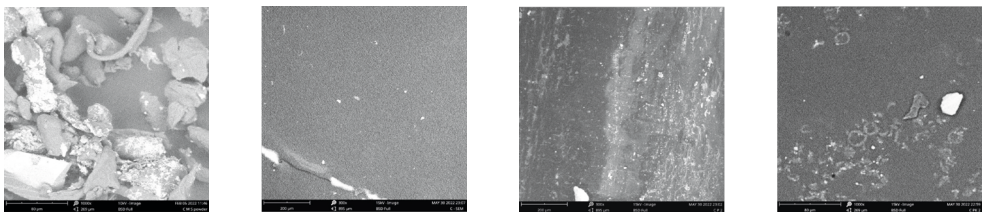

a b c d

Figure 2 SEM micrographs of CMS powder (a), CMS film (b), CMS/PVA film (c), and CMS/PVA/kaolin film (d)

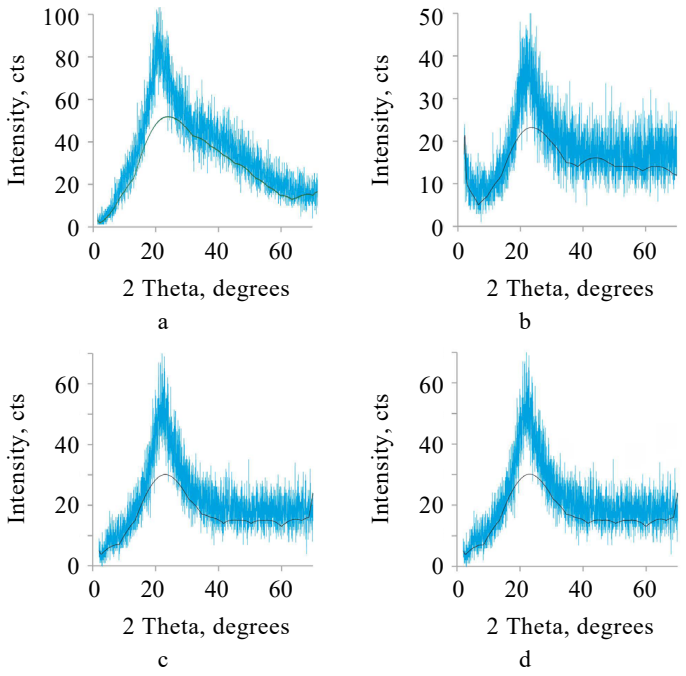

Figure 3 X-ray diffraction patterns of CMS powder (a), CMS film (b), CMS/PVA film (c), and CMS/PVA/kaolin film (d)

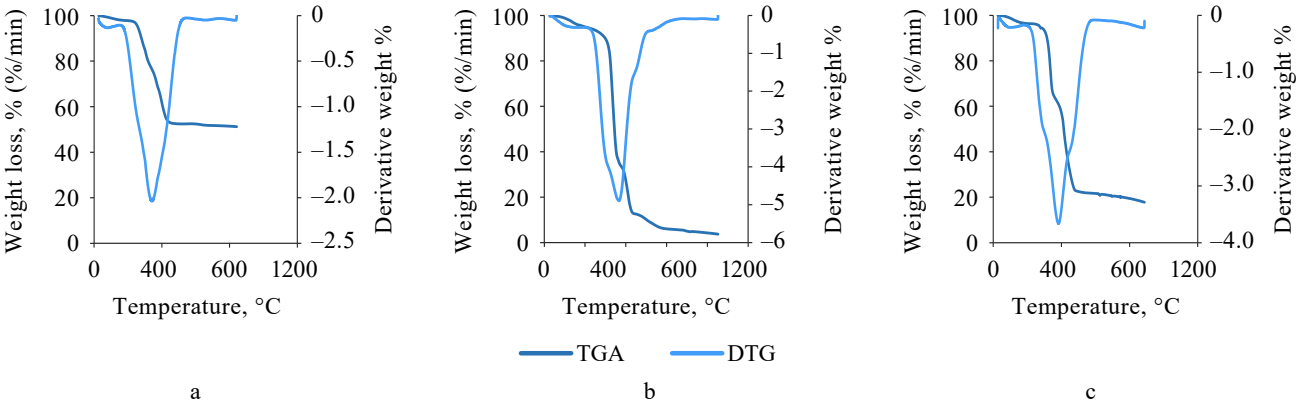

Figure 4 Thermogravimetric and derivative thermogravimetric curves of CMS powder (a), CMS film (b), CMS/PVA film (c), and CMS/PVA/kaolin film (d)

However, the incorporation of kaolin into the CMS/PVA films did not show any observable change in structural integrity. This can be seen from the non-distinguishable XRD peaks of the CMS/PVA and CMS/PVA/kaolin films, which was contrary to the scanning electron microscopy results. Neither did this finding agree with those reported by Yang *et al.* [33], who investigated the effect of additives on cross-linked CMS/PVA composite films. The authors observed that the addition of $CaCl_2$ and nano-SiO_2 to the cross-linked and PVA films improved their crystallinity and structural stability.

Thermal stability. Thermogravimetric analysis and derivative thermogravimetry were used to assess the thermal stability of carboxymethyl starch (CMS)-based composite films (Fig. 4). The thermal stability of CMS-based composite films is crucial to determine the maximum thermal conditions they can withstand without degrading or altering their structural characteristics [7].

The degradation process of the composite films occurred in three steps. The first step occurred at 25–200°C, with a weight loss of 0–6% for all the materials. The derivative thermogravimetry peaks were observed at 103, 160, and 105°C for the pure CMS film, CMS/PVA film, and CMS/PVA/kaolin film, respectively. The CMS film exhibited the lowest weight loss, while the CMS/PVA blend showed the highest weight loss. This initial degradation step corresponds to the loss of water molecules within the polymer matrix [34, 35]. The second step of degradation occurred at 200–350°C, with a weight loss of 5–10%. This step is attributed to the evaporation of volatile components like glycerol (melting point 290°C) [36]. The subsequent stage of degradation occurred at > 350°C and was attributed to the decomposition of composite components such as CMS, PVA, and/or kaolin [37]. This ultimate degradation step resulted in maximum weight loss for all the materials (Table 2).

Notably, the CMS film exhibited the lowest weight loss in this third stage apparently due to the absence of PVA and kaolin components.

PVA in the CMS film increased the maximum degradation temperature (DT_{max}) from 341.0 to 366.2°C, as can be observed in the derivative thermogravimetric peaks. However, the percentage weight loss for the CMS/PVA blend was significantly higher than that for the pure CMS film. In contrast, the CMS/PVA blend reinforced with kaolin exhibited a higher DT_{max} (383.3°C) and a lower percentage weight loss (39.1%) compared to the pure CMS and CMS/PVA films, indicating improved thermal stability.

Effect of polyvinyl alcohol on tensile mechanical properties of films. Figure 5 shows the effects of polyvinyl alcohol (PVA) on the tensile strength, percentage of elongation at break, and tensile modulus of the carboxymethyl starch (CMS) films. As can be seen, the addition of PVA (0–60%) into the CMS films resulted in a notable increase in tensile mechanical properties, with a 2.08-fold increase in tensile strength (Fig. 5a), a 1.31-fold increase in percentage of elongation at break (Fig. 5b), and a 1.58-fold increase in tensile modulus (Fig. 5c). The pure CMS film exhibited the lowest tensile strength, percentage of elongation at break (% EB), and tensile modulus, with values of 1.56 MPa, 25.40%, and 6.14 MPa, respectively. In contrast, the CMS/PVA film containing 60% of PVA demonstrated the highest values, with a tensile strength of 3.24 MPa, % EB of 33.3%, and tensile modulus of 9.32 MPa. This significant enhancement is attributed to the strengthening of intermolecular bonding between the CMS and PVA chains via hydrogen bonding [38]. The increased % EB values also indicate improved flexibility and toughness of the composite films. Similar findings were reported by Patil *et al.* [16], who investigated the effect of PVA incorporation (0–90%) into starch-based films. They observed a significant increase in tensile strength and the percentage of elongation at break of 1.24–1.93 and 1.93–3.74 fold, respectively. This consistency in results highlights the positive impact of PVA on the mechanical properties of CMS-based composite films.

Effect of kaolin on tensile mechanical strength of films. Figure 6 demonstrates the impact of kaolin on the tensile mechanical properties of the composites of carboxymethyl starch (CMS), polyvinyl alcohol (PVA), and kaolin. As can be seen, the introduction of 1.5 phr kaolin into the CMS/PVA film significantly increased its tensile strength by 18.8% from 3.24 to 3.85 MPa. Further increments in kaolin up to 4.5 phr resulted in a remarkable increase in tensile strength, reaching a maximum of 5.93 MPa (Fig. 6a). This enhancement may be attributed to a high degree of exfoliation and dispersion of kaolin in the polymer matrices of CMS and PVA [22]. However, a decrease in tensile strength to 5.82 MPa was observed at 5.5 phr kaolin. This reduction may be due to the kaolin content exceeding its compatibility limit and leading to the agglomeration and reduced interaction with the polymer matrix. Ariffin *et al.* [39] reported similar findings, where the flexural strength of polypropylene/kaolin composites exhibited an increase with rising kaolin contents, reaching an optimal value at 5 phr kaolin. However, further increases in kaolin beyond this threshold resulted in a decline in the mechanical properties of the composites.

The percentage of elongation at break (% EB) showed a slight decrease from 36.67 to 35.33% at 4.5 phr of kaolin (Fig. 6b), followed by a minor increase to

Table 2 Degradation steps of carboxymethyl starch-based composite films

Films	Step 1		Step 2		Step 3	
	DT peak, °C	Weight loss, %	DT peak, °C	Weight loss, %	DT_{max} peak, °C	Weight loss, %
CMS	103	1.14	256.4	4.8	341.0	23.6
CMS/PVA	160	4.05	294.5	9.6	366.2	64.6
CMS/PVA/Kaolin	103	1.33	302.3	6.9	383.3	39.1

DT is the degradation temperature; CMS is the carboxymethyl starch; PVA is the polyvinyl alcohol

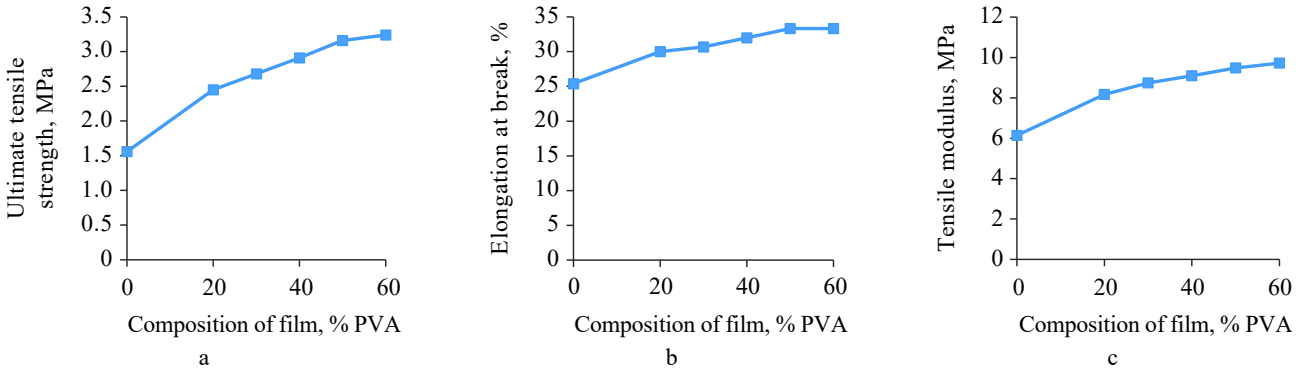

Figure 5 Plots of ultimate tensile strength (a), elongation at break (b), and tensile modulus (c) of carboxymethyl starch-based films versus percentage of polyvinyl alcohol

36.00% at 5.5 phr kaolin. This suggests that the addition of kaolin has a minimal impact on the flexibility of the composite films.

The effect of kaolin on tensile modulus (Fig. 6c) revealed a significant increase with rising kaolin concentrations, from 10.50 to 16.17 MPa. This enhancement in tensile modulus can be attributed to the presence of well-distributed rigid kaolin particles, as evident in the scanning electron microscopy results, which impose a mechanical restraint on the matrix by restricting its mobility and deformability [40].

Barrier properties. For a composite film to be considered suitable for packaging applications, it must possess sufficient barrier properties to prevent water vapor or air permeation, thereby ensuring the integrity of the packaged product [41]. The water vapor barrier property is typically measured in terms of water vapor permeability (WVP), where films with lower WVP values exhibit higher barrier properties.

Effect of polyvinyl alcohol on the water vapor permeability of films. Figure 7 shows the effect of polyvinyl alcohol (PVA) on the water vapor permeability (WVP) of carboxymethyl starch (CMS) films. As can be seen, the WVP of the CMS/PVA blend decreased by 28.9% with a PVA content from 0 to 60% (Fig. 7a). This is because the blending of PVA with CMS increases the intermolecular bonding between CMS and PVA via additional hydroxyl groups from PVA. This enhances their compatibility and lowers the penetration of water vapor molecules through the blend. The CMS/PVA blend containing 60% of PVA showed the lowest WVP (2.04×10^{-11} gm/m^{2}s·Pa), while the CMS film without PVA had the highest WVP (2.87×10^{-11} gm/m^{2}s·Pa).

Effect of kaolin on the water vapor permeability of films. The composite films showed a decrease in the water vapor permeability (WVP) from 1.5×10^{-11} to 0.945×10^{-11} gm/m^{2}s·Pa with the incorporation of 1.5–5.5 phr of kaolin (inorganic filler) (Fig. 7b). This result was in line with the studies by Yang *et al.* [33], who reported lower WVP values for cross-linked carboxymethyl starch-based composites with an increase in the inorganic filler (nano-SiO_2 particle). It might be that the polymer matrix system was reinforced by the exfoliation and intercalation of kaolin particles with carboxymethyl starch/polyvinyl alcohol chains. Consequently, this created a more tortuous pathway for water vapor molecules to diffuse through, thereby enhancing the barrier properties of the composite film [42].

Water vapor sorption characteristics. The water vapor sorption properties of carboxymethyl starch-based composite films were studied in terms of their sorption, diffusion, and permeability coefficients (Figs. 8 and 9). The effective diffusion coefficient was calculated from the slope of the early linear parts of the water vapor sorption curve.

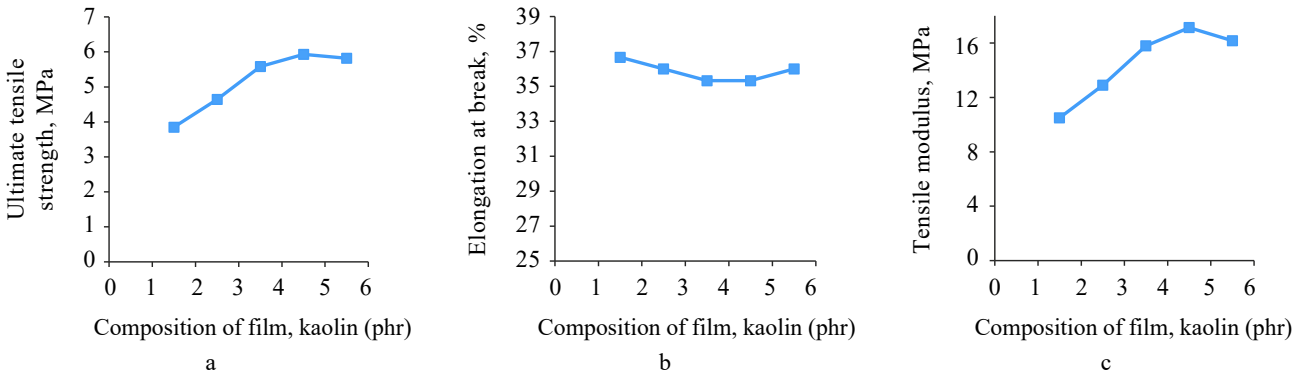

Figure 6 Plots of ultimate tensile strength (a), elongation at break (b), and tensile modulus (c) of carboxymethyl starch-based films versus kaolin content

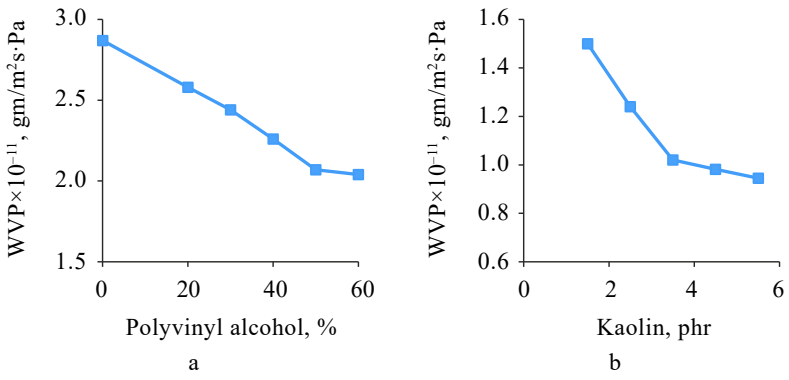

Figure 7 Effect of polyvinyl alcohol (a) and kaolin (b) on the water vapor permeability of carboxymethyl starch-based composite films

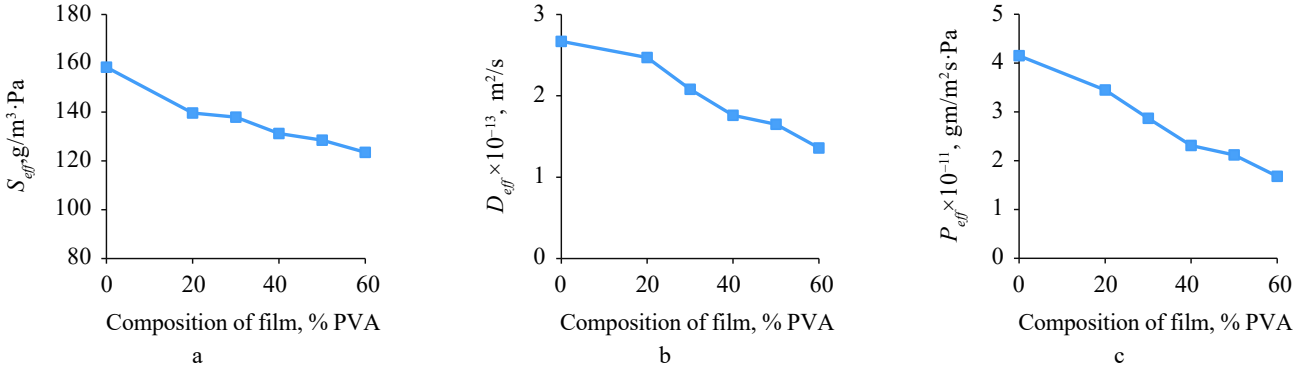

Figure 8 Plots of effective sorption S_{eff} (a), diffusion D_{eff} (b), and water vapor permeability P_{eff} (c) coefficients versus polyvinyl alcohol content

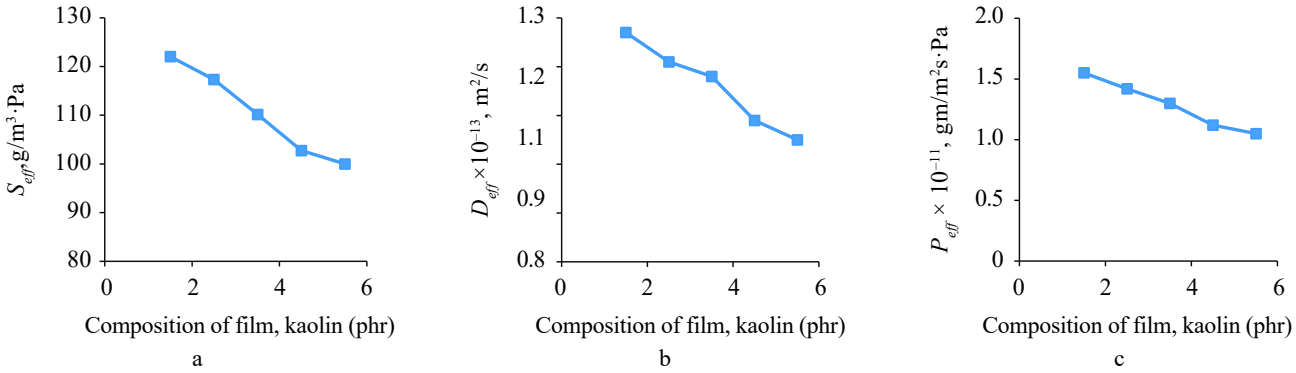

Figure 9 Plots of effective sorption S_{eff} (a), diffusion D_{eff} (b), and water vapor permeability P_{eff} (c) coefficients versus kaolin content

Effect of polyvinyl alcohol on the water vapor sorption. The influence of polyvinyl alcohol (PVA) on the water vapor sorption properties of the carboxymethyl starch composite films is illustrated in Fig. 8. The results revealed a progressive decrease in the effective sorption coefficients, diffusion coefficients, and water vapor permeability by 22% (Fig. 8a), 49.1% (Fig. 8b) and 59.5% (Fig. 8c), respectively, with increasing PVA concentrations (0–60%) in the films. Notably, the film containing 60% of PVA exhibited the lowest values for these parameters (S_{eff} 123.53 g/m³·Pa, D_{eff} 1.36×10^{-13} m²/s, and P_{eff} 1.68×10^{-11} g/m·Pa, respectively). This decrease can be attributed to the strong intermolecular interaction between carboxymethyl starch and PVA, which reduces the film's tendency to absorb moisture [43]. The formation of hydrogen bonds between the hydroxyl groups of starch and PVA leads to a more compact and dense film structure, thereby lowering the sorption, diffusion, and permeability coefficients [44]. The reduced water vapor permeability of the CMS/PVA composite films is desirable for packaging applications, as it helps maintain the quality and freshness of the packaged product by minimizing moisture absorption [45].

Effect of kaolin on the water vapor sorption. Figure 9 illustrates the impact of kaolin on the water vapor sorption properties of carboxymethyl starch (CMS) composite films. As can be seen, the incorporation of kaolin at concentrations of 1.5–5.5% resulted in a significant decrease in the sorption, diffusion, and permeability coefficients by 18.1% (Fig. 9a), 17.3% (Fig. 9b), and 32.3% (Fig. 9c), respectively. This reduction in the water vapor sorption properties of the blends indicated a decrease in the material's affinity for moisture [42]. This modification enhances the material's suitability for packaging applications, where minimal water vapor permeation is desired. The kaolin concentrations between 4.5 and 5.5 phr resulted in a slight decrease in water vapor sorption (2.7%), diffusion (3.7%), and permeability (6.3%) values. This subtle decline may indicate the peak kaolin concentration, beyond which further additions may not yield significant improvements. The dispersion of kaolin in the CMS/PVA polymer matrix creates a more tortuous pathway for water vapor molecules to diffuse through, thereby enhancing the material's water vapor resistance and barrier properties [42].

Biodegradation of carboxymethyl starch-based composite films. The biodegradability of polymers is a crucial aspect to consider in polymer applications, as these materials will ultimately be disposed of after their intended use. The ability of polymers to biodegrade naturally is essential for reducing the environmental impact and promoting sustainability [46]. The biodegradability of carboxymethyl starch (CMS)-based composite films was analyzed using the soil burial method (Figs. 10 and 11). This method provides a realistic environment for assessing biodegradability, as it simulates natural conditions and allows for the evaluation of microbial degradation [47]. The degree of biodegradability of the films

was studied by evaluating their weight loss for 56 days at periodic intervals of 7 days. As can be observed in Figure 10, all the film samples showed a significant increase in weight loss within the initial 7-day interval of burial. Specifically, the CMS/PVA blends (Fig. 10a) showed a 38–23% weight loss (decreasing with higher PVA contents, 0–60%), while the CMS/PVA/kaolin films exhibited lower weight loss (16–20%) dependent on the kaolin content (Fig. 10b). This rapid biodegradation can be attributed to the initial microbial colonization and degradation of the polymer surface [47].

However, the rate of biodegradation began to decrease during the subsequent days until the completion of the 56-day period. This decline can be due to the reduced availability of easily degradable materials and the increased complexity of the polymer structure [28]. Particularly, the rate of biodegradation of the CMS/PVA blends decreased by 22.2% with increasing PVA over the 56 days, while the pure CMS films exhibited the highest degradation rate of 90% (Fig. 11a). This suggests that CMS degrades at a faster rate than PVA, possibly due to its higher moisture absorption affinity. The absorbed moisture leads to swelling, creating a conducive environment for microbial growth on the film's surface [48]. In contrast, the incorporation of PVA into the CMS film appears to reduce biodegradability, potentially due to the formation of a more stable and compact polymer structure. This reduced biodegradability may result from PVA's ability to restrict the accessibility of microbes to the CMS chains, thereby slowing down the degradation process [49, 50].

In the CMS/PVA films reinforced with kaolin, the rate of biodegradation decreased by 30.4% with increasing kaolin contents (0–5.5 phr) (Fig. 11b). This is due to the formation of interfacial bonds between well-dispersed kaolin and the CMS/PVA matrix, which reinforces the polymer chain and renders it less accessible to the soil microbial attack [51]. Within the 56-day period, the films degraded quite significantly, if not completely, as evidenced by their substantial weight loss. This finding is crucial for the development of sustainable plastic packaging solutions, as it demonstrates the potential of these bioplastic films to degrade over time, reducing their environmental impact and promoting a more circular economy.

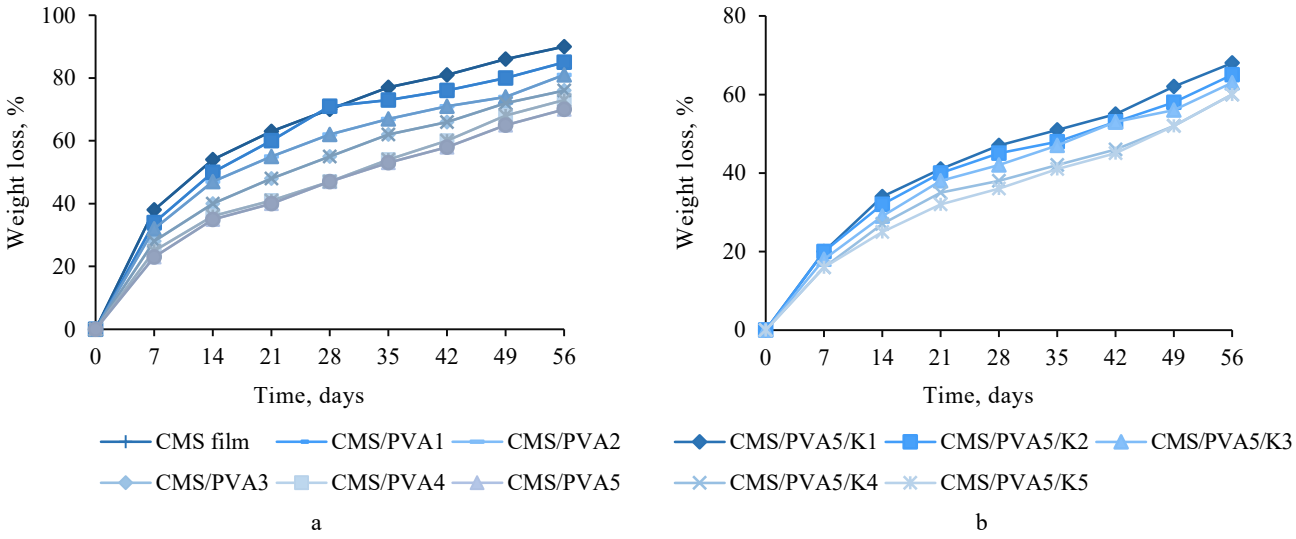

Figure 10 Soil burial biodegradability rates of carboxymethyl starch/polyvinyl alcohol (a) and CMS/PVA/kaolin composite (b) films for 56 days

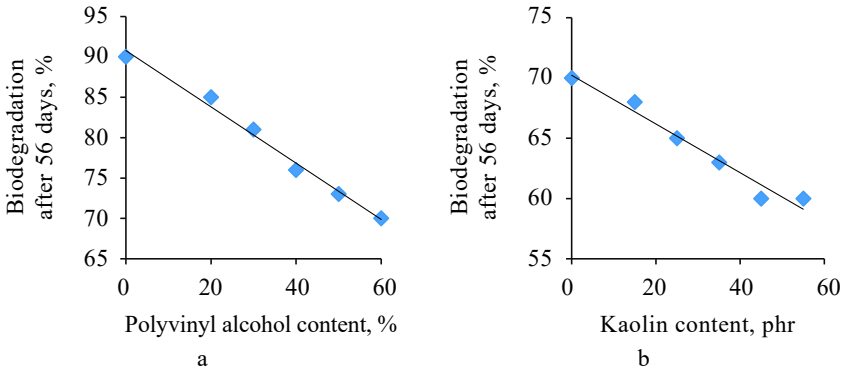

Figure 11 Degree of soil burial biodegradation of carboxymethyl starch-based films after 56 days versus polyvinyl alcohol (a) and kaolin (b) contents

CONCLUSION

In this study, we developed a composite film from carboxymethyl starch, polyvinyl alcohol, and kaolin for sustainable and eco-friendly bioplastic packaging. Blending carboxymethyl starch with polyvinyl alcohol at various concentrations and reinforcing the blend with kaolin yielded a bioplastic material with suitable properties for packaging applications.

The characterization results from scanning electron microscopy, X-ray diffraction, and thermogravimetric analysis revealed the composite's good surface microstructure, satisfactory crystallinity, and improved thermal stability, which affirmed the effective integration of the components.

The tensile mechanical test demonstrated significant improvements in the film's tensile strength and elongation at break with the addition of polyvinyl alcohol and kaolin, indicating enhanced durability. Furthermore, the inclusion of polyvinyl alcohol and kaolin substantially reduced the film's barrier properties in terms of water vapor permeability, making the bioplastic more effective at preventing moisture transfer.

Additionally, the water sorption ability of the composite film decreased with the incorporation of polyvinyl alcohol and kaolin, indicating improved resistance to water vapor absorption. Most importantly, the biodegradability test showed a significant level of biodegradation during the study period, which confirmed the composite's eco-friendly nature aligning with the principles of sustainability.

Conclusively, the carboxymethyl starch/polyvinyl alcohol/kaolin composite, with its improved functional properties, offers a viable alternative to conventional plastics in combating environmental concerns and plastic waste accumulation.

CONTRIBUTION

All the authors contributed equally and substantially to this research. Each author played a vital role in the conception, design, implementation, and interpretation of research findings, as well as in the overall preparation of this manuscript.

CONFLICT OF INTEREST

The authors state that there is no conflict of interest.

ACKNOWLEDGEMENTS

The authors wish to express their gratitude to the Head of Department of Chemistry, University of Benin for granting permission to use their laboratory facilities for this research and also to Mr. Isa Yakubu (Ahmadu Bello University) and Mr. Henry (University of Benin) for their technical assistance.

REFERENCES

1. Buryndin VG, Artyemov AV, Savinovskih AV, *et al*. Biostability of binder-free wood and plant plastics protected with antiseptics. Foods and Raw Materials. 2022;10(1):148–154. https://doi.org/10.21603/2308-4057-2022-1-148-154
2. Eremeeva NB. Nanoparticles of metals and their compounds in films and coatings: A review. Foods and Raw Materials. 2024;12(1):60–79. https://doi.org/10.21603/2308-4057-2024-1-588
3. Agarwal S. Major factors affecting the characteristics of starch-based biopolymer films. European Polymer Journal. 2021;160:11078. https://doi.org/10.1016/j.eurpolymj.2021.110788
4. Tabassum N, Rafique U, Qayyum M, Mohammed AAA, Asif S, *et al*. Kaolin–polyvinyl alcohol–potato starch composite films for environmentally friendly packaging: Optimization and characterization. Journal of Composite Science. 2024;8(1):29. https://doi.org/10.3390/jcs8010029
5. Shanmathy M, Mohanta M, Thirugnanam A. Development of biodegradable bioplastic films from Taro starch reinforced with bentonite. Carbohydrate Polymer Technologies and Applications. 2021;2:100173. https://doi.org/10.1016/j.carpta.2021.100173
6. Gómez-Aldapa CA, Velazquez G, Gutierrez MC, Rangel-Vargas E, Castro-Rosas J, *et al*. Effect of polyvinyl alcohol on the physicochemical properties of biodegradable starch films. Materials Chemistry and Physics. 2020;239:122–127. https://doi.org/10.1016/j.matchemphys.2019.122027
7. de Azevedo LC, Rovani S, Santos JJ, Dias DB, Nascimento SS, *et al*. Biodegradable films derived from corn and potato starch and study effect of silicate extracted from sugarcane waste ash. ACS Applied Polymer Materials. 2020;2(6):2160–2169. https://doi.org/10.1021/acsapm.0c00124
8. Compart J, Singh A, Fettke J, Apriyanto A. Customizing starch properties: A review of starch modifications and their applications. Polymers. 2023;15(16):3491. https://doi.org/10.3390/polym15163491
9. Omoike BA, Okieimen FE, Imoisi C, Abubakar MA. Characterization and evaluation of properties of cassava starch/poly(vinyl alcohol) films for food and pharmaceutical packaging applications. Singapore Journal of Scientific Research. 2024;14(1):34–42. https://doi.org/10.3923/sjsr.2024.34.42
10. Prasad J, Dixit A, Sharma SP, Mwakosya AW, Petkoska AT, *et al*. Nanoemulsion-based active packaging for food products. Foods and Raw Materials. 2024;12(1):22–36. https://doi.org/10.21603/2308-4057-2024-1-585
11. Spychaj T, Wilpiszewska K, Zdanowicz M. Medium and high substituted carboxymethyl starch: Synthesis, characterization and application. Starch – Stärke. 2013;65:22–33. https://doi.org/10.1002/star.201200159

12. Omoike BA, Okieimen FE, Imoisi C. Development of lemongrass oil-based starch/PVA/kaolin films: Antimicrobial properties and biodegradability. Science International. 2025;13(1):1–12. https://doi.org/10.17311/sciintl.2025.01.12
13. Bangar SP, Whiteside WS, Ashogbon AO, Kumar M. Recent advances in thermoplastic starches for food packaging: A review. Food Packaging and Shelf Life. 2021;30:100743. https://doi.org/10.1016/j.fpsl.2021.100743
14. Lee S, Kim ST, Pant BR, Song HH, Lee SK, *et al*. Carboxymethylation of corn starch and characterization using assymetrical flow field-flow fractionation coupled with multiangle light scattering. Journal of Chromatography A. 2010;1217:4623–4628. https://doi.org/10.1016/j.chroma.2010.04.082
15. Bhattacharyya D, Singhal RS, Kulkarni PR. Physicochemical properties of carboxymethyl starch prepared from corn and waxy amaranth starch. Carbohydrate Polymers. 1995;27:167–169. https://doi.org/10.1016/0144-8617(95)00062-C
16. Patil S, Bharimalla AK, Mahapatra A, Dhakane-Lad J, Arputharaj A, *et al*. Effect of polymer blending on mechanical and barrier properties of starch-polyvinyl alcohol based biodegradable composite films. Food Bioscience. 2021;44 (Part A):101352. https://doi.org/10.1016/j.fbio.2021.101352
17. Phattarateera S, Xin L, Amphong C, *et al*. Comparative studies of starch blends on the properties of PVA films. Carbohydrate Polymer Technologies and Applications. 2023;6:100340. https://doi.org/10.1016/j.carpta.2023.100340
18. Yurong G, Dapeng L. Preparation and characterization of corn starch/PVA/glycerol composite films incorporated with ε-polylysine as a novel antimicrobial packaging material. e-Polymers. 2020;20(1):154–161. https://doi.org/10.1515/epoly-2020-0019
19. Idris A, Muntean A, Mesic B, Lestelius M, *et al*. Oxygen barrier performance of poly(vinyl alcohol) coating films with different induced crystallinity and model predictions. 2021;11(10):1253. https://doi.org/10.3390/coatings11101253
20. Deng H, Su J, Zhang W, Khan A, Sani MA, *et al*. A review of starch/polyvinyl alcohol (PVA) blend film: A potential replacement for traditional plastic-based food packaging film. International Journal of Biological Macromolecules. 2024;273(Part 1):132926. https://doi.org/10.1016/j.ijbiomac.2024.132926
21. Gierszewska M, Jakubowska E, Olewnik-Kruszkowska E. Effect of chemical crosslinking on properties of chitosan montmorillonite composites. Polymer Testing. 2019;77:105872. https://doi.org/10.1016/j.polymertesting.2019.04.019
22. Rammak T, Boonsuk P, Kaewtatip K. Mechanical and barrier properties of starch blend films enhanced with kaolin for application in food packaging. International Journal of Biological Macromolecules. 2021;192:1013–1020. https://doi.org/10.1016/j.ijbiomac.2021.10.081
23. Kumari P, Kumari N, Mohan C, *et al*. Augmenting barrier efficiency in clay-based starch composite films for enhanced packaging sustainability. Polymers for Advanced Technologies. 2024;35(6):e6458. https://doi.org/10.1002/pat.6458
24. Labelle MA, Ispas-Szabo P, Vilotte F, *et al*. Carboxymethyl starch films as enteric coatings: Processing and mechanistic insights. Journal of Pharmaceutical Sciences. 2024;113(3):725–734. https://doi.org/10.1016/j.xphs.2023.09.002
25. Wilpiszewska K. Hydrophilic films based on starch and carboxymethyl starch. Green Sciences. 2019;21(2):26–30. https://doi.org/10.2478/pjct-2019-0016
26. Garavand Y, Taheri-Garavand A, Garavand F, Shahbazi F, Khodaei D, *et al*. Starch-polyvinyl alcohol-based films reinforced with chitosan nanoparticles: Physical, mechanical, structural, thermal and antimicrobial properties. Applied Sciences. 2022;12(3):1111. https://doi.org/10.3390/app12031111
27. Omoike BA, Okieimen FE, Imoisi C. Design and optimization of eco-friendly biocomposite films for packaging applications using response surface methodology. Tanzania Journal of Science. 2024;50(5):961–974.
28. Turan D. Water vapor transport properties of polyurethane films for packaging of respiring foods. Food Engineering Reviews. 2021;13:54–65. https://doi.org/10.1007/s12393-019-09205-z
29. Omoike BA, Okieimen FE, Imoisi C. Water vapour transport properties of cassava starch/poly(vinyl alcohol) films via experimental and fickian methods. Trends in Applied Sciences Research. 2024;19(1):225–232. https://doi.org/10.3923/tasr.2024.225.232
30. Chaisuwan K, Anurakumphan D, Hemmanee S, Ruamcharoen I, Leelakriangsak M. Soil burial degradation of starch-based films on microbial load and plant growth. Journal of Sustainability Science and Management 2023;18(3):110–124. https://doi.org/10.46754/jssm.2023.03.008
31. Rydz J, Šišková A, Eckstein AA. Scanning electron microscopy and atomic force microscopy: Topographic and dynamical surface studies of blends, composites, and hybrid functional materials for sustainable future. Advances in Materials Science and Engineering. 2019;2019:681785. https://doi.org/10.1155/2019/6871785
32. Nath D, Singh F, Das R. X-ray diffraction analysis by Williamson-Hall, Halder-Wagner and size-strain plot methods of CdSe nanoparticles- a comparative study. Materials Chemistry and Physics. 2020;239:122021. https://doi.org/10.1016/j.matchemphys.2019.122021
33. Yang L, Xie M, Fang J, Zhang T, Wang X, *et al*. Effect of additives on properties of cross-linked carboxymethyl starch/polyvinyl alcohol composite films. Journal of Applied Polymer Science. 2022;139(4):51546. https://doi.org/10.1002/app.51546

34. Manimaran M, Norizan MN, Kassim MHM, Adam MR, Norrrahim MNF, *et al*. Critical assessment of the thermal stability and degradation of chemically functionalized nanocellulose-based polymer nanocomposites. Nanotechnology Reviews. 2024;13(1):20240005. https://doi.org/10.1515/ntrev-2024-0005

35. Quilez-Molina AI, Meins JFL, Charrier B, Dumon M. Starch-fibers composites, a study of all-polysaccharide foams from microwave foaming to biodegradation. Carbohydrate Polymers. 2024;328:121743. https://doi.org/10.1016/j.carbpol.2023.121743

36. Luchese CL, Benelli P, Spada JC, Tessaro IC. Impact of the starch source on the physicochemical properties and biodegradability of different starch-based films. Journal of Applied Polymer Science. 2018;135(33):46564. https://doi.org/10.1002/app.46564

37. Basiak E, Lenart A, Debeaufort F. Effect of starch type on the physico-chemical properties of edible films. International Journal of Biological Macromolecules. 2017;98:348–356. https://doi.org/10.1016/j.ijbiomac.2017.01.122

38. Tan L, Sun B, Luo W, Liu S, Qiu B, *et al*. Enhanced mechanical property and water solubility of polyvinyl alcohol film via constructing hydrogen-bond network by adding carboxymethyl chitosan. Journal of Macromolecular Science, Part A. 2023;61(1):31–39. https://doi.org/10.1080/10601325.2023.2283045

39. Ariffin A, Ariff ZM, Jikan SS. Effects of kaolin and maleic anhydride contents on melt elasticity and flexural behaviour of polypropylene/kaolin and unplasticised poly(vinyl chloride)/kaolin composites. e-Polymers. 2010;10(1):095. https://doi.org/10.1515/epoly.2010.10.1.1069

40. Essabir H, Raji M, Bouhfid R, Qaiss AE. Hybrid nanocomposites based on graphene and nano-clay: Preparation, characterization, and synergistic effect. In: Qaiss AK, Bouhfid R, Jawaid M, editors. Graphene and Nanoparticles Hybrid Nanocomposites. Singapore: Springer; 2021, pp. 153–181. https://doi.org/10.1007/978-981-33-4988-9_5

41. Luo Q, Hossen MA, Zeng Y, Dai J, Li S, *et al*. Gelatin-based composite films and their application in food packaging: A review. Journal of Food Engineering. 2022;313:110762. https://doi.org/10.1016/j.jfoodeng.2021.110762

42. Dharini V, Selvam SP, Jayaramudu J, Emmanuel RS. Functional properties of clay nanofillers used in the biopolymer-based composite films for active food packaging applications – Review. Applied Clay Science. 2022;226:106555. https://doi.org/10.1016/j.clay.2022.106555

43. Ma N, Dong W, Qin D, Dang C, Xie S, *et al*. Green and renewable thermoplastic polyvinyl alcohol/starch blend film fabricated by melt processing. International Journal of Biological Macromolecules. 2024;279(Part 2):134866. https://doi.org/10.1016/j.ijbiomac.2024.134866

44. Castro JM, Montalbán MG, Martínez-Pérez N, Domene-López D, Pérez JM, *et al*. Thermoplastic starch/polyvinyl alcohol blend modification by citric acid–glycerol polyesters. International Journal of Biological Macromolecules. 2023;244:125478. https://doi.org/10.1016/j.ijbiomac.2023.125478

45. Abedi-Firoozjah R, Chabook N, Rostami O, Heydari M, Kolahdouz-Nasiri A, *et al*. PVA/starch films: An updated review of their preparation, characterization, and diverse applications in the food industry. Polymer Testing. 2023;118:107903. https://doi.org/10.1016/j.polymertesting.2022.107903

46. Moshood TD, Nawanir G, Mahmud F, Mohamad F, Ahmad MH, *et al*. Sustainability of biodegradable plastics: New problem or solution to solve the global plastic pollution? Current Research in Green and Sustainable Chemistry. 2022;5:100273. https://doi.org/10.1016/j.orgsc.2022.100273

47. Zee MV. Methods for evaluating the biodegradability of environmentally degradable polymers. In: Bastioli C. editor. Handbook of Biodegradable Polymers. Berlin, Boston: De Gruyter; 2020, pp. 1–22. https://doi.org/10.1515/9781501511967-001

48. Mittal A, Garg S, Premi A, Giri AS. Synthesis of polyvinyl alcohol/modified starch-based biodegradable nanocomposite films reinforced with starch nanocrystals for packaging applications. Polymers and Polymer Composites. 2020;29(5):405–416. https://doi.org/10.1177/0967391120922429

49. Lin YP, Dhib R, Mehrvar M. Recent advances in dynamic modeling and process control of PVA degradation by biological and advanced oxidation processes: A review on trends and advances. Environments. 2021;8(11):116. https://doi.org/10.3390/environments8110116

50. Lv Z, Meng X, Sun S, Jiang T, Zhang S, *et al*. Biodegradable carboxymethyl chitosan/polyvinyl alcohol hymexazol-loaded mulch film for soybean root rot control. Agronomy. 2023;13(9):2205. https://doi.org/10.3390/agronomy13092205

51. Abdullah ZW, Dong Y. Biodegradable and water resistant poly(vinyl) alcohol (PVA)/starch (ST)/glycerol (GL)/halloysite nanotube (HNT) nanocomposite films for sustainable food packaging. Frontiers in Materials. 2019;6:58. https://doi.org/10.3389/fmats.2019.00058

ORCID ID

Chinyere Imoisi https://orcid.org/0000-0001-9680-1635

Foods and Raw Materials. 2026;14(2)

ISSN 2308-4057 (Print)
ISSN 2310-9599 (Online)

Review Article
Open Access

Available online at http://jfrm.ru/en
https://doi.org/10.21603/2308-4057-2026-2-680
https://elibrary.ru/CMXWLM

Precision agriculture as a viable means of enhancing sustainable agricultural production

Simbo Diakite[1,*], Nyasha J. Kavhiza[1], Francess S. Saquee[1], Elena N. Pakina[1], Meisam Zargar[1], Ousmane Diarra[2,3], Prince E. Norman[4,], Brahima Traore[2,3], Fasse Samake[2,3], Cheickna Daou[2], Amadou H. Babana[3]**

[1] Institute of Agriculture, People's Friendship University of Russia, Moscow, Russia
[2] Institute of Applied Sciences – ISA, Bamako, Mali
[3] University of Sciences, Techniques and Technologies of Bamako, Bamako, Mali
[4] Sierra Leone Agricultural Research Institute (SLARI), Freetown, Sierra Leone

* e-mail: diakitesimbo88@gmail.com
** e-mail: norman.prince64@gmail.com

Received 01.12.2024; Revised 27.03.2025; Accepted 03.06.2025; Published online 20.10.2025

Abstract:
Effective management of finite resources in precision agriculture requires efficient technologies to generate reliable data about crops, pastures, soil, water sources, climate, pests, diseases, and other variables. These data enable farmers to make informed decisions to enhance efficiency and make their production more sustainable. This review aimed to assess the technological advances in precision agriculture in terms of their benefits, constraints, and potential for sustainable farming practices.
A total of 132 scientific papers were selected, analyzed, and discussed to explore the current status and the future of precision agriculture in relation to sustainable development. This review covers technologies utilized in planting, crop monitoring, resource management, decision support systems, and automation.
The application of artificial intelligence (AI)-driven technologies, including machine learning, computer vision, and sensor technologies, transforms traditional farming and contributes to resolving its limitations by providing farmers with real-time data and actionable insights. Ethical considerations, data security, and the digital divide are among the key challenges needing attention. Interdisciplinary collaboration is also needed to tackle complex issues associated with the sustainable implementation of advanced technologies, including AI in precision agriculture.
Precision agriculture technologies have a transformative impact on traditional farming. The integration of AI contributes to higher productivity and efficiency, as well as long-term sustainability of farming practices, ensuring food security for the growing population.

Keywords: Precision agriculture, sustainability, advanced techniques, production efficiency, technology adoptability

Please cite this article in press as: Diakite S, Kavhiza NJ, Saquee FS, Pakina EN, Zargar M, *et al.* Precision agriculture as a viable means of enhancing sustainable agricultural production. Foods and Raw Materials. 2026;14(2):357–376. https://doi.org/10.21603/2308-4057-2026-2-680

INTRODUCTION

Early forms of agriculture were predominantly subsistence-oriented and confined to small areas. However, as specialization gained momentum and farmers acquired more scientific knowledge, as well as mechanical ability, they enlarged their plots and improved techniques using standardized approaches. Thus, agriculture developed in the following stages: the pre-agricultural revolution [1], agricultural mechanization [2], the green revolution [3], and sustainable agriculture involving organic and precision farming [4, 5]. Each stage had its characteristics, benefits, and drawbacks (Table 1). Launched in the 1960s, the green revolution was based on a set of technical improvements aimed at eradicating hunger and malnutrition linked to exponential population growth [3]. In general, it has partially resolved the food security problems but also has had environmental implications. The agricultural intensification has increased due to the use of irrigation, fertilizers, pesticides, antibiotics, and growth promoters for animals. However, this has degraded the soil structure, polluted the ecosystems, and decreased agricultural and wild biological diversity due to its reliance on only a few high-yielding varieties of crops. These environmental shortcomings have

Copyright © 2025, Diakite *et al.* This is an open access article distributed under the terms of the Creative Commons Attribution 4.0 International License (https://creativecommons.org/licenses/by/4.0/), allowing third parties to copy and redistribute the material in any medium or format and to remix, transform, and build upon the material for any purpose, even commercially, provided the original work is properly cited and states its license.

Table 1 Stages in the evolution of agriculture

Development phase	Characteristics	Advantages	Disadvantages	Reference
The pre-agricultural revolution (before 1900)	Domestication of animals and plants, combining human and animal labor (draught power)	Economical; Minimal impact on the environment	A prolonged period of work; Low production (subsistence farming); Increased deforestation	[1]
Agricultural mechanization (1900–1930)	Use of machines (tractors, harvesters etc.) to mechanize the processes of cultivation and breeding, as well as the primary processing and transportation of products	Easier and more efficient operations; Larger cultivation area; Human labor freed up for lighter and/or more productive work	Increased environmental pollution from waste (exhaust gases, fuel vapors, antifreeze, brake fluid, soot); Loss of local biodiversity (in nature and agriculture); Higher cost of agricultural production	[2]
The green revolution (the 1960s)	Genetic modification of plants; Mechanization of production; Intensive use of chemicals (fertilizers and pesticides); Introduction of modern technology for planting crops, irrigation and harvesting processes	Increased production per unit area; Reduced food insecurity in the world; Improved quality of life	Mass production of cereals and legumes; High yields, but not enough nutritional value; A dramatic increase in energy consumption in agriculture; Contamination of the environment by high concentrations of chemicals (pesticides, fertilizers, etc.); Loss of genetic diversity in food crops and locally raised animals; High production costs	[3]
Sustainable agriculture (the 1980s), organic farming	Prohibition of pesticide use, genetically modified organisms, growth hormones, antibiotics, food additives; Use of adaptive varieties and breeds, special crop rotations, green manures, biological plant protection systems, probiotics, renewable energy and various near-natural technologies	Low/no pollution; Preserved health of plants, humans, animals and the entire planet (sustainable agriculture); Restored natural soil fertility, improved agrobiocenoses and ecosystems	Lower yields compared to farms using fertilizers and pesticides; Higher price of organic products	[4]
Precision agriculture (from the mid-1980s to date)	Use of geographical positioning system (GPS), geographic information systems (GIS), accurate field mapping, parallel driving systems, global navigator satellite systems (GNSSs), etc.	Increased awareness of variation in soil and crop conditions; Higher profitability and sustainability of agricultural operations; Lower negative environmental impact; Improved quality of the work environment and better awareness of the social aspects of farming, ranching, and relevant professions	Fuel saving; Work too difficult to adopt optimization; High production costs; Conservation of renewable and non-renewable resources; Environmental sustainability not assured	[5]

led to a shift towards sustainable agriculture, including organic and precision farming.

Precision agriculture emerged due to agriculturalists' ongoing efforts to lower unit costs and boost output per unit of input while considering the ecological principles [6, 7]. The main prerequisites for its rapid development were global positioning systems based on satellite and aerial photography, weather forecasting, variable rate fertilizer application, and plant health indicators. Another factor was the introduction of machines (used in data analysis and artificial intelligence) to predict crop planting even more accurately. Precision farming's defining feature is its reliance on cutting-edge technologies to achieve agronomic optimization at the plant or animal

level or at the intra-plot level. Its advantages are tied to the farmer's increased yields and/or enterprise profitability. Other advantages include enhanced animal welfare, better working conditions, and the potential to improve various aspects of environmental management. Precision farming thus contributes to the overall goal of sustainable agricultural production [7–10].

Unlike traditional farming methods, precision agriculture combines satellite navigation for unmanned aerial and proximal vehicles equipped with sensors and detectors which collect crop or livestock monitoring data. They are linked to computing platforms that process the pooled data and enable a decision that is adapted to an organism's need without increasing labor [5]. The data include information about stem size, leaf shape, hydrophysical and chemical properties of the soil, applied technology, and micro-climatic conditions around the plant. This information is transmitted to a computer via fixed or robot-mounted sensors and camera-equipped drones as images and individual plant data used for monitoring biotic and abiotic stresses. This individual plant information is made available to growers in real time as feedback so that they can make decisions about the distribution of water, pesticides, or fertilizers at a calibrated rate to the required specific area or site. In the same manner, it also helps in the planting, sowing, and harvesting processes [7, 11].

Despite the benefits of precision agriculture, farmers have not yet significantly embraced this technology. This could be due to lack of knowledge among farmers, inadequate financial means to start initial investments, or insufficient economic feasibility of investments due to small plot sizes [12, 13]. These aspects also affect the ratio of the technology's accessibility and availability, skilled mechanization workers, and maintenance costs.

The present review included the following stages: 1) determining the scope of the paper; 2) designating keywords that fit within the scope; 3) developing search strings based on the set keywords; 4) selecting literature databases to apply the developed search tools in; and 5) assessing the papers for their consistency with the defined scope. A total of 132 papers were selected, analyzed, and discussed exploring the current status as well as the future of precision agriculture in relation to sustainable development. Modern software was used to effectively illustrate the concepts explored in the paper. Thus, we reviewed the application and potential of precision agriculture for enhanced sustainable agricultural production.

RESULTS AND DISCUSSION

Overview of agriculture. Global agriculture is facing several major challenges caused by demographic issues, accelerated urbanization, epiphytotic diseases (fungi, bacteria, viruses, and nematodes), etc. [14–16]. One of these challenges is the supply of food for a burgeoning population while reducing its ecological carbon footprint and preserving natural resources for future generations. It was estimated that the current world population of about 8 billion could reach 10 billion by 2050 and would continue to increase by 1 billion every 12 years [17, 18]. This will increase the demand for energy and food, posing a serious threat to agriculture and the environment (Fig. 1).

According to the Population Reference Bureau and the United Nations Department of Economic and Social Affairs, the demographic growth puts pressure on the environmental resources (including their irrational use) in a quest to meet ever-increasing needs. This leads to other global problems such as environmental pollution, depletion of naturals resources, etc. [17, 18]. Another major

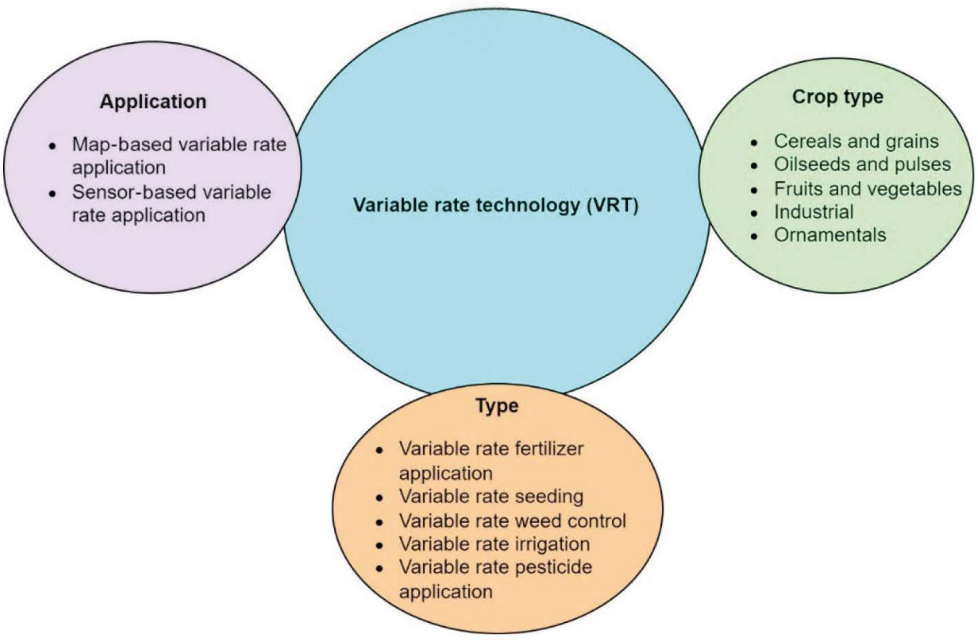

Figure 1 Segmentation analysis of the global variable rate technology market

consequence of the population growth is a shortage of food resources, which requires an increase in production through sustainable intensification (Fig. 2). Increasing the use of agricultural inputs can aggravate the problem of keeping the ecological balance. Therefore, there is a need to find ways to remediate soil cultivation and interrelationships between production systems and natural ecosystems. Unsustainable intensification in crop production can also lead to significant changes in the phytosanitary situation, which therefore requires proper adjustments and plant protection. These problems could cause changes in the populations of pathogens, pests that previously had no economic significance (including changes in their biological properties such as virulence), as well as beneficial flora and fauna [15, 16].

Another key problem is the anthropogenic activities which have led to the destruction of most natural ecosystems [19]. Furthermore, the rapid growth of human population and anthropogenic activities in the 20th century have contributed to an increase in desertification, pollution, and erosion, as well as a decrease in soil fertility. According to the United Nations Convention to Combat Desertification, about 33% of the world's soils are moderately or severely degraded due to erosion, salinity, intensified agriculture, deforestation, overgrazing, industrial pollution, uncontrolled irrigation systems, tillage practices, acidification, and nutrient depletion [20].

Beginning in the 1970s, urbanization has led to dramatic changes in the demand for agricultural products, diminishing agricultural land and causing labor shortage [21]. This phenomenon has its own characteristics in different regions and countries of the world.

Climate change has affected agricultural activities directly and indirectly in several ways. Its main impacts include the shifting of cropping calendar, increased susceptibility to biotic and abiotic stresses, and the spread of harmful microorganisms (as well as changes in their bioecological properties and interaction with plants) [22, 23]. According to Zhao *et al.* [24], each 1°C increase in the global mean temperature could reduce average global yields of wheat, rice, maize, and soybean by 6.0, 3.2, 7.4, and 3.1%, respectively.

Another limitation to agricultural production is caused by the proliferation of weeds [25], fungal diseases [26, 27], bacterial diseases [28], viral diseases, and pests, as well as the increased frequency of abiotic stresses (e.g., drought) in most farming systems [29]. According to the Food and Agriculture Organization, up to 40% of the world's food crops are destroyed by pests and diseases annually. This loss is estimated at $220 billion, causing famine for millions of people and negatively impacting agriculture, the main source of income for poor rural communities [30]. Weeds have also been reported to cause an average yield loss of 16 to 34% for spring wheat, rice, corn, potatoes, and soybeans [31]. According to Brás *et al.* [32], drought and heatwaves account for around 9 and 7.3% of cereal yield losses, respectively, as well as 3.8 and 3.1% of non-cereal yield losses, respectively.

The emergence and evolution of herbicide resistance in weeds since 1957 and fungicide resistance in many fungal and oomycete pathogens has become a serious problem since the introduction of site-specific inhibitors in the 1970s [33–35]. Several scenarios can lead to the

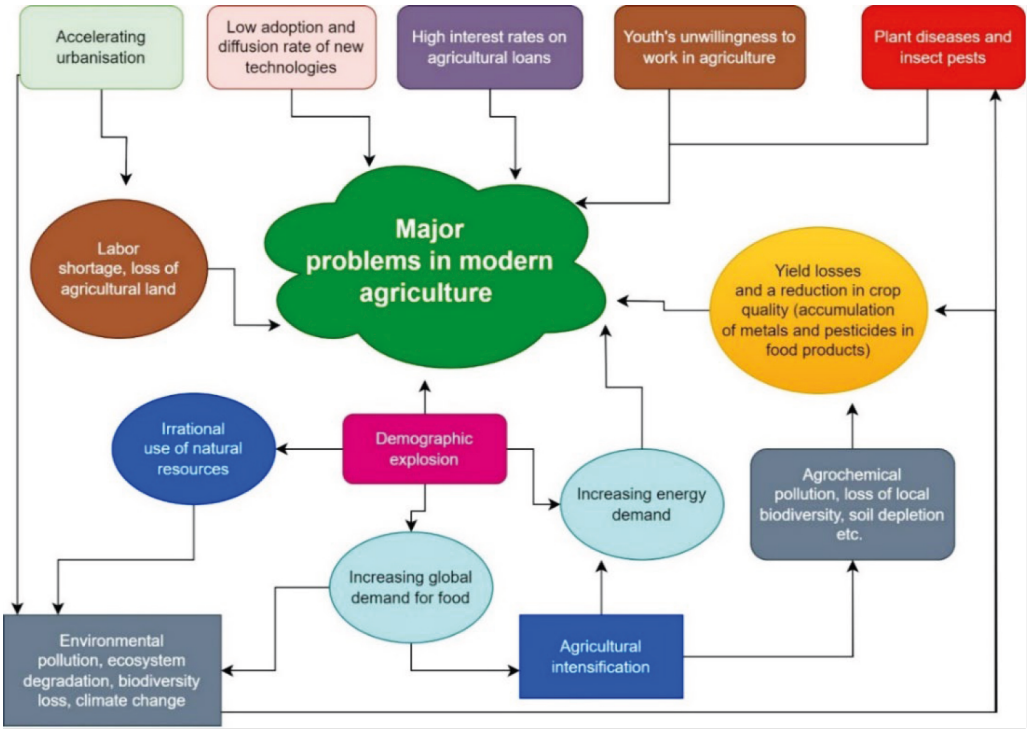

Figure 2 Major problems in modern agriculture

development of resistance: the repeated application of the same active ingredient in a field, the application of a reduced rate of pesticide, or the application of pesticides where the infestation is severe and the field cannot be recovered. According to the Health, Engineering and Agriculture Program (HEAP), about 245 species from 136 genera and 30 families of weeds are considered herbicide-resistant [37]. In the United States alone, crop losses directly due to pesticide resistance are estimated at about $1.5 billion annually [38].

Yield stability and reliable supply of high-quality seed are major challenges in agriculture. In Russia, the proportion of elite and first-generation (F1) hybrid seed represents about 5% of commercial malting barley crops, with over 90% of these varieties being 20–30-years-old [39]. Over time, the varieties lose their valued qualities and resistance to biotic and abiotic factors during long-term cultivation [40].

Improving the yield quality of agricultural products is one of the most important issues in agronomy, especially in Africa and Asia. According to Saquee *et al.* [23], micronutrient deficiencies in soils have led not only to crop loss but also to a decline in the nutritional status of most crops. Moreover, the yield and grain quality are also affected by climate change, the contamination of grains by heavy metals [41] and mycotoxins [42], as well as poor storage conditions [43, 44]. The accumulation of these toxic substances leads to yield losses, alters the product quality, and can therefore be found throughout the food value chain.

Precision agriculture can make an important contribution to solving the above problems. It can also be part of an environmentally sustainable agricultural system while maintaining profitability [8, 10].

History, concept, and advances in precision agriculture. Small landholdings were typical for agricultural production before technological advances. Farmers had a general understanding of their production system but did not measure variability. Mechanization and profit pressures led to the development large-scale, consistent, standard farming techniques. Accelerated agricultural development due to technological advancements occurred in the late 20th and early 21st centuries. As the agricultural market's profitability declines, producers seek technologies that minimize costs without reducing production [45, 46]. Thus, precision agriculture emerged in the early 1990s, taking various forms and depending on the knowledge and technology available at each stage. The first adopters of precision agriculture were the United States, Germany, United Kingdom, Netherlands, Denmark, Japan, and China, followed by Eastern Europe and Russia [9, 11, 12, 47]. In 1999, Dr. P. Robert, the "father of precision agriculture", defined it as an information- and technology-based farm management system aimed to identify, analyze, and manage differentiated spatial and temporal variations in the soil within a single field to optimize costs and increase production, as well as ecological stability, within a production system [48].

In recent years, precision agriculture has been extended to the dynamic sector of animal husbandry – precision animal husbandry, with its branches of precision dairy farming, precision pig farming, and precision poultry production. In similar terms, McBratney *et al.* [49] proposed that precision agriculture at the farm level aims to increase the number of better decisions per unit of space and time and their net benefits. The International Society of Precision Agriculture defines this method as a systematic production strategy that pools or aggregates spatial, temporal, and individual data. These data are processed and analyzed to produce information essential for making quality support management decisions, hence enhancing productivity, product quality, enterprise profitability, and sustainability of agricultural operations [50]. In addition, coordinated (precision) agriculture is a set of technical devices, software and hardware complexes, navigation, geo-information, and telecommunication technologies aimed at capturing, processing, and applying coordinated-related information to optimize agro-technological solutions for crop production [51].

Since the advent of precision agriculture, various advances have contributed to increased crop production and improved crop quality and profitability. One of such advances is artificial intelligence (AI). The application of AI in precision agriculture draws on advanced computational techniques, machine learning algorithms, computer vision, and sensor technologies to facilitate data-driven decision-making processes [52]. The paradigm shift from traditional, uniform farming techniques to a more personalized and adaptive approach marks the centrality of integrating AI in precision agriculture [53]. The advent of AI-driven technologies (including drones, satellites, and ground-based sensors) has empowered farmers with better understanding of crop health, soil conditions, and environmental factors. Using this information, they can make informed decisions on irrigation, fertilization, and pest control, thereby minimizing waste, optimizing resource allocation, and reducing the environmental footprint of agriculture [54].

Aerial photography from drones offers several tools to address these problems faster, leading to lower costs and higher sustainability [5, 55, 56]. Drones can handle a wide range of tasks in agriculture. In particular, they can monitor herds and agricultural plots, identify local areas of vegetation suppressed by various adverse factors in the field, and detect outbreaks of weeds, plant pathogens, and pests. They can also identify areas of fields subject to water erosion, detect agricultural engineering errors, specify microrelief maps of agricultural land, and provide technical support for implementing technologies. Drone sensors provide a wide range of accurate data on nitrogen, chlorophyll, biomass, moisture, and water stress. According to Dengeru *et al.* [57], mounted aerial vehicle spraying effectively reduces and mitigates farmers' health risks (exposure to toxic chemicals) during field spraying with handheld sprayers. Keshet *et al.* [58] demonstrated that drones could be used to help farmers

determine the presence of Levant voles and their damage in crop fields. They can better control the rodents using precision farming methods, e.g., apply rodenticides in specific areas, thereby increasing efficiency and decreasing the number of pesticides used.

The AI autonomous technologies and robotics play multifaceted roles in precision agriculture. Smart machines equipped with AI algorithms revolutionize the farming operations spanning from planting and crop maintenance to harvesting [59]. These technologies enhance operational efficiency and address constraints associated with labor shortages, thereby contributing to a more sustainable and economically viable future for agriculture. As precision agriculture is increasingly becoming data-centric, critical issues emerge that necessitate action, such as equitable access to technology, data security, and ethical considerations [60].

The incorporation of Machine Learning (ML) with Decision Support Systems (DSSs) contributes to the overall sustainability of farming practices and enhances resource management and informed decision-making for farmers [61], thereby empowering them with data-driven insights and predictive analytics. The ML algorithms are proficient in processing huge datasets, extracting meaningful patterns, and generating predictions. For instance, these algorithms provide more precise and localized weather predictions, compared to the traditional methods, by analyzing historical weather data, satellite imagery, and real-time meteorological information [62]. Accurate and reliable weather forecasts facilitate optimizing irrigation schedules, planning for adverse weather events, and mitigating the impact of climatic variations on crop yields [52]. In addition, the ML models can identify optimal planting dates and predict crop yields, as well as potential threats (e.g., disease outbreaks) by using weather patterns, crop-specific parameters, and historical datasets. The decision support systems enhance farmers' capabilities to make data-driven decisions based on historical data, current conditions, and predictive analytics [63]. These capabilities permit a deeper understanding of how crop rotations, soil conditions, and pest prevalence affect agricultural outcomes. As a result, farmers can adjust their practices and enhance long-term sustainability. The ML-driven decision support systems significantly optimize agricultural resources [64] by analyzing soil health, nutrient levels, and water usage datasets and making recommendations for precise fertilization and irrigation strategies.

Effective resource management is another useful application of AI for sustainable and efficient agriculture. Integrating AI technologies in precision agriculture has contributed to optimum utilization of water, fertilizers, and pesticides [65, 66]. The AI-driven smart irrigation systems leverage real-time data on soil moisture, weather forecasts, and crop requirements to precisely control the timing and amount of irrigation [67]. Through the dynamic adjustment of water delivery based on actual crop needs, smart irrigation minimizes water wastage, promotes water conservation, and ensures optimal crop hydration [68]. The AI contributes to precision agriculture by optimizing the application of fertilizers. The ML models analyze soil nutrient levels, composition, and historical yield data to recommend personalized fertilization plans for different sections of a field [69]. The use of AI in resource management makes the agriculture sector more environmentally sustainable [70, 71] by reducing water and fertilizer wastage and therefore minimizing environmental pollution, soil degradation, and the eutrophication of water bodies.

Advances in AI currently involve the integration of robotics and autonomous vehicles to further enhance the efficiency of resource management. AI algorithms enable farmers to apply resources precisely according to real-time data, reducing their reliance on manual labor. Incorporating AI technology in resource management has contributed to a transformative shift towards precision agriculture [72]. These interventions increase agricultural efficiency and productivity, promoting environmentally sustainable and resilient farming practices in the face of changing climate patterns.

Autonomous vehicles leverage AI algorithms to plant seeds at optimal depths and spaces, contributing to uniform crop growth. During harvesting, advanced sensors and robotic arms of these vehicles permit timely and selective picking, reducing waste and increasing overall yield efficiency [73]. Autonomous vehicles equipped with robotic systems and AI-driven algorithms identify and target pests or weeds with precision. They can perform automated weeding by distinguishing between weeds and crops. This technology reduces environmental impact by lowering the use of herbicides and pesticides, as well as addresses labor shortages, making weed management more sustainable and cost-effective [74]. Applying autonomous machines for repetitive tasks permits human labor to be directed towards more skilled and complex aspects of farming, increasing overall operational efficiency. Although the initial investment in automation technologies is high, it offers long-term economic viability benefits such as lower labor costs, higher productivity, and better yield quality. The integration of Internet of Things (IoT) technologies permits seamless connectivity between agricultural equipment and robotic systems [75, 76]. With these technologies, farmers can remotely monitor and control robotic systems, making adjustments based on real-time data and varying conditions. This level of control ensures that farming operations can be fine-tuned for real-time data exchange, adaptive decision-making, and optimal outcomes even from a distance [77].

Connectivity plays a crucial role in precision agriculture. It involves the integration of technologies and data exchange systems to create a networked ecosystem that transforms traditional farming practices. Connectivity, with advances in communication and sensor technologies, is a key contributor to precision agriculture [78]. For instance, the deployment of smart sensor equipment and IoT technologies enables farmers to collect real-time data on soil moisture, temperature, and crop

health [79, 80]. Interconnected technologies provide a continuous generation and flow of valuable information on irrigation, fertilization, and pest control. This forms a foundation for data-driven decision-making in precision agriculture. Connectivity technologies (including drones and satellites) provide a comprehensive view of the entire farm, aiding in crop monitoring, disease detection, and assessment of overall field health [81]. Connected systems leverage ML algorithms to analyze integrated data based on historical patterns and real-time inputs that enable the prediction of future trends for crop yields, weather conditions, and pest outbreaks [82]. Connectivity fosters information sharing on best practices, emerging technologies, and local insights among farmers, researchers, and agricultural experts through online platforms. Connectivity software enables farmers to plan, optimize resource, and implement sustainable farming practices by integrating data on crop rotation, resource usage, and yield history [83, 84].

The global satellite navigation system collects spatial information in the fields and allows the targeting of resources [8, 11]. It enables a number of precision agriculture technologies that can be divided into several categories based on the role they play in management decision-making and their level of complexity. In particular, they include positioning (e.g., georeferencing of field information), diagnostics and data management (e.g., soil sampling and yield monitoring), and application (e.g., variable rate technologies) technologies. Satellite geo-positioning (GPS) and geographic information systems (GIS) are the leading technologies used for many purposes, such as livestock and crop tracking, field monitoring and management, or geolocation at exact levels [26, 85, 86]. For instance, crops can be traced using satellite imagery, while drones can study soil moisture. Other geolocation tools facilitate the detailed tracking of livestock and pastures. Precision agriculture also draws on some other technologies such as sensors, big data, artificial intelligence (AI), visualization, the Internet of Things (IoT), and networks [87], as demonstrated in Fig. 3.

According to Loudjani *et al.* [8], the global market for precision farming technology has averaged €2.3 billion and is expected to grow by an average of 12% each year. Precision agriculture technologies can be divided into ground, aerial, and satellite. The ground technology suits production planning, mapping, scouting, and machine

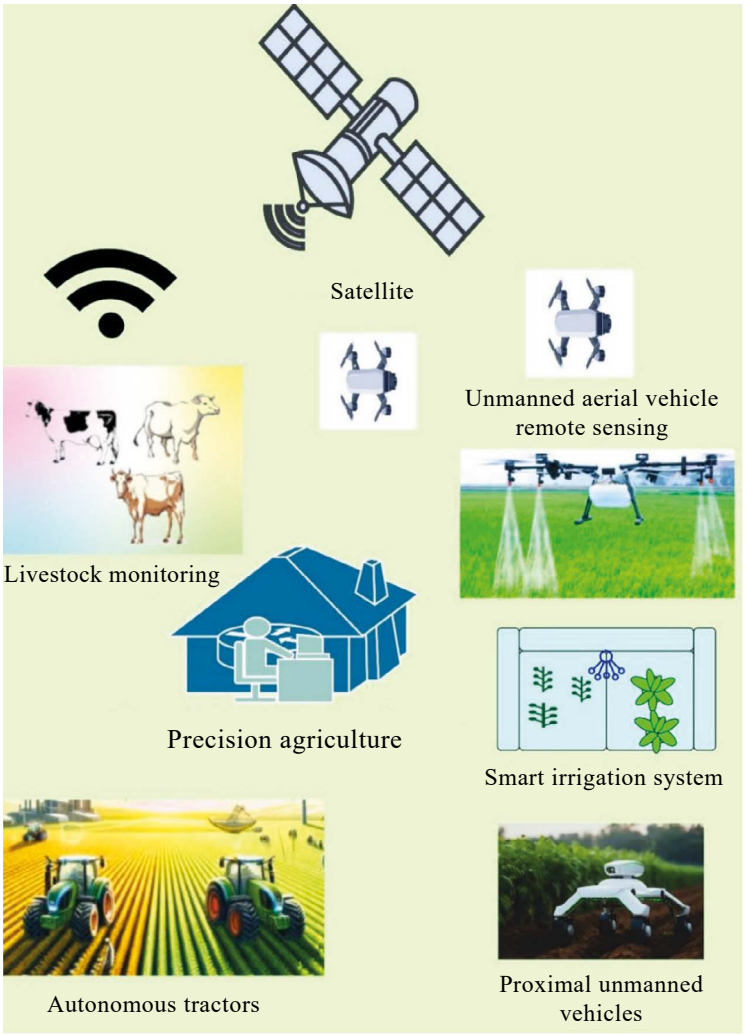

Figure 3 Precision agriculture concept

control. Aerial and satellite technologies are useful in resolving global problems, such as real-time yield state analysis from anywhere.

Remote sensing is a technique that allows growers to monitor yield health using satellite imagery. It provides up-to-date information on moisture stress, disease, structural anomalies, and nutrient levels. Modern precision agricultural satellite imaging has high spectral resolution, allowing growers to collect the most accurate data. Remote sensing enables visual observations to be recorded via digital media and georeferenced in a GIS database. Precision agriculture uses aerial photography and videography, with digital capture being the most common remote sensing method. According to Bill *et al.* [88], remote sensing has enormous potential for crop production at the farm level. Satellite remote sensing generates the General Yield Unified Reference Index (GYURI) by analyzing data from the Advanced Very-High-Resolution Radiometer (AVHRR), the Sentinel-2A/B satellite, and the Landsat 8 multispectral satellite. It has proven to be a valuable tool to estimate yield at the field level for spring barley, winter wheat, corn, and oilseeds [89, 90]. Therefore, remote sensing information can resolve many soil and crop management issues. In addition, this tool is more cost-effective than GPS or UAVs because it lacks extra fuel and labor costs.

There are different forms of ***variable rate technology (VRT*)**. The map-based VRT corrects the amount of applied fertilizers, pesticides, herbicides, and other products depending on the previously developed area map. The sensor-based VRT studies the soil in real-time and can assist in determining nitrogen insufficiency. The control system then determines the required quantity of inputs. VRT is a tool that enables farmers to apply the correct quantity of seeds, fertilizers, and crop protection products, leading to a positive environmental impact. In other words, VRT helps reduce losses resulting from the over- or underuse of agricultural resources by implementing precision application technologies [91]. The variable rate technology can be applied for variable rate fertilization, plant protection, seeding, and irrigation (Fig. 3).

Electronic field mapping is a land inventory tool that determines the resource potential of agricultural land. It allows farmers to accurately calculate the application rates of fuel, lubricant, fertilizer, and crop protection products on an area basis. An electronic map (raster or vector) and a related database are the best means of organizing farmland information in precision agriculture. In addition to showing field boundaries, a road network, and dwellings, electronic terrain maps include all the information about the terrain such as soil conditions, the application of fertilizers and crop protection products, crop rotation, yields, the amount of precipitation per year, etc. [91–93]. These maps have a multi-layer structure: fields, grasslands, pastures, orchards, disturbing objects (poles, trees, wells, etc.), soil agrochemical properties, measurement and sampling points, roads, etc. Each layer stores specific information in the form of objects. The lowest layer is usually a satellite image of the terrain. There are three main methods of collecting input data to produce these maps: 1) field measurement using a high-precision GNSS receiver (a more accurate method); 2) processing high-resolution satellite imagery (a less accurate but often faster and cheaper method); and 3) a combined method (an electronic map created from space imagery and edited in the field using a high-precision GPS receiver) [11].

Varying nutrient concentrations in the soil have been responsible for variation in crop yield. Proximal soil sensing allows farmers to obtain soil characteristics quickly and with less cost. This technique bridges the data gap between high-resolution point data and low-resolution remote sensing data. Intensive soil sampling is costly and time-consuming, labor-intensive and limited to point measurements [94]. Valente *et al.* [95] confirmed a need for a high soil sampling density to effectively determine the spatial variability of the soil's physical and chemical properties. Tripathi *et al.* [96] revealed that efficient, cost-effective, and easy-to-use tools are needed for specific soil management. For example, proximal soil sensors can acquire high data density rapidly and continuously, which is essential for delineating development areas. These sensors offer increased measurement density and complete coverage of the terrain. They can be divided into different categories depending on the type of sensor used, namely electrical, electromagnetic, optical, radiometric, mechanical, acoustic, pneumatic, and electrochemical [55, 56]. Proximal soil sensors are set near, or in direct contact with, the soil to measure its properties directly or indirectly. Electromagnetic induction uses the electromagnetic field induced in the soil column to calculate apparent electrical conductivity to indirectly establish the variability of different soil properties such as texture, moisture, and salinity [57].

Benefits of precision agriculture. Precision agriculture allows for an environmentally friendly way of farming by preventing overuse of fertilizers and crop protection chemicals, reducing climate and weather risks, achieving planned yields, and protecting the environment from pollution. The cutting-edge technologies in precision agriculture can optimize the usage of traditional resources. As a result, this agricultural management system contributes to the development of sustainable farming by addressing both economic and ecological problems. The main goal of precision agriculture is to increase the efficiency, productivity, and sustainability of farming operations. By having accurate information about soil moisture, nutrient levels, and pest infestations, farmers can apply fertilizers, irrigation, and pesticides in a more targeted and precise manner, thereby reducing waste and decreasing environmental impacts [51, 52]. With the precision agriculture techniques, farmers can make informed decisions based on real-time information, promoting more efficient, productive, and sustainable farming practices. The benefits of precision agriculture can be divided into three groups: agronomic, economic, and ecological benefits.

Ecological benefits of precision agriculture. Sound ecological principles need to be utilized to reduce the anthropogenic impacts and create scientific and technical support, as well as favorable conditions, for sustainable development in agriculture. Precision agriculture technologies enable farmers to mitigate the ecological footprint of agricultural activity through a more targeted use of inputs. They can also reduce losses due to over-application, nutrient imbalances, weed escapes, insect damage, etc. [97, 98]. Precision agriculture addresses some of the key issues of the late 20th and early 21st centuries such as environmental impact, risk, and degradation. This management practice also aims to ensure global sustainability and food security [8, 10]. Depending on the type of technique used, precision agriculture reduces the loss of soil fertility, with 30–50% of residual nitrogen in soils, as well as erosion, flood risk, soil compaction, carbon and ammonia emissions, water pollution, water consumption, and the use of herbicides (Table 2). Thus, the material and technical resources are used more rationally, with a positive environmental effect [8, 10].

However, the environmental benefits of precision agriculture are difficult to quantify for objective reasons. For instance, the complex nature of its implementation and impact on the agro-ecosystems makes it difficult to determine the environmental efficiency (reduction of production costs such as fuel, fertilizers, and plant protection products). Another reason is that the environmental conditionality of this technology by landscape and climatic conditions makes it possible to generalize the results obtained in the precision agriculture experiments. For this reason, precision agriculture techniques are not widespread, and it is quite difficult to obtain specific data confirming their effectiveness on a real-world scale. Furthermore, the ecological effects of precision agriculture depend on the level of a farm's intensification, and their evaluation can also be determined by the choice of technologies or farming systems used for comparison [99].

The ecological effects of precision farming technologies are measured by comparing differentiated single-field work with traditional continuous work (with the same level of applied effort), regardless of differences in fertility. Reducing the intensity of tillage (considering depth differentiation in a single field) offers, above all, a possibility of reducing fuel consumption. The ecological effect of differentiated seeding technology based on field heterogeneity is likely to be smaller than that of differentiated tillage, and quantifying it is much more difficult [8, 98, 99]. As a result, precision farming ensures savings in seed/planting material, fertilizer, and crop protection products, reducing the need for seeding zones. Obviously, this has little environmental potential. For example, smart sensor systems have resulted in nitrogen fertilizer savings of 10–80%, while residual nitrogen fertilizer levels in the soil have been reduced by 30–50% albeit maintaining wheat yield and grain quality [100]. In olive cultivation, the use of potassium, phosphate, and lime fertilizers was reduced by 31, 59, and 86%, respectively. This reduction in input use significantly lowered the environmental impact [101]. Precision technologies based on the spectrometric methods of soil and plant characterization can be used to optimize the seeding and fertilizer application rates without compromising crop yield and quality. The variable rate fertilizer application in individual soil fertility zones showed a higher tillering coefficient (up to 6.74%), higher grain yield (up to 14.55%), more ears per square meter (up to 27,6%), more protein (up to 6.2%), more grain (up to 12.56%), and a lower 1000 grain weight (up to 8.61%) compared to conventional flat-rate fertilization [102]. In addition, the site-specific seeding and variable rate fertilizer application saved approximately 14 kg N ha^{-1} compared to the conventional site-specific seeding and uniform rate fertilizer application [102].

Differentiated fertilizer application has a higher positive ecological effect. This precision method reduces the consumption of non-renewable energy and the deposition of heavy metals (uranium, cadmium) contained in fertilizers into the soil [99]. Quantifying these effects is difficult though. Furthermore, in some cases, the application of precision farming technologies is associated with an increase in fertilizer rates to enhance the economic efficiency of adaptive landscape farming. In Italy, the application of precision agriculture has led to a decrease in labor costs (–20%) and pesticides (–53%) while increasing the amount of nitrogen (+11%) and seeds distributed across the field (+5%) [48]. This indi-

Table 2 Expected environmental benefits of precision agriculture processes and techniques

Task	Technique	Environmental benefits
Fertilizer application	Soil nutrient mapping; Crop vegetation index; Micro-dams	Reducing environmental pollution; Increasing soil fertility; Reducing erosion
Irrigation	Soil texture mapping; Soil moisture sensors	Reducing erosion; Lower water consumption by meeting crop water requirements needs more precisely
Pesticide application	Disease detection using multi-sensor optics and volatile sensors	Improving soil condition and reducing erosion through reduced tillage; Lower risk of biodiversity loss; Reducing environmental pollution due to lower greenhouse gas emissions; Lower resistance
Yield quantification	Crop vegetation index	Higher yields due to precision spacing (pass to pass, headland rows) and speed; Reducing amount of residual pesticides in agricultural produce

cates that, in the face of a significant increase in total costs due to the capital invested in the technology, the farm aims to intensify production rather than reduce agricultural inputs [103].

Effective management of crop population ensures an optimized level of yield potential. As such, precision agriculture technology opens up additional opportunities to manage pest populations' resistance to plant protection agents. In practice, it is possible to implement the envisaged weed control strategies. Van Evert *et al.* [101], who studied precision agriculture technologies in potato production, reported a 23% reduction in pesticide use and a 15% reduction in nitrogen fertilizer use. Site-specific spraying can reduce herbicide usage by up to 70% while maintaining 100% weed control [104, 105]. In another study, the real-time sensor-based precision spraying system reduced the volume of pesticides (including herbicides, insecticides, and fungicides) applied to soybean and corn crops. Adopting this technology reduced costs 2.3 times compared to applying pesticides to the entire area with a conventional sprayer [51]. Thus, precision agriculture is a primary tool for protecting valuable agricultural landscapes and ensuring environmental stability in a single field and neighboring biomes. This provides additional opportunities to protect rare species of wild flora and fauna. The practical realization of its ecological potential depends largely on the choice of agro-technological policy and state legislative acts [99].

Economic and agronomic benefits of precision agriculture. The application of precision farming technologies requires additional costs to cover data collection and control (maps, global positioning systems, sensors, equipment, and software), as well as precise execution of agricultural practices and navigation (GPS-controlled machines and equipment). When introducing a system of precision farming, it is necessary to consider the expected costs of many factors and circumstances that ultimately provide the effect. Generalized data from global experience with individual precision agriculture technologies are given in Table 3 [99, 106].

Some cost-oriented measures are implemented once every 5–10 years, others annually. The attractiveness of precision agriculture technologies, as well as other innovations, is determined by the economic efficiency of an agricultural enterprise. When analyzing the economic efficiency of applying precision technologies, the expense of purchasing equipment and other production costs is compared to the level of expense reduction or yield gain over conventional technologies [99].

The use of economic analysis in precision agriculture is limited by the difficulty of identifying and quantifying positive and negative effects. The positive effects include: (a) a reduced workload and simplified processes for machine operators due to automation; (b) improved efficiency of product marketing due to transparent and accessible control of the entire process; (c) better general management of agricultural technologies based on information; and (d) improved conditions for managing individual processes and the entire farm [99, 107]. For example, German farmers, who implemented elements of precision agriculture, achieved a 30% increase in yield and a cost reduction of 30% for mineral fertilizers and 50% for inhibitors [108]. Precision farming can help farmers make the most of their resources without increasing their workload, thus improving efficiency. One method is to use a mapping tool that allows farmers to monitor field conditions and determine the optimal planting schedule [99, 107, 109].

Table 3 Precision agriculture technologies

Precision technology	Description	Merit
Parallel driving	Automatic control system; executive board; software; staff training costs	Time and fuel savings (driver can perform other tasks); improved overall productivity and quality of work
Differential seeding	Soil maps; seeders for differential seeding, depth and density changes; DGPS/RTK systems	Increased yields through improved seed density and distribution; reduced seed costs
Differential fertilizer application	Differential fertilizer application system; integrated GIS system; aerial photos; yield mapping; soil samples; soil map; staff training costs	Increased yields; time and fertilizer savings
Differentiated spraying based on weed map	Integrated injector sprayer; soil samples (soil map); personnel training costs; weed mapping with stand-alone weed visualization systems	Herbicide and time savings; increased yields
Differential irrigation	Water management software; drip irrigation piping; sensors	Water and nutrient conservation
Soil map differentiated tillage	Soil maps; sensors to determine soil composition; tillage tools	Increased yields; energy and time savings; improved machine efficiency
Measurement of crop chlorophyll content prior to harvest	Sensors for chlorophyll mapping of plants; yield mapping	Improved product quality; optimal time to start harvesting; improved grain quality with optimal moisture content
Harvesting logistics	Unified vehicle management system; new vehicle system; yield maps; logistics optimization system; auxiliary software tools for harvest scheduling	Increased yields; optimized harvest; fuel savings; reduced crop moisture content; time savings in transportation
Information management	Field map processing software	Reduced research costs in time and manpower; improved quality of the data obtained

From an economic perspective, a review of 234 studies published between 1988 and 2005 showed that precision agriculture was profitable in 68% of the cases [110]. Gusev and Volkova [111] analyzed 41 agricultural organizations in the Sverdlovskaya region and proposed a system of indicators to evaluate the effectiveness of precision technologies. Satellite-based vehicle monitoring systems are among the most commonly applied technologies. According to the authors, their use contributed to saving 6.3% on fuel consumption, with a total economic effect of 60.8 thousand rubles and a payback period of 0.64 years. The accurate application of agricultural technologies reduced the rates of seeds, fertilizers, and plant protection products by 1.1; 3.1; and 3.6%, respectively [111]. The most widespread are precision agriculture technologies that are relatively easy to use, do not require large investments in preparation or equipment, and have a short payback period [112].

In another study, precision agriculture reduced the costs of fertilizers, seeds, fuel, and lubricants by an average of 30% [99, 112]. The use of real-time kinematic navigation by Kelc *et al.* [113] saved 15.7% of time and 8.66% of fuel on a 3-meter-wide tillage machine, as well as 12.6% of time and 8.28% of fuel on a 6-meter-wide tillage machine.

In addition to reducing costs and increasing yields, precision farming enhances the physical and agrochemical properties of the soil and makes the shape of the field more suitable for performing agricultural operations. AquaCrop's automated multi-patterning can also contribute to farm-wide water savings due to reduced infiltration and drainage. This increases the final yield in the variable field due to a higher water content in the root zone [114].

Precision agriculture also has some benefits for social and working conditions. For example, automated systems are available for different models of tractors, which makes the work less tiring [113]. Similarly, the precision dairy farming technology improves automatic applications for individual cow management, thus reducing labor costs such as twice-daily milking. There is also an argument for improving animal welfare [8].

When introducing new precision machinery or technology, farm managers and workers need to improve their skills and master new specialized knowledge [115]. Training costs can vary considerably depending on the digital competence of a farmer. It was assumed that an "expert" only needed half the average learning time. According to Munz and Schuele [107], the farmers who were not at all familiar with digital technologies needed three times as much time for initial training. Overall, the proportion of learning costs in implementing the technology was very small (0.9–1.5%) and therefore was not considered an economically decisive determinant of success for a digital technology-driven operation.

Most modern approaches to the economic analysis of precision farming technology are limited to the evaluation of applied machinery and proper technologies in a single crop. At the same time, the overall agro-economic effect of integrating precision technologies at the farm level, considering synergistic effects, will be higher than the use of individual technology complexes [99].

The farm's size has a much greater effect on the economic success of technology application than changes in the product or input prices that cannot be controlled. Price-related ranges of variation become smaller as the farm size increases. This means that larger farms have greater resilience to market changes due to economies of scale in terms of added costs [107]. Small farms, however, can generally afford precision farming technologies only if they subcontract service companies, rather than buy the necessary equipment themselves. Applying a model-based sensitivity analysis to three farms of different sizes (11, 57, and 303 ha), Munz and Schuele [107] proved that larger farms had greater resilience to external factors due to economies of scale. Balogh *et al.* [115], who conducted 604 interviews and 30 semi-structured interviews in Hungary, also found that small farm size is a barrier to the faster spread of precision agriculture [115]. Therefore, the farms interested in adopting digital technologies need to (a) know their status quo well (e.g., the cost structure of the farm), (b) collect relevant data in sufficient detail during and after adoption (changes resulting from the implementation), and then (c) make changes based on the collected data. Since these approaches are often costly in practice, small farms (< 30 ha) are recommended to use service providers, while medium farms (30–70 ha) can join machine pools (resource pooling). Beyond that, government subsidies can help with the acquisition of these technologies [107]. In addition, the economic efficiency of precision farming technologies can be influenced by the range of machines selected, the comprehensiveness of their technological use, the level of their integration into the farm, and the rational use of the technology complex as part of business management [99]. Furthermore, economic efficiency can be affected by other factors such as the management system used in the farm or the prices of the initial set of information, production facilities, and manufactured agricultural products.

Unlike other innovation processes such as genetic engineering, public and consumer attitudes towards precision agriculture are generally positive or neutral [111, 115]. The knowledge-intensive nature of agricultural production and the attractiveness of agricultural professions are increasing, especially among the younger generation of farmers and specialists. However, the adoption of precision technologies into agricultural practice is relatively slow.

Factors affecting precision agriculture. ***High initial investment costs.*** The implementation of precision agriculture in crop production depends on the socio-demographic, financial, and contingent factors [116]. According to Mizik [117], the top five constraints to adopting small-scale precision technologies are a small land size, a high cost of adoption, technology challenges, a lack of professional support, and a lack of supportive policy. Le Hoang Nguyen *et al.* [118] examined

59 high-level journal articles to determine the factors that facilitate or hinder the adoption rate of precision agriculture technology. Of the reviewed studies, 63% reported driving factors at the farm level and 37%, at the individual level. The individual factors included the relative benefits of the technology, its observability and testing capability; the farmer's education, knowledge, and experience in using the technology; as well as the farmer's age, risk tolerance, and the complexity of the technology.

A smart irrigation control system costs about 54,540.8 USD without transportation and labor costs, which could limit its direct use by the farmers [109]. In another study, more than half (62.75%) of the respondents identified excessive cost as the main barrier to the adoption of precision farming technology in Italy [119]. Similarly, Pandeya *et al.* [120], who surveyed the farmers in Kentucky, reported high cost (20% of the respondents) as the main barrier, followed by complexity (15%) and lack of profitability (12%). Due to capital-intensive initial investment associated with precision farming technology, their adoption is mainly limited to large farms, while the expected benefits per hectare are not high enough to make a justifiable investment for small farms [121]. Moreover, there is a lack of information on precision farming technology. The information is mainly provided by equipment manufacturers, who are more interested in selling the equipment rather than in its economic efficiency. Jacobs *et al.* [122] conducted a survey in the Schweizer-Reneke region of South Africa and found that the adoption of precision agriculture was limited not only by high costs and a small size of cultivated area, but also by homogeneous fields.

Lack of skills and information asymmetry. The accuracy of methods using remotely sensed data (satellite, airborne, and drone) depends on many factors, including image resolution (spatial, spectral, and temporal), weather conditions, cultural and terrain conditions (e.g., growth stage, land cover), and analysis method (e.g., regression-based, machine learning, physical modeling). Given the complexity of image processing methods and the amount of technical expertise required for their application, a simple and robust workflow should be explored and developed for image pre-processing analysis and real-time applications. Major challenges and gaps remain in the development of tools and frameworks that can facilitate the use of satellite data by end users for real-time applications [123]. Another major barrier to adoption is the compatibility of precision farming equipment with conventional machinery, as well as between different components of precision farming technologies [124].

In addition, the following limitations to adoption are highlighted: (a) the farmers' inability to analyze and use the vast amount of data provided by precision agriculture technology; (b) the lack of scientific procedures to determine variable rate inputs; (c) the lack of evidence of the benefits of precision agriculture; (d) costly and time-consuming collection of data; and (e) the need to improve technology transfer [13].

Another barrier to adoption that requires significant investment is the lack of knowledge and skills to use the complex precision farming technologies and analyze the data [116, 124, 125]. Kendall *et al.* [126], who studied 27 Chinese farmers in Hebei and Shandong provinces, showed that although the farmers were open to engagement, they had limited knowledge about the use of precision technologies. Many of them highlighted the need for more professional information-sharing platforms and a greater role for extension agents. The farmers had doubts about the reliability and performance of technologies, including drones, due to battery issues and chemical efficacy.

In another study based on pilot interviews, 10 participants from the Beijing area found it difficult to discuss precision agriculture technologies due to their limited experience [127]. On a personal level, a farmer's decision to adopt precision farming technology also depends on their values and motivation. Not only subjective factors such as risk aversion affect their decision, but also such aspects as the farm's size and production conditions [47].

Poor collaboration among relevant stakeholders. No technological development can provide a total solution to the user until it has been commercialized as a service for extensive use. The interest in, and introduction of, precision agriculture has resulted in a mismatch between technological capabilities and scientific understanding of the relationship between input and output. The development of precision agriculture has been largely market-driven, but its future growth requires collaboration between the private and public sectors. The private sector must take responsibility for business development, product credibility, and consumer satisfaction. The public sector needs to coordinate the development and implementation of precision agriculture by providing support programs to meet the objectives [128]. Synergies between government, academia, and business are essential to facilitate the transfer and adoption of this technology by end users. The potential of this technology has already been demonstrated, but in practice, meaningful distribution is difficult as it requires large-scale commercialization to realize its benefits.

The utilization of AI technologies in precision agriculture is fraught with challenges. The creation of a unified and reliable dataset for AI algorithms is constrained by the quality and integration of diverse data sources such as satellite imagery, historical and sensor data. The biases that may inadvertently be introduced during model training lead to unfair outcomes with a complex interpretability challenge. The challenge of data privacy and security remains critical, especially as the amount of sensitive agricultural data increases. Another challenge is to provide farmers with equitable access to AI technologies, particularly smallholder farmers who may lack the resources or digital literacy required for effective adoption. Poor network connectivity or access to advanced hardware may also hinder the widespread adoption of AI-driven precision agriculture, particularly in the regions with limited technological infrastructure [52].

The vast amount of data generated through AI-driven technologies raises concerns about data privacy. Stakeholders including farmers must securely manage sensitive data and ensure proper control over data usage. Another ethical constraint is the ownership and sharing of agricultural data. Farmers, researchers, and technology service providers should establish clear guidelines on data ownership rights and mechanisms for fair data sharing without compromising individual interests. Advanced monitoring technologies, including drones and satellite imagery, are useful for farm surveillance and crop health, but the farmers' privacy needs to be protected against unwarranted intrusions. Ethical considerations regarding the impact of monitoring on individuals and local communities should be sensitive to cultural norms, community consent, and potential consequences of data collection. The adoption of AI technologies by farmers should ensure equitable access to these technologies to address the existing disparities. Insufficient digital literacy among farmers may pose ethical challenges. Through training and support, they can effectively navigate, and make informed decisions in, the AI-driven agricultural landscape [52].

Despite these constraints, various mitigating strategies have been noted. The explainable AI (XAI) techniques can resolve the constraint of algorithmic interpretability and provide the farmers with a better understanding of the recommendations provided by AI systems. The development of holistic and sustainable solutions to the multifaceted constraints of AI in precision agriculture necessitates the integration of expertise from diverse fields such as agriculture, computer science, ethics, and policy-making. The block chain technology can enhance data security and privacy by providing a decentralized and tamper-resistant system for managing agricultural data. Edge computing technologies contribute to resolving the infrastructure limitations by reducing the reliance on centralized computing resources and activating data processing closer to the source. Collaborative platforms for research and knowledge sharing help overcome the constraint of data quality and provide a collective understanding of best practices in AI-driven precision agriculture. Comprehensive policies and regulatory frameworks can serve as useful guides for the ethical and responsible implementation of AI in agriculture in terms of data privacy, security, and fairness. The digital divide among farmers can be overcome by fostering inclusive technology adoption programs that prioritize digital literacy and provide support for smallholder farmers [52].

Potential of precision agriculture for sustainable agricultural production. The potential of precision agriculture in sustainable development is quite broad. Since this form of advanced agriculture thrives on information technology, it enhances efficiency in the fields reducing the negative impacts associated with farming [92, 106]. For instance, accurate information on temporal and spatial weather conditions, crops type, and pest population enables the farmers to determine when to spray the pesticide and how much to apply, which increases efficiency and reduces the amount of pesticide released into the environment [42]. This then has a ripple effect and reduces the impact of pesticides on non-target species like bees (*Apis mellifera* L.), which play an important role in pollination [128]. Furthermore, variable rate fertilizer application allows for the provision of nutrients tailored to the different soil strata across the field. Unlike methods such as blanket fertilizer application or using the rough rule of thumb, this technology ensures that the nutrient-rich areas of the field do not receive excessive fertilizer. This reduces the risk of eutrophication whereby excess nitrates are deposited into surrounding water resources, consequently polluting them and adversely affecting marine life [129]. The acidification of the soils is also slowed this way.

In the context of climate change, specifically frequent droughts due to the El Nino Southern Oscillation effect in the global South, variable rate irrigation has been of tremendous benefit in high-value crop enterprises such as blueberry (*Vaccinium corymbosum* L.) farms. This technology enables the farmers to meet the crop water requirements while conserving water.

Precision agriculture and sustainable development have certain economic benefits [93]. As each stage of the industrial revolution has had profound effects on enhancing agricultural production, the fourth industrial revolution (information era), on which precision agriculture is premised, not only increases the returns but also potentially lowers the costs of production. The increased efficiencies in the fields allow for the optimum allocation of resources per unit area. In essence, this gives the farmers financial leverage to expand their operations and produce more, thus enhancing profitability of the enterprises.

CONCLUSION

Advances in precision agriculture have led to judicious use of energy and resources (labor, fertilizers, plant protection products, water, etc.) that could be exploited for increased agricultural production and productivity. The integration of machine learning with decision support systems, robotics, and artificial intelligence autonomous technologies in precision agriculture has contributed to higher yields and quality, as well as lower risks to humans and the environment. The utilization of satellite imagery, drones, ground-based sensors, and machine learning algorithms has enabled the farmers to analyze real-time data for proactive and informed decision-making. The precision obtained through efficient crop monitoring allows for early detection of diseases and pests, minimizing the environmental impact of interventions and contributing to higher crop productivity. The characteristic predictive analytics of machine learning and its decision support systems have enhanced the farmers' ability to analyze historical data, weather patterns, and crop-specific parameters that provide invaluable insights for resource optimization and long-term sustainability. Resource management, a critical aspect of sustainable agriculture, has been revolutionized through AI technologies.

The reduction of environmental impact through smart irrigation systems and precise fertilization strategies reveals AI's potential in addressing the constraints of resource scarcity and environmental degradation. The integration of automation and robotics in farming operations has led to a paradigm shift, enhancing economic viability and labor efficiency. Robotic systems, autonomous vehicles, and connected machinery streamline tasks (such as planting, crop maintenance, and harvesting), serving as the cornerstone for a more technologically-induced, productive agricultural sector. The application of connectivity in precision agriculture through interconnection between devices and data integration has demonstrated the significance of a holistic approach to farming. The real-time monitoring and exchange of knowledge among stakeholders at the collaborative platforms contribute to continuous sharing of useful information and sustainable practices. However, careful attention should be paid to the ethical issues of data privacy associated with these technological advancements, as well as the digital divide and the impact of automation on employment. The equitable distribution and alignment of the benefits of AI in precision agriculture are crucial for ethical considerations.

Based on this review, we see the future of the agricultural sector in harmonizing technological progress with the principles of environmental stewardship and societal well-being. Advances in explainable AI, edge computing, and inclusive technology offer exciting prospects to overcome the constraints of precision farming and shape a more resilient and equitable agricultural sector. The application of AI in precision agriculture is a technological evolution that provides a pathway to a more sustainable and productive future. Collaborative networking among stakeholders, interdisciplinary research, and responsible innovation are critical to harness the full potential of AI for the benefit of farmers, communities, and food systems. The lack of skills and information asymmetries that challenge precision agriculture can be resolved by engaging consultants and technical services providers. These consultants can serve as skills transfer agents to help farmers adopt precision technologies. They can fill the information gap related to the socio-economic factors such as age, level of education, and farming experience.

Roundtable discussions in 2016 with 32 scientists, administrators, and stakeholders from the public sector and industry (mainly from the United States but also from Brazil, Canada, Germany, Israel, New Zealand, South Korea, and the United Kingdom) resulted in the key steps to guide future efforts in precision agriculture. It is essential to strengthen research on sustainable agricultural practices through increased documentation, involvement of non-governmental organizations, and balanced funding (short- and long-term, basic and applied). It is also important to facilitate IP-neutral public-private partnerships, adapt research to the needs of small farms, encourage collaboration with diverse stakeholders, support emerging scientists, and promote projects aligned with sustainable agriculture goals [130]. Decision support systems should be tailored to the needs of local farmers involved in various farming enterprises. Considering the novelty of precision agriculture, these decision support systems need to be user-friendly. Another step towards precision farming is to increase the level of automation by installing on-board sensors so as to have diagnosis and variable rate application occurring simultaneously in real-time.

To overcome the challenge of landholding sizes and economies of scale, small farmers can pool their resources and acquire the equipment together as cooperatives to reduce the capital investment per farmer. Another benefit of common use is that the farmers can share their skills, knowledge, and experience with each other.

Policy implications are indispensable to precision agriculture adoption since policy drives all the other productive factors. There should be financial incentives for the early adopters of precision farming technologies. These incentives can be in the form of tax cuts, subsidies, or lower interest rates for the farmers acquiring these technologies for their farms.

CONTRIBUTION

All the authors were involved in the experimentation, data collection, management, and writing of the paper, as well as its reading and approval, prior to submission.

CONFLICT OF INTEREST

The authors declared no potential conflict of interest regarding the research, authorship, and/or publication of this article.

ACKNOWLEDGEMENTS

This work was supported by the RUDN University Strategic Academic Leadership Program. Special thanks to the editorial office for valuable comments that improved this manuscript.

REFERENCES

1. Barker G. The agricultural revolution in prehistory: Why did foragers become farmers? Oxford: Oxford University Press; 2006, pp. 382–414. https://doi.org/10.1093/oso/9780199281091.003.0015
2. Lowenberg-DeBoer J. The precision agriculture revolution. Foreign Affairs. 2015;94(3):105–112.
3. Evenson RE, Gollin D. Assessing the impact of the Green Revolution. 1960 to 2000. Science. 2003;300(5620):758–762. https://doi.org/10.1126/science.1078710
4. Gebbers R, Adamchuk VI. Precision agriculture and food security. Science. 2010;327(5967):828–831. https://doi.org/10.1126/science.1183899

5. Harwood RR. A history of sustainable agriculture. Sustainable agricultural systems. Boca Raton: CRC Press; 2020, pp. 3–19. https://doi.org/10.1201/9781003070474-2
6. Zargar M, Pakina E, Plushikov V, Vvedenskiy V, Bayat M. Efficacy of reducing lintour doses and biocontrol components for an effective weeds control in winter wheat (*Triticum aestivum*). Bulgarian Journal of Agricultural Science. 2017;23(3):980–987. https://elibrary.ru/UYGKAS
7. Tendulkar A. Introduction to precision agriculture: Overview, concepts, world interest, policy, and economics. In: Abd El-Kader SM, El-Basioni BMM, editors. Precision Agriculture Technologies for Food Security and Sustainability. IGI Global Scientific Publishing; 2021, pp. 1–22. https://doi.org/10.4018/978-1-7998-5000-7.ch001
8. Zarco-Tejada PJ, Hubbard N, Loudjani P. Precision agriculture: An opportunity for EU-farmers–potential support with the CAP 2014-2020. Joint Research Centre of the European Commission. 2014.
9. Franzen D, Mulla D. A history of precision farming. In: Zhang Q, editor. Precision agriculture technology for crop farming. London: CRC Press; 2015, pp. 1–19. http://doi.org/10.1201/b19336-1
10. Lieve VW. Precision-agriculture and the future of farming in Europe. Scientific Foresight Unit (STOA). Belgium: STOA; 2016, 1–42. https://doi.org/10.2861/020809
11. Balabanov VI. Development of robotized complex for crop production. Vestnik of federal state educational establishment of higher professional education "Moscow state agroengineering university named after V.P. Goryachkin" 2017;(6):52–55. (In Russ.) https://elibrary.ru/ZWKXXV
12. Bayat M, Engeribo A, Meretukov Z, Aigerim A, Temewei AG, *et al*. Response of common lambsquarters (*Chenopodium album* L.) to chemical weed control programs. Research on Crops. 2019;20(4):859–863. https://doi.org/10.31830/2348-7542.2019.127
13. Lowenberg-DeBoer J, Erickson B. Setting the record straight on precision agriculture adoption. Agronomy Journal. 2019;111(4):1552–1569. https://doi.org/10.2134/agronj2018.12.0779
14. Ritchie H, Rosado P, Roser M. Environmental impacts of food production. Our World in Data. 2022. [cited 2025 Jul 15] Available from: https://ourworldindata.org/environmental-impacts-of-food
15. Ngoma H, Lupiya P, Kabisa M, Hartley F. Impacts of climate change on agriculture and household welfare in Zambia: An economy-wide analysis. Climatic Change. 2021;167:55. https://doi.org/10.1007/s10584-021-03168-z
16. Diakite S, Pakina E, Zargar M, Aldaibe AAA, Denis P, *et al*. Yield losses of cereal crops by Fusarium Link: A review on the perspective of biological control practices. Research on Crops. 2022;23(2):418–436. https://doi.org/10.31830/2348-7542.2022.057
17. United Nations Department of economic and social affairs, population division. Global Population Growth and Sustainable Development. NY: United Nations Publication; 2021, 115 p.
18. The 2021 World population data sheet. PRB. [cited 2024 Nov 10] Available from: https://interactives.prb.org/2021-wpds/
19. Aragón FM, Rud JP. Modern industries, pollution and agricultural productivity: Evidence from Ghana. London: Internation Growth Centre; 2013, 50 p.
20. The Global Land Outlook 1. United Nations Convention to Combat Desertification. [cited 2024 Nov 5]. Available from: https://www.unccd.int/resources/global-land-outlook/glo1
21. Satterthwaite D, McGranahan G, Tacoli C. Urbanization and its implications for food and farming. Philosophical Transactions of the Royal Society B. 2010;365(1554):2809–2820. https://doi.org/10.1098/rstb.2010.0136
22. Devendra C. Climate change threats and effects: Challenges for agriculture and food security. Kuala Lumpur: Academy of Sciences Malaysia. 2012.
23. Saquee FS, Diakite S, Kavhiza NJ, Pakina E, Zargar M. The efficacy of micronutrient fertilizers on the yield formulation and quality of wheat grains. Agronomy. 2023;13(2):566. https://doi.org/10.3390/agronomy13020566
24. Zhao C, Liu B, Piao S, Wang X, Lobell DB, *et al*. Temperature increase reduces global yields of major crops in four independent estimates. The Proceedings of the National Academy of Sciences. 2017;114(35):9326–9331. https://doi.org/10.1073/pnas.1701762114
25. Chauhan BS. Grand challenges in weed management. Frontiers in Agronomy. 2020;1:3. https://doi.org/10.3389/fagro.2019.00003
26. Bayat M, Zargar M, Chudinova E, Astarkhanova T, Pakina E. In vitro evaluation of antibacterial and antifungal activity of biogenic silver and copper nanoparticles: The first report of applying biogenic nanoparticles against *Pilidium concavum* and *Pestalotia* sp. Fungi. Molecules. 2021;26(17):5402. https://doi.org/10.3390/molecules26175402
27. Różewicz M, Wyzińska M, Grabiński J. The most important fungal diseases of cereals–problems and possible solutions. Agronomy. 2021;11(4):714. https://doi.org/10.3390/agronomy11040714
28. Mansfield J, Genin S, Magori S, Citovsky V, Sriariyanum M, *et al*. Top 10 plant pathogenic bacteria in molecular plant pathology. Molecular Plant Pathology. 2012;13(6):614–629. https://doi.org/10.1111/j.1364-3703.2012.00804.x

29. He M, He CQ, Ding NZ. Abiotic stresses: General defenses of land plants and chances for engineering multistress tolerance. Frontiers in Plant Science. 2018;9:1771. https://doi.org/10.3389/fpls.2018.01771
30. Climate change fans spread of pests and threatens plants and crops, new FAO study. Food and Agriculture Organization of the United Nations (FAO). [cited 2024 Sept 11] Available from: https://www.fao.org/newsroom/detail/Climate-change-fans-spread-of-pests-and-threatens-plants-and-crops-new-FAO-study/en
31. Oerke EC. Crop losses to pests. The Journal of Agricultural Science. 2006;144(1):31–43. https://doi.org/10.1017/S0021859605005708
32. Brás TA, Seixas J, Carvalhais N, Jägermeyr J. Severity of drought and heatwave crop losses tripled over the last five decades in Europe. Environmental Research Letters. 2021;16(6):065012. https://doi.org/10.1088/1748-9326/abf004
33. Monteiro A, Santos S, Gonçalves P. Precision agriculture for crop and livestock farming–brief review. Animals. 2021;11(8):2345. https://doi.org/10.3390/ani11082345
34. Cook NM, Chng S, Woodman TL, Warren R, Oliver RP, *et al*. High frequency of fungicide resistance-associated mutations in the wheat yellow rust pathogen *Puccinia striiformis* f. sp. *tritici*. Pest Management Science. 2021;77(7):3358–3371. https://doi.org/10.1002/ps.6380
35. Krutyakov YA, Mukhina MT, Shapoval OA, Zargar M. Effect of foliar treatment with aqueous dispersions of silver nanoparticles on legume-*Rhizobium* symbiosis and yield of soybean (*Glycine max* L. Merr.). Agronomy. 2022;12(6):1473. https://doi.org/10.3390/agronomy12061473
36. Zargar M, Pakina E, Dokukin P. Agronomic evaluation of mechanical and chemical weed management for reducing use of herbicides in single vs. twin-row sugar beet. Journal of Advanced Agricultural Technologies. 2017;4(1):62–67. http://doi.org/10.18178/joaat.4.1.62-67
37. Zargar M, Bayat M, Saquee FS, Diakite S, Ramzanovich NM, *et al*. New advances in nano-enabled weed management using poly (epsilon-caprolactone)-based nanoherbicides: A review. Agriculture. 2023;13(10):2031. https://doi.org/10.3390/agriculture13102031
38. Pimentel D. Environmental and economic costs of the application of pesticides primarily in the United States Integrated pest management. In: Peshin R, Dhawan AK, editors. Integrated Pest Management: Innovation-Development Process. Dordrecht: Springer; 2014, pp. 89–111. https://doi.org/10.1007/978-1-4020-8992-3_4
39. Agafonov VP. Importance of barley production in economy and social development of the agro-industrial complex. Vestnik of Voronezh state agrarian university. 2017;9(16):3–12. (In Russ.)
40. Filenko GA, Skvortsova YuG, Firsova TI, Filippov EG. The effect of reproduction on productivity and sowing traits of spring barley. Grain Economy of Russia. 2018;(3):53–57. (In Russ.) https://doi.org/10.31367/2079-8725-2018-57-3-53-57
41. Haddad M, Nassar D, Shtaya M. Heavy metals accumulation in soil and uptake by barley (*Hordeum vulgare*) irrigated with contaminated water. Scientific reports. 2023;13:4121. https://doi.org/10.1038/s41598-022-18014-0
42. Peters J, van Dam R, van Doorn R, Katerere D, Berthiller F, *et al*. Mycotoxin profiling of 1000 beer samples with a special focus on craft beer. PLoS One. 2017;12(10):e0185887. https://doi.org/10.1371/journal.pone.0185887
43. Kumar D, Kalita P. Reducing postharvest losses during storage of grain crops to strengthen food security in developing countries. Foods. 2017;6(1):8. https://doi.org/10.3390/foods6010008
44. Altukhov AI, Zavalin AA, Milaschenko NZ, Trushkin SV. The problem of improving wheat quality in the country requires a complex solution. Bulletin of the Kursk State Agricultural Academy. 2020;(2):32–39. (In Russ.) https://elibrary.ru/PHACEU
45. Beluhova-Uzunova RP, Dunchev, D. M. Precision farming–concepts and perspectives. Problems of Agricultural Economics. 2019;3:142–155. https://doi.org/10.30858/zer/112132
46. Sahu B, Chatterjee S, Mukherjee S, Sharma C. Tools of precision agriculture: A review. International Journal of Chemical Studies. 2019;7(6):2692–2697.
47. Pathak HS, Brown P, Best T. A systematic literature review of the factors affecting the precision agriculture adoption process. Precision Agriculture. 2019;20:1292–1316. https://doi.org/10.1007/s11119-019-09653-x
48. Robert PC. Precision Agriculture: Research needs and status in the USA. Future directions of precision agriculture. Sheffield: Academic Press; 1999, pp. 19–33.
49. Mcbratney A, Whelan B, Ancev T, Bouma J. Future Directions of Precision Agriculture. Precision Agriculture. 2005;6(1):7–23. https://doi.org/10.1007/s11119-005-0681-8
50. International Society for Precision Agriculture. ISPA Forms Official Definition of "Precision Agriculture". Global Ag Tech Initiative. 2019.
51. Burlutskiy VA, Peliy AF, Borodina ES, Diop A, Batygin AS, *et al*. Efficiency of advanced sprayers for nutrient and pesticide application under precision cultivation of spring rapeseed (*Brassica napus*). Research on Crops. 2020;21(3):466–472. https://doi.org/10.31830/2348-7542.2020.074

52. Adewusi AO, Asuzu OF, Olorunsogo T, Iwuanyanwu C, Adaga E, *et al*. AI in precision agriculture: A review of technologies for sustainable farming practices. World Journal of Advanced Research and Reviews. 2024;21(01): 2276–2285. https://doi.org/10.30574/wjarr.2024.21.1.0314

53. Misra S, Ghosh A. Agriculture paradigm shift: A journey from traditional to modern agriculture. Biodiversity and Bioeconomy. Amsterdam: Elsevier; 2024, pp. 113–141. https://doi.org/10.1016/B978-0-323-95482-2.00006-7

54. Patel A, Mahore A, Nalawade RD, Upadhyay A, Choudhary V. Advancements in precision agriculture: Harnessing the power of artificial intelligence and drones in Indian agriculture. World Environment Day. 2023:43.

55. Doolittle JA, Brevik EC. The use of electromagnetic induction techniques in soils studies. Geoderma. 2014;223–225:33–45. https://doi.org/10.1016/j.geoderma.2014.01.027

56. Adamchuk VI, Allred BJ, Doolittle J, Grote K, Rossel R, *et al*. Tools for proximal soil sensing. In: Ditzler C, West L, editors. Soil Survey Manual. Natural Resources Conservation Service. Washington: U. S. Department of Agriculture; 2015, 18 p.

57. Dengeru Y, Ramasamy K, Allimuthu S, Balakrishnan S, Kumar APM, *et al*. Study on spray deposition and drift characteristics of uav agricultural sprayer for application of insecticide in redgram crop (*Cajanus cajan L. Millsp*.). Agronomy. 2022;12(12):3196. https://doi.org/10.3390/agronomy12123196

58. Keshet D, Brook A, Malkinson D, Izhaki I, Charter M. The use of drones to determine rodent location and damage in agricultural crops. Drones. 2022;6(12):396. https://doi.org/10.3390/drones6120396

59. Mishra H, Mishra D. Artificial intelligence and machine learning in agriculture: Transforming farming systems. Research Trends in Agriculture Science. 2023;1:1–16.

60. Wilgenbusch JC, Pardey PG, Hospodarsky N, Lynch BJ. Addressing new data privacy realities affecting agricultural research and development: A tiered-risk, standards-based approach. Agronomy Journal. 2022;114(5):2653–2668. https://doi.org/10.1002/agj2.20968

61. Liu Y, Gupta H, Springer E, Wagener T. Linking science with environmental decision making: Experiences from an integrated modeling approach to supporting sustainable water resources management. Environmental Modelling and Software. 2008;23(7):846–858. https://doi.org/10.1016/j.envsoft.2007.10.007

62. Salcedo-Sanz S, Ghamisi P, Piles M, Werner M, Cuadra L, *et al*. Machine learning information fusion in Earth observation: A comprehensive review of methods, applications and data sources. Information Fusion. 2020;63: 256–272. https://doi.org/10.1016/j.inffus.2020.07.004

63. Beriya A, Saroja VN. Data-driven decision making for smart agriculture. ICT India Working Paper. 2019;(8):1–16.

64. Karthikeyan A, Garg A, Vinod PK, Priyakumar UD. Machine learning based clinical decision support system for early COVID-19 mortality prediction. Frontiers in Public Health. 2021;9:626697. https://doi.org/10.3389/fpubh.2021.626697

65. Shaikh TA, Rasool T, Lone FR. Towards leveraging the role of machine learning and artificial intelligence in precision agriculture and smart farming. Computers and Electronics in Agriculture. 2022;198:107119. https://doi.org/10.1016/j.compag.2022.107119

66. Adebukola AA, Navya AN, Jordan FJ, Jenifer NJ, Begley RD. Cyber security as a threat to health care. Journal of Technology and Systems. 2022;4(1):32–64. https://doi.org/10.47941/jts.1149

67. Sinwar D, Dhaka VS, Sharma MK, Rani G. AI-Based Yield Prediction and Smart Irrigation. In: Pattnaik P, Kumar R, Pal S, editors. Internet of Things and Analytics for Agriculture, Volume 2. Singapore: Springer; 2020, pp. 155–180. https://doi.org/10.1007/978-981-15-0663-5_8

68. Abioye EA, Abidin MSZ, Mahmud MSA, Buyamin S, Ishak MHI, *et al*. A review on monitoring and advanced control strategies for precision irrigation. Computers and Electronics in Agriculture. 2020;173:105441. https://doi.org/10.1016/j.compag.2020.105441

69. Ewim DRE, Okwu MO, Onyiriuka EJ, Abiodun AS, Abolarin SM, *et al*. A quick review of the applications of artificial neural networks (ANN) in the modelling of thermal systems. Engineering and Applied Science Research. 2021;49(3):444–458.

70. Mouchou R, Laseinde T, Jen TC, Ukoba K. Developments in the application of nano materials for photovoltaic solar cell design, based on industry 4.0 integration scheme. In: Ahram TZ, Karwowski W, Kalra J, editors. Advances in Artificial Intelligence, Software and Systems Engineering: Proceedings of the AHFE 2021. Cham: Springer; 2021, pp. 510–521. https://doi.org/10.1007/978-3-030-80624-8_64

71. Owebor K, Diemuodeke OE, Briggs TA, Eyenubo OJ, Ogorure OJ, *et al*. Multi-criteria optimisation of integrated power systems for low-environmental impact. Energy Sources, Part A: Recovery, Utilization, and Environmental Effects. 2022;44(2):3459–3476. https://doi.org/10.1080/15567036.2022.2064565

72. Chowdhury S, Dey P, Joel-Edgar S, Bhattacharya S, Rodriguez-Espindola O, *et al*. Unlocking the value of artificial intelligence in human resource management through AI capability framework. Human Resource Management Review. 2023;33(1):100899. https://doi.org/10.1016/j.hrmr.2022.100899

73. Rajendran V, Debnath B, Mghames S, Mandil W, Parsa S, *et al*. Towards autonomous selective harvesting: A review of robot perception, robot design, motion planning and control. Journal of Field Robotics. 2024;41(7):2247–2279. https://doi.org/10.1002/rob.22230

74. Norsworthy JK, Ward SM, Shaw DR, Llewellyn RS, Nichols RL, *et al*. Reducing the risks of herbicide resistance: Best management practices and recommendations. Weed Science. 2012;60(SP1):31–62. https://doi.org/10.1614/WS-D-11-00155.1

75. Vermesan O, Bahr R, Ottella M, Serrano M, Karlsen T, *et al*. Internet of robotic things intelligent connectivity and platforms. Frontiers in Robotics and AI. 2020;7(MAR):104. https://doi.org/10.3389/frobt.2020.00104

76. Ukoba OK, Jen TC. Review of atomic layer deposition of nanostructured solar cells 4. Journal of Physics: Conference Series. 2019;1378(4):042060. https://doi.org/10.1088/1742-6596/1378/4/042060

77. Dong H, Zhang J, Zhao X. Intelligent wind farm control via deep reinforcement learning and high-fidelity simulations. Applied Energy. 2021;292:116928. https://doi.org/10.1016/j.apenergy.2021.116928

78. Habibzadeh H, Soyata T, Kantarci B, Boukerche A, Kaptan C. Sensing, communication and security planes: A new challenge for a smart city system design. Computer Networks. 2018;144:163–200. https://doi.org/10.1016/j.comnet.2018.08.001

79. Fantana NL, Riedel T, Schlick J, Ferber S, Hupp J, *et al*. Internet of things - converging technologies for smart environments and integrated ecosystems. In: Vermesan O, Friess P, editors. River Publishers Series in Communications. Aalborg: River Publishers; 2013, pp. 155–204.

80. Uddin SU, Chidolue O, Azeez A, Iqbal T. Design and analysis of a solar powered water filtration system for a community in black tickle-domino. 2022 IEEE International IOT, Electronics and Mechatronics Conference (IEMTRONICS). 2022:1–6. https://doi.org/10.1109/IEMTRONICS55184.2022.9795758

81. Lytos A, Lagkas T, Sarigiannidis P, Zervakis M, Livanos G. Towards smart farming: Systems, frameworks and exploitation of multiple sources. Computer Networks. 2020;172:107147. https://doi.org/10.1016/j.comnet.2020.107147

82. Petropoulos A, Siakoulis V, Stavroulakis E, Vlachogiannakis NE. Predicting bank insolvencies using machine learning techniques. International Journal of Forecasting. 2020;36(3):1092–1113. https://doi.org/10.1016/j.ijforecast.2019.11.005

83. Ikwuagwu CV, Ajahb SA, Uchennab N, Uzomab N, Anutaa UJ, *et al*. Development of an arduino-controlled convective heat dryer. UNN International Conference: Technological Innovation for Holistic Sustainable Development (TECHISD2020). 2020;180–195.

84. Little J, Knights P, Topal E. Integrated optimization of underground mine design and scheduling. Journal of The Southern African Institute of Mining and Metallurgy. 2013;113(10):775–785.

85. Santesteban LG. Precision viticulture and advanced analytics. A short review. Food Chemistry. 2019;279:58–62. https://doi.org/10.1016/j.foodchem.2018.11.140

86. Bayat M, Zargar M, Chudinova E, Astarkhanova T, Pakina E. In vitro evaluation of antibacterial and antifungal activity of biogenic silver and copper nanoparticles: The first report of applying biogenic nanoparticles against *Pilidium concavum* and *Pestalotia* sp. Fungi. Molecules. 2021;26(17):5402. https://doi.org/10.3390/molecules26175402

87. Javaid M, Haleem A, Singh RP, Suman R. Enhancing smart farming through the applications of Agriculture 4.0 technologies. International Journal of Intelligent Networks. 2022;3:150–164. https://doi.org/10.1016/j.ijin.2022.09.004

88. Bill R, Nash E, Grenzdörffer G, Wiebensohn J. Geographic Information Systems in Agriculture. In: Kresse W, Danko D, editors. Springer Handbook of Geographic Information. Cham: Springer; 2022, pp. 659–684. https://doi.org/10.1007/978-3-030-53125-6_24

89. Ferencz C, Bognár P, Lichtenberger J, Hamar D, Tarcsai G, *et al*. Crop yield estimation by satellite remote sensing. International Journal of Remote Sensing. 2004;25(20):4113–4149. https://doi.org/10.1080/01431160410001698870

90. Řezník T, Pavelka T, Herman L, Lukas V, Širůček P, *et al*. Prediction of yield productivity zones from Landsat 8 and Sentinel-2A/B and their evaluation using farm machinery measurements. Remote Sensing. 2020;12(12):1917. https://doi.org/10.3390/rs12121917

91. Global variable rate technology (vrt) market size by type (fertilizer vrt, crop protection chemical vrt), by crop type (cereals and grains, oilseeds and pulses), by application (map-based vrt, sensor-based vrt), by offering (hardware, variable-rate software), by geographic scope and forecast in 2019.Verified Market Research. [cited 2024 Sept 10]. Available from: https://www.verifiedmarketresearch.com/product/variable-rate-technology-vrt-market/

92. Kavhiza NJ, Vvedenskiy V, Behzad A, Bayat M, Kargar MH, *et al*. Weed mapping technologies in discerning and managing weed infestation levels of farming systems. Research on Crops. 2020;21(1):93–98. https://doi.org/10.31830/2348-7542.2020.015

93. Zargar M, Bayat M, Astarkhanova T. Study of postemergence-directed herbicides for redroot pigweed (*Amaranthus retroflexus* L.) control in winter wheat in southern Russia. Journal of Plant Protection Research. 2020;60(1):7–13. https://elibrary.ru/IPPUEQ

94. Perron I, Cambouris AN, Chokmani K, Vargas Gutierrez MF, Zebarth BJ, *et al*. Delineating soil management zones using a proximal soil sensing system in two commercial potato fields in New Brunswick, Canada. Canadian Journal of Soil Science. 2018;98(4):724–737. https://doi.org/10.1139/cjss-2018-0063

95. Valente DSM, de Queiroz DM, Pinto FDADC, Santos FL, Santos NT. Spatial variability of apparent electrical conductivity and soil properties in a coffee production field. Engenharia Agrícola. 2014;34(6):1224–1233. https://doi.org/10.1590/S0100-69162014000600017

96. Tripathi R, Nayak AK, Shahid M, Lal B, Gautam P, *et al*. Delineation of soil management zones for a rice cultivated area in eastern India using fuzzy clustering. Catena. 2015;133:128–136. https://doi.org/10.1016/j.catena.2015.05.009

97. Bongiovanni R, Lowenberg-DeBoer J. Precision agriculture and sustainability. Precision Agriculture. 2004;5:359–387. https://doi.org/10.1023/B:PRAG.0000040806.39604.aa

98. Nejad SM, Najafabadi SN, Aghighi S, Pakina E, Zargar M. Evaluation of *Phoma* sp. biomass as an endophytic fungus for synthesis of extracellular gold nanoparticles with antibacterial and antifungal properties. Molecules. 2022;27(4):1181. https://doi.org/10.3390/molecules27041181

99. Truflyak EV. Main elements of precision farming system. Izvestiya of Velikiye Luki State Agricultural Academy. 2016;(4):25–34. (In Russ.) https://www.elibrary.ru/VMHDCT

100. Diacono M, Rubino P, Montemurro F. Precision nitrogen management of wheat. A review. Agronomy for Sustainable Development. 2013;33:219–241. https://doi.org/10.1007/s13593-012-0111-z

101. Van Evert FK, Gaitán-Cremaschi D, Fountas S, Kempenaar C. Can precision agriculture increase the profitability and sustainability of the production of potatoes and olives? Sustainability. 2017;9(10):1863. https://doi.org/10.3390/su9101863

102. Kazlauskas M, Šarauskis E, Lekavičienė K, Naujokienė V, Romaneckas K, *et al*. The comparison analysis of uniform-and variable-rate fertilizations on winter wheat yield parameters using site-specific seeding. Processes. 2022;10(12):2717. https://doi.org/10.3390/pr10122717

103. Finco A, Bucci G, Belletti M, Bentivoglio D. The economic results of investing in precision agriculture in durum wheat production: A case study in central Italy. Agronomy. 2021;11(8):1520. https://doi.org/10.3390/agronomy11081520

104. Kempenaar C, Been T, Booij J, Van Evert F, Michielsen JM, Kocks C. Advances in variable rate technology application in potato in the Netherlands. Potato Research. 2017;60:295–305. https://doi.org/10.1007/s11540-018-9357-4

105. Ruigrok T, van Henten E, Booij J, van Boheemen K, Kootstra G. Application-specific evaluation of a weed-detection algorithm for plant-specific spraying. Sensors. 2020;20(24):7262. https://doi.org/10.3390/s20247262

106. Kavhiza NJ, Zargar M, Prikhodko SI, Pakina EN, Murtazova KMS, *et al*. Improving crop productivity and ensuring food security through the adoption of genetically modified crops in Sub-Saharan Africa. Agronomy. 2022;12(2):439. https://doi.org/10.3390/agronomy12020439

107. Munz J, Schuele H. Influencing the success of precision farming technology adoption–a model-based investigation of economic success factors in small-scale agriculture. Agriculture. 2022;12(11):1773. https://doi.org/10.3390/agriculture12111773

108. Zubarev YuN, Fomin DS, Chashchin AN, Zabolotnova MV. Use of uncleaned aircraft in agriculture. Perm Federal Research Centre Journal. 2019;(2):47–51. https://doi.org/10.7242/2658-705X/2019.2.5

109. Zhao W, Wu J, Shen Q, Yang J, Han X. Exploring the ability of solar-induced chlorophyll fluorescence for drought monitoring based on an intelligent irrigation control system. Remote Sensing. 2022;14(23):6157. https://doi.org/10.3390/rs14236157

110. Griffin TW, Lowenberg-DeBoer J. Worldwide adoption and profitability of precision agriculture implications for Brazil. Revista de Politica Agricola. 2005:14(4):20–37.

111. Gusev A, Skvortsov E, Volkova S. The study of the impact of introduction of precision farming technologies on the main production and economic indicators at agriculture organizations. AIP Conference Proceedings. 2022;2661(1):020012. https://doi.org/10.1063/5.0107626

112. Ghadamkheir M, Klyushin PV, Orujov E, Bayat M, Mu Madumarov M, *et al*. Influence of sulfur fertilization on infection of wheat take-all disease caused by the fungus *Gaeumannomyces graminis var. tritici*. Research on Crops. 2020;21(3):627–633. https://doi.org/10.31830/2348-7542.2020.098

113. Kelc D, Stajnko D, Berk P, Rakun J, Vindiš P, *et al*. Reduction of environmental pollution by using RTK-navigation in soil cultivation. International Journal of Agricultural and Biological Engineering. 2019;12(5):173–178. https://doi.org/10.25165/j.ijabe.20191205.4932

114. Perea GR, Daccache A, Díaz RJA, Poyato CE, Knox JW. Modelling impacts of precision irrigation on crop yield and in-field water management. Precision Agriculture. 2018;19:497–512. https://doi.org/10.1007/s11119-017-9535-4

115. Balogh P, Bujdos Á, Czibere I, Fodor L, Gabnai Z, *et al*. Main motivational factors of farmers adopting precision farming in Hungary. Agronomy. 2020;10(4):610. https://doi.org/10.3390/agronomy10040610

116. Blasch J, van der Kroon B, van Beukering P, Munster R, Fabiani S, *et al*. Farmer preferences for adopting precision farming technologies: A case study from Italy. European Review of Agricultural Economics. 2022;49(1):33–81. https://doi.org/10.1093/erae/jbaa031

117. Mizik T. How can precision farming work on a small scale? A systematic literature review. Precision Agriculture. 2023;24:384–406. https://doi.org/10.1007/s11119-022-09934-y

118. Le Hoang Nguyen L, Halibas A, Quang Nguyen T. Determinants of precision agriculture technology adoption in developing countries: A review. Journal of Crop Improvement. 2023;37(1):1–24. https://doi.org/10.1080/15427528.2022.2080784

119. Pandeya S, Gyawali BR, Upadhaya S. Factors influencing precision agriculture technology adoption among small-scale farmers in Kentucky and their implications for policy and practice. Agriculture. 2025;15(2):177. https://doi.org/10.3390/agriculture15020177

120. Troiano S, Carzedda M, Marangon, F. Better richer than environmentally friendly? Describing preferences toward and factors affecting precision agriculture adoption in Italy. Agricultural and Food Economics. 2023;11:16. https://doi.org/10.1186/s40100-023-00247-w

121. Weersink A, Fraser E, Pannell D, Duncan E, Rotz S. Opportunities and challenges for big data in agricultural and environmental analysis. Annual Review of Resource Economics. 2018;10:19–37. https://doi.org/10.1146/annurev-resource-100516-053654

122. Jacobs AJ, Van Tol JJ, Du Preez CC. Farmers perceptions of precision agriculture and the role of agricultural extension: A case study of crop farming in the Schweizer-Reneke region, South Africa. South African Journal of Agricultural Extension. 2018;46(2):107–118. https://doi.org/10.17159/2413-3221/2018/v46n2a484

123. Sishodia RP, Ray RL, Singh SK. Applications of remote sensing in precision agriculture: A Review. Remote Sensing. 2020;12(19):3136. https://doi.org/10.3390/rs12193136

124. Groher T, Heitkämper K, Walter A, Liebisch F, Umstätter C. Status quo of adoption of precision agriculture enabling technologies in Swiss plant production. Precision Agriculutre. 2020;21:1327–1350. https://doi.org/10.1007/s11119-020-09723-5

125. Barnes AP, Soto I, Eory V, Beck B, Balafoutis A, *et al*. Exploring the adoption of precision agricultural technologies: A cross regional study of EU farmers. Land Use Policy. 2019;80:163–174. https://doi.org/10.1016/j.landusepol.2018.10.004

126. Kendall H, Clark B, Li W, Jin S, Jones GD, *et al*. Precision agriculture technology adoption: A qualitative study of small-scale commercial "Family farms" located in the north China plain. Precision Agriculture. 2022;23:319–351. https://doi.org/10.1007/s11119-021-09839-2

127. Kendall H, Naughton P, Clark B, Taylor J, Li Z, *et al*. Precision agriculture in China: Exploring awareness, understanding, attitudes and perceptions of agricultural experts and end-users in China. Advances in Animal Biosciences. 2017;8(2):703–707. https://doi.org/10.1017/S2040470017001066

128. Leska A, Nowak A, Nowak I, Górczyńska A. Effects of insecticides and microbiological contaminants on *Apis mellifera* health. Molecules. 2021;26(16):5080. https://doi.org/10.3390/molecules26165080

129. Zhang N, Wang M, Wang N. Precision agriculture–a worldwide overview. Computers and Electronics in Agriculture. 2002;36(2–3):113–132. https://doi.org/10.1016/S0168-1699(02)00096-0

130. Yost MA, Sudduth KA, Walthall CL, Kitchen NR. Public–private collaboration toward research, education and innovation opportunities in precision agriculture. Precision Agriculture. 2019;20:4–18. https://doi.org/10.1007/s11119-018-9583-4

ORCID IDs
Simbo Diakite https://orcid.org/0000-0003-1462-1329
Nyasha J. Kavhiza https://orcid.org/0000-0002-8505-3253
Francess S. Saquee https://orcid.org/0000-0001-7653-6942
Elena N. Pakina https://orcid.org/0000-0001-6493-6121
Meisam Zargar https://orcid.org/0000-0002-5208-0861
Ousmane Diarra https://orcid.org/0009-0004-9514-9381
Prince E. Norman https://orcid.org/0000-0002-0150-8610
Brahima Traore https://orcid.org/0009-0006-0620-5658
Fasse Samake https://orcid.org/0009-0000-3964-9614
Cheickna Daou https://orcid.org/0009-0006-1836-1834
Amadou H. Babana https://orcid.org/0000-0001-6702-9922

Foods and Raw Materials. 2026;14(2)

ISSN 2308-4057 (Print)
ISSN 2310-9599 (Online)

Research Article
Open Access

Available online at http://jfrm.ru/en
https://doi.org/10.21603/2308-4057-2026-2-684
https://elibrary.ru/SYRDUP

Experimental recirculating carbon dioxide refrigeration unit

Evgeniy N. Neverov*, Pavel S. Korotkih, Alena K. Gorelkina, Irina V. Timoshchuk

Kemerovo State University, Kemerovo, Russia

* e-mail: neverov42@mail.ru

Received 06.12.2024; Revised 13.01.2025; Accepted 03.06.2025; Published online 20.10.2025

Abstract:
Turkey farming and meat processing are fast-developing areas of the Russian food industry. However, their development requires more advanced methods of meat storage and freezing. Traditional methods of air cooling often fail to preserve the original meat texture and nutritional value. This paper introduces a new refrigeration unit with CO_2 as a refrigerant. CO_2 snow and gas come in direct contact with turkey carcasses, thus accelerating the cooling process and improving the meat quality. CO_2 recirculation makes the refrigeration unit an economical solution to environmental issues. The refrigeration unit included a conveyor system, a vacuum chamber, and a CO_2 circulation system.

The research featured grade 1 turkey carcasses of 2.7 ± 0.1 kg frozen at different temperatures (–30, –50, and –70°C) and CO_2 flux rates (0–5 m/s). The share of CO_2 in the gas mix was ≥ 50%. The temperature and heat flux density were measured using thermocouples and heat flux probes.

As the temperature dropped from –30 to –70°C, the freezing time decreased from 48 to 33 min and to 29 min when the experiment involved enforced convection. The amount of CO_2 consumed increased from 7.5 to 13.5 kg without convection and from 6.5 to 12.0 kg with enforced convection. Compared to traditional methods, CO_2 provided uniform freezing and reduced mechanical damage to the meat structure.

The newly developed refrigeration unit with recirculated CO_2 demonstrated high efficiency in freezing turkey meat while reducing CO_2 consumption and providing uniform cooling of the carcass. It demonstrated could prospects for industrial use, which opens up new opportunities for further research and freezing process optimization.

Keywords: Refrigeration, CO_2 recirculation, quick freezing, convection, turkey meat, meat processing

Funding: The research was part of a comprehensive scientific innovative program initiated by Russian Federation Government Decree No. 1144-r, May 11, 2022: Developing and implementing new technologies in the E&P of solid minerals, industrial safety, bioremediation, and product development of deep coal processing: A consistent reduction of environmental impact and hazards (Agreement No. 075-15-2022-1201, September 30, 2022).

Please cite this article in press as: Neverov EN, Korotkih PS, Gorelkina AK, Timoshchuk IV. Experimental recirculating carbon dioxide refrigeration unit. Foods and Raw Materials. 2026;15(2):377–385. https://doi.org/10.21603/2308-4057-2026-2-684

INTRODUCTION

Turkey meat production is a poultry market sector with the most value-enhancing investments and a great growth potential. As the global population and urbanization continue to grow, so does consumers' awareness of turkey meat as a healthier option than other, more traditional meats. The growing demand triggers technical advancements in processing, packaging, distribution, shelf life, and availability of turkey meat.

Today, turkey farming is concentrated in North America and Europe, where the path of industrial development has led to advanced turkey farming infrastructure. They produce enough turkey meat to meet local demand and export the surplus [1]. Russia has recently seen an increase in the number of large-scale turkey farms while small and medium-sized businesses remain scarce. The resulting random distribution of turkey meat production across regions gives the turkey industry good development perspectives, considering that some regions lack any turkey meat farms altogether [2, 3]. New effective methods for frozen storage of turkey meat may lead to a more uniform distribution of this product across Russia's regions [4].

Turkey meat is nutritious and heart-healthy: it contains little cholesterol and fat, while being rich in protein. As the demand for turkey meat increases, consumers become more and more particular about its quality. Meat

Copyright © 2025, Neverov *et al.* This is an open access article distributed under the terms of the Creative Commons Attribution 4.0 International License (https://creativecommons.org/licenses/by/4.0/), allowing third parties to copy and redistribute the material in any medium or format and to remix, transform, and build upon the material for any purpose, even commercially, provided the original work is properly cited and states its license.

quality is a complex of sensory and biological indicators that determine its practical ability to meet nutritional requirements. As for turkey meat, its quality profile includes nutritional composition, color, texture, etc. All these qualities depend on the birds' welfare. Unlike other, more traditional meats, turkey has a significant share of flesh, which gives it excellent dietary characteristics. It is rich in vitamins B, phosphorus, iron, magnesium, potassium, and amino acids. The advantage of turkey meat is that it is basically muscle tissue with a lot of labile organic substances [5–7].

Russian industrial turkey farming is young but quick-developing. A potential capacity analysis of the Russian turkey meat market shows that the volume of domestic turkey production keeps growing in terms of slaughter weight: from 30,500 tons in 2009, it skyrocketed to 125,000 tons in 2013 and rose beyond 276,000 tons in 2017 to 418,000 tons in 2023 before peaking at 512,000 tons in 2024 [8].

Freezing preserves poultry meat for transportation or long-time storage. Low temperatures extend its shelf life by inhibiting microbial spoilage and deterioration. Meat properties that are to be preserved during storage include tenderness, water-holding capacity, color, and flavor. While improving tenderness, freezing damages other characteristics, depending on the size and distribution of ice crystals, which, in their turn, depend on the rate of freezing, temperature, and storage time. Although new technologies mitigate the negative effects of freezing, the complex nature of muscle tissue makes it difficult to predict the quality of defrosted meat.

For many decades, refrigeration of poultry meat has relied on air freezing. The temperature mode and flow patterns of the cooling medium vary depending on the shelf life, packaging, and type of product. However, free (unbound) water in muscle cells becomes crystallized during freezing, which makes mechanical damage to muscle tissue inevitable. As a result, the product loses some of its nutrients. Food science is still on the lookout for more effective and modern methods of poultry freezing [9–11].

Carbon dioxide (R744) as a refrigerant provides faster freezing compared to traditional units. Fast freezing is crucial for turkey meat with its high moisture content. It minimizes coarse crystallization, helping preserve the texture and taste while extending its shelf life [12, 13]. In addition, refrigerant R744 has low environmental burden. Yet, carbon dioxide has its disadvantages as a refrigerant, which means it requires a careful selection of the system for each particular case [14–16].

Carbon dioxide as a refrigerant has some advantages over hydrochlorofluorocarbon (HCFC). For instance, R744 has a lower compression ratio than HCFC, which increases its isentropic efficiency. The cross-sectional area of the suction pipe is proportional to the volumetric capacity. For R744, the suction line diameter is twice as small as that for R404A [17]. Table 1 shows the fitting criteria of R744 for various conditions and standards.

Systems that work on CO_2 can be divided into subcritical and transcritical ones. They have the same basic CO_2 cycle: compression – heat rejection – expansion. As a result, their thermodynamic diagrams are similar, too (Fig. 1). The main difference is in the heat rejection mode.

In a subcritical cycle, heat rejection occurs below the critical point (T_c = 31.2°C, P_c = 7.38 MPa for CO_2). In the diagram of enthalpy vs. pressure, this process

Table 1 R744 vs. alternatives: Compliance with conditions and criteria

Criterion	Compliance
Refrigeration capacity	Greater displacement
Operational conditions	Higher operating pressure and resting pressure
Refrigerant	High availability
Components	Become more available as production increases
Extra qualifications	Operators need extra qualifications
Price	Cheaper cooling agent, but higher the overall expenses
Safety	Advantages: low toxic, non-flammable Disadvantages: high pressure and difficulties associated with it

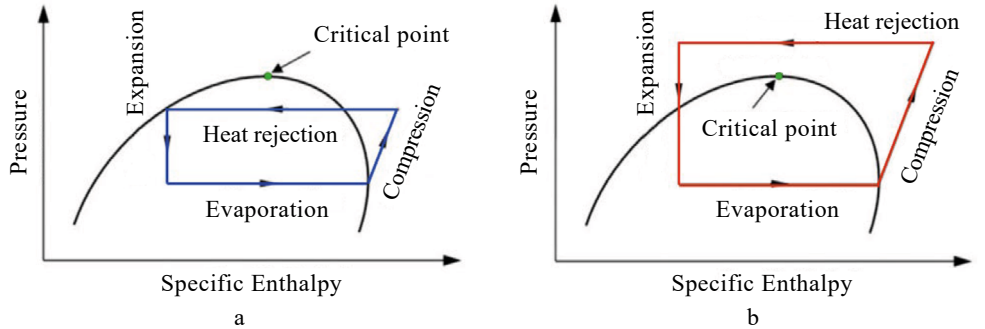

Figure 1 Working cycle of a refrigeration machine: Specific enthalpy and pressure in subcritical (a) vs. transcritical (b) systems

occurs partly within the area curbed by solid liquid (left of the critical point) and saturated vapor (right of the critical point). In the subcritical mode, heat rejection occurs as a condensation of the gaseous refrigerant at a nearly constant temperature.

In the transcritical CO_2 cycle, heat rejection occurs above the critical point, i.e., when the refrigerant is in its gaseous state. Unlike constant temperature condensation, it is a process of gas cooling [18, 19].

The systems differ in refrigeration capacity. In supercritical operation, the refrigeration capacity increases at a constant temperature as the pressure continues to grow. In the subcritical mode, the refrigeration capacity increases at lower discharge pressures.

The two systems also differ in power consumption. However, the general rule of "the lower the pressure, the lower the power consumption" is true for both systems. The change in power consumption is not proportional to the change in refrigeration capacity, which increases significantly. As a result, the amount of energy consumed by the compressor drive increases, too.

The highest performance coefficient is impossible in the supercritical mode at a minimal condensing pressure. The optimal performance coefficient (90–100 bar) depends on the evaporation conditions and the outlet temperature of the condenser. As a rule, the pressure for optimal performance is higher than for optimal efficiency [20, 21].

In transcritical systems, the pressure in the gas cooler has to be regulated to provide optimal performance while maintaining the pressure below the critical point.

R744 leaves the gas cooler at 40°C. This outlet temperature depends on the condenser size and the ambient temperature as much as the condensing temperature depends on these parameters.

Transcritical systems are designed to operate above the critical point some or all of the time. HCFC systems also go through a drop in efficiency when the ambient temperature increases. In R744 systems, the change is much greater during the transition from subcritical to transcritical cooling. Since heat rejection often occurs at ambient temperatures, some of the operating units may go subcritical in those Russian regions where the ambient temperature stays below 20–25°C.

For the transcritical mode, appropriate pressure control on the high-pressure side (condenser) is crucial as it optimizes the cooling capacity and efficiency. For example, by increasing the pressure on the high-pressure side, the machine increases its cooling capacity when operating above the critical point, which has a positive effect in the pre-cooling of poultry meat.

Like other food products, poultry has to cool down completely before packaging. Otherwise, water vapor condenses inside the package and causes molding or makes unwanted substances migrate into the product since some packaging is unsuitable for contact with warm food products. However, food enterprises see waiting for the product to cool down as a waste of time that creates practical and logistical problems. The cooling process occupies much place for many hours, which slows down the production cycles and may lead to financial losses [22, 23]. To prevent it, meat producers accelerate cooling by passing the product through a cooling tunnel with CO_2, which results in a high-quality product with a long shelf life and provides recirculation potential.

In this study, we developed and tested a refrigeration system for turkey carcasses with CO_2 as a refrigerant. The directs contact with CO_2 snow during freezing accelerated the cooling and improved the quality of meat while CO_2 recirculation minimized CO_2 losses.

STUDY OBJECTS AND METHODS

We used grade 1 turkey carcasses of 2.7 ± 0.1 kg (State Standard GOST 31473-2012).

To study the process of CO_2 freezing, we designed an experimental three-stage refrigeration unit with a heat-insulated chamber. To control the temperature, thermocouple units were installed under the turkey skin (5 ± 1 mm), inside the carcass (30 ± 5 mm), and in the inner surface of the opened turkey carcass (60 ± 10 mm) (Fig. 2). To measure the heat flux density, we placed remote heat flux probes PTP-9.9P on the surface of the carcasses.

The refrigeration unit was provided with an autonomous auxiliary low-power cooling system to prevent the pressure from increasing to emergency discharge values, when the refrigerant has to be released into the atmosphere. It also helped avoid complications caused by accidental power cut. The thermodynamic model was constructed using the Danfoss software.

Materials for the vacuum refrigeration chamber were selected based on the requirements for gas impermeability, thermal conductivity, resistance to aggressive environments, and mechanical strength. In some cases, we combined different materials. AISI 304 stainless steel served as the major material. This grade has high strength, corrosion resistance, and excellent tightness. Standard 100-millimeter-thick polyurethane foam boards provided thermal insulation.

The carcasses entered the chamber via a belt conveyor, after which the chamber was closed. Its hermetic doors were provided with PUREMIX CDM2B-40-300 double-acting pneumatic pushers, driven by a GANTA AC 260/025 air oil compressor. The chamber door was an AISI 304 steel sheet.

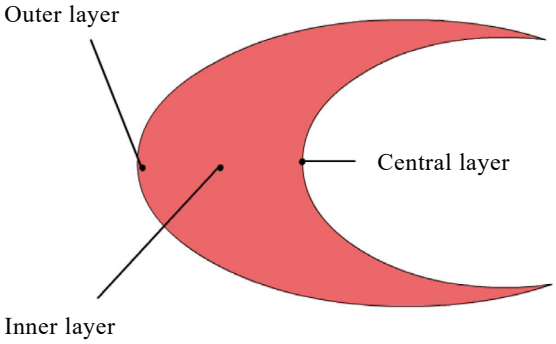

Figure 2 Temperature sensors in three layers of turkey carcass

To maintain the hermeticity along the perimeter, we used seals made of FVMQ fluorosilicone rubber. They are resistant to oils and solvents and retain their sealing ability at –80°C. The automated pneumatic system also included pneumatic stops, an air oil compressor, and compressed air preparation units. After closing the door, the limit switch gave a command to open the electromagnetic valve and turn on the Value VE-260 vacuum pump. It pumped air out of the chamber, preparing it for CO_2 intake.

The vacuuming process continued until 0.2 bar. The vacuum pump had a capacity of 170 L/min (10.2 m^3/h) to reduce the pressure in the 48-L experimental chamber to a targeted level in about 30 s.

At the next stage, liquid CO_2 was supplied to the chamber through nozzles [24]. Crystalline CO_2 settled on the product and at the bottom of the chamber. To increase the heat exchange rate, the chamber had ERA PROFIT 4 BB duct fans (100 mm across), which were responsible for artificial circulation of the gas environment.

We installed air flow velocity meters (anemometers) with an ATE-1019 remote sensor at the outlet of the fan ducts. Carbon dioxide passed through the fans, entered the side cavity of the chamber, circulated in the lower cavity, and passed through the perforated tray. The supply of CO_2 to the heat-insulated chamber stopped when the temperature in the center of the carcass reached –12°C.

Upon cooling, CO_2 snow sublimated into gas and was sucked off by the compressor through the liquid separator. The air compressor started, and the pneumatic pushers opened the doors. After the electric motor started, the conveyor started pushing the frozen product down the conveyor. The conveyor belts were strong enough and easy to clean. The latter is important because a conveyor belt consists of hinged parts that may accumulate residues of the frozen product.

Experiments on kinetics did not involve starting the conveyor and automatic doors.

RESULTS AND DISCUSSION

Figure 3 shows a diagram of a three-stage CO_2-operating subcritical-mode refrigeration unit. The first-stage compressor unit (*1*) sucked vapors out from the liquid separator (*7*) and compressed the gas to intermediate pressure 1 of 2.57 MPa. The gas entered heat exchanger I (*4*), where its temperature dropped to –15°C, after which it entered the second-stage compressor (*2*), where the gas was compressed to intermediate pressure 2 of 4.30 MPa. After that, the refrigerant moved to heat exchanger II (*4*), and then to the third-stage compressor (*3*), where the gas was compressed to the condensation pressure.

The superheated steam went to the oil separator (*5*), where oil separates from the steam. The oil then passed through oil filters to be distributed between three compressors. Hot steam entered the water-cooled condenser (*6*), where the steam condensed, and the resulting liquid entered liquid separator I (*7*). The gaseous refrigerant went back to the third-stage compressor. After that, the liquid refrigerant entered liquid separator II (*7*), where the process occurred once more. The purified refrigerant entered the linear receiver (*8*) and moved on to the chamber (*9*), with subsequent throttling and cooling. CO_2 snow sublimated into gas and was sucked out by the compressor through the liquid separator (*7*), after which the process repeated.

In the cascade heat exchanger, the evaporating third-stage refrigerant absorbed the heat removed by the condensing R744. The condensation temperature stayed below the critical point. Third-stage was a simple closed-loop chiller system controlled by the pressure in the first-stage low pressure receiver. It cooled down the load and removes heat from the condensing R744 in the first-stage cascade heat exchanger. This stage operated on R12 refrigerant. Figure 4 shows an operating cycle of the experimental three-stage refrigerator.

Table 2 summarizes the parameters of the refrigerant at the nodes.

Figure 5 shows a 3D model of the refrigerating unit (a) and the chamber in section (b).

The conveyor belt (*9.1*), driven by an electric motor (*9.2*), feeds the product to be frozen into the chamber (*9*), after which the chamber closes down with the help of double-acting pneumatic pushers (*9.3*), driven by an air oil compressor (*9.4*). After the door is closed, the vacuum pump (*9.5*) sucks air out until vacuum is reached, after which refrigerant R744 enters the chamber through

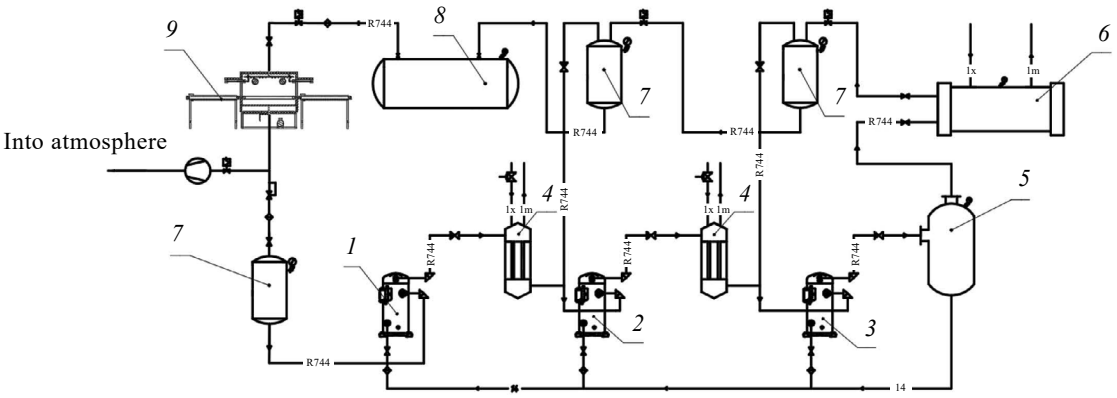

Figure 3 Three-stage CO_2-operating refrigerator

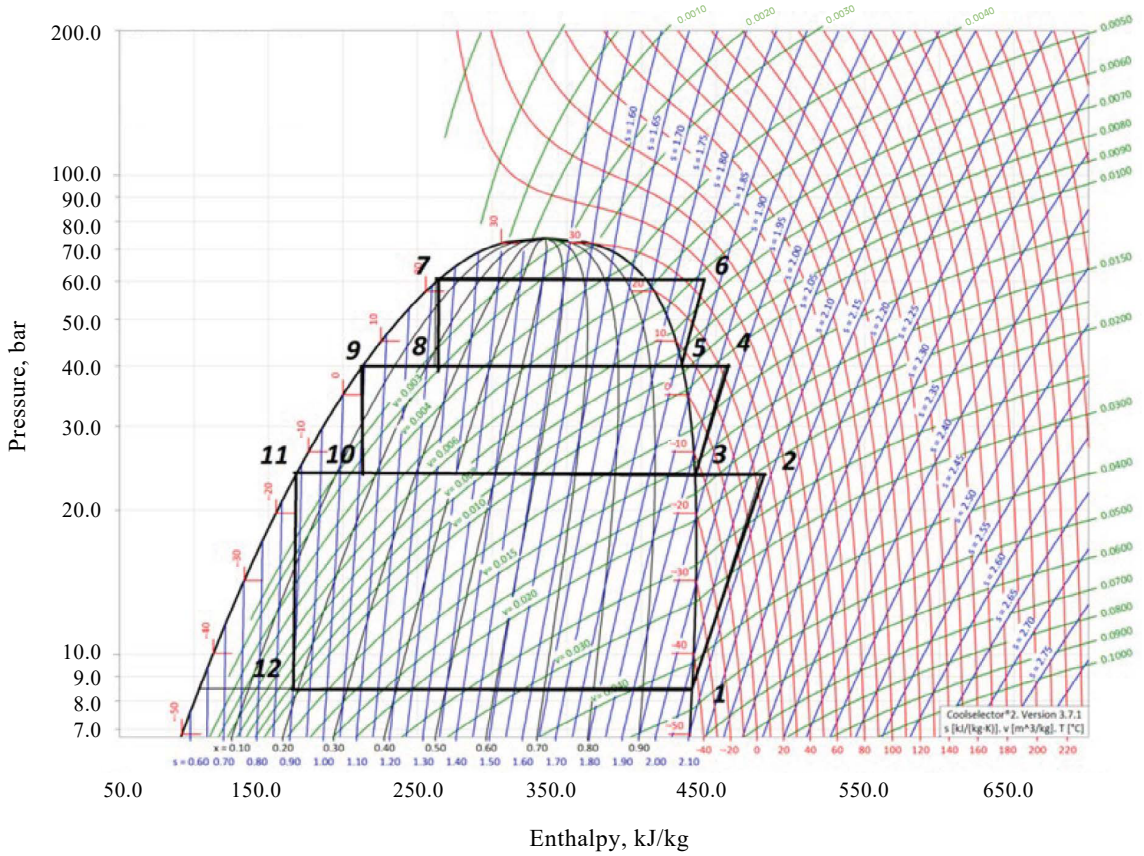

Figure 4 Three-stage CO_2-operating refrigerator: Operating cycle

Table 2 Refrigerant: Nodal parameters

P, MPa	h, kJ/kg	t, °C	V, m³
0.85	440	–50	0.045
2.57	480	25	0.021
2.57	440	–15	0.016
4.28	460	25	0.011
4.28	425	5	0.0085
6.00	445	35	0.0062
6.00	260	22	–
4.28	260	5	–
4.28	210	5	–
2.57	210	–15	–
2.57	170	–15	–
0.85	170	–50	–

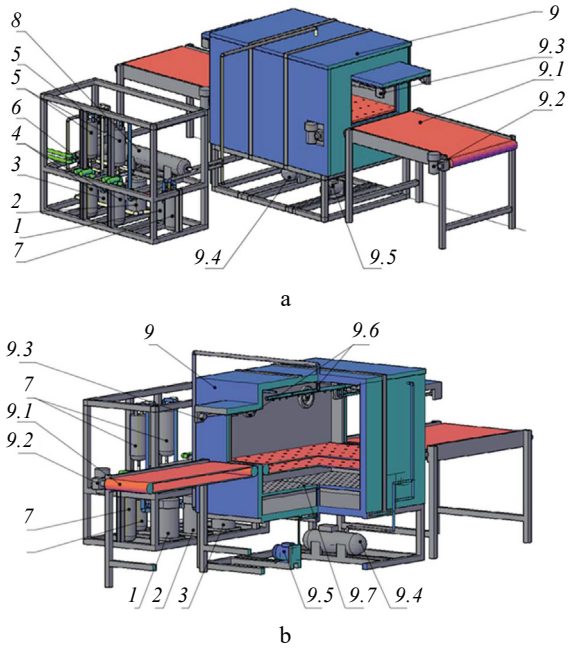

Figure 5 Three-stage CO_2-operating refrigerating unit: 3D model (a) and chamber in section (b)

nozzles. CO_2 snow settles on the product and on the bottom of the chamber. The duct fans (*9.6*) speed up the heat exchange by creating artificial air circulation. As the air passes through the fans, it enters the side cavity of the chamber, moves on to the lower cavity, and passes through the perforated tray (*9.7*). After cooling, CO_2 snow sublimates, and the compressor sucks it out with the help of the liquid separator. The air compressor starts, and the pneumatic pushers open the chamber doors.

We studied the freezing process of turkey carcasses under two conditions: with enforced convection at 3–5 m/s and without it. The experiment involved three cooling temperature modes: –30, –50, and –70°C. When the temperature dropped from –30 to –70°C, the freezing time decreased from 48 to 33 min. When forced convection was applied, it went down to 29 min. Without convection, the mass of CO_2 consumed increased from 7.5 to 13.5 kg; with convection, it rose from 6.5 to 12.0 kg.

Figure 6 shows thermograms of the turkey freezing process at –50 ± 2°C without forced convection. At the initial stage, the inner layer of the meat froze quite intensively, but a severe drop in the cooling rate started after 9 min at +10°C. After 21 min, when the temperature reached +3°C, the cooling slightly accelerated. The latter phenomenon was certainly a positive factor, since the product has to overcome the stage of ice formation and large crystals as quickly as possible to maintain its original quality. Moreover, water crystallization triggers the heat release and reduces the cooling rate.

The freezing process had three stages. As the outer and central layers froze, the boundary of the unfrozen areas shifted toward the inner layer, causing water crystallization in it. It took the outer layer 1–15 min to freeze. The central layer froze a little slower, 1–20 min. Water crystallization in the inner layer began after approximately 25 min. The product cooled down to the set temperature from minute 28 to the end of the freezing process.

Figure 7 shows a graph that illustrates the change in the heat flux density through the outer layer of a turkey carcass during cooling at a refrigerant temperature of –50 ± 2°C without forced convection.

Early in the freezing process, both the decrease in temperature and heat flux intensity were quite rapid due to the lack of preliminary cooling. The heat flux decreased moderately after 3 min. As the inner layer reached the target temperature (–12°C, 38 min), the heat rejection intensity became minimal.

The entire freezing process lasted 41 min and required 10 kg of CO_2. After the freezing, the temperature in the three control points was different, namely –21, –13, and –19°C for the outer, inner, and central layers of the turkey carcass, respectively (Fig. 6).

Figure 8 shows thermograms of the turkey meat freezing at –50 ± 2°C of the refrigerant entering the refrigeration chamber, with forced convection of 3–5 m/s. As expected, the forced convection accelerated the freezing process of the turkey carcass. The entire freezing process lasted 35 min.

The entire freezing process consisted of three stages: cooling to the cryoscopic temperature, freezing, and bringing the product to the targeted temperature. These stages are most clearly observed on the graph of temperature vs. time for the outer layer, where the temperature was the quickest to reach the cryoscopic temperature.

At the initial stage, the outer layer froze quite intensively, but the cooling rate dropped down after 10 min at 0°C, as seen from the flat area in Fig. 8. This process is associated with the early transition of water into ice, which reduces the latent heat. The duration of the phase transition in the outer layer depends on the heat rejection rate and the thickness of the product. In our case, crystallization continued for about 21 min, after which the cooling rate went up slightly.

During the freezing of the outer layer, the boundary of unfrozen areas shifted toward the central layer. As heat rejection from the central layer became more intensive, its temperature approached the cryoscopic value, and crystal formation started in the central part. The freezing process in the inner layer was quite intensive for 17 min, when the cooling rate slowed down due to the cryoscopic temperature.

The central layer froze similarly to the outer one because both were in direct contact with the circulating refrigerant.

After the freezing process was complete, we again detected non-uniformity of the temperature field. The tempe-

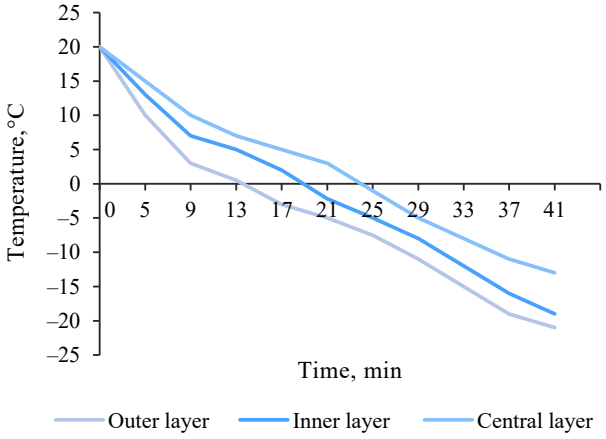

Figure 6 Freezing turkey meat at –50 ± 2°C

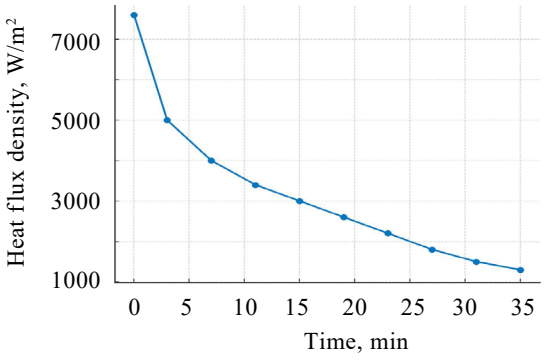

Figure 7 Heat flux density during freezing of turkey carcass with CO_2 at –50 ± 2°C

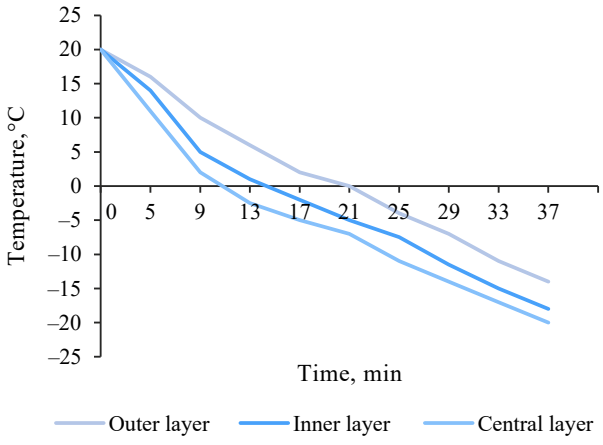

Figure 8 Freezing process of turkey meat at –50 ± 2°C and enforced convection speed of 3–5 m/s

rature values for the outer, inner, and central layers were –18, –12, and –16°C, respectively.

Figure 9 shows the change in heat flux density at –50 ± 2°C of the refrigerant entering the chamber, with an enforced convection rate of 3–5 m/s.

The heat flux density peaked, as expected, at the very onset of cooling when the temperature difference between the turkey carcass and the refrigerant was at its maximum, and the heat rejection process was intensive. The peak value was slightly higher compared to that recorded during the previous experiment, when the temperature was the same but with enforced CO_2 convection.

We used the experimental data on the heat flux density in the Newton-Richman formula to calculate the heat transfer coefficient. The highest value of the heat transfer coefficient was a_{max} = 109 W/(m²·K).

The correlation between the heat transfer coefficient and the time allowed us to conclude that the freezing of the outer layer coincided in time with the cooling of the central layer. The heat flow and the temperature decrease were quite intensive during this stage since the product had not gone through preliminary cooling, and the difference in temperature between the product and CO_2 was maximal. At the next stage, we also observed a moderate decrease in the heat flux level. The cooling of the central layer was almost complete, and the frozen outer layer spread in depth while freezing further. At the final stage, the heat rejection rate was the least intensive since the product continued to freeze down to a given temperature.

The freezing time for a turkey carcass at –30 ± 2°C (without convection) was almost the same as in the experiment with enforced CO_2 convection. Probably, the change in the amount of heat rejected under enforced convection conditions was not very significant compared to the heat of the water crystallization rejected during the freezing of the turkey carcasses.

The freezing lasted 48 min, with 7.5 kg CO_2 consumed. The lowest temperature (–20°C) was recorded in the outer layer at the end of the freezing. The temperature of the inner layer reached –13°C, which corresponded to the target temperature. The temperature in the central part of the turkey carcass was –19°C.

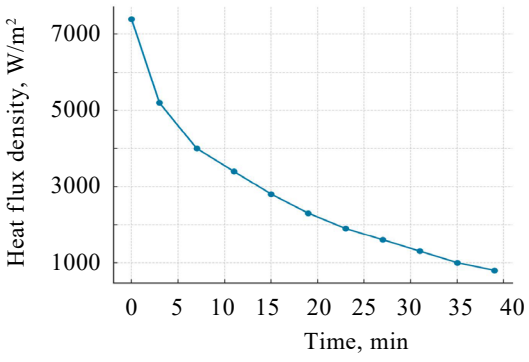

Figure 9 Heat flux density during freezing of turkey carcass with CO_2 at –50 ± 2°C and air convection rate of 3–5 m/s

In the enforced convection experiment, the complete freezing at –30 ± 2°C lasted 43 min, and the amount of carbon dioxide consumed was 6.5 kg. At the end of the freezing process, the lowest temperature in the outer layer was –20°C, i.e., the same as in the experiment without convection, but it was reached by 5 min faster. The inner and central layers also needed 5 min less to reach the temperatures recorded during the experiment without convection (–13 and –19°C, respectively).

Table 3 demonstrates the change in meat temperatures in different layers of the turkey carcass during refrigeration at different refrigerant temperatures, with and without enforced convection. It also presents data on CO_2 consumption required to achieve the target temperature in the inner layer.

In all cases, the freezing of the outer and central layers proceeded quite intensively since these layers were in direct contact with the refrigerant.

The inner layer froze mainly due to the heat rejection to the outer surfaces. The direct heat rejection through the outer layers had a much smaller effect on the intensity of the heat rejection from the inner layer.

Upon reaching the cryoscopic temperature, the inner layer froze less intensively because free (unbound) water in the intercellular space served as a solvent for mineral substances. As free water froze out, the concentration of salts in the unfrozen intercellular solution increased, shifting the cryoscopic temperature to the region of lower temperatures. In this case, water was freezing out gradually, increasing the concentration of the remaining solution. The central layer froze mainly by heat rejection to the internal cavity of the turkey carcass, which contacted

Table 3 Freezing turkey carcasses under different parameters

Enforced confection	Chamber temperature, °C	Layer	Treatment time, min				CO_2, kg
			30	35	40	50	
			Temperature, °C				
0	–30	outer	–7	–13	–15	–20	7.5
		inner	–3	–7	–9	–13	
		central	–5	–11	–13	–19	
	–50	outer	–11	–19	–21	–	10.0
		inner	–5	–11	–13	–	
		central	–8	–16	–19	–	
	–70	outer	–14	–20	–	–	13.5
		inner	–7	–14	–	–	
		central	–11.5	–18.0	–	–	
3–5	–30	outer	–10	–16	–18	–	6.5
		inner	–4	–9	–11	–	
		central	–7.5	–13.5	–16.5	–	
	–50	outer	–12	–18	–	–	9.0
		inner	–6	–12	–	–	
		central	–10	–16	–	–	
	–70	outer	–16	–	–	–	12.0
		inner	–10	–	–	–	
		central	–14	–	–	–	

with CO_2. After most unbound water crystallized, the temperature decrease accelerated again.

At the end of freezing, the temperature was different at different sensor points, i.e., the temperature field was uneven. The crystal formation directly depended on the freezing rate, which, in its turn, depended on the rate at which the interface moved between the liquid and solid phases from the surface of the frozen product to its thermal center.

At –70 ± 2°C, the process was very similar to the those described for –30 and –50°C, but it occurred much faster. The curves of the temperature fields showed that the freezing process without enforced convection was less intense and lasted 33 min. Enforced convection of the refrigerant at the fan outlet reduced the freezing time to 29 min. The CO_2 consumption was 13.5 and 12.0 kg, respectively, with or without enforced convection.

At a chamber temperature of –70°C and intensive convection, the preliminary cooling with CO_2 snow and temperature unification occurred most quickly. The preliminary cooling eliminated subsequent cracking of the carcass and, therefore, reduced weight loss associated with defrosting and cooking.

In the surface layer, crystals formed quite fast in all experiments due to its thinness and direct contact with CO_2. As crystallization started in the central layer, it prevented the rest of the product from supercooling since the linear speed of crystallization almost always exceeded the heat rejection rate, causing exchange diffusion between the layers. As the heat transfer coefficient changed, water moved from the inner, unfrozen layer to the outer, frozen one. Conversely, the freezing process made dissolved substances move from the outer layer to the inner one. Maximal freezing intensity was required to preserve moisture: if the heat rejection rate was insufficient, the inward movement of the frozen layer boundary was less than the exchange diffusion rate. A significant portion of the moisture began to move towards the surface of the product, freezing the moisture out of the product.

CONCLUSIONS

We developed a three-stage R744-operating refrigeration unit using heat inflow calculations and a careful selection of primary and auxiliary equipment. Based on direct contact of CO_2 with the product, the unit demonstrated an admirable economic efficiency, as well as prospects for automating the freezing of turkey carcasses. The refrigeration chamber was enlarged and provided with a conveyor belt and automatic doors. The CO_2 recirculation also added to its economic efficiency and compliance with environmental requirements.

The unit owed its high efficiency to direct contact of CO_2 snow and gas with frozen turkey. The enforced convection in the chamber made it possible to reduce the freezing time and ensure the uniformity of cooling, which helped preserve the quality of the product. CO_2 snow and gas allowed us to minimize mechanical damage to the meat structure, which often accompanies traditional freezing methods.

The automation system included pneumatic pushers and a vacuum pump, which boosted the productivity and reduced labor costs. The chamber performed well at various temperatures and air-gas flux rates, which makes the refrigerator a universal solution for all kinds of food industry enterprises.

To improve the freezing process, the phase changes of water in meat should be taken into account, with an outlook for the shortest phase transition time.

The study contributes to the evolution of food freezing. In addition to turkey meat, the new three-stage R744-operating refrigeration unit may be applied to a wide range of commercial foods. Further research will improve the efficiency and quality of the freezing process.

CONTRIBUTION

E.N. Neverov supervised the project; P.S. Korotkih collected, analyzed, and also interpretated the data; A.K. Gorelkina developed the experimental refrigerating chamber and conducted the experiments; I.V. Timoshchuk wrote the manuscript.

CONFLICT OF INTEREST

The authors declared no potential conflict of interest regarding the research, authorship, and/or publication of this article.

REFERENCES

1. Kálmán Á, Szőllősi L. Global Tendencies in turkey meat production, trade and consumption. Acta Agraria Debreceniensis. 2023;(2):83–89. https://doi.org/10.34101/actaagrar/2/12594
2. Zimnyakov VM, Varlamova YeN. The state and prospects of turkey meat production. Niva Povolzhya. 2017;(4): 55–62. (In Russ.) https://elibrary.ru/ZTIEKD
3. Askerov PF, Rabadanov AR, Kibirov KG, Tolparov EB, Bondarenko OV, *et al*. Role and importance of turkey meat production in poultry farming in Russia: Prospects for further development. Entomology and Applied Science Letters. 2021;8(3):15–20. https://doi.org/10.51847/IE9jQz8ugz
4. Nastasevich I, Lakitsevich B, Petrovich Z. Cold chain management in meat supplies: Old vs. new strategies. Theory and Practice of Meat Processing. 2017;2(4):20–34. (In Russ.) https://doi.org/10.21323/2414-438X-2017-2-4-20-34
5. Meretukova FN, Abregova NV. Quality indicators of semi-finished sous-vide products from turkey meat. New Technologies. 2021;17(2):48–55. (In Russ.) https://doi.org/10.47370/2072-0920-2021-17-2-48-55

6. Shakhnazarova LV, Stefanova IL, Klimenkova AYu. Use of turkey meat for the production of specialized food. Bird and poultry products. 2022;(4):64–68. (In Russ.) https://doi.org/10.30975/2073-4999-2022-24-4-64-68
7. Solaesa AG, García-Barroso C, Romero C, González C, Jiménez P, *et al*. Nutritional composition and technological properties determining the quality of different cuts of organic and conventional Turkey meat. Poultry Science. 2024;103(12):104331. https://doi.org/10.1016/j.psj.2024.104331
8. Russian turkey farming: confident growth continues. Scientific and practical journal for managers and specialists of the agro-industrial complex. [cited 2025 Apr 30] (In Russ.) Available from: https://zzr.ru/zzr-2025-03-001
9. Ishevsky AL, Davydov IA. Freezing as a method of food preservation. Theory and Practice of Meat Processing. 2017;2(2):43–59. https://doi.org/10.21323/2414-438X-2017-2-2-43-59
10. Anisimova KV, Protopopova KA, Spiridonov AB, Ipatova AF, Stepanova TO. Development of a laboratory installation for freezing meat, fish and fruit. AgroEcoInfo. 2023;(1):34. (In Russ.) https://elibrary.ru/XZTIYG
11. Ikram A, Arshad MT, Maqsood S, Safdar SZ, Rasheed A, *et al*. Modern approaches for ensuring the safety and integrity of frozen foods: An overview. Food and Agricultural Immunology. 2025;36(1):2491594. https://doi.org/10.1080/09540105.2025.2491594
12. Dang DS, Bastarrachea LJ, Martini S, Matarneh SK. Crystallization behavior and quality of frozen meat. Foods. 2021;10(11):2707. https://doi.org/10.3390/foods10112707
13. Young-Chan Y, Honggyun K, Karna R, Geun-Pyo H. Evaluation of the relationship between freezing rate and quality characteristics to establish a new standard for the rapid freezing of pork. Food Science of Animal Resources. 2021;41(6):1012–1021. https://doi.org/10.5851/kosfa.2021.e52
14. Maina P, Huan Z. A review of carbon dioxide as a refrigerant in refrigeration technology. South African Journal of Science. 2015;111(9/10):10. https://doi.org/10.17159/sajs.2015/20140258
15. Barta RB, Groll EA, Ziviani D. Review of stationary and transport CO_2 refrigeration and air conditioning technologies. Applied Thermal Engineering. 2021;185:116422. https://doi.org/10.1016/j.applthermaleng.2020.116422
16. Boupda O, Tessemo H, Fongang I, Nyami F, Lontsi F, *et al*. A review on technologies for the use of CO_2 as a working fluid in refrigeration and power cycles. Energy and Power Engineering. 2024;16(6):217–256. https://doi.org/10.4236/epe.2024.166011
17. Loktionov DG. Auto-refrigeration units on carbon dioxide. Scientific and Technical Support of Refrigeration Industry: Conf. proceedings. All-Russian Research Institute of Refrigeration Industry. Moscow, 2010;92–95. (In Russ.). https://elibrary.ru/RSDWYP
18. Shao L-L, Zhang C-L. Thermodynamic transition from subcritical to transcritical CO_2 cycle. International Journal of Refrigeration. 2016;64:123–129. https://doi.org/10.1016/j.ijrefrig.2016.01.018
19. Sharma DK, Hazarika MM, Ramgopal M. The optimum discharge pressure of CO_2-based refrigeration cycles operating under subcritical and transcritical conditions. International Journal of Ambient Energy. 2023;44(1):1232–1242. https://doi.org/10.1080/01430750.2023.2171483
20. Neverov EN, Korotky IA, Plotnikov IB, Korotkiy PS, Kozhaev AA. The study of the parameters of the heat transfer process at carbon dioxide sublimation. Bulletin of KSAU. 2020;(6):215–222. (In Russ.) https://doi.org/10.36718/1819-4036-2020-6-215-222
21. Ji H, Pei J, Cai J, Ding C, Guo F, *et al*. Review of recent advances in transcritical CO_2 heat pump and refrigeration cycles and their development in the vehicle field. Energies. 2023;16(10):4011. https://doi.org/10.3390/en16104011
22. Burak LCh. Prospects for the use of supercritical carbon dioxide technology in the food industry. Subject field overview. Polzunovskiy vestnik. 2025;(1):32–50. (In Russ.) https://doi.org/10.25712/ASTU.2072-8921.2025.01.004
23. Tosato G, Minetto S, Rossetti A, Hafner A, Schlemminger C, *et al*. Field data of CO_2 integrated refrigeration, heating, and cooling systems for supermarkets. Proceedings of the 14th IIR-Gustav Lorentzen Conf. on Natural Refrigerants. Kyoto, 2020:1162. https://doi.org/10.18462/iir.gl.2020.1162
24. Panão MRO, Franco PAG, Costa JJ. Effect of atomizer geometry on particle formation in dry-ice sprays. International Journal of Multiphase Flow. 2020;130:103358. https://doi.org/10.1016/j.ijmultiphaseflow.2020.103358

ORCID IDs
Evgeniy N. Neverov https://orcid.org/0000-0002-3542-786X
Pavel S. Korotkih https://orcid.org/0000-0002-4546-0276
Alena K. Gorelkina https://orcid.org/0000-0002-3782-2521
Irina V. Timoshchuk https://orcid.org/0000-0002-1349-2812

Foods and Raw Materials. 2026;14(2)

ISSN 2308-4057 (Print)
ISSN 2310-9599 (Online)

Research Article
Open Access

Available online at http://jfrm.ru/en
https://doi.org/10.21603/2308-4057-2026-2-685
https://elibrary.ru/UGBQOJ

Tetragonula laeviceps honey: Biochemical composition and kinetics of 5-hydroxymethylfurfural formation

Budianto[1,*], Anik Suparmi[2], Zefki O. Feri[3], Muh J. Arifin[4], Kiki Kristiani[5], Dewi Susanti[6], Tommy D. Irianto[6], Endang S. Furwanti[6], Desi W. Marniasari[6]

[1] Institute of Science and Technology Al-Kamal, Jakarta, Indonesia
[2] SMA Negeri 4 Tarakan, Tarakan, Indonesia
[3] State University of Yogyakarta, Yogyakarta, Indonesia
[4] SMK Negeri 3 Madiun, Madiun, Indonesia
[5] Sahid University Surakarta, Surakarta, Indonesia
[6] Poltekkes Kemenkes Pontianak, Pontianak, Indonesia

* e-mail: budianto_delta@yahoo.com

Received 10.06.2024; Revised 25.09.2024; Accepted 03.06.2025; Published online 20.10.2025

Abstract:
The emergence of a new bee species, *Tetragonula laeviceps*, in Indonesia has attracted scientific attention that promoted further exploration. We aimed to analyze changes in the biochemical composition of *T. laeviceps* honey stored at different temperatures and to study the kinetics of hydroxymethylfurfural formation.

T. laeviceps honey was stored at 25, 50, and 80°C for 6 h. The pollen sources were identified using the melissopalynology method, followed by a biochemical analysis using UHPLC-DAD-ESI/MS. The kinetics of hydroxymethylfurfural formation were analyzed using the Arrhenius equation applied to zero-, first-, and second-order reactions.

T. laeviceps honey was multifloral (three or more pollen types, each with < 16% frequency), with dominant *Zea mays* spp. *Mays* (L.) (40.24%) and *Vigna unguiculate sesquipedalis* (L.) (22.52%). Heating at 80°C significantly ($p < 0.05$) increased phenolic acids, flavonoid acids, total phenolics, total flavonoids, and hydroxymethylfurfural, as well as significantly ($p < 0.05$) degraded diastase, invertase, glucose oxidase, and DPPH. Heating at 50°C only had a significant impact on hydroxymethylfurfural and diastase. Ferulic acid and kaempferol compounds dominated in the phenolic and flavonoid acids in all the samples. The kinetics of hydroxymethylfurfural formation followed a first-order reaction, with specific rate constants of 0.1098/h (25°C), 0.0597/h (50°C), and 0.0053/h (80°C), involving an activation energy of 69.23 KJ/mol.

This study highlights the impact of storage and heating on the chemical composition of Klanceng honey. Our findings provide practical guidance for improving honey production and storage, while enhancing the commercial value of *T. laeviceps*.

Keyword: Klanceng honey, melissopalynology, activation energy, pollen, bioactive enzymes, phenolics, flavonoids

Please cite this article in press as: Budianto, Suparmi A, Feri ZO, Arifin MJ, Kristiani K, *et al. Tetragonula laeviceps* honey: Biochemical composition and kinetics of 5-hydroxymethylfurfural formation. Foods and Raw Materials. 2026;15(2):386–398. https://doi.org/10.21603/2308-4057-2026-2-685

INTRODUCTION

The emergence of a new bee species, *Tetragonula laeviceps*, has garnered significant attention among researchers and beekeepers. This species offers an extraordinary potential for exploration, particularly regarding the active biochemical compounds found in its honey [1]. However, the available information remains very limited. This lack of data indicates an urgent need for in-depth research to uncover the full potential of *T. laeviceps* honey, as well as its possible health benefits and commercial applications.

Honey research often focuses on the impact of storage and heating, as well as the kinetics of compound degradation [2]. One of the main challenges is gaining a deep understanding of the botanical sources of honey, which can affect its chemical composition and quality. The melissopalynology method, which is used to identify the pollen sources within honey [3], offers essential insights into the variety of plants visited by bees and how this influences the characteristics of honey. Unfortunately, many previous studies do not include this method, so information about the pollen's sources is

Copyright © 2025, Budianto *et al.* This is an open access article distributed under the terms of the Creative Commons Attribution 4.0 International License (https://creativecommons.org/licenses/by/4.0/), allowing third parties to copy and redistribute the material in any medium or format and to remix, transform, and build upon the material for any purpose, even commercially, provided the original work is properly cited and states its license.

often overlooked. In this study, we incorporated the melissopalynology method to understand the sources of pollen in honey and the variation in its composition related to different plants visited by bees.

Previous studies have extensively reported on the composition of active compounds in various types of honey. The kinetics of hydroxymethylfurfural (HMF) formation has also been a focus of research due to its importance as an indicator of honey quality [4, 5]. However, few studies have specifically explored individual phenolic compounds and flavonoids, or the kinetics of HMF formation, in the honey from *T. laeviceps*. This information may promote further research that can enrich our understanding of the honey produced by this bee species.

A high sugar content is the main challenge facing the optimization of the analysis protocol to determine individual phenolic and flavonoid compounds in honey. It can interfere with the analysis results by masking or affecting the detection of these compounds, complicating the extraction process [6]. This makes their separation from the honey matrix difficult, affecting the accuracy and reliability of the analysis [7]. Moreover, not all phenolic and flavonoid compounds are detected in honey, especially those in low concentrations (e.g., 3,4-dihydroxybenzoic acid and rutin).

Our study aimed to analyze changes in the biochemical composition of Klanceng honey during its storage at 25 and 50°C, as well as during its heating at 80°C for 6 h. Additionally, we studied the kinetics of HMF formation in *T. laeviceps* honey. Our results can provide deep and comprehensive insights into the quality of Klanceng honey.

In addition to enriching the scientific knowledge regarding the chemical composition and quality of Klanceng honey, our study can provide a practical guidance for beekeepers in optimizing honey production and storage processes. Our findings can also lay the groundwork for further research and broader commercial application, enhancing the economic value of *T. laeviceps* in both local and global markets.

STUDY OBJECTS AND METHODS

Two kilograms of Klanceng honey was taken from a bee farm in Jambangan village (Indonesia) on March 27, 2024. The sampling area was located at S7°40'39.47232" and E111°24'15.2247". The sample was placed in a large container for homogenization. Then, it was divided into three parts.

The samples were transferred into small glass containers, marked, and sealed until the analysis. Each sample was subdivided into three parts to be analyzed over 6 h of storing at 25 (control), 50, and 80°C.

Pollen observations were conducted using the acetolysis methods [8] with an addition of 30% glycerin. The mixture was stirred, and drops of the pollen-containing solution were placed on a microscope slide (CX-23 optilab). Melissopalynological analysis followed Bandeira *et al.* [9] and involved both melissopalynological and biochemical analyses to identify the food source of the Klanceng bee (*Tetragonula laeviceps*).

The geographical origin of the honey was determined according to Budianto *et al.* [10]. 200–300 pollen grains were analyzed and identified with a frequency categorized as follows: predominant (over 45%), secondary (16–45%), important minor pollen (3–15%), and minor pollen (less than 3%). The botanical origin was inferred from the pollen and honeydew frequencies. Within a 500 m radius, the plant spread percentage was calculated as:

$$\text{Plant spread} = \frac{\text{Number of plants found}}{\text{Total number of plants}} \quad (1)$$

As for nectar-producing plants, one or two flowers were sampled to check for nectar by opening the flower and examining the liquid nectar at the flower base without measuring its volume. Extrafloral nectar was assessed by examining the liquid nectar secreted by nectar glands that develop on stems, leaves, or other plant parts.

As for pollen-producing plants, one or two flowers were sampled to examine the pollen on the anther. The pollen, usually in powder form and of yellow color, was not weighed. According to Nuraeni *et al.* [11], honey types were classified as monofloral (one pollen species with > 45% frequency), bifloral (two pollen types with > 22.25% frequency each), and multifloral (three or more pollen types with < 16% frequency each).

Phenolic compound analysis. Due to the complexity of Klanceng honey, a cleanup step was necessary to remove interfering substances before Ultimate 3000 ultra-high-performance liquid chromatography (UHPLC). This method was adapted from Wang *et al.* [12] and involved diluting about 10 g of honey with five parts of acidifier water (pH = 2, adjusted with HCL) and homogenizing it with approximately 10 g of Amberlite XAD-2 resin for 30 min using a magnetic stirrer. The mixture was then passed through a glass column (25 × 2 cm) with a PTFE tap. Phenolic compounds remained in the column, while sugars and other polar substances were washed out using 100 mL of acidified water followed by 100 mL of distilled water. Sugar removal and optimal wash volumes were checked using high-performance liquid chromatography (HPLC) with an evaporative light scattering detector (ELSD). The setup included an HPLC Surveyor Plus system with a Surveyor autosampler, a Surveyor LC Pump, and an ELSD (Alltech 3300 ELSD). Sugars were separated chromatographically using an APS-2-Hypersil amine bonded phase column (250 × 4.6 mm; 5 µm) at 30°C with an isocratic elution of acetonitrile-water (80:20) at a flow rate of 0.85 mL/min. The phenolic fraction was eluted with about 75 mL of methanol and evaporated to dryness under reduced pressure at 40°C using a Multivapor P-6 concentrator. Then, it was redissolved in 3 mL of methanol, filtered through a 0.45-µm PTFE membrane, and analyzed by UHPLC-DAD-ESI/MS for the phenolic profile.

Phenolic profile by UHPLC-DAD-ESI/MS. Experiments were conducted using an Ultimate 3000 UHPLC system with a Q Exactive™ Focus Hybrid Quadrupole-

Orbitrap mass spectrometer and a HESI probe (ThermoFisher Scientific, USA). Separation was performed on Accucore PFP columns (50 × 2.1 mm, 2.6 µm and 100 × 2.1 mm, 2.6 µm). The mobile phase consisted of water with 0.1% formic acid (solvent A) and methanol with 0.1% formic acid (solvent B). The UHPLC gradient was as follows: 0–2 min, 98–50% A; 2–8 min, 50–30% A; 8–15 min, 30–2% A; 15–17 min, 2–98% A; 17–30 min, 98% A. The flow rate was 0.3 mL/min and the injection volume was 10 µL. All the samples were filtered with a 0.45 µm PTFE membrane filter before injection. The mass spectrometer operated in the negative mode with a spray voltage of 2.5 kV and a capillary temperature of 320°C. Mass spectra were scanned in the range of 120–1000 m/z.

Phenolic acids and flavonoids were identified and quantified based on their mass spectra, accurate mass, and retention time. Collision-induced dissociation was performed for confirmation, with a collision energy of 15–60 eV. Stock standard solutions of phenolic acids, flavonoids, and trans-resveratrol (100 mg/L) were prepared in methanol and calibration curves showed good linearity ($R^2 > 0.99$). The protocol efficiency was analyzed through recovery tests, with precision assessed from replicate measurements (n = 6) of the same honey sample, and expressed as a relative standard deviation (RSD).

Total phenolic content. Phenolic compounds were analyzed using the Folin-Ciocalteu reagent and following a modified method by Nikolaeva *et al.* [13]. Briefly, 100 µL of a honey ethanolic solution (1 g honey dissolved in 10 mL of 80% ethanol) was mixed with 4 mL of deionized water and 100 µL of the Folin-Ciocalteu reagent to incubate at room temperature (25°C) for 5 min. Next, we added 300 µL of a 20% sodium carbonate solution. The mixture was homogenized and incubated in the dark for 2 h at 25°C. The absorbance was then measured at 765 nm using a UV-visible spectrophotometer. The total phenolic content was calculated by comparing the sample's absorbance to a calibration curve made with gallic acid standard (0–620 mg/L in 10% ethanol) and expressed as 1 mg gallic acid equivalents per kg honey (mg GAE/kg).

Total flavonoid content. The analysis followed a modified method from Özkök *et al.* [14]. Briefly, 500 µL of a 10% honey ethanolic solution was mixed with 450 µL of $AlCL_2$ (25 g/L), 500 µL of $NaCH_3COOH$ (100 g/L), and 4 mL of deionized water. After incubating for 15 min at 25°C, a flavonoid-aluminum complex formed, and its formation was measured at 430 nm using a UV-visible spectrophotometer. A calibration curve was prepared using quercetin (0–130 mg/L) as the standard (1 mg quercetin equivalent per kg of honey), with results reported as the mean of duplicate assays.

Diastase activity. The analysis followed the procedure established by the International Honey Commission, using a spectrophotometer at an absorbance of 620 nm. The diastase number (DN) was equivalent to diastase units/gram honey.

$$DN = 35.2 \times \text{Absorbance (620)} - 0.46 \quad (2)$$

Invertase activity. The analysis followed the procedure established by the International Honey Commission, using an EnzyChrom control sample (EIT-100_AS). The test was carried out in the pH range of 4-5, using the spectrophotometric method at 560–570 nm, with a glucose calibration standard of 0–100 µm. The incubation time ranged from 20 to 30 min.

$$\text{Invertase} = \frac{A_{\text{sample}} - A_{\text{control}}}{slope \text{T}} \quad (3)$$

where A_{sample} is the absorbance of the sample; A_{control} is the absorbance of the control; T is the incubation time.

DPPH. The analysis followed a method modified by Amor *et al.* [15] to determine DPPH. A Klanceng honey sample was dissolved in hot water (40°C) and mixed with methanol with 2 mL of DPPH (0.1 mM). Distilled water was used for the control (substitute for extract). The samples were stored in the dark at room temperature (25°C) for 60 min. The analysis was performed using a spectrophotometer with an absorbance of 517 nm.

$$\text{DPPH} = \frac{A_{\text{control}} - A_{\text{sample}}}{A_{\text{control}}} \quad (4)$$

Antioxidants in the honey sample (IC_{50}) showed a decrease in the number of DPPH radicals (50%) from the initial concentration of the sample, mg/mL.

Hydroxymethylfurfural (HMF) was determined according to the Indonesian National Standard established in line with the International Honey Commission. Its working principle was to compare the difference in absorbance at 285 and 336 nm with a comparison solution of sodium bisulfite ($NaHSO_3$). For this, a 5 g sample was mixed with 0.50 mL of a Carrez I solution, and then 0.50 mL of Carez II was added to the mixture. After that, a few drops of alcohol were added to remove the foam. Then, 5 mL of the solution was taken for analysis. The samples (g) were measured by a spectrophotometer at 285 and 336 nm.

$$\text{HMF} = \frac{(A_{285} - A_{336}) \times \text{Dilution factor}}{\text{Sample weight}} \quad (5)$$

Glucose oxidase. The activity of glucose oxidase (GO) was determined according to the method described by Hamad *et al.* [16]. and expressed in µg H_2O_2/g honey. The test was conducted using colorimetry at a wavelength of 500 nm for 5 min.

Kinetics of biochemical degradation. The coefficient of determination (R^2) and the rate of degradation constant (K_t) were calculated based on the relationship between zero-order, first-order, and second-order reactions [17]:

$$\text{Zero-order reaction: } CA = C_0 - k_0 \times t \quad (6)$$

$$\text{First-order reaction: } CA = C_0 \times e^{-k_1 \cdot t} \quad (7)$$

$$\text{Second-order reaction: } CA = (k_2 \times t + \frac{1}{C_0})^{-1} \quad (8)$$

where C_0 is the initial concentration of Klanceng honey; *CA* is the biochemical concentration after being heated for *t*; *t* – the duration of heating, h; k_0, k_1, and k_2 – the rate constants of biochemical degradation reactions at zero order, first order, and second order. The half-life ($t_{1/2}$) is the time required for the degradation of 50% of the initial concentration (C_0). Its determination was adjusted to the order of the reactions that occur, namely based on the largest R^2 value.

$$\text{Zero-order reaction: } t_{1/2} = \frac{C_0}{2k_0} \quad (9)$$

$$\text{First-order reaction: } t_{1/2} = \frac{0.693}{k_1} \quad (10)$$

$$\text{Second-order reaction: } t_{1/2} = \frac{1}{C_0 \cdot k_2} \quad (11)$$

The type of reaction order was based on the largest R^2 value. The effect of temperature (*T*) and the value of *k* were determined by the Arrhenius equation (Eq. (11)). Activation energy (*Ea*) was determined by a linear regression of the Ln*k* curve to 1/*T*.

$$\text{Ln}k = \text{Ln°K} - \left(Ea/RT\right) \quad (12)$$

where *Ea* is the activation energy for the reaction, KJ/mol; *R* is the gas constant (8.314 J/mol°K); *T* is the reaction temperature, °K; *k* is the reaction constant.

Statistical test. The ANOVA test was employed to assess the average value, range of variation, and standard deviation. Concurrently, the post-hoc Tukey HSD test was utilized to detect disparities in biochemical degradation attributed to the heating effect, with a significance level at $p < 0.05$. The correlation analysis among biochemical compounds was conducted using SPSS version 26, employing a bivariate Spearman correlation with a two-tailed approach. Furthermore, the categorization of biochemical compounds based on heating temperatures was visualized using a Chord diagram generated with Origin Pro 2024.

RESULTS AND DISCUSSION

Plant origin. The melissopalynology method was employed to identify the source of pollen in honey, offering insights into the variety of plants visited by the Klanceng bee (*Tetragonula laeviceps*). The findings from the melissopalynological examination are presented in Table 1.

Based on the analysis of pollen frequency, we identified that secondary pollen originated from two plant species, namely *Zea mays* spp. *Mays* (L.) and *Vigna unguiculate sesquipedalis* (L.). Additionally, three important plant types indicated the presence of minor pollen, while the rest had only a small amount of pollen (less than 3%). Although our observations were limited to a 500 m radius, we did not find the species *Cocos nucifera* (L.). However, we noted a pollen frequency of 1.80%, which may indicate the potential presence of this species beyond our observation radius. These findings suggest a possibility of a broader range of movement for the Klanceng bee, which is consistent with our previous study [10].

The dwarf honey bee, also known as the *T. laeviceps* bee, is one of the two species of small wild honey

Table 1 Botanical origins of the Klanceng (*Tetragonula laeviceps*) bee's diet in Magetan (Indonesia) in 2024 (melissopalynological examination)

Local name	Scientific name	Family	Pollen frequency, %	Plant spread, %	Source	
					Pollen	Nectar
Corn	*Zea mays* spp. *Mays* (L.)	Poaceae	40.24	28.72	+	–
Noodle bean	*Vigna unguiculate sesquipedalis* (L.)	Fabaceae	22.52	25.02	+	–
Papaya	*Carica papaya* (L.)	Caricaceae	14.82	11.80	+	+
Egg plant	*Solanum melongena* (L.)	Lauraceae	9.47	10.80	+	+
Mango	*Mangifera indica* (L.)	Anacardiaceae	4.23	2.98	+	+
Water apple	*Syzygium aqueum* (L.)	Myrtaceae	2.15	2.45	+	+
Rambutan	*Nephelium lappaceum* (L.)	Sapindaceae	2.10	0.78	+	+
Coconut	*Cocos nucifera* (L.)	Araceae	1.80	n.d.	+	+
Guava	*Psidium guajava* (L.)	Myrtaceae	2.67	0.62	+	+
Cottonwood	*Ceiba pentadra* (L.)	Malvaceae	n.d.	1.24	–	+
Mahogany	*Swietenia macrophylla* (L.)	Maliaceae	n.d.	0.45	–	+
Avocado	*Persea Americana* (L.)	Lauraceae	n.d.	1.82	–	+
Melinjo	*Gnetum gnemon* (L.)	Gnetaceae	n.d.	1.43	–	+
Sapodilla	*Manikara zapota* (L.)	Sapotaceae	n.d.	0.87	–	+
Sengon	*Albizzia falcata* (L.)	Mimosoidae	n.d.	0.24	–	+
Breadfruit	*Artocarpus altilis* (L.)	Moraceae	n.d.	1.22	+	+
Red chili	*Capsicum annum* (L.)	Solaneceae	n.d.	5.43	+	+
Sonokeling	*Dalbergia latifolia* (L.)	Leguminoseae	n.d.	2.13	–	+
Lamboro	*Leucaena leucocephala* (L.)	Fabaceae	n.d.	2.00	+	+

n.d. – not detected

bees found in South and Southeast Asia. Its distribution is much wider than that of its sibling species, *Apis andreniformis*. Another species, *Apis florea*, which was first identified in the late 18th century, is unique due to its distinct morphology, foraging behavior, and defense mechanisms such as generating a piping sound. *A. florea* builds an open nest and forms small colonies, making them more vulnerable to predation compared to cavity-dwelling species with a larger number of defensive workers. The distinctive characteristics of the *T. laeviceps* bee, as shown in Fig. 1, include a body length of 7–8 mm and a wing length of 8–10 mm. Worker bees have lighter-colored wings compared to guard bees. Another notable feature is that the *T. laeviceps* bees produce a substantial amount of propolis.

Optimization of the analytical protocol for determining individual phenolic compounds. Amberlite XAD 2 sorbent was chosen for its effectiveness in extracting non-polar and low-polarity compounds from aqueous samples. It is therefore suitable for selectively isolating analytes from the honey matrix. One of the main challenges in analyzing phenolic compounds in honey is a high sugar content and other impurities. To address this, the honey samples were dissolved in acidified water to denature the proteins. The resulting impurities and denatured proteins were then removed by centrifugation. The supernatant was combined with Amberlite XAD 2 resin to wash away polar substances and sugars using a glass column. The removal of sugars from the column was verified using the HPLC-ELSD method for sugar detection and quantification. This process helped determine the optimal washing volumes, which were established at 100 mL of acidified water and 100 mL of distilled water.

The details of the analytical procedures used in this method are provided in Table 2. The recovery rates for each identified phenolic compound varied, amounting to 65–75% for phenolic acids and 75–100% for flavonoids.



a b c d

Figure 1 Distinctive characteristics of *Tetragonula laeviceps* bees: (a) body length; (b) shape and color of worker bees; (c) shape and color of guard bees; and (d) shape and size of propolis in the maintenance hive

Table 2 Parameters and analytical performance of the method used for quantifying individual phenolic compounds

Compounds	Liniarity, mg/L	Correlation coefficient (R^2)	Limit of detection, mg/L	Limit of quantification, mg/L	Precision, %	Recovery, %
Gallic acid	0.5–5.0	0.9977	0.0010	0.0050	3.8500	75
3.4-Dihydroxybenzoic acid	0.5–10.0	0.9985	0.0040	0.0120	4.8500	76
p-Hydroxybenzoic acid	0.5–7.5	0.9989	0.0100	0.0500	3.3400	74
Chlorogenic acid	0.5–10.0	0.9939	0.0010	0.0060	2.8800	75
Caffeic acid	0.5–10.0	0.9993	0.0010	0.0040	4.1200	76
Syringic acid	0.5–7.5	0.9989	0.0090	0.0750	3.7500	78
p-Coumaric acid	0.5–7.5	0.9987	0.0010	0.0040	4.7400	68
Ferulic acid	0.5–10.0	0.9996	0.0030	0.0095	1.5500	73
trans-Cinnamic acid	0.5–7.5	0.9994	0.0130	0.0675	4.6200	74
Catechin	0.5–7.5	0.9981	0.0010	0.0025	4.1500	68
Epicatechin	0.5–7.5	0.9992	0.0010	0.0035	3.9200	73
Naringin	0.5–5.0	0.9967	0.0010	0.0025	3.5400	73
Rutin	0.5–10.0	0.9998	0.0030	0.0135	3.8300	90
Hesperitin	0.5–5.0	0.9994	0.0000	0.0010	3.7400	87
Myricetin	0.5–7.5	0.9987	0.0010	0.0050	4.2300	84
Quercetin	0.5–7.5	0.9986	0.0070	0.0260	3.7300	67
Kaempferol	0.5–10.0	0.9996	0.0030	0.0125	3.9400	96
Isorhamnetin	0.5–7.5	0.9985	0.0030	0.0115	1.5500	89
Apigenin	0.5–5.0	0.9977	0.0020	0.0054	2.8400	87
Pinocembrin	0.5–7.5	0.9946	0.0010	0.0053	1.2300	91
Galangin	0.5–10.0	0.9974	0.0050	0.0162	0.8400	95
Chrysin	0.5–7.5	0.9971	0.0050	0.0152	1.1200	88
Pinostrobin	0.5–5.0	0.9984	0.0010	0.0035	4.5500	94

The precision values were consistently < 5%. Despite the satisfactory recovery results for most phenolic compounds, future research is recommended to implement the SPE (solid-phase extraction) procedure with commercial polymer sorbent cartridges to isolate phenolic compounds from the honey matrix, aiming to reduce the use and production of hazardous substances.

Quantification of phenolic acids and flavonoids in *Tetragonula laeviceps* honey using UHPLC-DAD-ESI/MS. We employed the UHPLC-DAD-ESI/MS technique to quantify phenolic acids and flavonoids in the honey samples following the initial isolation of the target compounds from the honey matrix. In total, 31 compounds derived from pollen, propolis, and flower nectar were identified in the honey samples. Of these, 24 compounds were quantified by comparing their retention times and MS spectra with available standards. Figure 2 illustrates a representative base peak chromatogram of a standard solution of phenolic compounds in honey heated at 25 (control), 50, and 80°C.

Out of the 24 target compounds, only 17 were succesfully identified and measured in all examined honey samples. These comprised 7 phenolic acids (chlorogenic, caffeic, 3.4-dihydroxybenzoic, *p*-hydroxybenzoic, *trans*-cinnamic, *p*-coumaric, and syringic) and 9 flavonoids (apigenin, chrysin, galangin, kaempferol, rutin, quercetin, isorhamnetin, pinocembrin, and pinostrobin). Meanwhile, catechin and epicatechin were found in very small amounts in all the samples, while gallic acid was detected in very small amounts in the experimental samples (50 and 80°C). Compounds such as naringin, hesperitin, myricetin, and *trans*-resveratrol were not identified.

In the absence of standards, the identification of additional compounds in honey extract relies on detecting deprotonated molecules, [M-H], and specific literature [18]. Utilizing the ChemSpider reference library to search for precise mass, we identified rhamnestin, abscisic acid, luteolin, pinobanskin, and pinobanskin-3-O-acetate in all the analyzed honeys. Table 3 summarizes the data for each target compound (phenolic acids, flavonoids, stilbens) and other significant compounds identified in the honey extracts.

The specific temperature regimes of 25, 50, and 80°C were chosen to simulate different storage and processing conditions that honey may undergo. These temperatures represent typical ambient storage (25°C), mild heating (50°C), and high heating (80°C), which are common in food processing and storage scenarios. The duration of 6 h allows for a significant period to observe biochemical changes, such as hydroxymethylfurfural (HMF) formation and enzyme degradation. Other temperatures and heating durations have indeed been studied in previous research, often focusing on different time scales or temperature ranges. Budianto *et al.* [10] examined the effect of heating Klanceng honey at high (70°C/7 h), medium (40°C/48 h), and low (25°C/48 h) temperatures.

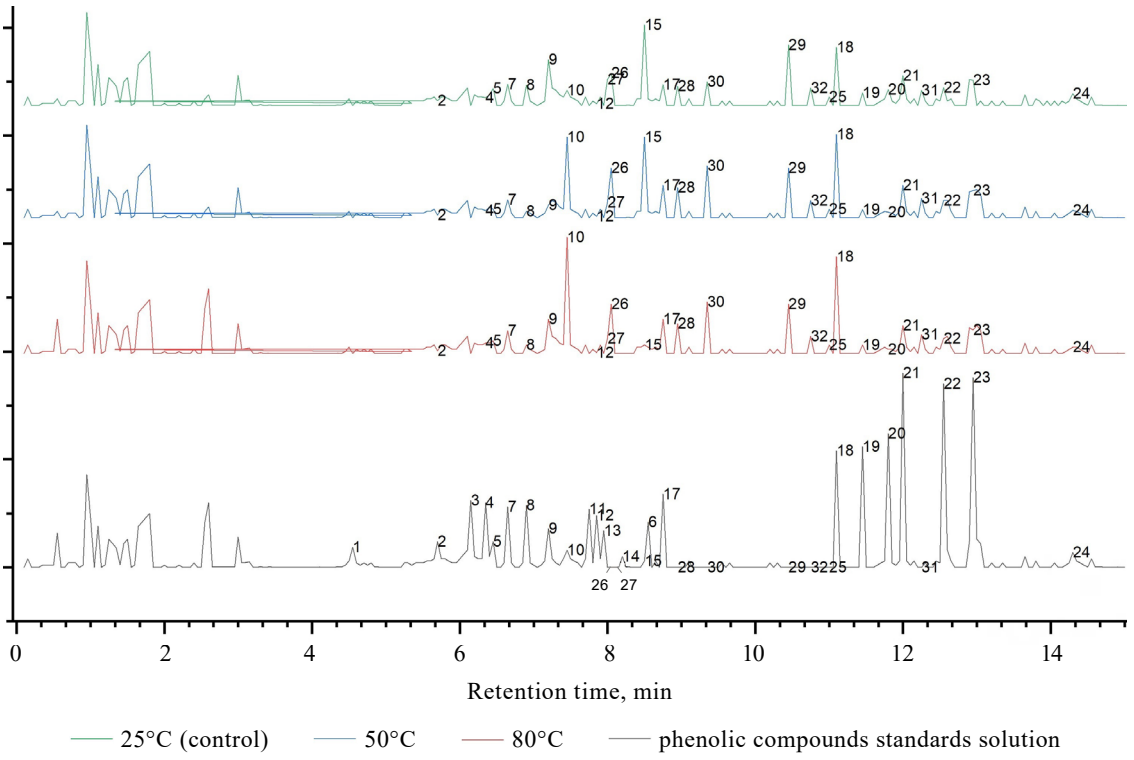

1 – gallic acid; 2 – 3.4-dihydroxybenzoic acid; 3 – catechin; 4 – 4-hydroxybenzoic acid; 5 – chlorogenic acid; 6 – epicatechin; 7 – caffeic acid; 8 – siric acid; 9 – *p*-coumaricacid; 10 – ferulic acid; 11 – naringin; 12 – rutin; 13 – hesperitin; 14 – *trans*-resveratrol; 15 – *trans*-cinnamic acid; 16 – myristetin; 17 – quercetin; 18 – kaempferol; 19 – isorhamnetin; 20 – apigenin; 21 – pinocembrin; 22 – galangin; 23 – chrysin; 24 – pinostrobin; 25 – rhamnetin; 26 – abscisic acid; 27 – eriodictyol; 28 – sakuranetin; 29 – alpinetin; 30 – pinobanksin; 31 – pinobanskin-3-O-acetate; 32 – luteolin

Figure 2 UHPLC chromatogram: Relative abundance, %, of biochemical components in relation to retention time

Table 3 Quantification of phenolic acids and flavonoids in *Tetragonula laeviceps* honey using UHPLC-DAD-ESI/MS

Peak number	Compounds	RT, min	Exact mass[b] $[M-H]^-$	Accurate mass $[M-H]^-$	ppm	Mass fragments (intensity, %)	Collision energy, eV
			Phenolic acids				
1	Gallic acid[a]	4.55	1.690.131	1.690.131	0.21	124 (100)	40
2	3.4-dihydroxybenzoic acid[a]	5.70	1.530.183	1.530.183	0.12	108 (100)	40
4	*p*-hydroxybenzoic acid[a]	6.35	1.370.234	1.370.234	0.12	91 (100)	35
5	Chlorogenic acid[a]	6.45	3.530.885	3.530.885	0.31	194 (100), 85	20
7	Caffeic acid[a]	6.65	1.790.345	1.790.345	0.13	132 (100)	35
8	Syringic acid[a]	6.95	1.970.443	1.970.443	0.12	184 (100), 167, 131, 123	30
9	*p*-coumaric acid[a]	7.25	1.630.394	1.630.394	0.21	113 (100)	30
10	Ferulic acid[a]	7.45	1.930.502	1.930.502	0.21	175, 149, 136, 134 (100)	30
15	*trans*-cinnamic acid[a]	8.50	1.470.446	1.470.446	0	118 (100), 103, 62	35
			Flavonoids				
3/6	Catechin[a]/epicatechin[a]	6.00/6.55	2.890.723	2.890.723	0.22	204, 151, 125, 124,109 (100)	35
11	Naringin[a]	7.70	5.791.724	5.791.724	0.24	469, 272 (100), 151	35
12	Rutin[a]	7.80	6.091.462	6.091.462	0.22	305 (100)	35
13	Hesperitin[a]	8.00	6.091.823	6.091.823	0.14	304 (100), 272, 153	20
16	Myricetin[a]	8.75	3.170.304	3.170.304	0.31	178, 151 (100), 137	40
17	Quercetin[a]	10.00	3.010.355	3.010.355	0.12	180, 151 (100), 107	40
18	Kaempferol[a]	11.12	2.850.421	2.850.421	0.32	154 (100), 117, 93	50
19	Isorhamnetin[a]	11.50	3.150.518	3.150.518	0.62	304 (100), 256, 152, 125	40
20	Apigenin[a]	11.80	2.690.452	2.690.452	0.51	152, 118 (100), 107	50
21	Pinocembrin[a]	12.06	2.550.667	2.550.667	0.42	214, 152 (100), 107	55
22	Galangin[a]	12.58	2.690.451	2.690.451	0.54	227, 151 (100), 117	65
23	Chrysin[a]	12.93	2.530.512	2.530.512	0.41	209,182, 143 (100), 107	50
24	Pinostrobin[a]	14.34	2.690.824	2.690.824	0.32	179, 137 (100)	50
			Stilbens				
14	*trans*-resveratrol[a]	8.22	2.270.712	2.270.712	0.42	190 (100), 143	35
			Other major compounds				
25	Rhamnetin	11.02	3.150.513	3.150.513	0.23	304 (100), 165, 121	40
26	Abscisic acid	8.07	2.631.283	2.631.283	0.22	178 (100), 191	35
27	Eriodictyol	8.03	2.870.563	2.870.563	0	125 (100)	55
28	Sakuranetin	8.93	2.850.772	2.850.772	0.13	135 (100)	55
29	Alpinetin	10.42	2.690.824	2.690.824	0.22	199 (100), 133	55
30	Pinobanskin	9.32	2.710.616	2.710.616	0.22	254, 243, 165 (100), 152	55
31	Pinobanskin-3-O-acetate	12.30	3.130.723	3.130.723	0.12	2713, 254 (100)	55
32	Luteolin	10.75	2.850.407	2.850.407	0.34	214, 151, 132 (100)	50

RT – retention time; [a] – compounds that were confirmed using available standards; [b] – calculated mass of the parent ion using a free chemical database (ChemSpider)

The results showed that high-temperature heating significantly reduced enzyme activity, while two years of storage increased the HMF values to > 40 ppm. Flanjak *et al.* [19] also found similar results with sage honey under almost identical heating durations and temperatures.

According to Table 4, heating at 80°C had a significant impact ($p < 0.05$) on the phenolic acid composition in the honey samples compared to heating at 50°C. Ferulic, *p*-coumaric, and caffeic acids were the most dominant compounds. We found that under certain conditions, heating can enhance the solubility or extraction of some phenolic compounds from the honey matrix. Similar conditions were observed in jojoba honey from Iran [17], sage honey from Croatia [19], and Klanceng honey from Indonesia [10]. However, some studies showed different results, such as those on Tualang and Kelulut honey in Malaysia [20].

The increase in flavonoid compounds due to heating also showed a similar pattern. The sample heated at 80°C exhibited a significant difference ($p < 0.05$) compared to the other samples. Kaempferol, quercetin, and pinocembrin dominated in the samples stored at 25°C and heated at 50°C. After heating at 80°C for 6 h, kaempferol, pinocembrin, and chrysin dominated. Heating at 50°C for 6 h did not cause significant changes in flavonoid compounds, a finding that aligns with previous studies [21]. However, other studies showed a significant impact with longer heating durations [21, 22]. Heating can increase the solubility of flavonoids from the honey matrix [23], as heat can break down cell walls or other structures that bind flavonoids, making them easier to extract and measure [24].

HMF showed a significant increase ($p < 0.05$) in all three samples, with the highest value in the sample heated

Table 4 The effect of heating on the composition of biochemical compounds in *Tetragonula laeviceps* honey (n = 6 for each temperature)

Compounds	25°C (control)	50°C	80°C
3.4-dihydroxybenzoic	0.021 ± 0.008^{b} (0.013–0.031)	0.025 ± 0.005^{b} (0.011–0.032)	0.056 ± 0.007^{a} (0.040–0.064)
p-hydroxybenzoic	0.072 ± 0.011^{b} (0.042–0.081)	0.075 ± 0.013^{b} (0.040–0.121)	0.091 ± 0.007^{a} (0.081–0.097)
Chlorogenic	0.092 ± 0.152^{b} (0.032–0.362)	0.092 ± 0.013^{b} (0.063–0.110)	0.210 ± 0.016^{a} (0.160–0.460)
Caffeic	0.162 ± 0.114^{b} (n.d.–0.252)	0.192 ± 0.022^{b} (0.162–0.266)	0.253 ± 0.015^{a} (0.210–0.412)
Syringic	0.062 ± 0.031^{b} (0.024–0.122)	0.073 ± 0.015^{b} (0.032–0.098)	0.243 ± 0.052^{a} (0.155–0.525)
p-coumaric	0.242 ± 0.110^{b} (0.102–0.514)	0.254 ± 0.052^{b} (0.105–0.367)	0.542 ± 0.157^{a} (0.218–0.675)
Ferulic	0.814 ± 0.332^{b} (0.322–1.327)	0.853 ± 0.072^{b} (0.322–1.327)	1.872 ± 0.332^{a} (1.322–2.127)
trans-cinnamic acid	0.055 ± 0.001^{b} (0.021–0.125)	0.059 ± 0.003^{b} (0.021–0.125)	0.982 ± 0.150^{a} (0.721–1.125)
∑ phenolic acids	1.520	1.623	2.536
Rutin	0.023 ± 0.010^{c} (0.011–0.042)	0.035 ± 0.006^{b} (0.021–0.075)	0.078 ± 0.005^{a} (0.051–0.095)
Quercetin	0.835 ± 0.245^{b} (0.543–1.322)	0.943 ± 0.254^{a} (0.552–1.115)	0.983 ± 0.154^{a} (0.452–1.125)
Kaempferol	2.352 ± 0.543^{b} (1.671–3.177)	2.321 ± 0.543^{b} (1.871–3.172)	3.742 ± 0.541^{a} (3.471–4.177)
Isorhamnetin	0.192 ± 0.062^{c} (0.122–0.313)	0.238 ± 0.062^{b} (0.222–0.289)	0.584 ± 0.032^{a} (0.122–0.813)
Apigenin	0.075 ± 0.022^{c} (n.d.–0.098)	0.157 ± 0.021^{b} (n.d.–0.198)	0.755 ± 0.222^{a} (n.d.-1.098)
Pinocembrin	0.731 ± 0.246^{b} (0.213–0.938)	0.945 ± 0.346^{b} (0.513–1.338)	1.405 ± 0.446^{a} (0.813–1.638)
Galangin	0.376 ± 0.125^{b} (0.115–0.534)	0.483 ± 0.146^{b} (0.213–0.738)	0.838 ± 0.246^{a} (0.513–1.338)
Chrysin	0.575 ± 0.182^{b} (0.218–0.793)	0.767 ± 0.246^{b} (0.213–0.939)	1.276 ± 0.346^{a} (0.813–1.538)
Pinostrobin	0.153 ± 0.014^{c} (n.d.–0.322)	0.234 ± 0.046^{b} (0.093–0.438)	0.665 ± 0.246^{a} (0.213–0.978)
∑ flavonoid acids	5.250	5.955	10.118
Total phenolic content, g GAE/kg	102.501 ± 0.105^{b} (97.343–105.474)	105.231 ± 0.101^{b} (97.342–113.474)	116.331 ± 0.452^{a} (101.342-123.474)
Total flavonoid content, mg QE/kg	79.092 ± 13.972^{c} (72.993–99.392)	109.201 ± 23.082^{b} (72.092–149.042)	112.271 ± 50.204^{a} (56.672–191.291)
DPPH, %	24.303 ± 2.302^{a} (18.232–36.447)	22.403 ± 4.401^{b} (15.791–26.876)	19.105± 3.207^{c} (17.982–24.764)
Diastase (DN)	18.301 ± 2.300^{a} (16.715–21.046)	16.304 ±3.303^{b} (14.923–20.097)	11.803 ±1.205^{c} (9.840–13.679)
Invertase, U/kg	94.304 ± 4.305^{a} (88.782–102.237)	74.208 ± 11.200^{a} (65.892–96.372)	16.203 ± 8.306^{b} (13.766–22.785)
HMF, mg/kg	4.321 ± 0.630^{c} (2.034–6.235)	7.305 ± 0.630^{b} (5.328–9.329)	16.302 ± 4.107^{a} (14.983–22.652)
Glucose oxidase, µg H_2O_2/g honey	226.634 ± 21.202^{a} (209.752–231.743)	212.861 ± 21.832^{a} (84.289–219.543)	33.339 ± 2.571^{b} (29.361–39.639)

The ANOVA test was followed by the Tukey HSD post hoc test with a significance level of $p < 0.05$. The same letters indicate no significant difference; DPPH – 1.1-diphenyl-2-picrylhydrazyl radical scavenging activity; HMF – 5-hydroxymethyl furan-2-carbaldehyde

at 80°C. The increase in total phenolic and total flavonoid contents did not show a significant difference at 50°C but was significantly different at 80°C. The significant increase in HMF values at 50 and 80°C indicates that HMF is highly sensitive to heating [19]. Therefore, it is an important indicator for assessing the quality of *T. laeviceps* honey and ensuring it has not been excessively heated [10]. The increase in HMF also shows the presence of cyclic aldehyde compounds obtained from the degradation of sugar compounds (Maillard reaction) [25]. HMF is formed during the acid-catalyzed dehydration of hexoses [5, 6]. Previous research recommends these parameters for heating and storage processes [26, 27].

Heating also caused a significant decrease in DPPH and diastase values in all three samples, although significant change in invertase and glucose oxidase values only occurred at 80°C. Antioxidants (DPPH) inhibit free radicals by donating electrons to oxidant compounds. These compounds participate in slowing down the damage caused by oxidation at a certain level. The decline in DPPH due to warming has been reported by many previous researchers [28–30]. Given the important role of these compounds, the researchers made DPPH a parameter to be tested. Glucose oxidase, which catalyzes the oxidation of glucose to H_2O_2 and gluconic acid, was also less sensitive to heating. Our study demonstrated that invertase is less sensitive to heating than diastase. Diastase comes from bee saliva, so the enzyme is identical to the purity of honey. The decrease in diastase activity disrupts maltose digestion and conversion of other sugars in honey. The enzyme is very sensitive to heat [5]. Storage for 6 months at 30°C reduces the concentration of diastase by half, so the researchers chose this parameter for the comparative test [31]. Invertase is an enzyme produced by the hypopharyngeal gland of bees that catalyzes the hydrolysis of sucrose into glucose and fructose. This enzyme is suspected to be sensitive to heat [10, 19]. Researchers are still debating if invertase and diastase remain effective during heating.

We used a chord diagram visualization from Origin Pro to provide a deeper understanding of the effect that heating had on the biochemical composition of *T. laeviceps* honey (Fig. 3). The diagram not only shows changes in the relative abundance of various biochemical components but also illustrates the relationships between these components that might be overlooked in tabular data representation. This visualization helps identify significant patterns and trends resulting from

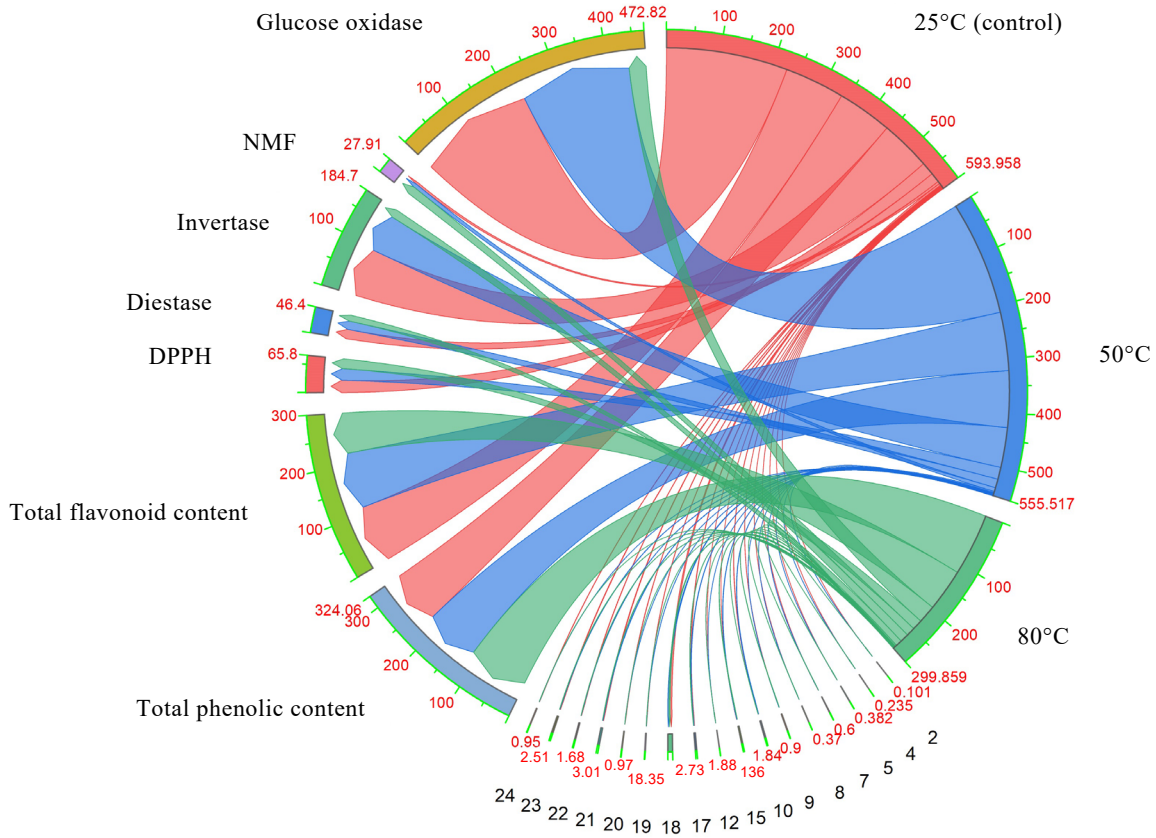

2 – 3.4-dihydroxybenzoic acid; 4 – 4-hydroxybenzoic acid; 5 – chlorogenic acid; 7 – caffeic acid; 8 – siric acid; 9 – *p*-coumaricacid; 10 – ferulic acid; 12 – rutin; 15 – *trans*-cinnamic acid; 17 – quercetin; 18 – kaempferol; 19 – isorhamnetin; 20 – apigenin; 21 – pinocembrin; 22 – galangin; 23 – chrysin; 24 – pinostrobin; DPPH – 1.1-diphenyl-2-picrylhydrazyl radical scavenging activity; HMF – 5-hydroxymethyl furan-2-carbaldehyde

Figure 3 The effect of heating on biochemical compounds in *Tetragonula laeviceps* honey

heating and facilitates the interpretation of the complex effect of heating on honey.

Based on the chord diagram data, significant differences in the values of invertase and glucose oxidase were observed among the all the samples under study. Of the total 600 bands measured, the invertase reached only 20 bands in the sample heated at 80°C, 100 bands in the control sample, and 64 bands in the honey heated at 50°C. Glucose oxidase exhibited similar patterns, with only 50/600, 230/600, and 200/600 bands in the 80°C sample, control honey, and 50°C sample, respectively. These findings indicate that heating at 80°C can reduce the presence of invertase and glucose oxidase in *T. laeviceps* honey.

The Spearman correlation analysis (Table 5) showed that phenolic acids had a strong positive correlation (> 0.9) with flavonoid acids, total phenolic, total flavonoid, and HMF content. Conversely, phenolic acids showed a strong negative correlation with diastase, invertase, DPPH, and glucose oxidase. All these relationships were significant at a confidence level of $p < 0.01$. They indicated that the changes in phenolic acids consistently correlated directly with the changes in flavonoid acids, total phenolics, total flavonoids, and HMF, while correlating inversely with the changes in diastase, DPPH, invertase, and glucose oxidase. These results are consistent with previous findings [32].

Table 6 shows changes in biochemical concentrations caused by heating for 6 h. As observed, these changes affected the reaction rate constant (k) of the biochemical degradation across different reaction orders. The reaction order indicates the magnitude of the effect of reactant concentration on the rate of the reaction. The order of the reaction was determined based on the experimental data (i.e., observed changes in concentration over time), rather than being directly related to the stoichiometric coefficients of the reactants.

A zero-order reaction indicates that the reaction rate is affected by the reaction rate constant, rather than the reactant concentration. The formation rate constants for HMF showed notable variations, with the k values of 0.0189/h, 0.2618/h, and 0.6296/h at 25, 50, and 80°C, respectively.

A first-order reaction shows that the reaction rate is affected by the reactant concentration. This condition can be observed in the relationship between ln(CA) and time (t), where CA is the concentration of the reactant at time t. The increase in HMF concentration was clearly visible at 80°C (0.0053/h), 25°C (0.1098/h), and 50°C (0.0597/h).

A second-order reaction shows the relationship between the reaction rate and the square of the reactant concentration. This means that the rate is proportional

Table 5 Correlation between biochemical compounds in Klanceng honey under heat treatment

Compounds	∑ phenolic acids	∑ flavonoid acids	Total flavonoid content, mg QE/kg	Total phenolic content, mg GAE/kg	DPPH, %	Diastase (DN)	Invertase, U/kg	HMF, mg/kg	Glucose oxidase
∑ phenolic acids	1	–	–	–	–	–	–	–	–
∑ flavonoid acids	0.970**	1	–	–	–	–	–	–	–
Total flavonoid content, mg QE/kg	0.944**	0.970**	1	–	–	–	–	–	–
Total phenolic content, mg GAE/kg	0.931**	0.931**	0.960**	1	–	–	–	–	–
DPPH, %	–0.945**	–0.932**	–0.961**	–0.974**	1	–	–	–	–
Diastase (DN)	–0.944**	–0.970**	–0.974**	–0.947**	0.935**	1	–	–	–
Invertase, U/kg	–0.970**	–0.957**	–0.947**	–0.973**	0.961**	0.947**	1	–	–
HMF, mg/kg	0.892**	0.905**	0.961**	0.987**	–0.948**	–0.947**	–0.933**	1	–
Glucose oxidase	–0.906**	–0.932**	–0.987**	–0.961**	0.962**	0.935**	0.935**	–0.961**	1

** Correlation is significant at the 0.01 level (2-tailed); HMF – 5-hydroxymethyl furan-2-carbaldehyde

Table 6 Heating effects and the kinetics of hydroxymethylfurfural (HMF) formation in Klanceng honey

Temperature, °C	Time, h	HMF, mg/kg	Temperature, °C	Time, h	HMF, mg/kg	Temperature, °C	Time, h	HMF, mg/kg
25	0	3.49 ± 0.02	50	0	3.49 ± 0.02	80	0	3.49 ± 0.02
	1	3.60 ± 0.30		1	6.20 ± 0.20		1	15.00 ± 0.07
	2	3.60 ± 0.31		2	6.80 ± 0.20		2	15.60 ± 0.30
	3	3.60 ± 0.31		3	8.80 ± 0.20		3	18.00 ± 0.40
	4	3.61 ± 0.24		4	7.70 ± 0.30		4	16.70 ± 0.20
	5	3.61 ± 0.21		5	8.20 ± 0.20		5	17.30 ± 0.20
	6	3.61 ± 0.27		6	8.80 ± 0.20		6	18.00 ± 0.40

Parameter	Temperature, °C	Zero Order		First Order		Second Order		*Ea*
		k/h	R^2	*k*/h	R^2	*k*/h	R^2	KJ/mol
HMF, mg/kg	25	0.0189	0.6714	0.1098	0.9176	0.0015	0.6727	69.2332
	50	0.2618	0.9324	0.0597	0.0138	0.9939	0.8578	
	80	0.6296	0.7924	0.0053	0.0203	0.9972	0.6028	

to $[CA]^2$. Table 6 shows the linear relationship between $1/CA$ and time (t), which is characteristic of a second-order reaction. In this context, CA represents the concentration of the reactant at time t. The reaction rate constants (k) for HMF formation at 25, 50, and 80°C were found to be 0.0015/h, 0.0138/h, and 0.0203/h, respectively, indicating that the reaction proceeds faster at higher temperatures.

The activation energy (Ea) for each parameter must be determined by comparing the most considerable R^2 values in determining the reaction order. If the order reaction has been determined, then the value of k used was based on the reaction. Based on the data above, the formation of HMF follows a first-order reaction, as indicated by the highest R^2 value compared to other reaction orders.

The addition of time (t) did not significantly impact the increase in HMF compared to changes in temperature (T), which had a greater influence on HMF formation. This strengthens the findings of previous researchers [33], although some studies proved that HMF was sensitive to duration and temperature. In our study, the formation of HMF followed the first-order reaction, which is in line with previous findings [34]. Some researchers report zero-order reactions. For example, in the same sample of Kelulut honey, heating at 40 and 50°C occurred at zero order and then rose to the first order at 70°C [35]. Boussaidet *et al.* [34], who studied honey in Southern Tunisia, found that the Ea ranged from 31 to 50 KJ/mol. However, significantly higher *Ea* values of 83.07, 91.70, and 89.57 KJ/mol were recorded in multi-floral honey from Kurdistan [36]. Also, Yap and Chin [35] creported an Ea value of 125 KJ/mol in honey from stingless bees, a species similar to *T. laeviceps*.

The heating of honey during production can reduce its quality, including its antimicrobial properties and enzyme activity, while increasing HMF levels. However, heating is still necessary to meet retail standards. The use of recrystallization methods can help prevent quality degradation during the process [37].

CONCLUSION

The Klanceng bee (*Tetragonula laeviceps*), with a body length of about 7–8 mm and a wing length reaching 8–10 mm, exhibits a diverse plant visitation pattern.

Using melissopalynology, we found that this bee collects pollen from various sources, including *Zea mays* spp. *Mays* (L.) and *Vigna unguiculata sesquipedalis* (L.) Although *Cocos nucifera* (L.) was not detected within the 500 m observation radius, a pollen frequency of 1.8% suggests its potential presence beyond this range. The Klanceng bee, belonging to the Tetragonula species, plays an important role in collecting pollen and nectar from various plants.

Heating *T. laeviceps* honey at 80°C significantly ($p < 0.05$) increased the contents of phenolic acids, flavonoid acids, total phenolic content, total flavonoid content, and hydroxymethylfurfural (HMF), as well as decreased the enzymes diastase, invertase, glucose oxidase, and DPPH. However, at 50°C, there was no significant impact, except for HMF and diastase. Ferulic and kaempferol compounds dominated the phenolic and flavonoid acids in all the treatments.

The kinetics of HMF formation in Klanceng honey followed a first-order reaction, meaning that the reaction rate was affected by the concentration of the reactants. The reaction rate constant (k) for HMF formation was 0.1098/h at 25°C, 0.0597/h at 50°C, and 0.0053/h at 80°C, with an activation energy of 69.23 KJ/mol. This activation energy indicated that a significant amount of energy was required for the reaction.

In this study, we primarily focused on the biochemical aspects and HMF kinetics of Klanceng honey, excluding microbial testing, which is also crucial for assessing honey quality. To provide a comprehensive evaluation and address honey quality in its entirety, we recommend that future research incorporate microbiological analysis as well.

CONTRIBUTION

All the authors were equally involved in the research analysis and manuscript writing.

CONFLICT OF INTEREST

The authors state that there is no conflict of interest.

REFERENCES

1. Agussalim, Umami N, Nurliyani, Agus A. The physicochemical composition of honey from indonesian stingless bee (*Tetragonula laeviceps*). Biodiversitas. 2021;22(8):3257–3263. https://doi.org/10.13057/biodiv/d220820
2. Rababah T, Al-U'datt M, Naqresh A, Gammoh S, Almajwal A, *et al*. Effect of temperature and time on the physicochemical and sensory properties of crystallized honey. ACS omega. 2024;9(18):20243–20252. https://doi.org/10.1021/acsomega.4c00570
3. Islam MK, Lawag IL, Green KJ, Sostaric T, Hammer KA, *et al*. An investigation of the suitability of melissopalynology to authenticate Jarrah honey. Current Research in Food Science. 2022;5:506–514. https://doi.org/10.1016/j.crfs.2022.02.014
4. Yang W, Zhang C, Li C, Huang ZY, Miao X. Pathway of 5-hydroxymethyl-2-furaldehyde formation in honey. Journal of Food Science and Technology. 2019;56(5):2417–2425. https://doi.org/10.1007/s13197-019-03708-7
5. Tarapoulouzi M, Mironescu M, Drouza C, Mironescu ID, Agriopoulou S. Insight into the recent application of chemometrics in quality analysis and characterization of bee honey during processing and storage. Foods. 2023;12(3):473. https://doi.org/10.3390/foods12030473
6. Vazquez L, Armada D, Celeiro M, Dagnac T, Llompart M. Evaluating the presence and contents of phytochemicals in honey samples: Phenolic compounds as indicators to identify their botanical origin. Foods. 2021;10(11):2616. https://doi.org/10.3390/foods10112616
7. Tsagkaris AS, Koulis GA, Danezis GP, Martakos I, Dasenaki M, *et al*. Honey authenticity: Analytical techniques, state of the art and challenges. RSC Advances. 2021;11(19):11273–11294. https://doi.org/10.1039/D1RA00069A
8. Margaoan R, Arădăvoaicei Ș, Sisea C, Cornea-Cipcigan M, Cordea M. Methods of microscopic slides preparation to identify the pollen grains derived from different bee products. Scientific Papers. Series D. Animal Science. 2023;66(1):412–421.
9. da Silva Ferreira Bandeira M, de Novais JS. Melissopalynological characterization of honeys from the Discovery Coast, Brazil. Palynology. 2020;44(3):539–550. https://doi.org/10.1080/01916122.2019.1631897
10. Budianto B, Feri ZO, Arifin MJ, Suparmi A, Kristiani K. The effect of processing and storage on Klanceng honey (*Tetragonula laeviceps*). Agronomía Mesoamericana. 2023;34(2):52131. https://doi.org/10.15517/am.v34i2.52131
11. Nuraeni S, Syaid NM, Sadapotto A. Identification of pollen as afood resource for honey bees (*Apis binghami*) in the village of Bonto Manurung, District of Tompobulu, Regency of Maros. IOP Conference Series: Earth and Environmental Science. 2023;1277:012033. https://doi.org/10.1088/1755-1315/1277/1/012033
12. Wang Y, Xing L, Zhang J, Ma X, Weng R. Determination of endogenous phenolic compounds in honey by HPLC-MS/MS. LWT. 2023;183:114951. https://doi.org/10.1016/j.lwt.2023.114951
13. Nikolaeva TN, Lapshin PV, Zagoskina NV. Method for determining the total content of phenolic compounds in plant extracts with folin–denis reagent and folin–ciocalteu reagent: Modification and comparison. Russian Journal of Bioorganic Chemistry. 2022;48(7):1519–1525. https://doi.org/10.1134/S1068162022070214

14. Özkök A, Özenirler Ç, Canlı D, Mayda N, Sorkun K. Monofloral features of turkish honeys according to mellissopalynologic, total phenolic acid and total flavonoid content. Gazi University Journal of Science. 2018; 31(3):713–723.

15. Amor SB, Mekious S, Benfekih LA, Abdellattif MH, Boussebaa W, *et al*. Phytochemical characterization and bioactivity of different honey samples collected in the Pre-Saharan region in Algeria. Life. 2022;12(7):927. https://doi.org/10.3390/life12070927

16. Hamad GM, Hafez EE, Abdelmotilib NM, Abdel-Hmeed KM, Ali SH, *et al*. Quality assessment, functional potentials, and safety evaluation of stored Egyptian honey as an environmental pollution bioindicator. Environmental Toxicology and Chemistry. 2020;39(10):1894–907. https://doi.org/10.1002/etc.4811

17. Molaveisi M, Beigbabaei A, Akbari E, Noghabi MS, Mohamadi M. Kinetics of temperature effect on antioxidant activity, phenolic compounds and color of Iranian jujube honey. Heliyon. 2019;5(1):e01129. https://doi.org/10.1016/j.heliyon.2019.e01129

18. Khaled O, Ryad L, Nagi M, Eissa F. Development and validation of a multiclass method for the determination of veterinary drug residues in honey. International Journal of Environmental Analytical Chemistry. 2025;105(13):3135–3152. https://doi.org/10.1080/03067319.2024.2339456

19. Flanjak I, Kenjerić D, Strelec I, Rajs BB, Primorac L. Effect of processing and storage on sage (*Salvia officinalis* L.) honey quality. Journal of microbiology, biotechnology and food sciences. 2022;11(6):e3375–e3375. https://doi.org/10.55251/jmbfs.3375

20. Muhammad NII, Sarbon NM. Physicochemical profile, antioxidant activity and mineral contents of honey from stingless bee and honey bee species. Journal of Apicultural Research. 2023;62(2):394–401. https://doi.org/10.1080/00218839.2021.1896214

21. Trinh VK, Duyen M, Nguyen HVH. Effects of heating temperature, storage temperature, and storage time on total phenolic content and antioxidant capacity of Vietnamese honey. 7th Analytica Vietnam Conference. 2022. p. 234–242.

22. Mat Ramlan NAF, Md Zin AS, Safari NF, Chan KW, Zawawi N. Application of heating on the antioxidant and antibacterial properties of Malaysian and Australian stingless bee honey. Antibiotics. 2021;10(11):1365. https://doi.org/10.3390/antibiotics10111365

23. Dimitriu L, Constantinescu-Aruxandei D, Preda D, Nichițean A-L, Nicolae C-A, *et al*. Honey and its biomimetic deep eutectic solvent modulate the antioxidant activity of polyphenols. Antioxidants. 2022;11(11):2194. https://doi.org/10.3390/antiox11112194

24. Rodríguez de Luna SL, Ramírez-Garza RE, Serna Saldívar SO. Environmentally friendly methods for flavonoid extraction from plant material: Impact of their operating conditions on yield and antioxidant properties. The Scientific World Journal. 2020;(1):6792069. https://doi.org/10.1155/2020/6792069

25. Belitz H-D, Grosch W. Sugars, sugar alcohols and honey. In: Food Chemistry. Berlin: Springer; 1999. p. 801–828.

26. White JW. The role of HMF and diastase assays in honey quality evaluation. Bee world. 1994;75(3):104–17.

27. Gruznov DV, Gruznova OA, Sokhlikov AB, Lobanov AV, Chesnokova IP. Changes in the chemical composition and antimicrobial activity of linden, buckwheat and sunflower honey stored at low temperatures. Current Research in Nutrition and Food Science. 2024;12(2):824–840. http://dx.doi.org/10.12944/CRNFSJ.12.2.27

28. Parcheta M, Świsłocka R, Orzechowska S, Akimowicz M, Choińska R, *et al*. Recent developments in effective antioxidants: The structure and antioxidant properties. Materials. 2021;14(8):1984. https://doi.org/10.3390/ma14081984

29. Zeb A. Concept, mechanism, and applications of phenolic antioxidants in foods. Journal of Food Biochemistry. 2020;44(9):e13394. https://doi.org/10.1111/jfbc.13394

30. Chaudhary P, Janmeda P, Docea AO, Yeskaliyeva B, Abdull Razis AF, *et al*. Oxidative stress, free radicals and antioxidants: Potential crosstalk in the pathophysiology of human diseases. Frontiers in Chemistry. 2023;11:1158198. https://doi.org/10.3389/fchem.2023.1158198

31. Adedayo OO, Ochigbo SS. Alterations in diastase activity and some physical properties of thermally treated honey from selected areas in Southern Nigeria. Journal of Raw Materials Research. 2017;11(2):1–17.

32. Turkut GM, Degirmenci A, Yildiz O, Can Z, Cavrar S, *et al*. Investigating 5-hydroxymethylfurfural formation kinetic and antioxidant activity in heat treated honey from different floral sources. Journal of Food Measurement and Characterization. 2018;12(4):2358–2365. http://dx.doi.org/10.1007/s11694-018-9852-y

33. Karadeniz F, Atalay D, Erge HS, Kaya S, Işık B, *et al*. Kinetics of 5-hydroxymethylfurfural (5-HMF) formation and colour change in date fruit fillings stored at different temperatures. Journal of Food Composition and Analysis. 2024;127:105986. https://doi.org/10.1016/j.jfca.2024.105986

34. Boussaid A, Chouaibi M, Attouchi S, Hamdi S, Ferrari G. Classification of Southern Tunisian honeys based on their physicochemical and textural properties. International Journal of Food Properties. 2018;21(1):2590–2609. https://doi.org/10.1080/10942912.2018.1540988
35. Yap SK, Chin NL. Kinetic modeling on quality parameters of raw *Kelulut* honey during dehydration process. Journal of Food Process Engineering. 2020;43(6):e13392. https://doi.org/10.1111/jfpe.13392
36. Mohammad NZ, Abdoulrahman K, Karim AY. Diastase Enzyme activity and Hydroxymethylfurfural production during thermal processing of honey. Diyala Agricultural Sciences Journal. 2023;15(2):1–10. https://dx.doi.org/10.52951/dasj.23150201
37. Ovsyannikov D, Oskin S, Lytnev A, Tsokur D. Modeling of honey heating in recrystallizer. Engineering for Rural Development. Proceedings of the Intern. Sci. Conf. Latvia University of Life Sciences and Technologies, 2020. p. 419–423. https://doi.org/10.22616/ERDev.2020.19.TF096

ORCID IDs
Budianto https://orcid.org/0000-0002-8277-6202
Anik Suparmi https://orcid.org/0000-0002-9720-8195
Zefki O. Feri https://orcid.org/0000-0002-3519-906X
Muh J. Arifin https://orcid.org/0000-0002-8147-3349
Kiki Kristiani https://orcid.org/0000-0002-3130-7115
Dewi Susanti https://orcid.org/0009-0008-0604-721X
Endang S. Furwanti https://orcid.org/0009-0001-8451-8100
Desi W. Marniasari https://orcid.org/0009-0003-6829-7285

Foods and Raw Materials. 2026;14(2)

ISSN 2308-4057 (Print)
ISSN 2310-9599 (Online)

Research Article
Open Access

Available online at http://jfrm.ru/en
https://doi.org/10.21603/2308-4057-2026-2-686
https://elibrary.ru/SJTJIR

Brinjal, turkey berry, and winged bean extracts: Total phenolic content and antioxidant activity

Sameera Priyadarshana, Konara Somawathie*, Mohamed Shafras, Darsiga Sivanandarajah

Sabaragamuwa University of Sri Lanka, Belihuloya, Sri Lanka

* e-mail: somawathiekm@appsc.sab.ac.lk

Received 24.09.2024; Revised 28.01.2025; Accepted 03.06.2025; Puplished online 18.11.2025

Abstract:
Despite the known impact of cooking on the food's nutritional value, the variation in bioavailability and bioaccessibility of bioactive compounds after digestion remains inadequately understood. This study aimed to compare the effect of different cooking methods on the total phenolic content and antioxidant activity of bioaccessible and bioavailable extracts of brinjal (*Solanum melongena* L.), turkey berry (*Solanum torvum* L.), and winged bean (*Psophocarpus tetragonolobus* L.).
Each vegetable was cooked by six methods using different combinations of coconut oil, coconut milk, and spices. The cooked vegetables were digested in vitro to evaluate their bioaccessible and bioavailable total phenolic content and antioxidant activity. The total phenolic content was determined by the Folin Ciocalteu method. Free radical scavenging activity, total antioxidant capacity, and reducing power were evaluated by the DPPH, ABTS, and FRAP assays, respectively.
All the cooking methods significantly increased the total phenolic content and antioxidant activity of the extracts compared to their raw forms. The vegetables cooked with oil, milk, and spices generally showed higher total phenolics and antioxidant activity than those cooked by the other methods. We found a strong positive correlation between the total phenolic content and various antioxidant parameters. The highest bioaccessibility index for phenolic compounds was registered in the brinjal extract cooked with oil and in the turkey berry and winged bean extracts cooked with oil, milk, and spices. Different cooking methods exhibited varying effects on the antioxidant activity of bioaccessible compounds. In bioavailable extracts, variability was observed for the total phenolic content and antioxidant activity among different cooking methods for brinjal, turkey berry, and winged bean.
The ABTS and FRAP assays showed the highest total phenolic content and antioxidant activity in all the vegetables cooked with coconut oil, milk, and spices.

Keywords: *Solanum melongena* L., *Solanum torvum* L., *Psophocarpus tetragonolobus* L., *in vitro* digestion, bioaccessibility, antioxidants, bioactive compounds, bioavailability, cooking methods

Funding: This study was funded from the research grant of Sabaragamuwa University of Sri Lanka (grant No. SUSL/RG/2016/19).

Please cite this article in press as: Priyadarshana S, Somawathie K, Shafras M, Sivanandarajah D. Brinjal, turkey berry, and winged bean extracts: Total phenolic content and antioxidant activity. Foods and Raw Materials. 2026;14(2):399–407. https://doi.org/10.21603/2308-4057-2026-2-686

INTRODUCTION

Vegetables exhibit multiple health benefits closely related to significant amounts of bioactive compounds in them. These include phenolic compounds, flavonoids, lignin, resveratrol, tannins, and alkaloids with antioxidant properties. Antioxidants are substances with an ability to inhibit or delay oxidative damage of nucleic acids, lipids, and proteins. Oxidative breakdown products such as reactive oxygen, nitrogen, and sulphur species link with chronic diseases. According to numerous studies, antioxidant-active compounds decrease the risk of various diseases, including cancer, cardiovascular disease, inflammation, diabetes, ulcers, osteoporosis, Alzheimer's disease, rheumatoid arthritis, cataracts, and age-related disorders [1].

Brinjal (*Solanum melongena* L.), originated from Asia, is one of the most widespread vegetables consumed around the world. Brinjal has a high free radical

Copyright © 2025, Priyadarshana *et al.* This is an open access article distributed under the terms of the Creative Commons Attribution 4.0 International License (https://creativecommons.org/licenses/by/4.0/), allowing third parties to copy and redistribute the material in any medium or format and to remix, transform, and build upon the material for any purpose, even commercially, provided the original work is properly cited and states its license.

scavenging capacity and is popular among consumers and researchers. Its high antioxidant activity is due to the presence of phenolic compounds, including delphinidin in the brinjal peel and chlorogenic acid in the flesh. Further, brinjal peels contain important bioactive compounds such as anthocyanins and flavonoids. The phenolic acids present in brinjal are classified into two classes: hydroxybenzoic acids and hydroxycinnamic acids. Caffeic and ferulic acids are the most common hydroxycinnamic acids in the plant kingdom, while *p*-coumaric, sinapic, and cinnamic acids are less common [2].

Turkey berry (*Solanum torvum* L.) is a vegetable commonly grown in all tropic countries. Originating from Central and South America, it is a member of the *Solanaceae* family. Turkey berry is not only used as a food product, but also in traditional medicine in Asia and Africa to prevent and cure a range of diseases. Turkey berry fruits contain high concentrations of various polyphenolic compounds, phenols, flavonoids, and tannins. These bioactive compounds account for turkey berry's high antioxidant activity [3].

Winged bean (*Psophocarpus tetragonolobus* L.) is a typical food crop and an underexploited food source for the tropics. It belongs to the *Fabaceae* family. Winged beans contain bioactive compounds with potential antioxidants, including vitamin C and E, polyphenols, and flavonoids. Studies have demonstrated anti-inflammatory, antimicrobial, anticarcinogenic, antitumoral, antimutagenic, anti-allergic, anti-aggregate, and anti-ischemic properties of winged beans [4].

Vegetables are generally cooked by different cooking processes before consumption. The cooking methods significantly impact their total phenolic content and antioxidant activity. Changes in bioactive concentrations and antioxidant capacities depend on the species and the method of cooking. The total phenolic content and antioxidant activity may vary between raw and cooked vegetables [5].

Health benefits of phenolics greatly depend on their bioaccessibility and bioavailability in the digestive tract and circulatory system. Bioaccessibility refers to a fraction of a compound released from the food matrix during digestion that becomes available for absorption in the gastrointestinal tract. Bioavailability is defined as a fraction of an ingested compound that reaches the circulatory system and is utilized by the body. Bioaccessibility and bioavailability of phenolic compounds are studied using *in vitro* (stimulated digestion) and *in vivo* models (animal model or human clinical trials). *In vitro* models are quick, technically simple, and inexpensive. They allow for screening numerous samples to study the efficiency of each digestion, absorption or transport mechanism [6, 7].

In this study, we aimed to compare the effect of different cooking methods on the total phenolic content and antioxidant activity of bioaccessible and bioavailable extracts of brinjal, turkey berry, and winged bean using *in vitro* models.

STUDY OBJECTS AND METHODS

Brinjal, turkey berry, and winged bean samples were collected from local markets. The vegetables were cleaned, washed, and cut into small slices separately. From each vegetable, seven portions of slices (30 g/portion) were weighed and separated. They were used to prepare seven different samples of each vegetable, namely raw, cooked with oil, cooked with milk, cooked with oil and milk, cooked with oil and spices, cooked with milk and spices, as well as cooked with oil, milk, and spices. The coconut oil, coconut milk, and spice mixtures used in the study were of the same brand.

Preparation of samples. ***Preparation of raw extracts.*** Thirty-gram portions of raw slices of each vegetable were individually blended with a small volume of distilled water and transferred to a clean cotton cloth separately. The extracts were collected by squeezing the samples in the cotton cloth. Each extract was topped up to 100 mL using distilled water. Finally, the extracts were collected into separate containers, labelled as R (raw) for respective vegetables, and stored at –18°C for further analysis.

Cooking with coconut oil. Thirty-gram portions of raw slices of each vegetable were stir-fried separately with 5 mL of coconut oil using an induction cooker at 80°C for 3 min. Mixtures of 0.50 g of chili powder, 1 g curry powder, 0.25 g turmeric powder, and 0.50 g salt were added to each portion. After that, the samples were cooked at 80°C for 6 min. The cooked samples were blended and transferred to a clean cotton cloth separately. The extracts were collected by squeezing the samples in the cotton cloth. Each extract was topped up to 100 mL using distilled water. Finally, the extracts of each vegetable were collected into containers, labelled as COS (cooked with oil and spices) for respective vegetables, and stored at –18°C for further analysis.

The same procedure was followed to cook 30 g portions of each vegetable without using the spices. The prepared samples were labelled as CO (cooked with oil) for respective vegetables and stored at –18°C for further analysis.

Cooking with coconut milk. Thirty-gram portions of raw slices of each vegetable were cooked separately with 10 mL of coconut milk for 3 min at 80°C. Mixtures of 0.50 g of chili powder, 1 g curry powder, 0.25 g turmeric powder, and 0.50 g salt were added into each portion. Then, 40 mL of coconut milk was added into all three preparations. The samples were mixed well and cooked at 80°C for 8 min. The cooked samples were blended and transferred to a clean cotton cloth separately. The extracts were collected by squeezing the samples. Each extract was topped up to 100 mL using distilled water. Finally, the extracts were collected into containers separately, labelled as CMS (cooked with milk and spices) for respective vegetables, and stored at –18°C for further analysis.

The same procedure was followed to cook 30 g portions of each vegetable without using the spices. The prepared samples were labelled as CM (cooked with

milk) for respective vegetables, and stored at –18°C for further analysis.

Cooking with coconut oil and coconut milk. Thirty-gram portions of raw slices of each vegetable were stir-fried with 5 mL of coconut oil separately using an induction cooker at 80°C for 3 min. Mixtures of 0.50 g of chili powder, 1 g curry powder, 0.25 g turmeric powder, and 0.50 g salt were added separately into each portion. Then, 50 mL of coconut milk was added into all three preparations and cooked at 80°C for 8 min. The cooked samples were blended and transferred to a clean cotton cloth separately. The extracts were collected by squeezing the samples. Each extract was topped up to 100 mL using distilled water. Finally, the extracts of each vegetable were collected into containers separately, labelled as COMS (cooked with oil, milk, and spices) for respective vegetables, and stored at –18°C for further analysis.

The same procedure was followed to cook 30 g portions of each vegetable without using the spices. The prepared samples were labelled as COM (cooked with oil and milk) for respective vegetables, and stored at –18°C for further analysis.

***In vitro* digestion process.** The below mentioned *in vitro* digestion process was carried out for differently cooked samples of brinjal, turkey berry and winged bean separately.

Oral phase. *In vitro* digestion was performed according to the method described by Minekus *et al.* [8] with some modifications. For this, 3-g portions of each cooked sample were mixed with 2.1 mL of a simulated salivary fluid (SSF) solution, partially blended with a blender, and transferred into a clean beaker. Subsequently, we added 0.3 mL of α-amylase of 1500 U/mL made up in the SSF electrolyte stock solution. Finally, 15 µL of 0.3 M $CaCl_2$ and 585 µL of water were added and mixed well. The beaker was kept in the heating water bath for 2 min at 37°C. The mixture obtained in this process is known as an oral bolus.

Gastric phase. To produce gastric chime, 6.00 mL of the oral bolus was mixed with 4.50 mL of a simulated gastric fluid (SGF), 0.96 mL of a porcine pepsin stock solution of 25000 U/mL made up in the SGF electrolyte stock solution, and 3 µL of 0.3 M $CaCl_2$. Then, 0.12 mL of 1 M HCl was added to obtain a pH value of 3.0 in the final mixture. The mixture was made up to 12.00 mL using distilled water. The beaker was kept in a shaking water bath for 2 h at 37°C.

Intestinal phase. The intestinal digestion was conducted in a 15 cm long dialysis tube. One end of the dialysis tube was closed using a twine thread and 12.00 mL of gastric chyme was added into it. Then, 6.6 mL of a simulated intestinal fluid (SIF) electrolyte was added and mixed well. After that, we added and mixed 3.00 mL of a pancreatin solution of 800 U/mL made up in the SIF electrolyte stock solution based on trypsin activity, 1.5 mL of a bile solution, and 24 µL of 0.3 M $CaCl_2$. Subsequently, 0.09 mL of 1 M NaOH was added to the mixture to get a final pH value of 7.0. Finally, the mixture was made up to 24.00 mL using distilled water. The dialysis tube was placed in a 100-mL beaker with 50.00 mL of distilled water. The beaker was kept in a shaking water bath for 2 h at 37°C. The content in the tube was filtered using 1-µm filter paper and the filtrate was stored at –18°C for further bioaccessibility analysis.

The outer solution of the tube was stored at –18°C for further bioavailability analysis.

Evaluation of total phenolic content and antioxidant activity. ***Total phenolic content.*** The Folin-Ciocalteu method was used to determine the total phenolic content as described by Swain and Hillis [9] with some modifications. Each cooked and digested vegetable sample (150 µL) was mixed with 2.4 mL of distilled water and 150 µL of 0.25 N Folin-Ciocalteu's reagent and allowed to react for 3 min. Then, 300 µL of sodium carbonate was added to this mixture. The final mixture was kept in the dark for 30 min. After that, absorbance was measured at 760 nm using a spectrophotometer. Each trial was done in three replicates and gallic acid was used to create a standard curve. The total phenolic content (TPC) was calculated using the following Eq. (1):

$$\text{TPC} = \frac{\text{Amount of gallic acid, µg}}{\text{Weight of vegetable sample, g}} \quad (1)$$

The result was expressed as mg of gallic acid equivalents (GAE) in 100 g of the food sample on a fresh weight basis.

DPPH assay. The antioxidant activity was measured using the DPPH (2,2-diphenyl-1-picrylhydrazyl) assay (free radical scavenging activity) as described by Brand-Williams *et al.* [10] with some modifications. For this, 2 mL of a DPPH solution (100 µM, 99% methanol) was added to different volumes (150, 300, 450, 600, and 750 µL) of each cooked and digested vegetable extract (0.01 mg/mL concentration). The mixtures were made up to 4 mL by adding distilled water. Then, we allowed them to stand for 30 min in a dark place at room temperature. After the incubation period, the absorbance was measured at 517 nm using a spectrophotometer. The DPPH radical scavenging activity (RSA, %) was calculated using the Eq. (2):

$$\text{RSA} = \frac{A_{\text{control}} - A_{\text{sample}}}{A_{\text{control}}} \times 100 \quad (2)$$

where A_{control} is the absorbance of the control; A_{sample} is the absorbance of a sample.

A graph was plotted [% inhibition (scavenging activity) against the concentration of samples] and 50% inhibition (IC_{50}) was obtained for the respective concentrations.

ABTS assay. The procedure explained by Re *et al.* [11] was used with some modifications. For this, 7.4 mM of ABTS radical solution and 2.6 mM potassium persulphate solution were used as the stock solution in the ABTS [2,2′-azino-bis-(3-ethylbenzothiazoline-6-sulfonic) acid] assay. The working solution was prepared by mixing the stock solutions equally and left to react for 12 h in the dark at room temperature. This solution was diluted by mixing 1 and 60 mL of the ABTS radical solution

and methanol, respectively. Then, 2.85 mL of the ABTS radical solution was left to react with 150 µL of an extract for 2 h in a dark place. The absorbance was read over 6 min at 734 nm using a spectrophotometer. The percentage inhibition of absorbance at 734 nm was calculated and the results were expressed as a percentage inhibition.

FRAP assay. The procedure explained by Benzie and Strain [12] was used with some modifications. For this, 300 mM of acetate buffer, 20 mM ferric chloride solution, and 10 mM 2,4,6-Tris(2-pyridyl)-s-triazine (TPTZ) solutions were prepared and mixed in a 10:1:1 ratio to prepare a ferric ion reducing antioxidant power (FRAP) reagent. The FRAP reagent was incubated at 37°C for 10 min. Then, 2.85 mL of the incubated FRAP reagent was left to react with 150 µL of a sample for 30 min in the dark. The absorbance of the colored product was measured at 593 nm using a UV-visible spectrophotometer. Trolox was used to create a calibration curve. The results were expressed as mg of Trolox equivalents in 1 g of a food sample.

Bioaccessibility and bioavailability indexes. Bioaccessibility index and bioavailability indexes were calculated using the following Eq. (3)–Eq. (6) [13, 14]:

$$\mathrm{PCBI} = \frac{\mathrm{PC_a}}{\mathrm{PC_b}} \times 100 \quad (3)$$

where PCBI is the phenolic compound bioaccessibility index, %; $\mathrm{PC_a}$ is the phenolic content in the bioaccessible extract; $\mathrm{PC_b}$ is the phenolic content in the cooked extract.

$$\mathrm{PBVI} = \frac{\mathrm{PC_a}}{\mathrm{PC_b}} \times 100 \quad (4)$$

where PBVI is the phenolic compounds bioavailability index, %; $\mathrm{PC_a}$ is the phenolic content in the bioavailable extract; $\mathrm{PC_b}$ is the phenolic content in the cooked extract.

$$\mathrm{AABI} = \frac{A_a}{A_b} \times 100 \quad (5)$$

where AABI is the antioxidant activity bioaccessibility index, %; A_a is the antioxidant activity of the bioaccessible extract; A_b is the antioxidant activity of the cooked extract.

$$\mathrm{AAVI} = \frac{A_a}{A_b} \times 100 \quad (6)$$

where AAVI is the antioxidant activity bioavailability index, %; A_a is the antioxidant activity of the bioavailable extract; A_b is the antioxidant activity of the cooked extract.

The AABI and AAVI were calculated individually for each result obtained via the DPPH, ABTS, and FRAP assays.

Statistical analysis. The data were expressed as mean ± SD (triplicate). Statistical analysis was performed using the Minitab 17 software. Statistical significance of the total phenolic content and antioxidant activity of the vegetables cooked with different methods was determined by one-way analysis of variance with Fisher's pairwise comparisons. Statistical significance of the bioaccessibility and bioavailability indexes was determined by one-way analysis of variance with a Tukey post hoc analysis. The differences were considered significant at $p < 0.05$. Pearson's correlation test was used to determine the correlation between the total phenolic content and antioxidant activity from different assays.

RESULTS AND DISCUSSION

Total phenolic content and antioxidant activity of vegetables cooked by different methods. ***Total phenolic content and antioxidant activity of raw samples.*** The tested cooking methods are common in Sri Lankan cuisines. The total phenolic content (TPC) and antioxidant activity of the raw and cooked vegetables are presented in Table 1. According to statistical analysis, the cooking methods had a significant ($p < 0.05$) effect on the TPC and antioxidant activity of brinjal, turkey berry, and winged beans. Compared to the raw vegetable extracts, the cooked vegetable extracts exhibited higher TPC and antioxidant activity, indicating the benefit of adapting Sri Lankan culinary methods. The TPC of raw brinjal used in our study reached 115.33 ± 5.25 mg GAE/100 g, lying within the range (78.3 to 125.4 mg GAE/100 g) reported by Chumyam *et al.* [15] in four eggplant cultivars.

The ABTS assay showed that the vegetables in our study had higher antioxidant activity than four cultivars of eggplant in the study by Chumyam *et al.* [15]. According to the DPPH assay, the turkey berry had higher antioxidant activity (IC_{50} value 4.71 ± 0.02%) compared to the study by Kortei *et al.* [16]. The TPC and IC_{50} values of winged beans were 147.55 ± 4.40 mg GAE/100 g and 4.28 ± 0.07 mg/mL, respectively.

Total phenolic content of cooked vegetables. There was a significant difference in the total phenolic content of brinjal and winged bean samples obtained by different cooking methods. However, the methods increased TPC values in a different order, namely COMS > CMS > COM > COS > CM > CO for brinjal and COMS > CMS > COS > COM > CM > CO for winged beans (COMS – cooked with oil, milk, and spices; CMS – cooked with milk and spices; COM – cooked with oil and milk; COS – cooked with oil and spices; CM – cooked with milk; and CO – cooked with oil). No significant difference was observed in the TPC values for turkey berry extracts between the samples cooked with oil, milk, and spices (1647.23 ± 1.15 mg GAE/100 g) and those cooked with milk and spices (1583.40 ± 2.32 mg GAE/100 g), as well as between the samples cooked with milk (1025.39 ± 1.56 mg GAE/100 g) and those cooked with oil (979.16 ± 4.72 mg GAE/100 g).

Among the cooking methods, cooking with oil showed the lowest TPC for all the vegetable extracts. Similarly, Gunathilake *et al.* [5] found that fried leafy vegetables had lower values of polyphenols, flavonoids, carotenoids, and antioxidant activity compared to boiled leafy vegetables.

Antioxidant activity by DPPH assay for cooked vegetables. The DPPH-determined antioxidant activity of cooked brinjal, turkey berry, and winged bean extracts showed significant difference between the cooking methods. Further, the turkey berry and winged bean extracts revealed the same order in accordance with the cooking methods, namely COMS > CMS > COS > CM > CO > COM, while brinjal showed a different order, COMS > CMS > COS > CO > COM > CM (COMS – cooked with oil, milk, and spices; CMS – cooked with milk and spices; COM – cooked with oil and milk; COS – cooked with oil and spices; CM – cooked with milk; and CO – cooked with oil).

Antioxidant activity by ABTS assay for cooked vegetables. The ABTS-determined antioxidant activity of differently cooked brinjal, turkey berry, and winged bean extracts showed significant difference between the cooking methods. They also revealed a different order of the methods, namely COMS > CMS > COS > COM > CO > CM for brinjal, COMS > COS > CMS > COM > CM > CO for turkey berry, and COMS > CMS > COS > COM > CM > CO for winged beans.

Antioxidant activity by FRAP assay for cooked vegetables. The FRAP-determined antioxidant activity of cooked brinjal extracts showed significant difference between the cooking methods. However, the antioxidant activity of turkey berry and winged beans revealed no significant difference in the cooking methods between the samples cooked with milk and those cooked with oil and milk, as well as between the samples cooked with oil and those cooked with oil and milk. Further, brinjal and turkey berry showed the same order in accordance with the cooking methods, namely COMS > CMS > COS > COM > CM > CO, while winged beans showed a different order, COMS > CMS > COS > CM > COM > CO.

According to the FRAP assay, the vegetable extracts showed higher antioxidant activity when cooked with spices: COMS > CMS > COS, compared to the other methods. The spices included turmeric, chili, and curry powders. Turmeric powder contains a variety of phenolic and bioactive compounds including curcumin, demethoxycurcumin, bisdemethoxycurcumin, ferulic acid, and vanillic acid [17]. Chili powder acts as an antioxidant due to the presence of metabolites with antioxidant capacities, such as capsaicinoids, ascorbic acid, vitamin E, provitamin A, carotenoids, xanthophylls, and phenolic compounds [18]. The curry powder contained coriander, cumin, fenugreek, and mustard seeds, as well as black pepper. Thus, the spices were rich in antioxidants including flavonoids, phenolic compounds, sulfur-containing compounds, tannins, alkaloids, phenolic diterpenes, and vitamins [19].

The vegetable samples cooked with oil, milk, and spices showed the highest total phenolic content and antioxidant activity determined by the DPPH, ABTS, and FRAP assays, except for the DPPH-determined antioxidant capacity of the brinjal extract. Cooking with coconut milk and coconut oil adds more types of polyphenolic and antioxidant compounds to the extract. Further, it helps in extracting both oil- and water-soluble antioxidant and polyphenolic compounds from the food matrix.

Relationship between phenolic compounds and antioxidant capacity. Table 2 depicts the correlation analysis between the total phenolic content and antioxidant capacity by DPPH, ABTS, and FRAP assays. The results showed a very strong correlation ($p < 0.05$) between the TPC and antioxidant capacity values of all the vegetable extracts, raw or cooked. This suggests that the phenolic compounds present in the extracts contributed significantly to the observed antioxidant effect and there was a significant linear relationship between the TPC and antioxidant capacity. Most plant polyphenols display significant antioxidant properties, mainly as free radical scavengers [20]. Many studies established a positive strong correlation between the TPC and antioxidant capacity [21]. The *r* values ranged from –1.00 to 1.00, showing a strong correlation between the variables, and the negative and positive values indicated an inverse and direct relationship between the variables. The TPC and DPPH (IC_{50}) values showed a negative strong relationship, with the IC_{50} value being inversely proportional to antioxidant capacity. The TPC and DPPH correlation for the brinjal and winged bean extracts was slightly less strong than that for the turkey berry extract. The TPC and ABTS correlation and the TPC and FRAP correlation for the winged bean extract were slightly stronger than those for the brinjal and turkey berry extracts.

Bioaccessibility indexes of phenolic compounds and antioxidant activity. We determined the effect of *in vitro* digestion on the total phenolic content and antioxidant capacity of the brinjal, turkey berry, and winged bean extracts cooked by different methods. Their bioaccessibility indexes are presented in Table 3.

Phenolic compound bioaccessibility index. The phenolic compound bioaccessibility index (PCBI) of the brinjal extract cooked by different methods ranged from 24.54 to 65.90%. This was in line with the results of Neto *et al.* [13], where the bioaccessibility of plant extract phenolic compounds varied from 30 to 100%. The brinjal extract cooked with coconut oil (CO) had the highest PCBI (65.90%) followed by the samples cooked with oil and milk (COM, 57.65%); milk (CM, 48.57%); oil and spices (COS, 44.50%); oil, milk, and spices (COMS, 31.38%); and milk and spices (CMS, 24.54%). Even though cooking with oil, milk, and spices and cooking with milk and spices showed higher total phenolic content (TPC) values before digestion, the PCBI for these methods were lower than for the other methods. The PCBI for turkey berry cooked by different methods varied from 13.38 to 32.51%. The turkey berry extract cooked with oil, milk, and spices showed the highest PCBI (32.51%) followed by the COS, CM, CMS, COM, and CO samples. The PCBI for winged bean ranged from 29.57 to 55.89%. The winged bean extract cooked with oil, milk, and spices showed the highest PCBI followed by the CMS, COS, CO, COM, and CM samples.

The digested samples of brinjal, turkey berry, and winged beans had lower TPC values regardless of the

Table 1 Effect of different cooking methods on total phenolic content and antioxidant capacity by DPPH, ABTS, and FRAP

Cooking methods	Brinjal				Turkey berry				Winged bean			
	TPC, mg GAE/100 g	DPPH, IC_{50} mg/mL	ABTS, %	FRAP, mg TE/g	TPC, mg GAE/100 g	DPPH, IC_{50} mg/mL	ABTS, %	FRAP, mg TE/g	TPC, mg GAE/100 g	DPPH, IC_{50} mg/mL	ABTS, %	FRAP, mg TE/g
R	115.33 ± 5.25^{g}	5.10 ± 0.02^{a}	31.85 ± 0.03^{g}	0.91 ± 0.06^{g}	862.78 ± 2.82^{e}	4.71 ± 0.02^{a}	27.43 ± 0.12^{g}	10.08 ± 0.01^{g}	147.55 ± 4.40^{g}	4.28 ± 0.07^{a}	36.21 ± 0.10^{g}	0.50 ± 0.01^{f}
CO	140.01 ± 7.13^{f}	3.70 ± 0.03^{d}	43.47 ± 0.04^{e}	2.20 ± 0.06^{f}	979.16 ± 4.72^{d}	4.44 ± 0.02^{c}	36.30 ± 0.12^{f}	14.34 ± 0.01^{f}	184.00 ± 5.98^{f}	4.05 ± 0.04^{c}	49.66 ± 0.03^{f}	1.65 ± 0.02^{e}
CM	252.63 ± 7.64^{e}	4.77 ± 0.03^{b}	41.23 ± 0.01^{f}	2.77 ± 0.04^{e}	1025.39 ± 1.56^{d}	4.01 ± 0.01^{d}	41.73 ± 0.01^{e}	23.38 ± 0.02^{d}	242.67 ± 7.96^{e}	3.76 ± 0.03^{d}	53.23 ± 0.03^{e}	2.18 ± 0.01^{d}
COM	304.99 ± 6.67^{c}	4.26 ± 0.04^{c}	46.84 ± 0.02^{d}	2.95 ± 0.05^{d}	1278.07 ± 1.72^{b}	4.54 ± 0.01^{b}	43.30 ± 0.08^{d}	29.92 ± 0.07^{d}	295.26 ± 10.02^{d}	4.19 ± 0.03^{b}	55.62 ± 0.05^{d}	1.75 ± 0.02^{e}
COS	279.64 ± 5.17^{d}	3.53 ± 0.02^{e}	49.76 ± 0.03^{c}	8.75 ± 0.04^{c}	1202.00 ± 113.80^{c}	3.78 ± 0.01^{e}	53.81 ± 0.12^{b}	38.74 ± 0.01^{c}	322.47 ± 6.36^{c}	3.33 ± 0.02^{e}	62.92 ± 0.01^{c}	2.99 ± 0.16^{c}
CMS	564.54 ± 5.34^{b}	2.67 ± 0.02^{g}	53.23 ± 0.03^{b}	10.10 ± 0.04^{b}	1583.40 ± 2.32^{a}	2.92 ± 0.02^{f}	51.24 ± 0.10^{c}	39.73 ± 0.02^{b}	370.13 ± 13.21^{b}	3.25 ± 0.02^{f}	67.41 ± 0.03^{b}	3.62 ± 0.01^{b}
COMS	596.60 ± 4.45^{a}	2.94 ± 0.03^{f}	56.11 ± 0.05^{a}	14.30 ± 0.04^{a}	1647.23 ± 1.15^{a}	2.18 ± 0.01^{g}	57.28 ± 0.11^{a}	42.43 ± 0.01^{a}	569.20 ± 7.94^{a}	3.17 ± 0.02^{g}	76.87 ± 0.02^{a}	4.43 ± 0.04^{a}

Results were expressed as mean ± SD (n = 3). The values followed by the same letters in the same column are not significantly different ($p < 0.05$); R – raw; CO – cooked with coconut oil; CM – cooked with coconut milk; COM – cooked with coconut oil and milk; COS – cooked with coconut oil + spices; CMS – cooked with coconut milk + spices; COMS – cooked with coconut oil and milk + spices

Table 2 Correlation analysis between total phenolic content and antioxidant parameters

Assays	Brinjal		Turkey berry		Winged bean	
	r	*p*-value	*r*	*p*-value	*r*	*p*-value
TPC and DPPH	–0.798	0.032	–0.885	0.008	–0.806	0.029
TPC and ABTS	0.868	0.011	0.859	0.013	0.944	0.001
TPC and FRAP	0.897	0.006	0.902	0.005	0.928	0.003

Seven paired mean samples from each assay were used in the comparison; *r* values denote Pearson's correlation value ($p < 0.05$)

Table 3 Bioaccessibility indexes for total phenolic content and antioxidant activity

Cooking methods	Brinjal				Turkey berry				Winged bean			
	TPC, mg GAE/100 g	DPPH, IC_{50} mg/mL	ABTS, %	FRAP, mg TE/g	TPC, mg GAE/100 g	DPPH, IC_{50} mg/mL	ABTS, %	FRAP, mg TE/g	TPC, mg GAE/100 g	DPPH, IC_{50} mg/mL	ABTS, %	FRAP, mg TE/g
CO	65.90^{a}	53.08^{d}	94.66^{f}	129.09^{b}	13.38^{f}	68.10^{b}	95.98^{e}	60.74^{b}	35.73^{d}	306.82^{b}	92.81^{a}	295.76^{d}
CM	48.57^{c}	71.41^{a}	105.21^{b}	171.48^{a}	25.34^{e}	62.36^{d}	89.82^{f}	32.72^{f}	29.57^{e}	284.85^{c}	90.96^{b}	136.70^{f}
COM	57.65^{b}	66.88^{c}	102.88^{d}	85.76^{d}	22.78^{e}	71.72^{a}	104.73^{b}	33.46^{e}	35.65^{d}	346.28^{a}	88.76^{c}	207.43^{e}
COS	44.50^{d}	53.48^{d}	106.07^{a}	77.60^{f}	25.93^{b}	64.95^{c}	96.95^{d}	52.74^{d}	39.42^{c}	277.50^{e}	86.11^{d}	375.92^{c}
CMS	24.54^{f}	47.94^{e}	103.95^{c}	98.02^{c}	24.88^{d}	50.52^{e}	110.28^{a}	55.42^{c}	47.04^{b}	273.11^{f}	78.34^{e}	533.43^{a}
COMS	31.38^{e}	68.69^{b}	97.38^{e}	82.10^{e}	32.51^{a}	39.14^{f}	103.91^{c}	75.75^{a}	55.89^{a}	278.07^{d}	74.39^{f}	376.75^{b}

The values followed by the same letters in the same column are not significantly different (Tukey's test, $p < 0.05$); CO – cooked with coconut oil; CM – cooked with coconut milk; COM – cooked with coconut oil and milk; COS – cooked with coconut oil + spices; CMS – cooked with coconut milk + spices; COMS – cooked with coconut oil and milk + spices

cooking method, compared to the TPC of the cooked samples. This may be due to the low pH in the stomach which caused a breakdown of phenolic compounds [22]. Further, each cooking method showed a significant difference in the TPC except for the winged bean extract cooked with oil or with oil and milk.

Antioxidant activity bioaccessibility index. The antioxidant activity bioaccessibility index (AABI) for the brinjal, turkey berry, and winged bean extracts cooked by different methods was based on DPPH, ABTS, and FRAP assays. The AABI < 100% indicated that the antioxidant activity became less bioaccessible, implying a loss of bioactive compounds during digestion. The AABI = 100% suggested that digestion did not significantly alter the bioaccessibility of bioactive compounds and the antioxidant capacity remained consistent before and after digestion. The AABI > 100% indicated that digestion improved the bioaccessibility through the release of bioactive compounds by breaking down the food matrix.

According to the DPPH assay, brinjal cooked with coconut milk and spices exhibited high antioxidant activity, while the digested brinjal extract cooked with milk showed a high AABI (71.41%). Further, all the methods of cooking brinjal revealed a significant difference, except for cooking with oil (53.08%) and cooking with oil and spices (40.25%). The AABI for the turkey berry extract varied from 39.14 to 71.72%. Even though cooking turkey berry with oil, milk, and spices showed the highest antioxidant capacity before digestion, it had a lower AABI (39.14%). This may be due to the breakdown of bioactive compounds during the digestion process [23]. The AABI for winged beans exceeded 100% for all the cooking methods. This indicated that the digestion process enhanced the release of bioactive compounds in the cooked winged beans.

The ABTS assay showed AABI values of over 100% for the brinjal extracts CM, COM, COS, and CMS, as well as for the turkey berry extracts cooked with COM, CMS, and COMS. This indicated that digestion improved the bioaccessibility through the release of bioactive compounds by breaking down the food matrix and making compounds more accessible.

According to the FRAP assay, AABI values of over 100% were registered in the brinjal extracts CO and CM, as well as in the winged bean extracts cooked by all the tested methods. However, the turkey berry extracts cooked by different methods showed AABI values of below 100%, with the sample COMS having the highest AABI value of 75.75%.

The selected vegetables cooked by different methods showed differences in the PCBI and AABI values. The differences in bioaccessibility could be due to several factors, such as possible interactions with other food components, the chemical state of the compounds, and their release from the food matrix [22].

Bioavailability indexes of phenolic compounds and antioxidant activity. *In vitro* bioavailability indexes for phenolic compounds and antioxidant activity are presented in Table 4.

Phenolic compound bioavailability index. The phenolic compound bioavailability index (PBVI) of the brinjal extracts ranged from 32.77 to 53.71%. The brinjal extract CO showed the highest phenolic compound bioaccessibility index (PCBI) and PBVI, while that COS had the lowest PCBI and PBVI. The turkey berry extract COMS exhibited the highest PCBI and PBVI. The winged bean extract CMS showed the highest PBVI (53.78%), while that COMS exhibited the lowest PBVI (37.62%), compared to the other cooking methods. The three vegetables cooked by different methods showed significant differences in total phenols, except for the winged beans CM and COM.

Antioxidant activity bioavailability index. The brinjal extract CM showed the highest antioxidant activity bioavailability index **(**AAVI) according to the DPPH (50.53%) and ABTS (55.74%) assays, while that cooked with coconut oil revealed the highest index according to the FRAP assay (149.09%). The turkey berry extracts cooked by different methods exhibited different antioxi-

Table 4 Bioavailability indexes for total phenolic content and antioxidant activity

Cooking methods	Brinjal				Turkey berry				Winged bean			
	TPC, mg GAE/100 g	DPPH, IC_{50} mg/mL	ABTS, %	FRAP, mg TE/g	TPC, mg GAE/100 g	DPPH, IC_{50} mg/mL	ABTS, %	FRAP, mg TE/g	TPC, mg GAE/100 g	DPPH, IC_{50} mg/mL	ABTS, %	FRAP, mg TE/g
CO	53.71^{a}	35.51^{e}	51.35^{b}	149.09^{a}	14.26^{e}	50.80^{b}	54.16^{d}	27.62^{c}	46.23^{c}	32.43^{e}	49.25^{c}	211.52^{a}
CM	32.77^{b}	50.53^{a}	55.74^{a}	114.80^{b}	13.76^{f}	45.41^{d}	48.21^{f}	35.80^{a}	41.75^{d}	38.56^{a}	51.12^{b}	157.34^{c}
COM	27.56^{d}	45.46^{b}	49.98^{d}	107.12^{c}	16.28^{d}	54.31^{a}	51.25^{e}	29.14^{b}	41.81^{d}	38.51^{a}	88.78^{a}	188.00^{b}
COS	30.54^{c}	40.25^{d}	50.60^{c}	39.43^{d}	19.30^{c}	48.46^{c}	55.29^{c}	23.00^{d}	48.42^{b}	36.20^{d}	46.41^{d}	113.71^{d}
CMS	22.93^{f}	33.50^{f}	49.84^{d}	37.43^{e}	19.78^{b}	38.07^{e}	59.04^{a}	22.43^{e}	53.78^{a}	37.44^{b}	42.52e	100.28^{e}
COMS	26.72^{e}	44.41^{c}	47.82^{c}	27.34^{f}	28.25^{a}	28.24^{f}	56.06^{b}	21.61^{f}	37.62^{e}	36.65^{c}	40.55f	80.36^{f}

The values followed by the same letters in the same column are not significantly different (Tukey's test, $p < 0.05$); CO – cooked with coconut oil; CM – cooked with coconut milk; COM – cooked with coconut oil and milk; COS – cooked with coconut oil + spices; CMS – cooked with coconut milk + spices; COMS – cooked with coconut oil and milk + spices

dant capacity according to different assays. The highest AAVI values were registered in the extracts cooked with oil and milk (DPPH), milk and spices (ABTS), and with milk (FRAP). The winged bean extracts showed the highest AAVI values when cooked with milk and with oil and milk (DPPH), with oil and milk (ABTS), and with oil (FRAP). Further, the FRAP assay revealed AAVI values of 100% for the winged bean extracts cooked by different methods, except for the sample COMS. This indicates that digestion improved the bioavailability through the release of bioactive compounds by breaking down the food matrix and making the compounds more accessible.

CONCLUSION

Our study revealed that the tested Sri Lankan domestic cooking methods significantly altered the total phenolic content and antioxidant capacity of brinjal, turkey berry, and winged bean extracts. In particular, all the cooking methods increased total phenolic compounds and the antioxidant activity of cooked vegetables compared to their raw forms. According to the ABTS and FRAP assays, all the vegetables exhibited the highest total phenolic content and the highest antioxidant activity when cooked with coconut oil, coconut milk, and spices (COMS). The cooking methods used in the experiments significantly influenced the bioaccessibility of phenolic compounds and antioxidant activity in brinjal, turkey berry, and winged beans. The highest bioaccessibility index for phenolic compounds was found in the brinjal extract cooked with coconut oil (CO) and in the turkey berry and winged bean COMS. Notably, the cooking methods that initially showed higher total phenolics and antioxidant activity did not always correspond to higher bioaccessibility, indicating that digestion might have altered the availability of these compounds.

Our study highlights the variability in the bioavailability of phenolic compounds and antioxidant activity across different cooking methods. According to our results, the choice of a cooking method is crucial for optimizing the bioavailability of health-promoting compounds. There is a need for further investigations on phenolic compounds in bioaccessible and bioavailable extracts cooked by different methods.

CONTRIBUTION

Sameera Priyadarshana was responsible for the conceptualization, methodology, and investigation. Konara Somawathie was involved in the conceptualization, funding acquisition, methodology, resources, supervision, as well as writing the original draft, reviewing, and editing. Mohamed Shafras performed project administration and supervision, as well as wrote, reviewed, and edited the original draft. Darsiga Sivanandarajah carried out formal analysis and wrote, reviewed, and edited the original draft.

CONFLICT OF INTEREST

The authors declare that there is no conflict of interest regarding the publication of this paper.

REFERENCES

1. Banwo K, Olojede AO, Adesulu-Dahunsi AT, Verma DK, Thakur M, *et al*. Functional importance of bioactive compounds of foods with potential health benefits: A review on recent trends. Food Bioscience. 2021;43:101320. https://doi.org/10.1016/j.fbio.2021.101320
2. Niño-Medina G, Urías-Orona V, Muy-Rangel MB, Heredia JB. Structure and content of phenolics in eggplant (*Solanum melongena*) – A review. South African Journal of Botany. 2017;111:161–169. https://doi.org/10.1016/j.sajb.2017.03.016
3. Darkwah WK, Koomson DA, Miwornunyuie N, Nkoom M, Puplampu JB. Review: Phytochemistry and medicinal properties of *Solanum torvum* fruits. All Life. 2020;13(1):498–506. https://doi.org/10.1080/26895293.2020.1817799
4. Bepary RH, Roy A, Pathak K, Deka SC. Biochemical composition, bioactivity, processing, and food applications of winged bean (*Psophocarpus tetragonolobus*): A review. Legume Science. 2023;5(3):e187. https://doi.org/10.1002/leg3.187
5. Gunathilake KDPP, Ranaweera KKDS, Rupasinghe HPV. Effect of different cooking methods on polyphenols, carotenoids and antioxidant activities of selected edible leaves. Antioxidants. 2018:7(9):117. https://doi.org/10.3390/antiox7090117
6. Bié J, Sepodes B, Fernandes PCB, Ribeiro MHL. Polyphenols in health and disease: Gut microbiota, bioaccessibility, and bioavailability. Compounds. 2023:3(1):40–72. https://doi.org/10.3390/compounds3010005
7. Dima C, Assadpour E, Dima S, Jafari SM. Bioavailability and bioaccessibility of food bioactive compounds; overview and assessment by *in vitro* methods. Comprehensive Reviews in Food Science and Food Safety. 2020;19(6):2862–2884. https://doi.org/10.1111/1541-4337.12623
8. Minekus M, Alminger M, Alvito P, Ballance S, Bohn T, *et al*. A standardised static *in vitro* digestion method suitable for food – An international consensus. Food & Function. 2014;5(6):1113–1124. https://doi.org/10.1039/c3fo60702j
9. Swain T, Hillis WE. The phenolic constituents of *Prunus domestica*. I.–The quantitative analysis of phenolic constituents. Journal of the Science of Food and Agriculture. 1959;10(1):63–68. https://doi.org/10.1002/jsfa.2740100110

10. Brand-Williams W, Cuvelier ME, Berset C. Use of a free radical method to evaluate antioxidant activity. LWT. 1995;28(1):25–30. https://doi.org/10.1016/s0023-6438(95)80008-5
11. Re R, Pellegrini N, Proteggente A, Pannala A, Yang M, *et al*. Antioxidant activity applying an improved ABTS radical cation decolorization assay. Free Radical Biology and Medicine. 1999;26(9–10):1231–1237. https://doi.org/10.1016/s0891-5849(98)00315-3
12. Benzie IF, Strain, J. [2] Ferric reducing/antioxidant power assay: Direct measure of total antioxidant activity of biological fluids and modified version for simultaneous measurement of total antioxidant power and ascorbic acid concentration. Methods in Enzymology. 1999;299:15–27. https://doi.org/10.1016/s0076-6879(99)99005-5
13. Neto JJL, de Almeida TS, de Medeiros JL, Vieira LR, Moreira TB, *et al*. Impact of bioaccessibility and bioavailability of phenolic compounds in biological systems upon the antioxidant activity of the ethanolic extract of *Triplaris gardneriana* seeds. Biomedicine & Pharmacotherapy. 2017;88:999–1007. https://doi.org/10.1016/j.biopha.2017.01.109
14. Dabulici CM, Sârbu I, Vamanu E. The bioactive potential of functional products and bioavailability of phenolic compounds. Foods. 2020;9(7):953. https://doi.org/10.3390/foods9070953
15. Chumyam A, Whangchai K, Jungklang J, Faiyue B, Saengnil K. Effects of heat treatments on antioxidant capacity and total phenolic content of four cultivars of purple skin eggplants. ScienceAsia. 2013;39(3):246–251. https://doi.org/10.2306/scienceasia1513-1874.2013.39.246
16. Kortei N, Suetor J, Aboagye G, Tettey C, Kpodo F, *et al*. Comparative study of the bioactive and chemical properties of three different *Solanum* spp. from Ghana. Food Research. 2020;4(5):1773–1784. https://doi.org/10.26656/fr.2017.4(5).010
17. Murthy HN, Paek KY. Bioactive compounds in underutilized vegetables and legumes. Reference Series in Phytochemistry. 2021. 681 p. https://doi.org/10.1007/978-3-030-57415-4_37
18. Puvača N. Bioactive compounds in dietary spices and medicinal plants. Journal of Agronomy, Technology and Engineering Management. 2022;5(2):704–711. https://doi.org/10.55817/uhfo5592
19. Yashin A, Yashin Y, Xia X, Nemzer B. Antioxidant activity of spices and their impact on human health: A review. Antioxidants. 2017:6(3):70. https://doi.org/10.3390/antiox6030070
20. Zeb A. Concept, mechanism, and applications of phenolic antioxidants in foods. Journal of Food Biochemistry. 2020;44(9):e13394. https://doi.org/10.1111/jfbc.13394
21. Ng Z-X, Chai J-W, Kuppusamy UR. Customized cooking method improves total antioxidant activity in selected vegetables. International Journal of Food Sciences and Nutrition. 2011;62(2):158–163. https://doi.org/10.3109/09637486.2010.526931
22. Pasli AA, Yavuz-Düzgün M, Altuntas U, Altin G, Özçelik B, *et al*. *In vitro* bioaccessibility of phenolics and flavonoids in various dried vegetables, and the determination of their antioxidant capacity via different spectrophotometric assays. International Food Research Journal. 2019;26(3):793–800.
23. Coelho M, Oliveira C, Coscueta ER, Fernandes J, Pereira RN, *et al*. Bioactivity and bioaccessibility of bioactive compounds in gastrointestinal digestion of tomato bagasse extracts. Foods. 2022;11(7):1064. https://doi.org/10.3390/foods11071064

ORCID IDs
Sameera Priyadarshana http://orcid.org/0009-0007-8651-2240
Konara Somawathie http://orcid.org/0009-0005-2872-5921
Mohamed Shafras http://orcid.org/0000-0002-4827-0275
Darsiga Sivanandarajah http://orcid.org/0000-0002-0598-1456

Foods and Raw Materials. 2026;14(2)

ISSN 2308-4057 (Print)
ISSN 2310-9599 (Online)

Research Article
Open Access

Available online at http://jfrm.ru/en
https://doi.org/10.21603/2308-4057-2026-2-682
https://elibrary.ru/JSGXVE

Stabilizing liposomes loaded with proteins, amino acids, vitamins, and microelements

Irina A. Tsepeleva, Alesya N. Yudina*, Alla A. Krasnoshtanova

Mendeleev University of Chemical Technology, Moscow, Russia

* e-mail: a.n.yudina@yandex.ru

Received 19.09.2024; Revised 17.01.2025; Accepted 03.06.2025; Published online 18.11.2025

Abstract:
Many protein-containing drugs have limited application in the prevention and treatment of diseases due to their instability in the gastrointestinal tract. Therefore, there is a need for complex liposomal drugs with stabilizing components that can enhance their therapeutic effect.

Our objects of study included soy lecithin, egg albumin, immunoglobulin, insulin, chitosan, amino acids, tocopherol, ascorbic acid, riboflavin, zinc sulfate, and iron (III) chloride. The concentrations of nutrients were determined by the colorimetric and titrimetric methods. We also used the peroxide value and the dynamic light scattering method.

Liposomes obtained by the injection method had a diameter of 4.7 ± 0.2 μm, which makes them suitable for oral drug administration. Protein incorporation at 98, 95, and 83% was achieved by 1.0 mg/mL insulin, 1.6 mg/mL globulin, and 30 mg/mL albumin, respectively. The most optimal concentration of albumin in liposomes was 30 mg/mL. The highest degrees of incorporation of amino acids and their mixtures were 94–98 and 90%, respectively. Stabilizing liposomes with vitamins B_2 and C, as well as zinc and iron, increased the liposomal incorporation of amino acid mixtures and ensured their release in the model gastrointestinal tract.

The protein corona increased the release of target components in the small intestine and improved liposome stability during storage. Modifying the surface of liposomes with chitosan decreased the release of albumin in the oral cavity, stomach, and intestine.

Complex liposomes proved to have better stability in the model gastrointestinal tract and during storage. The results obtained can be used to create complex nutriceuticals.

Keywords: Liposomes, soy lecithin, protein therapy, albumin, globulin, insulin, amino acids, vitamins, microelements

Please cite this article in press as: Tsepeleva IA, Yudina AN, Krasnoshtanova AA. Stabilizing liposomes loaded with proteins, amino acids, vitamins, and microelements. Foods and Raw Materials. 2026;14(2):408–424. https://doi.org/10.21603/2308-4057-2026-2-682

INTRODUCTION

Protein components are the most common functional elements involved in the life processes of the human body. They act as enzymes (biocatalysts of biochemical reactions), immunoglobulins regulating defense mechanisms against antigens, building blocks of muscle and connective tissues (collagen, keratin, elastin, fibrinogens, and thrombins), signal molecules (hormones, cytokines, and growth factors), as well as carriers of oxygen and carbon dioxide from tissues to the lungs (hemoglobin) [1].

Protein therapy has recently revolutionized the treatment of many diseases. Its main advantages are high specificity and lack of side effects. For quite a long time, the clinical rationale for the use of many therapeutic proteins was undermined by undesirable immune responses, which limited their effectiveness and affected their safety profile.

Currently, the protein-based pharmaceutical market is thriving, with sales exceeding $380 billion in 2023 and expected to rise to over $650 billion by 2030 [2].

Therapeutic proteins can be classified into four groups. The first group includes proteins with enzymatic or regulatory activity. They are mainly applied to replace deficient proteins in people with hereditary genetic diseases or mutations. The second group comprises proteins with targeting activity such as monoclonal antibodies that act as diagnostic tools for tumor lesions and other diseases. The third group includes vaccines based on protein or glycoprotein components of a pathogen,

Copyright © 2025, Tsepeleva *et al.* This is an open access article distributed under the terms of the Creative Commons Attribution 4.0 International License (https://creativecommons.org/licenses/by/4.0/), allowing third parties to copy and redistribute the material in any medium or format and to remix, transform, and build upon the material for any purpose, even commercially, provided the original work is properly cited and states its license.

capable of causing an immune response. Therapeutic proteins of the fourth group are recombinant proteins that are mainly used in diagnostics [3].

A disadvantage of protein-based pharmaceuticals is their limited stability in physiological fluids containing proteolytic enzymes (pepsin, trypsin, chymotrypsin). Another disadvantage is their low pH values in the stomach [4].

To overcome these drawbacks, protein-based drugs can be encapsulated in liposomes or hydrogels. The encapsulation material must be biocompatible, biodegradable, and stable under the conditions of prolonged release. In addition to the type of biomaterial, the choice of a way to introduce protein-based drugs is also important. For example, they can be introduced into a hydrogel either by forming a gel in the presence of a protein or by soaking the gel in a protein solution. The former technique can lead to denaturation of protein molecules due to impurities or by-products of gel formation. With the latter technique, proteins are usually displaced from the gel networks due to their heterogeneous size. Because of this limitation, only less than 0.1% can be incorporated when using this method [5].

Lipid-based delivery systems, or liposomes, are effective due to their ability to deliver antigens (peptides, proteins, and nucleic acid systems) to cells stimulating protective immune responses. Modern engineering of nanomedicines varying in composition, particle size, and surface charge can help in spatial and temporal drug delivery [6, 7].

In addition to high-molecular compounds, liposomes contain various low-molecular substances, such as amino acids, vitamins, microelements, carotenoids, etc.

The presence of various functional groups in amino acids makes it possible to synthesize a wide range of molecules to form liposomal aggregates with different morphologies [8–12]. In addition, natural L-amino acids can promote the biotransformation of other molecules [13, 14].

Denieva *et al.* [15] produced mixed liposomes based on natural amino acids (L-alanine, L-serine, and L-ornithine) and cationic lipids. They found that L-serine-based liposomes were capable of accumulating in the endoplasmic reticulum of cells for 1 h. Also, their transfection activity significantly exceeded that the commercial drug Lipofectamine-2000. The system proposed by the authors had a slight toxic effect (IC_{50} – 0.75 mg/mL, with a safe working concentration of 0.24 mg/mL).

Tosato *et al.* [16] formulated a dietary supplement based on 1.66 g of L-arginine and 500 mg of liposomal vitamin C. The authors showed its efficiency in restoring physical performance and reducing fatigue during the recovery from COVID-19.

Microelements and vitamins are also introduced into liposomal nanocontainers to increase their bioavailability, ensure prolonged release, and protect them from biodegradation in the digestive system [17]. For example, Liu *et al.* [18] applied liposomal co-encapsulation to extend the shelf life and improve the bioavailability of vitamins and a wide range of hydrophilic and hydrophobic molecules, such as peptides, proteins, and nucleic acid-based drugs, which are used for pharmaceutical, cosmetic, biochemical, and nutraceutical purposes.

Liposomal forms of vitamins have advantages over their free forms. In free form, vitamins have low absorption due to their passing through cell membranes and oxidation in the digestive system [19]. Liposomes loaded with vitamins are embedded in damaged areas of cell membranes, transferring the active compound into the cells. Another benefit of using liposomes as a transport carrier is that they are of the same nature as fat-soluble vitamins.

Since vitamin C is an acid, it can irritate the gastric mucosa, especially in people with peptic ulcers. This irritation can be avoided by enclosing the vitamin in liposomes. Nechaev *et al.* [20] developed liposomes loaded with vitamins C and E, which enhance each other's effects. The liposomes had stable quality, antioxidant effect, and good sensory indicators during 90 days of storage at 4 ± 2°C.

Lipovitam-Beta is an antioxidant drug of the new generation. The liposomal encapsulation of its active substances (beta-carotene, vitamins E and C) ensures their high bioavailability (over 90%, compared to 10–30% in traditional drugs) [21].

Vitamin B_2 (riboflavin) is involved in dehydrogenase reactions in the form of prosthetic groups FAD and FMN. Gupta *et al.* [22] studied the effect of liposomes on the photostability of riboflavin in an aqueous composition under fluorescent lighting. They found that the photostability of riboflavin was higher in the presence of neutral and negatively charged liposomes but lower in the presence of positively charged liposomes. In addition, higher concentrations of dimyristoylphosphatidylcholine in the liposomes increased the photostability of riboflavin.

Iron (II) and (III) ions are included in liposomes for a number of reasons. Firstly, in high doses, iron (II) and (III) cations have a negative effect on the intestinal mucosa, causing irritation. This effect can be avoided by taking iron (II) and (III) salts with food. However, taking iron with food reduces its bioavailability, with only 2–10% of absorption for non-heme iron (III) [23]. Secondly, the walls of the small intestine and duodenum mainly absorb the Fe^{2+} cation, but iron (II) ions are unstable in solutions and are oxidized to iron (III) ions. As a result, Fe^{2+}-based drugs cannot be used in liquid forms. Moreover, liquid forms of drugs based on Fe^{2+} and Fe^{3+} tend to stain tooth enamel, cause an unpleasant metallic taste, and pass through the gastrointestinal tract undigested [24].

The liposomal form of Fe^{3+} is an innovative method of delivering iron ions into the human body. It is a trivalent iron pyrophosphate enclosed in a double-layer lipid shell that has a similar structure to that of a cell membrane. When entering the lumen of the small intestine, liposomes containing iron (III) ions penetrate enterocytes by endocytosis and are transported into the

lymph. With the lymph, the liposomes enter mainly the liver, where iron (III) ions are released from the liposomal shell into active metabolism. The liposomal iron does not cause the typical side effects that traditional preparations of iron (II) and (III) salts do. The liposomal form of Fe^{3+} is highly efficient in patients with iron deficiency anemia associated with chronic and acute blood loss, deficiency of iron (II) or (III) ions in the diet, as well as anemia of chronic disease. Treating anemia of chronic disease with standard drugs based on Fe^{2+} and Fe^{3+} ions is ineffective due to changes in their absorption in the intestine and regulation of hepcidin. In inflammatory bowel diseases, iron-based drugs are usually administered intravenously, since their oral administration is ineffective. However, the liposomal form of iron (II) or (III) ions administered orally showed high efficiency in patients with Crohn's disease [25].

Zinc is another important microelement responsible for the normal functioning of innate immunity. Zinc exhibits antioxidant properties in relation to active forms of nitrogen and oxygen. It participates in the modulation of cytokine release and induces the proliferation of CD8+ T-cells, as well as maintains the integrity of the skin barrier and mucous membranes. In acquired immunity, zinc plays an important role in the growth of immune cells. It facilitates the intracellular binding of tyrosine kinase to T-cell receptors, promoting the development and activation of T lymphocytes. Zinc deficiency leads to a lower production of lymphocytes (especially T-cells), thymus atrophy, and disruption of cytokine synthesis, causing the development of oxidative stress and inflammatory processes [26].

Zinc enhances the antiviral properties of many mammalian cells by stimulating natural immunity. It is also an important structural component in a number of enzymes. Along with zinc-dependent protein complexes in liposomal compositions, this microelement can effectively fight viral infections by activating individual functional complexes of immune cells in the respiratory tract. Numerous studies have shown that taking zinc in combination with hydroxychloroquine significantly reduced the risk of death during COVID-19 [27].

The main requirements for liposomes are biodegradability, stability, the absence of immune response, a possibility of prolonged action, and non-toxicity. However, liposomes have a number of limitations due to their thermodynamic instability and tendency to aggregate in the human body. Liposomes lose their stability even with minor changes in environmental parameters, such as temperature, pH, or ionic strength. When stored in the dry form, they are destructed due to lipid peroxidation under the influence of oxygen. Therefore, scientists are faced with the task to obtain stabilized liposomal forms of bioactive substances and study the structural and functional properties of the resulting complexes [28].

Liposomes can be stabilized by creating additional shells (e. g., polymer-based) on top of the main bilipid layer. The resulting multilamellar liposomes have a more stable membrane and are much better able to retain the active compound during long-term storage. This is because their outer shells protect their deep bilipid layers from the effects of oxygen. Shells are often based on protein substances or polysaccharides (e. g., chitosan). Chitosan is easy to use for layer-by-layer adsorption of polyelectrolytes or ionotropic gelation and it contributes to effective particles. Even chitosan alone used in the outer shell can already increase the stability of liposomes. However, more significant results can be achieved by using an additional gelling agent such as polyacrylic acid [29]. This can reduce the intensity of liposome peroxidation during storage and improve the preservation of the active compound as it passes through the stomach.

Chitosan is commonly combined with sodium alginate to produce a shell for stabilized multilayer liposomes. The chitosan-alginate complex can effectively bind to the hydrophilic surface of the bilipid layer and release liposomal particles under certain pH values in the small intestine [30].

Also common are liposomal shells based on casein and whey protein in functional nutrition. Such shells are less resistant and stable in the stomach. However, their advantages include high accessibility and lower susceptibility to peroxidation [31, 32].

Liposomes can also be stabilized with α-tocopherol, an antioxidant that prevents lipid peroxidation. In addition, vitamin E has a cholesterol-like effect, ordering unsaturated bilayers and disordering saturated ones. It forms stabilizing complexes by interacting with free fatty acids. Finally, introducing vitamin E into liposomal nutraceuticals can make them effective dietary supplements [33].

Currently, most protein drugs are administered parenterally, which allows for higher bioavailability compared to the oral route. However, this approach has a number of disadvantages that deteriorate the quality of human life. Therefore, the pharmaceutical industry is seeking to develop oral delivery methods for more cost-effective and flexible forms of drugs [34].

In view of the above, we aimed to obtain protein and amino acid preparations to be incorporated into liposomes, as well as to study their properties and ways of stabilization [35, 36].

STUDY OBJECTS AND METHODS

Our study objects included: moslecithin – soy lecithin (65% phospholipid fraction; Ekobio Plus, Russia); egg albumin (99% active ingredient; Roskar Poultry Farm, Russia); Globfel-4 globulin – γ- and β-globulin fractions of horse blood serum hyperimmunized with industrial strains of panleukopenia and infectious rhinotracheitis viruses, calicivirus, and chlamydia in cats (Vetbiokhim, Russia); Actrapid® HM – a short-acting insulin preparation (genetically engineered soluble human insulin, 100 IU/mL; Novo Nordisk, Denmark); chitosan (200 kDa, 85% deacetylation; Sigma-Aldrich, USA); LifeEvit vitamin E in capsules (400 mg alphatocopherol acetate; Saneka Pharmaceuticals, Slovak Republic); amino acids: serine, histidine, proline, alanine, lysine, and arginine (99.5% active ingredient; PanEco,

Russia); ascorbic acid (99.5% active ingredient; Dia-M, Russia); riboflavin (99% active ingredient; Pharmstandard-Ufa Vitamin Plant, Russia); zinc sulfate, chemically pure (Khimmed, Russia); and iron chloride (III), chemically pure (Ruskhim, Russia).

The protein content in the solutions was measured by the microbiuret method. The method was based on the spectrophotometric determination of the optical density of the colored product (biuret complex) resulting from the interaction between copper ions and groups of peptide bond atoms under alkaline conditions at 330 nm. The total amino acid content was determined by a reaction with ninhydrin to form a violet-colored complex [37]. The riboflavin content was measured by the optical density at 445 nm. The ascorbic acid content was determined by the reduction reaction of 2.6-dichlorophenolindophenol, measuring the optical density at 510 nm. The trivalent iron content was determined by a reaction with thiocyanate ion in a strongly acidic medium to form a red-colored complex with maximum absorption at 500 nm. The zinc content was determined by the titrimetric method by a reaction with 0.1 M solution of sodium EDTA salt, 1 mL of which corresponded to 13.63 mg of zinc chloride [38]. The liposomal stability in the gastrointestinal model and during storage was assessed by determining the peroxide value based on the ability of hydroiodic acid to reduce peroxides with the release of molecular iodine. The amount of molecular iodine was determined by titration with sodium thiosulfate in the presence of starch [39]. The size of microparticles and the zeta potential of the suspensions formed by them were determined automatically by the dynamic light scattering method on a Photocor Compact Z particle size analyzer (Photocor, Russia).

The thermal method for preparing liposomes. Samples of lecithin were homogenized in different volumes of distilled water with lipid contents of 0.75, 1.00, 2.00, and 3.00 wt. %. The homogenate was hydrated for 2 h. Then, 3.0 vol. % glycerol was added to the resulting suspension and thermostatted for 30 min at 65–70°C with constant stirring in a magnetic stirrer. The mixture was then kept at the specified temperature for 1 h. The prepared solutions were analyzed for liposome formation using microscopy after 1 week [40].

The injection method for preparing liposomes. The injection method is based on the spontaneous formation of bilayer vesicles when the liposomal base enters the hydrophilic solvent medium due to injection-induced pressure difference. This technique was used as described in [41]. In particular, 50 mg of egg lecithin was dissolved in 1.0 mL of 96% ethanol and added to 15 mL of 0.01 M phosphate buffer (pH 7.5). Previously, the material to be incorporated in the liposomes had been dissolved in the buffer by constant stirring in a magnetic stirrer. The prepared solution was allowed to stand overnight at room temperature and then analyzed by microscopy at a magnification of 400×.

The thin film hydration method. The thin-film hydration method is used for loading hydrophilic substances into liposomes. It is based on the rehydration of lipid films in the presence of a buffer containing the substances to be loaded. Phospholipids are dissolved in an organic solvent, usually chloroform, which is then evaporated under reduced pressure until a thin lipid film is obtained. Then, an aqueous phase is added to the film, with the hydrophilic ingredients dissolved, and a liposomal dispersion is formed [42].

Evaluation of liposome stability during storage. One of the main causes of liposome destruction is lipid peroxidation. The degree of destruction of liposomal particles during storage or use depends on their initial oxidation, which is indicated by their peroxide value. Liposomes were incubated for 8 weeks at 6°C in a hermetically sealed container. Their samples were taken throughout the storage period to determine the peroxide value [39].

***In vitro* digestion modeling.** The human gastrointestinal tract was modelled in accordance with the International Standardized Protocol for Digestion of Foods [43, 44]. The conditions for simulating digestion at each stage were as follows:

– the oral cavity: simulated salivary fluids (SSFs), pH 7.0;
– the stomach: simulated gastric fluids (SGFs), pH 3.0, 2 h, pepsin (1:1000 enzyme:substrate ratio by weight);
– the intestine: simulated intestinal fluids (SIFs), pH 7.0, 2 h, trypsin + α-chymotrypsin (1:1000 enzyme:substrate ratio). A mixed solution of trypsin and chymotrypsin had been previously prepared at a 4:1 ratio of their activities, respectively, according to the Protocol.

At all the stages, the solutions were kept in a shaker thermostatted at 37°C and stirred at 100 rpm.

To construct a parallel release profile, 0.3 g of liposomes was placed into a test tube and 2 mL of a simulating solution (SGFs or SIFs) was added to the tube. The liposomes were incubated for a given time, after which they were separated from the solution by centrifugation at 11,000 rpm for 30 min.

To construct a sequential release profile, 0.6 g of liposomes was placed into a test tube and 3 mL of a solution simulating the oral cavity (SSFs) was added to the tube. The mixture was incubated at 37°C for 15 min, after which the liposomes were separated by centrifugation at 11,000 rpm for 30 min. A solution simulating the stomach (SGFs) was then added to the microparticles and they were incubated for 90 min under the same conditions. The liposomes were separated by centrifugation in the same mode. Finally, a solution simulating the small intestine (SIFs) was added and the liposomes were incubated for 120 min under the same conditions. They were separated again, as described above.

At the end of the modeling, all the supernatants were analyzed for the concentrations of incorporated components by standard methods. Based on the data, we determined the degree of release of the target components under the influence of the gastrointestinal enzymes at each stage [44].

Modification of liposomes with chitosan. A chitosan solution was added dropwise with stirring to an

emulsion of liposomes obtained by the injection method (5 mg/mL) in a potassium phosphate buffer solution (pH 7.4) until a given concentration of chitosan in the emulsion was achieved. After that, the liposome-chitosan complexes were incubated for 1 h with vigorous stirring at room temperature. The modified liposomes were separated by centrifugation at 10,000 rpm for 7 min.

Modification of liposomes with ovalbumin ("protein corona"). Stock solutions of egg albumin with concentrations of 10–100 mg/mL were prepared in 0.01 M potassium phosphate buffer (pH 7.4). Liposomes were obtained by the injection method. The resulting emulsion was added dropwise to the protein solution in a volume ratio of 1:1 and mixed. The mixture was incubated at room temperature for 4 h and then centrifuged at 10,000 rpm for 7 min. To remove unbound protein, the liposomes were washed twice with distilled water and then centrifuged under the same conditions.

RESULTS AND DISCUSSION

Comparative analysis of the injection and thermal methods for obtaining soy lecithin liposomes. There are numerous methods for producing liposomes, but many of them are difficult to scale up for industrial use. Therefore, we aimed to compare the thermal and injection methods since both can be easily adapted for industrial production of liposomal forms of drugs.

To prepare liposomes by the thermal method, soy lecithin was used at concentrations of 0.75, 1.00, 2.00, and 3.00 wt. %. The resulting liposomes were examined microscopically with a magnification of 400×. The most optimal concentrations of soy lecithin were 1.0 and 3.0 wt. %. Therefore, these concentrations were used for further experiments (Fig. 1).

As can be seen in Fig. 1, the obtained liposomes were significantly heterogeneous in size. Therefore, they were homogenized using an IKA T25 digital ULTRA-TURRAX laboratory homogenizer. The select the best process time, solutions with a lipid content of 1.0 and 3.0 wt. % were homogenized for 15–120 s with an interval of 15 s. The homogenized particles were microscopically examined at each stage (Fig. 2). The sample homogenized for 90 s had even, rounded particles of approximately the same size. A further increase in time caused intense foam formation. Thus, 1.5 min was determined as the most optimal time, after which the size and shape of the preparations remained unchanged.

This experiment also showed that the suspensions with a phospholipid content of under 3.0 wt. % were most effectively homogenized, so this concentration was used for further analyses. The resulting liposomes were dried at 50°C.

According to laser light scattering, the size of the thermally obtained liposomes was 4–10 μm, which exceeded the permissible microparticle diameter of 100 nm–5 μm for oral drug delivery [45].

Next, we determined changes in the size and ζ-potential of the liposomes during incubation in various sections of the gastrointestinal tract for a parallel profile. For this, the stages of the gastrointestinal tract (oral cavity, stomach, and intestine) were simulated (Table 1).

We found that over time, the liposomes significantly increased in size in the gastrointestinal model. For example, exposure to the stomach environment for 120 min caused a ten-fold increase in size. At the same time, the ζ-potential of the liposomes decreased. This was due to the destruction of liposomes, as well as changes in the configuration of negatively charged polar groups

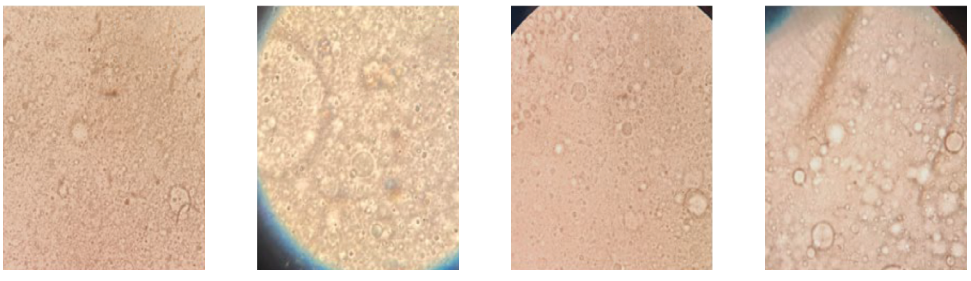

Figure 1 Liposomes prepared by the thermal method with soy lecithin contents of: (a) 0.75%; (b) 1.00%; (c) 2.00%; and (d) 3.00% (400× magnification)

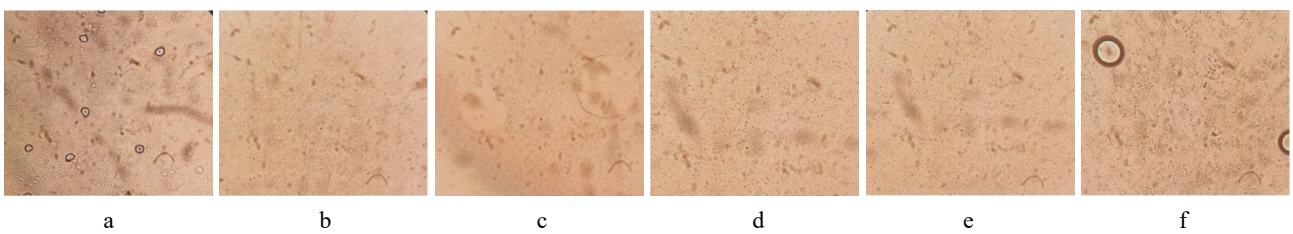

Figure 2 Liposomes prepared by the thermal method with 3% lecithin after homogenization for: (a) 15 s; (b) 45 s; (c) 75 s; (d) 90 s; (e) 105 s; and (f) 120 s (400× magnification)

Table 1 Changes in the size and ζ-potential of thermally obtained liposomes in model sections of the gastrointestinal tract for a parallel profile

Sample	ζ-potential, mV	Size, μm
Initial	36 ± 4	7.0 ± 0.4
Simulated salivary fluid (SSF) (15 min)	25 ± 2	17.5 ± 0.9
Simulated gastric fluid (SGF) (60 min)	25 ± 2	75.3 ± 3.8
Simulated gastric fluid (SGF) (120 min)	8 ± 1	115.5 ± 5.8
Simulated intestinal fluid (SIF) (30 min)	28 ± 3	65.4 ± 3.3
Simulated intestinal fluid (SIF) (60 min)	24 ± 2	43.3 ± 2.2

Table 2 Changes in the size and ζ-potential of thermally obtained liposomes in model sections of the gastrointestinal tract for a sequential profile

Sample	ζ-potential, mV	Size, μm
Simulated salivary fluid (SSF) (15 min)	34 ± 2	17.2 ± 0.9
Simulated gastric fluid (SGF) (120 min)	24 ± 1	68.3 ± 3.4
Simulated intestinal fluid (SIF) (60 min)	32 ± 2	46.7 ± 2.3

Table 3 Changes in the size and ζ-potential of liposomes obtained by injection in model sections of the gastrointestinal tract for a parallel profile

Sample	ζ-potential, mV	Size, μm
Initial	36 ± 4	4.7 ± 0.2
Simulated salivary fluid (SSF) (15 min)	25 ± 2	12.4 ± 0.6
Simulated gastric fluid (SGF) (60 min)	25 ± 2	45.3 ± 2.3
Simulated gastric fluid (SGF) (120 min)	8 ± 1	76.7 ± 3.8
Simulated intestinal fluid (SIF) (30 min)	28 ± 3	55.7 ± 2.8
Simulated intestinal fluid (SIF) (60 min)	24 ± 2	68.4 ± 3.4

Table 4 Changes in the size and ζ-potential of liposomes obtained by injection in model sections of the gastrointestinal tract for a sequential profile

Sample	ζ-potential, mV	Size, μm
Simulated salivary fluid (SSF) (15 min)	33 ± 2	12.4 ± 0.6
Simulated gastric fluid (SGF) (120 min)	25 ± 1	48.2 ± 2.4
Simulated intestinal fluid (SIF) (60 min)	21 ± 1	56.4 ± 2.8

of phospholipid molecules during oxidation. Moreover, the decrease in ζ-potential was caused by changes in the orientation near the surface of the bilayer membrane. As the liposomes passed through each of the gastrointestinal sections, their absolute ζ-potential values dropped to below 30 mV, which indicated liposomal adhesion. The greatest decrease was observed in the acidic environment of the stomach.

Then, we analyzed changes in the size and ζ-potential of the liposomes in the gastrointestinal model for a sequential profile. Samples were collected after the maximum incubation time for each gastrointestinal section – the oral cavity, stomach, and small intestine (Table 2).

The results for the sequential profile were similar to those for the parallel profile (increased particle size and decreased ζ-potential due to liposome destruction). The intestinal environment caused the particles to aggregate, with a decrease in the absolute value of ζ-potential and a slight decrease in size.

Since the preparation of liposomes by the thermal method was time-consuming (about 7 days), we aimed to study the injection method to speed up the process.

As lecithin has low solubility in ethyl alcohol, hexane was used as a solvent and then removed from the mixture by evaporation. We studied changes in the size and ζ-potential of liposomes in the model sections of the gastrointestinal tract for the parallel and sequential profiles (Tables 3 and 4).

We found similar tendencies in the behavior of the liposomes in the gastrointestinal model, regardless of the method of their preparation. However, the liposomes obtained by the injection method had a smaller diameter (4.7 ± 0.2 μm) compared to those obtained by the thermal method. This makes them more promising agents for oral drug delivery. Another advantage of the injection method is its shorter time. Therefore, liposomes were obtained by the injection method for further analyses.

Studying the degree of protein incorporation into liposomes. To determine the effectiveness of liposomes as target protein delivery systems, we studied the conditions that ensured the highest degree of protein incorporation. Albumin, globulin, and insulin were used as model proteins. They were encapsulated by passive diffusion into the pre-prepared liposomes. The liposomes were then separated by centrifugation for 20 min at 8000 rpm. The residual concentration of proteins in the supernatant was determined by the microbiuret method and the degree of their incorporation into liposomes was calculated (Figs. 3 and 4).

The most optimal concentration of albumin for liposomal incorporation was 30 mg/mL, with the incorporation degree of 83% (Fig. 3).

The most optimal concentration of insulin for liposomal encapsulation was 1.0 mg/mL, which was equivalent to a mixture of Actrapid® and 0.1 M phosphate buffer (1:4), pH 7.0. This concentration contributed to 98% of encapsulation (Fig. 4).

For immunoglobulin, the most optimal concentration was 1.6 mg/mL, which was equivalent to a 10-fold

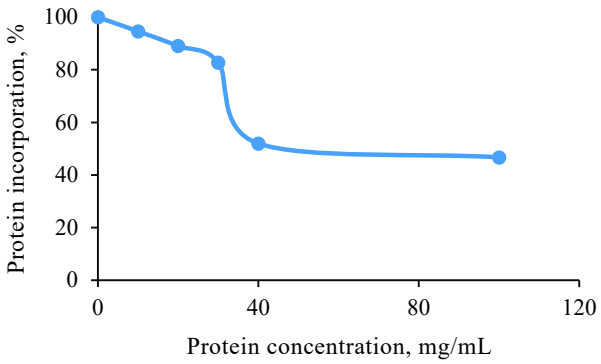

Figure 3 The degree of albumin incorporation into liposomes vs. the initial concentration of albumin in the solution

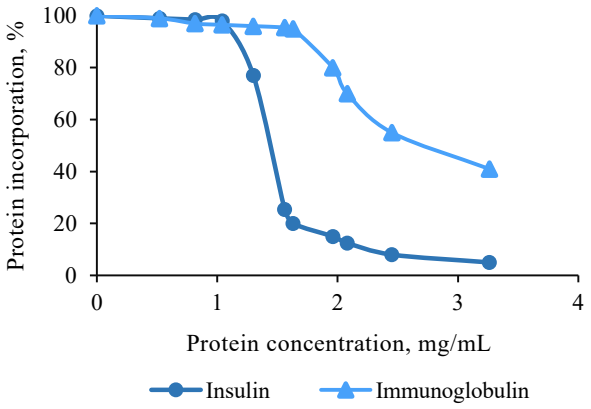

Figure 4 The degree of insulin and immunoglobulin incorporation into liposomes vs. the initial concentration of the proteins in the solution

dilution of Globfel-4 in 1.5 M phosphate buffer, pH 7.0. The degree of immunoglobulin incorporation was 95% (Fig. 4).

Based on the results, the capacity of liposomes was 207.0 mg/g for albumin, 8.5 mg/g for insulin, and 13.0 mg/g for immunoglobulin. The differences between the proteins might be due to their charge at the pH applied, as well as the size of their molecules. In particular, the isoelectric point is near pH 4.9 for albumin, 5.4 for insulin, and 5.2 for immunoglobulin.

The release of target components in the gastrointestinal tract is an important aspect to determine the efficiency of drugs in liposomal form. Therefore, we aimed to study the behavior of protein-loaded liposomes in the model gastrointestinal sections.

Studying protein release from liposomes in the in vitro models of human gastrointestinal tract. An experiment similar to the one for unloaded liposomes was carried out to analyze the release of incorporated proteins in parallel and sequential profiles. Liposomal vesicles were incubated in the respective model sections of the gastrointestinal tract and separated by centrifugation. The residual protein concentrations in the supernatants were measured by the biuret method to calculate the degree of protein release. The results are presented in Fig. 5 for the parallel profile and in Fig. 6 for the sequential profile.

In the parallel profile, the degree of albumin release from the liposomes reached 17% in the oral cavity (with 11% released in the first 5 min of incubation), 38% in the stomach, and 53% in the intestine. Insulin showed the highest degree of release in the stomach (about 50%), 30% in the intestine (28% in the first 30 min), and about 15% in the oral cavity. Similar results were obtained for immunoglobulin: 16% released in the oral cavity, 38% in the stomach, and 50% in the small intestine.

The sequential profile showed the following patterns of protein release. The lowest degree of release was observed in the oral cavity for all the proteins (11, 15, and 17% for albumin, insulin, and immunoglobulin,

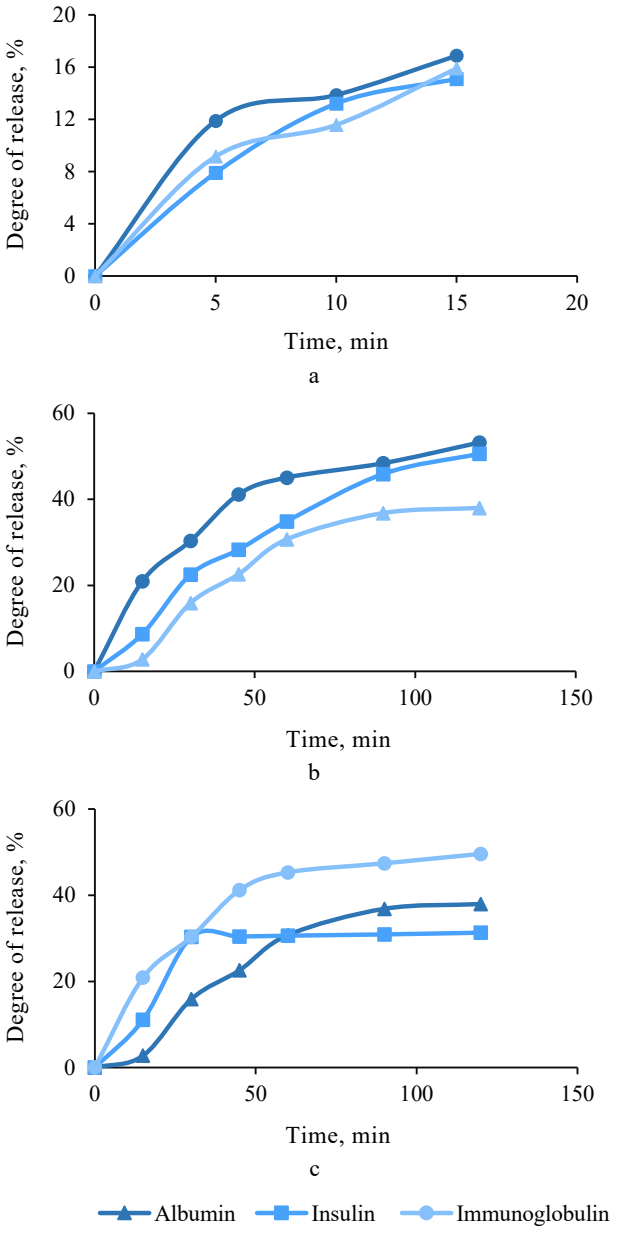

Figure 5 Parallel profile of protein release from liposomes *in vitro* in the models: (a) oral cavity (SSF); (b) stomach (SGF); and (c) intestine (SIF)

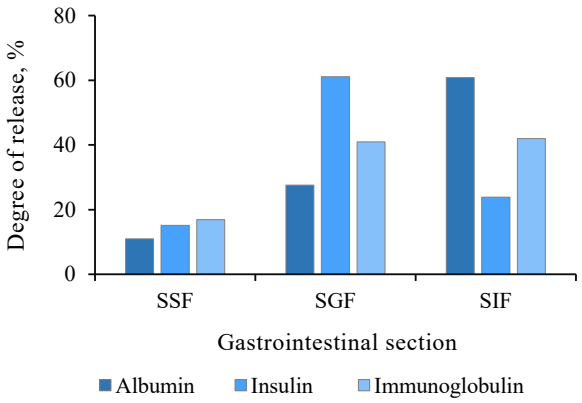

Figure 6 Sequential profile of protein release in the model gastrointestinal sections

respectively). Yet, there were some differences in the subsequent model sections. Albumin and immunoglobulin showed the greatest release (64 and 42%, respectively) in the small intestine, while in the stomach their release reached 28 and 41%, respectively. The maximum amount of insulin (61%) was released in the stomach. The differences between the proteins might be due to their charge at the pH of the model gastrointestinal environment. In the stomach model, albumin was less positively charged compared to the other proteins.

According to our results, the liposomes loaded with albumin showed the greatest loading capacity and degree of release in the gastrointestinal tract. Therefore, they were used for further analyses. However, due to the high degree of albumin release in the stomach, the liposomes need to be stabilized.

Currently, there is a trend towards producing complex liposomal preparations containing several high- and low-molecular components. In this study, we used amino acids, vitamins, and microelements as low-molecular components. In each case, we determined the capacity of liposomes for these components, as well as their release from liposomes in the model gastrointestinal sections in a sequential profile.

Incorporation of amino acids into liposomes. Amino acids such as arginine, alanine, proline, serine, lysine, tryptophan, and histidine are used in medicine to prevent and treat various diseases. Their incorporation into liposomes can enhance the therapeutic effect of other medicinal substances. When used together with proteins, they can improve the amino acid score of the resulting drugs.

Arginine, alanine, proline, and serine are nonessential amino acids. Arginine is one of the key metabolites in nitrogen metabolism processes. It participates in the synthesis of creatine, which is part of muscle tissue, and also strengthens the immune system [46]. Alanine is a source of energy. It promotes the synthesis of carbohydrates, the removal of toxins from the liver, and the absorption of glucose. The intake of these amino acids is important for increased physical activity or stress. Proline and serine are neuromodulators. They are present in significant amounts in the human brain and regulate memory functions and the nervous system as a whole. Their deficiency can lead to disorders of the nervous system, Alzheimer's disease, and encephalopathy [47]. Lysine, tryptophan, and histidine are essential amino acids. Lysine and histidine are the main components of neuronal proteins, tRNA, and nucleoprotein complexes of ribosomes, stimulating RNA synthesis in nerve cells [48]. Their deficiency can lead to anemia, enzyme deficiency, and epileptic seizures. When tryptophan enters the blood, it binds to albumin, facilitating the transfer of amino acids to the central nervous system through the blood-brain barrier. Tryptophan deficiency causes the development of pellagra and dementia.

The amino acids were incorporated into liposomes by the injection method. For each amino acid, we determined a concentration that ensured its complete incorporation into the liposomes. For this, the liposomes were separated by centrifugation and the residual concentration of the amino acid in the supernatant was determined by the ninhydrin method. Based on the data, we calculated the degree of amino acid incorporation and the capacity of the liposomes (Fig. 7, Table 5).

As can be seen, the highest degree of incorporation was observed for tryptophan (94%), histidine (98%), proline (91%), and lysine (95%).

In order to create complex liposomal preparations, the liposomes were loaded with mixtures of two and all seven amino acids. Their ratios were based on the previously established liposomal capacities and the amino acid score (Table 6). The experiment was carried out as described above.

As can be seen, the co-incorporation of amino acids into the liposomes increased the percentages of the target components compared to individual amino acids. The arginine-serine mixture had the highest degree of incorporation (96%).

Next, we studied the release of the amino acids under gastrointestinal tract conditions in a sequential profile. The experiment was carried out as described above for the protein-loaded liposomes. Figure 8 shows the release of individual amino acids, while Fig. 9 shows the release of amino acid mixtures.

According to our results, significant amounts of the amino acids (up to 35%) were released in the oral cavity and the stomach, while their residual amounts (up to 20%) were released in the intestine. The release of amino acid mixtures decreased to 10–12% in the oral cavity, except for the histidine-proline mixture (48%). Their release in the stomach remained high, with 75% for the arginine-serine mixture. The lysine-tryptophan mixture showed maximum release in the intestine. Thus, incorporating amino acids into liposomes without additional components did not have a stabilizing effect in the model gastrointestinal tract.

Incorporation of vitamins into liposomes. Vitamins B_2 and C were chosen as auxiliary components incorporated into liposomes to increase the stability, therapeutic activity, and bioavailability of the target

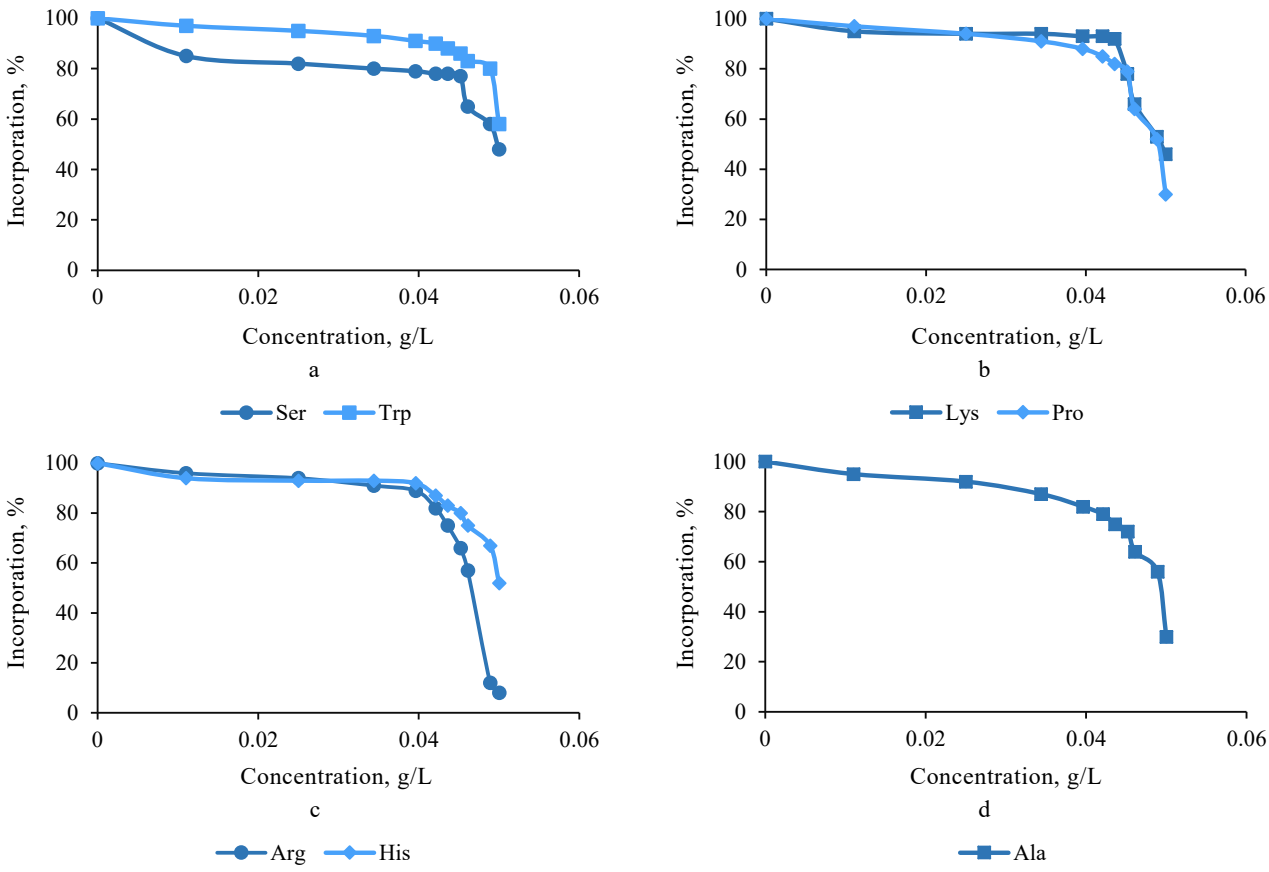

Figure 7 Incorporation of amino acids into liposomes vs. their concentration in the initial emulsion

Table 5 Amino acid incorporation into liposomes

Amino acid	Concentration, mg/L	Incorporation, %	Capacity, mg/mg
Ala	25.0	89	0.122
Ser	38.0	86	0.160
Trp	40.0	94	0.149
His	40.0	98	0.141
Pro	34.4	91	0.141
Arg	40.0	88	0.141
Lys	42.2	95	0.155

Table 6 Incorporation of amino acid mixtures into liposomes

Amino acid mixture	Concentration of amino acids in the mixture, mg/L	Incorporation, %	Specific content of amino acids, mg/g
Arg Ser	8.6 38.4	96	0.167
Lys Ala	42.0 17.6	84	0.211
His Pro	16.3 40.0	89	0.200
Trp Lys	4.0 40.0	79	0.156
Arg Ser Lys Ala His Pro Trp	8.6 2.5 3.6 1.5 1.4 4.2 0.3	90	0.078

preparation. These vitamins participate in the proliferation of B- and T-cells, increase the expression of cytokines, and improve the differentiation of immune cells with the formation of leukocytes [49].

The experiments were carried out as described above. The vitamins were incorporated in the concentrations corresponding to their average daily requirement (0.2 μg/mL for riboflavin and 3.4 μg/mL for ascorbic acid).

Table 7 shows the degree of incorporation of vitamins B_2 and C into the liposomes loaded with individual amino acids and their mixtures. As can be seen, vitamin B_2 had the highest degree of incorporation with serine (95%), tryptophan (91%), histidine (92%), and lysine (94%). The incorporation of vitamin C exceeded 90% with all the amino acids under study.

The co-incorporation of both vitamins (B_2 and C) into the liposomes loaded with amino acid mixtures was 88%. This might be due to a partial loss of vitamin activity during the preparation and storage of the liposomal mixtures, as well as the biodegradation of the liposomal form. As a result, these preparations could not provide the average daily requirements for vitamins B_2 and C.

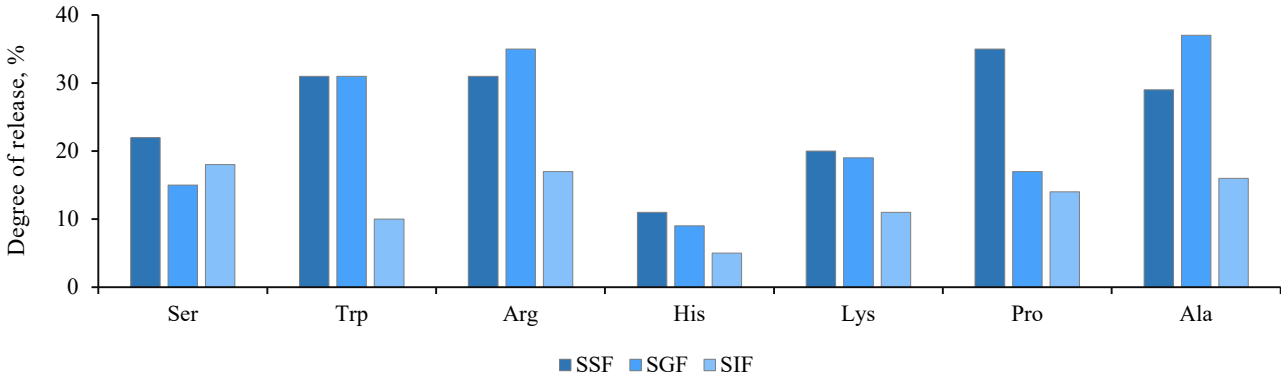

Figure 8 Release of amino acids from liposomes in model gastrointestinal tract in a sequential profile

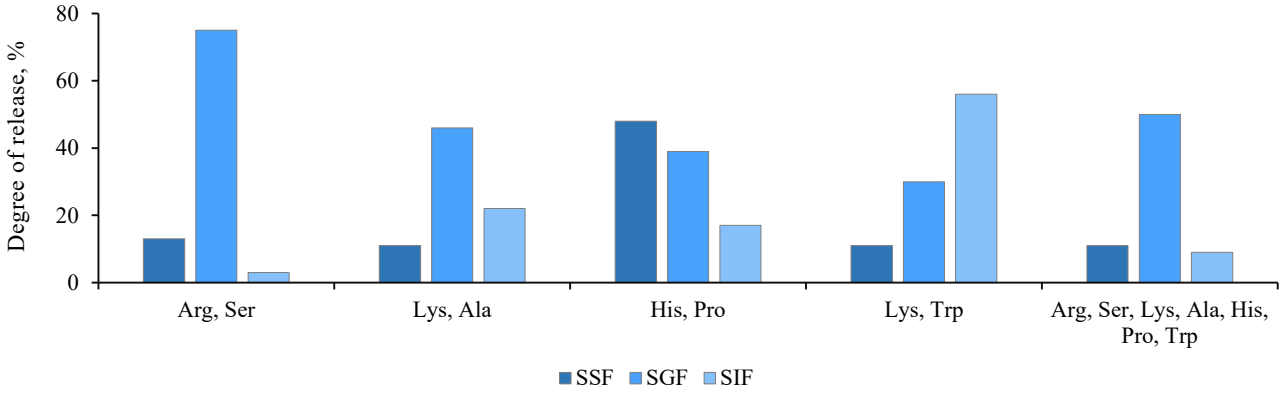

Figure 9 Release of amino acid mixtures from liposomes in model gastrointestinal tract in a sequential profile

Table 7 Incorporation of vitamins B_2 and C into liposomes loaded with amino acids

Amino acid	Incorporation, %		Liposome capacity, μg/mg	
	Vitamin B_2	Vitamin C	Vitamin B_2	Vitamin C
Arg	84	99	0.596	11.94
Ala	88	95	0.625	11.46
Ser	95	98	0.674	11.82
Trp	91	97	0.646	11.70
His	92	98	0.653	11.82
Pro	86	91	0.610	10.98
Lys	94	98	0.667	11.82

Incorporation of microelements into liposomes. Zinc and iron (III) were used as soluble salts to study the effect of microelements on the stability of liposomes. Their bioavailability for the human body is quite low (3–5% for iron and 48% for zinc). The problem of iron absorption is associated with the fact that excess iron ions bind to ferroportin, causing its degradation and storing Fe^{3+} in the form of ferritin. Therefore, the bioavailability of iron (III) ions can be improved by their co-incorporation into liposomes together with B vitamins. Zinc should be combined with vitamin C to improve the absorption of both components in the lymphoid system of the small intestine, without causing any side effects for the other organs [50].

The liposomes were obtained as described above. The microelements were added in the concentrations corresponding to their daily requirements (4.67 μg/mL for Fe^{3+} and 3.00 μg/mL for Zn^{2+}).

According to the results, the degrees of incorporation of iron (III) and zinc ions into the liposomes loaded with amino acids were 98 and 94%, respectively. Noteworthily, the incorporation of amino acids was at least 94%, which might be due to their binding to the metal ions.

Modeling the digestion of liposomes loaded with amino acids and a vitamin-and-mineral complex. We analyzed the release of amino acids from the liposomes loaded with albumin, vitamins B_2 and C, as well as Fe^{3+} and Zn^{2+} ions, in the model gastrointestinal tract (Fig. 10).

The total degree of amino acid release was 90%. Noteworthily, the incorporation of vitamins and microelements led to their stabilization in the oral cavity and stomach, with release degrees of 15 and 27%, respectively. This improved their release and bioassimilation in the small intestine.

Formation of the protein corona. According to literature, the interaction of proteins with lipid vesicles leads not only to liposomal encapsulation, but also to the formation of a protein corona on the surface. The term "protein corona" was proposed in 2007 to describe the spontaneous aggregation and coating of proteins around the surface of nanoparticles [51]. Further studies have

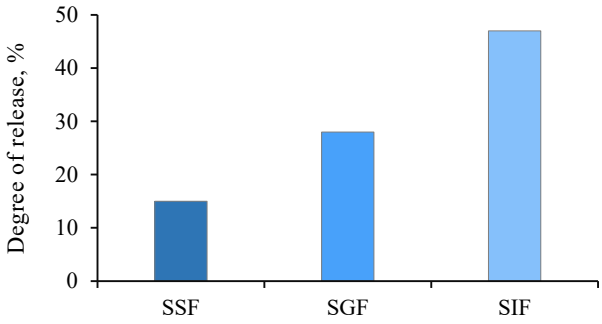

Figure 10 Amino acid release from liposomes with a vitamin-and-mineral complex under *in vitro* digestion conditions

Table 8 Changes in the size and ζ-potential of liposomes depending on the concentration of the albumin solution used for surface modification

Egg albumin solution, mg/mL	Size, μm	ζ-potential, mV
0	4.7 ± 0.2	37 ± 2
10	8.0 ± 0.4	36 ± 2
20	10.6 ± 0.5	34 ± 2
30	12.8 ± 0.6	33 ± 2
40	15.2 ± 0.8	31 ± 3
100	19.0 ± 1.0	28 ± 2

shown that protein adsorption plays an important role in many biological processes [52]. Fundamentally, a protein corona consists of an internal and an external layers. The internal layer ("hard corona") includes tightly bound protein molecules, while the external layer ("soft corona") is represented by proteins that are in dynamic equilibrium with the solution [53].

Protein coronas, which form on the surface of microparticles by changing the surface charge, can help improve the permeability of the intestinal epithelium. This can facilitate the oral administration of drugs and their absorption *in vivo* [54].

Egg albumin was used for a protein corona to form. It has a negative charge at neutral pH and can be adsorbed on the surface of a cationic carrier due to electrostatic attraction. This changes the positive charge of the surface and forms electrically neutral particles.

As we studied the formation of a protein corona on the surface of liposomes, we determined changes in the size and ζ-potential of the particles depending on the concentration of the albumin solution (Table 8).

As can be seen, higher concentrations of egg albumin in the solution for surface modification caused an increase in the liposome size and a decrease in the absolute value of ζ-potential, which indicated the formation of a protein corona. No particles had a charge closer to neutral. This might be due to the heterogeneous albumin coating of the liposomes.

The size distribution of the resulting liposomes is shown in Fig. 11. We found that high concentrations of albumin increased the number of large liposomes. For example, the sample with an albumin concentration of 100 mg/mL had only 10% of liposomes with a diameter of less than 15 μm.

The formation of a protein corona on the surface of the liposomes can improve the bioavailability of orally administered drugs. Since liposomes under 5 μm in size are used for oral administration, the concentration of albumin should not exceed 10 mg/L for a protein corona to form.

Effect of surface modification on the properties of liposomes. The liposome surface can be modified with chitosan to improve prolonged release of protein and, therefore, its bioavailability. In this experiment, aliquots of the liposomal emulsion were mixed with equal volumes of chitosan solutions at various concentrations. Egg albumin was used as a model protein.

We analyzed changes in the size of liposomes depending on the concentration of chitosan used for modification (Table 9). As can be seen, higher concentrations of chitosan increased the average size of liposomal particles. These findings were confirmed by the distribution of liposomes by size (Fig. 12).

A 0.1% chitosan solution was chosen for further analyses since this concentration provided a significant proportion of liposomes up to 6 μm in size, which is important for oral drug administration.

Effect of antioxidants on the stability of liposomes. Storage of liposomes is challenging due to their instability and high degradability. The stability of liposomes depends on many factors, such as the composition of lipids, the size and shape of particles, the density of packaging, as well as temperature and humidity.

Lipid peroxidation is one of the main causes of liposome destruction [55]. Antioxidants such as vitamin E can be used to reduce the risk of lipid peroxidation and improve the stability of liposomes.

For this experiment, liposomes were loaded with albumin. During their preparation by the injection method, alpha-tocopherol acetate was added to the liposomal mixture at concentrations of 5, 10, and 20 mg per 1 g of lecithin. We analyzed changes in the size and ζ-potential of the liposomes depending on the content of vitamin E, as well as their size distribution (Table 10, Fig. 13).

According to the data, the liposomal emulsions without tocopherol and those with 5 and 10 mg/g of tocopherol were stable and not prone to aggregation. Increasing the content of vitamin E to 20 mg/g caused the liposomes to grow in size (from 4.7 to 18.5 μm).

Next, we studied the behavior of the liposomes modified with a protein corona, chitosan, and vitamin E in the model gastrointestinal tract in a sequential profile (Fig. 14). As can be seen, the liposomes stabilized with vitamin E showed maximum release in the small intestine. This can improve the availability of the drug.

Finally, we analyzed changes in the peroxide value to determine the stability and degree of destruction of liposomes during long-term storage (Fig. 15). According to the results, 10 mg vitamin E/g liposomal base was most effective in reducing the degree of liposome degradation during storage.

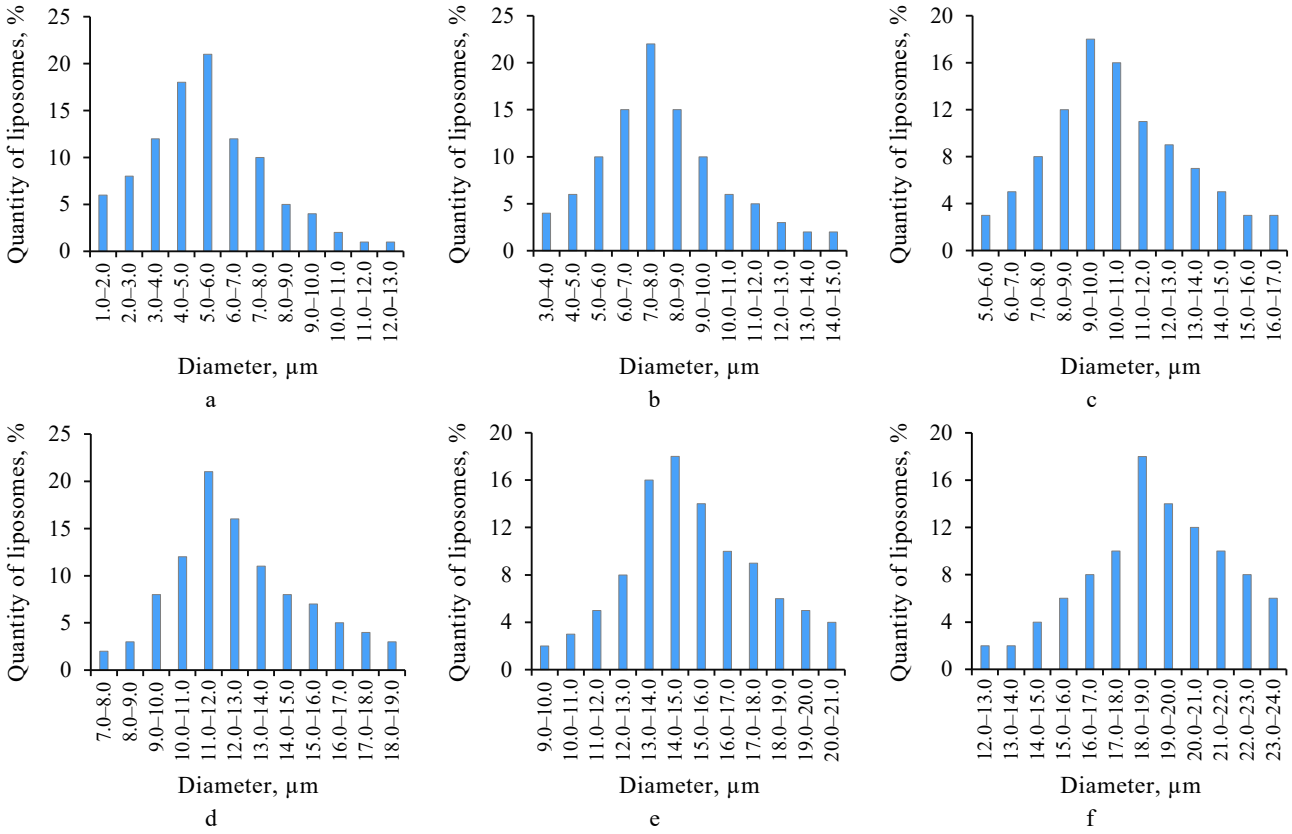

Figure 11 Liposome size distribution after surface modification with albumin at various concentrations, mg/mL: (a) 0; (b) 10; (c) 20; (d) 30; (e) 40; and (f) 100

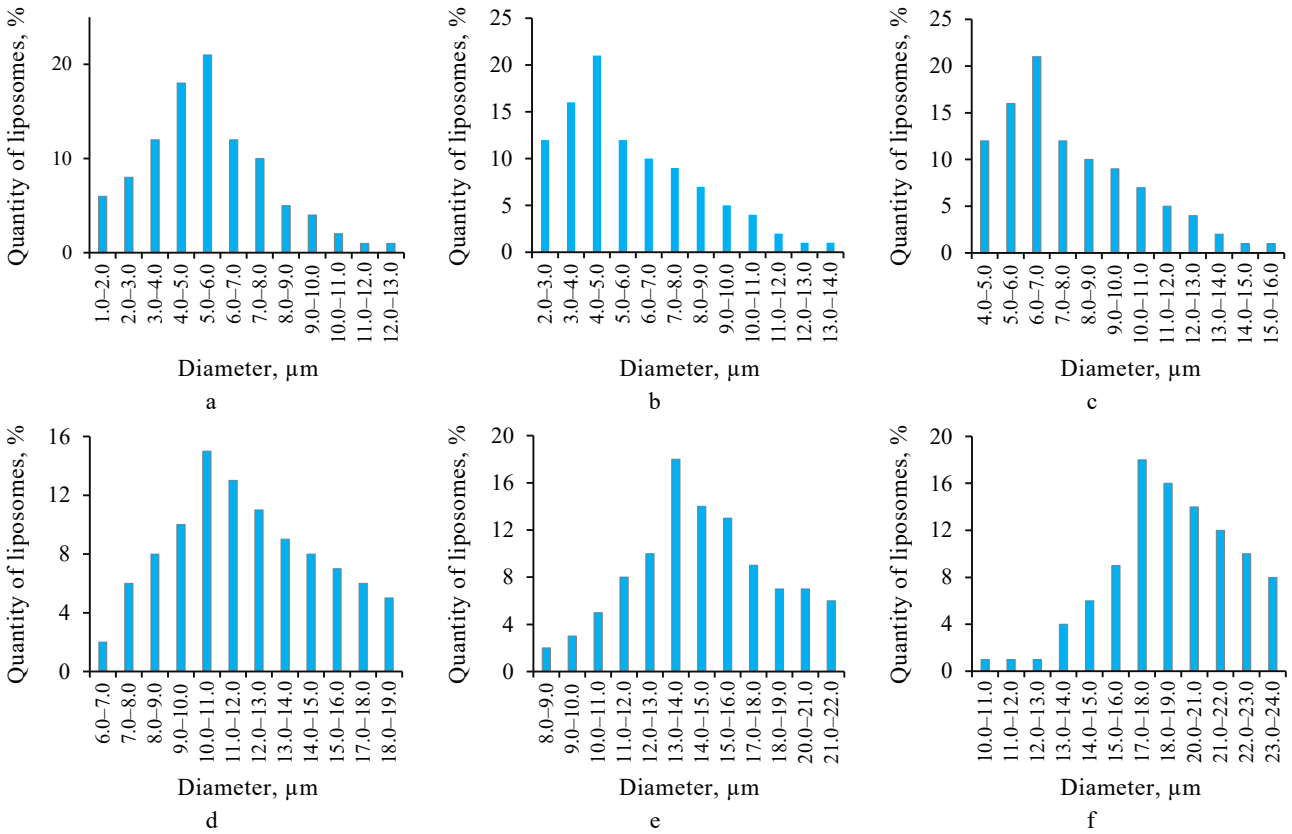

Figure 12 Distribution of liposomes by size depending on chitosan concentration, %: (a) 0; (b) 0.10; (c) 0.15; (d) 0.30; (e) 0.40; and (f) 0.50

Table 9 Changes in the liposome size depending on the chitosan concentration used for modification

Chitosan, %	Size, μm
0	4.7 ± 0.2
0.10	5.8 ± 0.3
0.15	7.8 ± 0.4
0.30	12.1 ± 0.6
0.40	14.9 ± 0.7
0.50	18.8 ± 0.9

Table 10 Changes in the size and ζ-potential of liposomes depending on the content of vitamin E

Vitamin E, mg/g	ζ-potential, mV	Size, μm
0	37 ± 2	4.7 ± 0.2
5	32 ± 2	5.2 ± 0.3
10	28 ± 2	12.8 ± 0.6
20	25 ± 1	18.5 ± 0.9

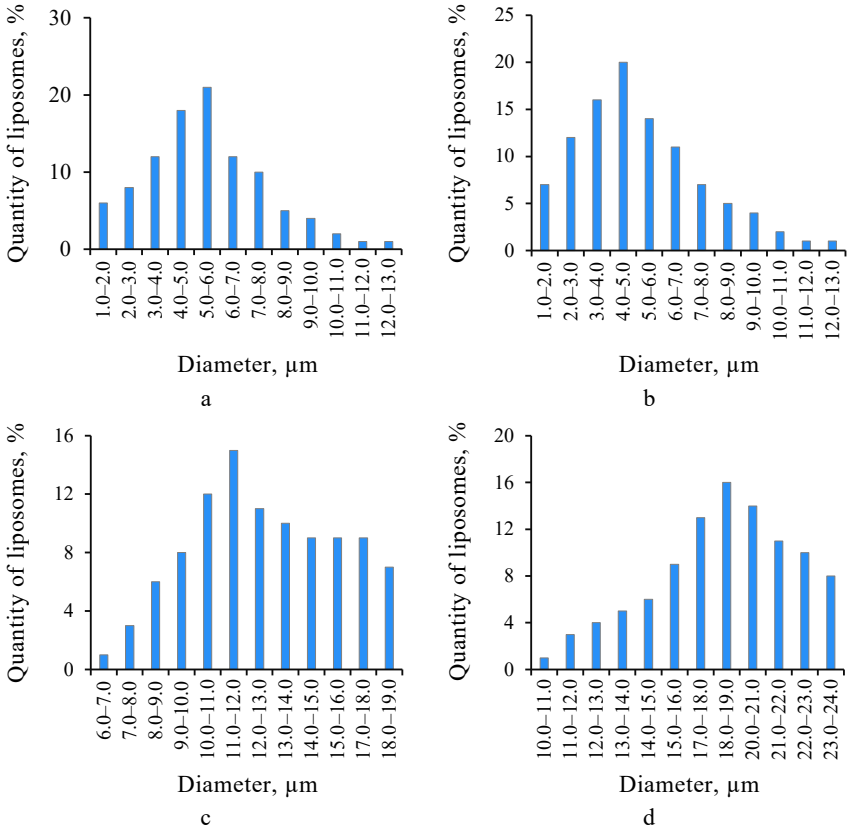

Figure 13 Liposome size distribution with vitamin E modification at concentrations, mg/g: (a) 0; (b) 5; (c) 10; and (d) 20

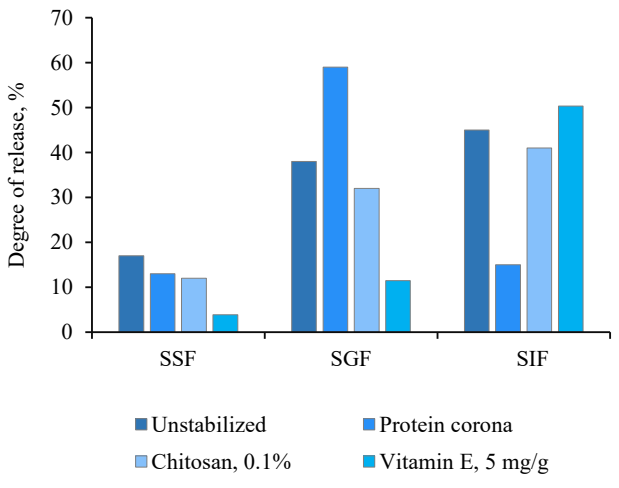

Figure 14 Release of egg albumin from liposomes stabilized in different waysna

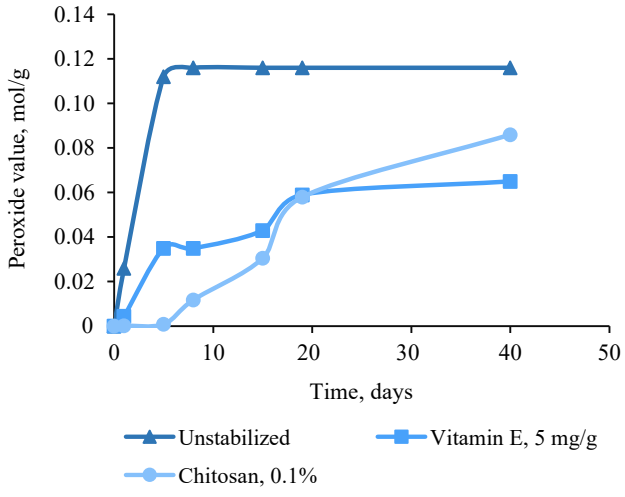

Figure 15 Changes in peroxide value during long-term storage of liposomes

CONCLUSION

Our study showed that the liposomes obtained by the thermal and injection methods had similar properties. However, the injection method produced liposomes with a smaller diameter (4.7 ± 0.2 μm), which made them more promising agents for oral drug delivery. Other advantages of the injection method over the thermal method are ease of use and a shorter duration.

Protein therapy is a promising tool for the future of medicine. Therefore, ways need to be found to prevent the destruction of protein molecules in the gastrointestinal tract. We analyzed the degrees of protein incorporation into liposomes using albumin, insulin, and globulin as model proteins. The most optimal concentrations of albumin, insulin, and globulin were 30, 1.0, and 1.6 mg/mL, respectively. These concentrations ensured their incorporation at 83, 98, and 95%, respectively.

We determined the concentrations of amino acids (arginine, alanine, proline, serine, lysine, tryptophan, and histidine) and their mixtures that ensured their maximum incorporation into liposomes. Among individual amino acids, the highest degrees of incorporation were 94% for tryptophan, 98% for histidine, 91% for proline, and 95% for lysine. Among the mixtures, maximum incorporation was observed for the arginine-serine mixture (96%) and for the mixture of all the amino acids (90%).

The liposomes were stabilized by incorporating vitamins B_2 and C, as well as microelements (zinc and iron (III) ions) in the form of easily digestible salts. We found that a vitamin and mineral complex increased the degree of incorporation of amino acid mixtures into liposomes to 94%.

We studied the release of amino acids from the liposomes loaded with amino acids, albumin, vitamins B_2 and C, and microelements (iron (III) and zinc ions) in the model gastrointestinal tract. The degree of amino acid release was 99%, with 54% released in the small intestine, which indicated a significant degree of drug stabilization and accessibility.

Our results showed a positive effect of the protein corona on the bioavailability of liposomes for oral drug administration. In particular, the protein corona changed the charge of nanoparticles, thereby facilitating drug absorption *in vivo*.

We analyzed the release of albumin, insulin, and globulin under simulated gastrointestinal conditions in both parallel and sequential profiles. Encapsulated albumin had the highest release (64%) in the small intestine, which indicated its efficiency for oral drug delivery and protection in the acidic environment of the stomach. For insulin and globulin, the release degrees were 28 and 50%, respectively.

Antioxidants can be incorporated to improve the stability of liposomes during storage. According to our results, 10 mg of vitamin E per 1 g of liposomal base was the most effective concentration for reducing the degree of liposome degradation during storage.

Modifying the surface of liposomes with chitosan decreased the degree of albumin release in the oral cavity, the stomach, and the intestine by 30, 16, and 11%, respectively.

CONTRIBUTION

A.A. Krasnoshtanova supervised the study, managed the data, and edited the manuscript. I.A. Tsepeleva designed the concept, developed the methodology, conducted the study, and wrote a draft of the manuscript. A.N. Yudina edited the manuscript.

CONFLICT OF INTEREST

The authors declared no conflict of interest regarding the publication of this article.

REFERENCES

1. Ye C, Chi H. A review of recent progress in drug and protein encapsulation: Approaches, applications and challenges. Materials Science and Engineering: C. 2018;83:233–246. https://doi.org/10.1016/j.msec.2017.10.003
2. El-Fakharany EM, El-Gendi H, Saleh AK, El-Sayed MH, Alalawy AI, *et al*. The use of proteins and peptides-based therapy in managing and preventing pathogenic viruses. International Journal of Biological Macromolecules. 2024;270(Part 2):132254. https://doi.org/10.1016/j.ijbiomac.2024.132254
3. Pogmore JP, Uehling D, Andrews DW. Pharmacological targeting of executioner proteins: Controlling life and death. Journal of Medicinal Chemistry. 2021;64(9):5276–5290. https://doi.org/10.1021/acs.jmedchem.0c02200
4. Li X, Yu J, Dong Y, Shen X, Hou R, *et al*. Protein acetylation and related potential therapeutic strategies in kidney disease. Pharmacological Research. 2023;197;106950. https://doi.org/10.1016/j.phrs.2023.106950
5. Choudhury A, Sonowal K, Laskar RE, Deka D, Dey BK. Liposome: A carrier for effective drug delivery. Journal of Applied Pharmaceutical Research 2020;8(1):22–28. https://doi.org/10.18231/j.joapr.2019.v.8.i.1.003
6. Almeida B, Nag OK, Rogers KE, Delehanty JB. Recent progress in bioconjugation strategies for liposome-mediated drug delivery. Molecules. 2020;25(23):5672. https://doi.org/10.3390/molecules25235672
7. Bobrysheva TN, Anisimov GS, Zolotoreva MS, Evdokimov IA, Budkevich RO, *et al*. Encapsulated polyphenols in functional food production. Foods and Raw Materials. 2025;13(1):18–34. https://doi.org/10.21603/2308-4057-2025-1-620

8. Wang Y, Fernandes RMF, Marques EF. From single gemini surfactants in water to catanionic mixtures with the bile salt sodium taurodeoxycholate: Extensive micellar solutions, coacervation and liquid crystal polymorphism as revealed by phase behavior studies. Journal of Molecular Liquids. 2019;285:330–337. https://doi.org/10.1016/j.molliq.2019.04.067
9. Morais D, Tanoeiro L, Marques AT, Concalves T, Duarte A, *et al*. Liposomal delivery of newly identified prophage lysins in a *Pseudomonas aeruginosa* model. International Journal of Molecular Sciences. 2022;23(17):10143. https://doi.org/10.3390/ijms231710143
10. Liu P, Chen G, Zhang J. A review of liposomes as a drug delivery system: Current status of approved products, regulatory environments, and future perspectives. Molecules. 2022;27(4):1372. https://doi.org/10.3390/molecules27041372
11. Yüzer MO, Gençcelep H. Sesame seed protein: Amino acid, functional, and physicochemical profiles. Foods and Raw Materials. 2023;11(1):72–83. https://doi.org/10.21603/2308-4057-2023-1-555
12. Halavach TM, Kurchenko VP, Tarun EI, Romanovich RV, Mushkevich NV, *et al*. Chitosan complexes with amino acids and whey peptides: Sensory and antioxidant properties. Foods and Raw Materials. 2024;12(1):13–21. https://doi.org/10.21603/2308-4057-2024-1-584
13. McGregor C, Perrin C, Monck M, Camilleri P, Kirby AJ. Rational approaches to the design of cationic gemini surfactants for gene delivery. Journal of the American Chemical Society. 2001;123(26):6215–6220. https://doi.org/10.1021/ja005681c
14. Yang P, Singh J, Wettig S, Foldvari M, Verrall RE, *et al*. Enhanced gene expression in epithelial cells transfected with amino acid-substituted gemini nanoparticles. European Journal of Pharmaceutics and Biopharmaceutics. 2010;75(3):311–320. https://doi.org/10.1016/j.ejpb.2010.04.007
15. Denieva ZG, Koloskova OO, Gileva AM, Budanova UA, Sebyakin YuL. Mixed cationic liposomes based on *L*-amino acids as effective means of delivery of therapeutic molecules into cells. Biologiceskie Membrany. 2023;40(3):203–216. https://doi.org/10.31857/S0233475523030052
16. Tosato M, Calvani R, Picca A, Ciciarello F, Galluzzo V, *et al*. Effects of L-arginine plus vitamin C supplementation on physical performance, endothelial function, and persistent fatigue in adults with long COVID: A single-blind randomized controlled trial. Nutrients. 2022;14(23):4984. https://doi.org/10.3390/nu14234984
17. Eremeeva NB. Nanoparticles of metals and their compounds in films and coatings: A review. Foods and Raw Materials. 2024;12(1):60–79. https://doi.org/10.21603/2308-4057-2024-1-588
18. Singh H, Thompson A, Liu W, Corredig M. Liposomes as food ingredients and nutraceutical delivery systems. Encapsulation Technologies and Delivery Systems for Food Ingredients and Nutraceuticals. United Kingdom: Woodhead publishing series in food science, technology and nutrition; 2012, pp. 287–318. https://doi.org/10.1533/9780857095909.3.287
19. Praskova JA, Kiseleva TF, Reznichenko IYu, Frolova NA, Shkrabtak NV, *et al*. Biologically active substances of *Vitis amurensis* Rupr.: Preventing premature aging. Food Processing: Techniques and Technology. 2021;51(1):159–169. (In Russ.) https://doi.org/10.21603/2074-9414-2021-1-159-169
20. Nechaev AP, Samoilov AV, Bessonov VV, Nikolaeva YuV, Tarasova VV, *et al*. Influence of antioxidants in native and micellized forms on shelf life of emulsion fat product. Problems of Nutrition. 2020;89(5):101–109. (In Russ.) https://doi.org/10.24411/0042-8833-2020-10070
21. Zaitsev VV, Shestakova SV, Voevodina YuA, Ryzhakina TP. Physiological reaction of hemostasis in piglets caught in unfavorable environmental conditions for the inclusion of the lipipital preparation lipovitam-beta in their diet. Research Journal of Pharmaceutical, Biological and Chemical Sciences. 2019;10(1):2068–2074. https://elibrary.ru/YSEIBV
22. Gupta A, Kalyanram P, Stadler I. Interaction of riboflavin-5-phosphate with liposome bilayers. Journal of Nanotoxicology and Nanomedicine. 2018;3(1):49–59. https://doi.org/10.4018/JNN.2018010103
23. Brzezińska J, Szewczyk A, Brzezicha J, Prokopowicz M, Grembecka M. Evaluation of physicochemical properties of beetroot-based dietary supplements. Foods. 2021:10(8):1693. https://doi.org/10.3390/foods10081693
24. Lo JO, Benson AE, Martens KL, Hedges MA, McMurry HS, *et al*. The role of oral iron in the treatment of adults with iron deficiency. European Journal of Haematology. 2023;110(2):123–130. https://doi.org/10.1111/ejh.13892
25. Fedorova TA, Borzykina OM, Strelnikova EV, Danilov AYu, Ivanets TYu. Correction of iron deficiency anemia in patients with menorrhagia. Gynecology. 2017;19(1):68–73. https://doi.org/10.17116/repro201723450-55
26. Taherinia S, Heidari Z, Salehidoost R, Karimifar M, Arab A, *et al.* Associations between empirically derived dietary patterns and oxidative stress and inflammation in adults with primary hypothyroidism: A case-control study. BMC Endocr Disord. 2023;23:105. https://doi.org/10.1186/s12902-023-01348-9
27. Zinc and Hydroxychloroquine in COVID19 and Sars-CoV2. Clinical Trials Registry – ICH GCP. [cited 2024 Oct 10]. Available from: https://ichgcp.net/clinical-trials-registry/

28. Robson AL, Dastoor PC, Flynn J, Palmer W, Martin A, *et al*. Advantages and limitations of current imaging techniques for characterizing liposome morphology. Frontiers in Pharmacology. 2018;9:80. https://doi.org/10.3389/fphar.2018.00080
29. Ivanov LV, Scherbak AV, Kravchenko VG, Derimedved LV, Suprun EV. Study of mechanisms of cytotoxicity spectrum expansion of pegylated liposomal delivery systems. World Science. 2019;3(6):26–36. (In Russ.) https://doi.org/10.31435/rsglobal_ws/30062019/6573
30. Ding Y, Yang R, Yu W, Hu C, Zhang Z, *et al.* Chitosan oligosaccharide decorated liposomes combined with TH302 for photodynamic therapy in triple negative breast cancer. Journal of Nanobiotechnology. 2021;19:147. https://doi.org/10.1186/s12951-021-00891-8
31. Kianfar E. Protein nanoparticles in drug delivery: Animal protein, plant proteins and protein cages, albumin nanoparticles. Journal of Nanobiotechnology. 2021;19:159. https://doi.org/10.1186/s12951-021-00896-3
32. Kurchenko VP, Halavach TM, Sushynskaya NV, Tarun EI, Dudchik NV, *et al*. Multicomponent composites of cyclodextrin nanocomplexes with biologically active substances for functional foods. Food Processing: Techniques and Technology. 2022;52(2):375–389. (In Russ.) https://doi.org/10.21603/2074-9414-2022-2-2370
33. Kenchappa V, Wahl M, Heinle H. Liposomes as carriers of resveratrol and vitamin E: Evaluating ameliorative antioxidant effect using chemical and cellular test systems. International Journal for Vitamin and Nutrition Research. 2022;92(5–6):342–348. https://doi.org/10.1024/0300-9831/a000680
34. Wang S, Chen Y, Guo J, Huang Q. Liposomes for tumor targeted therapy: A review. International Journal of Molecular Sciences. 2023;24(3):2643. https://doi.org/10.3390/ijms24032643
35. Kurakin MS, Ozherel'eva AV, Motyreva OG, Krapiva TV. A new approach to the development of food products. Food Processing: Techniques and Technology. 2021;51(3):434–448. (In Russ.) https://elibrary.ru/ZDZMEX
36. Moliboga EA, Sukhostav EV, Kozlova OA, Zinich AV. Functional food market analysis: Russian and international aspects. Food Processing: Techniques and Technology. 2022;52(4):775–786. (In Russ.) https://doi.org/10.21603/2074-9414-2022-4-2405
37. Gumerov TY, Mingaleeva ZS, Reshetnik OA. Recipes development and evaluation of quality and safety indicators for cereal products. Food Industry. 2022;7(1):70–81. (In Russ.) https://doi.org/10.29141/2500-1922-2022-7-1-9
38. Marukhlenko AV, Maksimova TV, Pleteneva TV, Morozova MA. Development and validation of method for the quantitative determination of zinc in its chelate complexes using energy dispersive x-ray fluorescence spectroscopy. Drug development & registration. 2021;10(4):154–161. (In Russ.) https://doi.org/10.33380/2305-2066-2021-10-4-154-161
39. Brodkorb A, Egger L, Alminger M, Alvito P, Assunção R, *et al*. INFOGEST static in vitro simulation of gastrointestinal food digestion. Nature Protocols. 2019;14:991–1014. https://doi.org/10.1038/s41596-018-0119-1
40. Liu W, Hou Y, Jin Y, Wang Y, Xu X, *et al*. Research progress on liposomes: Application in food, digestion behavior and absorption mechanism. Trends in Food Science and Technology. 2020;104:177–189. https://doi.org/10.1016/j.tifs.2020.08.012
41. Lisovaya EV, Lisovoy VV, Victorova EP. Methods for obtaining liposomal systems to be used in the food industry. New Technologies. 2020;16(5):28–33. (In Russ.) https://doi.org/10.47370/2072-0920-2020-16-5-28-33
42. Zhang H. Thin-film hydration followed by extrusion method for liposome preparation. Methods in Molecular Biology. 2017;1522:17–22. https://doi.org/10.1007/978-1-4939-6591-5_2
43. Minekus M, Alminger M, Alvito P, Ballance S, Bohn T, *et al*. A standardised static *in vitro* digestion method suitable for food – an international consensus. Food & Function. 2014;5:1113–1124. https://doi.org/10.1039/c3fo60702j
44. Hur SJ, Lim BO, Decker EA, McClements DJ. *In vitro* human digestion models for food applications. Food Chemistry. 2011;125(1):1–12. https://doi.org/10.1016/j.foodchem.2010.08.036
45. Kornilov KN, Roeva NN, Voronich SS. Ecological valuation of modified starches by the method of dynamic laser light scattering. Ecological Systems and Devices. 2020;7:31–40. (In Russ.) https://doi.org/10.25791/esip.07.2020.1169
46. Kuznetsova LA, Basova NE. The role of arginine and endothelial nitric oxide synthase in the pathogenesis of COVID-19 complicated by metabolic syndrome. Acta Biomedica Scientifica. 2022;7(6):51–70. (In Russ.) https://doi.org/10.25687/1996-6733.prodanimbiol.2021.2.38-51
47. Davis DA, Cox PA, Banack SA, Lecusay PD, Garamszegi SP, *et al*. L-serine reduces spinal cord pathology in a vervet model of preclinical ALS/MND. Journal of Neuropathology & Experimental Neurology. 2020;79(4):393–406. https://doi.org/10.1093/jnen/nlaa002
48. Holeček M. Histidine in health and disease: Metabolism, physiological importance, and use as a supplement. Nutrients. 2020;12(3):848. https://doi.org/10.3390/nu12030848

49. Reznichenko IYu, Donchenko TA. Formation of a diets taken into account the biological value of cookies. Polzunovskiy VESTNIK. 2024;(1):120–125. (In Russ.) https://doi.org/10.25712/ASTU.2072-8921.2024.01.014
50. Kononova IN, Kareva EN. Fourth-generation folic acid active metabolite Quatrefolic® and micronized, microencapsulated iron Lipofer®: Innovative approaches for iron and folic acid deficiencies in women (a review). Russian Journal of Woman and Child Health. 2022;5(1):18–27. (In Russ.) https://doi.org/10.32364/2618-8430-2022-5-1-18-27
51. Tretiakova DS, Khaidukov SV, Onishchenko NR, Vodovozova EL, Babayants AA, *et al*. Lipophilic prodrug of methotrexate in the membrane of liposomes promotes their uptake by human blood phagocytes. Acta Naturae. 2020;12(1):99–109. https://doi.org/10.32607/actanaturae.10946
52. Sybachin AV, Stepanova DA. Modification of multiliposomal nanocontainers with albumin as a method for increasing their resistance to enzymatic hydrolysis. Kolloidnyj Zhurnal. 2021;83(2):222–229. (In Russ.) https://doi.org/10.31857/S0023291221020117
53. Shipunova VO, Deyev SM. Artificial scaffold polypeptides as an efficient tool for the targeted delivery of nanostructures in vitro and *in vivo*. Acta Naturae. 2022.14(1):54–72. https://doi.org/10.32607/actanaturae.11545
54. Ding R, Zhao Z, He J, Tao Y, Zhang H, *et al*. Preparation, drug distribution, and in vivo evaluation of the safety of protein corona liposomes for liraglutide delivery. Nanomaterials. 2023;13(3):540. https://doi.org/10.3390/nano13030540
55. Demchenko EA, Savenkova TV, Mizinchikova II. Effects of oils and fats on the quality characteristics, nutritional value, and storage capacity of cookies. Food Processing: Techniques and Technology. 2021;51(4):674–689. (In Russ.) https://doi.org/10.21603/2074-9414-2021-4-674-689

ORCID IDs
Irina A. Tsepeleva https://orcid.org/0009-0003-8980-4741
Alesya N. Yudina https://orcid.org/0009-0004-3290-8459
Alla A. Krasnoshtanova https://orcid.org/0000-0002-1095-2641

Foods and Raw Materials. 2026;14(2)

ISSN 2308-4057 (Print)
ISSN 2310-9599 (Online)

Research Article
Open Access

Available online at http://jfrm.ru/en
https://doi.org/10.21603/2308-4057-2026-2-683
https://elibrary.ru/KCYFOG

Soft-shell clam from the waters of the Kandalaksha Bay: Use for food purposes

Yulia V. Shokina[1,*], Pavel V. Lutsyk[1], Ekaterina I. Reshetnik[2], Svetlana L. Gribanova[2], Yulia I. Derzhapolskaya[2], Ma Yiqian[3]

[1] Murmansk State Technical University, Murmansk, Russia
[2] Far Eastern State Agrarian University, Blagoveshchensk, Russia
[3] Harbin Leshi Agricultural Technology Co., Ltd., Harbin, China

* e-mail: shokinayuv@mstu.edu.ru

Received 24.01.2025; Revised 20.05.2025; Accepted 03.06.2025; Published online 20.11.2025

Abstract:
The edible part of the soft-shell clam contains a lot of protein and little fat, which makes it a good source of protein. We studied the chemical composition and nutritional value of the edible part of the soft-shell clam (*Mya arenaria* Linnaeus, 1758) living in the waters of the Kandalaksha Bay. Capillary electrophoresis was used to analyze the amino acid profile for its protein. The protein-water ratio of 17.81% and the protein-water-fat ratio of 17.69% classify soft-shell clams as a medium-protein, low-fat raw material with a high potential for food purposes. It had limiting amino acids (methionine and cysteine totaling 75.93%) and a high content of essential amino acids (valine, histidine, leucine, isoleucine, tyrosine, phenylalanine, and threonine, scoring over 100% each). The biological value of the protein was 72.34%, with a coefficient of difference between amino acid scores of 27.66%. The edible part of the soft-shell clam proved hygienically safe. Nitrosamines, pesticides, polychlorinated biphenyls, and salts of heavy metals (lead, arsenic, cadmium, and mercury) did not exceed the maximum allowable concentrations established for food products. The degree of protein digestibility was 46.8% for the edible part of the soft-shell clam frozen for 6 months at –18°C and slowly air-defrosted. Based on our results, soft-shell clams can be considered an excellent and safe source of high-quality protein and therefore be used in functional food technologies after further studies.

Keywords: Bivalve mollusk, flash freezing, amino acid profile, chemical composition, nutritional value, biological value, protein digestibility

Please cite this article in press as: Shokina YuV, Lutsyk PV, Reshetnik EI, Gribanova SL, Derzhapolskaya YuI, *et al.* Soft-shell clam from the waters of the Kandalaksha Bay: Use for food purposes. Foods and Raw Materials. 2026;14(2):425–431. https://doi.org/10.21603/2308-4057-2026-2-683

INTRODUCTION

The Strategy for the development of the Russian Fishery Complex up to 2030 contains several programs for developing aquaculture. One of them aims to cultivate bivalve mollusks and echinoderms, which are steadily in high demand both in the Russian and foreign markets. The main residents of the project are the Russian Far East – Primorsky Krai (90% of production) and the Azov-Black Sea basin (10% of production). Intensive technologies for growing mollusks are expected to collect at least 1.5 tons of biomass per hectare. Russia and its export markets in Southeast Asia are to become the main consumers of mollusks.

Since 2015, the export of fish and seafood from Russia to China, Japan, and South Korea has been growing steadily. These countries traditionally specialize in the fishing and industrial processing of mollusks, which are classified as delicacies. From 2014 to 2018, Russia saw a 62-fold increase in its export of crustaceans to China (from 3.7 to 230.6 million US dollars) and a three-fold increase in its export of mollusks (from 14.0 to 42.7 million US dollars). In 2018 alone, the total export of fish, crustaceans, and mollusks from Russia to China amounted to 1.63 billion US dollars. All the seafood exported to China was grown or caught in the Russian Far East [1].

The growth of interest in bivalve mollusks has been observed in recent years worldwide. Bivalves are primarily an excellent source of vitamin B_{12}, omega-3 fatty acids, choline, iron, selenium, zinc, and other micro- and macronutrients [2], as well as native protein and collagen [3–6].

Copyright © 2025, Shokina *et al.* This is an open access article distributed under the terms of the Creative Commons Attribution 4.0 International License (https://creativecommons.org/licenses/by/4.0/), allowing third parties to copy and redistribute the material in any medium or format and to remix, transform, and build upon the material for any purpose, even commercially, provided the original work is properly cited and states its license.

Experts from the All-Russian Association of Fishermen (VARPE) and the NTech company have recorded a significant increase in sales of the main types of shellfish. In the first seven months of 2024, retail sales increased by 54.5% in physical terms (25.6% in monetary terms) for frozen scallops, by 50.4% (45%) for squid, and by 2.4% (16.2%) for mussels. In total, the sales of these shellfish grew by 19.11% in physical terms and by 25.18% in monetary terms. This growth is more significant than that of the food market as a whole, which, according to NTech, increased by 19.7 and 7.2%, respectively. VARPE explains the high demand for shellfish by the increased popularity of pan-Asian cuisine among Russians [7].

The most promising species of bivalve mollusks for commercial use today are mollusks that live or grow in the shallow sandy waters of the Sea of Japan, the Sea of Okhotsk, and the Yellow Sea. These seas are the commercial stocks of *Anadara broughtonii*, *Spisula sachali nensis*, *Mactra chinensis*, and other mollusks at depths from 2 to 15 m [8].

The growing global demand for mollusks has promoted long-term studies of the lifestyle and production of soft-shell clams (*Mya arenaria* Linnaeus, 1758) that live in coastal sea waters and bays (Kandalaksha and Kola) adjacent to the Kola Peninsula [9–11]. According to these studies, unused reserves of this bivalve mollusk in the Far North of Russia have potential for industrial production and processing.

Dredging is the main method of extracting soft-shell clams, while freezing is the most common industrial method of their processing [12]. Bivalves – fresh or defrosted – are used to make a wide range of culinary products [13].

Today, amateur and industrial production, as well as the protection, of soft-shell clams is not regulated by the government. This increases the availability and economic attractiveness of fishing in Russia's Northern Fishery Basin.

The soft-shell clam (*Mya arenaria*), also known as "sand shell", is a bivalve mollusk that burrows into the ground to a depth of 10 m [12, 14].

Over the last 300–700 years, the species of *Mya arenaria* has re-explored the territories that its ancestors inhabited many millions of years ago. According to scientists, its dominance in the infauna of local water bodies has not affected their endemics [14]. Soft-shell clams inhabit the silty-sandy soils of the littoral of the subarctic and arctic regions of the Atlantic Ocean, including the waters of the Barents and White Seas. In the White Sea, the mollusks were found in the waters of the Onega, Dvina, and Kandalaksha bays. They prefer clean fast-flowing reservoirs, which leads to their increased population and facilitates the counting.

Soft-shell clams can withstand water temperatures from –2 to +28°C, with optimal values from +6 to +14°C. They can also withstand water salinity ranging from 25 to 35‰, with an endurance level of 5‰. They are resistant to anaerobic environmental conditions and able to survive significant oxygen deficiency for a long time.

Potential soft-shell clam fishing areas on the Kola Peninsula are the waters of the White Sea in the Gulf of Chupa of the Kandalaksha Bay, which has a high density of mollusk settlements [12]. The length of mollusks caught in this area ranges from 43 to 74 mm. Their mass ranges from 11 to 44 g, with the edible part accounting for 16–20% of the mass. 100 g of the edible part contains 13.66–16.90% of protein, up to 0.6% fat, (83.08 ± 0.40)% water, and (1.52 ± 0.005)% mineral substances (ash). Nitrogenous compounds in the edible part of the mollusk are represented by nitrogen-terminal amino acids and volatile bases, the mass fractions of which are 6 and 85 mg %, respectively [12].

Despite the abundance of data on the functional and technological properties of bivalves, as well as their composition [2–4, 12, 15], research is lacking on the hygienic safety and nutritional value of soft-shell clams living in the waters of the Kandalaksha Bay, which are of scientific and commercial value.

We aimed to study the indicators of nutritional value and hygienic safety of the soft-shell clam bivalve mollusk (*Mya arenaria*) living in the waters of the Kandalaksha Bay to justify its use for food purposes.

To achieve this aim, we sought to:

– investigate the sensory characteristics of soft-shell clams exposed to flash freezing for preservation;
– explore the chemical composition and nutritional value of soft-shell clams;
– evaluate the functional and technological properties of the mollusk using the protein-water ratio (PWR, %) and the protein-water-fat ratio (PWFR, %) coefficients to identify the most promising processing methods;
– study the amino acid composition of the soft-shell clam protein, including the mass fraction of essential amino acids (EAA), and calculate its biological value indicators (EAA scores, EAA rationality coefficient, amino acid composition rationality coefficient, EAA score difference (*ΔDAS*), EAA score difference coefficient (CDAS), biological value, and EAA comparable redundancy);
– experimentally determine the degree of digestibility of the protein in the edible part of the mollusk;
– examine the hygienic safety of the edible part of the soft-shell clam against the Technical Regulation *On the Safety of Fish and Fish Products* (TR EAEU 040/2016);
– make conclusions on the expediency of food use of the soft-shell clam inhabiting the Kandalaksha Bay.

STUDY OBJECTS AND METHODS

We studied bivalve soft-shell clams (*Mya arenaria* Linnaeus, 1758) living in the Gulf of Chupa of the Kandalaksha Bay (Murmansk Region, Russia). The mollusks were sampled in July 2015 and August 2018. Seasonal changes were not considered in the study.

Chemicals and reagents. All the chemicals used in the study were of analytical grade, produced by Russian chemical enterprises, and met the state standards of the Russian Federation.

Sample preparation. Soft-shell clam bivalve mollusks (*Mya arenaria*), 43 to 74 mm and 11 to 48 g (Fig. 1),



Figure 1 *Mya arenaria* Linnaeus, 1758 (compiled by the authors)

were collected during the expedition. Immediately after the collection, the alive soft-shell clams (about 7 kg) were frozen by the contact method to a temperature in the center of the mollusk to be –18 ± 1°C. They were transported to the laboratory and stored at the same temperature [12].

Before research, the mollusks were thawed in the air at a temperature not exceeding +8°C to a temperature in the center of the mollusk to be –1°C [12]. Then, the mollusks were cleaned manually, and the free liquid was removed. The edible part of the mollusks (about 20% of the total weight) was collected to study the chemical composition, hygienic safety, and protein digestibility. The samples were ground using a micro grinder or blender immediately prior to analysis. The frozen mollusks were stored for a maximum of 8 months.

Proximate composition analysis. The chemical composition of the edible part of the mollusk was determined using standard methods according to State Standard 7636-85. The mass fraction of water was determined by drying a crushed sample at 105°C to constant weight. The mass fraction of fat was determined by weight extraction in a Soxhlet extractor. The mass fraction of ash was obtained by mineralizing a pre-ashed sample at 600°C. The total and non-protein nitrogen contents were determined by the Kjeldahl method modified in terms of sample mineralization with concentrated sulfuric acid. For this, we used a Pro-Nitro A setup and a Selekta Bloc Digest apparatus. Crude protein was determined by multiplying the amount of total nitrogen by a factor of 5.80, which is used to determine total crude protein in jellyfish [3]. Native protein was found by multiplying the difference between total and non-protein nitrogen by 5.8. The obtained concentrations were expressed in terms of wet and dry weight. The protein-water ratio (PWR, %) and protein-water-fat ratio (PWFR, %) were calculated using Eq. (1), (2), respectively.

$$\mathrm{PWR} = \frac{P}{W} \times 100 \quad (1)$$

$$\mathrm{PWFR} = \frac{P}{W + F} \times 100 \quad (2)$$

where P is the mass fraction of protein, %; W is the mass fraction of water, %, where F is the mass fraction of fat, %.

Amino acid analysis. The amino acid composition of the edible part of the mollusk was determined by capillary electrophoresis using the Kapel system according to State Standard R 55569-2013. All determinations were made in triplicate. The amino acid content (threonine, cysteine + methionine, valine, phenylalanine + tyrosine, isoleucine + leucine, lysine) was expressed in g per 100 g of product and in g per 100 g of protein.

Amino acids. Capillary electrophoresis was used to define the mass fractions of proteinogenic amino acids in the form of phenylisothiocarbamyl derivatives – the total content (free and bound forms) of individual amino acids. Since during decomposition of a sample, asparagine and glutamine were hydrolyzed to aspartic and glutamic acids, respectively, their contents were the total contents of these acids with the respective amides. Since leucine and isoleucine were not separated under analysis conditions, we determined their sum.

The Kapel capillary electrophoresis system with a high voltage source of positive polarity was equipped with: a quartz capillary of 75 cm long and 50 μm in inner diameter, a photometric or spectrophotometric detector capable of measuring at 250 to 260 nm, and a computer with Elforan software that registers IT processing of electrophoregrams. The Kapel system is registered in the State Register of Measuring Instruments. Table 1 shows the ranges of measured concentrations of amino acids.

Amino acid scores. Contents of essential amino acids (EAA) in the soft-shell clam protein were measured by calculating the EAA C_j score, a unit fraction or % (Eq. (3)). The calculation followed the World Health Organization (WHO) reference model of amino acid requirements for children of preschool and school age (3–10 years old) and adults [9].

$$C_j = \frac{A_j}{A_{reference}} \quad (3)$$

where A_j is the EAA content in 100 g of protein, g; $A_{referens}$ is the EAA content in 100 g of native protein according to FAO/WHO, g.

Protein digestibility. The digestibility index of the soft-shell clam protein was determined by the accelerated Jaramillo method. The biological value of protein is characterized, among other things, by the degree of digestion in the human body. The rate at which proteins are attacked by gastrointestinal enzymes (such as pepsin and trypsin) characterizes the degree of protein digestion. The degree of protein digestion (DPD, %) was calculated using the Eq. (4):

$$\mathrm{DPD} = \frac{N_{digested}}{N_{total}} \times 100 \quad (4)$$

where $N_{digested}$ is the amount of nitrogen in the digested part of the protein; N_{total} is the total amount of nitrogen in the protein.

The amount of nitrogen in the digested part of the protein was calculated as a difference between total

Table 1 Amino acid concentrations measured by the Kapel capillary electrophoresis system

Amino acid	Measurement range, mg/dm³	Amino acid	Measurement range, mg/dm³
Alanine (Ala)	0.5–150	Leucine + Isoleucine (Leu+Ile)	0.5–150
Arginine (Arg)	0.5–250	Lysine (Lys)	0.5–100
Asparagine (Asn)	1.0–50	Methionine (Met)	0.4–50
Aspartic acid (Asp)	0.5–50	Proline (Pro)	0.25–500
Valine (Val)	0.4–150	Serine (Ser)	0.3–300
Histidine (His)	0.5–50	Threonine (Thr)	0.5–50
Glycine (Gly)	0.2–50	Tryptophan (Trp)	1.0–50
Glutamine (Gln)	0.5–50	Tyrosine (Tyr)	1.0–150
Glutamic acid (Glu)	1.0–50	Phenylalanine (Phe)	1.0–150

All determinations were performed in triplicate. The amino acid contents were expressed in g per 100 g of product and in g per 100 g of protein

nitrogen in the product and nitrogen in the undigested part of the protein according to the Eq. (5):

$$\text{DPD} = \frac{N_{total} - N_{residual}}{N_{total}} \times 100 \quad (5)$$

where $N_{residual}$ is the content of the residual (undigested) part of the protein.

The content of total and residual (undigested) nitrogen was determined using the accelerated Jaramillo method. For this, a sample of the test product was mineralized in a metal sleeve when heated with a mixture of caustic and sodium acetate. After that, the released ammonia was quantitatively absorbed by a 0.1 N solution of sulfuric acid. The acid that was not bound by ammonium hydroxide at the end of mineralization was determined by back titration with a 0.1 N sodium hydroxide solution in the presence of an indicator.

The amount of residual nitrogen was calculated by the Eq. (6):

$$N_{residual} = \frac{(A - a) \times 1.4}{H \times 1000} \times 100 \quad (6)$$

where A is the volume of 0.1 N sulfuric acid solution in a receiving glass, mL; a is the amount of 0.1 N sodium hydroxide solution used for titration of 0.1 N sulfuric acid solution, mL; 1.4 is the conversion factor for nitrogen; and H is the weight of the sample under analysis.

Hygienic safety indicators. The hygienic safety indicators were determined at the State Regional Center of Standardization, Metrology and Testing in Murmansk Region, the Test Performance Center for Industrial Production of Crude Products and Raw Materials (Murmansk, Russia). Frozen mollusks (–18°C in the center) with a total mass of 1 kg were sampled according to Method M-02-1009-2008 (Sampling Act dated November 19, 2018). They were analyzed for mass concentrations of toxic compounds whose maximum content is regulated in accordance with the Technical Regulation *On the Safety of Fish and Fish Products* (TR EAEU 040/2016) and Technical regulation *On food safety* (TR CU 021/2011) by standardized methods:

– lead and cadmium (mg/kg of product) were measured by atomic absorption according to the guidelines for control State Standard 30178-96;
– arsenic (mg/kg of product) was determined by atomic absorption by electrothermal atomization according to method M-02-1009-2008;
– mercury (mg/kg of product) was measured by destruction of a sample with a mixture of nitric and sulfuric acids, followed by precipitation of mercury with copper iodide, and colorimetric determination in the form of copper tetraiodomercurate against a standard scale according to State Standard 26927-86;
– nitrosamines (the sum of nitrosdimethylamine NDMA and nitrosdiethylamine NDEA, mg/kg of product) were determined by the fluorimetric chemiluminescent method according to MUK 4.1.011-93; and
– pesticides (polychlorinated biphenyls, mg/kg) were measured by capillary gas-liquid chromatography with an electron capture detector according to the methodological guidelines MUK 4.1.1023-01.

Measurement of temperature in the shell. The temperature in the thickness of the mollusk, including frozen ones, was measured using a high–precision, ultrafast TESTO 735-1 electronic thermometer (Table 2) registered in the Russian State Register of Measuring Instruments (Fig. 2).

Statistical analysis. Experimental results were expressed as mean values with standard deviation (n = 3). The least squares method was used to calculate the standard deviation.

RESULTS AND DISCUSSION

Table 3 shows the sensory properties of the soft-shell clams stored for eight months at –(18 ± 1)°C in a polymer non-hermetic container. The test samples were air-defrosted immediately before analysis.

Table 2 Characteristics of measuring instruments

Characteristic	TESTO 735-1 electronic thermometer	K/T probe (primary converter to the electronic thermometer)
Controlled temperature range, °C	from –20 up to 800	from –200 before 1370
Temperature sensitivity limit, °C	0.05	0.10
Measurement error	± 0.2°C, or ± 0.3%	± 0.3°C



Figure 2 Testo 735-1 electronic thermometer (compiled by the authors)

Table 3 Sensory properties of the frozen bivalve mollusk *Mya arenaria* after air defrosting

Indicator	Description
Appearance	The shells are intact, without contamination; no change after defrosting
Color	The shells are from milky white to grayish white; the body is from transparent pinkish white to slightly nontransparent grayish white
Consistency of the edible part	Juicy, tender
Taste	The taste is characteristic of fresh mollusk, slightly iodine; no off-flavors
Mass fraction of mineral impurities (sand, silt, etc.), %	Not more than 0.1 per total mass of the mollusk

Table 4 demonstrates the mass fractions of the main nutrients in the composition of the mollusk tissues. The protein-water ratio and the protein-water-fat ratio calculated to determine the preferred processing method for raw soft-shell clams were 17.81% and 17.69%, respectively. Figure 3 shows the amino acid profile of the protein in the edible part of the soft-shell clam. The hygienic safety indicators for the mollusk are shown in Figs. 4–8.

As can be seen in Figs. 4–8, the values of the hygienic safety indicators in the edible part of the mollusk were 6.5–87.0 times lower than the established limits.

Table 4 Chemical composition of the frozen bivalve mollusk *Mya arenaria* after air defrosting

Indicator	Result in g per 100 g of the edible part
Water	83.08 ± 0.40
Protein	13.66 ± 0.05
Fat	0.60 ± 0.02
Carbohydrate	1.16
Ash (minerals)	1.520 ± 0.005
Mass fraction of total nitrogen (TN), %	2.425 ± 0.550
Mass fraction of non-protein nitrogen (NPN), %	0.240 ± 0.110
Crude protein (CP), %	14.07 ± 3.17

Carbohydrate data are mean ± standard deviation (n = 3). The content of carbohydrates, %, was calculated according to the Eq.: Carbohydrate = 100 – (moisture + protein + fat + ash)

Our study demonstrated good preservation of frozen bivalve soft-shell clams. After 6 months of storage at –(18 ± 1)°C, the mollusks showed excellent sensory properties after air defrosting (Table 3). They had no noticeable or quality-reducing changes in appearance, color, flavor, and consistency, which is especially important for food purposes.

The edible part of the mollusk had a high protein content (Table 4). Our data were consistent with those in other studies. For example, Chinensis and Broughtonii [8] reported a protein content of 12.22 to 15.82 g in 100 g of the edible part of bivalve mollusks commercially harvested in the Sea of Japan.

Due to the low (less than 1%) fat content, soft-shell clams can be used for dietetic and functional products. Their protein-water ratio and protein-water-fat ratio coefficients classify them as medium-protein, low-fat raw material. The best ways to process them for food purposes are cooking, freezing, or manufacturing sterilized multi-component canned foods (including those with vegetables, cereals, etc.).

Table 4 shows that after two weeks of storage at –18°C, the contents of native protein and non-protein nitrogenous compounds were 90 and 10%, respectively.

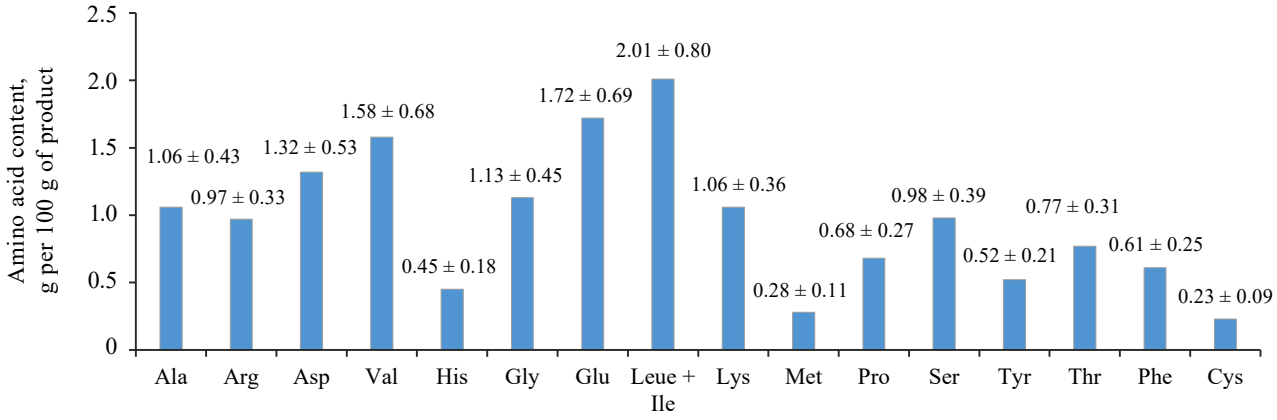

Figure 3 Amino acid profile of the protein in the edible part of the soft-shell clam. Data are mean ± standard deviation (n = 3)

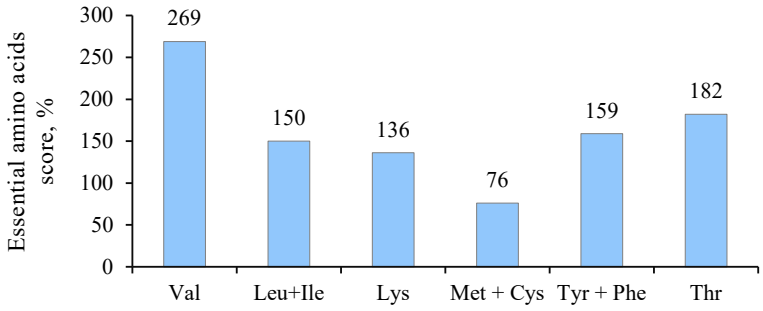

Figure 4 Essential amino acid scores in the protein of the edible part of *Mya arenaria*

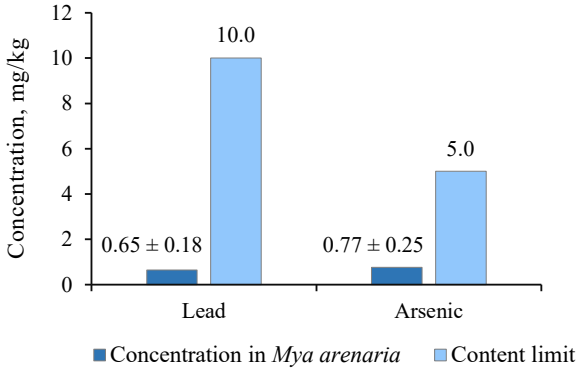

Figure 5 Concentrations of arsenic and lead in the soft-shell clams. Data are mean ± standard deviation (n = 3)

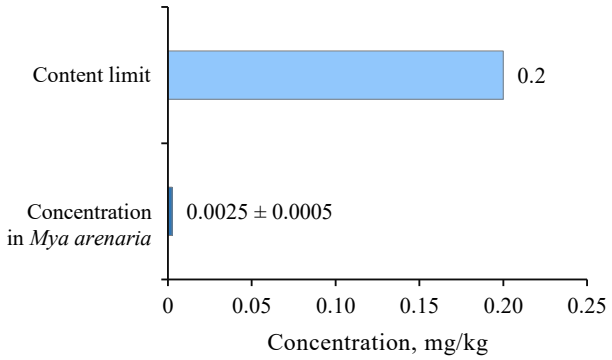

Figure 6 Concentrations of mercury in the soft-shell clams. Data are mean ± standard deviation (n = 3)

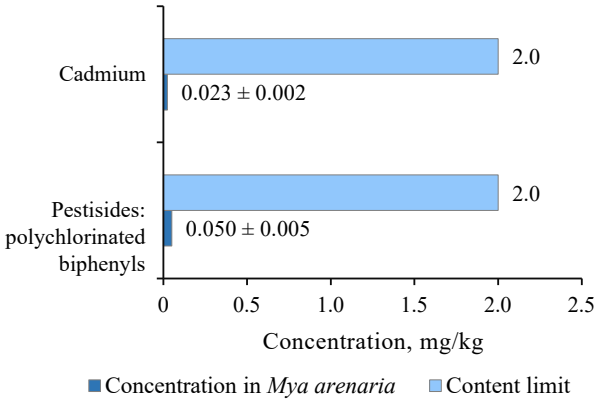

Figure 7 Concentrations of cadmium and pesticides in the soft-shell clams. Data are mean ± standard deviation (n = 3)

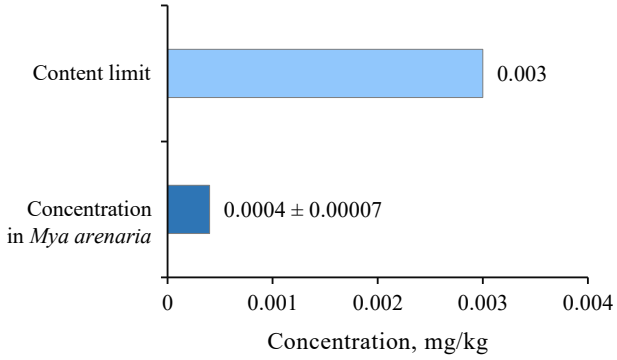

Figure 8 Concentrations of nitrosamines in the soft-shell clams. Data are mean ± standard deviation (n = 3)

This ratio of protein and non-protein nitrogen is conventional for many aquatic organisms and can indicate freshness and high quality of frozen raw materials – mollusk.

The amino acid profile shows the biological value of protein in the mollusk. The protein in its edible part contains essential amino acids and histidine, with the exception of tryptophan which was not determined. Among the essential amino acids, the pair "methionine + cysteine" (76%) was the limiting one. This result was consistent with that in the study of bivalve mollusks in the Sea of Japan (73%) [8].

The soft-shell clam protein may be considered defective in the absence of information about the tryptophan content.

The digestibility of the protein in the edible part that has not undergone thermal cooking was at a fairly high level of 50%.

An analysis of the hygienic safety of the consumed part of the mollusk revealed full compliance with the established standards. In the samples, none of the tested compounds reached the maximum permissible level. Moreover, the concentration of the detected contaminants was significantly lower than the established limits.

CONCLUSION

The edible part of *Mya arenaria* Linnaeus, 1758 is hydrated, high in valuable protein, and low in fat. The protein content per its dry weight is more than 80%. The protein of the soft-shell clam contains essential amino acids, except for tryptophan, the content of which was not determined. The dominant essential amino acids are glutamic acid, leucine + isoleucine, and valine. *Mya arenaria* living in the waters of the Kandalaksha Bay of the White Sea can be used as raw material for food production.

The biological value of shellfish products can be rised by combining them with other proteins rich in tryptophan.

CONTRIBUTION

All the authors were involved in the experimentation, data collection, management, and writing of the paper, as well as its reading and approval, prior to submission.

CONFLICT OF INTEREST

The authors state that there is no conflict of interest.

ACKNOWLEDGEMENTS

The research was supported by the World-Class Scientific and Educational Center "Russian Arctic: New Materials, Technologies and Research Methods".

REFERENCES

1. Shishkina NP. Prospects for food exports to China. Scientific Journal of Baikal State University. 2020;4(1):18–27. (In Russ.) https://doi.org/10.17150/2587-7445.2020.4(1).18-27
2. España MSA, Rodríguez EMR, Romero CD. Comparison of mineral and trace element concentrations in two molluscs from the Strait of Magellan (Chile). Journal of Food Composition and Analysis. 2007;20(3–4):273–279. https://doi.org/10.1016/j.jfca.2006.06.007
3. Chen DW, Su J, Liu XL, Yan DM, Lin Y, *et al*. Amino acid profiles of Bivalve mollusks from Beibu Gulf, China. Journal of Aquatic Food Product Technology. 2012;21(4):369–379. https://doi.org/10.1080/10498850.2011.604820
4. Karnjanapratum S, Benjakul S, Kishimura H, Tsai YH. Chemical compositions and nutritional value of Asian hard clam (*Meretrix lusoria*) from the coast of Andaman Sea. Food Chemistry. 2013;141(4):4138–4145. https://doi.org/10.1016/j.foodchem.2013.07.001
5. Doyle TK, Houghton JDR, McDevitt R, Davenport J, Hays GC. The energy density of jellyfish: Estimates from bomb-calorimetry and proximate composition. Journal of Experimental Marine Biology and Ecology. 2006;343(2):239–252. https://doi.org/10.1016/j.jembe.2006.12.010
6. Dietary protein quality evaluation in human nutrition. Report of an FAQ Expert Consultation. Auckland: FAO Food and Nutrition Paper; 2011. 66 p.
7. Sales of shellfish have increased dramatically in Russia. Who started buying and why? RGRU. (In Russ.) Available from: https://rg.ru/2024/11/14/prodazhi-molliuskov-rezko-vyrosli.html?ysclid=m7hvy1yxqx834-337085
8. Tabakaeva OV, Tabakaev AV, Piekoszewski W. Nutritional composition and total collagen content of two commercially important edible bivalve molluscs from the Sea of Japan coast. Journal of Food Science and Technology. 2018;55:4877–4886. https://doi.org/10.1007/s13197-018-3422-5
9. Karnjanapratum S, Benjakul S, Kishimura H, Tsai YH. Chemical compositions and nutritional value of Asian hard clam (*Meretrix lusoria*) from the coast of Andaman Sea. Food Chemistry. 2013;141(4):4138–4145. https://doi.org/10.1016/j.foodchem.2013.07.001
10. Smolkova OV. Linear growth and yield of bivalve mollusks *Mya Arenaria* Linnaeus, 1758 in the conditions of the littoral of the Barents and White Seas. IOP Conf. Series: Earth and Environ. Sci. 2021;937:022078. https://doi.org/10.1088/1755-1315/937/2/022078
11. Smolkova OV. Production characteristics of settlements bivalve *Mya arenaria* Linne, 1758 of the Barents Sea. Transactions of the Kola Science Centre of RAS. 2021;12(3):141–150. (In Russ.) https://doi.org/10.37614/2307-5252.2021.3.9.017
12. Shokina YuV, Kravets PP, Lutsyk PV. Evaluation of techno-chemical properties of the bivalve mollusk *Mya Arenaria* as fishery perspective object and aquaculture of the Kandalaksha Bay. Vestnik of MSTU. 2015;18(4):667–671. (In Russ.) https://elibrary.ru/VNUJPL
13. Murray MT, Pizzorno J, Pizzorno L. The Encyclopedia of Healing Foods. NY: Atria Books; 2005, 912 p.
14. Gerasimova AV, Ushanova EV, Filippov AA, Filippova NA, Stogov IA, *et al*. Long-term changes in cohort structure of the soft-shell clam *Mya arenaria* in the White Sea: Growth rate affects lifespan and mortality. Marine Biology Research. 2018;14(1):51–64. https://doi.org/10.1080/17451000.2017.1346259
15. Wright AC, Fan Y, Baker GL. Nutritional value and food safety of bivalve molluscan shellfish. Journal of Shellfish Research. 2018;37(4):695–708. https://doi.org/10.2983/035.037.0403

ORCID IDs

Yulia V. Shokina https://orcid.org/0000-0002-6513-1912
Ekaterina I. Reshetnik https://orcid.org/0000-0002-3166-9992
Svetlana L. Gribanova http://orcid.org/0000-0003-1448-4328
Yulia I. Derzhapolskaya http://orcid.org/0000-0002-1851-0063

Foods and Raw Materials. 2026;14(2)

ISSN 2308-4057 (Print)
ISSN 2310-9599 (Online)

Research Article
Open Access

Available online at http://jfrm.ru/en
https://doi.org/10.21603/2308-4057-2026-2-687
https://elibrary.ru/NCUESU

Whey and water-ethanol solution as extractants of biologically active substances: Comparative analysis

Anna A. Stepanova[1], Alice D. Mitina[1], Natalia S. Velichkovich[1,*], Oksana V. Kozlova[1], Timothy A. Larichev[1], Larisa A. Proskuryakova[1], Vladimir V. Martirosyan[2]

[1] Kemerovo State University, Kemerovo, Russia
[2] Scientific Research Institute for the Baking Industry, Moscow, Russia

* e-mail: velichkovich@yandex.ru

Received 19.05.2025; Revised 26.06.2025; Accepted 05.08.2025; Published online 27.11.2025

Abstract:
Industrial whey wastes contain organic substances that cause serious harm to the environment, which makes whey recycling a relevant research objective. Whey can serve as an extractant of biologically active substances from plant raw materials. This research compared a 70% aqueous-ethanol solution and whey as extractants of bioactive components from a plant blend of *Heracleum sibiricum* L., *Syringa vulgaris* L., *Arctium tomentosum* Mill., *Achillea millefolium* L., *Thymus vulgaris* L., and *Pulmonaria officinalis* L. The method of high-performance liquid chromatography revealed catechin, chlorogenic acid, astragalin, ferulic acid, coumaric acid, and some trace amounts of other compounds. The samples subjected to water-ethanol extraction demonstrated a better quantitative and qualitative profile than those processed with whey: 637.92 vs. 380.45 mg/kg for chlorogenic acid, 93.05 vs. 2.34 mg/kg for coumaric acid, and 53.12 vs. 3.09 mg/kg for astragalin. Whey proved unable to extract catechin and ferulic acid. However, whey made it possible to obtain compounds that water-ethanol solution failed to extract, namely rutin and caffeic acid. By fractionating the extracts and isolating individual biologically active substances, we obtained chlorogenic acid (90.0%), ferulic acid (92.0%), and coumaric acid (88.0%) with water and ethanol, as well as caffeic acid (84.5%) and rutin (78.0%) with whey. Both ethanol and whey proved industrially relevant and demonstrated good prospects for commercial extraction of biologically active substances from various plant raw materials.

Keywords: Extraction, biologically active substances, whey, plant extract, extractant, fractionation, blending

Funding: This research was supported by the Russian Science Foundation, grant No. 23-16-00113.

Please cite this article in press as: Stepanova AA, Mitina AD, Velichkovich NS, Kozlova OV, Larichev TA, *et al.* Whey and water-ethanol solution as extractants of biologically active substances: Comparative analysis. Foods and Raw Materials. 2026;14(2):432–442. https://doi.org/10.21603/2308-4057-2026-2-687

INTRODUCTION

The recent decades have seen a growing scientific interest in medicinal plants with therapeutic effects. New methods for the extraction, isolation, and analysis of phytochemical components make it possible to utilize their pharmacological potential in all their diversity [1–3]. Such advanced analytical techniques as high-performance liquid chromatography and gas chromatography-mass spectrometry have revolutionized the authentication and analysis of bioactive molecules [4–6]. In combination with genomic technologies, e. g., DNA barcoding, these techniques optimize the phytochemical synthesis in order to increase the yield and range of bioactive compounds, thus promoting novel plant-based therapies [7, 8]. The high therapeutic potential of plant materials is applied to treating diabetes mellitus and some cancers, as well as Alzheimer's and Parkinson's diseases, not to mention various microbial and fungal infections [9–11]. The holistic properties of plant extracts result from a complex mix of bioactive compounds, i. e., alkaloids, flavonoids, terpenes, phenols, etc. Each of these compounds provides therapeutic benefits, enhanced by their synergistic interactions. The synergetic effect and natural origin, combined with lower risks of side effects, make plant compounds promising alternatives to synthetic pharmaceuticals [12, 13].

In addition, the food industry is currently facing external problems caused by epidemics, military conflicts, etc. In this respect, medicinal plants offer a solution to the so-called hidden hunger issue, i. e., a deficiency of

Copyright © 2025, Stepanova *et al.* This is an open access article distributed under the terms of the Creative Commons Attribution 4.0 International License (https://creativecommons.org/licenses/by/4.0/), allowing third parties to copy and redistribute the material in any medium or format and to remix, transform, and build upon the material for any purpose, even commercially, provided the original work is properly cited and states its license.

phytonutrients in the national diet [14, 15]. A comprehensive use of plant components upgrades traditional products into functional foods. Their chemical composition contains non-traditional plant components responsible for bioactive properties with a long-term physiological antioxidant, antiseptic, immunomodulatory, radioprotective, or anticancer effects [16–19].

Countries that boast plant biodiversity have certain advantages in the fields of national economic growth and healthcare. By stimulating R&D in herbal medicines and plant food products, they turn their natural resources into innovative solutions in the food industry and healthcare [8, 20].

Phytoextraction is a complex process that depends on a number of factors. Extraction remains the main chemical method of producing bioactive compounds from plant raw materials [21]. An effective extraction technique produces a maximal yield of target components that render the resulting extracts with the highest biological activity possible. However, the yield of biologically active substances and their activity also depend on the solvent used. Traditional solvents applied in phytoextraction include methanol, ethanol, acetone, and water. Bioactive compounds differ in solubility, which means that the process of solvent selection should take into account the specifics of plant materials and target compounds. Therefore, choosing an optimal extraction solvent is a difficult matter that depends on each individual plant material [22].

Environmental protection and sustainability are another issue to be considered in relation to extraction and processing. Whey is a non-conventional raw material that can act as an extractant for bioactive substances of plant origin. It may reduce environmental burden by replacing inorganic extractants. As whey is rich in organic substances, its industrial wastes are bad for the environment. Its recycling as an industrial extractant is a relevant solution to all the above-mentioned problems. However, whey requires a detailed comparative analysis with other extractants to confirm its effectiveness.

Surprisingly, the whey extractant issue has gained a rather narrow scientific coverage. Velichkovich *et al.* [23] tested plant extracts obtained with whey for flavonoid compounds, antioxidant activity, and effective extraction parameters.

Melnikova *et al.* [24] obtained dairy-plant extracts from yacon tubers (*Polymnia sonchifolia*) using a curd whey ultrafiltrate. The resulting optimal parameters included 50–60 min extraction time, 40–60°C, and pH 4–5. The optimal ratio of yacon pulp and whey ultrafiltrate ranged from 1:4 to 1:6. The method improved the efficiency of nutrient extraction, thus increasing the nutritional and biological value of the finished product.

Kaledina *et al.* [25] extracted vitamin C and rutin from green tea, thyme, and rose hips using unsalted cheese and curd whey. The optimal parameters included 30 min extraction time and 40–60°C. The optimal amount of raw material was 1–10% of extractant mass.

Khalanskaya *et al.* [26] extracted bioactive substances from aloe, hawthorn, and licorice using whey and skim milk permeate. The optimal parameters included 30 min extraction time and 40–60°C. The most effective ratio of raw material to solvent was 1:2.

Lodygin *et al.* [27] used whey to isolate bioactive components from milk thistle, peppermint leaves, sage leaves, and purple echinacea. The optimal processing parameters included 2 h extraction time, 55–60°C, and 70 rpm. The optimal whey-to-plant ratios were 1:8 for milk thistle and peppermint and 1:10 for sage and purple echinacea. The experimental whey extracts demonstrated a higher antioxidant activity than the aqueous ones. The yield of phenolic compounds was higher at the ratio of 1:8. The sage extracts yielded much more phenolic compounds than the extracts of purple echinacea.

Sargin *et al.* [28] obtained a water-fat extract from plant raw materials. The procedure involved calendula, St. John's wort, and chamomile as herbs or inflorescences and a water-fat emulsion as an extractant, i. e., whole natural milk, milk or curd whey, or their mixes. The plant raw material was soaked in deionized water until swollen. The water-fat emulsion had a 3–15% fat content. The extraction relied on the percolation method. The ratios of plant raw materials to the extractant ranged from 1:25 to 1:10; the extraction time was 2–24 h at 10–80°C. The 1:1 ratio of calendula flowers and a milk-and-whey mix served as an example. The optimal processing parameters included 2 h, 80°C, and 1:10 calendula-extractant ratio. Using the HPLC method, they detected 8% terpenoids and 4.5% tannins in the extracts. The extraction of St. John's wort herbs and flowers with a 1:1 mix of milk and curd whey had the following optimal parameters: 24 h, 10°C, 1:10 of raw material and extractant. The resulting extract contained a total 12% of terpenoids and tannins, 10% carotene, and 3.2% vitamin C. The optimal parameters for extracting bioactive substances from chamomile with whey included 3 h, 40°C, and a chamomile-to-whey ratio of 1:20. The liquid chromatography revealed 13.5% tannins and terpenoids, 14.1% carotenes, 2.7% polyphenols, and 2.1% vitamin C.

Daudova & Ramazanova used milk whey to extract bioactive compounds from barberry [29] and cranberry [30]. The berries were ground, extracted with milk whey, and filtered. The optimal ratios of raw materials to extractant were 1:10–1:20 at 40 or 60°C for 60–90 min. The purified extract could be used as a food additive in bakery products.

Doronin *et al.* [31] produced pectin powder from beet roots, using curd and cheese whey as extractant. They ground the beet and treated it with acidified citric acid to a pH of 3.5–3.8 at 95–100°C for 60–90 min. The extraction with curd or cheese whey lasted for 60–80 min at 90–95°C and 0.2–0.3 MPa; the ratio of pulp, water, acidified citric acid, and curd/cheese whey was 1:2:5–1:2:6. Another extract was obtained by extracting crushed beet leaves with curd or cheese whey at 1:7–1:12, 65–70°C, and 0.2–0.3 MPa for 60–80 min. Both extracts were mixed at 80–90–20–10, evaporated to 12–15% solids, and dried to 3–5% moisture. The resulting content of soluble pectin was 1.1–1.57%.

This study focused on a comparative analysis of ethanol and whey extracts of a blend of lilac, lungwort, yarrow, burdock, hogweed, and thyme. The research objective was to assess the effect of the extractant on the yield of bioactive substances.

STUDY OBJECTS AND METHODS

The research involved 70% water-ethanol solution and whey as extractants. The list of plant materials included hogweed (*Heracleum sibiricum* L.), lilac (*Syringa vulgaris* L.), burdock (*Arctium tomentosum* Mill.), lungwort (*Pulmonaria officinalis* L.), thyme (*Thymus vulgaris* L.), and yarrow (*Achillea millefolium* L.) [32, 33]. The extracts were obtained from the plant blend using whey and water-ethanol solution.

To compare the extractants used to extract bioactive compounds from the plant blend, we isolated the bioactive substances individually in several stages:

– composing a plant blend based on the metabolomic analysis of the extracts;
– obtaining extracts from the blend using whey and a 70% water-ethanol solution;
– phytochemical analysis;
– fractionation;
– isolating individual bioactive substances from one major peak per fraction; and
– drying the bioactive substances separately.

Metabolomic analysis of the extracts to compose the blend. We used the method of high-efficiency liquid chromatography (HPLC) to define the metabolome of the plant materials. The process involved a LC-20AB Shimadzu Prominence chromatograph (Shimadzu, Japan) with a binary pump, an SPD-M20A diode array detector, and a Zorbax 300SB-C18 4.6 Column (250 mm, 5 µm; Agilent Technologies, USA). The separation temperature was 40°C in the gradient elution mode. The data for the mobile phase were as follows: 0.1% eluent A, trifluoroacetic acid (TFA) in bi-distilled water, acetonitrile B, 1 mL/min flow rate, 254, 280, and 325 nm analytical wavelengths. The components were identified by their retention times and the spectra of standard substances. Their concentration was calculated using calibration equations. The metabolome analysis made it possible to compile a plant blend for further research.

Obtaining extracts from the blend with whey and 70% water-ethanol solutions. To prepare cheese whey, we heated it to 45°C and centrifuged it to separate the milk fat. After that, the solution was brought to 95°C and held for 15 min to coagulate the remaining whey protein and provide additional pasteurization. The heated whey was centrifuged to separate it into liquid (extract) and thick (protein) fractions. The resulting extract was passed through a cotton-gauze filter for additional purification [23]. This cheese whey was used as extractant. The extraction parameters were as follows: 3 h, 90 ± 1°C, 2.5 g raw material to 450 mL whey or 70% water-ethanol solution. Upon extraction, we filtered the extracts through a sterile cotton gauze and an ash-free filter. They were stored in the dark at +2 to +6°C in 500 mL conical flasks with rubber stoppers.

Phytochemical composition. The phytochemical analysis of the blends relied on the analytical HPLC method described above.

Fractionation. The blends were evaporated in a vacuum rotary evaporator at 40°C with silica gel (5 g silica gel per 80 mL extract) until the solvent was completely removed (Fig. 1).

The resulting mix was dried and loaded into the column of a Büchi Pur-C150 preparative chromatograph (Büchi, Switzerland). The processing parameters were as follows: flash mode, FP ECOFLEX Si 40 g, ELSD and UV detectors (254, 270, 280, and 320 nm). Vials from each peak were collected separately and evaporated.

We conducted the elution in a gradient mode in the hexane-methylene chloride and methylene chloride-methanol systems, increasing the content of the more polar solvent by 20% for each subsequent column volume (Table 1).

We defined the total fraction yield gravimetrically, analyzed their composition by analytical HPLC, and expressed in g/kg and mg/kg of plant material, respectively.

Isolating individual bioactive substances from one major fraction peak. To isolate individual bioactive substances from fractions of Blends 1 and 2, we used the preparative liquid chromatography method in a Büchi Pure C-850 chromatograph and a Prep Pure C18 column (100 Å; 5 µm; 250×20 mm; Büchi, Switzerland). The isolation parameters included gradient elution mode and



Figure 1 Evaporating the blends

Table 1 Gradient elution

Column volumes	Solvent, vol. %		
	Hexane	Methylene chloride	Methanol
0.0	100.0	0.0	0.0
1.0 ± 0.2	80.0	20.0	0.0
1.0 ± 0.2	80.0	20.0	0.0
1.0 ± 0.2	60.0	40.0	0.0
1.0 ± 0.2	60.0	40.0	0.0
1.0 ± 0.2	40.0	60.0	0.0
1.0 ± 0.2	40.0	60.0	0.0
1.0 ± 0.2	20.0	80.0	0.0
1.0 ± 0.2	20.0	80.0	0.0
1.0 ± 0.2	0.0	100.0	0.0
1.0 ± 0.2	0.0	100.0	0.0
0.0	0.0	100.0	0.0
1.0 ± 0.2	0.0	80.0	20.0
1.0 ± 0.2	0.0	80.0	20.0
1.0 ± 0.2	0.0	60.0	40.0
1.0 ± 0.2	0.0	60.0	40.0
1.0 ± 0.2	0.0	40.0	60.0
1.0 ± 0.2	0.0	40.0	60.0
1.0 ± 0.2	0.0	20.0	80.0
1.0 ± 0.2	0.0	20.0	80.0
1.0 ± 0.2	0.0	0.0	100.0
3.5 ± 0.2	0.0	0.0	100.0

40°C; for mobile phase: 0.1% eluent A, TFA in bi-distilled water, acetonitrile B, 10 mL/min flow rate; 254, 270, 280, and 320 nm analytical wavelengths.

The fractions collected after separating the large fractions of Blends 1 and 2 were analyzed and purified by HPLC on an LC-20AB Shimadzu Prominence analytical chromatograph with a binary pump (Shimadzu, Japan). To study and purify each bioactive substance isolated from the blend fraction, we used an SPD M20A diode-matrix detector and a Zorbax 300SB-C18 4.6 column (250 mm, 5 µm; Agilent, USA).

Drying the individual bioactive substances. The drying procedure involved a sublimation unit at the following constant lyophilization conditions: 0.3 mbar, –20°C at the final drying stage, –80°C cooler temperature [34].

RESULTS AND DISCUSSION

To study the metabolomic composition of the plant extracts, we used the following chromatographic standards: 3,4-dihydroxybenzoic acid (protocatechuic acid), hyperoside, gallic acid, apigenin-7-O-glucoside, quercetin 3-D-glucoside, luteolin-7-glucoside (cinaroside), (+)-catechin, astragalin (kaempferol-3-glucoside), chlorogenic acid, acacetin, ellagic acid, rutin hydrate, p-coumaric acid, caftaric acid, rosemarinic acid, chicoric acid, trans-caffeic acid, trans-ferulic acid, rutin, ferulic acid (3-methoxy-4-hydroxycinnamic acid), caffeic acid (3,4-dihydroxycinnamic acid), genistin, daidzein, formononetin, oenothein B, morin (3,5,7,2',4'-pentahydroxyflavone), 2,5-dihydroxybenzoic acid, and neochlorogenic acid.

The chromatographic profiles obtained were summarized as a graph (Fig. 2).

The metabolome profile included astragalin, 2,5-dihydroxybenzoic acid, isoquercetin, chlorogenic acid isomer, hyperoside, and gallic acid. The maximal astragalin content belonged to lilac inflorescences (1230.88 µg/g) while its leaves contained the maximal value of isoquercetin (931.00 µg/g). High levels of astragalin were also found in different parts of hogweed, the leaves of which also contained 2,5-dihydroxybenzoic acid (1038.80 µg/g). Chlorogenic acid isomer was detected only in lungwort (350.00 µg/g). The herbal part of thyme and lilac inflorescences had almost the same quantity of gallic acid, i. e., 24.00 and 23.00 µg/g, respectively. The yarrow samples were rich in hyperoside (335.00 µg/g). Hogweed, lilac, and lungwort contained the highest volumes of bioactive substances.

The metabolomic analysis made it possible to compile two blends of the plants (Table 2). The blends consisted of the same plant materials in the same proportions but had different extractants.

Figure 3 shows the blends obtained as a result of extracting plant materials with whey and 70% water-ethanol extractant.

Figures 4, 5 and Table 3 summarize the phytochemical composition of Blends 1 and 2. We identified the components by their retention times and the spectra of such standard substances as 3,4-dihydroxybenzoic acid, 2,5-dihydroxybenzoic acid, hyperoside, gallic acid, apigenin-7-O-glucoside (cosmosiin), catechin, astragalin, ferulic acid, caffeic acid, chlorogenic acid, neochlorogenic acid, acacetin, quercetin-3D-glucoside, ellagic acid, rutin, luteolin-7-glucoside (cinaroside), p-coumaric acid, caftaric acid, rosemarinic acid, chicoric acid, oenothein B, genistein, daidzein, formononetin, and morin. The concentration was calculated using calibration equations (3–5% mean error).

According to the HPLC analysis, the greatest number of phenolic components belonged to Blend 1. Onnonin and formononetin were not detected.

Figure 4 and Table 3 show that Blend 1 contained significant amounts of chlorogenic acid (637.92 mg/kg), ferulic acid (507.43 mg/kg), catechin (416.38 mg/kg), and coumaric acid (93.05 mg/kg).

Traces of 3,4-dihydroxybenzoic and rosemarinic acids were below the detection limit (BLD) in Blend 2 (Fig. 5, Table 3). However, Blend 2 proved to be rich in phenolic acids, e. g., chlorogenic acid (380.45 mg/kg), caffeic acids (265.91 mg/kg), and rutin (104.08 mg/kg). Blend 2 also contained coumaric acid (2.34 mg/kg) and astragalin (3.09 mg/kg).

To summarize, the phytochemical composition studied by the HPLC method showed that Blend 1 contained a lot of catechin, chlorogenic acid, coumaric acid, and ferulic acid while Blend 2 was rich in chlorogenic acid, caffeic acid, and rutin.

The HPLC fractionation demonstrated that the qualitative and quantitative profiles of fractions in Blend 1 (Fig. 6, Table 4) were quite diverse, as represented by

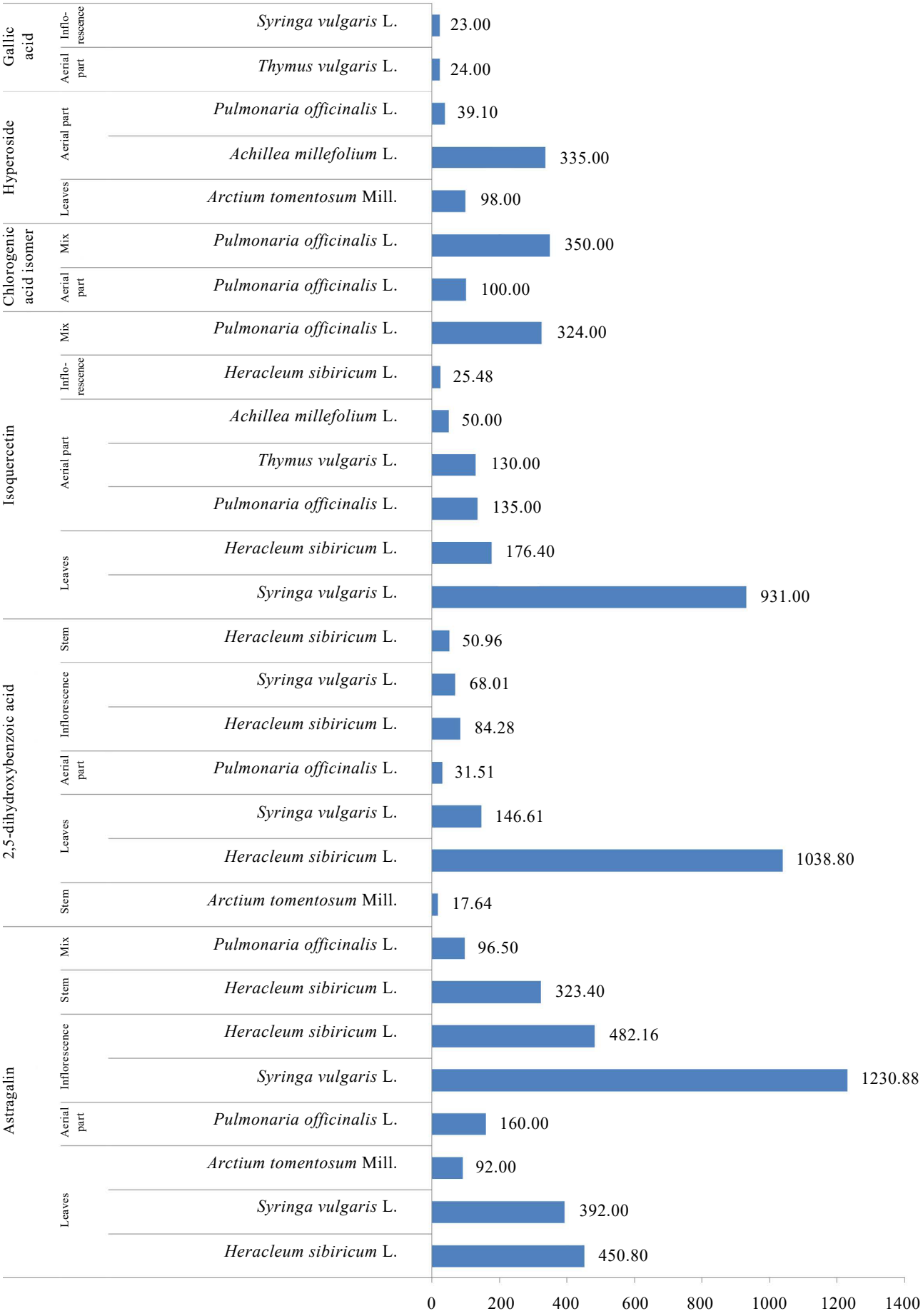

Figure 2 Metabolomic analysis of bioactive substances in plant extracts, μg/g

Table 2 Composition of blends

Blend	Extractant	Composition
1	70% water-ethanol	Hogweed, lilac, burdock, yarrow, thyme, lungwort
2	Whey	



Figure 3 Blends for phytochemical composition analysis

coumaric acid (fraction 2, № 4–6), chlorogenic acid (fraction 2, № 4–5), formononetin (fraction 5), catechin (fractions 5–8), ferulic acid (fractions 6–9), astragalin (fractions 7–8), and rosemarinic acid (fraction 9).

Fraction 2 contained chlorogenic acid in very small quantities; fraction 5 contained coumaric acid and formononetin below the detection limit.

Fraction 5, Blend 1 had the highest amount of catechin (5.20 ± 0.23 mg/kg); in fraction 6, it was below the detection limit. The biggest amount of catechin was contained in fraction 7 (12.91 ± 1.53 mg/kg) and fraction 8 (6.77 ± 1.48 mg/kg).

Fractions 6–9 were rich in ferulic acid: from 2.30 ± 0.08 mg/kg in fraction 8 to 8.26 ± 0.29 mg/kg in fraction 7. Fraction 6 contained 5.36 ± 0.17 mg/kg ferulic acid whereas fraction 9 had 5.78 ± 0.23 mg/kg ferulic acid.

Fractions 7 and 8 contained 2.43 ± 0.12 mg/kg and 3.24 ± 0.12 mg/kg astragalin, respectively.

Rosemarinic acid was detected nowhere but in fraction 9, where it was below the detection limit.

Fractions 1, 3–5, 8, and 10 in Blend 1 contained some unidentified compounds.

The qualitative and quantitative analysis of bioactive substances in the fractions of Blend 2 (Fig. 7, Table 5) revealed that fraction 1 contained traces of 3,4-dihydroxybenzoic acid (below the detection limit), as well as a number of unidentified compounds. Unidentified compounds were also detected in fractions 4 (vials 14–18, fraction yield 1.68 ± 0.07 g/kg), fraction 6 (vials 23–25, fraction yield 9.19 ± 0.28 g/kg), and fraction 8 (vials 28–35, fraction yield 12.38 ± 0.60 g/kg).

In fraction 2, we identified only two compounds, i. e., chlorogenic and caffeic acids. The content of chlorogenic acid in fraction 2 was 38.42 ± 1.58 mg/kg. Caffeic acid was present in trace amounts.

Fraction 3, Blend 2 was a mix of phenolic acids, i. e., chlorogenic, caffeic, and coumaric acids. The content of chlorogenic acid was 24.56 ± 1.10 mg/kg while that of

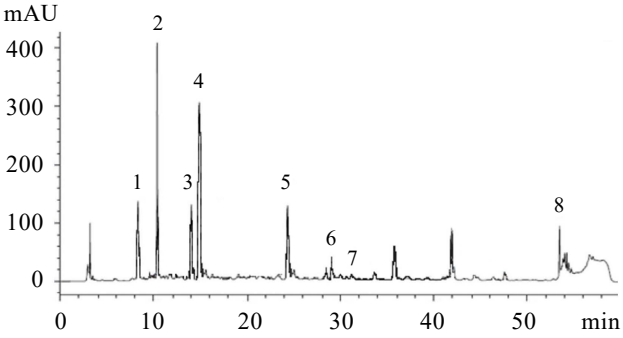

Figure 4 Blend 1, HPLC chromatogram: (1) catechin; (2) chlorogenic acid; (3) coumaric acid; (4) ferulic acid; (5) astragalin; (6) rosemarinic acid; (7) daidzein; and (8) formononetin

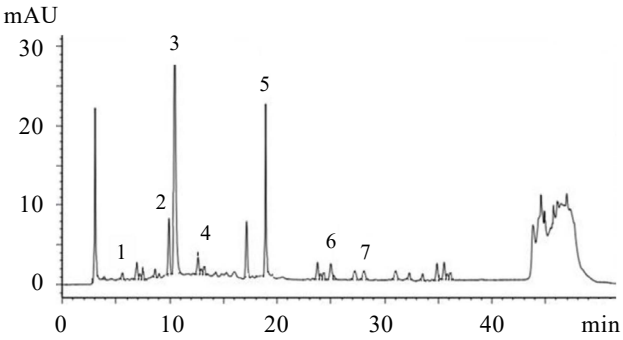

Figure 5 Blend 2, HPLC chromatogram: (1) 3,4-dihydroxybenzoic acid; (2) caffeic acid; (3) chlorogenic acid; (4) coumaric acid; (5) rutin; (6) astragalin; and (7) rosemarinic acid

Table 3 Phytochemical composition of blends

Bioactive substance	Retention time, min	Content, mg/kg	
		Blend 1	Blend 2
3,4-dihydroxybenzoic acid	5.10	–	traces
Catechin	8.99	416.38	–
Chlorogenic acid	10.35	637.92	380.45
Caffeic acid	10.76	–	265.91
Coumaric acid	14.56	93.05	2.34
Ferulic acid	15.44	507.43	–
Rutin	19.70	–	104.08
Astragalin	24.58	53.12	3.09
Rosemarinic acid	28.24	traces	b.l.d.
Daidzein	31.80	b.l.d.	–
Formononetin	53.87	b.l.d.	–

b.l.d. – below the detection limit

caffeic acid was as low as 5.89 ± 0.21 mg/kg. Coumaric acid was present in fraction 3 in trace amounts.

The HPLC analysis of fractions 4 and 5 revealed caffeic acid (1.29 ± 0.05 and 86.67 ± 3.07 mg/kg, respectively) and coumaric acid (0.98 ± 0.04 and 0.52 ± 0.02 mg/kg, respectively). Fraction 4 was rich in chlorogenic acid (5.73 ± 0.28 mg/kg).

Fraction 6 also contained rutin (67.92 ± 2.40 mg/kg) and astragalin (below the detection limit).

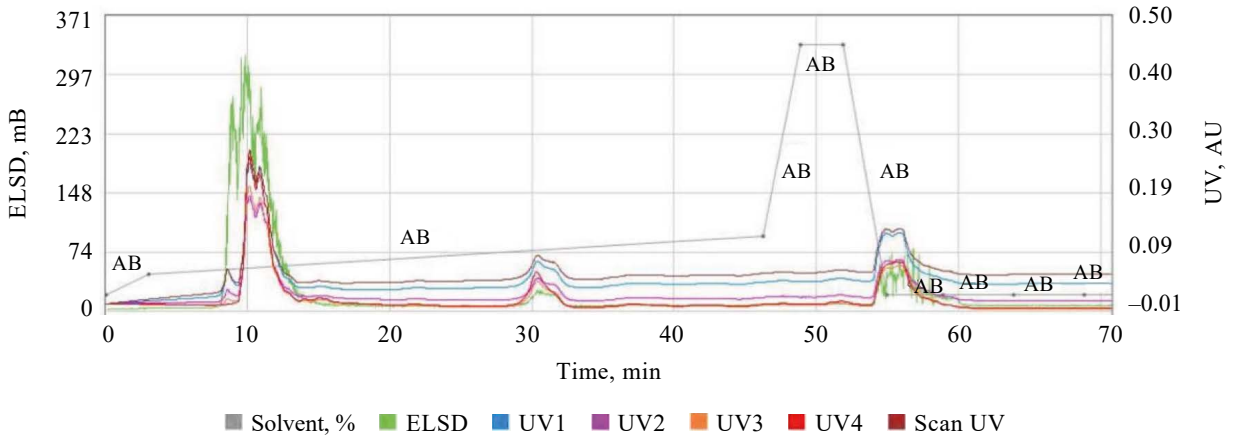

Figure 6 Preparative separation in Blend 1, chromatogram: UV1 λ = 254 nm; UV2 λ = 270 nm; UV3 λ = 280 nm; and UV4 λ = 320 nm

Table 4 Composition of fractions in Blend 1

Fraction	Vial	Yield of fraction, g/kg	Bioactive substances	Yield, g/kg
1	2	8.93 ± 0.41	n.i.	n.d.
2	3–4	11.79 ± 0.53	Coumaric acid Chlorogenic acid	33.74 ± 1.25 b.l.d.
3	5–7	14.94 ± 0.53	n.i.	n.d.
4	8–10	13.45 ± 0.46	n.i. Chlorogenic acid n.i. Coumaric acid	n.d. 18.29 ± 0.54 n.d. 14.33 ± 0.51
5	12–16	7.19 ± 0.26	Catechin n.i. Coumaric acid n.i. n.i. Formononetin	5.20 ± 0.23 6.95 ± 0.21 b.l.d. n.d. n.d. b.l.d.
6	16–20	3.41 ± 0.11	Catechin Ferulic acid n.i. Coumaric acid	b.l.d. 5.36 ± 0.17 n.d. 13.98 ± 0.64
7	21–25	2.11 ± 0.08	Ferulic acid Astragalin Catechin	8.26 ± 0.29 2.43 ± 0.12 12.91 ± 1.53
8	26–29	28.19 ± 1.02	n.i. n.i. Catechin Ferulic acid Astragalin	n.d. n.d. 6.77 ± 1.48 2.30 ± 0.08 3.24 ± 0.12
9	30–36	12.57 ± 0.43	Rosemarinic acid Ferulic acid	b.l.d. 5.78 ± 0.23
10	37–41	16.23 ± 0.58	n.i.	n.d.

n.i. – not identified; n.d. – not detected; and b.l.d. – below the detection limit

In Fraction 7 was revealed nothing but rutin (38.18 ± 1.52 mg/kg).

The total of ten fractions in Blend 1contained coumaric (fraction 2), chlorogenic (fraction 4), and ferulic acids (fractions 8–9). Blend 2 had eight fractions which contained rutin (fraction 7) and caffeic acid (fraction 5).

Fractions 2, 4, 8, and 9, Blend 1 were selected to isolate individual bioactive substances. Coumaric acid was isolated from fraction 2, and chlorogenic acid was isolated from fraction 4. Since fractions 8 and 9 in Blend 1 were rich in ferulic acid, we decided to isolate it from these fractions. Fractions 5 and 7, Blend 2 were used to isolate caffeic acid and rutin. Table 6 demonstrates the isolation results for individual bioactive substances.

Thus, Blend 1 yielded chlorogenic acid (90.0% mass fraction), ferulic acid (92.0%), and coumaric acid (88.0%)

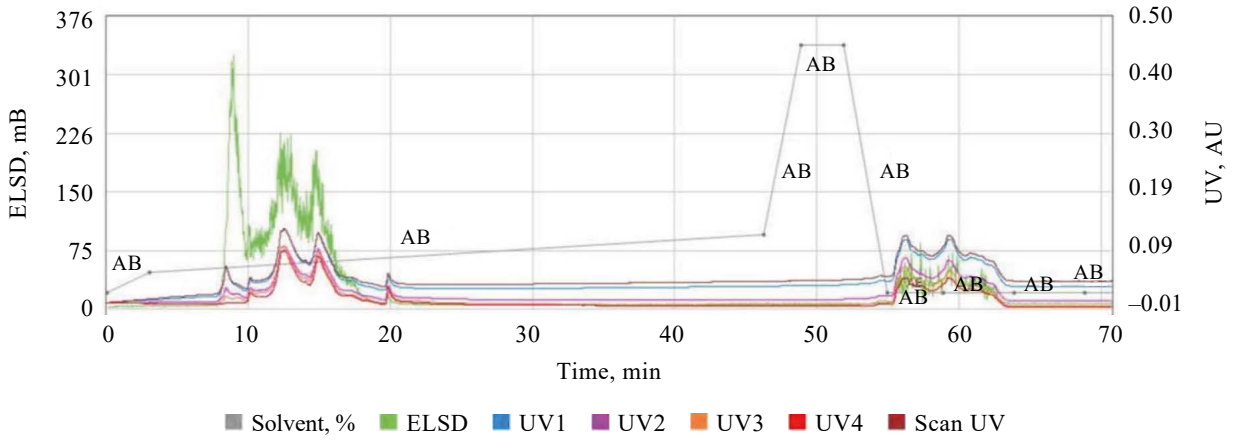

Figure 7 Preparative separation in Blend 2, chromatogram: UV1 λ = 254 nm; UV2 λ = 270 nm; UV3 λ = 280 nm; and UV4 λ = 320 nm

Table 5 Composition of fractions in Blend 2

Fraction	Vial	Yield, g/kg	Bioactive substances	Yield, g/kg
1	1–3	1.77 ± 0.04	3,4-dihydroxybenzoic acid	b.l.d.
			n.i.	n.d.
			n.i.	n.d.
			n.i.	n.d.
2	4–7	1.18 ± 0.05	Chlorogenic acid	38.42 ± 1.58
			Caffeic acid	b.l.d.
3	8–12	7.73 ± 0.37	Chlorogenic acid	24.56 ± 1.10
			Caffeic acid	5.89 ± 0.21
			Coumaric acid	b.l.d.
4	14–18	1.68 ± 0.07	Chlorogenic acid	5.73 ± 0.28
			Caffeic acid	1.29 ± 0.05
			Coumaric acid	0.98 ± 0.04
			n.i.	n.d.
5	19–22	33.17 ± 1.32	Caffeic acid	86.67 ± 3.07
			Coumaric acid	0.52 ± 0.02
6	23–25	9.19 ± 0.28	n.i.	n.d.
			n.i.	n.d.
			Rutin	67.92 ± 2.40
			Astragalin	b.l.d.
7	25–28	0.57 ± 0.02	Rutin	38.18 ± 1.52
8	28–35	12.38 ± 0.60	n.i.	n.d.

n.i. – not identified; n.d. – not detected; and b.l.d. – below the detection limit

Table 6 Bioactive substances isolated from blends

Blend	Bioactive substance	Concentration, vol. % (purity)
1	Chlorogenic acid	90.0 ± 3.5
	Ferulic acid	92.0 ± 4.0
	Coumaric acid	88.0 ± 4.0
2	Caffeic acid	84.5 ± 4.2
	Rutin	78.0 ± 3.8

in individual form. Blend 2 yielded caffeic acid (84.5%) and rutin (78.0%).

Individual bioactive substances were obtained as white crystalline powder by freeze-drying (Fig. 8). All bioactive substances had a low moisture content (Table 7), which means they could retain their biological properties during long-time storage.

Sublimation made it possible to obtain individual bioactive substances as solids with a moisture content of 3.8–4.5%. A comparative analysis of the obtained extractants proved that Blend 1 (70% water-ethanol solution) contained more biologically active substances than Blend 2 (whey). Unlike Blend 1, Blend 2 contained rutin and caffeic acid. Unlike Blend 2, Blend 1 had traces of catechin, ferulic acid, and some other bioactive substances. Figure 9 compares bioactive substances isolated from the two blends.

The samples with 70% water-ethanol extractant yielded more bioactive substances than the whey extractant: chlorogenic acid (637.92 vs. 380.45), coumaric acid (93.05 vs. 2.34), astragalin (53.12 vs. 3.09), catechin (416.38 vs. 0), ferulic acid (507.43 vs. 0). However, the whey extractant made it possible to isolate some

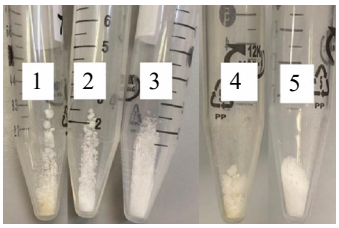

Figure 8 Lyophilized bioactive substances: (1) rutin; (2) chlorogenic acid; (3) coumaric acid; (4) caffeic acid; and (5) ferulic acid

Table 7 Mass fraction of moisture in fractions

Bioactive substance	Moisture mass fraction, %
Chlorogenic acid	4.0 ± 0.1
Caffeic acid	3.8 ± 0.1
Ferulic acid	4.3 ± 0.2
Coumaric acid	4.5 ± 0.2
Rutin	4.2 ± 0.2

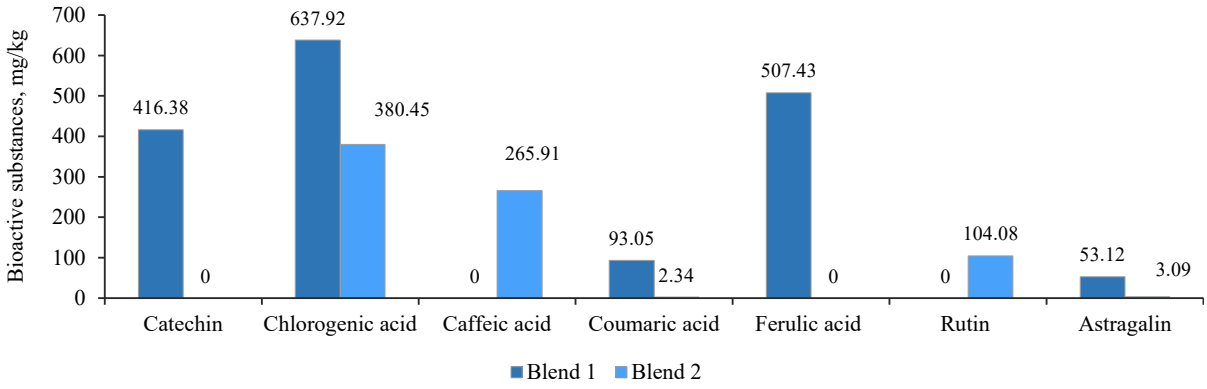

Figure 9 Quantities of bioactive substances in Blend 1 (70% water-ethanol extractant) and Blend 2 (whey)

substances that the 70% water-ethanol extractant failed to isolate, i. e., caffeic acid (265.91) and rutin (104.08).

To summarize, the water-ethanol extractants proved more effective in extracting bioactive substances in larger volumes. Yet, the industrial use of way might still be feasible, given that whey is a massive waste product of dairy production and its drain causes significant harm to the environment. In addition, whey was able to isolate some biologically active substances (rutin and caffeic acid) that the water-ethanol solution failed to extract.

CONCLUSION

The focus of phytochemical extraction research is shifting towards more efficient but environmentally friendly and scalable methods. While maximizing the yield and purity of bioactive substances, these methods ensure the sustainability of the extraction process.

Ethanol extraction is effective due to its wide solubility range. It is a neutral solvent capable of extracting a wide range of compounds, including both hydrophilic (water-soluble) components and lipophilic ones. Its antimicrobial properties reduce the risks of contamination and preserve the quality of extracts. Ethanol is relatively safe and economical. It evaporates after extraction, thus facilitating the concentration processes. These characteristics make ethanol a popular extractant of bioactive ingredients, especially those with high antioxidant activities [35].

Whey remains an unconventional extractant. However, its status as a major pollutant makes it a prospective candidate for industrial recycling. Today, whey wastes are recycled for the biologically active substances they contain, which may complicate the purification of the finished products. But whey can also be used to extract bioactive substances from plant materials. While few studies report whey as an effective extractant, some do feature the whey extraction of terpenoid fractions, phenolic compounds, vitamin C, and rutin.

We studied the phytochemical composition of plant blends that had the same component composition but different extractants, i. e., 70% water-ethanol solution (Blend 1) and whey (Blend 2). Blend 1 contained large amounts of catechin, chlorogenic acid, coumaric acid, and ferulic acid. Blend 2 was rich in chlorogenic acid, caffeic acid, and rutin. We also fractionated the blends. Blend 1 yielded ten fractions, which mainly contained coumaric acid (fraction 2), chlorogenic acid (fraction 4), and ferulic acid (fractions 8–9). Blend 2 yielded eight fractions, some of which contained rutin (fraction 7) and caffeic acid (fraction 5).

We also isolated some individual bioactive substances from the fractions obtained. Blend 1 yielded chlorogenic acid (90.0%), ferulic acid (92.0%), and coumaric acid (88.0%). Blend 2 yielded caffeic acid (84.5%) and rutin (78.0%).

The bioactive substances underwent freeze-drying to a moisture mass fraction of 3.8–4.5%, which makes them a valuable ingredient with a long-term shelf-life to be used in feed for live-stock animals.

The alcohol extractant proved superior to the whey extractant in terms of quantity and diversity of bioactive

substances extracted. However, the whey extractant was able to isolate substances that the water-ethanol solution failed to affect. The fact that whey was able to extract caffeic acid and rutin proved its efficiency as a solvent and rendered it with some prospects for future studies. Both ethanol and whey proved industrially relevant as extractants of biologically active substances from plant materials.

CONTRIBUTION

The authors were equally involved in writing the manuscript and bear equal responsibility for any potential plagiarism.

CONFLICT OF INTEREST

The authors declared no conflict of interest regarding the publication of this article.

REFERENCES

1. Velichkovich NS, Dunchenko NI, Stepanova AA, Kozlova OV, *et al.* The phytochemical composition of Kuzbass medicinal plants. Foods and Raw Materials. 2025;13(2):219–232. https://doi.org/10.21603/2308-4057-2025-2-649
2. Milentyeva IS, Le VM, Kozlova OV, Velichkovich NS, Fedorova AM, *et al.* Secondary metabolites in *in vitro* cultures of Siberian medicinal plants: Content, antioxidant properties, and antimicrobial characteristics. Foods and Raw Materials. 2021;9(1):153–163. https://doi.org/10.21603/2308-4057-2021-1-153-163
3. Asyakina L, Atuchin V, Drozdova M, Kozlova O, Prosekov A. Ex Vivo and In Vitro Antiaging and Antioxidant Extract Activity of the *Amelanchier ovalis* from Siberia. International Journal of Molecular Sciences. 2022;23(23):15156. https://doi.org/10.3390/ijms232315156
4. Babich OO, Samsuev IG, Tcibulnikova AV, Zemlyakova ES, Popov AD, *et al.* Properties of plant extracts and component composition: Column chromatography and IR spectroscopy. Foods and Raw Materials. 2024;12(2): 373–387. https://doi.org/10.21603/2308-4057-2024-2-615
5. Kozlova OV, Velichkovich NS, Faskhutdinova ER, Neverova OA, Petrov AN. Methods for extracting immune-response modulating agents of plant origin. Food Processing: Techniques and Technology. 2023;53(4):680–688. (In Russ.) https://doi.org/10.21603/2074-9414-2023-4-2468
6. Donno D, Mellano MG, Gamba G, Riondato I, Beccaro GL. Analytical strategies for fingerprinting of antioxidants, nutritional substances, and bioactive compounds in foodstuffs based on high performance liquid chromatography–mass spectrometry: An overview. Foods. 2020;9(12):1734. https://doi.org/10.3390/foods9121734
7. Prosekov AYu, Golubtsova YuV, Shevyakova KA. Influence of technological raw food treatment on the effectiveness of species identification. Food Industry. 2014;(6):8–10. (In Russ.) https://elibrary.ru/SFJBBP
8. Allaoui HE, Ahmadi KE, Abdouni AE, Dira I, Bastrioui ME, *et al.* Trends and insights in medicinal plant extract research: A ten-year bibliometric and visualization study. Horticulturae. 2024;10(11):1163. https://doi.org/10.3390/horticulturae10111163
9. Omeroglu PY, Acoglu B, Ozdal T, Tamer CE, Copur OU. Extraction techniques for plant-based bio-active compounds. Natural Bio-Active Compounds. Singapore: Springer; 2019. pp. 465–492.
10. Sukhikh S, Babich O, Prosekov A, Patyukov N, Ivanova S. Future of chondroprotectors in the treatment of degenerative processes of connective tissue. Pharmaceuticals. 2020;13(9):220. https://doi.org/10.3390/ph13090220
11. Chaachouay N, Zidane L. Plant-derived natural products: A source for drug discovery and development. Drugs and Drug Candidates. 2024;3(1):184–207. https://doi.org/10.3390/ddc3010011
12. Fokina AD, Vesnina AD, Frolova AS, Chekushkina DYu, Proskuryakova LA, *et al*. Bioactive anti-aging substances: Geroprotectors. Food Processing: Techniques and Technology. 2024;54(2):423–435. (In Russ.) https://doi.org/10.21603/2074-9414-2024-2-2517
13. Salmerón-Manzano E, Garrido-Cardenas JA, Manzano-Agugliaro F. Worldwide research trends on medicinal plants. International Journal of Environmental Research and Public Health. 2020;17(10):3376. https://doi.org/10.3390/ijerph17103376
14. Priss O, Pugachov M, Pugachov V, Yaremko I, Shchabelska V. The development of the world economy and the impact of the global food crisis 2022–2023. Economic Affairs. 2023;68(01s):35–42. https://doi.org/10.46852/0424-2513.1s.2023.5
15. Dolganyuk V, Sukhikh S, Kalashnikova O, Ivanova S, Kashirskikh E, *et al.* Food proteins: Potential resources. Sustainability. 2023;15(7):5863. https://doi.org/10.3390/su15075863
16. Hutsol T, Priss O, Kiurcheva L, Serdiuk M, *et al.* Mint plants (Mentha) as a promising source of biologically active substances to combat hidden hunger. Sustainability. 2023;15(15):11648. https://doi.org/10.3390/su151511648
17. Milentyeva IS, Fedorova AM, Larichev TA, Altshuler OG. Biologically active compounds in *Scutellaria baicalensis* L. callus extract: Phytochemical analysis and isolation. Foods and Raw Materials. 2023;11(1):172–186. https://doi.org/10.21603/2308-4057-2023-1-564

18. Kostyuchenko MN, Kosovan AP, Martirosyan VV, Tyurina OE, Peshkina IP, *et al.* Development of technology and range of functional bakery products using endemic raw materials for the population of the arctic zone of the Russian Federation. Food Industry. 2025;(6):80–84. (In Russ.) https://doi.org/10.52653/PPI.2025.6.6.017
19. Dyshlyuk LS, Fedorova AM, Loseva AI, Eremeeva NI. Callus cultures of *Thymus vulgaris* and *Trifolium pratense* as a source of geroprotectors. Food Processing: Techniques and Technology. 2021;51(2):423–432. https://doi.org/10.21603/2074-9414-2021-2-423-432
20. Vesnina A, Prosekov A, Atuchin V, Minina V, Ponasenko A. Tackling atherosclerosis via selected nutrition. International Journal of Molecular Sciences. 2022;23(15):8233. https://doi.org/10.3390/ijms23158233
21. Truong H, Nguyen DH, Ta NTA, Anh VB, Tuong HD, *et al*. Evaluation of the use of different solvents for phytochemical constituents, antioxidants, and *in vitro* anti-inflammatory activities of *Severinia buxifolia*. Journal of Food Quality. 2019;2019(1):1–9. https://doi.org/10.1155/2019/8178294
22. Asyakina LK, Fedorova AM, Dyshlyuk LS. Optimization of the parameters of *in vitro* extraction of root cultures *Scutellaria galericulata, Scutellaria baicalensis, Potentilla alba*. Food Industry. 2021;(10):82–85. (In Russ.) https://doi.org/10.52653/ppi.2021.10.10.001
23. Velichkovich NS, Stepanova AA, Kozlova OV, Lutz VA, Larichev TA. Extraction of bioactive substances from medicinal plants with whey: Selecting optimal parameters. Food Processing Techniques and Technology. 2024;54(3):633–644. (In Russ.) https://doi.org/10.21603/2074-9414-2024-3-2532
24. Melnikova EI, Korenman YaI, Niftaliev SI, Rudnichenko ES, Korneeva MM, *et al*. Method for obtaining milk and plant extract from yacon tubers. Patent RU 2345543 C1. 2009. (In Russ.) https://elibrary.ru/ZXFQNK
25. Kaledina MV, Fedosova AN, Shramko MI, Salatkova NP, Martinova IA. Fermented milk drinks with herbal extracts on the basis of whey. Newsletter of North-Caucasus Federal University. 2013;(6):92–96. (In Russ.) https://elibrary.ru/RXANWJ
26. Khalanskaya DM, Lodygin AD, Kurchenko VP. Effect of technological factors on the extraction of biologically active substances from plant raw materials. Proceedings of the International Scientific and Practical Conference on Molecular Genetics and Biotechnology in Obtaining and Using Synthetic and Natural Biologically Active Substances. Stavropol; 2017:290–293. (In Russ.) https://elibrary.ru/ZISHHT
27. Lodygin A, Khalanskaya D, Evdokimov I, Kurchenko V, Lodygina S, *et al*. Application of whey for plant biologically active substances extraction. Journal of Hygienic Engineering and Design. 2024;46:73–79.
28. Sargin BV, Bobkov GV, Pavlov SA. Method for preparing extracts of herbal raw material by water-in-oil extraction in natural extractants. Patent RU 2491947 C2. 2013. (In Russ.) https://elibrary.ru/XZIHCD
29. Daudova TN, Ramazanova LA. Method for obtaining milk and plant extract from pepperidge berries. Patent RU 2355193 C1. 2009. (In Russ.) https://elibrary.ru/XPYEQZ
30. Daudova TN, Ramazanova LA. Method for obtaining milk and plant extract from high cranberries. Patent RU 2358475 C1. 2009. (In Russ.) https://elibrary.ru/ZHJXRZ
31. Doronin AF, Demidov DA, Demidova TI, Shevernitskaya ON, Muratov VS. Method for production of powdered product of garden beet. Patent RU 2409280 C1. 2011. (In Russ.) https://elibrary.ru/ZFWZWX
32. Asyakina LK, Loseva AI, Milentyeva IS, Prosekov AYu, Minina VI. Prospects for using Siberian federal district plants in the production of functional food products. Bulletin of the South Ural State University. Series: Food and Biotechnology. 2022;10(4):5–17. (In Russ.) https://elibrary.ru/AVIQIC
33. Babich O, Larina V, Krol O, Ulrikh E, Sukhikh S, *et al. In vitro* study of biological activity of *Tanacetum vulgare* extracts. Pharmaceutics. 2023;15(2):616. https://doi.org/10.3390/pharmaceutics15020616
34. Lee S, Jo K, Jeong SKC, Choi YS, Jung S. Production of freeze-dried beef powder for complementary food: Effect of temperature control in retaining protein digestibility. Food Chemistry. 2024;433:137419. https://doi.org/10.1016/j.foodchem.2023.137419
35. Lee JE, Jayakody JTM, Kim JI, Jeong JW, Choi KM, *et al.* The influence of solvent choice on the extraction of bioactive compounds from Asteraceae: A comparative review. Foods. 2024;13(19):3151. https://doi.org/10.3390/foods13193151

ORCID IDs
Anna A. Stepanova https://orcid.org/0000-0001-7774-8859
Alice D. Mitina https://orcid.org/0009-0004-7824-3982
Natalia S. Velichkovich https://orcid.org/0000-0002-9061-1256
Oksana V. Kozlova https://orcid.org/0000-0002-2960-0216
Timothy A. Larichev https://orcid.org/0000-0003-0166-2527
Larisa A. Proskuryakova https://orcid.org/0000-0002-9583-9161
Vladimir V. Martirosyan https://orcid.org/0000-0002-4026-5789

Foods and Raw Materials. 2026;14(2)

ISSN 2308-4057 (Print)
ISSN 2310-9599 (Online)

Research Article
Open Access

Available online at http://jfrm.ru/en
https://doi.org/10.21603/2308-4057-2026-2-688
https://elibrary.ru/QADNGU

Geroprotective potential of *Thymus vulgaris* L. callus culture and its metabolites

Anastasiya M. Fedorova*, Arina A. Shevel, Svetlana V. Kovalenko, Ekaterina S. Miller, Anna I. Loseva, Olga G. Altshuler, Alexandra V. Zaushintsena, Vladimir P. Yustratov

Kemerovo State University, Kemerovo, Russia

* e-mail: anastasija.fedorova-af2014@yandex.ru

Received 02.04.2025; Revised 23.06.2025; Accepted 05.08.2025; Published online 27.11.2025

Abstract:
Healthy aging and active longevity need an integrated approach to a healthy lifestyle. Proper nutrition can effectively prevent the development of chronic diseases that lead to premature aging. Therefore, food scientists are searching for new bioactive substances with geroprotective potential to be introduced into functional food products and dietary supplements. We aimed to study the bioactivity of the *Thymus vulgaris* L. callus culture extract and its metabolites as potential geroprotectors.

We studied a hydroalcoholic extract of the *T. vulgaris* callus culture (70% ethanol) and its individual bioactive substances (thymol, oleanolic and ursolic acids), with *Caenorhabditis elegans* used as a model organism. IR spectroscopy and high-performance liquid chromatography were employed to analyze the effect of the extract and its metabolites on the growth of *C. elegans* larvae, as well as on the nematodes' lifespan and resistance to oxidative and thermal stress.

The extract of the *T. vulgaris* callus culture increased the length and surface area of the nematode body, producing an anabolic effect. In a 100-fold dilution, the extract enhanced the survival and stress resistance of the nematodes. Thymol, oleanolic and ursolic acids were obtained from the extract at 95% purification. Thymol completely inhibited the growth of nematode larvae, with no offspring produced from the eggs. At 10 μM, thymol increased the survival of the nematodes by a factor of 1.8 and also improved their stress resistance. In the presence of oleanolic acid (10 and 50 μM), some nematodes laid eggs; oleanolic acid increased the nematode lifespan be a factor of 1.9. Oleanolic acid (200 and 100 μM) and ursolic acid (50 and 100 μM) increased the survival of the nematodes exposed to thermal stress compared to the control.

The extract of the *T. vulgaris* callus culture and its metabolites (thymol, oleanolic and ursolic acids) have geroprotective potential for use in food supplementation. However, there is a need for further research.

Keywords: Geroprotectors, callus culture extract, thymol, oleanolic acid, ursolic acid, *Caenorhabditis elegans*

Funding: This study was part of the state assignment on "The development of bioactive additives consisting of plant metabolites *in vitro* to protect the population from premature aging" (project FZSR-2024-0008).

Please cite this article in press as: Fedorova AM, Shevel AA, Kovalenko SV, Miller ES, Loseva AI, *et al.* Geroprotective potential of *Thymus vulgaris* L. callus culture and its metabolites. Foods and Raw Materials. 2026;14(2):443–460. https://doi.org/10.21603/2308-4057-2026-2-688

INTRODUCTION

According to the World Health Organization, 2022 saw the global population aged 65 and over accounting for 9.4% of the total population. Across the countries, the proportion of older people reached 16.85% in Russia (similarly to Australia, Iceland, Belarus, and Montenegro), 14.5% in China, and about 19% in the USA and the UK [1]. The number of older people is growing every year worldwide. A country or a region is considered to be aging when its population aged 60 years and over reaches 10%. Whether aging is an inevitable destructive biological process remains controversial. Aging, however, leads to an increase in age-related diseases, including metabolic disorders, cancer, and neurodegeneration [2].

Aging is a complex process influenced by genetic, environmental, and lifestyle factors [3]. In 2023, a group of scientists led by K. Lopez-Otin added three new hallmarks of aging to the original 9 hallmarks, providing a more comprehensive framework for anti-aging research. They include genomic instability, telomere attrition, epigenetic alterations, loss of proteostasis, disabled macroautophagy, deregulated nutrient-sensing, mitochondrial dysfunction, cellular senescence, stem cell exhaustion,

Copyright © 2025, Fedorova *et al.* This is an open access article distributed under the terms of the Creative Commons Attribution 4.0 International License (https://creativecommons.org/licenses/by/4.0/), allowing third parties to copy and redistribute the material in any medium or format and to remix, transform, and build upon the material for any purpose, even commercially, provided the original work is properly cited and states its license.

altered intercellular communication, chronic inflammation, and dysbiosis [4].

Currently, geroprotectors are actively used to combat or prevent premature aging by counteracting the hallmarks mentioned above [4, 5]. One of them is metroformin, which is primarily known as an antidiabetic agent [6]. Nicotinamide mononucleotide is another anti-aging agent that plays a vital role in various biological processes, including cell death, aging, gene expression, neuroinflammation, and DNA repair, as reported by Nadeeshani *et al*. [7]. Quercetin is a flavonoid that exhibits antioxidant activity *in vitro*. It has a positive effect on the lifespan of *Caenorhabditis elegans* and its survival under oxidative stress, on the expression of the *SOD-3* gene, and on the accumulation of lipid inclusions *in vivo* [8].

Thus, targeting the hallmarks of aging can slow down or reverse the aging process.

Some of the major challenges of the modern world are how to prevent aging and prolong an active life. They call for a complex approach integrating a healthy lifestyle, proper nutrition, physical activity, good mental health, and preventive healthcare [9]. Proper nutrition is one of the most effective measures to prevent the development of chronic diseases that lead to premature aging [10].

Therefore, there is a need to search for new bioactive substances (bioactive geroprotectors) to be included in the human diet as part of functional foods or dietary supplements.

Today, plant materials rich in bioactive geroprotectors are used to produce effective and safe drugs to prevent cardiovascular, oncological, and skin diseases, as well as diseases associated with premature wear, fragility, and other aging processes in the body [11–14]. Among various bioactive geroprotectors, polyphenols are increasingly attracting scientists due to their rejuvenating effect. According to many studies, polyphenols exhibit anti-inflammatory and antioxidant effects by stimulating cell regeneration [15, 16]. In addition, they can regulate the immune function and inflammatory response, as well as increase resistance to diseases such as lupus [17], rheumatoid arthritis [18], and multiple sclerosis [19]. Finally, polyphenols isolated from plants benefit human health by slowing down the aging of various organs and tissues, such as the brain, muscles, skin, heart, liver, and gut [20].

Thymus vulgaris L. is one of many plants containing a wide range of polyphenols. Growing in the Mediterranean region, this plant has been shown to protect the brain from neurodegeneration and neuroinflammation risk factors. Shimada *et al*. [21] described the inhibitory effect of three pentacyclic terpenes (ursolic, betulinic, and oleanolic acid) isolated from *T. vulgaris* on glutaminase activity. Glutaminase inhibitors are a potential therapeutic agent for the prevention and treatment of neurodegenerative diseases. Other researchers identified the anti-inflammatory activity of linalool and geraniol contained in *T. vulgaris* essential oil against lipopolysaccharide-induced neuroinflammation in BV-2 microglial cells [22].

In addition, thymol and para-cymene, both individually and in combination, contributed to the attenuation of cholinergic brain damage that leads to neurodegenerative diseases [23]. Warman *et al*. [24] established the effect of *T. vulgaris* essential oil on the attenuation of chronic low-grade inflammation of the brain caused by aging and the protection of blood telomeres in aged C57BL/6J mice. The oil was also found to exhibit spasmolytic and antimicrobial effects [25]. Many studies confirm the positive effect of *T. vulgaris* extracts on cardiovascular, oncological, and inflammatory diseases [26]. Furthermore, these extracts are also used to treat respiratory problems [27], relieve gastrointestinal spasms, and improve digestion [28]. Thus, *T. vulgaris* has been shown to have functional potential for preventing the development of chronic diseases that lead to premature aging.

T. vulgaris grows in the central and southern regions of the European part of Russia, in the Caucasus, and in the south of Eastern and Western Siberia [29]. However, its natural resources are insufficient to meet the needs of the whole population. Therefore, biotechnological cultivation of callus cultures [30] should be applied to preserve biodiversity and produce a sufficient amount of plant materials for obtaining bioactive substances. Plant cell cultures are increasingly being used as alternative sources of valuable secondary metabolites [31, 32]. Callus culture is one of the models of microclonal propagation of plants. It is a system of plant tissues consisting of thin-walled parenchymatous cells grown on artificial nutrient media [33].

The bioactivity of the *T. vulgaris* callus culture extract and its metabolites can be assessed using various models including nematodes, fruit flies, mice, rats, or primates [34]. Today, *C. elegans* nematodes are promising model organisms for fundamental research. Their aging is manifested through decreased mobility, tissue degeneration, and cessation of reproduction. This makes them effective models for preclinical trials of bioactive substances [35]. In addition, their anatomical and physiological features allow for short-term studies of their lifespan. According to Zhang *et al*. [36], bioactive substances extracted from *Portulaca oleracea* with ethyl acetate increased the average lifespan of nematodes by 5.3, 12.7, and 16.5% at concentrations of 250, 500, and 1,000 μg/mL, respectively. Also, the higher concentrations increased the worms' motility.

Many studies of *C. elegans* have shown the influence of metabolic pathways on aging. These nematodes have complex conservative pathways and gene expression programs. Their longevity and response to stress are controlled by such pathways as stress reactions (reactive oxygen species, heat shock). Oxidative stress is the main factor of aging in vertebrates, with reactive oxygen species accelerating the aging process. Song *et al*. [37] found that the nematodes incubated with raspberry extract had reduced levels of free radicals for five days. The SKN-1 protein is a transcription factor involved in the modulation of oxidative stress and, therefore, the

lifespan of the worms. During stress, the protein is phosphorylated and its accumulation in the nucleus activates the genes such as *gcs-1, gst-4,* and *gst-7.* These genes regulate metabolism, aging, and oxidative stress [38].

Thus, the nematodes *C. elegans* are used to study the effects of polyphenols on their viability and longevity. According to studies, bioactive substances at different concentrations have varying effects on the metabolism and physiological processes of the worms, increasing their life expectancy, reducing thermal and oxidative stress, etc.

In this study, we aimed to investigate the biological activity of the *T. vulgaris* callus culture extract and its individual bioactive substances (potential geroprotectors) for preventative functional food supplementation. In particular, we analyzed the geroprotective potential of the extract and three of its bioactive substances (thymol, oleanolic and ursolic acids) *in vivo.*

STUDY OBJECTS AND METHODS

Our study objects included: 50% alcohol solutions of the hydroalcoholic extract of *Thymus vulgaris* L. callus culture (70% ethanol), which were diluted with sterile distilled water at ratios of 1:10,000, 1:1,000, and 1:100; individual bioactive substances (thymol, oleanolic and ursolic acids) as solutions in dimethyl sulfoxide (DMSO) at concentrations of 200, 100, 50, and 10 μM.

The cultivation of the *T. vulgaris* callus culture, the hydroalcoholic extraction of its biomass, and the chemical analysis of the extract were performed at the early stages of our study at the Laboratory for Biotesting of Natural Nutraceuticals, Kemerovo State University, as described in [39].

The bioactive substances were isolated from the hydroalcoholic extract as follows. The extract was evaporated on an IKA RV 8 rotary vacuum evaporator (IKA-Werke GmbH & Co. KG, Staufen, Germany) at under 40°C. Deionized water, which had been sparged with an inert gas, was added to the residue evaporated to 1/4 of the initial volume and the vacuum evaporation was continued until a dry residue was obtained. The residue was then treated three times with dichloromethane (EKOS-1, Russia) for 5 min, each time with vigorous stirring. The resulting extracts were combined, and anhydrous sodium sulfate (Organic Mir, Russia) was added at 20.0 g per liter of the dichloromethane extract. The mixture was left to settle for 3 h and filtered through a degreased paper filter with a pore size of 8–12 μm (State Standard 12026-76; Ekokhim, Russia) followed by a membrane filter with a pore size of 0.45 μm (Membrane Solutions, LLC, USA).

The residue was used to isolate the flavonoid fraction, while the supernatant (filtrate) was used to isolate thymol.

IR spectra were recorded on an SF-2000 device (SPEKTR, Russia) for those bioactive substances of the *T. vulgaris* callus culture extract which were at least 95% pure.

Thymol was purified further by vacuum evaporation. For this, the supernatant was evaporated in a vacuum evaporator until the initial volume was reduced tenfold. The resulting solution of thymol in dichloromethane was subjected to column chromatography using aluminum oxide (activity II according to Brockmann) as a sorbent [40]. For this, aluminum oxide was dried in a drying cabinet at 150°C for 12 h, cooled in a desiccator, and then deactivated with 3% water by weight. The solution was eluted with dichloromethane using a BioLogic low-pressure chromatograph (BioRad, Hercules, CA, USA) on a 30×150 mm chromatographic column with a fraction collector, resulting in 1 mL of the eluate.

The purification of individual bioactive substances from the residue of the flavonoid fraction (flavonoids and their glycosides, phenolic carboxylic acids, triterpenoids) included the following stages. First, the residue was dissolved in 96% ethanol (RFK, Russia). The ethanol fraction was passed through an AN-1 anion exchanger (State Standard 20301-74). Then, it was washed with water-ethanol eluents (up to 50% ethanol), desorbed using 0.1 M HCl, and fractionated using a Sephadex LH-20 sorbent (GE Healthcare, Chicago, Illinois, USA) in an ethanol gradient of 10–80%. As a result, we obtained two bioactive substances – oleanolic and ursolic acids.

Figure 1 shows the stages of isolation and purification of metabolites from the extract of the *T. vulgaris* callus culture.

The isolated individual bioactive substances were identified using IR spectroscopy and HPLC (degree of oxidation on a glassy carbon electrode):

1. IR spectroscopy was performed on an FSM-1202 spectrometer (Infraspek, St. Petersburg, Russia). IR spectra were recorded in potassium bromide disks (Fluka, Germany). The conditions included a transmission mode of 4000–400 cm^{-1}, a resolution of 4 cm^{-1}, and 30 scans. Air was used as a reference sample and it was recorded before the analysis of each test sample. FSpec (4.0.0.2) and Aspec (1.1) softwares were used to control the process and analyze the spectral data.
2. The oxidation of the bioactive substances on a glassy carbon electrode was measured on a Tsvet Yauza-04 HPLC chromatograph, with an UV/Vis detector and a photodiode array at wavelengths of 255, 280, and 370 nm. The process was controlled and the data were analyzed using MultiChrom 3.1.1550 (Ampersend, Russia), with a Kromasil C18 110A column (5 μm, 250×4.6 mm; MERCK, USA) and a KJO-4282 analytical guard pre-column.

The bioactivity of the *T. vulgaris* callus culture extract and its individual bioactive substances was tested on nematodes *Caenorhabditis elegans*. The *C. elegans* N2 Bristol strain was provided by the Laboratory of Innovative Drug Development and Agrobiotechnology, Moscow Institute of Physics and Technology (National Research University, Dolgoprudny, Russia).

The nematodes were cultivated on solid agar according to the method described in [41]. They were fed on *Escherichia coli* OP50 strain provided by the Engelhardt Institute of Molecular Biology, Russian Academy of Sciences (Russia). To obtain a starter culture, one *E. coli*

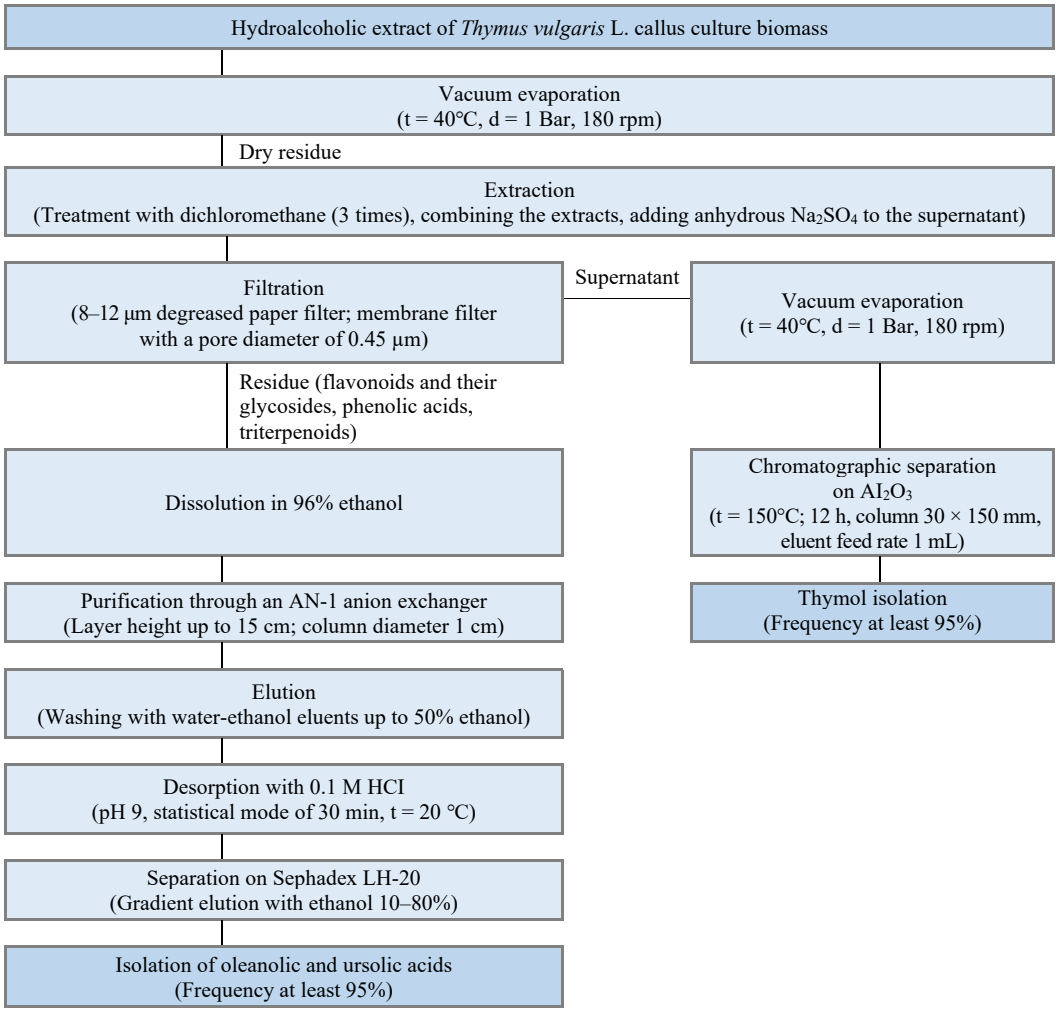

Figure 1 Isolation and purification of bioactive substances from the extract of the *Thymus vulgaris* L. callus culture

colony was grown in 5 cm^3 of LB medium (AppliChem GmbH, Germany) for 12 ± 0.5 h at 37 ± 0.5°C with vigorous stirring (120 rpm). At least 100 *C. elegans* worms were used in the experiments to test the *T. vulgaris* callus culture extract, as well as each individual bioactive substance.

To synchronize the nematodes, 5–10 mL of sterile water was added to an agar Petri dish with the nematodes and mixed several times until all the nematodes and their eggs were adhesively attached to the agar. The liquid was poured into a 50-mL tube and centrifuged for 2 min at 1,200 rpm. The supernatant was removed and the sediment was washed with 10 mL of distilled water. The supernatant was removed again and then 5 mL of a freshly prepared mixture of 1 mL of 10 N NaOH, 2.5 mL of sodium hypochlorite, and 6.5 mL of water was added to the sediment. The sediment was vigorously mixed for 5 min with a pause every 2 min to hydrolyze the nematodes. Upon completion, 5 mL of M9 medium (1,000 mL ddH_2O, 3 g KH_2PO_4, 5 g NaCl, 6 g Na_2HPO_4, 1 mL 1 M $MgSO_4$) was added to neutralize the reaction. The mixture was centrifuged for 2 min at 2500 rpm. The supernatant was removed and the sediment was resuspended in 10 mL of fresh sterile water. The neutralization and centrifugation were repeated 3 times. The sediment was washed for the fourth time with 10 mL of S medium (1,000 mL S base, 10 mL 1 M potassium citrate pH 6, 10 mL trace metal solution, 3 mL 1 M $CaCl_2$, 3 mL 1 M $MgSO_4$). The supernatant was removed, 10 mL of epy S medium was added, and the test tube with nematode eggs was left on a slow shaker for 24 h at room temperature until the nematodes entered the L1 development stage.

The *T. vulgaris* callus culture extract and its individual bioactive substances were tested in a liquid S medium to evaluate the growth rate of *C. elegans* larvae. For this, the substances at 100 μmol/mL (final) and the extract at a 100-fold dilution were added to the L1 nematodes simultaneously with the addition of *E. coli* OP50 bacteria. This time was considered the starting point (0 h) for assessing the effect of the tested compounds on the time it took *C. elegans* larvae to reach the sexually mature L4 development stage and lay eggs (the end point).

The growth parameters of the tested *C. elegans* larvae, including the nematodes' body surface area, length and width, were compared with those of the control nematodes. The effect of the extract and its bioactive substances on each of the mentioned parameters

of nematode ontogenesis was validated at three points of postembryonic development, including 72, 96, and 108 h. The experiments were carried out in 48-well plates (Eppendorf, USA) in 300 µL of a liquid S medium for culturing nematodes at 20 ± 0.5°C in a Binder climatic chamber (Germany). The plates were covered with a protective film to prevent evaporation of the culture liquid medium (SSI, USA). The experiments were carried out under sterile conditions in a FastFlow laminar flow hood (Italy).

An overnight culture of *E. coli* OP50, which had been washed from LB broth and resuspended in the S medium to a final bacterial concentration of 0.5 mg/mL, was added to the synchronized L1 nematodes in the S medium. Each well of the plate was filled with 270 µL of the nematode suspension with *E. coli* and then 30 µL of the test extract and its bioactive substances was added to the wells according to the dropping scheme. The plate was sealed with film and left to incubate for 72 h at 20 ± 0.5°C. Upon incubation, morphological changes in the nematodes were analyzed using an Axio Observer Z1 microscope (Karl Zeiss, Germany), with a series of images taken at a fixed magnification.

The plate was placed in a climate chamber and left to incubate for another 24 h at 20 ± 0.5°C. Then, the nematodes were tested for changes in the microscope at the same magnification. After 108 h of incubation, the procedure was repeated for the last time. The growth rates of the nematode larvae incubated in the presence of the tested extract and its individual bioactive substances were compared with those for the control nematodes (without the tested compounds).

The freeware CellProfiler 4.2.1 was used for image analysis [42]. First, the images were pre-processed to compensate for uneven illumination and remove undesirable artifacts such as well edges. Next, the nematodes and their clusters were separated by foreground/background segmentation. Then, 60 nematodes were manually selected for machine learning to identify them and separate their clusters. The resulting model was used to segment the nematodes in all the images using the UntangleWorms module [43]. The StraightenWorms and MeasureObjectSizeShape modules were used to measure the area, length, and width of the nematodes.

The nematode images were made to meet the requirements of the CellProfiler software. For this, the images were pre-processed with the ImageJ freeware to compensate for uneven illumination of the wells and to remove artifacts such as well edges, *E. coli* OP50 residues, eggs or L1 nematodes in the wells. The artifacts were "painted over" with the Pen tool (dark gray color) using the codes #a9a9a9, rgb (169, 169, 169), and cmyk (0, 0, 0, 34) to align the image background. The contrast parameter (Brightness/Contrast) was adjusted in the low-contrast images, where it was difficult to distinguish the nematodes from the background.

The digital data obtained from the nematode images during machine learning (StraightenWorms and MeasureObjectSizeShape modules) was filtered by leaving only those values that differed from the average by no more than a standard deviation. As a result of filtering, the number of measured nematode parameters (area, length, width) significantly reduced.

The digital images of the nematodes were converted to the metric scale of measurement. Using the ZenPro software of the Axio Observer Z1 microscope (Karl Zeiss, Germany), we determined the coefficient of converting pixels into millimeters (2.05×10^{-3}). So, the length and width of the nematodes in pixels were multiplied by this coefficient. To convert the area to the metric scale, the pixel values were multiplied by the square of this coefficient.

The effect of the *T. vulgaris* callus culture extract and its individual bioactive substances (0, 10, 50, 100, and 200 µM) on the lifespan of *C. elegans* was assessed in 10-, 100-, and 1000-fold dilutions based on the number of surviving worms. The experiment was conducted in 96-well plates in the liquid S medium for culturing nematodes. The number of live and dead nematodes was counted every 4–7 days during 59 days. The experiment was considered complete when there were no live nematodes left in the control group [41].

To determine the effect of the *T. vulgaris* callus culture extract and its individual bioactive substances on the resistance of *C. elegans* to oxidative and thermal stress, we modified the experiment for cultivating *C. elegans* in the liquid medium. After adding 15 µL of the bioactive substances, the plate was left for incubation at 20 ± 0.5°C for 5 days. Then, live and dead worms were counted in each well of the plate. To study the worms' resistance to oxidative stress, 15 µL of 1 M hydrogen peroxide (working concentration 100 mM) was added to each well and the incubation continued at 20 ± 0.5°C. To study the resistance of *C. elegans* to thermal stress, the plate was left for incubation at 20 ± 0.2°C. The first and second counts of live and dead nematodes were made after 24 and 48 h of incubation, respectively. The worms' resistance to oxidative and thermal stress in the presence of bioactive substances was compared with the results for the control nematodes, which were incubated without the tested compounds [44, 45].

All the experiments were conducted in triplicate. The obtained data were expressed as an average of three measurements with standard deviation. The data were analyzed using the Microsoft Office Excel 2007. The statistical analysis was performed using the ANOVA with the Scheffe's criterion.

RESULTS AND DISCUSSION

Isolation and purification of metabolites from the hydroalcoholic extract of the *Thymus vulgaris* L. callus culture. Thymol, oleanolic acid, and ursolic acid were isolated and purified from the extract of *T. vulgaris* L. callus culture using chromatography, with at least 95% of purification.

IR spectroscopy of the metabolites. The IR spectroscopy results for the bioactive substance thymol obtained from the extract of the *T. vulgaris* callus culture are presented in Fig. 2 and Table 1.

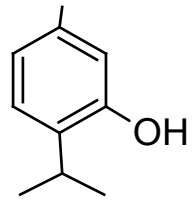

a

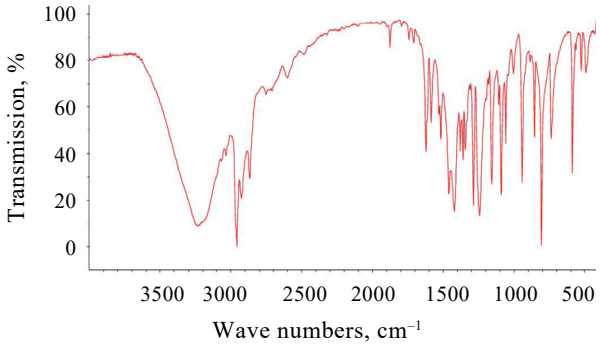

b

Figure 2 Structure (a) and IR spectrum (b) of thymol isolated from the extract of *Thymus vulgaris* L. callus culture

Table 1 Characteristic vibrational frequencies and their correlation with the main structural fragments of thymol isolated from the *Thymus vulgaris* L. callus culture extract

Structure	Wave numbers, cm^{-1}	Type of vibrations/bonds in structural fragments
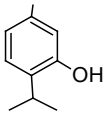	2960	Asymmetric stretching vibrations of C-H in methyl groups
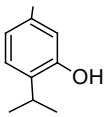	2865	Symmetric stretching vibrations of methyl groups
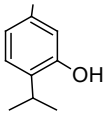	2926	Asymmetric stretching vibrations of the methylene group
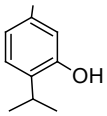	1583, 1460, 1420	Stretching vibrations of C=C bonds in a ring
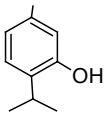	1422	Asymmetric C-C-O vibrations
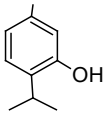	1380, 1361, 1344	Symmetric stretching C-C-O vibrations
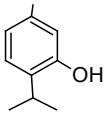	856, 806, 738	Out-of-plane deformation vibrations of C-H bonds in an aromatic ring
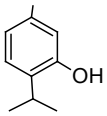	588	Out-of-plane deformation vibrations of the O-H group

As can be seen, the IR spectrum of thymol (2-isopropyl-5-methylphenol) has the following distinctive features. The absorption band at 2960 cm^{-1} is due to asymmetric stretching vibrations of C-H in methyl groups, while the band at 2865 cm^{-1} results from symmetric stretching vibrations of the molecule's methyl groups. The band at 2926 cm^{-1} is caused by asymmetric stretching vibrations of the methylene group. The first and second overtones (1877, 1744, and 1709 cm^{-1}) are due to the presence of substituents in the para- and meta- positions. Stretching vibrations of the C-C ring are at 1583, 1460, and 1420 cm^{-1}. The triplet bands at 1380, 1361, and 1344 cm^{-1} characterize an isopropyl fragment. The band around 1422 cm^{-1} is due to in-plane deformation vibrations of the O-H group. Out-of-plane deformation vibrations of C-H bonds in the aromatic ring are at 856, 806, and 738 cm^{-1}. Out-of-plane deformation C-C vibrations in the aromatic ring are at 745 cm^{-1}. A broad band of out-of-plane deformation vibrations of the O-H group is found around 588 cm^{-1}.

The IR spectroscopy results for oleanolic acid obtained from the extract of the *T. vulgaris* callus culture are presented in Fig. 3 and Table 2.

As can be seen, the IR spectrum of oleanolic acid isolated from the extract of *T. vulgaris* callus culture has the following distinctive features. The band with the absorption maximum at 3386 cm^{-1} is specific for the associated O-groups. The band at 2931 cm^{-1} is due to symmetric stretching vibrations of C-H in methyl fragments (groups). The band at 2867 cm^{-1} also corresponds to symmetric stretching vibrations of C-H in methyl fragments (groups). The strong intensity band at 1716 cm^{-1} is due to stretching vibrations of C=O in the carboxyl group.

The band at 1451 cm^{-1} is due to scissor vibrations of C-H in methylene groups, which is specific for cyclohexane structures. The band at 1377 cm^{-1} corresponds to deformation vibrations of C-H in geminal methyl groups. The bands at 1252 and 1162 cm^{-1} are due to stretching vibrations of the C-O-H bond. The broad band at 1050 cm^{-1} is caused by planar deformation vibrations of the C-O bond. The band at 960 cm^{-1} results from methylene vibrations of C-H. Finally, the bands at 861 and 771 cm^{-1} are formed by pendulum vibrations of methylene groups.

The IR spectroscopy results for ursolic acid obtained from the extract of the *T. vulgaris* callus culture are presented in Fig. 4 and Table 3.

As can be seen, the IR spectrum of ursolic acid (3β-hydroxyurs-12-ene-28-oic acid) isolated from the extract of *T. vulgaris* callus culture has the following distinctive features.

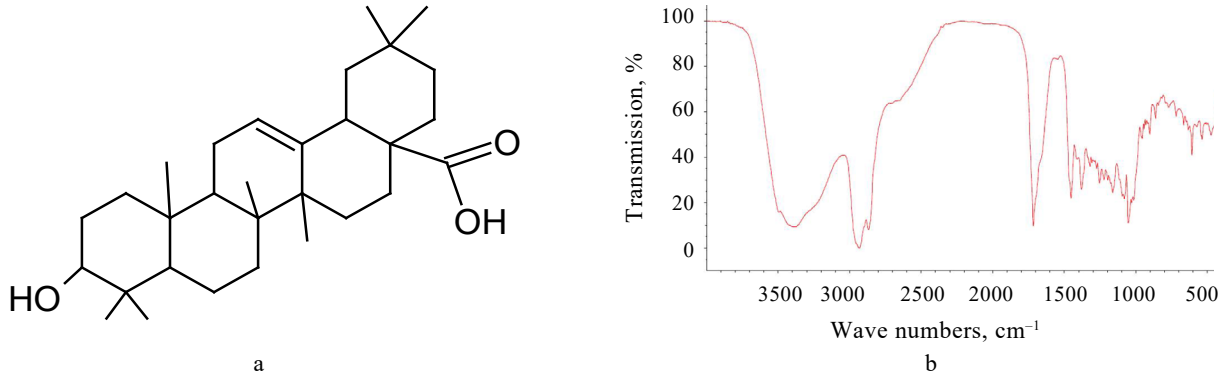

a b

Figure 3 Structure (a) and IR spectrum (b) of oleanolic acid isolated from the extract of *Thymus vulgaris* L. callus culture

Table 2 Characteristic vibrational frequencies and their correlation with the main structural fragments of oleanolic acid isolated from the *Thymus vulgaris* L. callus culture extract

Structure	Wave numbers, cm^{-1}	Type of vibrations/bonds in structural fragments
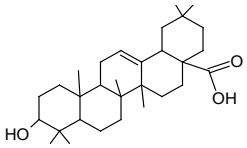	3433	Associated OH groups
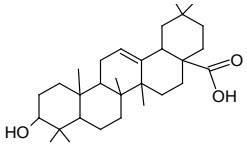	2962	Stretching symmetric C-H vibrations in methyl groups
	1652	Stretching vibrations of C=O in a carboxyl group
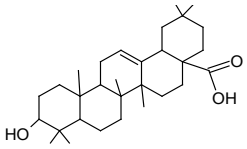	1451	Scissor vibrations of C-H in methylene groups
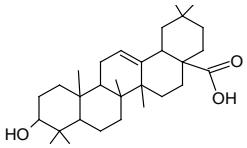	1377	Deformation vibrations of C-H in methylene structures
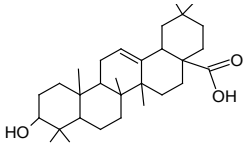	1320	Planar deformation vibrations of C-O
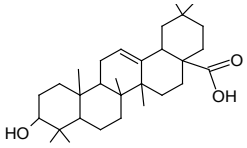	1252, 1162	Stretching vibrations of the C-O bond
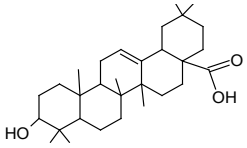	960	Planar deformation vibrations of the hydroxyl (alcohol) group in ring A
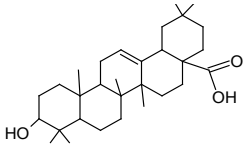	861, 771	Pendulum vibrations of methylene groups

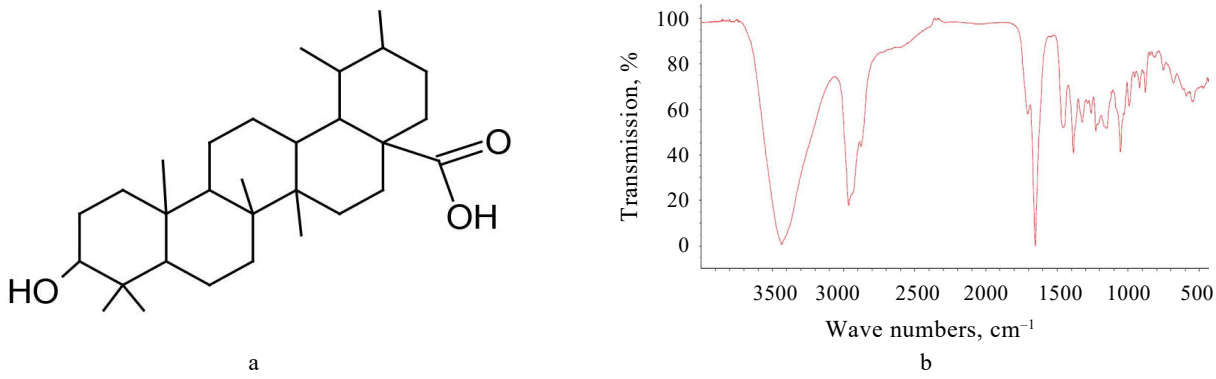

a b

Figure 4 Structure (a) and IR spectrum (b) of ursolic acid isolated from the extract of *Thymus vulgaris* L. callus culture

Table 3 Characteristic vibrational frequencies and their correlation with the main structural fragments of ursolic acid isolated from the *Thymus vulgaris* L. callus culture extract

Structure	Wave numbers, cm^{-1}	Type of vibrations/bonds of structural fragments
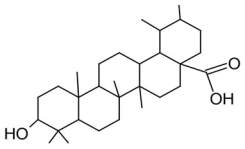	3433	Associated OH groups
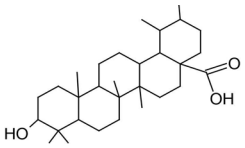	2962	Stretching symmetrical vibrations of C-H in methyl fragments
	1652	Stretching vibrations of C=O in a carboxyl group
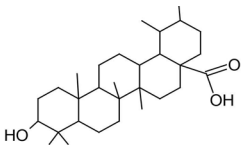	1453	Scissor vibrations of C-H in methylene groups
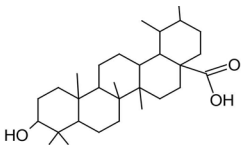	1384	Deformation vibrations of C-H in methyl structures
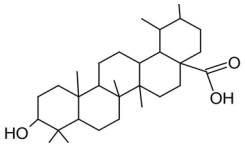	1320	Planar deformation vibrations of C-O
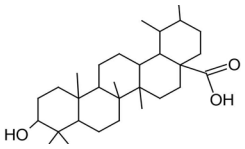	1261, 1226	Stretching vibrations of the C-O bond
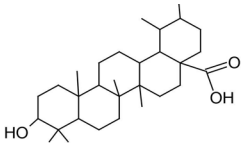	993	Planar deformation vibrations of the hydroxyl (alcohol) group in ring A
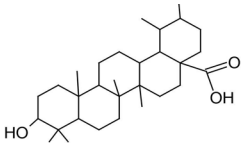	880, 730	Pendulum vibrations of methylene groups

The band with the absorption maximum at 3433 cm^{-1} is specific for the associated OH groups. The band at 2962 cm^{-1} is due to symmetric stretching vibrations of C-H in methyl fragments (groups). The band at 2877 cm^{-1} also corresponds to symmetric stretching vibrations of C-H in methyl fragments (groups). The strong intensity band at 1652 cm^{-1} is caused by stretching vibrations of C=O in the carboxyl group.

The band at 1453 cm^{-1} is caused by scissor vibrations of C-H in the methylene groups, which is specific for cyclohexane structures. The band at 1384 cm^{-1} is due to deformation vibrations of C-H in geminal methyl structures. The band at 1320 cm^{-1} results from planar deformation vibrations of O-H. The bands at 1261 and 1226 cm^{-1} are caused by stretching vibrations of the C-O-H bond. The broad band at 1053 cm^{-1} is formed by planar deformation vibrations of the O-C-C, C-O bond. The band at 993 cm^{-1} is due to methylene vibrations of C-H. Finally, the bands at 881 and 749 cm^{-1} are caused by pendulum vibrations of the methylene fragments of ursolic acid.

According to the results, the spectral activity of the individual bioactive substances corresponds to their structural features. Their characteristic features, including those in the fingerprint zone of the IR spectrum, are also consistent with their cultivation, extraction, and preparation.

HPLC identification of the metabolites. The HPLC results for the bioactive substances isolated from the extract of *T. vulgaris* callus culture are presented in Fig. 5.

The biological activity of the extract of *T. vulgaris* L. callus culture and its metabolites. ***The effect of the extract and its bioactive substances on the growth of C. elegans larvae.*** The effect of the *T. vulgaris* callus culture extract and its individual bioactive substances

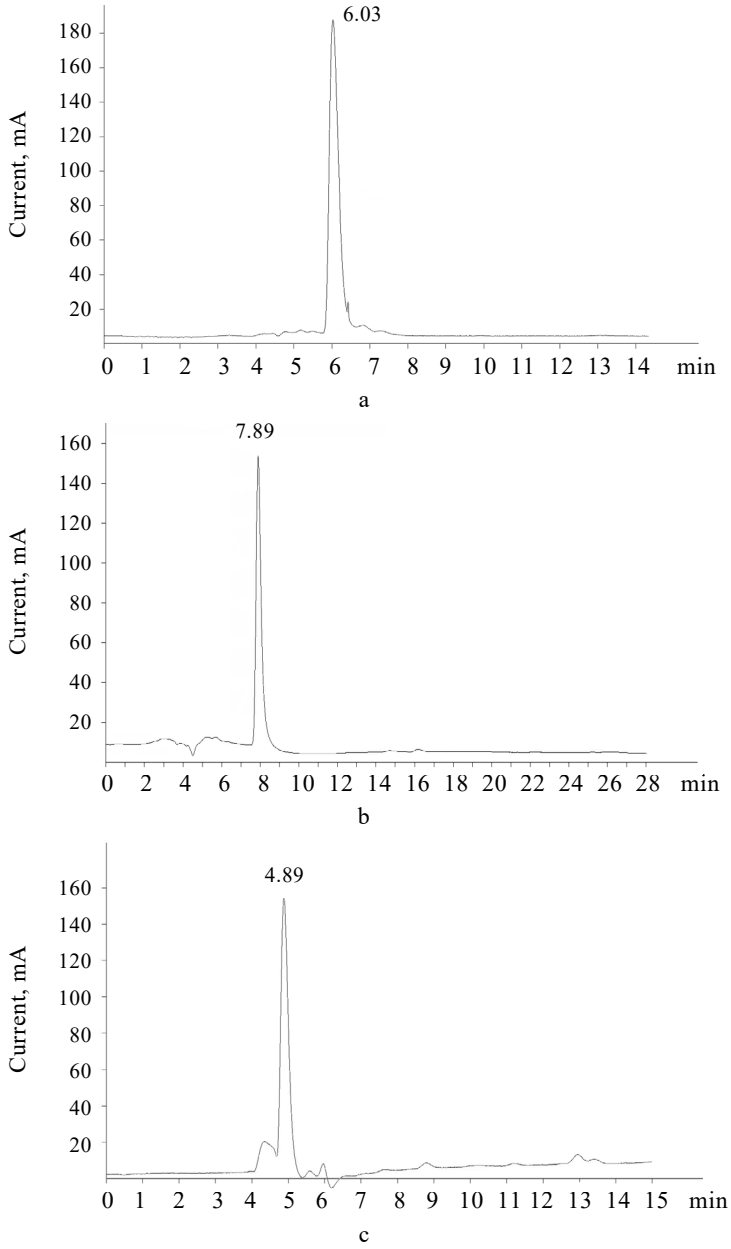

Figure 5 HPLC chromatogram: (a) oleanolic acid; (b) ursolic acid; and (c) thymol

(thymol, oleanolic and ursolic acids) at 100 μM on the growth of *C. elegans* larvae was determined as a duration of larval development from stage L1 (larvae) to stage L4 (sexually mature nematodes). The control nematodes were incubated without adding the tested compounds. The results are presented in Table 4.

When cultivated on solid agar, it usually takes a *C. elegans* larva (stage L1) three days to reach a sexually mature stage of development (L4), when it lays eggs formed in the intestinal cavity. In a liquid medium, however, neither the control nor the test nematodes laid eggs after 72 h. The control worms had a slight shift in ontogenesis and laid eggs after 96 h of incubation. None of the tested bioactive substances accelerated the development of the L1 larva to stage L4 compared to the control. However, the compounds had a different effect on the growth rate of nematode larvae, namely:

1. In the presence of ursolic acid (sample 4), the entire population of nematodes reached stage L4 after 96 h, laying eggs with a new generation of L1 larvae.
2. In the presence of oleanolic acid (sample 3), only part of the nematode population began laying eggs after 96 h (some even produced an insignificant number of new L1 larvae), but some nematodes did not reach stage L4 even after 108 h.
3. In the presence of thymol (sample 2), larval growth was fully inhibited and none of the nematodes reached stage L4 even after 108 h, with no new larvae produced.

To further study the effect of the *T. vulgaris* extract and its metabolites on the growth rate of nematode larvae, we also determined their body surface area, length, and width.

To determine the body surface area of the L4 nematode larvae, we performed image processing with machine learning, using the programs described in the methods section above. Initially, the images were preprocessed in the ImageJ program to compensate for uneven lighting and to remove undesirable artifacts for subsequent machine learning.

Then, the nematodes and their clusters were separated from the image background using foreground/background segmentation. The next step was machine learning of 60 nematode images using the UntangleWorms, MeasureObjectSizeShape, and StraightenWorms modules of CellProfiler 4.2.1. Its aim was to write an algorithm for identifying and segmenting the nematodes from the entire pool.

Applying the machine learning algorithm, we obtained a number of nematode parameters, including their area, length, and width. After filtering, these data in pixels were converted to metric units (mm). The larva body surface area was recorded until the nematodes reached stage L4.

The effects of the *T. vulgaris* callus culture extract and its metabolites (thymol, oleanolic and ursolic acids) on the nematodes' surface area, length, and width are presented in Figs. 6–8.

As can be seen in Fig. 6, the extract of the *T. vulgaris* callus culture increased the surface area of the nematodes throughout the entire experiment, with the maximum area after 108 h of incubation. The delay in the larval growth from L1 to L4 correlated with the increased surface area over time. The area of the control nematodes remained unchanged during 108 h of obser-

Table 4 Development from larva (L1) to adult nematodes (L4)

Sample	Name of sample	72 h	96 h	108 h
1	*Thymus vulgaris* L. callus culture extract	–	+	n.a.
2	Thymol	–	–	–
3	Oleanolic acid	–	–/+	+/–
4	Ursolic acid	–	+	n.a.
Control		–/+	+	n.a.

"+" – L1 larvae are present; "–/+" – small numbers of L1 in the population; "+/–" – not all the nematodes have laid eggs or produced a new L1 generation; n.a. – not available

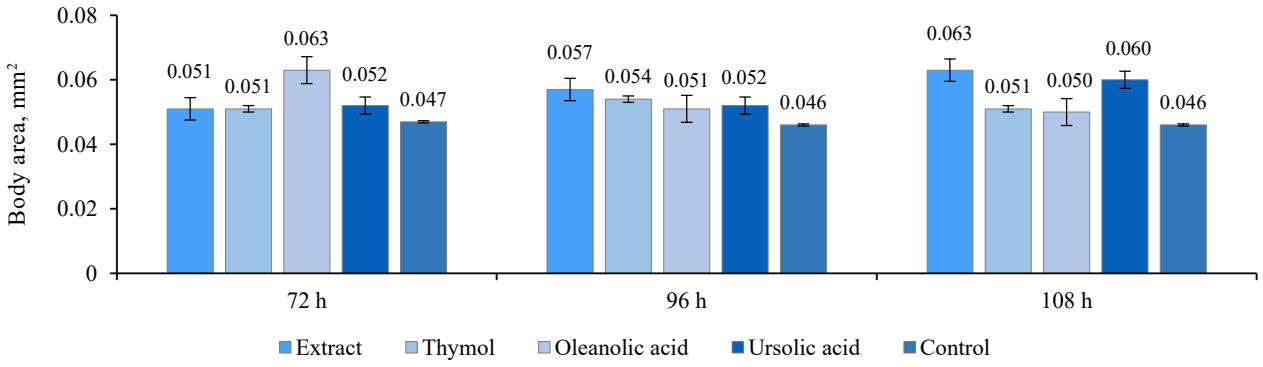

Figure 6 Effect of the *Thymus vulgaris* L. callus culture extract and its bioactive substances on the *Caenorhabditis elegans* body surface area

vation. Regardless of the effect that the extract and its bioactive substances had on the growth rate of the larvae, their surface area exceeded the area of the control larvae throughout the experiment.

The fastest larva development was observed in the presence of oleanolic acid, with all L4 nematodes producing a new generation of L1 larvae after 72 h. In the presence of ursolic acid, the fastest developing larvae to stage L4 in 96 h had a decreased surface area. Thymol had an insignificant effect on the surface area of the larvae, with only a 1.17-fold increase over 96 h of incubation, compared to the control nematodes.

As can be seen in Fig. 7, the body length of the tested nematodes significantly exceeded the length of the control nematodes after 72, 96, and 108 h of incubation.

The *T. vulgaris* extract increased the length of the nematodes during 108 h of incubation. Also, it might have had an anabolic effect expressed in a larger surface area. In the presence of ursolic acid, the maximum length of the larvae was observed after 72 h. It was higher than the length of the control nematodes by an average of 23.3%. The longest length was registered in the presence of oleanolic acid after 108 h of incubation. Furthermore, the effect of oleanolic acid was greater than that of thymol and ursolic acid by factors of 1.16 and 1.24, respectively.

According to Fig. 8, the width of the control larvae remained unchanged throughout the experiment (108 h). No significant differences against the control were found in the presence of the *T. vulgaris* extract and thymol. Oleanolic and ursolic acids had an insignificant effect on the body width of the nematode larvae, increasing it only 1.01 times compared to the extract, thymol, and the control group.

The effect of T. vulgaris callus culture extract and its individual bioactive substances on the lifespan of C. elegans. The effect of the *T. vulgaris* extract and its metabolites on the lifespan of *C. elegans* was determined as the number of surviving worms.

The extract was tested in 10-, 100-, and 1000-fold dilutions (Fig. 9).

We found that the extract of *T. vulgaris* callus culture in a 10-fold dilution was toxic to the nematodes: they died after 3 weeks of incubation in its presence. In a 100-fold dilution, the extract had little effect on the lifespan of the nematodes. Their survival began to decline on day 36 of incubation, and on day 40, they all died. In a 1,000-fold dilution, the extract had no effect on the lifespan of the nematodes in comparison with the control group.

The effects of the bioactive substances isolated from the *T. vulgaris* extract at concentrations of 0, 10, 50, 100, and 200 μM on the lifespan of *C. elegans* are presented in Figs. 10–12.

As shown in Fig. 10, thymol at 10 μM increased the survival of the nematodes on day 8 by a factor of 1.8 compared to the control group. Overall, however, thymol at various concentrations had no positive effect on the

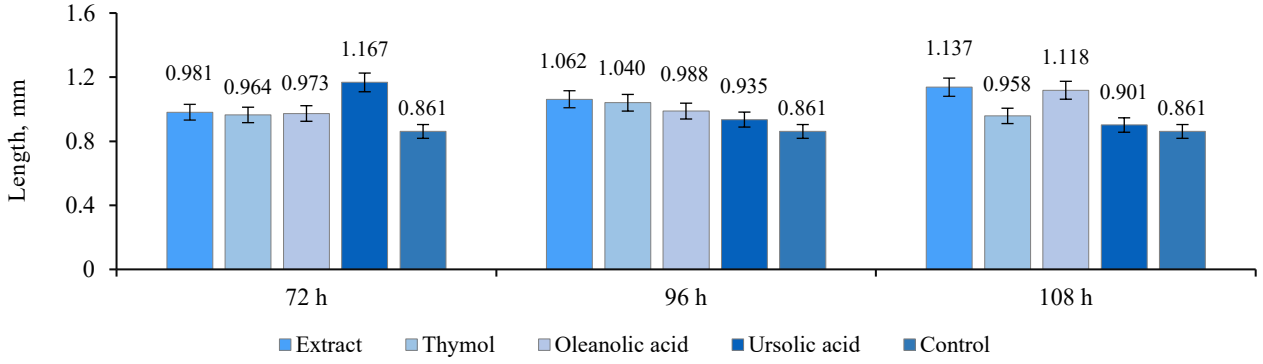

Figure 7 Effect of the *Thymus vulgaris* L. callus culture extract and its bioactive substances on the *Caenorhabditis elegans* length

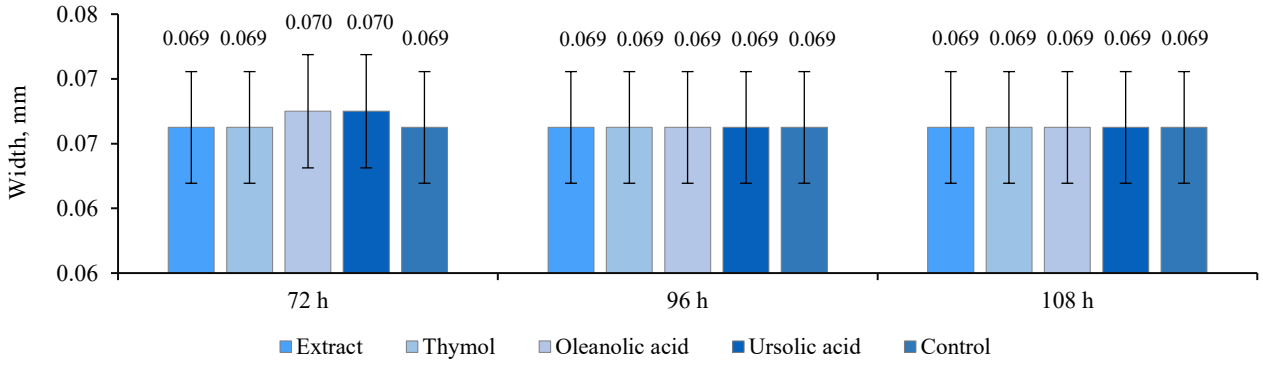

Figure 8 Effect of the *Thymus vulgaris* L. callus culture extract and its bioactive substances on the *Caenorhabditis elegans* width

lifespan of *C. elegans*. Moreover, it turned out to be toxic since the nematodes began to die on day 13 of incubation.

According to Fig. 11, oleanolic acid at 10 and 50 μM increased the lifespan of the nematodes by a factor of 1.9. On day 61 of the experiment, 16% of the nematode population remained alive and active. Higher concentrations of oleanolic acid (100 and 200 μM) had a negative effect on the lifespan of *C. elegans*.

As shown in Fig. 12, ursolic acid had no significant effect on the lifespan of the nematodes. At concentrations of 50 and 100 μM, it had a positive effect from day 3 to day 30 of nematode incubation. After day 30, the lifespan of the worms became comparable with that of the control group.

We found no publications on the effect of the *T. vulgaris*. callus culture extract on the lifespan of *C. elegans*.

Our data confirmed that thymol, oleanolic acid, and ursolic acid can influence and increase the lifespan of the nematodes [46–48].

The effect of T. vulgaris callus culture extract and its individual bioactive substances on stress (oxidative and thermal) resistance of C. elegans. The effect of the *T. vulgaris* callus culture extract and its metabolites on the resistance of *C. elegans* to oxidative stress was assessed by counting the nematodes that died within 24 and 48 h at 20°C after the addition of 1 M hydrogen peroxide (working concentration 100 mM) under oxidative stress conditions.

Figure 13 shows the results for the *T. vulgaris* callus culture extract in 10-, 100-, and 10.00-fold dilutions.

As can be seen in Fig. 13, the 10.00-fold dilution of the *T. vulgaris* extract increased the resistance of *C. elegans* to oxidative stress. Their survival rate was 1.5 times higher compared to the control. However, after 48 h of incubation, the extract lost its effect on the resistance of the nematodes to oxidative stress. Furthermore, the *T. vulgaris* extract did not show any stress-resistant effect on *C. elegans* under heat stress during 24 and 48 h.

Figure 14 shows the effect of the individual bioactive substances at concentrations of 0, 10, 50, 100, and 200 μM on the resistance of *C. elegans* to oxidative stress during 24 and 48 h of exposure.

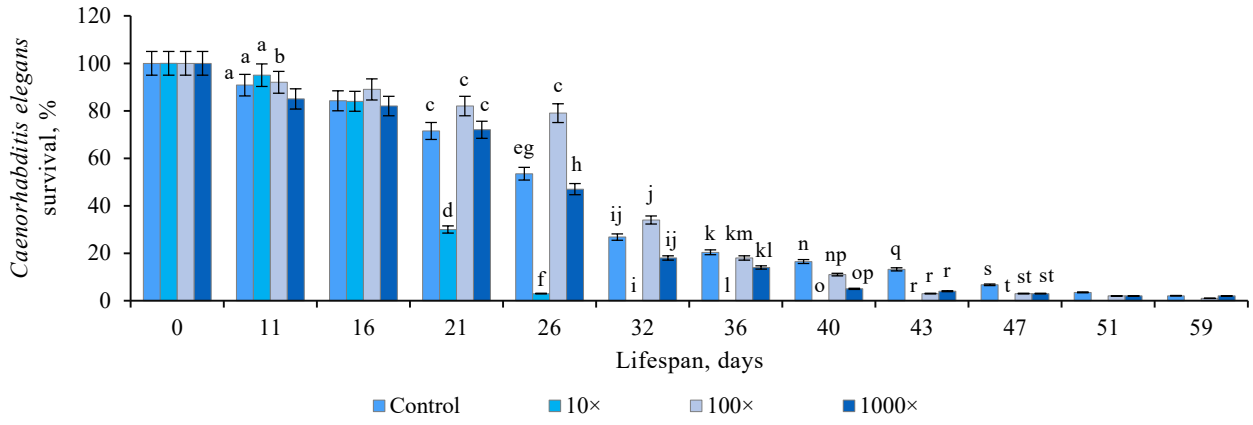

Different letter indices denote statistically significant differences between the samples (within a parameter) according to ANOVA with Scheffe's post hoc test. Identical letter indices denote the absence of significant differences

Figure 9 Effect of *Thymus vulgaris* L. callus culture extract on the lifespan of *Caenorhabditis elegans* nematodes

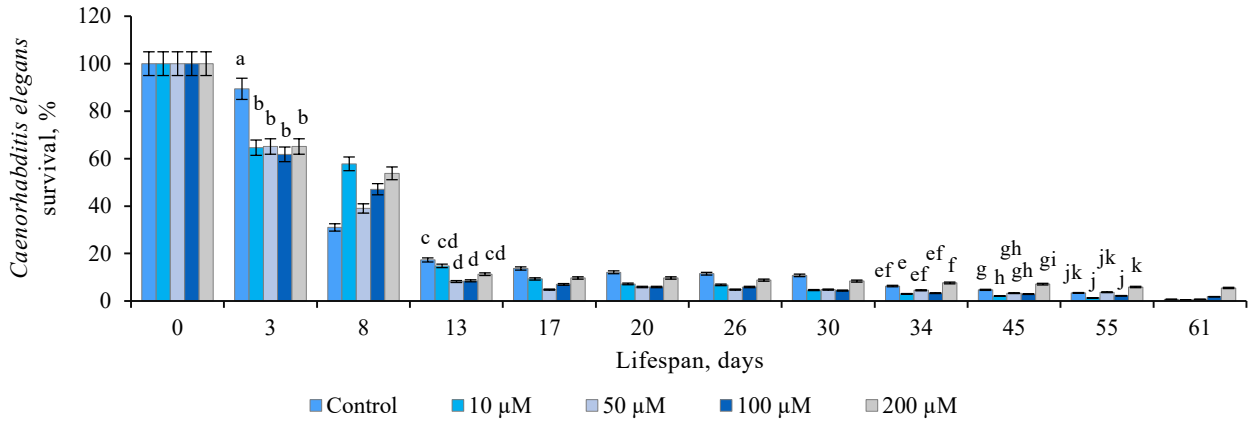

Different letter indices denote statistically significant differences between the samples (within a parameter) according to ANOVA with Scheffe's post hoc test. Identical letter indices denote the absence of significant differences

Figure 10 Effect of thymol isolated from *Thymus vulgaris* L. callus culture extract on the lifespan of *Caenorhabditis elegans* nematodes

As can be seen, oleanolic and ursolic acids at all tested concentrations (10–200 μM) affected the survival of *C. elegans,* compared to the control. Thymol showed an insignificant effect on the resistance of the nematodes to oxidative stress. At 50 μM, this substance increased the survival of the nematodes 1.01 times compared to the control, but at the other concentrations, it had no effect on *C. elegans* stress resistance.

The analysis of *C. elegans* resistance to oxidative stress during 48 h of exposure revealed that thymol and

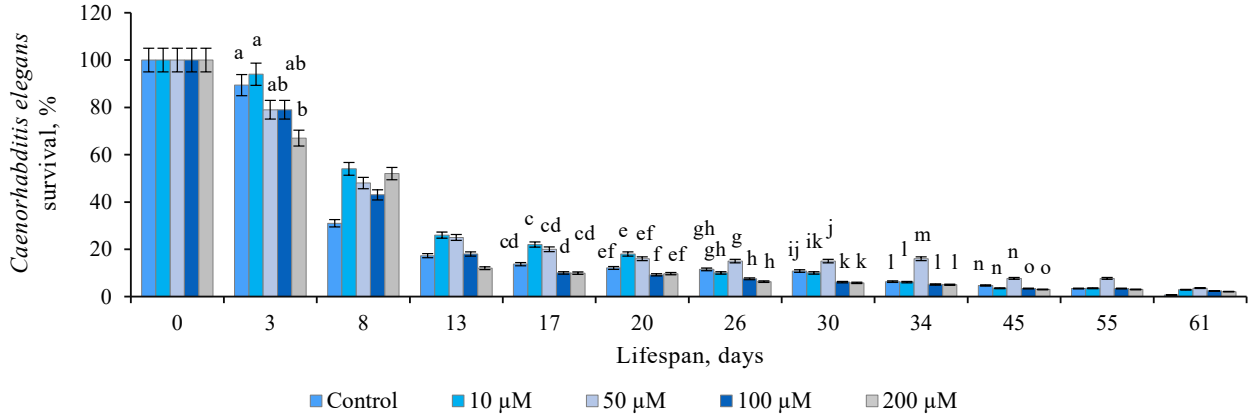

Different letter indices denote statistically significant differences between the samples (within a parameter) according to ANOVA with Scheffe's post hoc test. Identical letter indices denote the absence of significant differences

Figure 11 Effect of oleanolic acid isolated from *Thymus vulgaris* L. callus culture extract on the lifespan of *Caenorhabditis elegans* nematodes

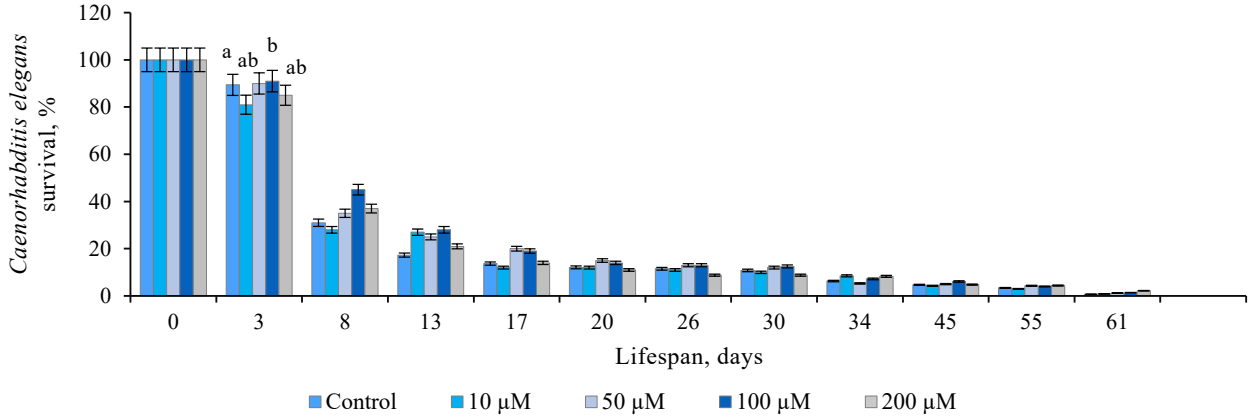

Different letter indices denote statistically significant differences between the samples (within a parameter) according to ANOVA with Scheffe's post hoc test. Identical letter indices denote the absence of significant differences

Figure 12 Effect of ursolic acid isolated from *Thymus vulgaris* L. callus culture extract on the lifespan of *Caenorhabditis elegans* nematodes

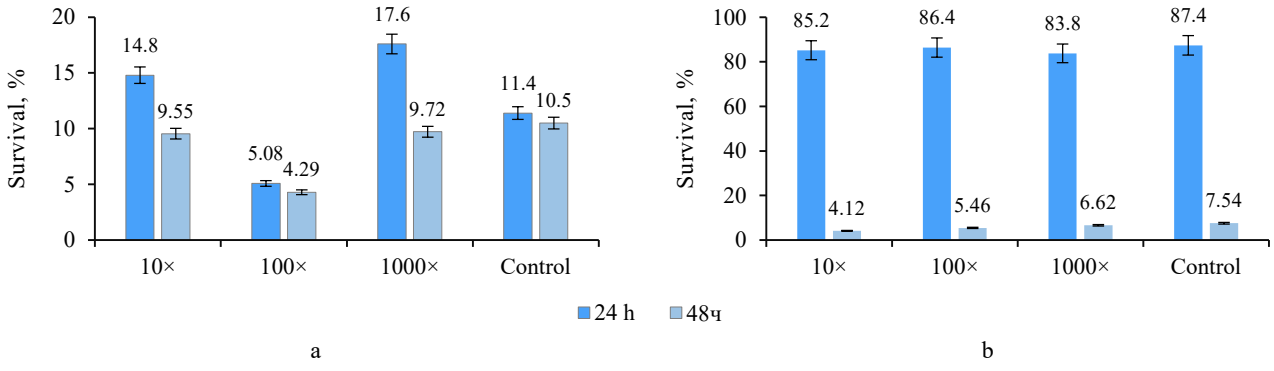

Figure 13 Effect of *Thymus vulgaris* L. callus culture extract on the stress resistance of *Caenorhabditis elegans*: (a) oxidative stress; (b) thermal stress

oleanolic acid at 10–200 μM increased the survival rate of the nematodes 1.1 times compared to the control. Ursolic acid showed the same result but only at 10–100 μM. At a concentration of 200 μM, ursolic acid decreased the survival of the nematodes compared to the control.

Figure 15 shows the effect of the individual bioactive substances at concentrations of 0, 10, 50, 100, and 200 μM on the resistance of *C. elegans* to thermal stress during 24 and 48 h of exposure.

During 24 h of *C. elegans* exposure to thermal stress, thymol at 10 μM increased the survival rate of the nematodes by a factor of 1.01 compared to the control. However, at higher concentrations of 50 to 200 μM, thymol led to a decrease in the survival rate. Oleanolic

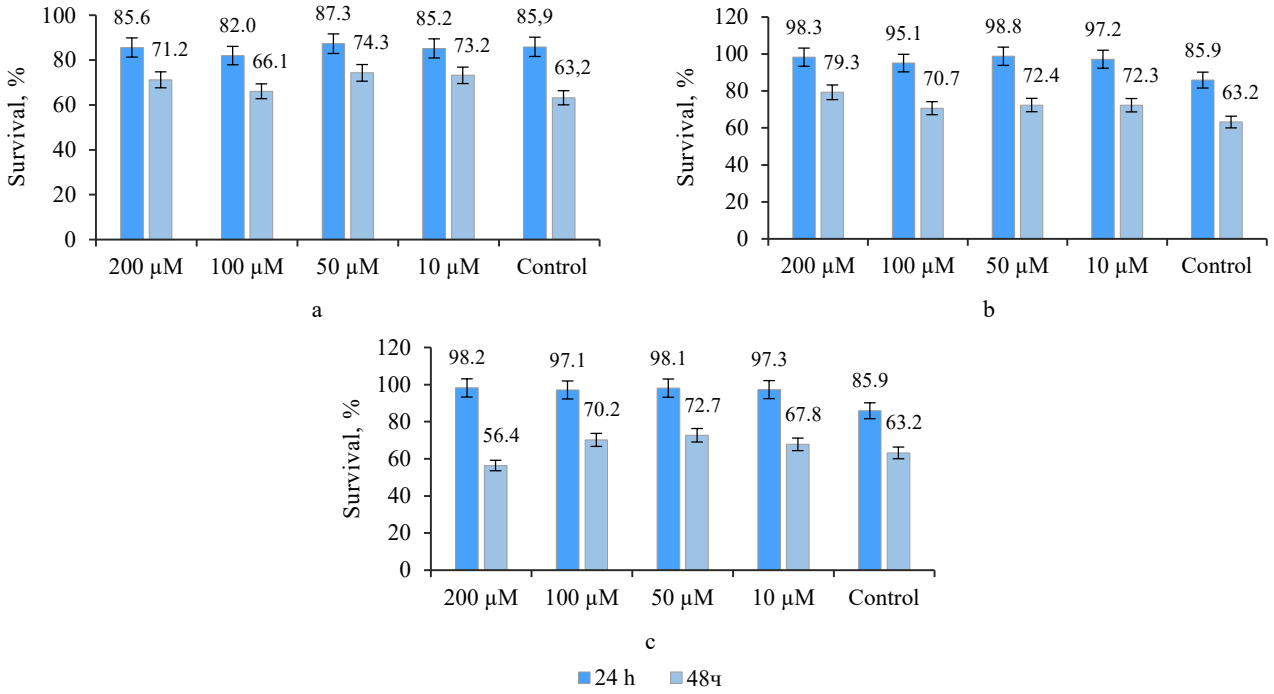

Figure 14 Effect of individual bioactive substances on *Caenorhabditis elegans* resistance to oxidative stress: (a) thymol; (b) oleanolic acid; and (c) ursolic acid

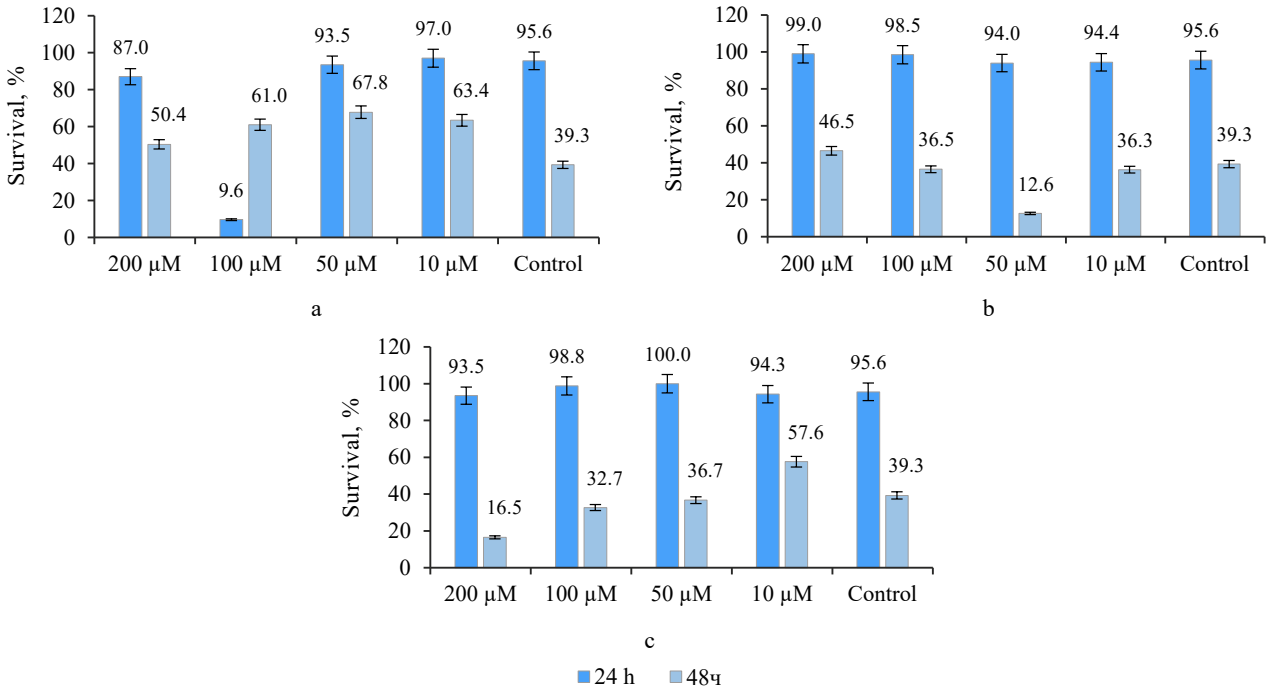

Figure 15 Effect of individual bioactive substances on *Caenorhabditis elegans* resistance to thermal stress: (a) thymol; (b) oleanolic acid; and (c) ursolic acid

acid increased the survival rate only at high concentrations of 200 and 100 μM, compared to the control. Ursolic acid at 100 and 50 μM showed a significant increase in the survival of the nematodes, compared to the control.

During 48 h of *C. elegans* exposure to thermal stress, thymol at concentrations of 10–200 μM led to a high survival rate of the nematodes. Oleanolic acid at 10 μM increased their survival rate by a factor of 1.18, compared to the control, but significantly decreased it at its other concentrations. Ursolic acid at 10 μM insignificantly increased the survival rate of the nematodes exposed to thermal stress, compared to the control. Yet, its higher concentrations of 50 to 200 μM decreased the number of surviving nematodes.

We found no publications on the effect of the *T. vulgaris* callus culture extract on the resistance of *C. elegans* to oxidative and thermal stress.

Our findings on *C. elegans* stress resistance under the influence of thymol, oleanolic acid, and ursolic acid are consistent with those reported in scientific literature [46]. For example, Zhang *et al*. [47] demonstrated that oleanolic acid can increase stress resistance and reduce intracellular reactive oxygen species in *C. elegans*. A study by Yue *et al*. [48] shows that ursolic acid can reduce the level of reactive oxygen species during oxidative stress in the nematodes. Naß *et al*. [49] also reported that ursolic acid increased resistance to oxidative and thermal stress.

Our data differed from the data reported by other authors since we used different concentrations of the metabolites and a different source of their isolation.

To sum up, our results suggest that a 70% hydroalcoholic extract of the *T. vulgaris* callus culture and its individual bioactive substances (thymol, oleanolic and ursolic acids) have geroprotective potential since they can affect the growth rate of *C. elegans* larvae, as well as the lifespan and resistance of the nematodes to oxidative and thermal stress. This makes them good candidates for use in functional foods and preventative dietary supplements.

CONCLUSION

Our study found that the *Thymus vulgaris* L. callus culture is a promising source of metabolites such as thymol, oleanolic acid, and ursolic acid. These substances have a number of bioactive properties, including a positive effect on the growth of *Caenorhabditis elegans* larvae, as well as their lifespan and survival under oxidative and thermal stress.

Effects on the growth rate of *C. elegans* larvae:

– the *T. vulgaris* callus culture extract increased the length of the nematodes during 108 h of incubation and, possibly, exhibited an anabolic effect by increasing their body surface area;
– in the presence of ursolic acid, the entire population of the nematodes developed from larvae to sexually matured nematodes (stage L4) after 96 h, laying eggs with a new generation of L1 larvae;
– in the presence of oleanolic acid, some nematodes began laying eggs after 96 h and even produced an insignificant number of new larvae, but all the nematodes did not reach stage L4 even after 108 h;
– thymol fully inhibited the growth of nematode larvae, with no larvae reaching the reproductive L4 stage even after 108 h. The eggs formed in that period failed to hatch into larvae;
– in the presence of ursolic acid, the fastest development of larvae to stage L4 in 96 h was accompanied by a decrease in the nematodes' body area; and
– under the action of ursolic acid, the nematodes reached their maximum length after 72 h, exceeding the length of the control nematodes by an average of 23.3%.

Effects on the lifespan of *C. elegans*:

– in a 100-fold dilution, the *T. vulgaris* callus culture extract increased the lifespan of the nematodes;
– in the presence of thymol at 10 μM, the survival of the nematodes on day 8 increased by a factor of 1.8 compared to the control group; and
– oleanolic acid at 10 and 50 μM increased the lifespan of the nematodes by a factor of 1.9. On day 61 of the experiment, 16% of the nematodes remained alive and active.

Effects on the resistance of *C. elegans* to oxidative and thermal stress:

– in a 1000-fold dilution, the *T. vulgaris* callus culture extract increased the survival of the nematodes under oxidative stress by a factor of 1.5 compared to the control;
– at all concentrations (10–200 μM), thymol, oleanolic acid, and ursolic acid affected the survival of the nematodes under oxidative stress, compared to the control;
– during 24 h of incubation under thermal stress, thymol at 10 μM increased the percentage of surviving nematodes by a factor of 1.01; oleanolic acid increased nematode survival only at 200 and 100 μM; and ursolic acid significantly increased nematode survival at 100 and 50 μM, compared to the control; and
– during 48 h of incubation under thermal stress, thymol at 10–200 μM showed a high percentage of nematode survival; oleanolic acid at 10 μM increased nematode survival by a factor of 1.8; and ursolic acid at 10 μM insignificantly increased nematode survival, compared to the control.

CONTRIBUTION

A.M. Fedorova and A.A. Shevel designed the research concept; the formal analysis was performed by E.S. Miller; S.V. Kovalenko, A.I. Loseva, A.V. Zaushintsena, O.G. Altshuler, and V.P. Yustratov developed the methodology; A.M. Fedorova wrote, reviewed, and proofread the manuscript. All the authors have read and approved the manuscript.

CONFLICT OF INTEREST

The authors declared no potential conflict of interest regarding the research, authorship, and/or publication of this article.

REFERENCES

1. Lopez-Otín C, Blasco MA, Partridge L, Serrano M, Kroemer G. Hallmarks of aging: An expanding universe. Cell. 2023;186(2):243–278. https://doi.org/10.1016/j.cell.2022.11.001
2. Zhong Y, Jin C, Zhang X, Zhou R, Dou X, *et al*. Aging imaging: The future demand of health management. European Journal of Nuclear Medicine and Molecular Imaging. 2023;50:3820–3823. https://doi.org/10.1007/s00259-023-06377-z
3. Dominguez LJ, Veronese N, Baiamonte E, Guarrera M, Parisi A, *et al*. Healthy aging and dietary patterns. Nutrients. 2022;14(4):889. https://doi.org/10.3390/nu14040889
4. Zeppa SD, Agostini D, Ferrini F, Gervasi M, Barbieri E, *et al*. Interventions on gut microbiota for healthy aging. Cells. 2023;12(1):34. https://doi.org/10.3390/cells12010034
5. Fedorova AM, Dyshlyuk LS, Milentyeva IS, Loseva AI, Neverova OA, *et al*. Geroprotective activity of trans-cinnamic acid isolated from the Baikal skullcap (*Scutellaria baicalensis*). Food Processing: Techniques and Technology. 2022;52(3):582–591. (In Russ.) https://doi.org/10.21603/2074-9414-2022-3-2388
6. Ma T, Tian X, Zhang B, Li M, Wang Y, *et al*. Low-dose metformin targets the lysosomal AMPK pathway through PEN2. Nature. 2022;603(7899):159–165. https://doi.org/10.1038/s41586-022-04431-8
7. Nadeeshani H, Li J, Ying T, Zhang B, Lu J. Nicotinamide mononucleotide (NMN) as an anti-aging health product – Promises and safety concerns. Journal of Advanced Research. 2022;37:267–278. https://doi.org/10.1016/j.jare.2021.08.003
8. Vesnina A, Milentyeva I, Minina V, Kozlova O, Asyakina L. Evaluation of the *in vivo* anti-atherosclerotic activity of quercetin isolated from the hairy roots of *Hedysarum neglectum* Ledeb. Life. 2023;13(8):1706. https://doi.org/10.3390/life13081706
9. Sukhikh S, Babich O, Prosekov A, Patyukov N, Ivanova S. Future of chondroprotectors in the treatment of degenerative processes of connective tissue. Pharmaceuticals. 2020;13(9):220. https://doi.org/10.3390/ph13090220
10. Roberts SB, Silver RE, Das SK, Fielding RA, Gilhooly CH, *et al*. Healthy aging-nutrition matters: Start early and screen often. Advances in Nutrition. 2021;12(4):1438–1448. https://doi.org/10.1093/advances/nmab032
11. Fokina AD, Vesnina AD, Frolova AS, Chekushkina DYu, Proskuryakova LA, *et al*. Bioactive anti-aging substances: Geroprotectors. Food Processing: Techniques and Technology. 2024;54(2):423–435. (In Russ.) https://doi.org/10.21603/2074-9414-2024-2-2517
12. Babich O, Larina V, Krol O, Ulrikh E, Sukhikh S, *et al*. *In vitro* study of biological activity of *Tanacetum vulgare* extracts. Pharmaceutics. 2023;15(2):616. https://doi.org/10.3390/pharmaceutics15020616
13. Babich O, Dyshlyuk L, Noskova S, Sukhikh S, Prosekov A, *et al*. *In vivo* study of the potential of the carbohydrate-mineral complex from pine nut shells as an ingredient of functional food products. Bioactive Carbohydrates and Dietary Fibre. 2019;18:100185. https://doi.org/10.1016/j.bcdf.2019.100185
14. Asyakina L, Atuchin V, Drozdova M, Kozlova O, Prosekov A. *Ex vivo* and *in vitro* antiaging and antioxidant extract activity of the *Amelanchier ovalis* from Siberia. International Journal of Molecular Sciences. 2022;23(23):15156. https://doi.org/10.3390/ijms232315156
15. Luo J, Si H, Jia Z, Liu D. Dietary anti-aging polyphenols and potential mechanisms. Antioxidants. 2021;10(2):283. https://doi.org/10.3390/antiox10020283
16. Si H, Liu D. Dietary antiaging phytochemicals and mechanisms associated with prolonged survival. The Journal of Nutritional Biochemistry. 2014;25(6):581–591. https://doi.org/10.1016/j.jnutbio.2014.02.001
17. Islam MA, Khandker SS, Kotyla PJ, Hassan R. Immunomodulatory effects of diet and nutrients in systemic lupus erythematosus (SLE): A systematic review. Frontiers in Immunology. 2020;11:1477. https://doi.org/10.3389/fimmu.2020.01477
18. Long Z, Xiang W, He Q, Xiao W, Wei H, *et al*. Efficacy and safety of dietary polyphenols in rheumatoid arthritis: A systematic review and meta-analysis of 47 randomized controlled trials. Frontiers in Immunology. 2023;14:1024120. https://doi.org/10.3389/fimmu.2023.1024120
19. La Rosa G, Lonardo MS, Cacciapuoti N, Muscariello E, Guida B, *et al*. Dietary polyphenols, microbiome, and multiple sclerosis: From molecular anti-inflammatory and neuroprotective mechanisms to clinical evidence. International Journal of Molecular Sciences. 2023;24(8):7247. https://doi.org/10.3390/ijms24087247
20. Liu Y, Fang M, Tu X, Mo X, Zhang L, *et al*. Dietary polyphenols as anti-aging agents: Targeting the hallmarks of aging. Nutrients. 2024;16(19):3305. https://doi.org/10.3390/nu16193305
21. Shimada A, Ueno H, Inagaki M. Glutaminase inhibitory activities of pentacyclic triterpenes isolated from *Thymus vulgaris* L. Nat Prod Res. 2021;36(11):2864–2868. https://doi.org/10.1080/14786419.2021.1921766

22. Horváth G, Horváth A, Reichert G, Böszörmenyi A, Sipos K, *et al*. Three chemotypes of thyme (*Thymus vulgaris* L.) essential oil and their main compounds affect differently the IL-6 and TNF*α* cytokine secretions of BV-2 microglia by modulating the NF-*κ*B and C/EBP*β* signalling pathways. BMC Complementary Medicine and Therapies. 2021;21(1):148. https://doi.org/10.1186/s12906-021-03319-w

23. Sammi SR, Trivedi S, Rath SK, Nagar A, Tandon S, *et al*. 1-Methyl-4-propan-2-ylbenzene from *Thymus vulgaris* attenuates cholinergic dysfunction. Molecular Neurobiology. 2017;54(7):5468–5481. https://doi.org/10.1007/s12035-016-0083-0

24. Warman DJ, Jia H, Kato H. Effects of thyme (*Thymus vulgaris* L.) essential oil on aging-induced brain inflammation and blood telomere attrition in chronologically aged C57BL/6J mice. Antioxidants. 2023;12(6):1178. https://doi.org/10.3390/antiox12061178

25. Micucci M, Protti M, Aldini R, Frosini M, Corazza I, *et al*. *Thymus vulgaris* L. essential oil solid formulation: Chemical profile and spasmolytic and antimicrobial effects. Biomolecules. 2020;10(6):860. https://doi.org/10.3390/biom10060860

26. Pereira O, Peres A, Silva A, Domingues M, Cardoso S. Simultaneous characterization, and quantification of phenolic compounds in *Thymus x citriodorus* using a validated HPLC–UV and ESI-MS combined method. Food Research International. 2013;54(2):1773–1780. https://doi.org/10.1016/j.foodres.2013.09.016

27. Alarcón R, Pardo-de-Santayana M, Priestley C, Morales R, Heinrich M. Medicinal and local food plants in the south of Alava (Basque Country, Spain). Journal of Ethnopharmacology. 2015;176:207–224. https://doi.org/10.1016/j.jep.2015.10.022

28. Li X, He T, Wang X, Shen M, Yan X, *et al*. Traditional uses, chemical constituents and biological activities of plants from the genus *Thymus*. Chemistry & Biodiversity. 2019;16(9):e1900254. https://doi.org/10.1002/cbdv.201900254

29. Efremov AP. Medicinal plants and fungi of central Russia. The complete Determinant Atlas. Moscow: Phyton XXI; 2024, 504 p. (In Russ.)

30. Ozyigit II, Dogan I, Hocaoglu-Ozyigit A, Yalcin B, Erdogan A, *et al*. Production of secondary metabolites using tissue culture-based biotechnological applications. Frontiers in Plant Science. 2023;14:1132555. https://doi.org/10.3389/fpls.2023.1132555

31. Babich O, Sukhikh S, Pungin A, Ivanova S, Asyakina L, *et al*. Modern trends in the *in vitro* production and use of callus, suspension cells and root cultures of medicinal plants. Molecules. 2020;25(24):5805. https://doi.org/10.3390/molecules25245805

32. Babich O, Sukhikh S, Pungin A, Ivanova S, Asyakina L, *et al*. Correction: Babich et al. Modern trends in the in vitro production and use of callus, suspension cells and root cultures of medicinal plants. Molecules. 2022;27(17):5513. https://doi.org/10.3390/molecules27175513

33. Grevtsova SA, Aylyarova MK, Rekhviashvili EI, Kabulova MYu. Callus culture of linear scouring (S. linear) – As an alternative source of clonal micropropagation. Innovative technologies in crop production and ecology: Proceedings of the international scientific and practical conference dedicated to the 80th anniversary of the birth of the scientist, microbiologist, agroecologist, honored worker of higher education of Russia, honored scientist of north Ossetia, Dr Agri Sci, professor Alexander Timofeevich Farniev. Vladikavkaz, 2017;116–118. (In Russ.) https://elibrary.ru/YPARSJ

34. Vesnina A, Prosekov A, Atuchin V, Minina V, Ponasenko A. Tackling atherosclerosis via selected nutrition. International Journal of Molecular Sciences. 2022;23(15):8233. https://doi.org/10.3390/ijms23158233

35. Busquets O, Ettcheto M, Pallàs M, Camins A, Folch J, *et al*. Experimental models for aging and their potential for novel drug discovery. Current Neuropharmacology. 2018;16(10):1466–1483. https://doi.org/10.2174/1570159X15666170707155345

36. Zhang W, Zheng B, Deng N, Wang H, Li T, *et al*. Effects of ethyl acetate fractional extract from *Portulaca oleracea* L. (PO-EA) on lifespan and healthspan in *Caenorhabditis elegans*. Journal of Food Science. 2020;85(12):4367–4376. https://doi.org/10.1111/1750-3841.15507

37. Song B, Zheng B, Li T, Liu RH. Raspberry extract ameliorates oxidative stress in *Caenorhabditis elegans* via the SKN-1/Nrf2 pathway. Journal of Functional Foods. 2020;70:103977. https://doi.org/10.1016/j.jff.2020.103977

38. Havermann S, Humpf HU, Wätjen W. Baicalein modulates stress-resistance and life span in *C. elegans* via SKN-1 but not DAF-16. Fitoterapia. 2016;113:123–127. https://doi.org/10.1016/j.fitote.2016.06.018

39. Dyshlyuk LS, Fedorova AM, Loseva AI, Eremeeva NI. Callus cultures of *Thymus vulgaris* and *Trifolium pratense* as a source of geroprotectors. Food Processing: Techniques and Technology. 2021;51(2):423–432. https://elibrary.ru/UCGPFZ

40. Ayvazov BV. Intro to chromatography. Moscow: Vysshaya shkola; 1983, 240 p. (In Russ.)

41. Faskhutdinova ER, Sukhikh AS, Le VM, Minina VI, Khelef MEA, *et al*. Effects of bioactive substances isolated from Siberian medicinal plants on the lifespan of *Caenorhabditis elegans*. Foods and Raw Materials. 2022;10(2): 340–352. https://doi.org/10.21603/2308-4057-2022-2-544
42. McQuin C, Goodman A, Kamentsky L, Cimini BA, Karhohs KW, *et al*. CellProfiler 3.0: Next-generation image processing for biology. PLoS Biology. 2018;16(7):e2005970. https://doi.org/10.1371/journal.pbio.2005970
43. Wählby C, Kamentsky L, Liu ZH, Riklin-Raviv T, Conery AL, *et al*. An image analysis toolbox for high-throughput *C. elegans* assays. Nature Methods. 2012;9(7):714–716. https://doi.org/10.1038/nmeth.1984
44. Vesnina A, Milentyeva I, Minina V, Kozlova O, Asyakina L. Evaluation of the *in vivo* anti-atherosclerotic activity of quercetin isolated from the hairy roots of *Hedysarum neglectum* Ledeb. Life. 2023;13(8):1706. https://doi.org/10.3390/life13081706
45. Le V, Sukhikh A, Milentyeva I, Asyakina L, Prosekov A, *et al*. Effects of rutin produced by *Filipendula ulmaria* callus cultures on the lifespan and stress resistance in *Caenorhabditis elegans*. Caspian Journal of Environmental Sciences. 2023;21:313.
46. Henrique Moniz AM, Xavier Junior FH, Melo Martins Silva G, Reis de Melo ACG, Silva MMCL, *et al*. *Lippia origanoides* essential oil increases longevity and ameliorates *β*-amyloid peptide-induced toxicity in *Caenorhabditis elegans*. Natural Product Research. 2023;39(4):695–703. https://doi.org/10.1080/14786419.2023.2287183
47. Zhang J, Lu L, Zhou L. Oleanolic acid activates *daf-16* to increase lifespan in *Caenorhabditis elegans*. Biochemical and Biophysical Research Communications. 2015;468(4):843–849. https://doi.org/10.1016/j.bbrc.2015.11.042
48. Yue Z, Liu H, Liu M, Wang N, Ye L, Guo C, *et al*. *Cornus officinalis* extract enriched with ursolic acid ameliorates UVB-induced photoaging in *Caenorhabditis elegans*. Molecules. 2024;29(12):2718. https://doi.org/10.3390/molecules29122718
49. Naß J, Efferth T. Ursolic acid ameliorates stress and reactive oxygen species in *C. elegans* knockout mutants by the dopamine Dop1 and Dop3 receptors. Phytomedicine. 2021;81:153439. https://doi.org/10.1016/j.phymed.2020.153439

ORCID IDs
Anastasiya M. Fedorova https://orcid.org/0000-0002-8071-4411
Arina A. Shevel https://orcid.org/0009-0000-3630-2826
Svetlana V. Kovalenko https://orcid.org/0009-0006-2889-4458
Ekaterina S. Miller https://orcid.org/0000-0002-7538-8076
Anna I. Loseva https://orcid.org/0000-0003-4037-2653
Olga G. Altshuler https://orcid.org/0000-0001-7035-673X
Alexandra V. Zaushintsena https://orcid.org/0000-0003-4645-828X
Vladimir P. Yustratov https://orcid.org/0000-0002-1779-4332

GUIDE FOR AUTHORS FORMATTING REQUIREMENTS FOR ARTICLES

We publish original, previously unpublished English language articles that possess scientific novelty in the field of food industry and related branches of science. The Journal publishes scientific papers, peer reviews, brief scientific communications, letters to the editor, and related news items.

The main requirements for submitted articles are: validity of factual material, clarity and brevity, reproducibility of experimental data. The manuscript should meet the specified formatting standards. Please make sure that the section "Results and discussion" of your article states the novelty of your research.

All manuscripts submitted to the *Foods and Raw Materials* should be written in US English. The manuscript should contain no less than 10 pages in Microsoft Word text editor, abstract, tables, figures, and references included.

Format instructions

– 20 mm margins;
– single line spacing without automatic hyphenation;
– no extra interspaces between words or gaps between paragraphs;
– Times New Roman, size 10.

Structure

(1) **The type of your manuscript** should be clarified in the upper left corner (scientific article, review article, short message, note or letter, etc).

(2) **Title** (< 10 words) should be informative and reflect the main results of the research. The title of the article should be in lowercase letters, with the exception of the first letter and proper names. Please avoid abbreviations.

(3) **First and last names of the authors** are separated by commas. Paternal and middle names should be contracted to the first letter. Spelling should coincide with your ORCID id. Please mark the name of the author responsible for correspondence with an asterisk*.

(4) **Affiliation** is a formal name of the institution, city, postal address with postal code. The names and locations of institutions or companies should be given for all authors. If several institutions are listed, match the institution and the corresponding author with superscript numbers. Please include the e-mail address of the author responsible for correspondence.

(5) **Abstract** (200–250 words) cannot exceed 2000 characters with spaces. The abstract should be original and completely reflect the main results and novelty of the article. The best way to structure your abstract is to let it follow the structure of the article itself: relevance, tasks and objectives, methods, results, and conclusions. Please avoid meaningless introductory phrases and vague, general statements.

(6) **Keywords** provide < 10 keywords identifying the subject and the result of the research. Remember that it is key words that enable your potential readers to find your article on the Internet.

(7) **Funding** indicates how the research and the publication of this article were funded. If the study was performed with the support of a grant, specify the number of the grant and its name. State the name of your employer if the study was performed as part of your routine work and did not receive additional funding.

(8) **Introduction** gives a brief review of the publications related to the matter and proves its relevance. Referenced sources should be indexed in international scientific databases. In-text references should be given in square brackets and numbered [beginning with №1] in order of their appearance in the text. If several sources are quoted, they are given in chronological order. Make sure your introduction reflects the objectives of your research.

(9) **Study objects and methods:**

– Experimental research papers should contain a full description of the subject of the study, consecutive stages of the experiment, equipment, and reagents. Do not forget to specify the original company names of equipment and reagents manufacturers in brackets. If the method you use is not widely known or has been considerably modified, please provide a brief description.

– Theoretical research papers should specify objectives, approximations and assumptions, conclusions and equations. Please do not overload your text with intermediate data and description of well-known methods (such as numerical methods of solving equations) unless you have introduced some novelty into them.

– Review studies should include a paragraph that specifies the selection algorithm for sources to be reviewed. The paragraph describes databases (Scopus, Web of Science, Elibrary; bibliographies, conferences, etc.), types of publications (articles, reviews, ports, books, etc.), publication sources (journals, books, conference proceedings, etc.), period when they were published, justification of the search strategy, exclusion criteria, etc.

(10) **Results and discussion** should provide a concise description of experimental data. Rather than repeating the data given in tables and graphs, the text should seek to reveal the principles detected. While describing your research results, it is recommended to use the Past Indefinite verb tense. The discussion should not reiterate the results. The discussion should contain an interpretation of the obtained research results (compliance of the results with the research hypothesis, generalisation of the research results, suggestions for practical application and future research).

Each **table** should be made in MS Word (Table – Add Table) or MS Excel and contain no less than three columns. Provide a number and a title for each table.

The Journal publishes color photographs and diagrams.

Mathematical equations should start with a separate line and be typed in the MathType frame as a whole. Mind that it is not allowed to compile formulae from composite elements (e.g. one part of the formula is a table, another part is a text, and some other part is an embedded frame). Please maintain the common settings for fonts, the size of characters and their placement in MathType formulas. Please avoid manual change for individual symbols or formula elements.

(11) **Conclusion** briefly summarises the main results of your research. Naturally, the conclusion should contain the answer to the question posed by the introduction.

(12) **Contribution** should indicate the actual contribution of each author in the research process. *Foods and Raw Materials* observes the CRediT taxonomy of the authors' contributions.

(13) **Conflict of interest** should indicate a real or potential conflict of interest. If there is no conflict of interests, you should write that "the author declares that there is no conflict of interest".

(14) **Acknowledgements** contains expression of gratitude to those who contributed to the research.

(15) **AI declaration**. You are expected to disclose the use of AI tools at all stages of manuscript preparation, including: text generation, even in such formal parts as introduction, discussion, conclusions, or annotations; data preparation or validation, e.g., statistical analysis, visualization, or data synthesis; translation, paraphrasing, or editing; searching for relevant publications or compiling references; processing/creating figures, graphs, charts, audio/video materials, etc.

(16) **References** should be formatted according to the standard defined by the editors. The references are given in the order of their appearance in the text. Make sure you have included the DOI, if available.

Please avoid references to publications that are not readily available, e.g. institutional regulations, state standards, technical requirements, unpublished works, proceedings of conferences, extended abstracts of dissertation, and dissertations. Make sure you do not cite unpublished articles. It is not recommended to use more than three references to web resources. Please avoid citing publications that are more than 10 years old.

Self-citation should be well-justified and cannot exceed 10% of the references. Please make sure that at least 50% of the works you cite are less than 5 years old and published in periodicals registered in such data bases as Scopus, Web of Science, etc.

If you mention no references to fresh, 2–3-year-old papers, it might reduce your chances for publication. The references should reflect the actual impact of representatives of the international scientific community on the issue.

The manuscript should be carefully checked and signed by all authors on the first page of the main text. The article will not be published if it fails to meet the requirements. All articles are subject to general editing.

Correspondence and submission of all documents is done by e-mail: *fjournal@mail.ru* or *jfrm.ru/en*

The editors expect to receive accompanying documents in Russian or English.

For submission instructions, subscription and all other information visit this journals online at *jfrm.ru/en/*

Foods and Raw Materials. 2026;14(2)
ISSN 2310-9599 (Print)
ISSN 2308-4057 (Online)
Available online at https://jfrm.ru/en/
DOI: https://doi.org/10.21603/2308-4057-2026-2

CONTENTS

Prosekov Alexander Yu. Food security and globalization 247

Omran Azza A., Hassan Nadra S.Y., Hanaa Abd Elaziz M. Alternative sweets from cooked pulses and date products: Nutritional and quality characteristics 252

Kaledin Anatoly P., Stepanova Marina V., Sotnikova Larisa F., Zaitsev Sergei Yu., Melikova Yulia N., Kuryndina Anastasia S., Vilmis Daria A. Carcinogenesis of malignant neoplasms in cats: Development factors 264

Dolganyuk Vyacheslav F., Kashirskikh Egor V., Sukhikh Stanislav A., Kremleva Olga E., Ulrikh Elena V., Malkov Danil I., Babich Olga O. Effect of cultivation conditions on polysaccharide synthesis by *Skeletonema pseudocostatum* 276

Perevozchikova Maria A., Domsky Igor A., Sergeev Alexey A., Economov Alexander V., Dolgikh Mikhail A., Dolgikh Alexander V. Hematological profile of wild boar *Sus scrofa* (Linnaeus 1758) (*Suina, Suidae*) in the Kirov Region, Russia 285

Tan Kimberly Weng Kuan, Yong Phaik Har, Ng Zhi Xiang Synergistic anti-glycation and antioxidant interaction among different mushroom extract combinations 300

Parada Romina B., Marguet Emilio R., Campos Carmen A., Vallejo Marisol Controlled fermentation in improving the functional properties of *Brassica* with *Undaria* 321

Mamay Dmitriy S., Babenyshev Sergey P., Evdokimov Ivan A., Mamay Angelina V., Lisitsyn Vyacheslav A. Empirical predicting permeate flux in skim milk microfiltration 331

Soloshenko Vladimir A., Mager Sergey N. Prospects for livestock farming in Siberia and Far East of Russia 339

Omoike Bright A., Okieimen Felix E., Imoisi Chinyere Developing composite films from carboxymethyl starch, polyvinyl alcohol, and kaolin for sustainable packaging applications 344

Diakite Simbo, Kavhiza Nyasha J., Saquee Francess S., Pakina Elena N., Zargar Meisam, Diarra Ousmane, Norman Prince E., Traore Brahima, Samake Fasse, Daou Cheickna, Babana Amadou H. Precision agriculture as a viable means of enhancing sustainable agricultural production 357

Neverov Evgeniy N., Korotkih Pavel S., Gorelkina Alena K., Timoshchuk Irina V. Experimental recirculating carbon dioxide refrigeration unit 377

Budianto, Suparmi Anik, Feri Zefki O., Arifin Muh J., Kristiani Kiki, Susanti Dewi, Irianto Tommy D., Furwanti Endang S., Marniasari Desi W. *Tetragonula laeviceps* honey: Biochemical composition and kinetics of 5-hydroxymethylfurfural formation 386

Priyadarshana Sameera, Somawathie Konara, Shafras Mohamed, Sivanandarajah Darsiga Brinjal, turkey berry, and winged bean extracts: Total phenolic content and antioxidant activity 399

Tsepeleva Irina A., Yudina Alesya N., Krasnoshtanova Alla A. Stabilizing liposomes loaded with proteins, amino acids, vitamins, and microelements 408

Shokina Yulia V., Lutsyk Pavel V., Reshetnik Ekaterina I., Gribanova Svetlana L., Derzhapolskaya Yulia I., Yiqian Ma Soft-shell clam from the waters of the Kandalaksha Bay: Use for food purposes 425

Stepanova Anna A., Mitina Alice D., Velichkovich Natalia S., Kozlova Oksana V., Larichev Timothy A., Proskuryakova Larisa A., Martirosyan Vladimir V. Whey and water-ethanol solution as extractants of biologically active substances: Comparative analysis 432

Fedorova Anastasia M., Shevel Arina A., Kovalenko Svetlana V., Miller Ekaterina S., Loseva Anna I., Altshuler Olga G., Zaushintsena Alexandra V., Yustratov Vladimir P. Geroprotective potential of *Thymus vulgaris* L. callus culture and its metabolites 443